

# FINAL REPORT

Cooperative Technology Demonstration: Polymer-Enhanced  
Subsurface Delivery and Distribution of Permanganate

ESTCP Project ER-200912

February 2013

Michelle Crimi  
**Clarkson University**

Jeffrey A.K. Silva  
**Polymer Methods in Remediation**

Tom Palaia  
**CH2M HILL**

*This document has been cleared for public release*



# REPORT DOCUMENTATION PAGE

*Form Approved*  
OMB No. 0704-0188

Public reporting burden for this collection of information is estimated to average 1 hour per response, including the time for reviewing instructions, searching existing data sources, gathering and maintaining the data needed, and completing and reviewing this collection of information. Send comments regarding this burden estimate or any other aspect of this collection of information, including suggestions for reducing this burden to Department of Defense, Washington Headquarters Services, Directorate for Information Operations and Reports (0704-0188), 1215 Jefferson Davis Highway, Suite 1204, Arlington, VA 22202-4302. Respondents should be aware that notwithstanding any other provision of law, no person shall be subject to any penalty for failing to comply with a collection of information if it does not display a currently valid OMB control number. **PLEASE DO NOT RETURN YOUR FORM TO THE ABOVE ADDRESS.**

<b>1. REPORT DATE (DD-MM-YYYY)</b> 13-02-2013		<b>2. REPORT TYPE</b> Final Cost and Performance Report		<b>3. DATES COVERED (From - To)</b> 04/2009 - 12/2012	
<b>4. TITLE AND SUBTITLE</b>  Polymer-Enhanced Subsurface Delivery and Distribution of Permanganate				<b>5a. CONTRACT NUMBER</b> W912 HQ-09-C-0006	
				<b>5b. GRANT NUMBER</b>	
				<b>5c. PROGRAM ELEMENT NUMBER</b>	
<b>6. AUTHOR(S)</b> Crimi, Michelle; Silva, Jeffrey, A.K.; Palaia, Thomas, A.				<b>5d. PROJECT NUMBER</b> ER-200912	
				<b>5e. TASK NUMBER</b>	
				<b>5f. WORK UNIT NUMBER</b>	
<b>7. PERFORMING ORGANIZATION NAME(S) AND ADDRESS(ES)</b>  Clarkson University 8 Clarkson Avenue Potsdam, NY 13699				<b>8. PERFORMING ORGANIZATION REPORT NUMBER</b>	
<b>9. SPONSORING / MONITORING AGENCY NAME(S) AND ADDRESS(ES)</b> SERDP/ESTCP 4800 Mark Center Drive Suite 17D08 Alexandria, VA 22350-6386				<b>10. SPONSOR/MONITOR'S ACRONYM(S)</b> ESTCP	
				<b>11. SPONSOR/MONITOR'S REPORT NUMBER(S)</b> ER-200912	
<b>12. DISTRIBUTION / AVAILABILITY STATEMENT</b>  Approved for public release; distribution is unlimited					
<b>13. SUPPLEMENTARY NOTES</b>					
<b>14. ABSTRACT</b> The goal of this project was to demonstrate and validate the use of a water-soluble polymer with permanganate for in situ chemical oxidation (ISCO) of organic contaminants to improve the sweep efficiency of permanganate through heterogeneous media and to control manganese dioxide particles to enhance contaminant destruction. Two test plots were treated at Marine Corps Base Camp Lejeune's Site 88 to treat TCE. Permanganate only was delivered to one plot to serve as a control, while permanganate with the polymers xanthan gum (for improved sweep) and sodium hexametaphosphate (for manganese dioxide byproduct control) were delivered to the second plot. With polymer, the sweep efficiency doubled from 37% in the permanganate-only plot to 67% in the permanganate + polymer plot with one pore volume of amendment delivered. With polymer, preferential flow was reduced and there was no resulting negative impact to injection pressure. Total costs of polymer-amended ISCO above traditional ISCO are estimated at approximately \$58 per cubic meter of treated media. Additional benefits of implementation can include lower injection volume and field time requirements and lower probability of contaminant rebound.					
<b>15. SUBJECT TERMS</b>					
<b>16. SECURITY CLASSIFICATION OF:</b>			<b>17. LIMITATION OF ABSTRACT</b>	<b>18. NUMBER OF PAGES</b>	<b>19a. NAME OF RESPONSIBLE PERSON</b> Michelle Crimi
<b>a. REPORT</b>	<b>b. ABSTRACT</b>	<b>c. THIS PAGE</b>			<b>19b. TELEPHONE NUMBER (include area code)</b> 315-268-4174

# CONTENTS

<b>List of Tables</b>	<b>iii</b>
<b>List of Figures</b>	<b>iv</b>
<b>Acronyms</b>	<b>ix</b>
<b>Acknowledgements</b>	<b>xii</b>
<b>Executive Summary</b>	<b>xiii</b>
<b>1.0 Introduction</b>	<b>1</b>
1.1 Background	1
1.2 Objective of the Demonstration	1
1.3 Regulatory Drivers	1
<b>2.0 Technology</b>	<b>2</b>
2.1 Technology Description	2
2.2 Advantages and Limitations of the Technology	16
<b>3.0 Performance Objectives</b>	<b>17</b>
<b>4.0 Site Description</b>	<b>18</b>
4.1 Site Location and History	18
4.2 Site Geology/Hydrogeology	21
4.3 Contaminant Distribution	34
<b>5.0 Test Design</b>	<b>39</b>
5.1 Conceptual Experimental Design	39
5.2 Baseline Characterization	39
5.3 Treatability Study Results	45
5.4 Design and Layout of Technology Components	52
5.5 Field Testing	60
5.6 Sampling Methods	62
5.7 Sampling Results	65
<b>6.0 Performance Assessment</b>	<b>111</b>
6.1 Performance Criteria: Evaluate Occurrence of Contaminant Rebound Post-Treatment	112
6.2 Performance Objective: Improved Contaminant Treatment Effectiveness	112
6.3 Performance Objective: Increased Penetration of Permanganate into Lower Permeability Layers/Strata	112
6.4 Performance Objective: Decreased Flow Bypassing of Areas of High Contaminant Mass	113
6.5 Performance Objective: Decrease Impact of MnO <sub>2</sub> Deposition of Injection Pressures	114
6.6 Performance Objective: Improved Understanding of Impacts of the Enhanced Delivery Approach on Groundwater Quality	114

<b>7.0</b>	<b>Cost Assessment</b>	<b>115</b>
7.1	Cost Model	115
7.2	Cost Drivers	120
7.3	Cost Analysis	121
<b>8.0</b>	<b>Implementation Issues</b>	<b>124</b>
<b>9.0</b>	<b>References</b>	<b>128</b>

**Appendix A: Points of Contact**

**Appendix B: Raw Data for Soil and Groundwater Samples Collected  
Pre-, Post-, and 1 Year Post-treatment**

**Appendix C: DPT Data Plots**

**Appendix D: Treatability Study Plan**

**Appendix E: Treatability Study Report**



## LIST OF TABLES

<b>Table 2-1</b>	<b>Impacts of MnO<sub>2</sub> on Subsurface Permeability: Laboratory and Field Evaluations</b>
<b>Table 2-2</b>	<b>Experimental Conditions</b>
<b>Table 2-3</b>	<b>Range of Response Values and Statistical Significance of Reaction Variables</b>
<b>Table 2-4</b>	<b>Advantages and Limitations of Enhanced Permanganate ISCO using Water Soluble Polymers</b>
<b>Table 3-1</b>	<b>Demonstration Performance Objectives</b>
<b>Table 4-1</b>	<b>Hydraulic Conductivity Calculated at Each Slug Test Location</b>
<b>Table 4-2</b>	<b>Analytical Results for Contaminants (GC-MS) in Soils</b>
<b>Table 4-3</b>	<b>Analytical Results for Contaminants (GC-MS) in Groundwater</b>
<b>Table 4-4</b>	<b>Site Characterization Summary</b>
<b>Table 5-1</b>	<b>Operating Conditions for Characterizing Permeability Reduction using Xanthan</b>
<b>Table 5-2</b>	<b>Schedule of Plot Testing and Sampling</b>
<b>Table 5-3</b>	<b>Total Number and Types of Samples to be Collected</b>
<b>Table 5-4</b>	<b>Analytical Methods for Sample Analysis</b>
<b>Table 5-5</b>	<b>Control Plot Operation (permanganate only)</b>
<b>Table 5-6</b>	<b>Test Plot Operation (permanganate + polymer)</b>
<b>Table 5-7</b>	<b>Project Schedule</b>
<b>Table 5-8</b>	<b>QA/QC Samples</b>
<b>Table 5-9</b>	<b>Pre-treatment VOCs Concentrations for Control and Test Plot from Cores Collected During the Drilling of Injection Wells and CMT Wells</b>
<b>Table 6-1</b>	<b>Performance Objectives</b>
<b>Table 7-1</b>	<b>Cost Model for PA-ISCO</b>
<b>Table 7-2</b>	<b>Cost Analysis Design Basis for Template Site MCIEAST-MCB CAMLEJ, North Carolina</b>

## LIST OF FIGURES

- Figure 2-1. Simplified illustration of the cross-flow mechanism.**
- Figure 2-2. Viscosity-time plot.**
- Figure 2-3. PCE Concentration time plot.**
- Figure 2-4. Results of 1-D transport experiments for Xanthan/KMnO<sub>4</sub> solutions.**
- Figure 2-5. 2-D tank experiment showing xanthan biopolymer improving sweep efficiency within a fining downward heterogeneity structure.**
- Figure 2-6. UTCHEM simulation showing the potential benefits of polymer addition at the NTC Orlando-SA17 area.**
- Figure 2-7. Demonstration of 418 nm Response Metrics.**
- Figure 2-8. Percentage of particles < 0.10 μm for all sample conditions at high stabilization aid concentration and t = 24 hours.**
- Figure 2-9. Average particle size and zeta potential for each stabilization aid condition at pH 7 with base groundwater.**
- Figure 2-10. Representative data for 525 nm measurements (to determine permanganate concentration) vs. time.**
- Figure 2-11. Mass of Mn (as MnO<sub>2</sub>) per kg of media with distance from 1-D column influent.**
- Figure 2-12. Percent decrease in MnO<sub>2</sub> deposition in source zone w/1,000 mg/L SHMP.**
- 
- Figure 4-1. Test area at MCIEAST-MCB CAMLEJ, North Carolina, OU 15, Site 88.**
- Figure 4-2. Closer view of test area located within and immediately west of the footprint of the former Building 25.**
- Figure 4-3. Test Area Conceptual Site Model.**
- Figure 4-4. Test Geologic Cross Section.**
- Figure 4-5. Example HRP results.**
- Figure 4-6. Boring log for DPT01.**
- Figure 4-7. Grain size analysis for surficial aquifer media.**
- Figure 4-8. Geologic cross-section within the test area based on most recent characterization activities.**
- Figure 4-9. Potentiometric map of the Surficial Aquifer.**
- Figure 4-10. Potentiometric map of the Upper Castle Hayne Aquifer.**
- Figure 4-11. PCE concentrations in the Surficial Aquifer (2007).**
- Figure 4-12. PCE concentrations in the Upper Castle Hayne Aquifer (2007).**

- Figure 5-1. Pilot test system layout.**
- Figure 5-2. Pressure response to injection flow rates determined during the step-injection testing for the (A) control plot and the (B) test plot.**
- Figure 5-3. Wellbore pressure response to increasing flow rate within the test and control plots.**
- Figure 5-4. Schematic representation of the Upper Castle Hayne Aquifer used to calculate maximum injection pressures for the formation.**
- Figure 5-5. Characterizing shear-thinning character of polymer-amended solutions.**
- Figure 5-6. Wellhead pressure response calculated as a function of injection flow rate.**
- Figure 5-7. Calculated steady-state viscosity and shear rate profiles for the optimal PA-ISCO fluid.**
- Figure 5-8. Layout of demonstration plots.**
- Figure 5-9. Injection well design.**
- Figure 5-10. MLS monitoring well design.**
- Figure 5-11. Schematic of the PA-ISCO demonstration process equipment.**
- Figure 5-12. Photograph showing 40% NaMnO<sub>4</sub> solution totes.**
- Figure 5-13. Xanthan gum/SHMP mixing system.**
- Figure 5-14. Automated process control system.**
- Figure 5-15. Fluid injection and filtering system.**
- Figure 5-16. Injection wellhead manifold and pressure monitoring.**
- Figure 5-17. Location of DPT cores. CP-DPT indicates control plot cores. TP-DPT indicates test plot cores. DPT A, B, and C are one-year post-treatment cores collected for the test plot and DPT X, Y, and Z are one-year post-treatment cores collected for the control plot.**
- Figure 5-18. Sediment cores used to vertically characterize the presence/absence of permanganate within the control plot.**
- Figure 5-19. Location of DPT transects.**
- Figure 5-20. General stratigraphy and distribution of permanganate observed within the control plot (along Transect CP-A – CP-A')**
- Figure 5-21. General stratigraphy and distribution of permanganate observed within the control plot (along Transect CP-B – CP-B')**
- Figure 5-22. General stratigraphy and distribution of permanganate observed within the control plot (along Transect CP-C – CP-C')**
- Figure 5-23. General stratigraphy and distribution of permanganate observed within the test plot (along Transect TP-A – TP-A')**

- Figure 5-24.** General stratigraphy and distribution of permanganate observed within the test plot (along Transect TP-B – TP-B')
- Figure 5-25.** General stratigraphy and distribution of permanganate observed within the test plot (along Transect TP-C – TP-C')
- Figure 5-26.** Semivariogram and model variogram fit parameters used in kriging of permanganate distributions.
- Figure 5-27.** Presence/absence of permanganate as observed post-injection in the DPT boring locations.
- Figure 5-28.** Results of ordinary kriging of the post-injection permanganate data representing the distribution of permanganate within the control plot after a 1 pore volume injection. Integrated sweep efficiency (volume contacted by permanganate divided by total volume) was 33%.
- Figure 5-29.** Results of ordinary kriging of the post-injection permanganate data representing the distribution of permanganate within the test plot after a 1 pore volume injection. Integrated sweep efficiency (volume contacted by permanganate divided by total volume) was 67%.
- Figure 5-30.** Example of polymer-improved sweep efficiency within a 2-D sand tank.
- Figure 5-31.** TCE and PCE concentrations measured in CMT wells 1 and 2 at each screened interval. Values, which are the average of duplicates, are presented for pre-treatment, during treatment, and post-treatment. Delivery occurred until the beginning of Day 6.
- Figure 5-32.** TCE and PCE concentrations measured in CMT wells 3 and 4 at each screened interval. Values, which are the average of duplicates, are presented for pre-treatment, during treatment, and post-treatment. Delivery occurred until the beginning of Day 6.
- Figure 5-33.** Soil VOCs concentrations (TCE and PCE) along with permanganate distribution for transect TP-A – TP-A'
- Figure 5-34.** Soil VOCs concentrations (TCE and PCE) along with permanganate distribution for transect CP-A – CP-A'
- Figure 5-35.** Conductivity (mS/cm) and ORP (mV) for CMT 1 (test plot) at each depth.
- Figure 5-36.** Conductivity (mS/cm) and ORP (mV) for CMT 3 (control plot) at each depth.
- Figure 5-37.** Total solids (mg/L) for CMT 1 and CMT 2 (test plot) at each depth.
- Figure 5-38.** Total solids (mg/L) for CMT 3 and CMT 4 (control plot) at each depth.
- Figure 5-39.** Chromium concentrations (mg/L) for CMT 1 and CMT 2 (test plot) at each depth.
- Figure 5-40.** Chromium concentrations (mg/L) for CMT 3 and CMT 4 (control plot) at each depth.

- Figure 5-41.** Concentrations (mg/L) of common cations measured in CMT 1 at each depth.
- Figure 5-42.** Concentrations (mg/L) of common cations measured in CMT 2 at each depth.
- Figure 5-43.** Concentrations (mg/L) of common cations measured in CMT 3 at each depth.
- Figure 5-44.** Concentrations (mg/L) of common cations measured in CMT 4 at each depth.
- Figure 5-45.** Concentrations (mg/L) of common anions measured in CMT 1 and CMT 2 at each depth.
- Figure 5-46.** Concentrations (mg/L) of common anions measured in CMT 3 and CMT 4 at each depth.
- Figure 5-47.** Manganese concentrations (mg/L) measured in test plot CMT 1 and CMT 2.
- Figure 5-48.** Manganese concentrations (mg/L) measured in control plot CMT 3 and CMT 4.
- Figure 5-49.** Manganese as water-extractable, Ba-extractable, and as  $\text{MnO}_2$  for example test plot cores post-treatment with distance from injection
- Figure 5-50.** Manganese as water-extractable, Ba-extractable, and as  $\text{MnO}_2$  for example control plot cores post-treatment with distance from injection
- Figure 5-51.** Manganese as water-extractable, Ba-extractable, and as  $\text{MnO}_2$  for test and control plot cores collected immediately post-treatment with respect to depth (relative to the center point of the screened interval).
- Figure 5-52.** Manganese as water-extractable, Ba-extractable, and as  $\text{MnO}_2$  for test and control plot cores collected one year post-treatment with respect to depth (relative to the center point of the screened interval).
- Figure 5-53.** Mn as  $\text{MnO}_2$  with distance from injection for test and control plots immediately post-treatment (Test, ImmPost and Control, ImmPost) and one year post-treatment (Test, 1YrPost and Control, 1YrPost).
- Figure 5-54.** The relationship of total sodium to total manganese for the test and control plots immediately post-treatment (on the left) and one year post-treatment (on the right).
- Figure 5-55.** The ratio of Na to Mn with  $\text{MnO}_2$  concentration for test and control plots immediately post-treatment (Test, ImmPost and Control, ImmPost) and one year post-treatment (Test, 1YrPost and Control, 1YrPost).
- Figure 5-56.** Mn extraction for test and control plot immediately post-treatment and one-year post-treatment by depth.
- Figure 5-57.** Anion exchange capacity (left) and cation exchange capacity (right) for test and control plot immediately post-treatment and one-year post-treatment.

**Figure 5-58.** Cation exchange capacity for the test plot one year post-treatment with respect to distance from injection (left) and depth (right).

**Figure 5-59.** Polymer concentration as indicated by viscosity measured on year post-treatment in CMT 1 and CMT 2 with depth as designated by the port number.

**Figure 5-60.** Sodium concentrations for the control plot's CMT 3 and 4.

**Figure 5-61.** Sodium concentrations for the test plot's CMT 1 and 2.

**Figure 5-62.** Sodium as water-extractable, Ba-extractable, and associated with  $\text{MnO}_2$  solids structure for the test plot cores collected immediately post-treatment (left) and one year post-treatment with respect to depth (relative to the center point of the screened interval).

## ACRONYMS

<b>APHA</b>	American Public Health Association
<b>AST</b>	Aboveground storage tank
<b>bgs</b>	Below ground surface
<b>CDISCO</b>	Conceptual design for ISCO (modeling tool)
<b>COC</b>	Contaminant of concern OR Chain of custody
<b>CEC</b>	Cation exchange capacity
<b>CPT</b>	Cone penetrometer test
<b>CSM</b>	Conceptual site model
<b>CSP</b>	Certified safety professional
<b>CVOC</b>	Chlorinated volatile organic compound
<b>c.y.</b>	Cubic yard
<b>c-DCE</b>	cis-dichloroethylene
<b>DNAPL</b>	Dense nonaqueous phase liquid
<b>DO</b>	Dissolved Oxygen
<b>DoD</b>	Department of Defense
<b>DOT</b>	Department of Transportation
<b>DPT</b>	Direct push technology
<b>EC</b>	Electrical conductivity
<b>ECD</b>	Electrical conductivity detector
<b>ERD</b>	Enhanced reductive dechlorination
<b>EPA</b>	Environmental Protection Agency
<b>FS</b>	Feasibility study
<b>GC-MS</b>	Gas chromatography – mass spectroscopy
<b>gpm</b>	gallon per minute
<b>HASP</b>	Health and Safety Plan
<b>SHMP</b>	Hexametaphosphate (used interchangeably with SHMP)
<b>HDPE</b>	High density polyethylene
<b>HRP</b>	High-resolution piezocone
<b>ID</b>	Inner diameter
<b>IDW</b>	Investigative derived waste
<b>ISCO</b>	In situ chemical oxidation
<b>k</b>	Hydraulic conductivity
<b>KMnO<sub>4</sub></b>	Potassium permanganate
<b>LPM</b>	Low permeability media
<b>MCIEAST-MCB</b>	Marine Corps Installations East – Marine Corps Base Camp Lejeune
<b>MCL</b>	Maximum contaminant level
<b>MIP</b>	Membrane interface probe
<b>MLS</b>	Multi-level sampling
<b>Mn</b>	Manganese
<b>MnO<sub>2</sub></b>	Manganese dioxide
<b>MnO<sub>4</sub><sup>-</sup></b>	Permanganate anion
<b>mV</b>	Millivolts

<b>MW</b>	Monitoring well
<b>NAPL</b>	Nonaqueous phase liquid
<b>NCAD</b>	North Carolina Administrative Code
<b>NOD</b>	Natural oxidant demand
<b>ORP</b>	Oxidation/Reduction potential
<b>OU</b>	Operable unit
<b>PA-ISCO</b>	Polymer-amended ISCO
<b>PCE</b>	Tetrachloroethylene (perchloroethylene)
<b>PCS</b>	Process control system
<b>pH</b>	Negative base-10 logarithm of hydronium ion activity
<b>PI</b>	Principal investigator
<b>PITT</b>	Partitioning interwell tracer test
<b>PLC</b>	Process logic controlled
<b>PPE</b>	Personal protection equipment
<b>psig</b>	pounds per square inch gauge
<b>PVC</b>	Polyvinyl chloride
<b>QA/QC</b>	Quality assurance / quality control
<b>RABITT</b>	Reductive Anaerobic In Situ Treatment Technology
<b>RI</b>	Remedial investigation
<b>SEAR</b>	Surfactant enhanced aquifer remediation
<b>SERDP</b>	Strategic Environmental Research and Development Program
<b>SHMP</b>	Sodium hexametaphosphate
<b>SPCC</b>	Spill Prevention, Control, and Countermeasure Plan
<b>SS</b>	Suspended solids
<b>TCE</b>	Trichloroethylene
<b>TOC</b>	Total organic carbon
<b>TCE</b>	Trichloroethylene
<b>TTI</b>	Target treatment interval
<b>UST</b>	Underground storage tank
<b>VC</b>	Vinyl chloride
<b>VOC</b>	Volatile organic chemical
<b>VSE</b>	Vertical sweep efficiency
<b>ZVI</b>	Zero valent iron



## ACKNOWLEDGEMENTS

Several organizations and individuals cooperated to make this collaborative demonstration possible. Clarkson University, Colorado School of Mines (CSM), and CH2M HILL collaborated to develop, design, and implement the demonstration, which was funded by The United States Department of Defense Environmental Security Technology Certification Program (ESTCP). The Clarkson technical lead and project coordinator was Dr. Michelle Crimi. Key Clarkson personnel included Bradley Martin, Jessica Dzara, Kawalpreet Kaur, Guannan Jiang, Dustin Whyman, and Gerlinde Wolf. Dr. Jeffrey Silva, formerly of CSM and currently a Senior Hydrologist at HIES, was the project technical lead for CSM. Key CSM personnel included Sean Davenport and Dr. John McCray. Mr. Tom Palaia was technical lead for CH2M HILL. Chris Bozzini, Monica Fulkerson, Simon Kline, and Brooke Propst from CH2M HILL's Charlotte (CLT), North Carolina office provided local site management, coordination with the Base, field oversight, and field sampling support. The CLT staff was instrumental in obtaining Base approval for the project and for implementing the field portion of the project. Narendra De and Tom Palaia from CH2M HILL's Denver office provided technical direction, design, and field management support throughout the project. The DEN office staff was instrumental in the planning, engineering design, and monitoring of the project. Of exemplary note were Monica's and Narendra's (while Monica was out on maternity leave) perseverance in project management and agility in adapting to change which allowed the field effort to come in on time. The entire project team greatly appreciates the efforts of CH2M HILL to make several important aspects of this project happen. Dr. Saebom Ko, a postdoctoral researcher with the U.S. EPA Kerr Laboratories in Ada, OK served as a co-investigator and key collaborator. Her volunteer efforts were deeply appreciated. The demonstration/validation project took place at Marine Corps Installations East – Marine Corps Base Camp Lejeune. The site staff was excellent hosts. Carus Corporation generously donated the permanganate and sodium hexametaphosphate for this demonstration/validation.

## EXECUTIVE SUMMARY

The Department of Defense Environmental Security Technology Certification Program (ESTCP) funded the demonstration and validation of polymer-amended ISCO (PA-ISCO). PA-ISCO is the use of water-soluble polymers to enhance *in situ* chemical oxidation (ISCO) using permanganate. The demonstration was conducted at the Marine Corps Installations East – Marine Corps Base Camp Lejeune’s Site 88, at which chlorinated solvents (trichloroethylene [TCE] and tetrachloroethylene [PCE]) are found in the subsurface. The two main goals of the project were: (1) to reduce the effects of site heterogeneities on oxidant delivery; and (2) manage the deposition of MnO<sub>2</sub> (permanganate oxidation byproduct) to improve the delivery of oxidant. With respect to these objectives, experiments were carried out using two polymers. Xanthan gum was used to improve sweep efficiency of the oxidant through lower permeability areas. Sodium hexametaphosphate (SHMP) was used to reduce the instance of MnO<sub>2</sub> precipitation and build-up. Through previous laboratory development funded by the DoD’s Strategic Environmental Research and Development Program (SERDP), the effectiveness of both polymers was tested. Both were deemed viable candidates for field study.

The test site consisted of two injection wells. One injection well received only permanganate (control plot); the other injection well received a mixture of oxidant and polymers (test plot). Multilevel wells were used to monitor groundwater prior to treatment, during treatment, and post-treatment. Real-time groundwater quality measurements included specific conductivity, oxidation-reduction potential (ORP), permanganate, and viscosity. Groundwater samples were collected from the multilevel monitoring wells for laboratory measurements of pH, ORP, solids concentration, cations, anions, cation exchange capacity (CEC), and anion exchange capacity (AEC) toward understanding how polymer addition affects groundwater quality. Twelve to fifteen soil cores per injection well were extracted at various distances from the injection site immediately following treatment. One year post-treatment, groundwater and soil cores were collected to investigate long-term effects of treatment on soil and groundwater chemistry and the fate of the polymer.

Comparisons between test and control plots were used to assess treatment performance. Key indicators of performance for the polymer included:

- Movement of permanganate into lower permeability layers/strata
- Preferential flow around areas of high contaminant mass due to MnO<sub>2</sub> deposition
- Potential for rebound
- Treatment effectiveness
- Injection pressure
- Groundwater quality

The addition of polymer improved oxidant movement into lower permeability strata, reduced preferential flow, and greatly improved the overall sweep efficiency of the PA-ISCO fluid compared to the permanganate control plot where polymer was not used. As a result, a greater percentage of the aquifer was contacted by the oxidant. Specifically, one pore volume of solution was introduced to each plot; the use of polymer resulted in a test plot sweep efficiency of 67%, double that of the control plot (sweep efficiency = 33%). Because a greater portion of the aquifer

was swept, overall treatment was more effective and there was lower rebound. It is important to note that even with polymer, the oxidant solution did not contact 100% of the contaminated media in one pore volume. Rebound could still be expected if an insufficient volume of oxidant is applied. The volume appropriate for treatment should be determined on a site-by-site basis. However, based on this demonstration, the use of polymer can reduce the necessary volume of solution by more than an order of magnitude. Importantly, the polymer-amended solution did not negatively affect injection pressure during this demonstration.

Groundwater quality data collected included parameters associated with the soil that can affect groundwater concentrations of contaminant and key cations and anions. Most geochemical outcomes using polymer were similar to those without polymer; however, changes due to ISCO were slower to appear downgradient of the polymer-treated plot. Two possible reasons for this observation include retention within, and flow around, the viscous polymer solution. Polymer was still present at the site one year post-treatment. Geochemical analyses indicated the polymer was “retreating” from its leading edge and releasing the geochemical signature of the amended oxidant solution rather than being flushed through the treated zone by upgradient solution as was measured in the control plot. This has important implications with respect to appropriate monitoring of treatment performance. Byproducts of permanganate oxidation (e.g.,  $MnO_2$  solids) and short-term mobilization of metals (e.g., chromium) observed at some ISCO sites may be sequestered within the viscous PA-ISCO solution during treatment and held within the treated zone post-treatment until viscosity dissipates. Long-term post-treatment viscosity could also be leveraged in future PA-ISCO applications to sequester permanganate within the treatment zone providing longer-term treatment to address contaminant rebound from low permeability media (e.g., fine silts or clays) that are not swept during the initial PA-ISCO treatment.

Lessons learned beyond those tied to specific performance objectives included:

- Results of the control plot exemplified the surprising extent to which preferential flow occurs in the subsurface, even within lithology that appears the same or similar.
- Site characterization and monitoring efforts must be designed based on site-specific factors. In order to prepare an appropriate treatment system design and to capture treatment outcomes effectively, operational and performance monitoring strategies must match the operational goals and the physico-chemical characteristics of the amendments applied.
- Soil core data were more valuable than groundwater data with respect to making accurate pre- and post-treatment subsurface evaluations of treatment performance.
- Simple geochemical field measurements such as conductivity and ORP provided valuable, real-time information with respect to operational performance. High data density using real-time monitoring approaches added significant value with respect to making real-time, cost-saving decisions in the field.
- Automated amendment delivery schemes, while costly, will add value to field operations by allowing for round-the-clock, unmanned injection. This will be particularly valuable at sites where unescorted activity is not possible.

Key differences in the cost of PA-ISCO relative to traditional ISCO included polymers and polymer mixing equipment and associated shipping. Further, an automated process control system was employed to allow 24-hr injection, which was important for maintaining the viscosity of the injection solution at design levels. Key drivers of total project cost included the

nature and extent of contamination, degree of heterogeneity, and rate of injection achievable (average hydraulic conductivity).

There were no apparent regulatory barriers to PA-ISCO for the polymers and oxidants employed. Technical and/or implementation issues associated with PA-ISCO included:

- Uncertainty regarding the influence of polymer on hydraulic conductivity over the long-term within the treated area.
- Uncertainty regarding the degree of heterogeneity the polymer can overcome.
- Concern over the potential for daylighting evoked by the use of a higher viscosity solution.
- Improved sweep efficiency could be achieved by increasing injection volume for any delivered amendment, particularly for more reactive (short-lived) amendments. Polymer can significantly reduce required injection volumes; however, low volume delivery is not appropriate for most remediation approaches that involve the delivery of aqueous phase amendments, including ISCO. This translates to longer duration delivery and increased field time per injection event.
- The dry powdered form of xanthan gum and SHMP used in this demonstration required expensive (~20% of total equipment cost) hydrodynamic mixing equipment. Procuring polymer in liquid form that could be trucked to the site in tanker trailers may be more cost-effective, particularly for larger-scale operations.

## **1.0 INTRODUCTION**

### **1.1 BACKGROUND**

*In situ* chemical oxidation (ISCO) using permanganate is an established remediation technology being applied at hazardous waste sites throughout the United States and abroad. Field applications of ISCO continue to grow and have demonstrated that ISCO can achieve destruction of contaminants and achieve clean-up goals. However, some field-scale applications have had uncertain or poor *in situ* treatment performance. Poor performance is often attributed to poor uniformity of oxidant delivery caused by zones of low permeability media (LPM) and site heterogeneity and excessive oxidant consumption by natural subsurface materials. A second permanganate ISCO challenge is the management of manganese dioxide (MnO<sub>2</sub>) particles, which are a byproduct of the reaction of permanganate with organic contaminants and naturally-reduced subsurface materials. These particles have the potential to deposit in the well and subsurface and impact flow in and around the well screen, filter pack, and the surrounding subsurface formation. This is a particular challenge for sites with excessive oxidant consumption due to the presence of natural materials or large masses of non-aqueous phase liquids (NAPLs). This demonstration/validation focused on (1) diminishing the detrimental effects of site heterogeneities with respect to the uniformity of oxidant delivery, and (2) managing MnO<sub>2</sub> aggregation and deposition.

### **1.2 OBJECTIVES OF THE DEMONSTRATION**

This project goal was to demonstrate and validate the use of a water-soluble polymer with permanganate for *in situ* chemical oxidation (ISCO) of organic contaminants with the dual primary objectives of (1) improving the sweep efficiency of permanganate through heterogeneous media containing lower permeability media, and (2) controlling manganese dioxide (MnO<sub>2</sub>) particles to improve oxidant delivery and flow, thereby enhancing contaminant destruction. A secondary project objective was to compare post-delivery/treatment groundwater quality for “permanganate only” and “permanganate + polymer” test areas.

### **1.3 REGULATORY DRIVERS**

This project addresses contaminants amenable to ISCO using permanganate; most commonly chlorinated solvents such as trichloroethylene (TCE) and tetrachloroethylene (PCE). Over 3,000 DoD sites are contaminated by chlorinated solvents, including dense nonaqueous phase liquid (DNAPL) present at high mass density, which challenge many remediation technologies, as well as very low concentrations emanating from contaminant trapped in lower permeability layers that the majority of treatment technologies have difficulty accessing. The U.S. Environmental Protection Agency’s (EPA’s) maximum contaminant level for TCE and PCE is 5 µg/L. This concentration is lower than typically present at sites containing even very dilute concentrations of these contaminants. These MCLs, and others related to contaminants amenable to permanganate ISCO, are the regulatory driver for advancing approaches for their treatment. Specific to the site for this particular demonstration, Marine Corps Installations East – Marine Corps Base Camp Lejeune (MCIEAST-MCB CAMLEJ), remediation activities are conducted in accordance with the North Carolina Groundwater Quality Standards specified in 15A North Carolina Administrative Code (NCAC) 2L .0202.

## 2.0 TECHNOLOGY

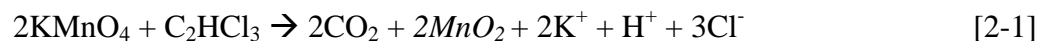
### 2.1 TECHNOLOGY DESCRIPTION AND DEVELOPMENT

#### 2.1.1 Challenges to ISCO using Permanganate

ISCO using permanganate is an established remediation technology being applied at hazardous waste sites throughout the United States and abroad. A wide variety of organic contaminants have been successfully oxidized by permanganate, with high treatment effectiveness (e.g., > 90% mass destruction) for common contaminants such as chlorinated ethenes (e.g., TCE, PCE) with very fast reaction rates (e.g., 90% destruction in minutes). Field applications of ISCO continue to grow and have demonstrated that ISCO can achieve destruction of contaminants and achieve clean-up goals. However, some field-scale applications have had uncertain or poor in situ treatment performance. Two challenges with any in situ remediation technology are (1) treatment amendment delivery limitations due to site heterogeneities, and (2) minimizing unfavorable impacts of technology implementation. With respect to permanganate ISCO, these challenges specifically relate to (1) the ability to deliver into low permeability media (LPM) (vs. preferential flow and bypassing of the LPM), and (2) deposition of oxidation reaction byproduct manganese dioxide (MnO<sub>2</sub>) particles, preventing effective distribution and contact with contaminants.

Poor amendment (i.e., permanganate) sweep efficiencies are typically the result of the injection process whereby the injected amendments are delivered into preferential flow paths within zones of higher permeability. This leads to the treatment amendment bypassing LPM and rebounding contaminant concentrations within a groundwater aquifer following treatment. The efficiency and efficacy of engineered remediation strategies that involve the introduction of chemical amendments such as oxidants into the subsurface is dependent on achieving an efficient subsurface sweep applied amendment within the contaminated zone. When injected under an applied pressure gradient the resulting subsurface distribution is impacted greatly by the architecture of the subsurface permeability field because the amendments will seek preferential flow paths through more permeable media, resulting in a less efficient sweep of the target zone by the injected amendments. The extent to which this occurs in a given heterogeneous system largely depends on the physicochemical properties of the injected fluid, the mode of introduction (e.g., injection rates, orientation and placement of well screens), the permeability distribution, the location of the contaminant zone (in high-permeability zones, within clay zones, etc), and the interaction of the fluid with the solid media at the pore-scale. Therefore, understanding the interplay between the site-specific heterogeneity of the subsurface and the injected remediation fluids is crucial to optimizing the distribution of applied amendments in the subsurface, thereby enhancing the contact between the amendment and the target contaminant. Mobility control methods exist that can mitigate the effects of permeability heterogeneity.

In addition to difficulties due to naturally existing site heterogeneities, MnO<sub>2</sub> particles, a product of the reaction of permanganate with organic materials (Eqn. 2-1), can create secondary site heterogeneities that may provide an added hindrance to the technology's effectiveness.



MnO<sub>2</sub> particles are of interest because they have the potential to deposit in the well and subsurface and impact the flow regime in and around the permanganate injection system, including the well screen, filter pack, and the surrounding subsurface formation. Permeability changes may result due to MnO<sub>2</sub> particle deposition, which has been observed in laboratory and field evaluations (e.g., West et al., 1998, 2000; Li and Schwartz, 2000; Lowe et al., 2000; Reitsma and Marshall, 2000; Lee et al., 2003). It is postulated that differences observed in MnO<sub>2</sub> deposition and permeability effects are attributable to differences in natural and design conditions associated with these studies. **Table 2-1** presents a summary of laboratory and field evaluations where impacts of MnO<sub>2</sub> deposition have been observed and documented. The stability of these MnO<sub>2</sub> particles in solution, which is an indicator of their potential to be controlled and transported with groundwater flow, can be impacted by several reaction matrix conditions. These include reactant/particle concentrations, pH, turbulence, the presence of anions/cations in solution, and the presence of stabilizing colloids or polymers (Morgan and Stumm 1964; Perez Benito et al. 1989, 1990, 1991, 1992a,b; Insausti et al. 1992, 1993; Doona and Schneider 1993; Chandrakanth and Amy 1996), providing a foundation for managing particle aggregation and deposition.

**Table 2-1. Impacts of MnO<sub>2</sub> on Subsurface Permeability: Laboratory & Field Evaluations**

Study Description	Impacts of MnO <sub>2</sub>	Reference
Field evaluation: A 5-spot recirculation network was employed to deliver 3000 mg/L NaMnO <sub>4</sub> to treat up to 600 mg/L TCE in groundwater. NaMnO <sub>4</sub> was added to contaminated groundwater above ground, filtered at 5 and 1 um respectively, then injected into a central injection well.	After approximately 5 days of operation, increasing injection well pressures (up to 18 psig) caused reduced recirculation rates (down to 4 gpm). Redevelopment of the injection well recovered the well efficiency, however increasing injection pressures and reduced recirculation rates were again rapidly observed.	Lowe et al., 2000
Field evaluation: 2-4 wt% of KMnO <sub>4</sub> was used to treat TCE at 100 to 800 mg/L in groundwater.	Hydraulic conductivities measured 10 months after completion of the ISCO test showed order of magnitude decreases in several wells, especially the oxidant injection well.	West et al., 1998, 2000
Laboratory study: 1-D column and 2-D test cell studies were conducted to examine flushing efficiencies resulting from reaction of permanganate with typical aquifer materials containing dense nonaqueous phase liquid (DNAPL) contamination. The distribution of MnO <sub>2</sub> was evaluated.	The distribution of MnO <sub>2</sub> in column studies indicates that the majority of Mn was located close to or at the DNAPL zone. Precipitates tended to plug the column – flushing become more difficult as the experiment progressed. The 2-dimensional studies demonstrated flow bypass zones with high DNAPL saturation once the permanganate initially came into contact with the DNAPL. Contaminant removal efficiencies were less in 2D systems where flow was able to bypass areas with MnO <sub>2</sub> build-up.	Li and Schwartz, 2000
Laboratory study: 2-D experimental studies examined flow processes during DNAPL oxidation, with varying rates of reaction due to varied initial permanganate concentrations introduced to the system.	Substantial MnO <sub>2</sub> build-up was observed around the DNAPL emplacement zone. With lower initial permanganate concentration and slower reaction rates, more MnO <sub>2</sub> was deposited downgradient from the point of contact of oxidant with the DNAPL. Flow-regimes were impacted by the MnO <sub>2</sub> deposition.	Reitsma and Marshall, 2000
Laboratory study: 3-D experimental studies examined DNAPL contaminant destruction and MnO <sub>2</sub> deposition with treatment using 1250 mg/L KMnO <sub>4</sub> .	The DNAPL oxidation process became less efficient with time, likely due to reduction in permeability caused by increasing MnO <sub>2</sub> deposition that inhibited contact between the permanganate and DNAPL. Large amounts of unreacted permanganate left the treatment zone during oxidant flushing.	Lee et al., 2003

### 2.1.2 Enhanced Permanganate ISCO

Methods to mitigate the potential for preferential flow and bypassing effects would increase remediation effectiveness and reduce costs of environmental restoration efforts through reduced occurrence of rebound. This project's goal was to validate the use of water-soluble polymers with permanganate for ISCO of organic contaminants with the dual objectives of (1) improving the sweep efficiency of permanganate through heterogeneous media containing LPM, and (2) controlling manganese dioxide (MnO<sub>2</sub>) particles to improve oxidant delivery and flow, thereby enhancing contaminant destruction. A secondary project objective was to compare post-delivery/treatment groundwater quality for "permanganate only" and "permanganate + polymer" test areas.

**Objective 1: Improve oxidant sweep efficiency.** Mobility control includes a class of strategies involving the modification of in-situ fluid viscosities. This strategy was developed by the petroleum industry for enhanced oil recovery to overcome preferential flow and other by-passing effects produced by geological heterogeneities. Mobility control mechanisms have been used by the petroleum industry since the 1960's to improve chemical flood efficiency and maximize oil production from lower permeability strata. Traditional mobility control techniques in petroleum reservoir engineering have involved the use of polymers, which increase the viscosity of the injected solutions. The increased viscosity of the injected fluid minimizes the effects of the aquifer heterogeneities by promoting strong transverse fluid movement, or cross-flow, across heterogeneous reservoir units (Lake, 1989; Sorbie, 1991), providing an enhanced sweep efficiency. The occurrence and benefits of cross-flow during polymer flooding for oil recovery is well documented (see Seright and Martin, 1991, Sorbie, 1991 and references therein) and a summary of recent applications in environmental restoration may be found in Jackson et al. (2003).

A simplified illustration of the cross-flow mechanism is provided below (**Figure 2-1**) for linear flow of a viscous Newtonian fluid in a two-layered aquifer system (permeability  $k_1 > k_2$ ).

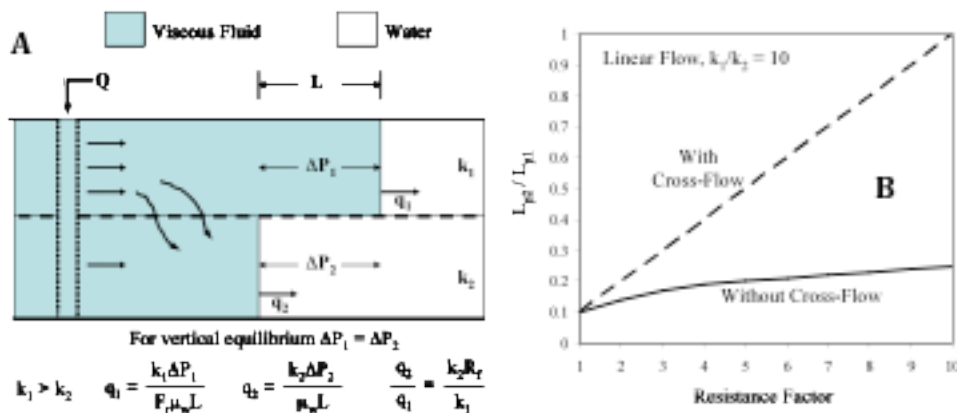


**Figure 2-1.** Simplified illustration of the cross-flow mechanism (from Seright and Martin, 1991).  $k_1 > k_2$ . The cross-flow condition occurs more readily with injected polymer.



When a viscous fluid is injected into the subsurface, a transverse pressure gradient is induced between higher and lower permeability strata causing fluid to flow from the more permeable strata into less permeable strata in an attempt to attain vertical equilibrium (i.e.,  $DP_1 = DP_2$ ). The result is a smoothing of the viscous liquid frontal advance within heterogeneous porous media and diminished viscous fingering (i.e., enhanced sweep efficiency) as the fluid propagates away from the point of injection. The effects of the cross-flow mechanism are better shown in **Figure 2-1B**, where the calculated ratio of the positions of the viscous fronts in both layers ( $L_2/L_1$ , see **Figure 2-1A**) are plotted for the case of no cross-flow versus that with unrestrained cross-flow for an increasing resistance factor ( $R_f$ ).  $R_f$  is the ratio of the fluid injectivity ( $Q$  divided by the difference in pressure between the point of injection and a defined distant point of reference) of water to that of the viscous fluid and can be thought of as a fluid-specific measure of resistance to flow. As shown, an increase in the amendment resistance to flow decreases the relative positions of the viscous fronts between layers when cross-flow occurs (i.e.,  $L_2/L_1$  approaches unity). The effect of cross-flow in real geologic systems would fall between these two curves because the resistance to transverse flow is not negligible. The net result is that preferential flow and by-passing of low permeability media is reduced, improving amendment sweep efficiency.

Technically, the term “mobility control” relates to defining an optimum mobility ratio (i.e., mobility of injected fluid greater than that of the displaced fluid) to displace a viscous pore fluid (oil or viscous NAPLs) from porous media. When a viscous fluid is used to displace pore water and promote lateral dispersion of the injected fluid within variable permeability media (as is the case in this research), the term “heterogeneity control” is more appropriate. Viscosity modification of engineered remediation amendments, whether by the addition of polymers or other modifications to amendment formulations, should promote similarly favorable heterogeneity control results for amendment emplacement in environmental systems as those observed in the petroleum industry. Moreover, heterogeneity control strategies can be applied to improve the efficiency of a variety of *in situ* remediation technologies, including *in situ* chemical oxidation.

Fundamental study of the applicability of heterogeneity control within near-surface geologic systems was completed under SERDP Project ER-1486 at the Colorado School of Mines. The principal goal of the project was to examine the fundamental processes associated with polymer-enhanced sweep efficiencies as a means to promote enhanced contact between the injected amendments and the target contamination. An additional objective of ER-1486 was to examine the compatibility of polymers and two remediation amendment categories (i.e., chemical oxidants and bioamendments).

Xanthan gum has been identified a highly promising polymer for use with permanganate oxidant solutions, in that it maintains a stable and predictable viscosity within the oxidant solution (**Figure 2-2**), and exhibits a low oxidant demand for permanganate (Smith et al., 2008). When the xanthan gum/permanganate solution contacts PCE (aqueous or non-aqueous phase liquid), solution viscosity rapidly decreases (**Figure 2-2**). This coupled with the low oxidant demand for the polymer suggests that the oxidation of PCE initiates partial oxidation of the xanthan molecule at specific locations along the polymer chain, impacting the viscosity. However, as a part of design, during subsurface injection a continuous and stable bank of xanthan/permanganate

solution will exist behind the PCE contact zone that will continue to impart heterogeneity control within the aquifer.

**Figure 2-3** shows that xanthan gum does not greatly inhibit PCE oxidation. Calculated second order rate constants for the PCE/KMnO<sub>4</sub>/xanthan gum system averaged around 0.036 M<sup>-1</sup> sec<sup>-1</sup> for xanthan concentrations between 1600 and 142 mg/L. This is nearly the same as that determined for the no-xanthan case (PCE/KMnO<sub>4</sub> system) where the rate constant was 0.04 M<sup>-1</sup> sec<sup>-1</sup>. Both measured rate constants are consistent with those reported in the scientific literature.

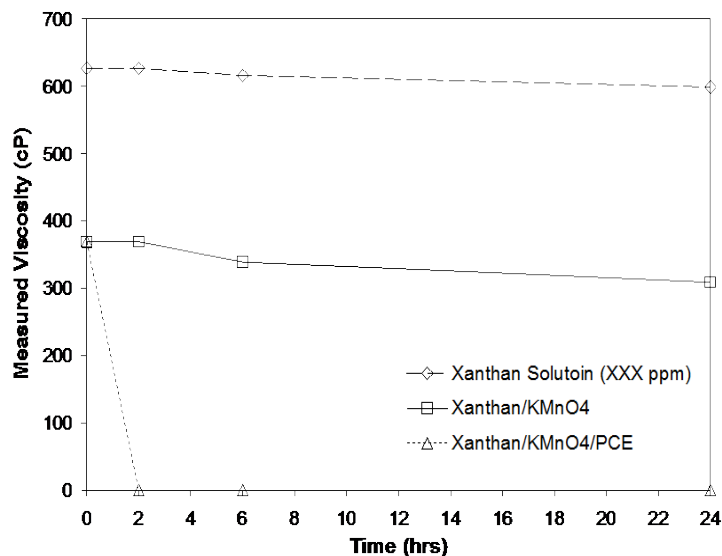


**Figure 2-2.** Viscosity-time plot.

Of additional importance to polymer/oxidant compatibility, and to implementation design, is to assess the comparative transport of xanthan gum and permanganate within porous media when introduced together in solution. The results of 1-D column experiments have shown that polymer and oxidant transport similarly, and conservatively, within a clean silica sand. Observed sharpening of the polymer and oxidant breakthrough profiles, compared to the conservative tracer, reflects the polymer mitigating pore-scale heterogeneities within the column. These results are presented as **Figure 2-4**. Similar column experiments were performed in natural soil possessing elevated natural oxidant demand (NOD) characteristics. The results of these experiments are also presented in **Figure 2-4**. The observed early breakthrough for both the conservative tracer and xanthan gum elution profiles, and tailing of the xanthan gum elution profile, are indicative of a reduction in media permeability due to MnO<sub>2</sub> precipitation as a result of oxidation of natural organic matter. This slight permeability reduction resulted in some mechanical filtering of xanthan gum which temporarily delayed its approach to C/C<sub>0</sub> = 1 (i.e., the time needed for effluent xanthan concentrations to equal that of the influent). However, the viscosity of the effluent did reach its inlet value at 2.5 pore volumes, suggesting that the oxidation of NOD ultimately did not affect the viscosity of the polymer during transport. These results also indicate that although the strength of the polymer front was 80% reduced during the

initial flushed pore volumes, as a result of retention, the continued introduction of xanthan gum/KMnO<sub>4</sub> solution restored the integrity of the polymer bank within this new permeability condition. It should be noted that the media used in these experiments was collected from within a sewage wastewater leach field and therefore possessed a significantly greater NOD than would reasonably exist within a groundwater aquifer. Additional experiments such as these have been budgeted as a part of this proposal using site media so as to assess and potentially incorporate the mechanics of these phenomena within an implementation design basis.

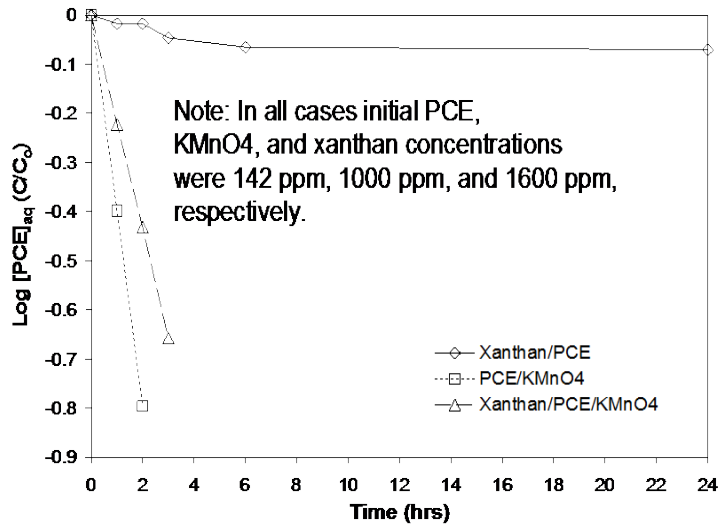


Figure 2-3. PCE Concentration time plot.

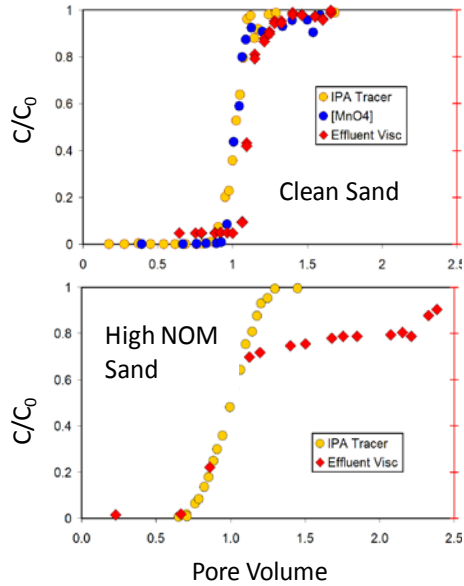
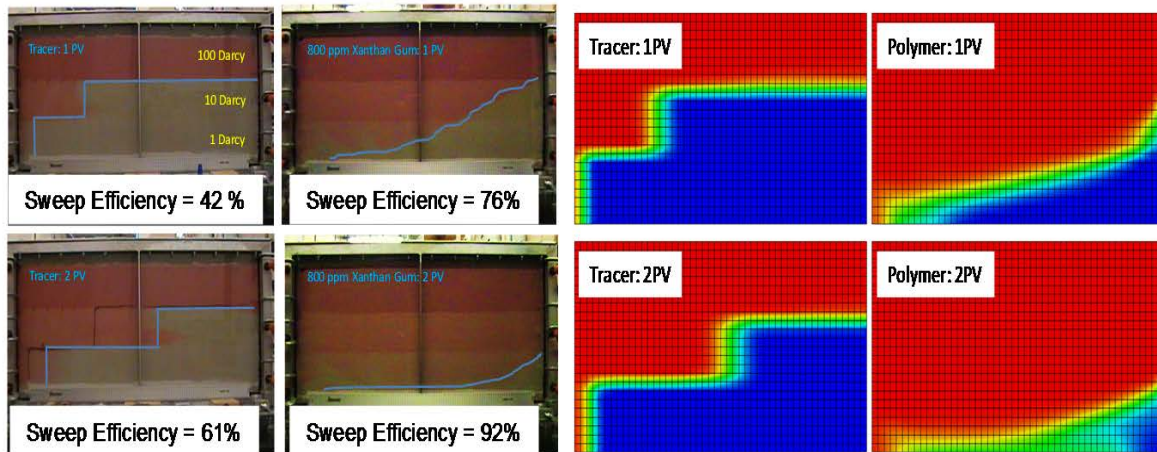


Figure 2-4. Results of 1-D transport experiments for xanthan/KMnO<sub>4</sub> solutions. Xanthan biopolymer transport in clean sand was found to be similar to that of a conservative tracer (i.e., no unexpected retention of polymer).

An example of polymer-improved sweep efficiency in a 2-D experimental tank is presented in **Figure 2-5**. Here, the permeability structure is layered in a fining downward sequence. Permeabilities varied over three orders of magnitude (i.e., 100 – 1 darcy). The addition of 800 ppm xanthan gum is shown to provide a sweep efficiency (i.e., swept area of the tank divided by the total tank area) of 92% at 2 pore volumes, compared to the no polymer case of 61%. Furthermore, there was a 500% sweep efficiency improvement of the lowest permeability layer after 2 pore volumes flushing. These results indicate that the addition of polymers to remediation amendments can greatly improve amendment delivery efficiency to lower permeability strata and reduce the volume of amendment required to achieve such delivery.

To further demonstrate the benefits of polymer addition on the resulting distribution of  $\text{KMnO}_4$ , the UTCHEM simulator was used to simulate fluids propagation (with and without polymer addition) within a contaminated aquifer section at the NTC Orlando-SA17 Area (**Figure 2-6**). Model input parameters were based on those measured as a part of SERDP project ER-1486. The permeability field consisted of three continuous layers of silty fine-sand ( $k = 100$  millidarcy) surrounded by a fine-med sand ( $k = 1000$  millidarcy). The frontal advance rate was 20 ft/day and the simulation time was 2 days. As shown in Figures A4, the addition of xanthan gum greatly improves the distribution of oxidant in this system and forces oxidant into the lower permeability media (LPM). Slower frontal advance rates and/or elevated polymer concentrations will improve oxidant sweep efficiencies further. Ultimately, simulations like these are critical to tailor polymer solution characteristics and injection rates to a specific site as a part of implementation design to maximize the benefits of polymer-induced heterogeneity control.



**Figure 2-5.** 2-D tank experiment showing xanthan biopolymer improving sweep efficiency within a fining downward heterogeneity structure (3-order of magnitude permeability contrast, 500% sweep improvement of lowest permeability layer. Numerical simulation of this experiment is also presented.

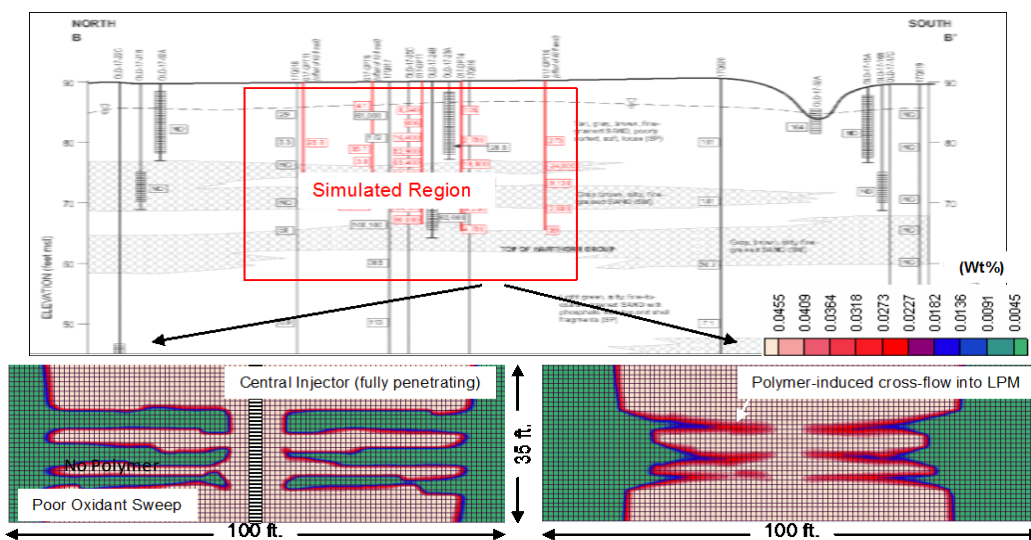


**Figure 2-6.** UTCHEM simulation showing the potential benefits of polymer addition at the NTC Orlando-SA17 area.

***Objective 2: Control Manganese Dioxide Particles.*** SERDP Project ER-1484 determined that  $MnO_2$  particles in groundwater can be controlled using polymers to specifically allow for their facilitated transport through porous media. Since it is not particle size alone that determines the ability of these particles to be transported, physico-chemical interactions must be considered; therefore the experimental studies examined the interactions of potential stabilization aids (e.g., ionic/nonionic, organic/inorganic water soluble polymers) with  $MnO_2$  particles, as well as the interactions of potential stabilization aids with porous media and groundwater. The ideal particle stabilizer will (1) interact minimally with porous media, (2) react minimally with the oxidant permanganate, (3) interact minimally with other groundwater components, (4) be acceptable to the regulatory community, and (5) be cost-effective.

Batch experimental studies were conducted to evaluate four polymer stabilization aids with respect to particle stability in solution over time and the influence groundwater conditions have on stabilization (experimental conditions included in **Table 2-2**). Measurements of each reaction solution included spectrophotometric evaluation of particle behavior (optical measurement of particle suspension and settling), particle filtration (filtered at each pore size of 5, 1, 0.4 and 0.1 mm), and optical (laser) measurement of particle size and zeta potential.

Spectrophotometric measurements were made at 418 nm and assessed for multiple responses. Because the 418 nm data reflect the measurement of particles suspended in solution, they provide a qualitative indication of particle behavior. An increase in the 418 nm measurements indicates an increasing concentration of suspended particles, whereas a decrease indicates that particles have settled from solution. An ideal stabilization aid will prevent particle settling. Responses measured using the 418 nm data include (1) maximum absorbance value ( $A_{max}$ ), (2) time of maximum absorbance ( $T_{max}$ ), (3) time of maximum absorbance minus time of minimum absorbance ( $T_{max}-T_{min}$ ), and (4) particle settling rate ( $k_{s-obs}$ ) (**Figure 2-7**). A higher maximum absorbance value indicates a higher concentration of particles suspended in solution.  $T_{max}$  and  $T_{max}-T_{min}$  characterize the particle growth and settling behavior. Favorable particle

stabilization is indicated by a highly positive value for the  $T_{\max}-T_{\min}$ , corresponding with a relatively late  $T_{\max}$  value in general (i.e., particles are suspended for a longer duration). Particle settling rates were calculated by fitting the 418 nm data after the reaction between oxidant and reductant was complete (~4 hours) to a power curve;  $y = Ax^B$ , where  $y$  is absorbance at 418 nm,  $x$  is time,  $A$  and  $B$  are model fitting parameters, and  $B$  provides the rate of particle settling in terms of decreasing 418 nm absorbance vs. time. Values for these indicator measurements are included in **Table 2-3**. Sodium hexametaphosphate (SHMP), gum arabic, and xanthan gum all improve particle stability as evidenced by higher  $A_{\max}$  values, higher  $T_{\max}$  values, higher  $T_{\max}-T_{\min}$  values, and lower  $k_{s-\text{obs}}$  values.

**Table 2-2. Experimental Conditions**

Variable	Condition A		Condition B		Condition C			
Particle concentration	10 mg/L		100 mg/L		---			
pH	7		3		---			
Ionic variation	Base groundwater		Base groundwater + Ca <sup>2+</sup>		Base groundwater + PO <sub>4</sub> <sup>3-</sup>			
Solids content	None		20 wt. %		---			
Redox conditions	1:1 initial ratio of MnO <sub>4</sub> <sup>-</sup> to reductant		Oxidizing (excess MnO <sub>4</sub> <sup>-</sup> )		Reducing (excess reductant)			
Stabilization Aids	Dowfax		Hexametaphosphate		Gum arabic		Xanthan Gum	
Stabilization Aid Concentration (mg/L)	23,540	3,300	1,000	100	1,000	100	25	10

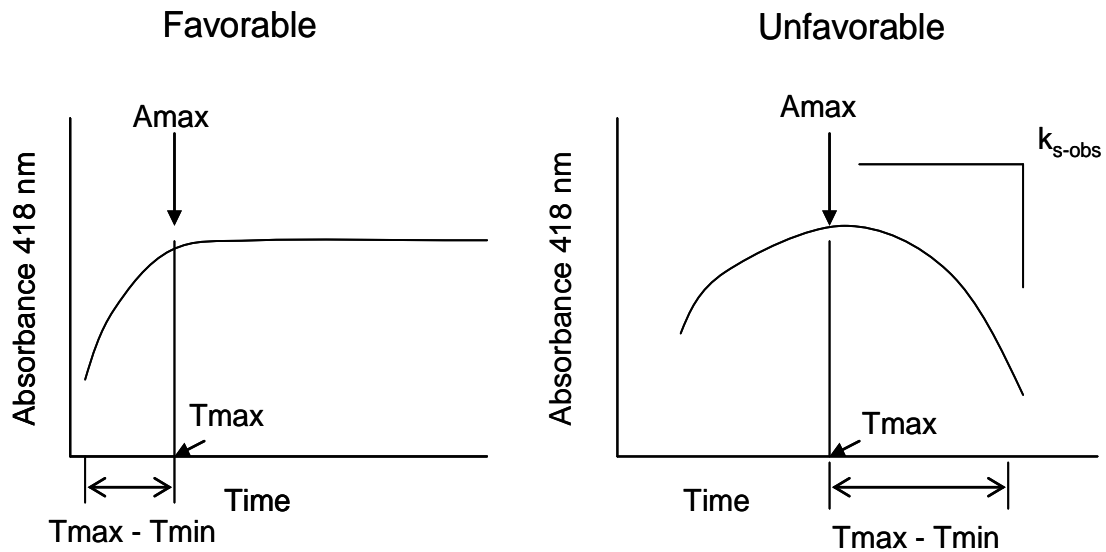


**Figure 2-7.** Demonstration of 418 nm response metrics.

**Table 2-3. Range of Response Values and Statistical Significance of Reaction Variables (check indicates the condition or interaction has a statistically significant impact on the response)**

		<b>Amax</b>	<b>Tmax</b>	<b>Tmax-Tmin</b>	<b>K<sub>s-obs</sub><sup>a</sup></b>
<b>No Stabilization</b>	Response range	0.2 – 1.2	2 – 8	-71 – -50	0.75 – 1.02
	Particle Conc (PC)	√	√	√	√
	pH				
	Groundwater (GW)			√	
	PC x pH (interaction)				
	PC x GW			√	
	pH x GW				
<b>Dowfax</b>	Response range	0.5 – 3.2	1 – 21	-71 – -30	0.5 – 1.10
	PC	√	√	√	
	pH	√	√	√	
	GW	√			
	Dowfax Conc (D-C)	√	√	√	
	PC x pH		√	√	
	PC x GW	√			
	PC x D-C		√	√	
	pH x GW	√			
	pH x D-C				
	GW x D-C	√			
<b>SHMP</b>	Response range	0.3 – 2.0	10 – 40	-20 – +10	0.1 – 0.7
	PC	√		√	√
	pH		√	√	
	GW				√
	SHMP Conc (SHMP-C)		√	√	√
	PC x pH		√	√	√
	PC x GW		√	√	√
	PC x SHMP-C			√	
	pH x GW				
	pH x SHMP-C				√
	GW x SHMP-C		√	√	√
<b>Gum arabic</b>	Response range	1.0 – 3.6	20 – 44	+5 – +38	-0.1 – +0.4
	PC	√			
	pH	√	√	√	√
	GW	√			
	Gum Arabic Conc (GA-C)	√			
	PC x pH	√		√	
	PC x GW	√		√	
	PC x GA-C	√			
	pH x GW				
	pH x GA-C		√	√	
GW x GW-C					
<b>Xanthan gum</b>	Response range	0.7 – 3.4	10 – 58	-50 – +55	0.15 – 0.80
	PC	√	√	√	√
	pH		√	√	√
	GW	√	√	√	
	Xanthan Conc (X-C)				√
	PC x pH				
	PC x GW	√			√
	PC x X-C				√
	pH x GW				
pH x X-C				√	
GW x X-C				√	

<sup>a</sup>A positive k<sub>s-obs</sub> value, as applied here, indicates particle settling has occurred during the 72 hour reaction period, whereas a negative k<sub>s-obs</sub> value indicates particle growth continues through reaction.



The particle filtration and optical measurement data concur with the conclusions of the spectrophotometric evaluations. The use of SHMP, gum arabic, and xanthan gum result in a greater percentage of particles < 0.10  $\mu\text{m}$  (Figure 2-8) under a range of experimental conditions; as well as a smaller average  $\text{MnO}_2$  particle size and more favorable (highly negative) zeta potential for particle stabilization (Figure 2-9). While results are similar and favorable for several stabilization aids, SHMP is of particular interest because it does not exert a non-productive demand for permanganate (Figure 2-10).

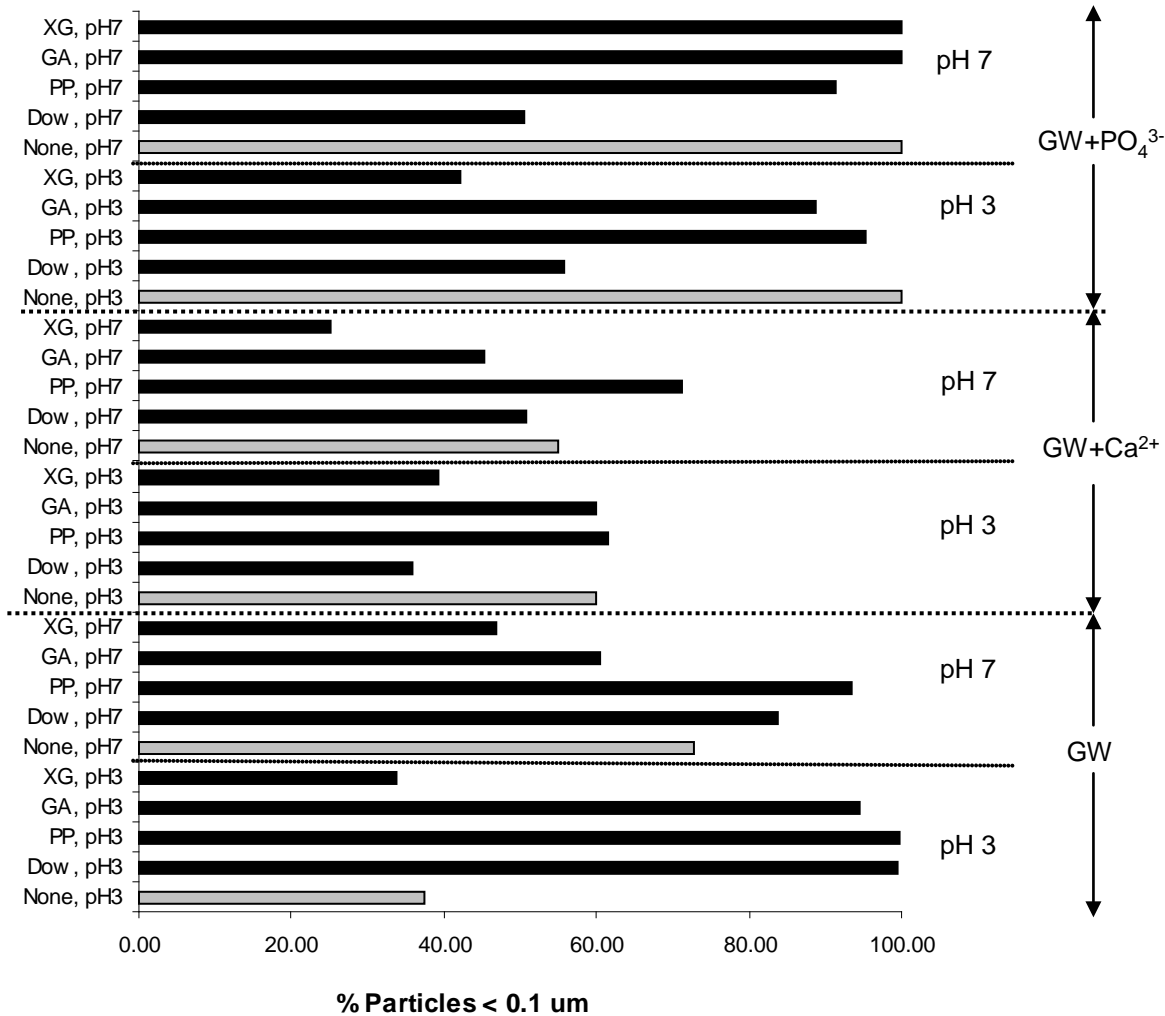


**Figure 2-8.** Percentage of particles < 0.10  $\mu\text{m}$  for all sample conditions at high stabilization aid concentration and  $t = 24$  h. None = no stabilization aid; Dow = Dowfax; PP = polyphosphate (or sodium hexametaphosphate (SHMP)); GA = gum arabic; XG = xanthan gum.

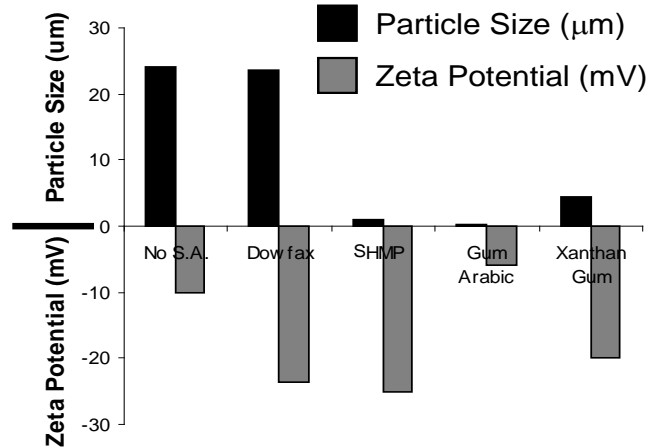


**Figure 2-9.** Average particle size and zeta potential for each stabilization aid condition at pH 7 with base groundwater. High particle concentration samples are presented.

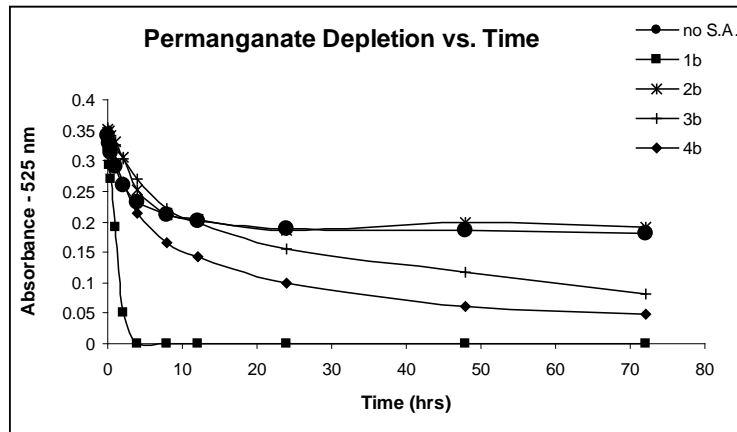


**Figure 2-10.** Representative data for 525 nm measurements (to determine permanganate concentration) vs. time. “No S.A.” refers to no stabilization, “1b” refers to Dowfax, “2b” is SHMP, “3b” is gum arabic, and “4b” is xanthan gum. All samples are for the base groundwater condition (no excess  $\text{Ca}^{2+}$  or  $\text{PO}_4^{3-}$ ) at pH 3. SHMP results mimic those of the “no stabilization” condition, indicating it does not exert a demand for the permanganate.

The batch experimental studies have established the proof of concept for using polymers to improve particle stability in solution, enhancing their potential to be more readily transported in groundwater. Additional experiments evaluated transport of  $\text{MnO}_2$  both with and without SHMP in 1-D transport systems of varied media content (i.e., organic matter, clay, mineralogy) to determine if the enhanced stability is maintained during transport through porous media. **Figure 2-11** shows deposition of  $\text{MnO}_2$  with distance from the influent end TCE NAPL source. Note that the majority of deposition occurs in or near the NAPL source with some differences in deposition based on media type. **Figure 2-12** shows the decrease of  $\text{MnO}_2$  deposition in the source zone (which is Section 1 of **Figure 2-11**) with use of 1,000 mg/L of SHMP with the permanganate solution.

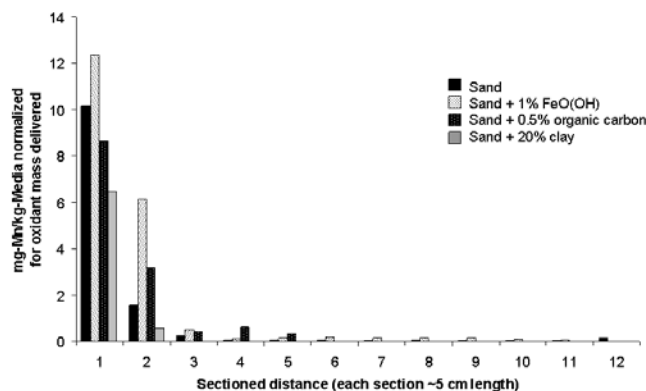


**Figure 2-11.** Mass of Mn (as MnO<sub>2</sub>) per kg of media with distance from 1-D column influent. Each section is approximately 5 cm of column length. Results are normalized for the total mass of permanganate delivered to the column. Delivery mass differed for columns due to plugging and restricted flow in Sand + Goethite and Sand + Clay columns.

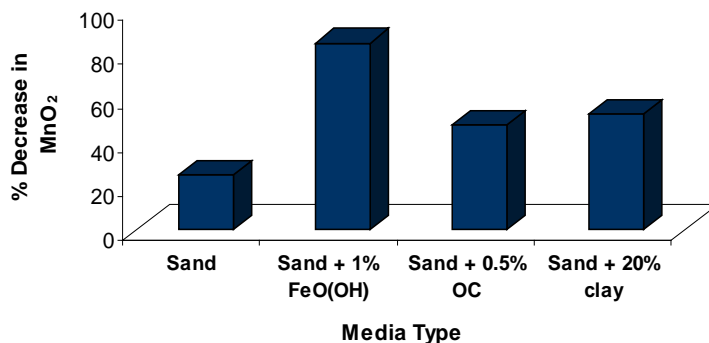


**Figure 2-12.** Percent decrease in MnO<sub>2</sub> deposition in source zone with 1,000 mg/L SHMP

**Summary.** This project focuses on (1) diminishing the effects of site heterogeneities with respect to the uniformity of oxidant delivery, and (2) managing MnO<sub>2</sub> aggregation and deposition, which is a significant challenge for sites with excessive oxidant consumption due to the presence of natural materials or large masses of dense non-aqueous phase liquids (DNAPLs). We are demonstrating/validating the use of water-soluble polymers (xanthan gum and sodium hexametaphosphate (SHMP)) to improve the delivery and distribution of permanganate oxidant solutions within heterogeneous contaminated aquifers. Xanthan gum biopolymers have a long history of use in the petroleum industry, and their contribution toward improving the sweep efficiency of injected fluids by minimizing the effects of the aquifer heterogeneities is well-documented (Lake, 1989; Sorbie, 1989 and references therein). SERDP Project ER-1486 has verified that xanthan gum can significantly enhance the sweep efficiency of permanganate through heterogeneous media. Additionally, SERDP Project ER-1484 has found SHMP to stabilize MnO<sub>2</sub> particles in solution, preventing particle aggregation and inhibiting permeability reductions due to in situ deposition. Both of these projects have shown xanthan gum and SHMP to be compatible with permanganate solutions and amenable to co-injection.

## 2.2 ADVANTAGES AND LIMITATIONS OF THE TECHNOLOGY

Table 2-4 summarizes the advantages and limitations associated with introducing each polymer to a standard permanganate ISCO operation.

**Table 2-4. Advantages and Limitations of Enhanced Permanganate ISCO using Water Soluble Polymers**

<b>Xanthan Gum</b>	
<b>Advantages</b>	Improves injected fluid's sweep efficiency within heterogeneous porous media. Increased injection fluid viscosity promotes mobility reduction in the principal flow direction (longitudinal for vertically installed wells) and encourages transverse fluid movement (or cross-flow) of fluids between strata of differing permeability.
	Improved sweep efficiency results in improved distribution of co-injected remediation agent and improved contact between the amendment and the target contaminant
	In the presence of permanganate, xanthan gum will slowly oxidize into simple sugars. During our Treatability Study we found that, depending on the specific concentrations of oxidant and polymer, the co-injected solution will lose roughly half its initial viscosity in one week after emplacement. Initially, the enhanced viscosity will hydraulically isolate the treatment zone, improving contact times. As the polymer is oxidized the hydraulic properties of the treatment area should be largely restored.
	Xanthan gum costs are approximately 60% permanganate costs. Costs relative to permanganate depend on xanthan gum type and concentration employed, which depend on media characteristics. Because of the relatively lower permeability of this demonstration area, relative cost here is higher than may be typical.
<b>Limitations</b>	Increased injected fluid viscosity results in reduced fluid mobility during transport within porous media. "Mobility" refers to the fluid-specific component of hydraulic conductivity. Therefore, a reduction in mobility results in a reduction in hydraulic conductivity. This hydraulic conductivity reduction can limit the rate of fluid injection within shallow aquifer systems
	Larger polymer molecules can become trapped within narrow pores during transport with porous media, reducing the permeability to polymer and in severe cases to water. This entrapment mechanism becomes more pronounced as the intrinsic permeability of the porous media decreases and the mean pore diameter approaches the effective hydrodynamic diameter of the polymer molecule (which is generally considered to be about 1 micron (Dominguez and Willhite, 1977)). Permeability reduction compounds the reduced injectivity of the polymer-amended fluid resulting from the increased viscosity. Therefore, the effects of mobility reduction and permeability reduction must be accounted for during implementation design.
	Polymer mixing and filtration equipment costs must be added to the design and treatment costs. Costs for this demonstration, which depend on scale, are ~\$20K for the added equipment.
<b>SHMP</b>	
<b>Advantages</b>	Maintains MnO <sub>2</sub> particles suspended in solution, inhibiting their deposition in the subsurface. This can result in improved contact with contaminant and increased remediation efficiency.
	Does not react with permanganate therefore there is no additional demand for oxidant.
	Aside from an additional line to introduce SHMP to permanganate solution prior to subsurface delivery, there are no additional modifications to a typical permanganate system design for implementation.
	SHMP costs are approximately 40% of the permanganate costs. Costs relative to permanganate depend on the SHMP concentration employed, which depends on media characteristics. Because of the relatively low permeability of this demonstration area and high concentration of SHMP to be employed, relative cost here is higher than may be typical.
<b>Limitations</b>	The impacts of adding excess "salt" to the subsurface system are expected to be minimal and harmless, yet they have not been investigated.
	The addition of SHMP will increase total dissolved solids concentrations in the treatment zone and possibly downgradient.

### 3.0 PERFORMANCE OBJECTIVES

Table 3-1 shows the demonstration's performance objectives, data requirements, success criteria, and results. The results are discussed in more detail in Section 6.0.

**Table 3-1. Performance Objectives**

Performance Criteria	Data Requirements	Success Criteria (with use of polymer)	Results
<b>Quantitative Performance Objectives</b>			
Increased penetration of oxidant into lower permeability layers/strata	<ul style="list-style-type: none"> <li>- Examination of soil cores for evidence of permanganate or MnO<sub>2</sub></li> <li>- If LPM of thickness appropriate for discrete groundwater sampling is present, then MnO<sub>4</sub><sup>-</sup> /MnO<sub>2</sub> concentrations measured in groundwater over space and time</li> </ul>	<ul style="list-style-type: none"> <li>- 50% longer distance of permanganate penetration into lower permeability layers/strata</li> <li>- 25% higher permanganate concentration at expected time of arrival in each monitoring well</li> <li>- Demonstrated improvement in vertical sweep efficiency within lower permeability layers/strata</li> <li>- Demonstrated improvement in overall vertical sweep efficiency in test plot</li> </ul>	Objective met
Decreased flow bypassing (increased lateral sweep efficiency) of areas of high contaminant mass	<ul style="list-style-type: none"> <li>- Examination of soil cores for evidence of permanganate or MnO<sub>2</sub> in media with high contaminant concentration</li> <li>- Soil core extractions for MnO<sub>2</sub> and measurements of MnO<sub>4</sub><sup>-</sup> and MnO<sub>2</sub> in groundwater over time and distance</li> <li>- Soil core extractions for contaminant with distance</li> </ul>	<ul style="list-style-type: none"> <li>- 50% lower mass of MnO<sub>2</sub> in given mass of media (indicative of inhibition of deposition that can increase bypass)</li> <li>- 25% greater mobile MnO<sub>2</sub> concentration at given time point in monitoring well</li> <li>- 50% lower mass of contaminant in high concentration cores</li> </ul>	Objective partially met; sweep was improved, however not specifically associated with high contaminant mass
Evaluate long-term potential for and short-term occurrence of contaminant rebound	<ul style="list-style-type: none"> <li>- Contaminant concentrations in groundwater over time and distance</li> <li>- Contaminant concentrations in soil cores pre- and post-treatment</li> </ul>	<ul style="list-style-type: none"> <li>- Data collected and are representative of test plots</li> <li>- Post-treatment groundwater monitoring results remain below baseline concentrations</li> </ul>	Objective partially met
Improved contaminant treatment effectiveness	<ul style="list-style-type: none"> <li>- Contaminant concentrations in groundwater over time and distance from injection</li> <li>- Contaminant mass in soil over time and distance</li> </ul>	Statistically significant reduction in contaminant mass as compared to a control plot	Objective met
<b>Qualitative Performance Objectives</b>			
Decreased impact of MnO <sub>2</sub> on injection pressure	Injection well pressure over time	No increase in injection pressure attributable to MnO <sub>2</sub>	Objective met
Improved understanding of impacts of polymers on groundwater quality	pH, ORP, key metals, solids concentrations, conductivity, bioactivity	Note differences	Objective met

## 4.0 SITE DESCRIPTION

### 4.1 SITE LOCATION AND HISTORY

MCIEAST-MCB CAMLEJ Operable Unit (OU) 15, Site 88 was selected for the technology demonstration because it best fulfilled the preferred technical criteria, including chloroethene concentration, depth to groundwater, minimum interference, utility access, bulk hydraulic conductivity, and heterogeneous lithology.

The test area is located in Jacksonville, North Carolina. MCIEAST-MCB CAMLEJ covers approximately 236 square miles and is a training base for the United States Marine Corps. The test area is located within OU 15, Site 88, which consists of the former Base Dry Cleaning facility (former Building 25), located approximately 500 feet east of the intersection of Post Lane Road and McHugh Boulevard (**Figure 4-1**). The test area is located within and immediately west of the footprint of the former Building 25 (**Figure 4-2**).

Former Building 25 operated as a dry cleaning facility from the 1940s until 2004 when operations ceased and the building was demolished. Five 750-gallon underground storage tanks (USTs) were installed on the north side of the building to store dry cleaning fluids. Initially, Varsol™, a petroleum hydrocarbon-based stoddard solvent, was used in dry cleaning operations at Building 25. Due to flammability concerns, Varsol's use was discontinued in the 1970s and was replaced with tetrachloroethene (PCE). PCE was stored in a 150-gallon aboveground storage tank (AST) adjacent to the north wall of Building 25, in the same vicinity as the USTs. PCE was reportedly stored in the AST from the 1970s until the mid-1990s. Facility employees have reported that during this time, spent PCE was disposed of in floor drains that discharged into the sanitary sewer system on the north side of the building (**Figure 4-2**).

In December 1986 and again in March 1995, self-contained dry cleaning machines were installed in Building 25, eliminating the need for bulk storage of PCE. The USTs and AST were removed in November 1995.

During removal of the USTs and ASTs, chlorinated volatile organic compounds (VOCs) were detected in soil and groundwater samples. Subsequent investigations conducted in 1996 and 1997 identified subsurface soil contamination under and near Building 25, and along a line of borings paralleling the underground sanitary sewer line north of Building 25, which was attributed to the leakage of solvent-contaminated wastewater (Baker, 1998a). Groundwater analytical results identified wide-spread chlorinated solvent contamination (PCE, trichloroethene [TCE], and cis-1,2-dichloroethene [cis-1,2-DCE]), which had impacted the Surficial Aquifer (less than 25 ft below ground surface [bgs]) and the upper portion of the Castle Hayne Aquifer (25-80 ft bgs). A distinct contaminant plume was identified, which suggested Building 25 was the source area. The results also suggested the presence of a dense non-aqueous phase liquid (DNAPL) in this area.





Figure 4-1. Test area at MCIEAST-MCB CAMLEJ, North Carolina, OU 15, Site 88.



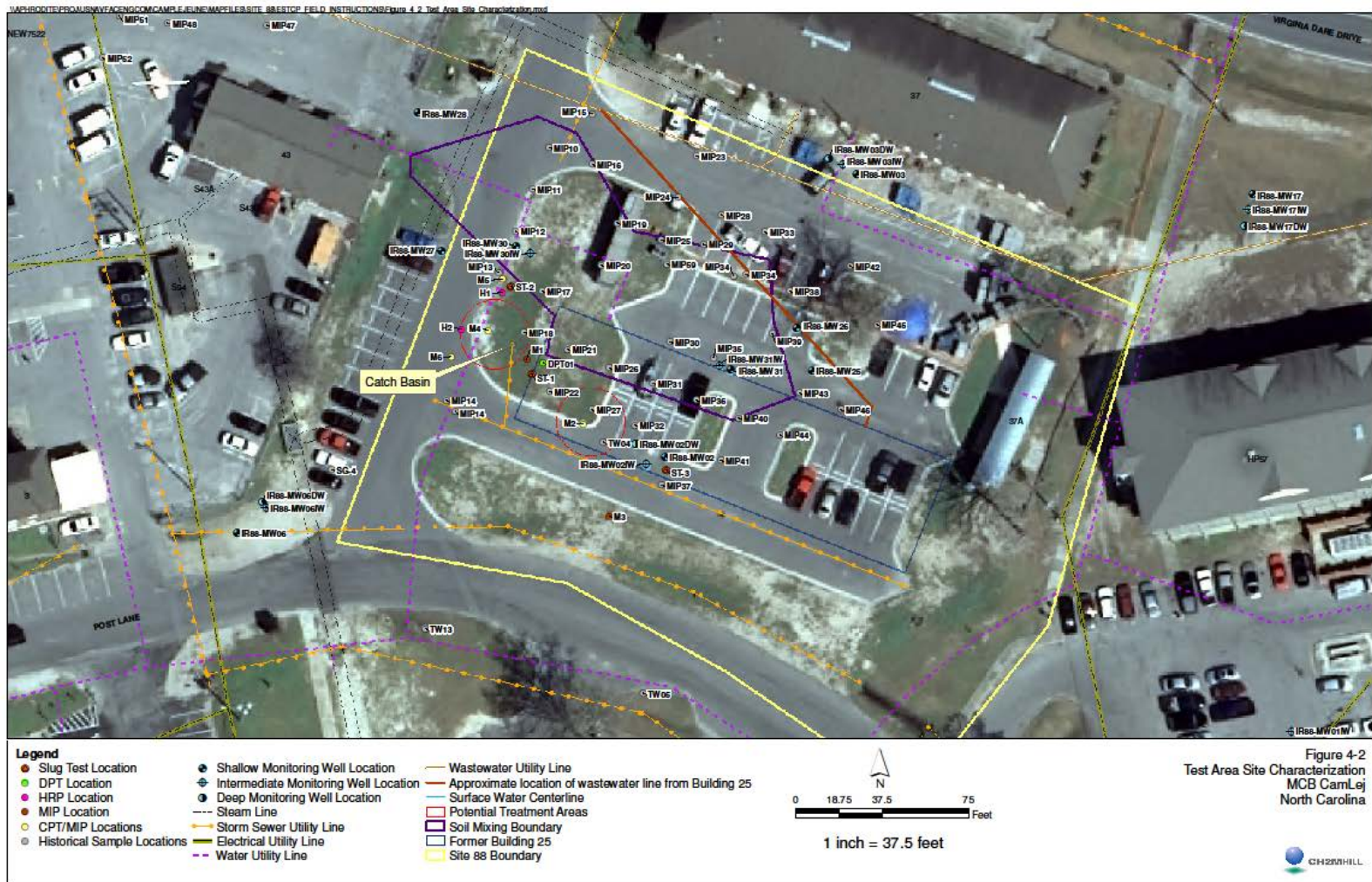


Figure 4-2. Closer view of test area located within and immediately west of the footprint of the former Building 25.



In 2005, shallow soil mixing with clay and zero valent iron (ZVI) was implemented at Site 88 in the vicinity of former Building 25, as shown on **Figures 4-2** and **4-3**, to contain and treat the DNAPL source area. Approximately 7,050 cubic yards of impacted soil was treated. Within the soil mixing zone, PCE concentrations in the soil were reduced by greater than 99 percent. Despite the significant source area mass flux reduction, residual groundwater contamination remains over a large portion of the surrounding and downgradient areas. Additional investigation and remediation activities conducted at Site 88 include:

- Free Phase DNAPL Recovery, 1998: Conducted north of Building 25
- Partitioning Inter-well Tracer Test (PITT), 1998: Conducted adjacent to the north wall of Bldg. 25
- Surfactant-Enhanced Aquifer Remediation (SEAR), 1998-1999: Conducted adjacent to the north wall of Building 25
- Reductive Anaerobic *In-Situ* Treatment Technology (RABITT), 2001: Conducted at monitoring wells IR88-MW05 and IR88-MW05IW, approximately 200 ft northwest of the test area

## 4.2 SITE GEOLOGY AND HYDROGEOLOGY

### 4.2.1 Geology

Southeastern North Carolina and MCIEAST-MCB CAMLEJ are within the Tidewater region of the Atlantic Coastal Plain physiographic province. The MCIEAST-MCB CAMLEJ area is underlain by a westward (inland) thinning wedge of marine and non-marine sediments ranging in age from early Cretaceous to Holocene. Along the coastline, several thousands of feet of interlayered, unconsolidated sediment are present, consisting of gravel, sand, silt, clay deposits, calcareous clays, shell beds, sandstone and limestone that was deposited over pre-Cretaceous crystalline basement rock.

Site 88 is underlain by a thick sequence of coastal plain soils consisting of unconsolidated sands, silts, clays, and partially indurated shelly sands. Soils within the Surficial Aquifer are generally comprised of silty sands, ranging in thickness from 20 to 30 feet, which overlie a discontinuous layer of clayey silt or clay approximately 20 ft bgs. A clayey silt and clay confining layer, ranging in thickness from 4 to 10 feet, underlies the former location of Building 25 at a depth of approximately 20 ft bgs and extends westward as far as Building 3, whereupon it pinches out and is not encountered again until the 88MW-15 well cluster (**Figure 4-3**). Within the Castle Hayne Aquifer, a fine grained layer overlies massive beds of fine to medium grained sand with sporadic zones of partial cementation and shell fragments extending to a depth of roughly 180 feet bgs. At Site 88, the Castle Hayne Aquifer is divided into the upper Castle Hayne (25-80 feet), the middle Castle Hayne (80-130 feet), and the lower Castle Hayne (130-180 feet). A plastic clay layer, known as the Beaufort confining unit, was encountered beneath the Castle Hayne Aquifer; the Beaufort confining unit defines the vertical limit of subsurface investigation at Site 88.

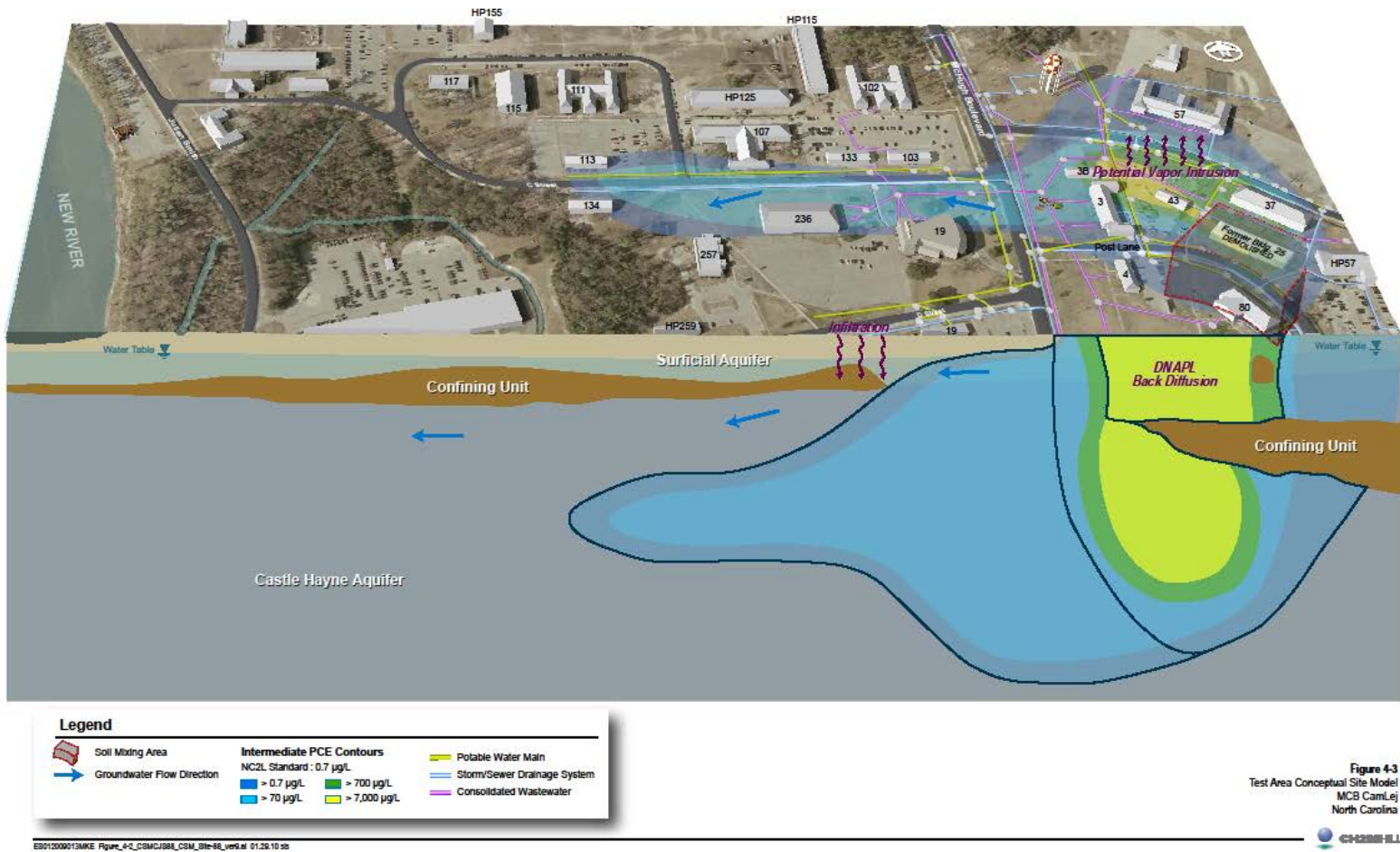


Figure 4-3. Test area conceptual site model

The general geologic setting in the vicinity of the test area is presented on **Figure 4-4**. The lithology in the test area was further investigated during site characterization activities conducted in Nov and Dec 2009. Cone penetrometer testing (CPT) was conducted at locations M2, M4, M5 and M6, shown on **Figure 4-2**, to delineate stratigraphic layers in the subsurface. High-resolution piezocone (HRP) profiling was conducted at location H1 to obtain detailed lithologic and hydraulic information. Example HRP results are provided in **Figure 4-5**. Additionally, a continuous soil core was collected from 10 to 50 ft bgs via direct push technology (DPT) at soil boring location DPT01, as shown on **Figure 4-2**. The boring log for DPT01 is provided in **Figure 4-6**.

The data collected during site characterization indicates alternating fine grained silty sand and sand to approximately 20 ft bgs in the vicinity of the test area. Soil particle size analysis has been completed for this shallower area. These data are included as **Figure 4-7**. The fine grained sediments are underlain by a more dense silty clay and clay layer approximately 7 to 12 feet thick to a depth of approximately 30 ft bgs. Below this unit are alternating layers of silty sand and sand. The sands become more dominate with depth and fewer fines are present, generally between 40 to 60 ft bgs. The boring log for deep monitoring well 88-MW02DW, located adjacent to the test area, indicates that fine grained silty sand is again present between 60 to 88 ft bgs, which is underlain by a layer of partially cemented sand and shells exists from 88 to 90 ft. A geologic cross-section within the vicinity of the test area based on site characterization activities is presented in **Figure 4-8**.

#### **4.2.2 Hydrogeology**

The hydrogeologic setting at Site 88 is that of a two aquifer system, the Surficial Aquifer and the Castle Hayne Aquifer, with the two aquifers typically separated by a low permeability clayey silt aquitard (Duke, 1999). This low permeability unit is present under former Building 25 within the test area, and, as noted above, is discontinuous to the west of former Building 25.

In November 2009, depth-to-water measurements were taken across Site 88. In the vicinity of the test area, the water table was found to occur from 7.25 to 10.10 ft bgs. The depth to water in monitoring wells screened within the Upper Castle Hayne Aquifer in the vicinity of the test area, ranged from 14.46 to 15.62 ft bgs.

**Figure 4-9** shows the potentiometric surface of the Surficial Aquifer measured in November 2009, as represented by the shallow monitoring wells (less than 25 ft bgs). **Figure 4-9** shows a highly variable water table surface, which is likely due in part to the heterogeneous nature of the shallow sediments, and also the anthropogenic effects relating to the soil mixing activities. The soil mixing involved addition of a mixture of zero-valent iron and bentonite clay that significantly reduced the hydraulic conductivity of the mixed soil. Shallow groundwater flow in the test area is to the southwest, with a horizontal hydraulic gradient of approximately 0.002 ft/ft. A downward vertical hydraulic gradient of approximately 0.25 ft/ft between the Surficial Aquifer and the Upper Castle Hayne Aquifer in the test area was calculated, based on the November 2009 depth-to-water measurements collected in the IR88-MW02 cluster.

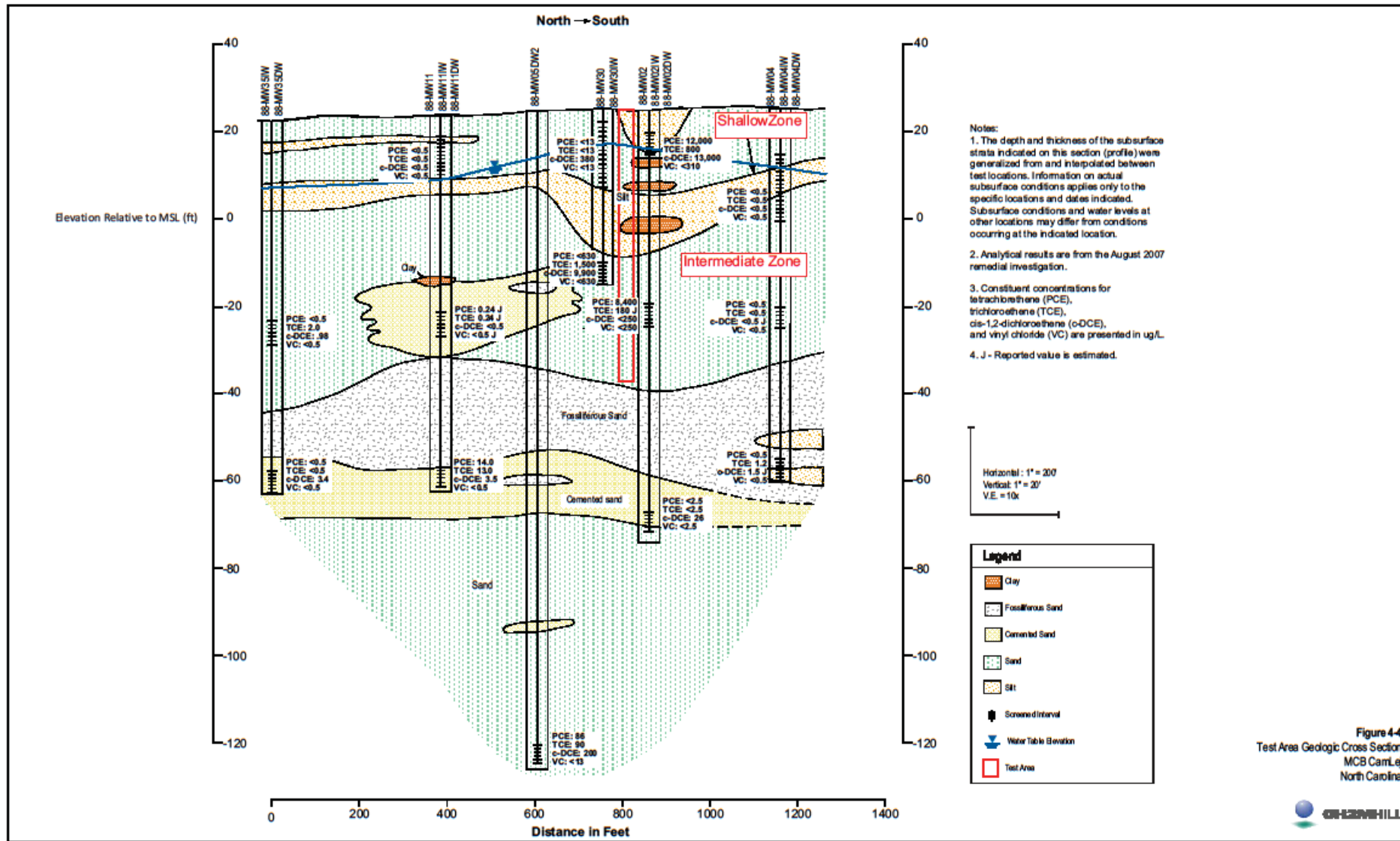


Figure 4-4. General geologic setting in vicinity of test area



# DIRECT SENSING

H-1A

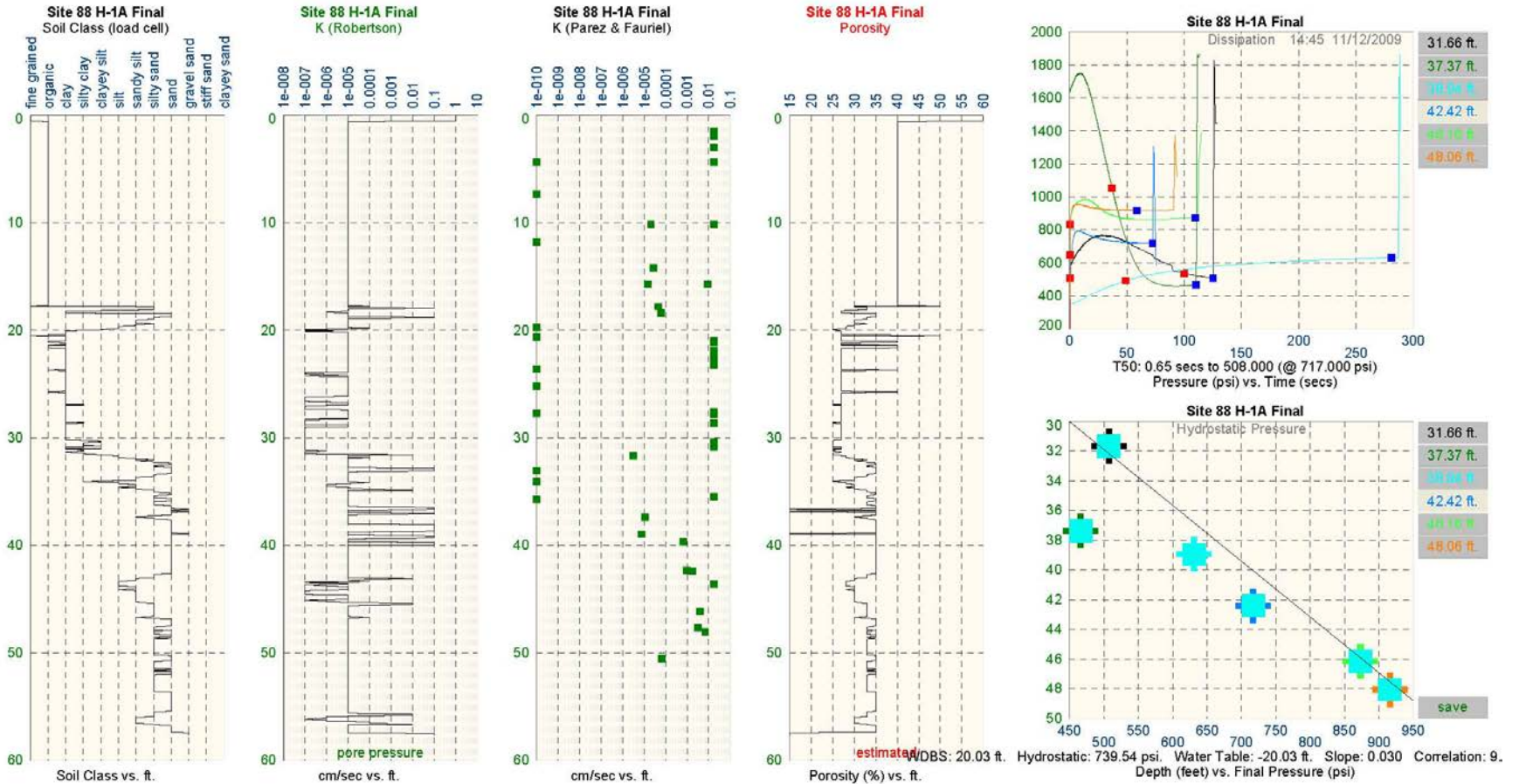


Figure 4-5. Example HRP results



CH2MHILL

**Boring Number: DPT-01**

Sheet: 1 of 2

Client: Clarkson University  
 Project: ESTCP  
 Location: Site 88, MCB Camp Lejeune  
 Project Number:

Driller: Drill Pro  
 Drilling Method: DPT  
 Sampling Method: macro-core  
 Logged by: B. Propst  
 Start/Finish Date: 11-12-09

Depth (ft)	Sample Information				Soil Log	Soil Description	Comments
	Sample #	Sample Type	Recovery (%)	SPT (6"-6"-6")			
0						Ground Surface	
0 - 5		HA	100			<b>Silty Sand (SM)</b> Brown, dry, loose, fine grained	
5 - 10						No sample collected	
10 - 15	DP-1	DP	100			<b>Sand (SP)</b> Tan/brown, wet, loose, fine grained  <b>Sand (SP)</b> Gray, wet, loose, fine grained	
15 - 20	DP-2	DP	100				
20 - 25	DP-3	DP	100			<b>Silty Sand (SM)</b> Light brown, wet, loose, fine grained	
25 - 28						<b>Sandy Clay (CL)</b> Light brown, wet, soft, fine grained	
28 - 30	DP-4	DP	100			<b>Clay (CH)</b> Light gray, high plasticity, soft to medium stiff	
30 - 33						<b>Sandy Clay (CL)</b> Brown, wet, stiff	

**Figure 4-6.** Boring Log for DPT01



CH2MHILL

### Boring Number: DPT-01

Sheet: 2 of 2

Client: Clarkson University  
 Project: ESTCP  
 Location: Site 88, MCB Camp Lejeune  
 Project Number:

Driller: Drill Pro  
 Drilling Method: DPT  
 Sampling Method: macro-core  
 Logged by: B. Propst  
 Start/Finish Date: 11-12-09





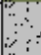
Depth (ft)	Sample Information				Soil Log	Soil Description	Comments
	Sample #	Sample Type	Recovery (%)	SPT (6"-6"-6")			
35	DP-5	DP	100		 Sand (SP) Light gray, wet, medium dense, fine grained		
35					 Silty Sand (SM) Brown, wet, medium dense, fine grained		
40	DP-6	DP	100		 Silty Sand (SM) Gray, wet, loose to medium dense, fine grained		
45	DP-7	DP	100		 Sand (SP) Olive gray, wet, loose to medium dense, fine grained		
50	DP-8	DP	100		 Sand (SP) Gray, wet, loose, medium grained		
50						Terminate boring at 50' bgs	
55							
60							

Figure 4-6. Boring log for DPT01 (cont'd)

# Particle Size Distribution Report

**Project:** Soil Laboratory Testing

**Report No.:** CT2989SL-01-01-10

**Client:**

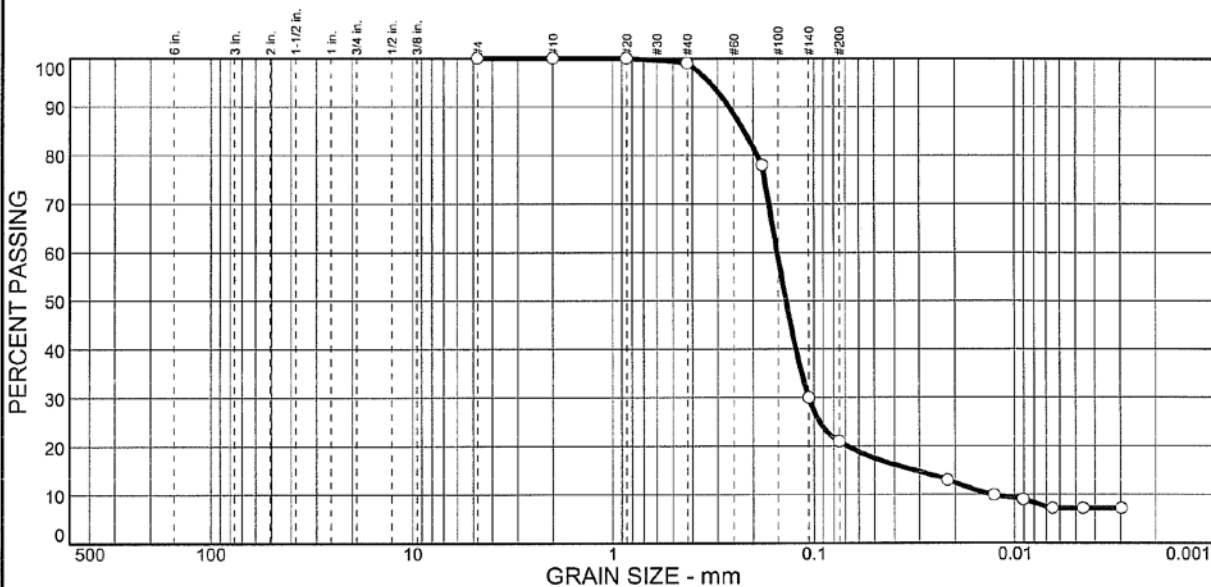
**Date:** 1/29/10

**Sample No:** CT2989S1

**Source of Sample:** Not Specified

**Location:** --

**Elev./Depth:**





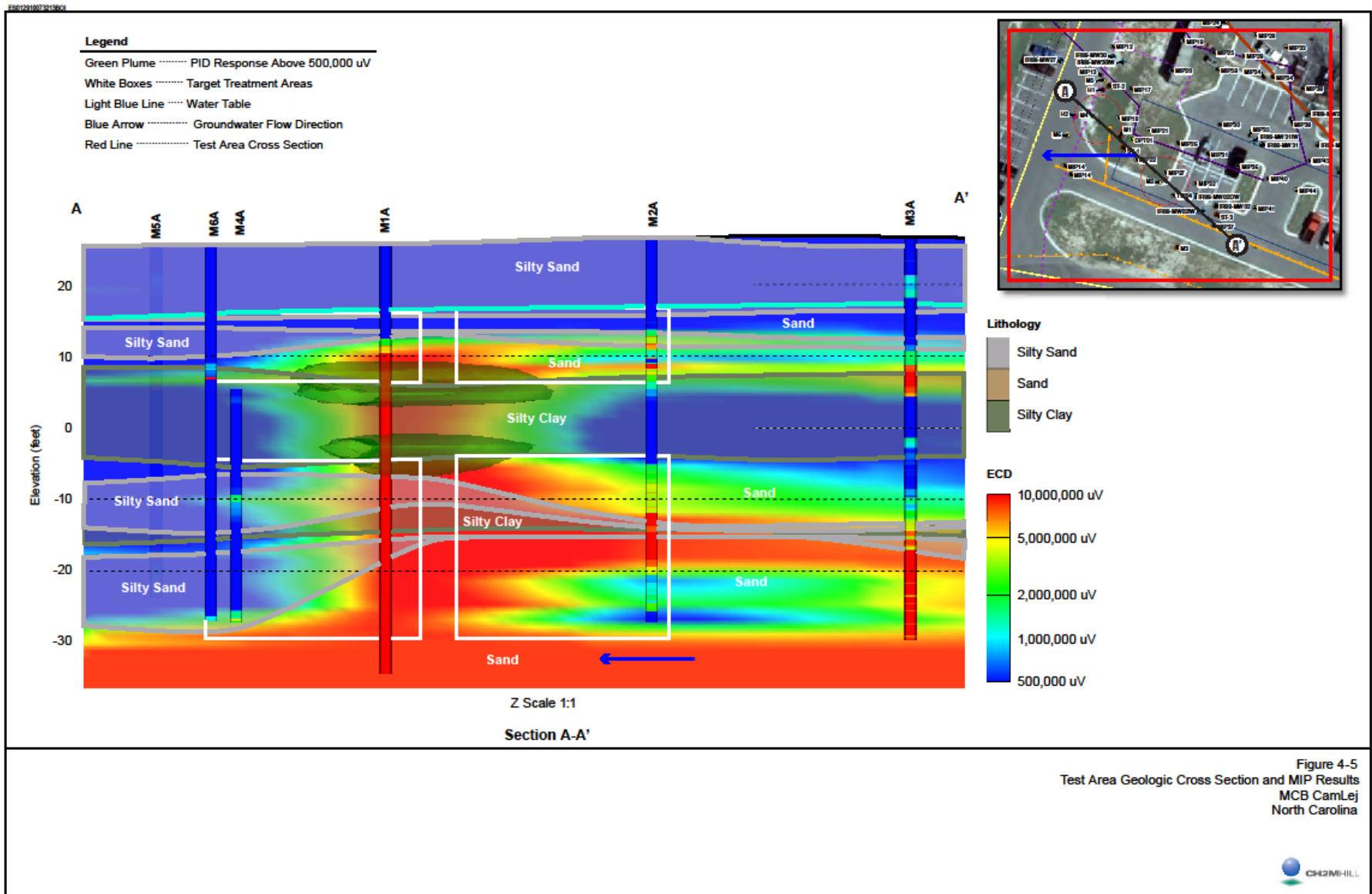
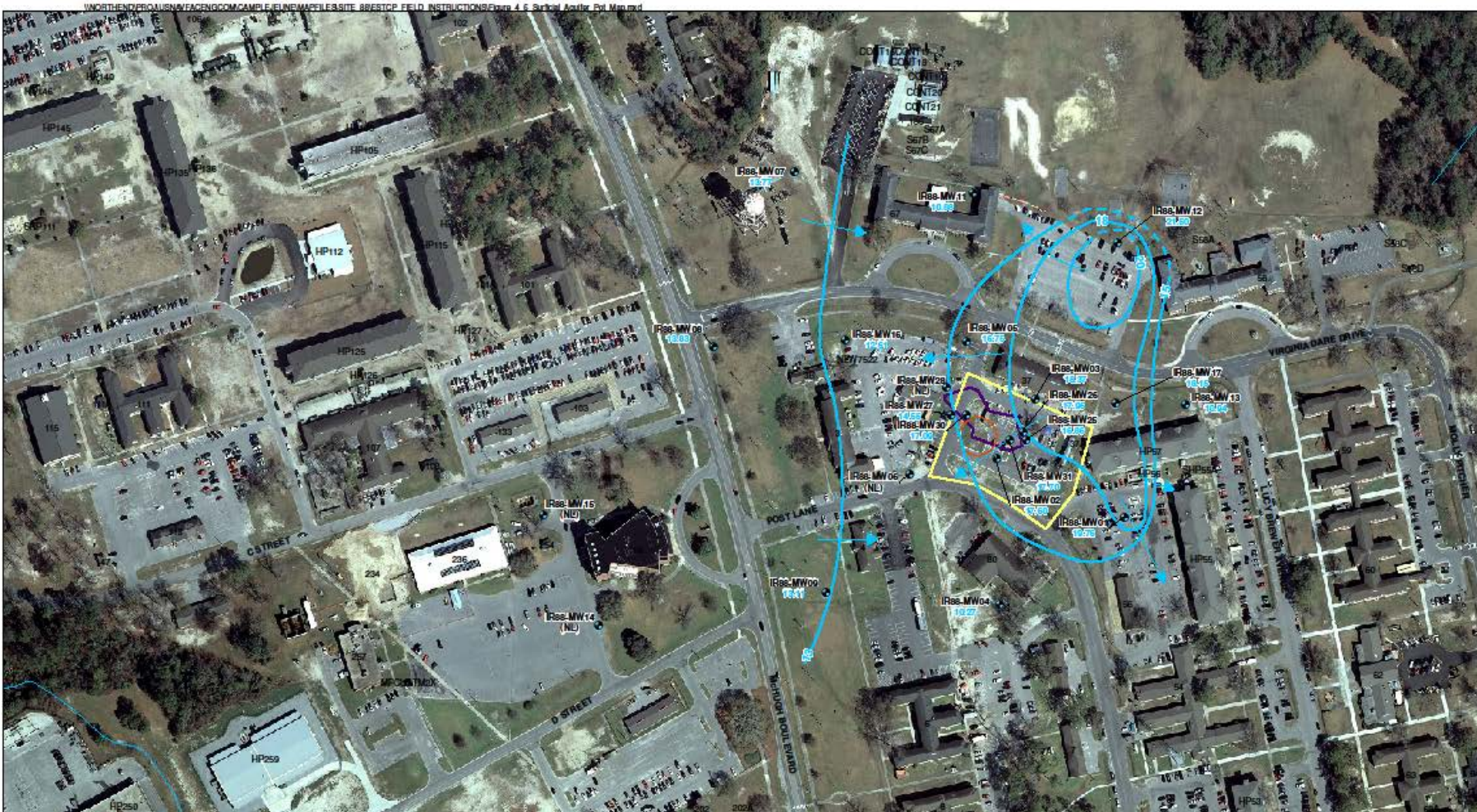


**Figure 4-8.** Geologic cross-section within the test area based on most recent characterization activities





- Legend**
- Shallow Monitoring Well Location
  - Shallow Aquifer Potentiometric Contour
  - - - Shallow Aquifer Potentiometric Contour (inferred)
  - ➔ Groundwater Flow Direction
  - Surface Water Centerline
  - Site 88 Boundary
  - Test Area
  - Soil Mixing Boundary
- NL = Not Located

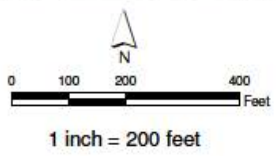


Figure 4-6  
Potentiometric Map  
Surficial Aquifer  
MCB CamLej  
North Carolina



Created by: Brooke Props/CLT Checked by: Kell Halberg/CLT

Figure 4-9. Potentiometric map of the Surficial Aquifer

**Figure 4-10** shows the potentiometric surface of the Upper Castle Hayne Aquifer in November 2009, as represented by the intermediate zone wells (45 to 55 ft bgs). The groundwater flow pattern for this aquifer is less complex than that of the Surficial Aquifer, with groundwater flow generally to the west, with an approximate horizontal hydraulic gradient in the vicinity of the test area of 0.0004 ft/ft. A downward vertical gradient of 0.0015 ft/ft between the Upper Castle Hayne and Middle Castle Hayne Aquifers within the test area was calculated, based on the November 2009 depth-to-water measurements collected in the IR88-MW02 cluster.

Aquifer testing was conducted during site characterization activities in November and December 2009. A pneumatic slug test method was employed through DPT-installed steel rod piezometers at three locations across the test area, ST-1, ST-2, ST-3, shown on **Figure 4-2**. A groundwater sampler equipped with a screen was pushed using DT to the terminating depth of the testing interval. The drill rods were then pulled up to expose two feet of the screen and conduct the slug test.

Hydraulic conductivity was calculated using the Hvorslev method. The hydraulic conductivity values calculated at each slug test location are summarized in **Table 4-1**. The hydraulic conductivity in the Surficial Aquifer ranged from 1.5 ft/day to 5.2 ft/day, with an average hydraulic conductivity of 2.8 ft/day. The hydraulic conductivity in the Upper Castle Hayne Aquifer just below the confining unit ranged from 0.9 ft/day to 4.9 ft/day, with an average hydraulic conductivity of 2.5 ft/day.

As previously mentioned, HRP profiling was conducted at location H1 to obtain detailed hydraulic information. HRP technology involves the advancement of a probe that continuously logs pore pressure (measured as hydraulic head) and periodically logs pore pressure dissipation during stoppage time. The data are then electronically processed and used to estimate vertical gradients, soil type, and hydraulic conductivity. HRP conductivity values generally ranging from  $1 \times 10^{-5}$  centimeters per second (cm/s) (0.03 ft/day) to 0.001 cm/s (3 ft/day) in the Surficial Aquifer. In the Upper Castle Hayne Aquifer, HRP conductivity values were generally higher, ranging from  $1 \times 10^{-4}$  cm/s (0.3 ft/day) to 0.01 cm/s (30 ft/day).



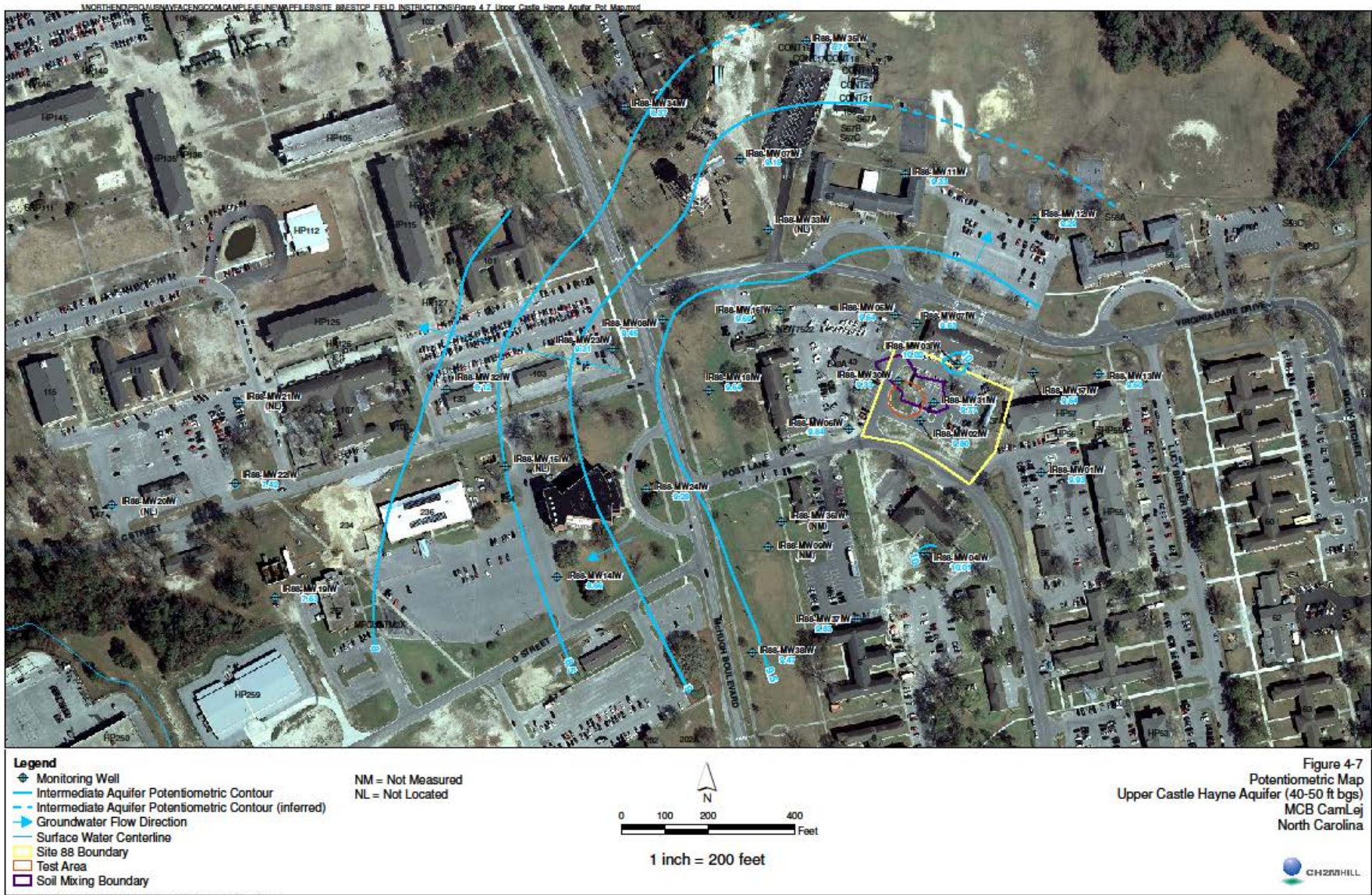


**Figure 4-10.** Potentiometric map of the Upper Castle Hayne Aquifer

**Table 4-1. Hydraulic Conductivity Calculated at Each Slug Test Location**

Location	Interval Depth (ft bgs)	Test	Conductivity Results (ft/day)	Average Conductivity (ft/day)
ST-1	33-35	1	4.9	4.6
		2	4.8	
		3	4.2	
	38-40	1	2.6	2.5
		2	2.5	
		3	2.5	
	43-45	1	9.8	9.8
		2	9.8	
		3	9.8	
ST-2	14-16	1	2.2	2.0
		2	1.5	
		3	2.1	
	33-35	1	0.9	1.0
		2	1.0	
		3	1.0	
		4	1.0	
	42-44	1	6.1	6.0
		2	6.1	
		3	5.9	
		4	5.9	
		5	6.0	
	47-49	1	10.7	10.9
		2	10.7	
		3	11.0	
		4	11.0	
	54-56	1	8.7	9.0
		2	8.7	
		3	9.1	
		4	9.4	
		5	9.2	
		6	9.2	
	61-63	1	2.3	2.8
		2	2.4	
3		2.8		
4		3.7		
ST-3	14-16	1	5.2	4.0
		2	2.7	
	33-35	1	1.5	1.5
		2	1.4	
	45-47	1	16.6	17.0
		2	16.4	
		3	18.1	
	54-56	1	8.2	7.4
		2	7.5	
		3	8.0	
		4	6.9	
		5	6.3	
	60-62	1	3.9	3.2
2		2.5		
ST-4 (offset from ST-1)	14-16	1	0.6	0.6
		2	0.6	
		3	0.6	
		4	0.5	

### 4.3 CONTAMINANT DISTRIBUTION

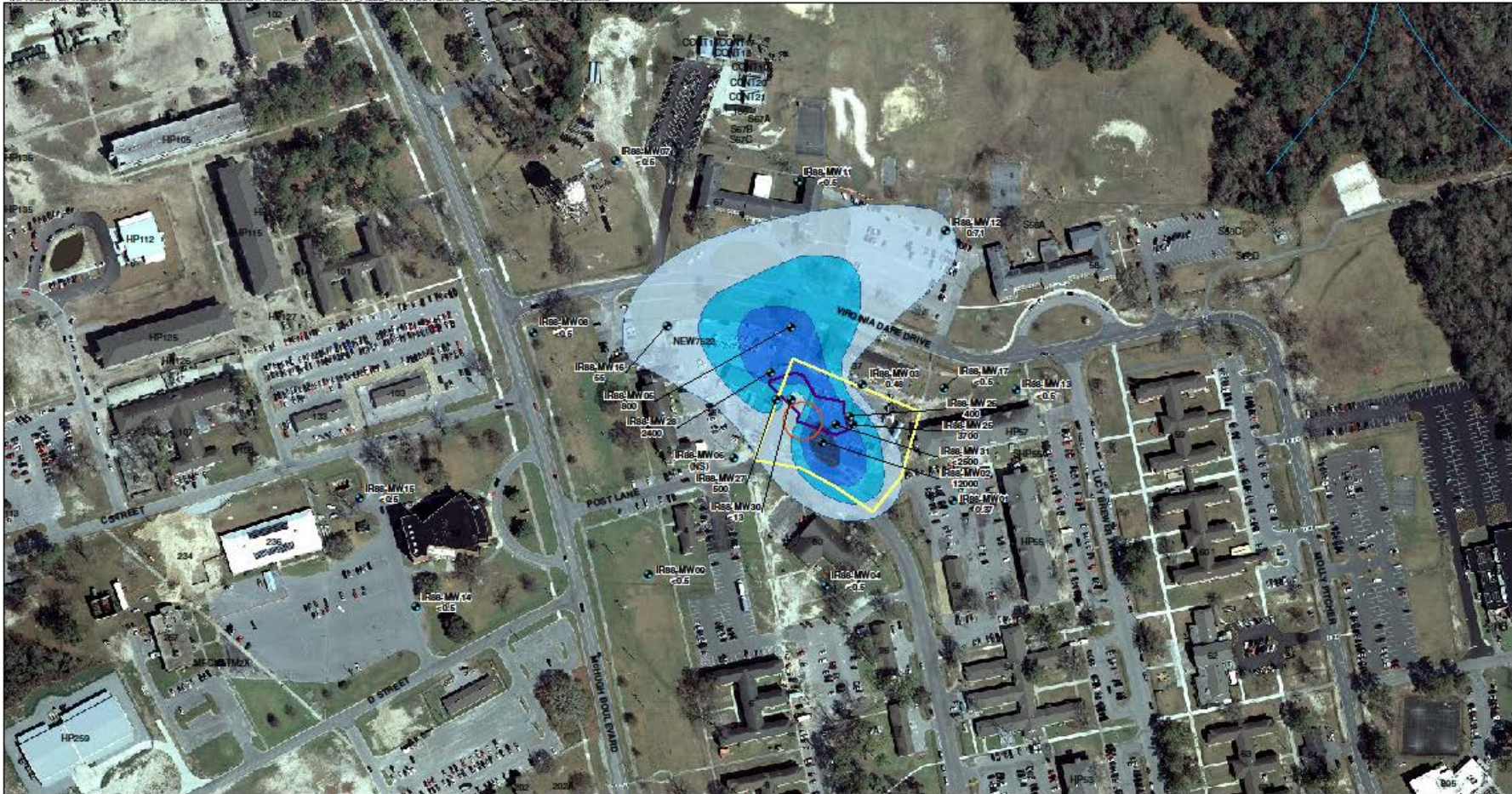
Based on the chemical data gathered for Site 88, former Building 25 is the source of the chlorinated VOCs that are currently observed in the groundwater within the shallow, intermediate, deep and very deep aquifer zones. The contaminants of concern (COCs) for Site 88 are PCE and its anaerobic biodegradation daughter products TCE, cis-1,2-DCE, and vinyl chloride.

Data obtained from groundwater samples collected as part of the RI in August 2007, indicate the maximum chlorinated VOC concentration within the shallow aquifer in the vicinity of former Building 25 and the test area, was reported at well IR88-MW02 with PCE and cis-1,2-DCE concentrations of 12,000 micrograms per liter ( $\mu\text{g/L}$ ) and 13,000  $\mu\text{g/L}$  respectively. Concentrations in the source area decrease significantly with depth, as shown by the 88-MW02 cluster, on **Figure 4-4**. **Figures 4-11** and **4-12** show the post-treatment distribution of PCE in the Surficial and Upper Castle Hayne Aquifers across the test area and Site 88 (2007).

During site characterization activities conducted in November and December 2009, membrane interface probe (MIP) profiling was conducted at six locations, M1 through M6 shown on **Figure 4-4**, to delineate contaminant concentrations within the test area. Analytical results are shown on **Figure 4-8**. MIP results indicate that the highest contaminant concentrations in the Surficial Aquifer exist from 16 to 18 ft bgs at location M1, immediately above an apparent confining unit. MIP results in this area are indicative of DNAPL. Results suggest that contamination in the shallow zone extends approximately 45 feet to the southeast towards location M2. MIP results consistently indicate higher contaminant concentrations throughout the Upper Castle Hayne Aquifer between 40 and 50 ft bgs at locations M1, M2, and M3. Again, the highest contaminant concentrations were detected at location M1 from approximately 33 to 35 ft bgs, immediately below an apparent confining unit. In both the Surficial and Upper Castle Hayne Aquifers, contaminant concentrations appear to decrease significantly to the west towards location M6.

Two groundwater and three soil samples were collected from soil boring DPT01. DPT soil samples were obtained using a 5-foot long, 1.5-inch inner diameter (ID) acetate macro-core sampler. As each borehole was advanced, continuous soil cores were collected and soil samples were collected directly from the acetate liners. The groundwater samples were collected by pushing the groundwater sampler equipped with a screen to the terminating depth of the sampling interval. The drill rods were then pulled up to expose two feet of the screen. A peristaltic pump was used to purge the groundwater and collect the groundwater sample. DNAPL, which was dark in color, was observed in the groundwater sample collected in the shallow interval (14-16), immediately above the confining unit. The DNAPL was collected and submitted for laboratory analysis.





- Legend**
- Shallow Monitoring Well Location
  - Surface Water Centerline
  - ▭ Site 88 Boundary
  - ▭ Test Area
  - ▭ Soil Mixing Boundary
- Shallow PCE Contours**  
 NC2L Standard : 0.7  $\mu\text{g/L}$
- ▭ > 0.7  $\mu\text{g/L}$
  - ▭ > 700  $\mu\text{g/L}$
  - ▭ > 70  $\mu\text{g/L}$
  - ▭ > 7,000  $\mu\text{g/L}$

Note: Concentration contours have been interpolated between monitoring well locations. Actual concentrations may differ from those shown on this figure.

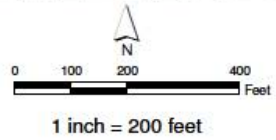


Figure 4-8  
 Tetrachloroethene  
 Surficial Aquifer  
 MCB CamLej  
 North Carolina



Figure 4-11. PCE concentrations in the Surficial Aquifer (2007)



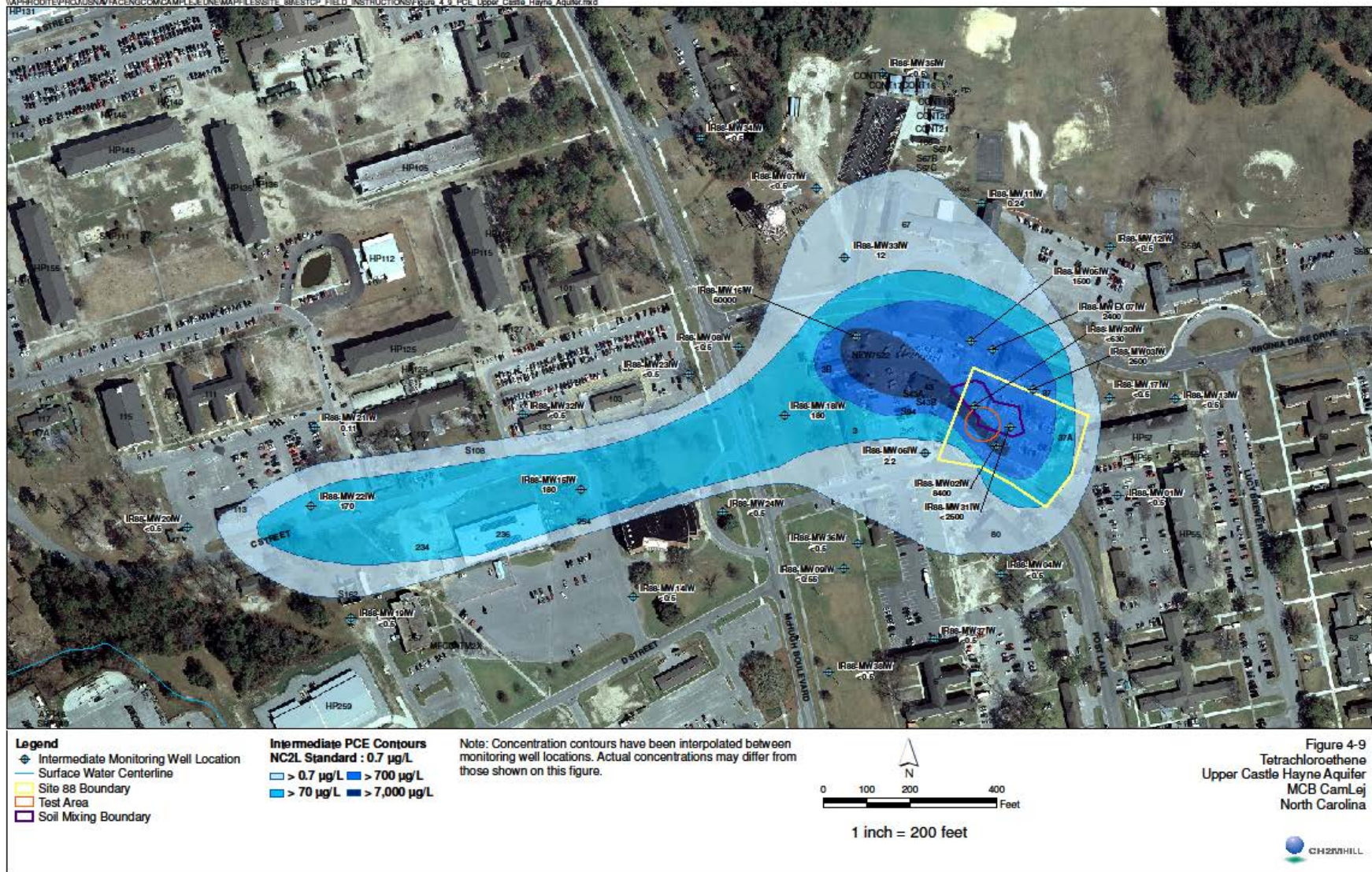


Figure 4-12. PCE concentrations in the Upper Castle Hayne Aquifer (2007)



Analytical results are summarized in **Tables 4-2 and 4-3**. PCE and cis-1,2-DCE were detected at maximum concentrations of 7,100 micrograms per kilogram ( $\mu\text{g}/\text{kg}$ ) and 10,000  $\mu\text{g}/\text{kg}$ , respectively, in the soil sample collected immediately above the confining unit. Below the confining unit, PCE ranged from below the laboratory detection limit (720  $\mu\text{g}/\text{kg}$ ) to 1,300  $\mu\text{g}/\text{kg}$  and cis-1,2-DCE ranged from below the laboratory detection limit (5.2  $\mu\text{g}/\text{kg}$ ) to 22  $\mu\text{g}/\text{kg}$ . PCE was detected in the groundwater sample collected immediately above the confining unit (14-16 ft bgs) at a concentration of 220,000  $\mu\text{g}/\text{L}$ . Below the confining unit (33-35 ft bgs), PCE was detected at a concentration of 230,000  $\mu\text{g}/\text{L}$ . These groundwater concentrations are indicative of DNAPL, which is consistent with observed site conditions described above and the results of the MIP data collected from M1 adjacent to DPT01. Site characterization results for the test area are summarized in **Table 4-4**.

**Table 4-2. Analytical Results for Contaminants (GC-MS) in Soils**

Sample ID	DPT01-16-18	DPT01-33-35	DPT01-53-55
Sample Date	11/12/2009	11/12/2009	11/12/2009
<b>Volatile Organic Compounds (<math>\mu\text{g}/\text{kg}</math>)</b>			
2-Butanone	49	14 U	10 U
Acetone	2300 U	48	40
Carbon Disulfide	14	14 U	10
Tetrachloroethene	7,100	720 U	1,300
Toluene	7.6	6.9 U	5.2 U
Trichloroethene	600	12	540 U
cis-1,2-Dichloroethene	10,000	22	5.2 U
trans-1,2-Dichloroethene	21	6.9 U	5.2 U
Vinyl Chloride	38	6.9 U	5.2 U

Notes:

U- Analyte not detected

**Table 4-3. Analytical Results for Contaminants (GC-MS) in Groundwater**

Sample ID	DPT01-14-16	DPT01-33-35
Sample Date	11/12/2009	11/12/2009
<b>Chemical Name</b>		
<b>Volatile Organic Compounds (<math>\mu\text{g}/\text{L}</math>)</b>		
Acetone	75,000	50,000 U
Tetrachloroethene	220,000	230,000
Trichloroethene	10,000 U	13,000 U
cis-1,2-Dichloroethene	10,000 U	13,000 U
Vinyl Chloride	10,000 U	13,000 U

Notes:

U- Analyte not detected

**Table 4-4. Site Characterization Summary**

<b>Depth Interval of Study Area</b>	<b>7 ft bgs to 18 ft bgs</b>	<b>33 ft bgs to 62 ft bgs</b>
Predominant Soil Type	Sand	Sand
Fine-grained Soil Type	Silty Sand (7 to 11 ft bgs) Sand (11 to 18 ft bgs)	Silty Sand (33 to 40 ft) Sand (40 to 60 ft bgs)
Depth to Water, ft bgs	7.5	15.5
Hydraulic Conductivity, ft/day	0.5 to 5.2 Average: 1.8 Heterogeneity: 10.4 Vertical Conductivity: 0.00013 Anisotropy: 13,846	0.9 to 18.1 Average: 6.6 Heterogeneity: 20.1
Hydraulic Gradient, ft/ft	Horizontal: 0.002, southwest Vertical: 0.25, downward	Horizontal: 0.0004, west Vertical: 0.0015, downward
PCE Concentration in Groundwater, µg/L	220,000	230,000
PCE Concentration in Soil, µg/kg	7,100 (16-18 ft bgs)	ND < 720 (33 -35 ft bgs) 1,300 (53-55 ft bgs)
Depth Interval with Greatest Mass of Contaminant as indicated by MIP, ft bgs	16 to 18	33 to 35
Visual or Analytical Evidence of DNAPL?	Yes	No

## 5.0 TEST DESIGN

The objectives for this demonstration were: (1) to mitigate the effects of site heterogeneities with respect to the uniformity of permanganate delivery using the polymer xanthan gum, and (2) to manage MnO<sub>2</sub> aggregation and deposition using the polymer SHMP. A secondary project objective was to compare post-delivery/treatment groundwater quality for “permanganate only” and “permanganate + polymer” test areas. The objectives were to be pursued concurrently in separate treatment and control plots (**Figure 5-1**) within the Upper Castle Hayne aquifer. This section provides a detailed description of the system design and testing conducted to address these objectives. Laboratory studies supporting the design have been completed and are available in the project’s Treatability Study Report.

### 5.1 CONCEPTUAL EXPERIMENTAL DESIGN

Two plots were utilized to implement the demonstration and achieve the project objectives. One was a control plot (permanganate only), one was a SHMP + xanthan test plot (permanganate + SHMP + xanthan; hereafter referred to as permanganate + polymer) (**Figure 5-1**). An injection well was installed in the center of each test plot for substrate delivery. Multi-level sampling (MLS) wells were installed at various distances from the injection wells and screened at four depth intervals to monitor the water quality of the targeted zones.

### 5.2 BASELINE CHARACTERIZATION

Baseline characterization activities took place in two parts: (1) preliminary site screening activities and (2) sampling activities that took place during the well field installation after the site was selected for the demonstration. Both activities allowed an assessment of pre-treatment site conditions that contributed to implementation design calculations. The results of these activities are included in Section 4 of this report and included the following activities:

1. Soil sample collection to support treatability study activities
2. Potable water injection test
3. Groundwater sample collection
4. High resolution piezocone (HRP) survey
5. Membrane Interface Probe (MIP) survey

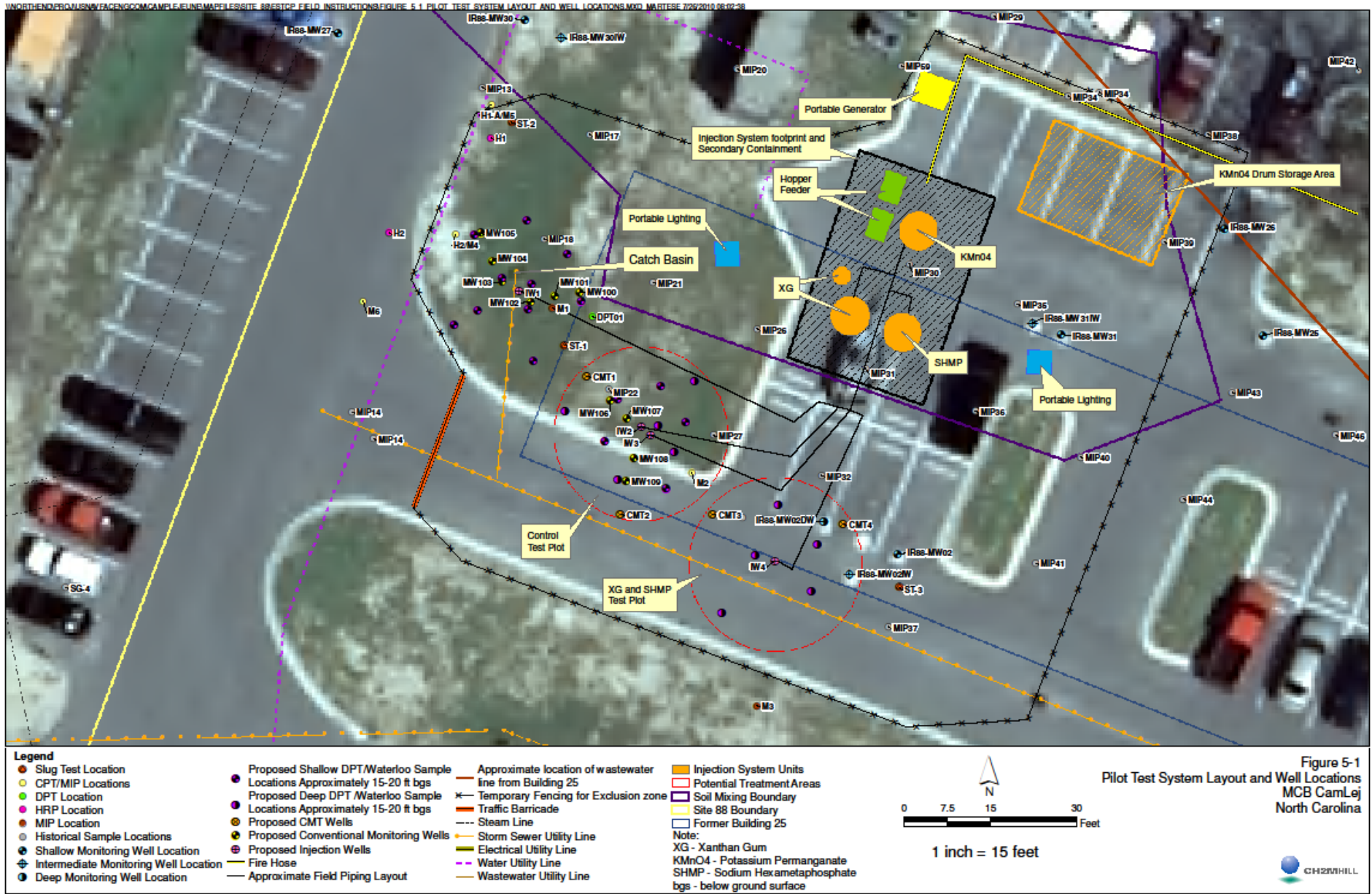


Figure 5-1. Pilot test system layout

### 5.2.1 Baseline Soil Sampling

During well installation, baseline cores were collected from each plot to characterize pre-treatment conditions. Soil samples were analyzed for VOCs, natural oxidant demand, total organic carbon (TOC), grain size distribution, pH, ORP, cation exchange capacity (CEC), and manganese content (see **Tables 5-1, 5-2, and 5-3**). At Site 88, a confining unit separates the Surficial Aquifer from the Upper Castle Hayne Aquifer at approximately 25 ft bgs. All borings advanced beyond this depth (all those associated with xanthan test and control plots) required the installation of isolation casings from the ground surface into the confining unit (at least one foot) to prevent cross-contamination. Baseline sampling allowed for collection of media used for treatability studies described in Section 5.3 and provided reference data to compare changes in groundwater quality due to the demonstration. Raw data are presented in Appendix B and are discussed in Section 5.7.

### 5.2.2 Baseline Groundwater Sampling

Prior to implementation of the demonstration, groundwater samples were collected from each MLS well within each plot to measure pre-treatment water quality (see **Tables 5-1, 5-2, and 5-3**) using the low-flow sampling techniques that are standard for MCIEAST-MCB CAMLEJ. Raw data are presented in Appendix B and are discussed in Section 5.7

### 5.2.3 Potable Water Injection Testing

Step-injection tests were performed using the two central injection wells (i.e., IW3 and IW4) to evaluate the initial hydraulic properties of each plot and to optimize injection flow rates used during the demonstration. In these tests, potable water was injected at a constant volumetric rate while the well pressure response was monitored and recorded using an in-well pressure transducer (Level Troll 500, In-Situ, Inc.). Injection continued until the pressure response to injection stabilized. Thereafter, the rate of injection was increased and the pressure within the well was again monitored and recorded until the pressure response stabilized. This procedure continued until stable pressure responses were collected at 5-6 flow rates (**Figure 5-2**).

Plotting injection flow rate (in ft<sup>3</sup>/day) as a function of the stabilized pressure response (i.e., pressure head in feet of water) provides an estimate of the aquifer transmissivity (ft<sup>2</sup>/day) as the slope of this function as shown in **Figure 5-3**. Calculated transmissivities were observed to be similar for both demonstration plots, suggesting a similar degree of permeability heterogeneity exists between these test plots. This result is significant for this demonstration in that the similar heterogeneity condition provides a good basis for comparing sweep-efficiencies between the control and test plots. The results of this hydraulic testing are presented in **Tables 5-4 and 5-5**, in which transmissivity and hydraulic conductivity are calculated at each flow rate condition.

The results of the step-injection tests provide calculated hydraulic conductivities that are within the range of values measured via slug-testing during the initial site characterization. However, these values were considered most appropriate for demonstration design purposes because they were measured under direct injection and provide a better integrated average conductivity across the injection well screen.

**Table 5-1. Schedule of Plot Testing and Sampling**

Time Since Treatment, t (weeks)	Activity	Location	Measurements
<b>Pre-Demonstration</b>			
t = -9	Soil core collection (sonic)	10 Control locations to 60 ft bgs 10 Test locations to 60 ft	See Table 5-2
t = -1	Injectability testing (stepped)	Test and control injection wells	Flow vs. time
t = -1	Well sampling	Injection and 2 MLS wells – control and test wells	See Table 5-2
<b>Delivery Performance</b>			
t = 0	Well sampling	Injection and 2 MLS wells – control and test wells	See Table 5-2
<b>Post-Demonstration</b>			
t = 1-2	Well Sampling	Injection and 2 MLS wells – control and test wells	See Table 5-2
t = 1-2	Soil core collection (DPT)	16 locations to 60 ft bgs	See Table 5-2

**Table 5-2. Total Number and Types of Samples to be Collected**

Component	Test Plot	Matrix	# Samples	Analytes	Location
Pre-Demonstration Sampling	Control	Groundwater	9	TCL, VOCs, pH, ORP, total solids, suspended solids, major cations/anions, TOC	1 injection well, 2 MLS wells
		Soil	5	TCL, VOCs, NOD, TOC, pH, ORP, CEC, microbial density, diversity, activity, Mn speciation	Soil cores from 5 points to 60 ft bgs.
	Test	Groundwater	9	TCL, VOCs, pH, ORP, total solids, suspended solids, major cations/anions, TOC	1 injection well, 2 MLS wells
		Soil	5	TCL, VOCs, NOD, TOC, pH, ORP, CEC, microbial density, diversity, activity, Mn speciation	Soil cores from 5 points to 60 ft bgs.
Delivery Performance Sampling	Control	Groundwater	8	TCL, VOCs, pH, ORP, total solids, suspended solids, major cations/anions, TOC	2 MLS wells
	Test	Groundwater	8	TCL, VOCs, pH, ORP, total solids, suspended solids, major cations/anions, TOC	2 MLS wells
Post-Demonstration Sampling	Control	Groundwater	9	TCL, VOCs, pH, ORP, total solids, suspended solids, major cations/anions, TOC	1 injection well, 2 MLS wells
		Soil	5	TCL, VOCs, NOD, TOC, pH, ORP, CEC, microbial density, diversity, activity, Mn speciation	Soil cores from 5 points to 60 ft bgs.
	Test	Groundwater	9	TCL, VOCs, pH, ORP, total solids, suspended solids, major cations/anions, TOC	1 injection well, 2 MLS wells
		Soil	5	TCL, VOCs, NOD, TOC, pH, ORP, CEC, microbial density, diversity, activity, Mn speciation	Soil cores from 5 points to 60 ft bgs.

Notes: Field measurements of dissolved oxygen, pH, ORP, specific conductivity, temperature, and turbidity will be collected using a portable multi-parameter meter and flow-through cell.

**Table 5-3. Analytical Methods for Sample Analysis**

Matrix	Analyte	Method	Container	Preservative	Holding Time
Groundwater	MnO <sub>4</sub>	APHA 4500	Spec vial	None	Immediate
	TCL VOCs	EPA 8260B and 5030	(3) 40-ml Vial	HCl pH< 2; Cool to 4°C	7 Days
	pH, ORP	APHA 4500, 2580	(1) 250-ml poly	Cool to 4°C	3 Days
	Total Solids Suspended Solids	APHA 2540		Cool to 4°C	ASAP (7 days max)
	Major Cations/Metals	APHA 3125		Cool to 4°C	30 Days
	Major Anions	APHA 4110		Cool to 4°C	2 Days
	Total Organic Carbon	APHA 5310B		Cool to 4°C	15 Days
	Field Parameters, including: MnO <sub>2</sub> MnO <sub>4</sub> Chloride Xanthan gum viscosity ORP/temperature/pH/specific conductivity/turbidity	Field spectrometer at 418 nm Field spectrometer at 525 nm Chloride-specific probe Viscometer Multi-parameter meter with flow-through cell	--	--	--
Soil	TCL VOCs	EPA 8260B and 5035	(3) Encore Samplers	Cool to 4°C	48 hours
	NOD	Siegrist et al., 2009	(3) 4-oz jar, minimum	Cool to 4°C	30 Days
	TOC, Grain Size, Bulk Density, Porosity	EPA 9060		Cool to 4°C	30 Days
	pH, ORP	EPA 9045D		Cool to 4°C	3 Days
	Cation Exchange Capacity	Sparks et al., 1996		Cool to 4°C	10 Days
	Microbial Density, Diversity, Activity	Kieft and Phelps (1997); Phelps et al. (1994a,1994b) Weaver et al. (1994)		Cool to 4°C	3 Days
	Mn Speciation	Chao, 1972		Cool to 4°C	30 Days

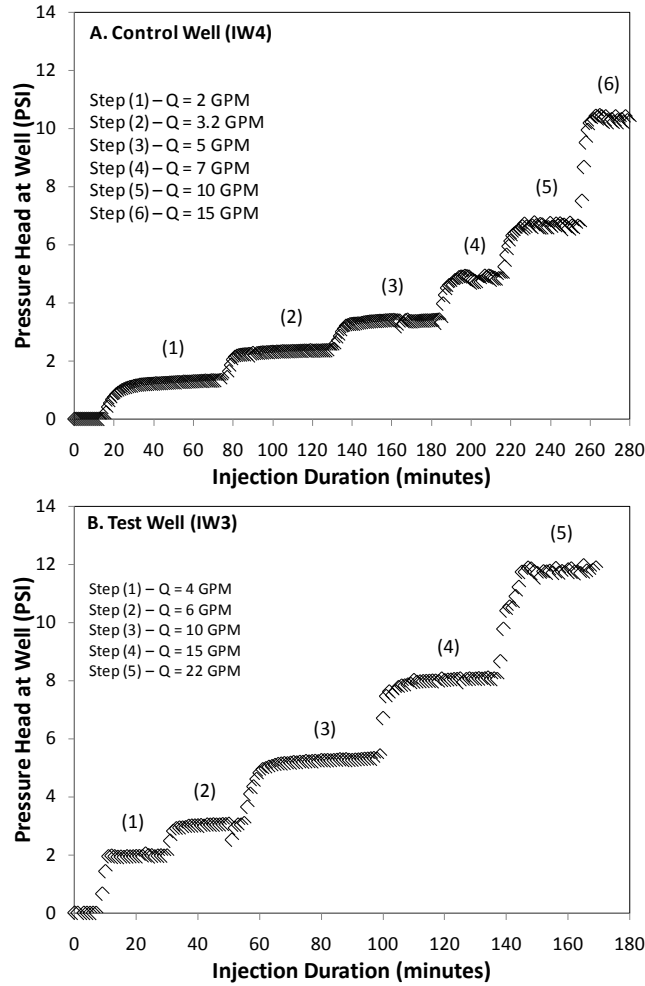


**Figure 5-2.** Pressure response to injection flow rates determined during the step-injection testing for the (A) control plot and the (B) test plot.

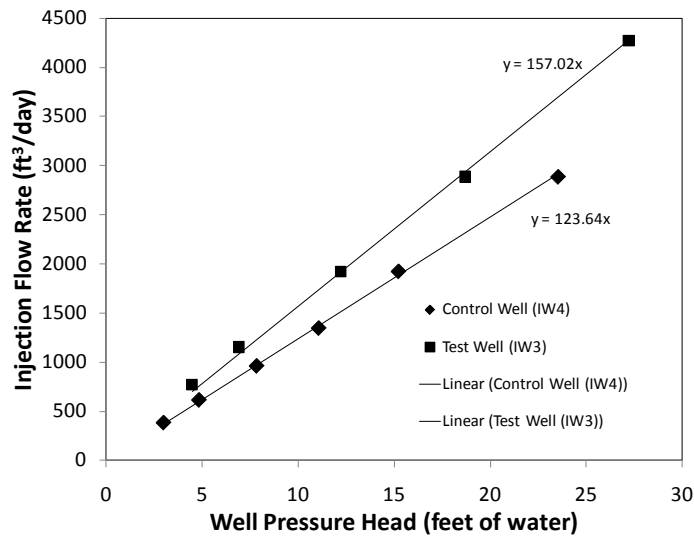


**Figure 5-3.** Wellbore pressure response to increasing flow rate within the test and control plots.



**Table 5-4. Results of the Step-Injection Hydraulic Testing (Test Plot, IW3)**

Q (GPM)	P (PSI)	P (ft)	T (ft <sup>2</sup> /day)	K (ft/day)	K (cm/sec)
0	0				
4	1.94	4.47	172.10	6.88	2.43E-03
6	3	6.92	166.94	6.68	2.36E-03
10	5.3	12.22	157.49	6.30	2.22E-03
15	8.1	18.68	154.57	6.18	2.18E-03
22.2	11.8	27.22	157.03	6.28	2.22E-03

Note: P(ft) is the pressure head in feet of water. K determined using 25 ft as the saturated thickness (b), as  $K = T/b$ .

**Table 5-5. Results of the Step-Injection Hydraulic Testing (Control Plot, IW4)**

Q (GPM)	P (PSI)	P (ft)	T (ft <sup>2</sup> /day)	K (ft/day)	K (cm/sec)
2	1.3	3.00	128.41	5.14	1.81E-03
3.2	2.1	4.84	127.19	5.09	1.79E-03
5	3.4	7.84	122.75	4.91	1.73E-03
7	4.8	11.07	121.72	4.87	1.72E-03
10	6.6	15.22	126.47	5.06	1.78E-03
15	10.2	23.53	122.75	4.91	1.73E-03

Note: P(ft) is the pressure head in feet of water. K determined using 25 ft as the saturated thickness (b), as  $K = T/b$ .

### 5.3 TREATABILITY STUDY RESULTS

The objectives of the Treatability Study as it relates to the polymer-amended ISCO (PA-ISCO) demonstration using xanthan gum were to:

1. Determine an optimal solution formulation for demonstrating polymer-enhanced delivery and sweep-efficiency improvement at our selected test site.
2. Collect rheological and transport related data needed to support implementation design.
3. Test our proposed polymer/oxidant mixing strategy at the bench-scale prior to scaling up this strategy at the field scale.

#### 5.3.1 Solution Formulation

An optimal solution formulation is one that provides an optimal permanganate concentration to account for sediment and contaminant oxidant demand, a range of viscosities appropriate for improving sweep efficiencies and demonstrating heterogeneity control within the Castle Hayne

formation, and adequate rheological stability over a practicable injection time frame (i.e., 3-5 days). This effort began measuring polymer/oxidant solution viscosities as a function of applied shear rate for several polymer/oxidant solution mixtures as described in the ER-0912 Treatability Study Report. The goal here was to generate baseline viscosity/shear rate profiles and assess the effect of salinity (as permanganate) on solution viscosities. The results of these initial measurements indicated that, for a given xanthan gum concentration, initial solution viscosities were not greatly sensitive to permanganate concentration within a range of 500 – 5,000 mg/L permanganate.

The next step toward determining an optimal xanthan/permanganate solution was to measure the viscosity/shear rate function over time. Permanganate will eventually oxidize portions of the xanthan gum molecule, reducing solution viscosities over time. Our anticipated maximum polymer/oxidant injection period was less than 5 days. Therefore, viscosities were measured over a 6-day period. The results of this work indicated that the degree and rate of viscosity loss increased with increasing xanthan gum concentration and with increasing permanganate concentration. The most rheologically stable combination of xanthan gum and permanganate were those for 500 mg/L permanganate, regardless of the xanthan concentration. However, a 500 mg/L permanganate concentration was determined to be too low for the oxidant demand of the Castle Hayne sediments (i.e., sediment oxidant demand averaged 0.8 g/kg). The use of the CDISCO design tool (developed under ESTCP Project ER-0623, In Situ Chemical Oxidation for Groundwater Remediation: Technology Practices Manual) suggested that a 5,000 mg/L permanganate concentration was optimal to meet at 15 foot radius objective within 5 days of operation in the field (scheduling and budget constraint).

Physical two-dimensional tank experiments and numerous numerical simulations performed during the conduct of SERDP Project ER-1486 have shown that the optimal range of fluid viscosities for improving sweep efficiencies is between 10 and 30 centipoise (cP). Increasing fluid viscosities above 30 cP results in a diminished return on additional sweep efficiency improvement. Further, increased viscosities can limit rates of fluid injection. Therefore, the goal of selecting an appropriate xanthan gum concentration resulted in selecting a concentration that provided this range of viscosities in a 5,000 mg/L permanganate solution. In this work we found that a polymer concentration between 1,000 mg/L and 500 mg/L would meet our viscosity goals. The final optimal xanthan gum concentration was determined with the implementation design calculations described below.

One-dimensional column tests were also performed to characterize the potential for permeability reduction as a result of polymer entrapment and/or manganese dioxide plugging. Permeability reductions will be accounted for when selecting injection flow rates. Details of these procedures were presented in the ER-0912 Treatability Study Report. The test sediment used was collected from the 40-50 foot depth within the Castle Hayne aquifer. The initial conditions and results of these experiments are presented in **Table 5-6**. Injection flow rates in each case were fixed at 1 cm/min which provided shear rate conditions similar to that anticipated during field-scale injection operations.

**Table 5-6. Operating Conditions for Characterizing Permeability Reduction Using Xanthan**

Test Condition	Original Hydraulic Conductivity (ft/day)	Original Media Permeability (darcy)	Final Hydraulic Conductivity (ft/day)	Final Permeability (darcy)	Permeability Reduction Factor
Col-1 (Oxidant Only)	11.9	4.2	11.9	4.2	1
Col-2 (KMnO4/Xanthan)	10.8	3.81	0.43	3.2	1.2
Col-3 (KMnO4/Xanthan)	11.2	3.95	0.31	2.6	1.5
Col-4 (KMnO4/Xanthan/SHMP)	9.6	3.39	0.48	3.3	1.02

The first experiment (Col-1) was performed to assess the permeability reduction potential for the oxidant only. For this sediment the permeability was not reduced indicating that permeability reduction as a result of MnO<sub>2</sub> precipitation was not a factor. Experiments Col-2 and Col-3 were duplicate experiments for a 1,000 mg/L xanthan gum and 5,000 mg/L oxidant solution. For Col-2, the polymer/oxidant solution was injected for just 8 pore volumes and permeability was reduced by a factor of 1.2. For Col-3, the solution was injected for 20 pore volumes. The pressure drop across the test column in this case was found to slowly increase over the injection period, resulting in an end-point permeability reduction factor of 1.5. These permeability reduction factors are similar to those measured for a silica sand media of similar intrinsic permeability in the absence of oxidant. This suggests that the presence of permanganate and the presence of MnO<sub>2</sub> particles generated as a result of oxidation of the sediment organic matter, does not significantly affect xanthan transport. A fourth experiment was performed that included 5000 mg/L SHMP in addition to the polymer and oxidant. In this case the sediment permeability was found to be reduced by only a factor of 1.02 over a 20 pore volume injection. It would appear that the same electrostatic repulsion characteristics useful in managing the precipitation and aggregation of MnO<sub>2</sub> particles have a similar effect on mitigating xanthan gum surface adsorption and aggregation processes that encourage xanthan entrapment and permeability reduction. Based on these results SHMP will be included in the polymer/oxidant solution during field-scale implementation at a concentration of 5,000 mg/L.

Treatability tests were performed to evaluate the ability of SHMP to control MnO<sub>2</sub> generated as a result of permanganate oxidation of PCE, and are also summarized in the ER-0912 Treatability Study Report. Initial batch scale tests were conducted to determine the optimum permanganate to SHMP mixture to employ. MnO<sub>2</sub> suspended in solution were measured for systems containing site soil and 5,000 mg/L permanganate. As mentioned previously, the design tool CDISCO was used to optimize design under site-specific conditions, and results suggested that a 5,000 mg/L permanganate concentration was optimal to meet at 15 foot radius objective within 5 days of operation in the field. Replicate systems that also contained SHMP concentrations of 500, 1,000, and 2,000 mg/L were prepared and MnO<sub>2</sub> suspended in solution was also measured in these systems. The batch results indicated that the higher concentration of SHMP maintained a higher concentration of MnO<sub>2</sub> suspended.

Next, two 1-D transport columns were packed with field porous media with near identical flow conditions, as verified using a tracer test. Site groundwater containing PCE at solubility (using field NAPL introduced to groundwater above saturation) was introduced to the columns for 3 pore volumes of throughput. Water was circulated through the columns until the influent and effluent PCE concentrations of both columns were within 5% of each other (in the low mg/L range).

To one column, 5,000 mg/L of permanganate only was delivered, while 5,000 mg/L permanganate + 2,000 mg/L SHMP were delivered to the other. Solutions were delivered until back pressure, presumably due to solids generation and loading, prevented additional flow. This occurred just prior to pore volume of throughput in the permanganate only column, where permanganate was observed to reach approximately ¼ of the way into the column. However, restricted flow occurred later in the SHMP + permanganate column, with approximately 2 pore volumes of fluid delivered where permanganate was observed nearly ½ way through the column. MnO<sub>2</sub> were measured in the effluent of these columns and a significantly greater concentration (>10x) were present in the effluent of the permanganate + SHMP compared to the permanganate only columns. Manganese was extracted from sections of the porous media after completion of the flow-through studies. The permanganate-only column had more than two times the mass of Mn as MnO<sub>2</sub> per kg of porous media compared to the permanganate + SHMP column. Because the column still experienced restricted flow and as an added safety factor, a concentration of 5,000 mg/L SHMP was selected for use in the field. Batch tests evaluate that the higher concentration does result in a higher concentration of MnO<sub>2</sub> suspended in solution.

### 5.3.2 Estimating Maximum Injection Pressures

The maximum allowable injection pressure for the upper Castle Hayne Formation was estimated using matrix failure calculations by first calculating the pressure required to initiate formation damage. Injection operations within both test plots would be operated below this maximum pressure condition. These calculations were used to guide field characterization and implementation design, as described below. A schematic representation of the upper Castle Haynes Formation used in support of these calculations is provided as **Figure 5-4**.

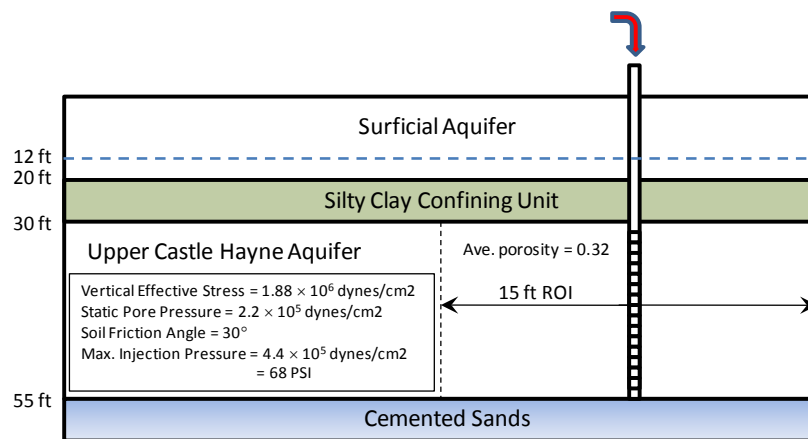


**Figure 5-4.** Schematic representation of the Upper Castle Hayne Aquifer used to calculate maximum injection pressures for the formation.

The total vertical stress (or total overburden pressure) was determined as the sum of the vertical stresses contributed by the weight of the media (i.e. the vertical effective stress,  $\sigma_{v,eff}$ ) and that of the water column (i.e., pore pressure,  $P_{pore}$ ) above the top of the injection well screen, or by:

$$\sigma_{v,tot} = \sigma_{v,eff} + P_{pore} = h_{tot}\rho_m g(1 - \phi) + h_{sat}\rho_w g\phi \quad [5.1]$$

where  $h_{tot}$  is the media thickness from ground surface to the top of the well screen,  $\rho_m$  and  $\rho_w$  are the mineral and water densities, respectively,  $g$  is the gravitational constant and  $\phi$  is the media porosity. By Equation 5.2, formation damage is then considered to initiate when  $P_{pore}$  meets or exceeds  $\sigma_{v,tot}$ , or when as the effective stress attains a zero or negative value.

However, the effective stress possesses both vertical and horizontal components. The vertical effective stress relates to the inter-granular stress imposed by the weight of the media (i.e. normal stress). The horizontal effective stress describes the strength of the media in terms of its internal resistance to shearing (Abramson et al., 2001; Payne et al., 2008). For normally-consolidated aquifer materials, the vertical effective stress is usually the dominant component (Hubbert and Willis, 1957; Payne et al., 2008), and therefore the horizontal effective stress ( $\sigma_{h,eff}$ ) becomes the limiting factor for the onset of formation damage and hydraulic fracturing.

By adopting Mohr-Coulomb failure theory, the limiting (i.e., maximum) injection pressure ( $P_{max}$ ) associated with the horizontal effective stress can be determined as:

$$P_{max} = \frac{\sigma_{h,eff}}{2} , \text{ where} \quad [5.2]$$

$$\sigma_{h,eff} = \sigma_{v,eff}(1 - \sin \theta) , \text{ and} \quad [5.3]$$

$$\sigma_{v,eff} = \sigma_{v,tot} - P_{pore} \quad [5.4]$$

In Equation 5.3,  $\theta$  is the soil friction angle, which was selected to be 30 degrees in these calculations, and is a reasonable value for the site sediments based on comparison of media properties presented by Payne et al. (2008). For the conditions identified in Figure 5-1, the maximum injection pressure for the upper Castle Hayne aquifer was determined to be 68 PSI (gauge pressure applied at the wellhead). A 40% factor of safety of was applied to account for potential well completion irregularities and errors associated with the selection of the soil friction angle. This reduces the maximum injection wellhead pressure to 50 PSI. Therefore, the injection system and all associated plumbing for this demonstration was designed to accommodate, at most, a 50 PSI backpressure at the wellhead.

### 5.3.3 Optimizing Injection Flow Rates and Polymer Concentration

To provide the best comparison of sweep-efficiency between the control plot and the test plot, the injection flow rate in both plots should be the same. Therefore, our objective here was to optimize the injection rate for the polymer-amended solution (i.e., test plot) first. In this analysis, the following form of the radial Darcy's Law equation was employed (confined condition):

$$Q_{inj} = 2\pi b \frac{k_{int}\rho g}{R_k\mu} \cdot \frac{(h_{well}-h_o)}{\ln\left(\frac{r_o}{r_{well}}\right)} \quad [5-5]$$

where  $b$  is the saturated thickness (25 feet),  $k_{int}$  is the intrinsic permeability,  $R_k$  is the permeability reduction factor,  $\mu$  is the viscosity of the injected fluid,  $r_{well}$  is the radius of the injection well,  $r_o$  is the radial distance at which the pressure effects of injection are negligible,  $h_{well}$  is the pressure head at the injection well,  $h_o$  is the pressure head at  $r_o$ , and  $\rho$  and  $g$  are the solution density and gravitational constant, respectively.

As discussed previously, solutions of xanthan gum are shear-thinning (i.e., the solution viscosity decreases with increasing shear rate). To account for this fluid behavior, PA-ISCO fluid viscosity was measured as a function of the applied rate of shear. The results of these measurements are presented in **Figure 5-5**.

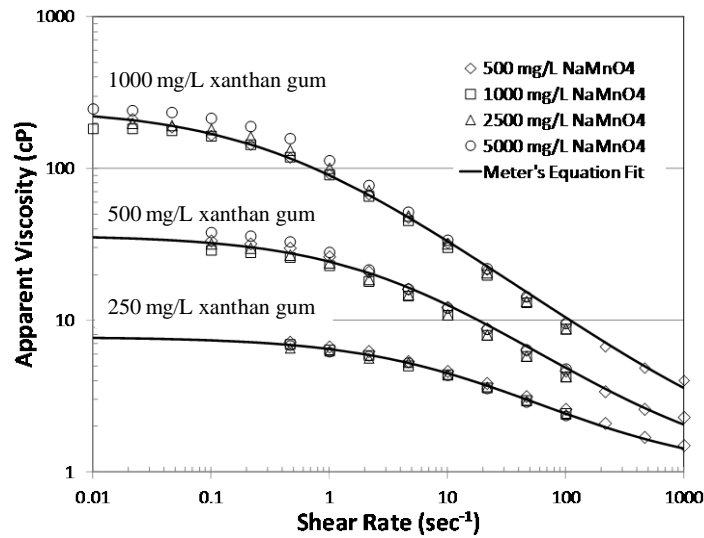


**Figure 5-5.** Characterizing shear-thinning character of polymer-amended solutions.

Solution viscosity ( $\mu_p$ ) was modeled as a function of shear rate ( $\gamma$ ) using Meter's equation (Meter and Bird, 1964):

$$\mu_p = \mu_w + \frac{\mu^0 - \mu_w}{1 + \left(\frac{\gamma}{\gamma_{1/2}}\right)^{P_a-1}} \quad [5-6]$$

where  $\mu^0$  is the polymer solution viscosity at zero shear rate (read from the Newtonian plateau region of lowest measurable shear rate change),  $\mu_w$  is the water viscosity (here assumed to be 1 cP),  $\gamma_{1/2}$  is the shear rate at which the polymer solution viscosity is half that of the zero shear rate viscosity, and  $P_a$  is an empirical coefficient which governs the abruptness of the change of viscosity with shear rate. The results of the Meter's Equation fits are presented in **Table 5-7**.

Equation 5-6, and the parameters presented in **Table 5-7**, were used as input into Equation 5-5 to evaluate injection pressures as a function of the rate of injection and polymer concentration for these shear-thinning fluids. A spreadsheet model was used to facilitate these calculations. Meter's equation parameters for alternate polymer concentrations were interpolated from the values presented in **Table 5-7**.

**Table 5-7. Results of Meter's Equation Fits to Measured Viscosity-Shear Rate Data**

Xanthan Gum Concentration (mg/L)	Zero Shear Rate Viscosity (cP)	$P_\alpha$	$\gamma_{1/2}$ (sec <sup>-1</sup> )
1000	248	1.6	0.37
500	36	1.6	3
250	7.7	1.6	11

The results of these calculations are presented in **Figure 5-6**. Note the non-linear pressure response to injection flow that results from the shear-thinning nature of the polymer solutions used. By this analysis a 1000 mg/L xanthan gum solution (containing 5000 mg/L NaMnO<sub>4</sub>) could be injected into the upper Castle Haynes formation at a maximum rate of 6 gallons per minute before meeting the maximum formation pressure estimated in Section 5.2.3. However, preparing a concentrate solution in the field with which meter in a 1000 mg/L solution into the process control system was determined to be impractical. Furthermore, a 1000 mg/L xanthan solution would provide a range of fluid viscosities that were in excess of the optimal range needed to demonstrate sweep-efficiency improvement at this site (i.e. between 10 and 30 cP). Utilizing equations 5-5, 5-6, and incorporating the following Carreau Equation which relates the porous media equivalent shear rate ( $\gamma_{eq}$ ) to the Darcy velocity ( $q$ ):

$$\gamma_{eq} = C \left( \frac{3n+1}{4n} \right)^{\frac{n}{n-1}} \cdot \frac{q}{\sqrt{k_{int}\phi}} \quad [5-7]$$

where  $n = P_\alpha - 1$ , it was determined that a 500 mg/L xanthan gum solution injected at a rate of 6 gallons per minute (GPM) provided the ideal range of fluid viscosities within the ROI of the test plot (as demonstrated in **Figure 5-7**). At 6 GPM, it was additionally determined that a 1 pore volume injection would require 5 days (the pore volume of each demonstration plot was estimated to be approximately 59,000 gallons or 8000 ft<sup>3</sup>), which was additionally optimal for our demonstration time frame. Therefore, the results of these calculations and those performed during our treatability study work indicated that the optimal solution formulation for this demonstration would contain a 500 mg/L xanthan gum concentration and 5,000 mg/L NaMnO<sub>4</sub>. SHMP would also be added to this solution at a concentration of 5,000 mg/L to stabilize MnO<sub>2</sub> particles formed during injection.

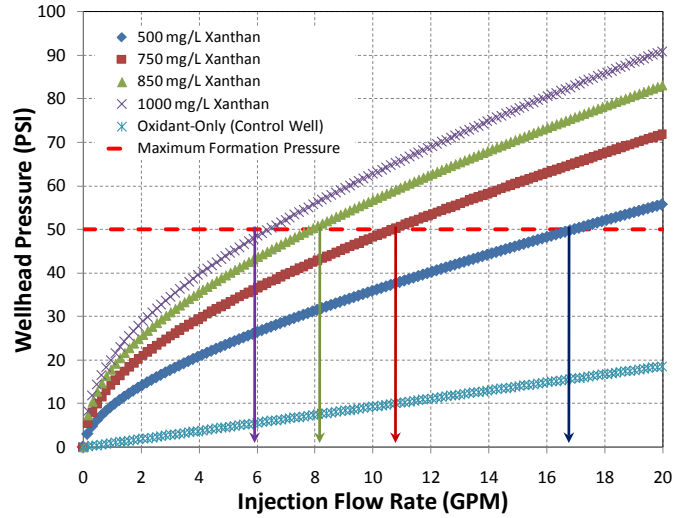


**Figure 5-6.** Wellhead pressure response calculated as a function of injection flow rate.

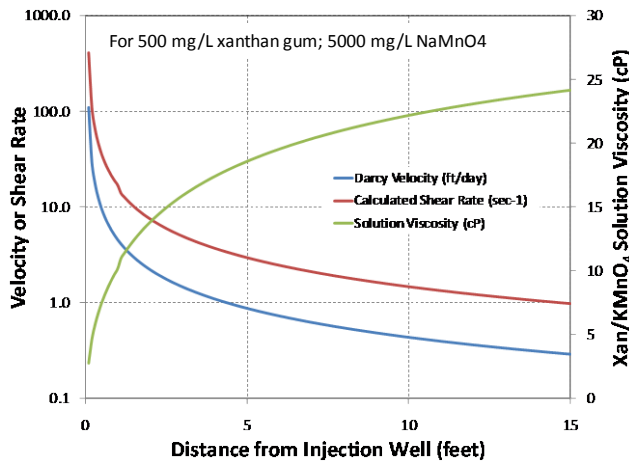


**Figure 5-7.** Calculated steady-state viscosity and shear rate profiles for the optimal PA-ISCO fluid.

#### 5.4 DESIGN AND LAYOUT OF TECHNOLOGY COMPONENTS

As described in Section 5.1, two side-by-side demonstration plots of approximately 30-feet in diameter were delineated and injection wells installed in the center of these plots to provide a 15-foot ROI (**Figure 5-8**). A process control and mixing system was then designed and constructed around these plots to enable the demonstration. Injection operations occurred sequentially, starting with the control plot (no polymer case) followed by the test plot. This section describes the components of the demonstration system.



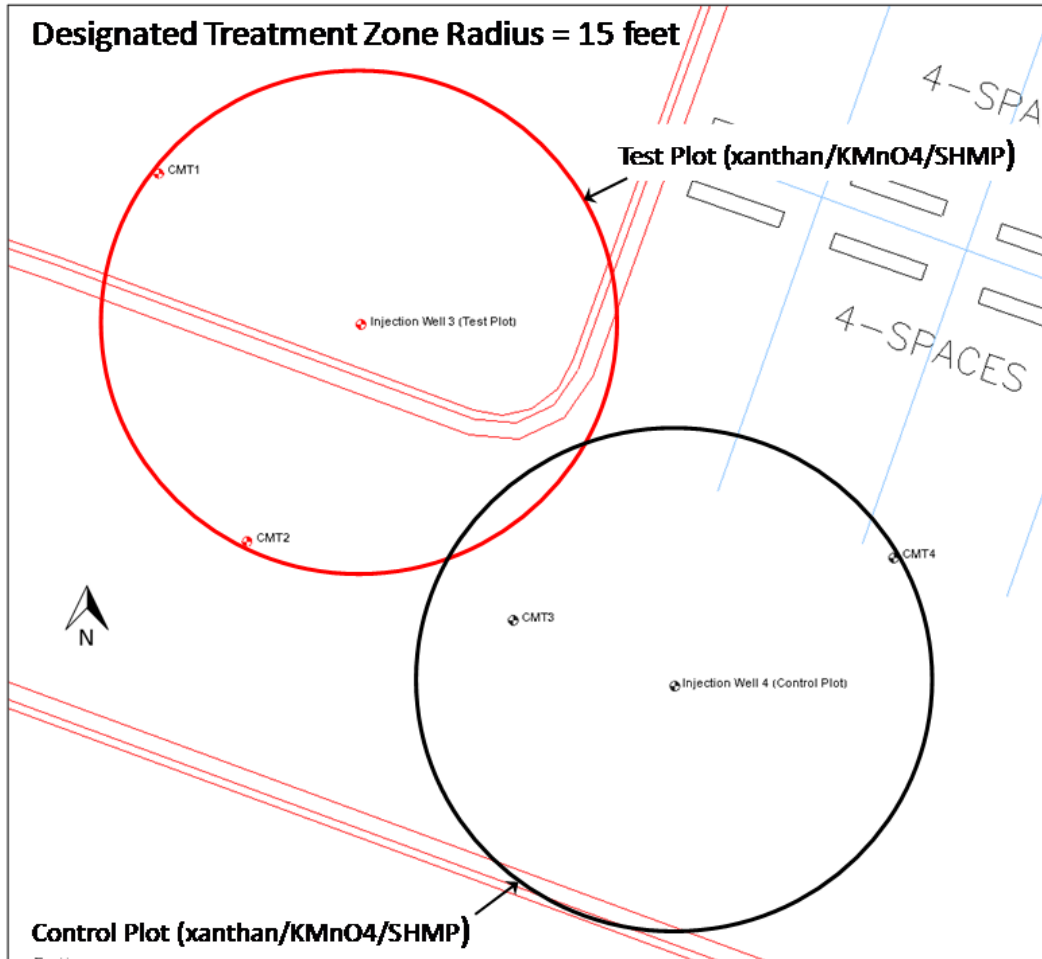


Figure 5-8. Layout of demonstration plots.

#### 5.4.1 Control Plot

The control plot consisted of one injection well located at the center of the plot and two multi-level sampling (MLS) wells installed around the perimeter of the plot at a distance of approximately 15 feet from the injection well. The injection well was screened from 35 to 55 feet bgs within the upper Castle Haynes formation. Both MLS wells were installed to sample the same depth interval of the injection well and included four sampling ports with this depth interval. Specific MLS well screens were installed to target individual stratigraphic units within this interval.

#### 5.4.2 SHMP and Xanthan Gum Test Plot

The test plot also included a single injection well located at the center of the plot (screened 35-55 ft bgs within the upper Castle Haynes formation) and two MLS wells. As was the case for the control plot, the two test plot MLS wells were installed at a distance 15 feet from the injection wells with four depth-discrete sampling ports. The depths and screen lengths of the MLS wells sampling ports were determined in the field based on site stratigraphy. Similar to the control plots, the MLS well screens targeted individual isolated stratigraphic units and/or zones with unique permeability.

### 5.4.3 Well Specifications

All wells were installed and developed using Roto-sonic drilling technology. During installation, soil was geologically logged from ground surface to the total depth of the well. Injection wells were constructed with 4-inch diameter stainless steel screens (20-slot) affixed to schedule 80 polyvinyl chloride (PVC) risers and completed below grade and within individual well vaults. A removable injection manifold was constructed on-site to facilitate plumbing connections and allow for wellhead pressure monitoring during injection operations (see **Figure 5-9**). Each MLS well was constructed from Solinst Continuous Multichannel Tubing (CMT) material (see **Figure 5-10**) and was fabricated in the field by manually cutting sampling ports at the desired depth and length after the borehole was logged and desired screen intervals are identified. Each sampling port was isolated from the port above by installing poured bentonite seals. After installation and prior to sampling, all wells were developed according to local and state requirements.

### 5.4.4 Design and Layout of Process Equipment

The schematic diagram of the process/flow system used to deliver  $\text{NaMnO}_4$ , xanthan gum, and SHMP to the demonstration plots is presented as **Figure 5-11**. The dosing equipment consisted of standard off-the-shelf construction materials (e.g., PVC piping, flexible hosing with cam lock fittings, and poly tanks), inline mixing and monitoring equipment, and basic controls for automated 24-hr operation and shutdown capability. All equipment was contained within individual secondary containment basins. The injection flow system designed to allow for an injection rate between 0.5 and 10 GPM under a 50 psig backpressure at the wellhead. The various chemical metering systems were designed to maintain a set dosing rate regardless of the rate of injection. Photographs of the various individual system, taken during the demonstration, are presented as **Figures 5-12 through 5-16**.

**Water source.** A fire hydrant, located approximately 250 feet away from the demonstration plots, was used as the water source for the process system and was equipped with a back-flow preventer and a pressure regulation system. The fire hydrant provided sufficient line pressure to drive the fluid process system while also providing a source of water to support xanthan/SHMP batch mixture preparation. Water was delivered from the fire hydrant to the process control/mixing system through flexible hose with Cam-Lok connections.

**Sodium Permanganate Dosing Unit.** Sodium permanganate was donated to the project by Carus Corp (RemOx® L ISCO Reagent) and was shipped to the site in six 263 gallon totes as a 40 % liquid concentrate solution. These totes were placed within a separate secondary containment upon arrival at the demonstration site. The sodium permanganate dosing system utilized a chemical metering pump to feed liquid permanganate into the main process line at a rate necessary to dilute the concentrate down to 5000 mg/L within the main process line. The system was capable of continuous and unattended over-night operation.

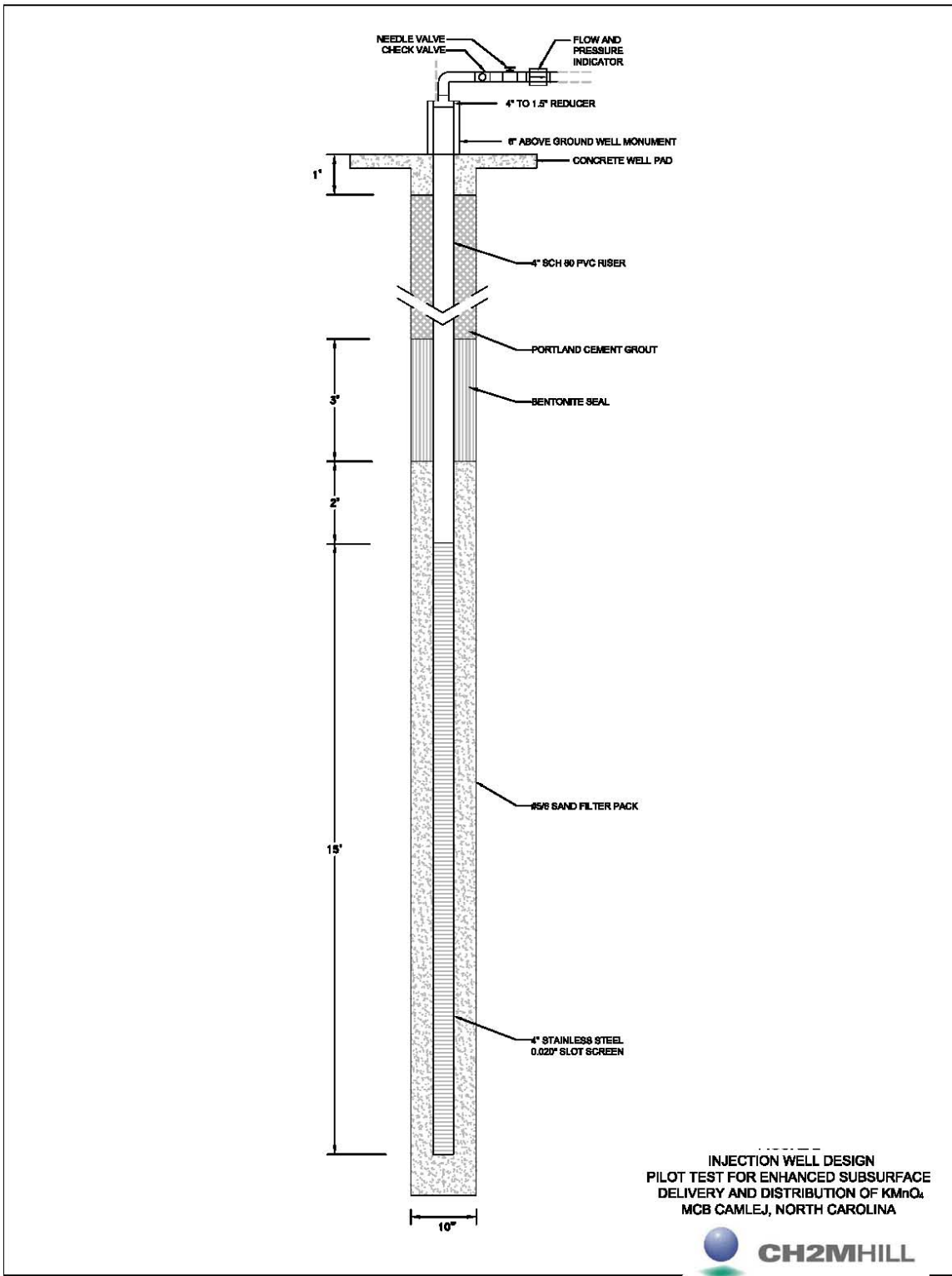


Figure 5-9. Injection well design.

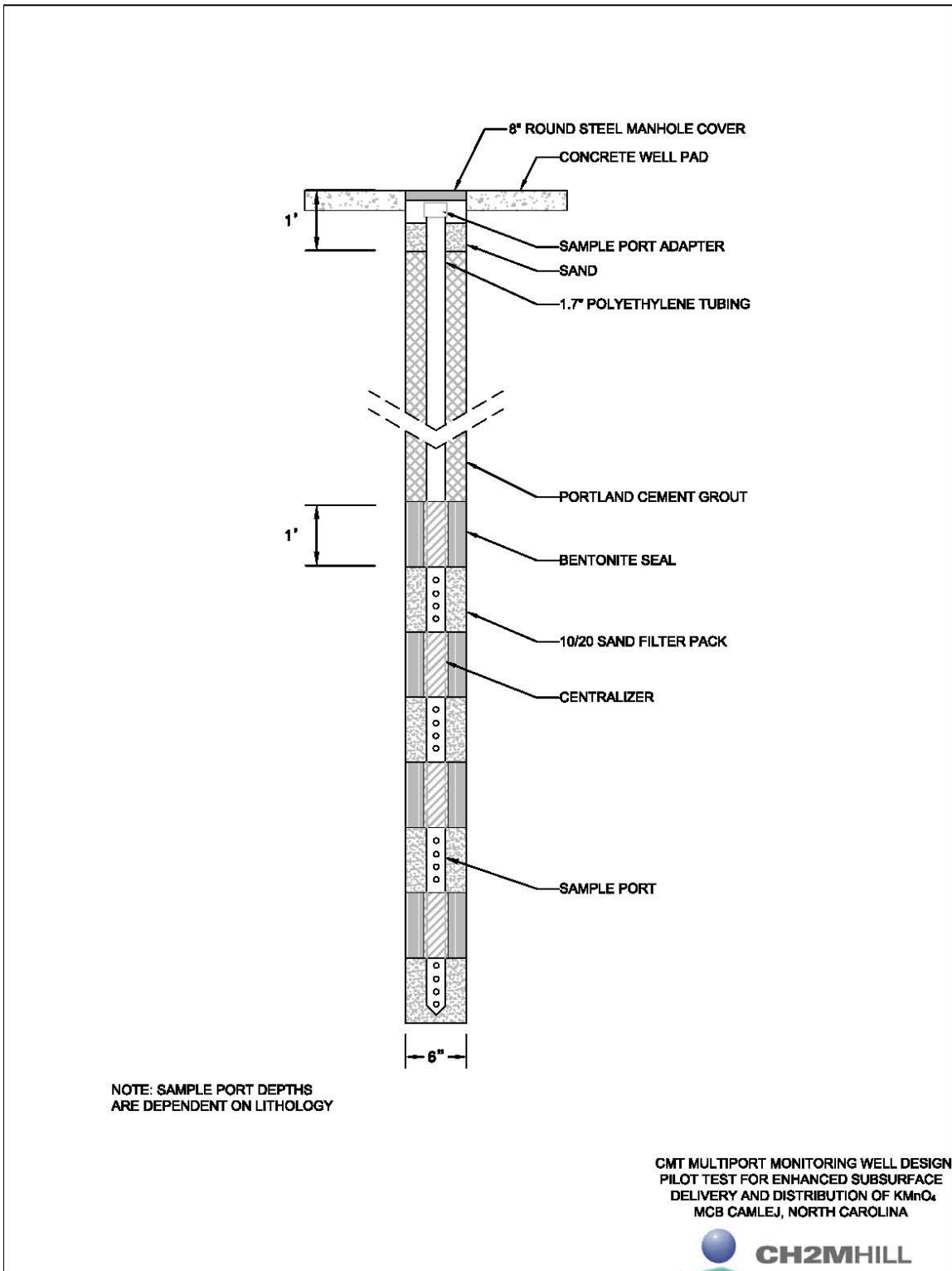
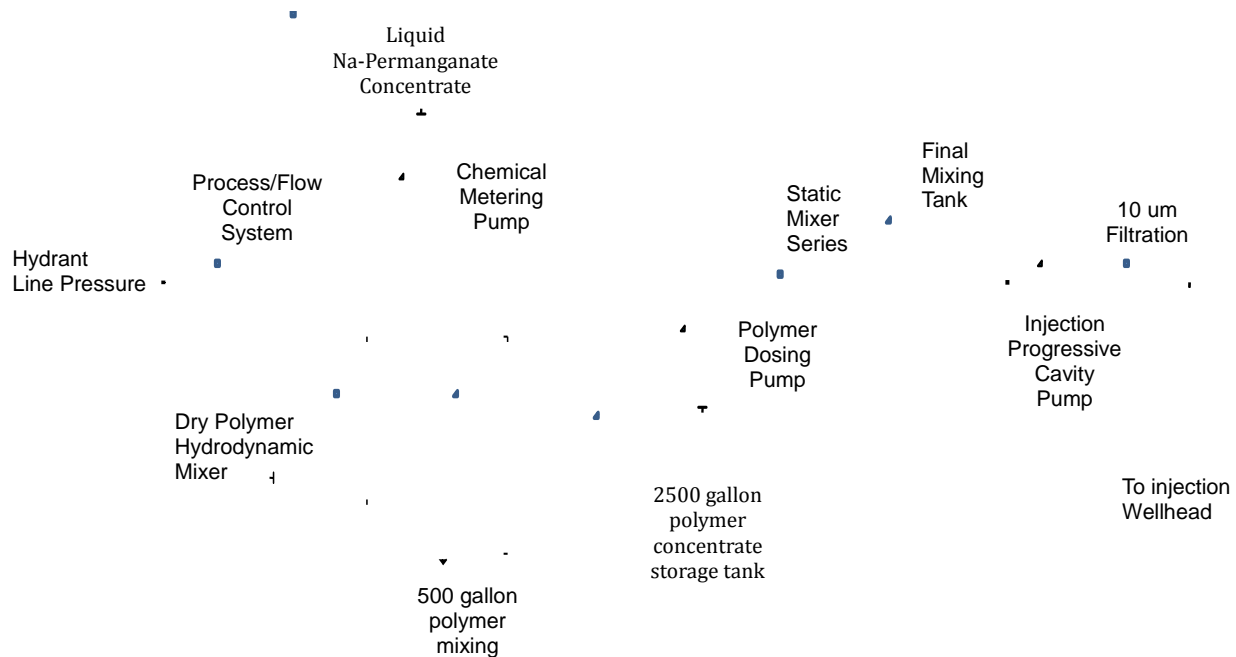


Figure 5-10. MLS monitoring well design.



**Figure 5-11.** Schematic of the PA-ISCO demonstration process equipment.



**Figure 5-12.** Photograph showing 40%  $\text{NaMnO}_4$  solution totes.





**Figure 5-13.** Xanthan gum/SHMP mixing system.



**Figure 5-14.** Automated process control system.





**Figure 5-15.** Fluid injection and filtering system.



**Figure 5-16.** Injection wellhead manifold and pressure monitoring.

***Xanthan/SHMP Mixing Unit.*** The xanthan/SHMP process equipment consisted of a hydrodynamic shear mixing unit, a 500 gallon batch preparation and mixing tank, a 2,600 gallon primary storage tank, and a transfer pump (to transfer fluids from the 500 gallon batch preparation tank to the primary storage tank). The polymer mixing unit consisted of a stainless steel hopper, educator, an internal shearing device, and a gear pump to drive fluids through the shear mixer. The hydrodynamic mixer was plumbed in a re-circulation loop, drawing fluids from the bottom of the mixing tank and introducing fluids at the top of the tank. Xanthan gum (Kelzan-T, CP Kelco, Houston, TX) and SHMP were delivered to the site in dry powder form within 50 lb bags. The xanthan powder and SHMP were manually applied to the hopper to prepare 500 gallon batches of fluid with a final concentration of 5,000 mg/L xanthan gum and 30,000 mg/L SHMP. Each batch was homogenized using the hydrodynamic mixer for 1 hour before transferring fluids to the storage tank. A high-capacity progressive cavity pump was used to dose the concentrated xanthan/SHMP solution into the main process line at a position 2-feet downstream of the permanganate dosing location. In-line hydrodynamic mixers were used to homogenize both chemical feeds before entering an additional 500 gallon poly-tank.

***Injection System.*** The 500 gallon tank positioned at the end on the process control system served as a “resting” tank to allow the polymer time to swell and homogenize in the presence of the sodium permanganate solution before being injected into the subsurface. An overhead mixer was installed in this tank to assist further homogenization. Fluid injection into the subsurface was accomplished via a second progressive cavity pump that withdrew fluids from the bottom of the “resting” tank. As a positive displacement pump, the cavity pump allowed injection at a constant rate regardless of the backpressure on the outlet end of the pump. A pressure transducer was installed to shut down the pump when the backpressure exceeded 50 psi as a safety precaution.

***Media Filtration.*** Prior to reaching the injection wells, all substrate and permanganate solution was directed through one of two parallel 10 micron stainless steel strainers to remove debris and help break up any large polymer aggregates that may have formed during the hydration/mixing process. This is a precautionary step included due to the lower permeability of the aquifer sediments. The system was designed so that when one strainer is exhausted, the solution is routed to the secondary strainer to maintain injection. The exhausted strainer could then be cleaned and re-installed into the filter housing. The strainers, however, were never exhausted during the demonstration and no cleaning/re-installation was necessary.

***Injection wells.*** An injection manifold (2 lines) was built to include instrumentation to monitor and control the injection flow rate. Instrumentation included a flow control valve, flow indicator transmitter/totalizer, pressure gauge, and sample port.

## **5.5 FIELD TESTING**

Field operations commenced on 20 October 2010 with the delivery of the process control and mixing systems, the NaMnO<sub>4</sub> concentrate, xanthan gum, and SHMP. Maple Leaf Environmental Equipment, Ltd (MLE) was contracted by CH2M HILL to construct the process/control systems as skid-mounted systems at their facility in Brockville, Ontario, Canada. MLE also provided all connection hoses and poly tanks used in this demonstration. The polymer mixing equipment and associated dosing pumps were purchased by the Colorado School of Mines (CSM) as a part of

their project budget. A portable diesel generator supplied power for the demonstration and overhead lighting was rented to allow operations at night.

### **5.5.1 Control Plot Operations**

Control plot operations began on 28 October 2010 following step-injection testing. The permanganate chemical metering pump was set to dose the 40% v/v sodium permanganate concentrate at a rate that provided a 5000 mg/L permanganate concentration leaving the process system. At startup and throughout the 5-day injection period, liquid samples were collected from a sampling port located on the injection wellhead manifold. Permanganate concentration was measured on-site using a portable UV/Vis (HACH DR/2010). Solution standards were prepared on site prior to injection operations to calibrate the UV/Vis spectrophotometer. Samples were collected from additional points along the process and injection system during the initial phases of injection to help fine tune the rate of dosing at the metering pump. The rate of injection was fixed at 6 GPM. Control plot injection was terminated on 02 November 2010, which constituted a 5-day (or 1 pore volume) injection duration.

Prior to startup and throughout the injection period, groundwater samples were collected at the two multi-level monitoring well locations positioned at the edge of the test plot using low-flow sample collection methods. Water quality parameters and permanganate concentrations at each of 4 depth intervals were monitored throughout the injection period.

### **5.5.2 TEST PLOT OPERATIONS**

Mechanical problems with the gear pump used to recirculate and prepare the xanthan gum/SHMP concentrate solution necessitated a delay of further field activities until the pump could be repaired. Field staff remobilized to the site on 05 December 2010 to initiate test plot operations.

Test plot operations began on 07 December 2010 with the preparation of the xanthan gum/SHMP concentrate solution. This concentrate was prepared within the 500 gallon polymer mixing tank and then transferred into the 1,500 gallon poly storage tank. The working volume of each batch prepared was 350 gallons. Water was added to the batch tank via a dedicated bypass line on the process control skid and a volumetric totalizer was used to measure the volume of water added. Xanthan gum and SHMP were introduced as dry powders to the stainless steel hopper that was mounted upon the hydrodynamic mixing unit. A total of 14.6 pounds of xanthan gum, and 87.5 pounds of SHMP powder were introduced per batch to provide a concentrated solution containing 5,000 mg/L xanthan gum and 30,000 mg/L SHMP. These powdered components were weighed on site using a top-loading scale. Once the dry xanthan and SHMP were added to the batch, the hydrodynamic mixer continued to re-circulate the concentrated solution within the batch tank for a period of 1.5 hours before the batch was transferred to the 1,500 gallon storage tank. A total of 3 concentrate batches were prepared prior to initiating injection operations to provide enough fluid for overnight injection. Additional 350 gallon batches were then prepared daily during the course of injection operations.

The polymer dosing pump (progressive cavity pump) was set for a 1/10 dilution of the polymer concentrate solution, providing a 500 mg/L xanthan gum and a 3,000 mg/L SHMP solution upon exiting the process flow system. As was the case for the control plot, the NaMnO<sub>4</sub> concentrate was metered down to deliver a 5,000 mg/L concentration upon exiting the process flow system. The rate of injection of the PA-ISCO fluid formulation was set at 6 GPM, in keeping with the rate used for the control plot.

Test plot injection was initiated on 08 December 2010. As was the case for the control plot, samples of injected fluid were collected from the injection wellhead manifold throughout the injection period and analyzed for permanganate concentration. In this case, the samples were also measured for solution viscosity using a portable viscometer (Brookfield LVDV-E). Viscosity standards were prepared on-site using various dilutions of the polymer concentrate solution. Test plot injection ended on 13 December 2012 for a 5-day (or 1 pore volume) injection.

## 5.6 SAMPLING METHODS

### 5.6.1 Soil and Groundwater Sampling

Post-treatment samples were collected as described in Section 5.2.1 Baseline Soil Sampling and 5.2.2 Baseline Groundwater Sampling, and shown in **Tables 5-1 to 5-3**. Samples were collected for each CMT well and from each port within the CMTs (depths are shown on **Figure 5-17**). Raw data are included in Appendix B.

Groundwater samples were collected from each plot during and immediately post-treatment. A total of 12 DPT sediment cores were collected per demonstration plot. These sediment cores were collected at 5-foot intervals between 20 and 60 feet below ground surface (bgs). This coring interval contained the lower portion of the silty clay upper confining unit, the upper Castle Hayne Formation, and the upper portion of the cemented sands that acted as a lower confining unit within the upper Castle Hayne.

As shown in **Figure 5-17**, these cores were collected along three transects centering on the injection well in both demonstration plots. This approach provided a means of investigating the lateral distribution of injected permanganate and served to allow a volumetric assessment of sweep-efficiencies between the two demonstration plots. DPT sediment coring began within 12 hours of injection cessation and continued for up to 3 days post-injection.

One year post-treatment, an additional round of groundwater samples was collected from each well depth. Also, three DPT cores were collected for each plot at a distance approximately 5, 10, and 15 feet from injection (shown as A, B, and C for the test plot and X, Y, and Z for the control plot in **Figure 5-17**).

In addition the physical and chemical parameters measured as per Tables 5-1 to 5-3, the sediment cores were additionally logged for sediment stratigraphy and the presence and absence of permanganate (i.e. purple color and/or MnO<sub>2</sub> staining). A photographic example of the sediment cores collected is presented in **Figure 5-18**.



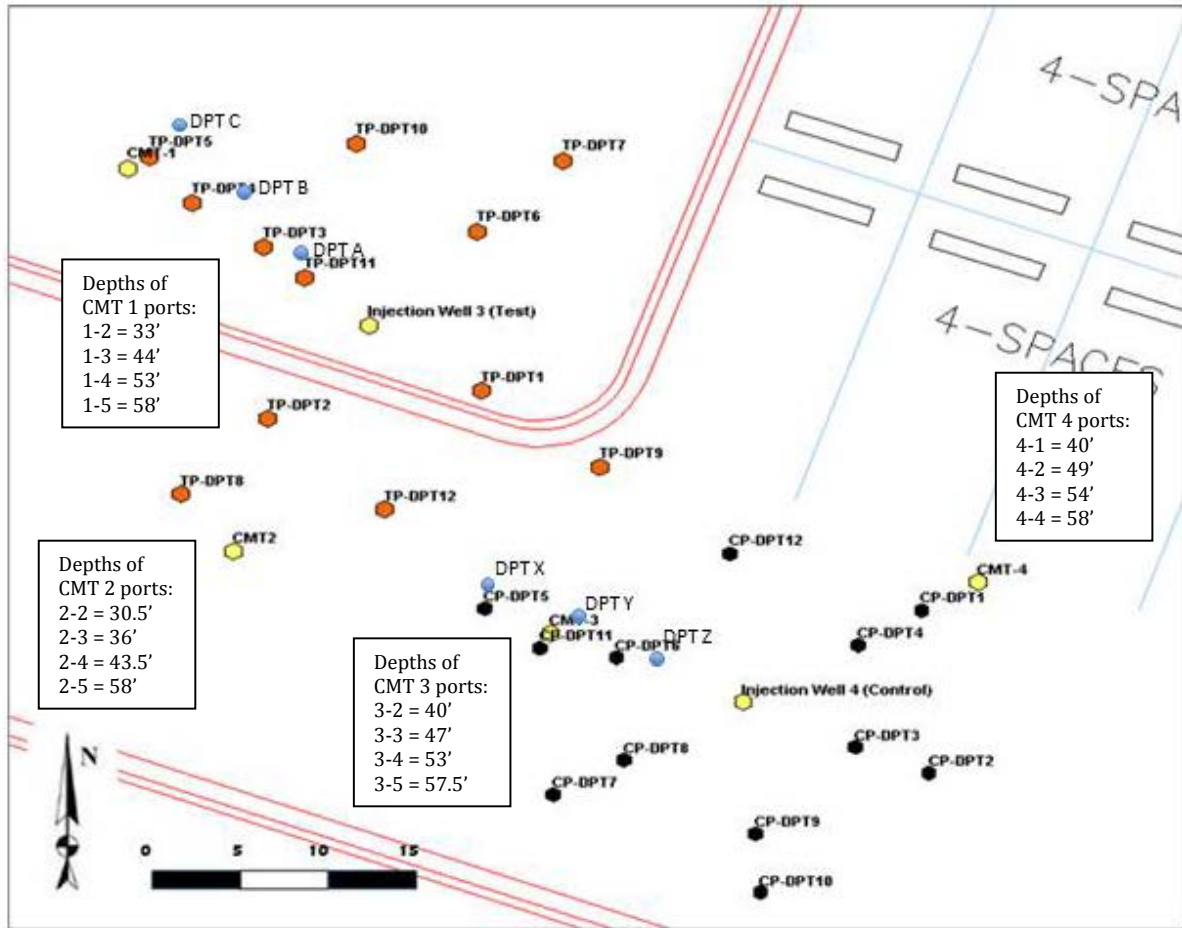


**Figure 5-17.** Location of DPT cores. CP-DPT indicates control plot cores. TP-DPT indicates test plot cores. DPT A, B, and C are one-year post-treatment cores collected for the test plot and DPT X, Y, and Z are one-year post-treatment cores collected for the control plot.



**Figure 5-18.** Sediment cores used to vertically characterize the presence/absence of permanganate within the control plot.

### 5.6.2. Quality Assurance

Field blanks and duplicate samples were collected and submitted for laboratory analysis. **Table 5-8** describes each quality assurance/quality control (QA/QC) sample and the required frequency of collection.

**Table 5-8. QA/QC Samples**

<b>Sample Type</b>	<b>Description</b>	<b>Frequency</b>	<b>Analytes</b>
Field Blank	Designed to detect contamination in the decontamination water. A field blank is decontamination water collected directly in the sample bottle. It is handled like a sample and transported to the laboratory for analysis.	One field blank from each source of decontamination water for each sampling event, where a sampling event is defined as one week	TCL VOCs, MnO <sub>4</sub>
Field Duplicate	Designed to check precision of data in the laboratory. A field duplicate is a sample collected in addition to the native sample at the same sampling location during the same sampling event.	10% of field samples	TCL VOCs, MnO <sub>4</sub>

### 5.6.3 Decontamination Procedures

Appropriate personnel, drilling and well equipment and materials, and sampling equipment and materials decontamination procedures were followed as described below.

**Personnel Decontamination:** Personnel decontamination is discussed in the Health and Safety Plan included in this project's Demonstration Plan.

**Drilling Equipment and Well Construction Materials:** Before mobilizing to the site, all drilling tools were cleaned with a high-pressure hot-water power washer or steam jenny, or hand washed with a brush using detergent to remove oil, grease, and hydraulic fluid from the exterior of the unit. Degreasers were not used. All drilling tools were decontaminated prior to installation of each monitoring well. Decontamination of all equipment, tools, and well materials consisted of hot-water pressure washing to remove all visible evidence of soil, encrustations, or films. Well materials, augers, drill rods, and split-spoon samplers were rinsed with de-ionized water after pressure washing and prior to use.

**Sampling Equipment:** Any stainless-steel sampling equipment was decontaminated prior to sampling and between all samples to prevent the introduction of contaminants into the sample. This generally included washing equipment with a laboratory detergent, then rinsing with tap water, de-ionized water, and isopropanol. Water sampling, water level measuring, and sample preparation equipment brought onsite was cleaned prior to and after each use. During cleaning and decontamination operations, the substitution of higher grade water for tap water was permitted and did not need be noted as a variation. Personnel decontaminated PPE in accordance with the Health and Safety Plan included in this project's Demonstration Plan.



## 5.7 SAMPLING RESULTS

Appendix B contains all raw data for all field samples collected, including groundwater and soil core results. A general discussion of results is presented below. Data were analyzed to determine if performance metrics were met and are discussed further in Section 6.0.

### 5.7.1 Permanganate Distribution and Sweep Efficiency

Sediment stratigraphy and permanganate presence/absence data collected during the DPT coring events were compiled and reconstructed in cross-sections for each investigation transect to better visualize the distribution of permanganate. A map showing the locations of these transect cross-sections is provided as **Figure 5-19**. The actual cross-sections are provided below as **Figures 5-20** through **5-25**.

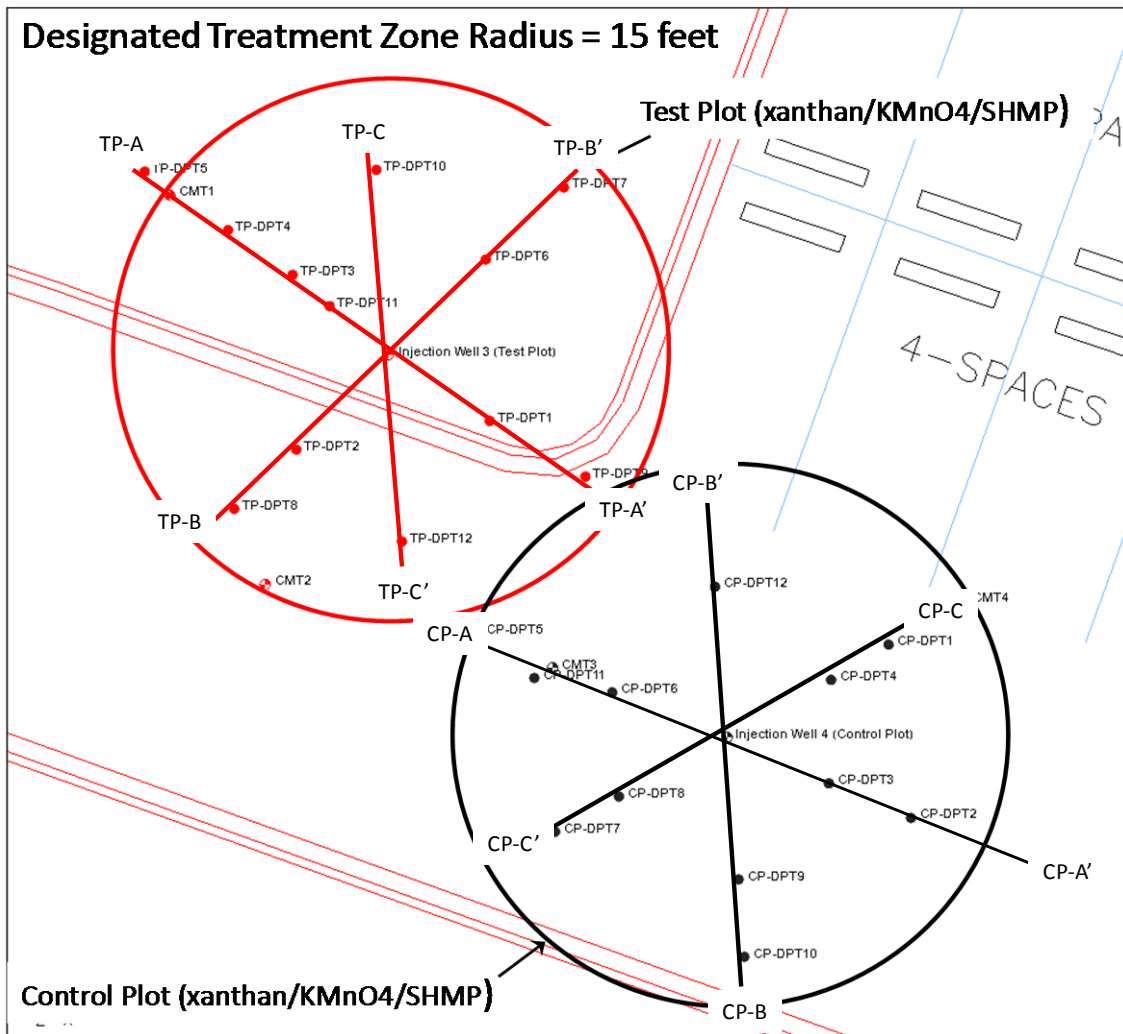


**Figure 5-19.** Location of DPT transects.

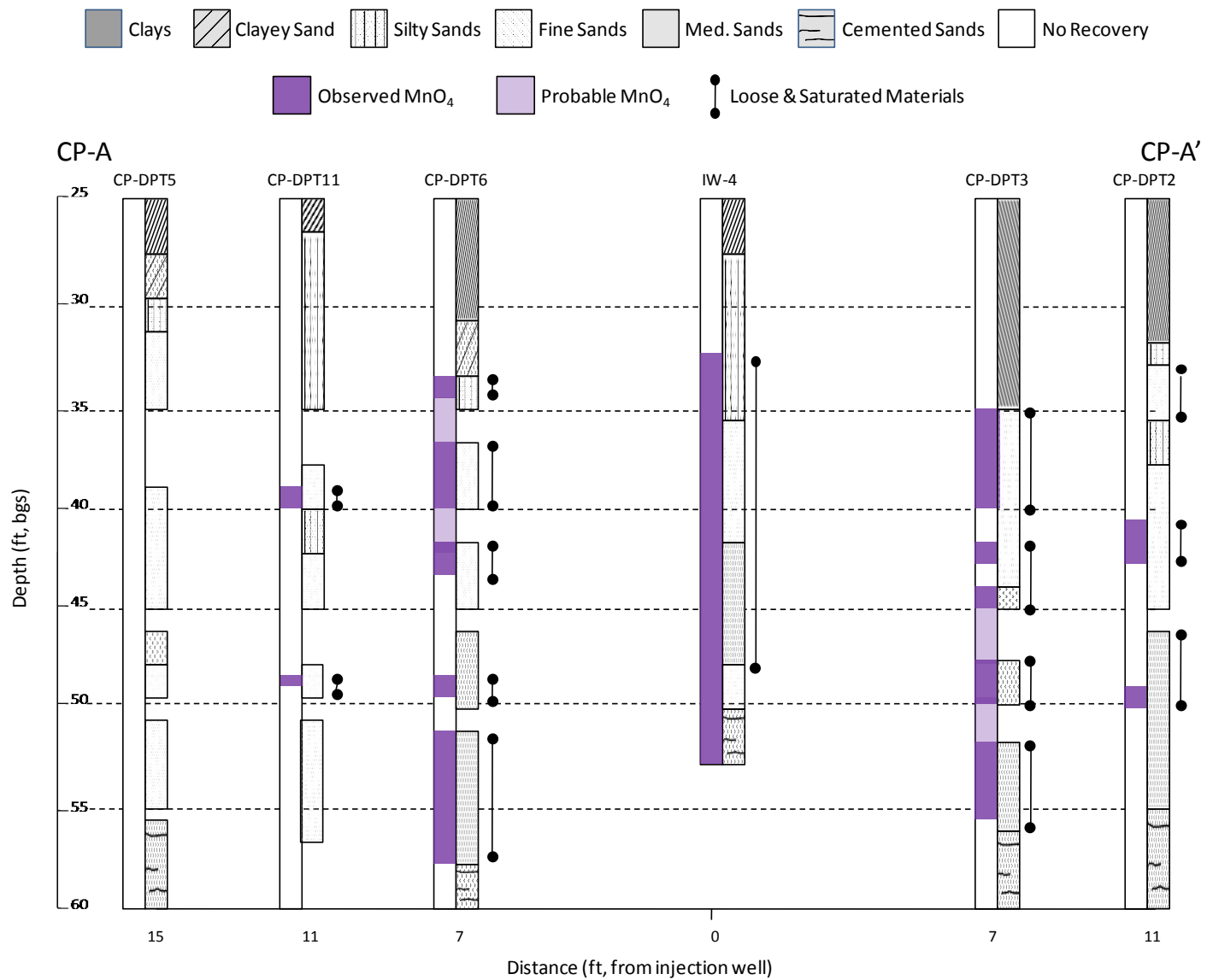


**Figure 5-20.** General stratigraphy and distribution of permanganate observed within the control plot (along Transect CP-A-CP-A').

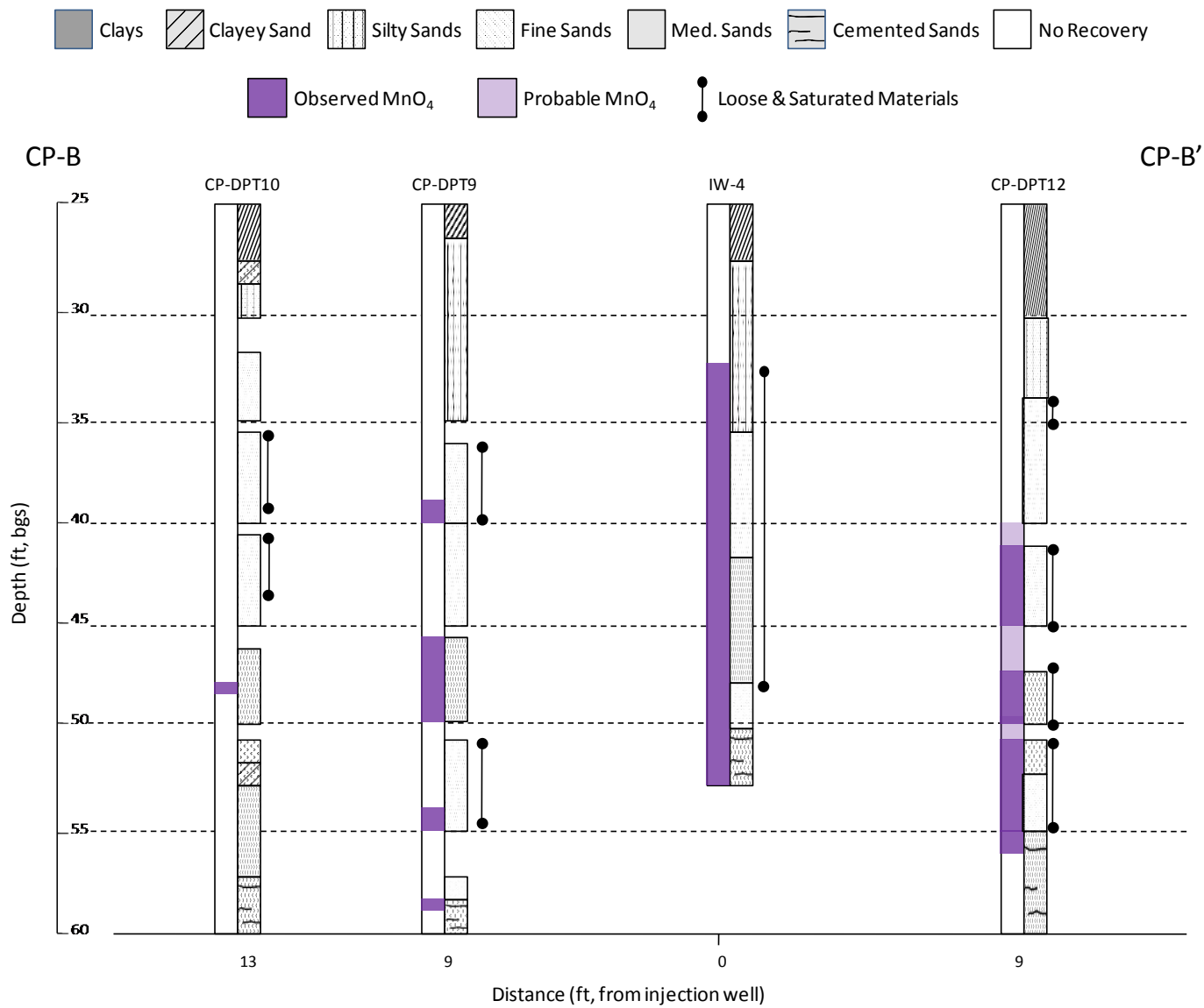


**Figure 5-21.** General stratigraphy and distribution of permanganate observed within the control plot (along Transect CP-B-CP-B').

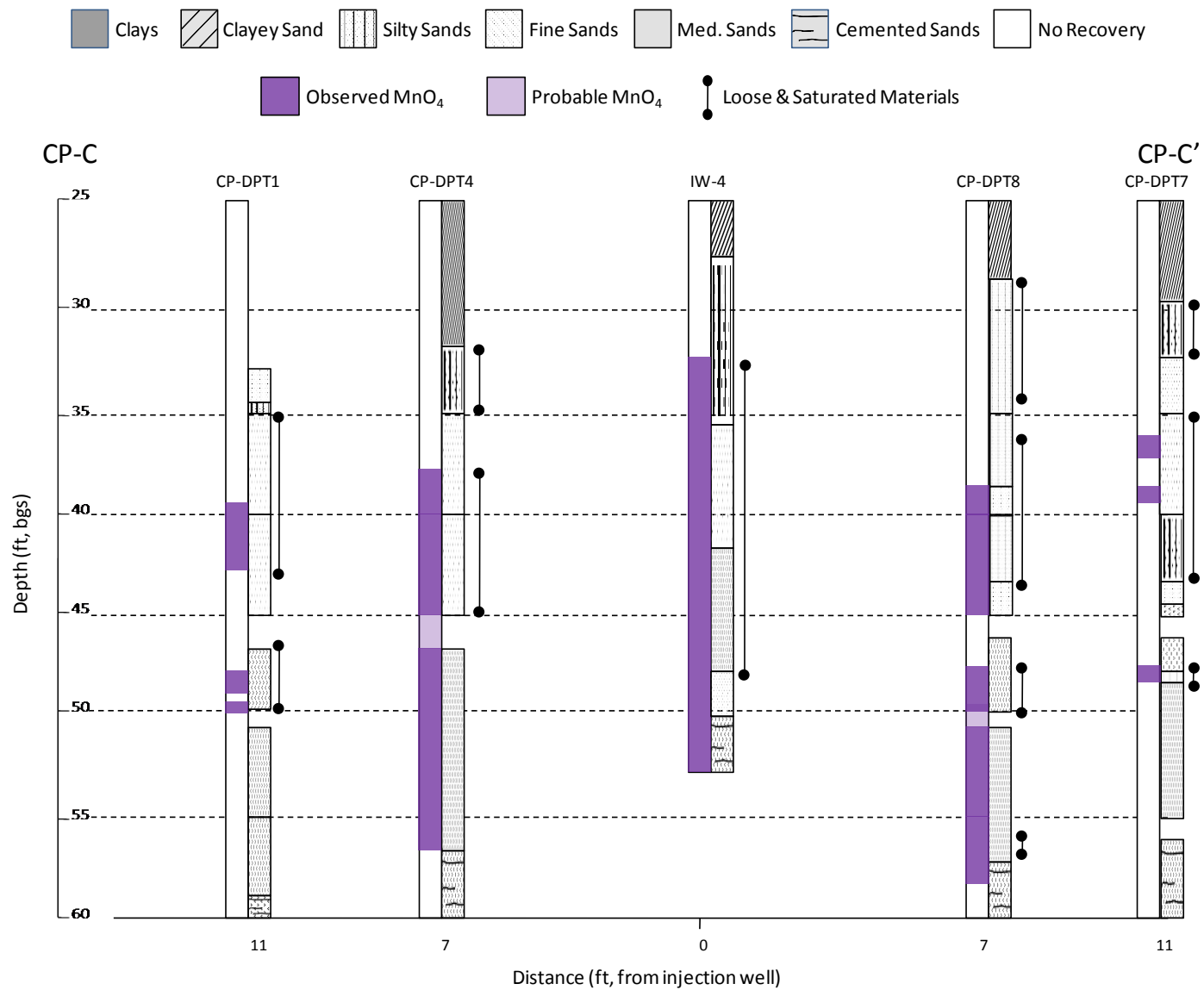


**Figure 5-22.** General stratigraphy and distribution of permanganate observed within the control plot (along Transect CP-C-CP-C').

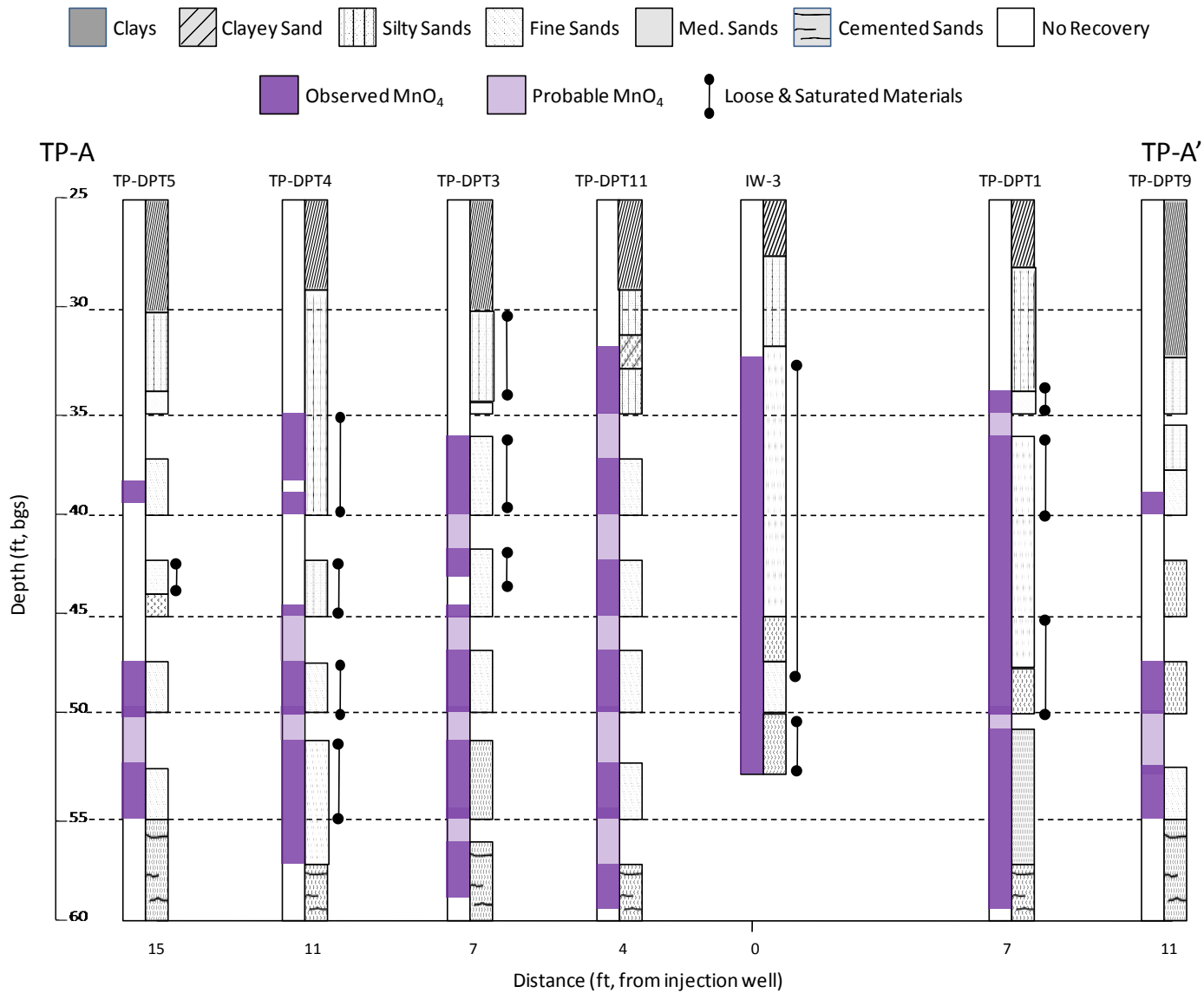


**Figure 5-23.** General stratigraphy and distribution of permanganate observed within the test plot (along Transect TP-A-TP-A').

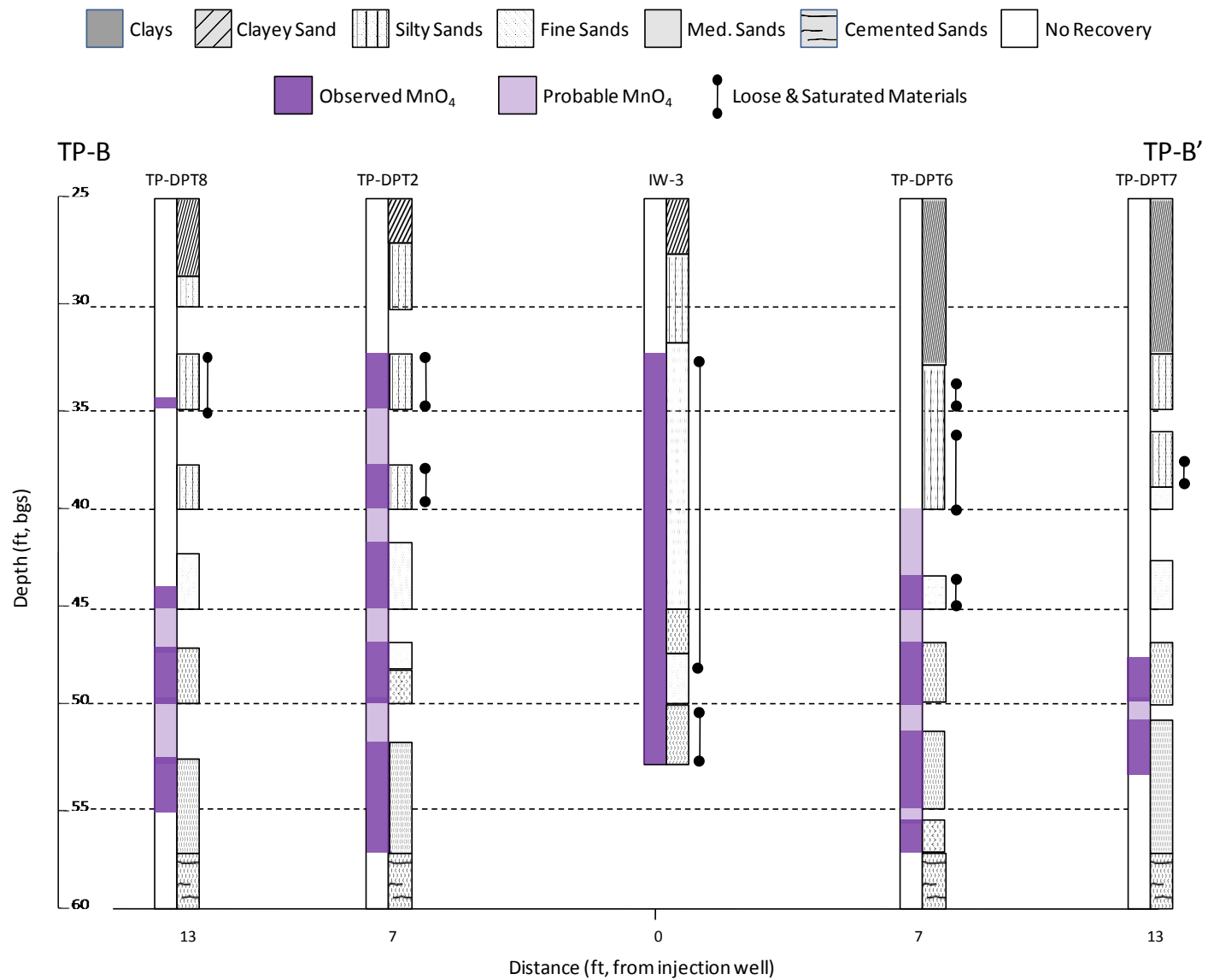


**Figure 5-24.** General stratigraphy and distribution of permanganate observed within the test plot (along Transect TP-B -TP-B').



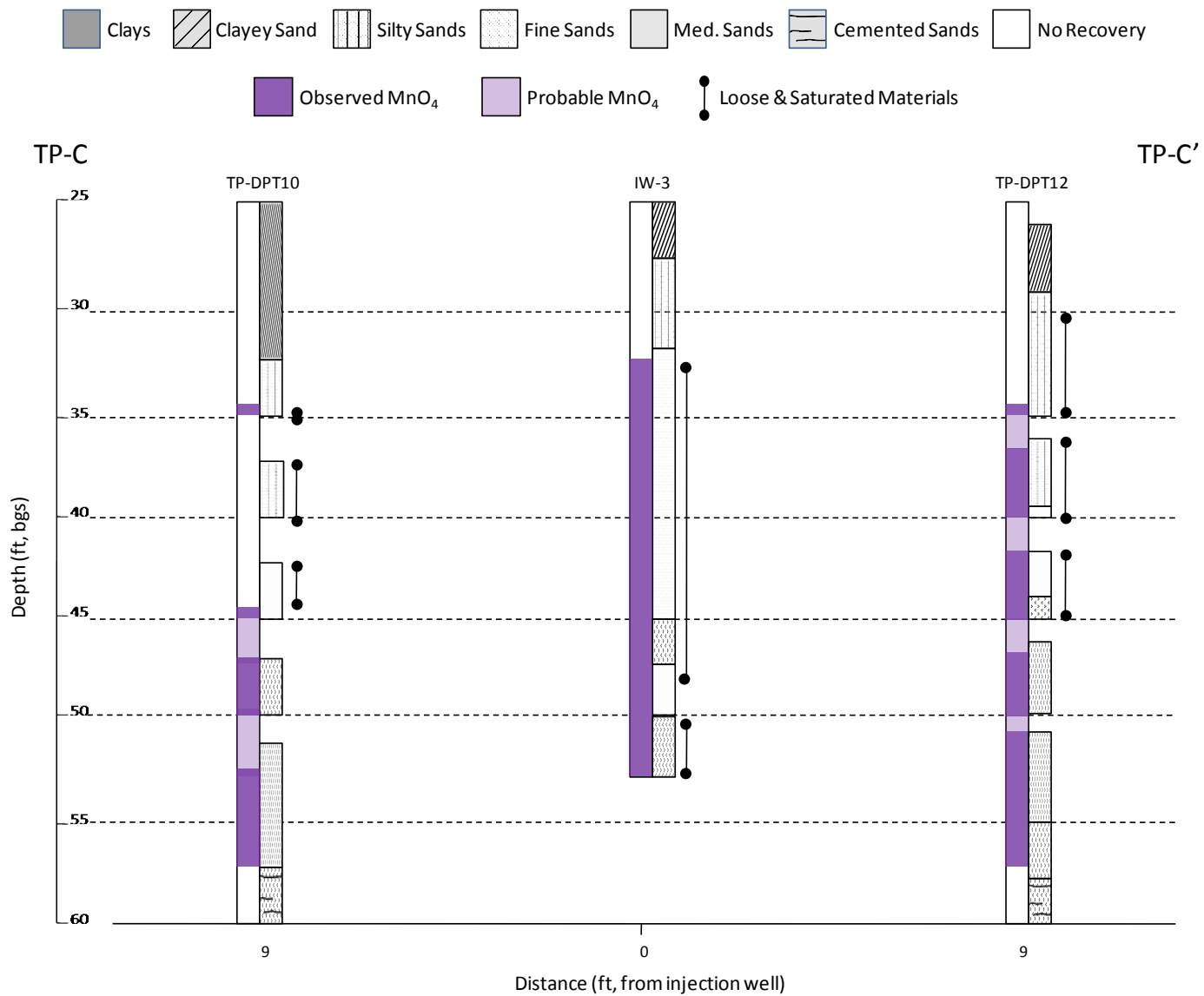


**Figure 5-25.** General stratigraphy and the distribution of permanganate observed within the test plot (along Transect TP-C-TP-C').

The permanganate presence/absence data, and the permanganate/MnO<sub>2</sub> concentration data, collected during each post-injection coring event were used to produce a three-dimensional (3D) dataset representing the 3D distribution of permanganate at the end of injection operations. This dataset was input into the Groundwater Modeling System (GMS, v. 8.1) software package (additional details pertaining to the kriging approach used are presented in **Figure 5-26**), the results of which are presented in **Figure 5-27**. DPT location coordinates were determined from distance measurements taken in the field during the coring event and utilizing triangulation calculations from the known locations of nearby monitoring wells. Ordinary kriging of the permanganate dataset was then used to provide a 3D volumetric representation of the distribution of permanganate within both demonstration plots. In both cases the experimental variogram was a general semivariogram utilizing 8 lags with a 2 foot separation distance.

GMS could not provide a cylindrical grid space. Therefore, a square (or cube) grid space (dimensions: X = 28 feet, y = 28 feet, z = -35 feet) was used to represent the control volume for each demonstration plot. Ordinary kriging of the permanganate data presented in **Figure 5-27**, using the modeling parameters shown in **Figure 5-26**, was used to populate the grid volume. The results of this kriging procedure are presented in **Figures 5-28 and 5-29** as isosurface projections.

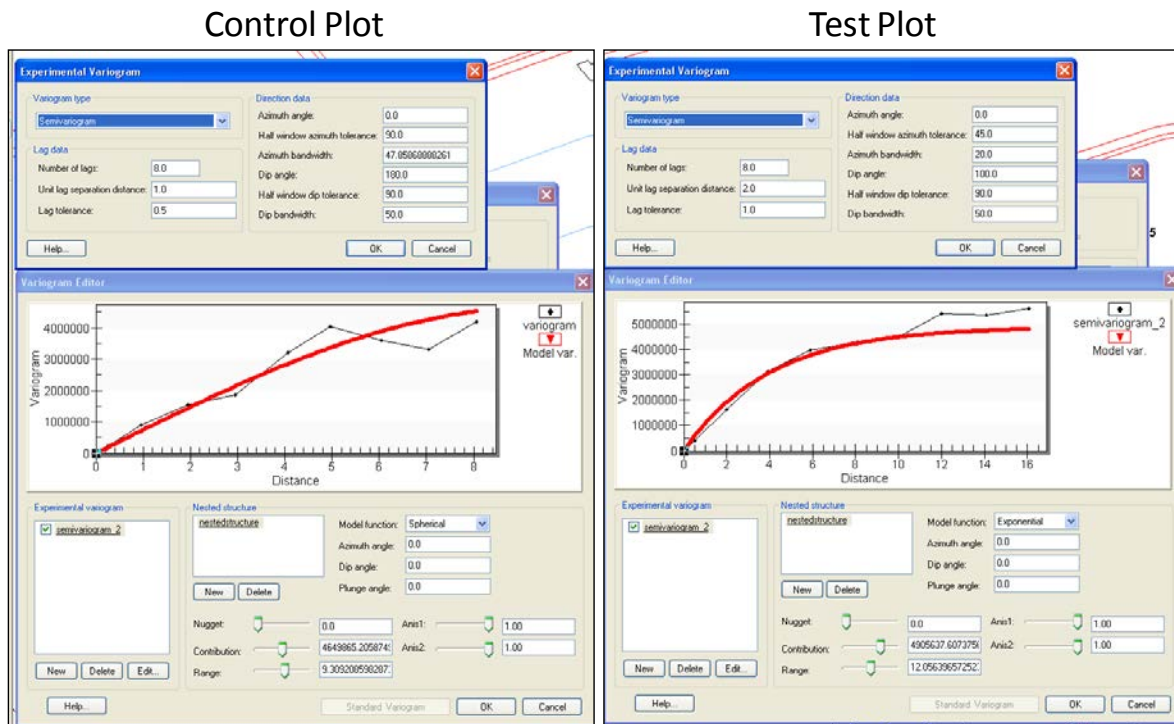


**Figure 5-26.** Semivariogram and model variogram fit parameters used in kriging of permanganate distributions.

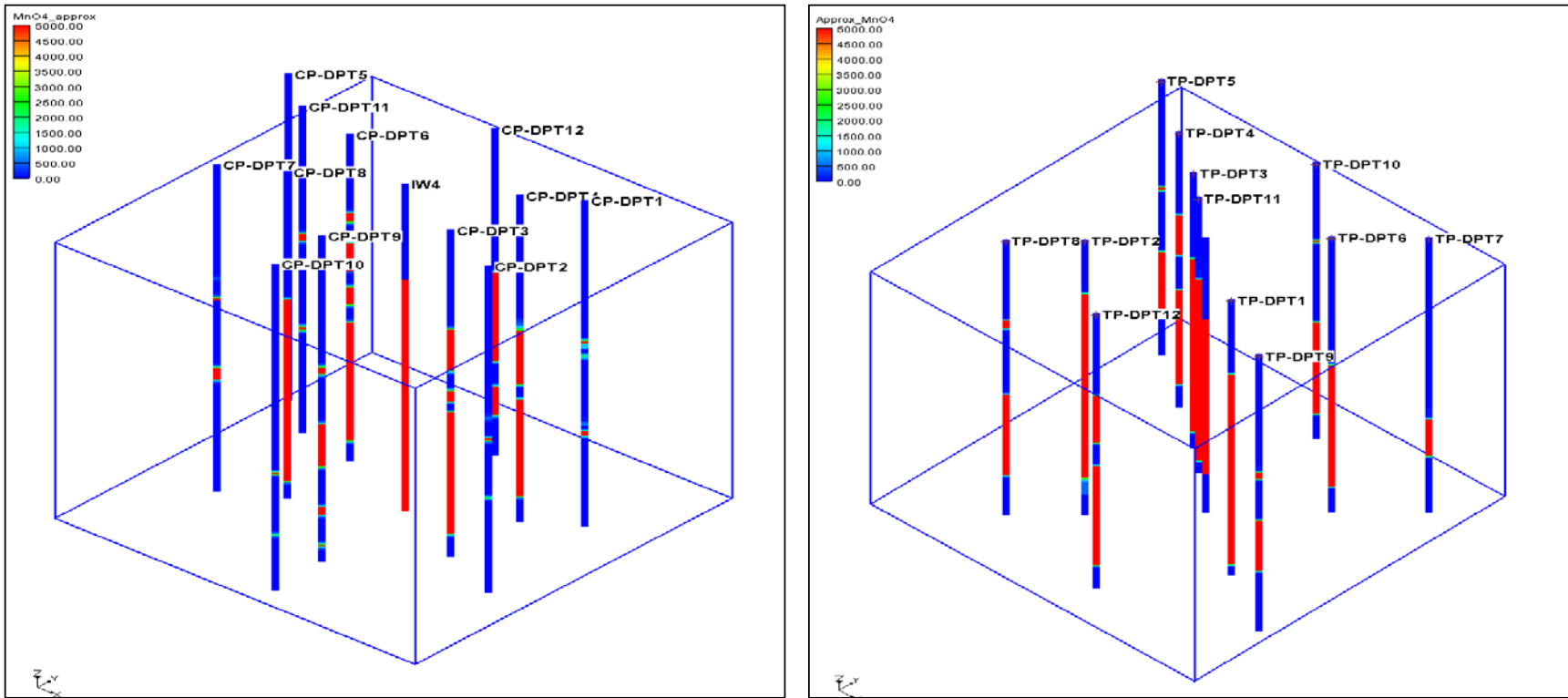


**Figure 5-27.** Presence/absence of permanganate as observed in the post-injection DPT boring locations.

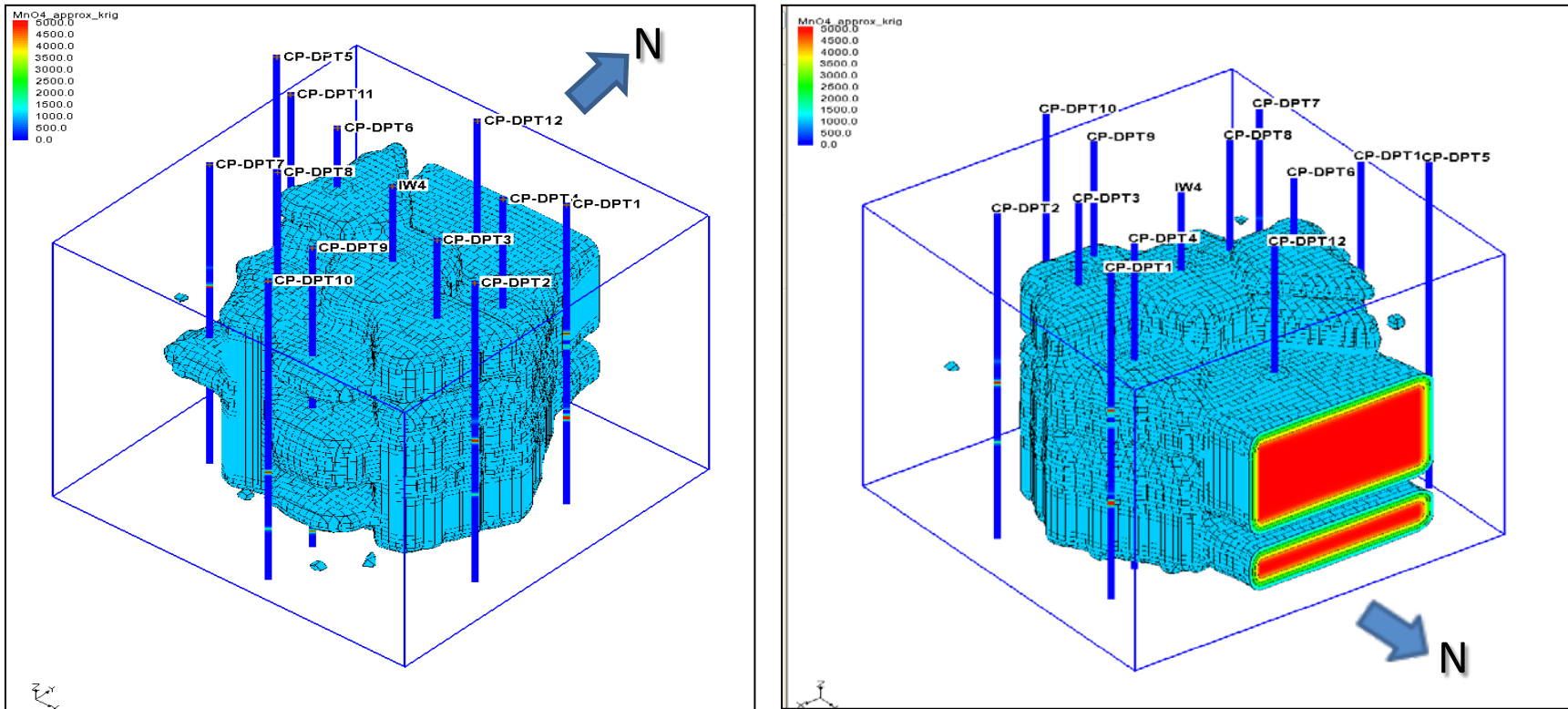


**Figure 5-28.** Results of ordinary kriging of the post-injection permanganate data representing the distribution of permanganate within the control plot after a 1 pore volume injection. Integrated sweep efficiency (volume contacted by permanganate divided by total volume) was 33%

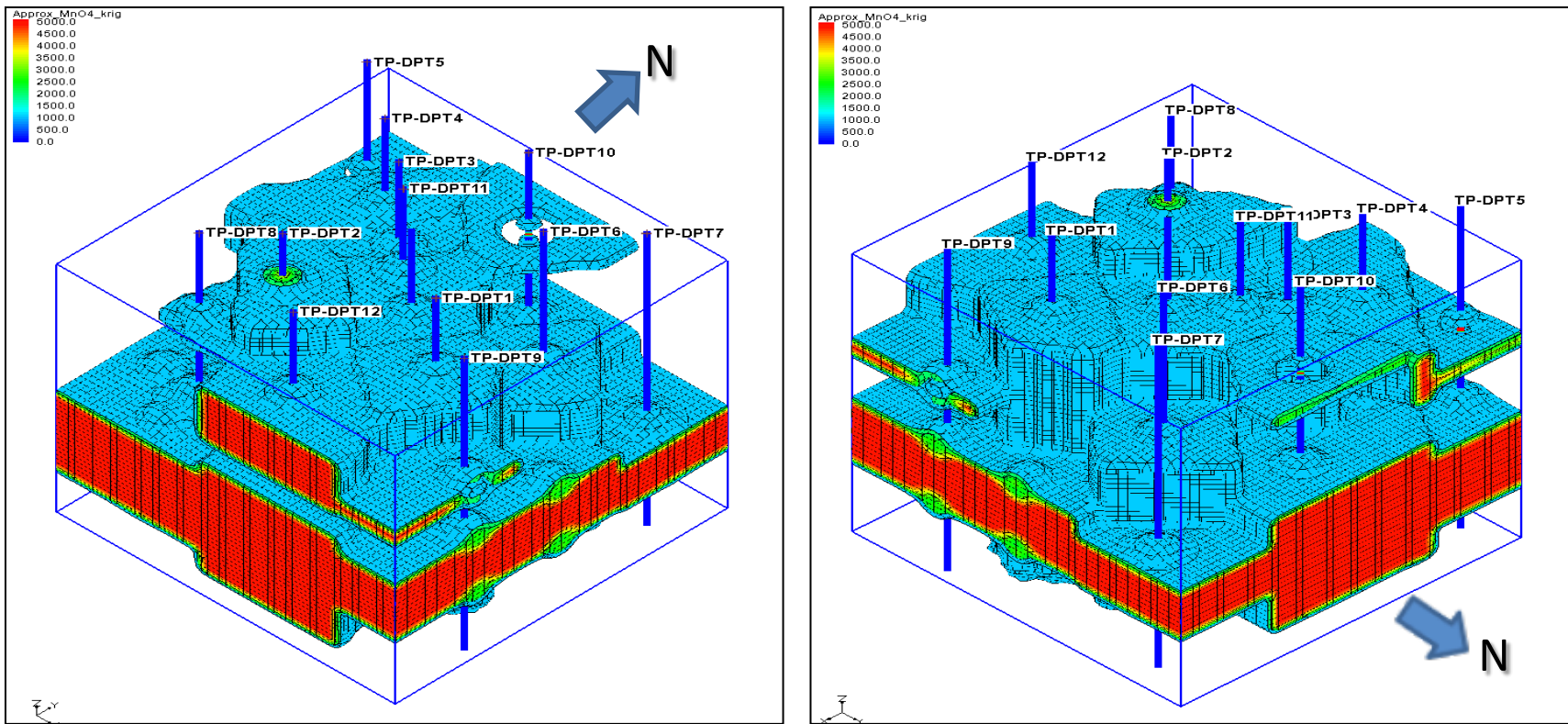


**Figure 5-29.** Results of ordinary kriging of the post-injection permanganate data representing the distribution of permanganate within the test plot after a 1 pore volume injection. Integrated sweep efficiency (volume contacted by permanganate divided by total volume) was 67%.

**Control Plot Results:** In the absence of polymer addition, it was anticipated that the injected permanganate solution would follow paths of least resistance associated with the higher permeability sands. However, upon examining the control plot cross-sections it is clear that injected permanganate also penetrated the less permeable finer sands and silty sands within the treatment zone. This result negates meaningful statistical correlation between the presence of permanganate and media permeability based on media textural classification for this site. Closer examination of the DPT boring logs, however, indicated that the presence of permanganate within the upper Castle Hayne formation sediments is more closely related to the vertical location of sediments that were observed in the core borings to be “loose and saturated”. These sediments were observed to be very fluid and, in many cases, were found to be positioned between more densely compacted sediments of similar grain size (i.e. textural category) within the collected cores and appear to have provided preferential flow paths for injected fluid propagation. The occurrence of variable density depositional facies is typical of the Tidewater region of the Atlantic Coastal Plain and appears to be a common feature of the upper Castle Hayes sediments in the area of the demonstration site.

The distribution of permanganate is shown to become more vertically discontinuous with distance from the injection well and after a 1 pore volume injection, permanganate occurred within distinct depth intervals at a distance of 11 feet from the point of injection (cf. cross-sections CPA-CPA' and CPC-CPC', **Figures 5-20** and **5-22**, respectively). In transect cross-section CPB-CPB', a more vertically continuous occurrence of permanganate was observed at boring CP-DPT12. It is likely that the bulk of the injected permanganate followed this preferential flow path to the north of the control plot and outside the control plot boundary in the vicinity of CP-DPT12.

As shown in **Figure 5-28**, in the absence of polymer addition the injected permanganate did not extend to the eastern, southern, and western edges of the control plot volume. Rather, it appears that the injected permanganate preferentially flowed toward and exited the control volume to the north during the injection period. This representation agrees with the results presented in the permanganate distribution cross section CPB-CPB' (**Figure 5-21**). Permanganate was not encountered in groundwater samples collected from CMT 4 (positioned at the northeastern “edge” of the control plot) at any depth interval during the injection period. However, permanganate was encountered in groundwater samples collected at CMT 3 (positioned to the west of the injection well and within the control plot, **Figure 5-20**) beginning day 2 of the injection period at the 2<sup>nd</sup> depth interval of four total from ground surface (~35 ft), but was not encountered within similar samples collected from the remaining depth intervals throughout the remainder of the injection period. These results speak to the degree to which permeability heterogeneity can control the distribution of injected fluids within even a moderately heterogeneous aquifer such as the upper Castle Hayne. Mitigating this type of preferential flow on the subsurface distribution of injected remedial fluids is a key function of viscosity-modification via polymer amendment.

Integration of the isosurface contours within the grid domain (for permanganate concentrations > 0 mg/L) provided the total volume swept within the control volume. This swept volume divided by the total volume of the simulation domain provides the sweep efficiency for the permanganate



treatment in the absence of polymer addition. The volumetric sweep efficiency for the control plot injection was thus determined to be 33%.

**Test Plot Results:** As shown in **Figures 5-23** through **5-25**, the subsurface distribution of permanganate within the test plot is significantly more uniform and vertically continuous for the polymer-amended fluid, suggesting a more uniform displacement front during injection. Also, contrary to the results of the control plot, the distribution of permanganate is observed to be less dependent on the locations of loose and saturated sediments. It appears, then, that the addition of polymer to the permanganate fluid formulation mitigated the bypassing of strata within the heterogeneous aquifer, regardless of the degree of compaction of the sediments, and contacted more of the soil within the treatment volume.

As shown in **Figure 5-29**, the addition of polymer to the injected permanganate solution provided improved sweep efficiency compared to the control plot injection. While some preferential flow is observed within portions of the test plot volume, the overall distribution of permanganate was greatly improved. The sweep efficiency for the test plot injection was determined to be 67%, or a 109% improvement over the control plot injection (i.e., no polymer case).

It is important to remember that (per design) this demonstration was limited to a 1 pore volume injection, as defined by the 59,000 gallon pore volume contained within the control volume of each demonstration plot. With viscosity modification, the effects of heterogeneity can be mitigated but not eliminated (Silva, 2011; Silva et al., 2012a), and a longer injection period would have been required to maximize sweep efficiency improvement.

As an example to further demonstrate this statement, the results of a five-layer two-dimensional (2D) sand tank experiment (research performed during the conduct of SERDP Project ER-1486) are provided in **Figure 5-30**. As shown, the addition of xanthan gum biopolymer mitigates the effects of heterogeneity relative to the no-polymer case. However, 100% sweep efficiency could not be achieved after injecting just 1 pore volume of polymer-amended fluid. In fact, 1.5 pore volumes were required to completely sweep this layered heterogeneous system, compared to a 6 pore volume injection for the non-polymer-amended case (Silva, 2011; Silva et al, 2012b). The maximal permeability contrast for this 2D tank experiment was 82.5/5 darcy, or 16.5, which is similar to the range of maximum permeability contrast observed for the upper Castle Hayne formation during hydraulic testing associated with the initial site characterization (i.e., a factor of 10 to 17 permeability contrast). Therefore, it is likely that an optimal sweep efficiency improvement for the test plot would require a 1.5 to 2 pore volume injection volume.

It has become common, during more typical ISCO treatments, for practitioners to inject less than 1 pore volume (often closer to 0.25 pore volumes) within a designated treatment volume to avoid longer field durations. Injected oxidant concentrations are typically greater than that used in this demonstration, with the objective of injecting enough oxidant mass within the overall treatment zone to overcome unproductive demands. This method of treatment relies on the groundwater gradient to distribute oxidant down-gradient. However, with this mode of treatment the subsurface distribution of oxidant can be greatly dependent on the degree of permeability heterogeneity, and achieving contact between the oxidant and target contaminant can be less

efficient due to oxidant following preferential flow paths within more permeable strata. PA-ISCO represents an alternative treatment approach that focuses on improving contact efficiency by improving sweep efficiency. PA-ISCO can require a longer period of injection. However, cost savings can be realized by achieving more effective treatment via improved contact efficiency, a lower number of injection points, and a more efficient use of oxidant during treatment.

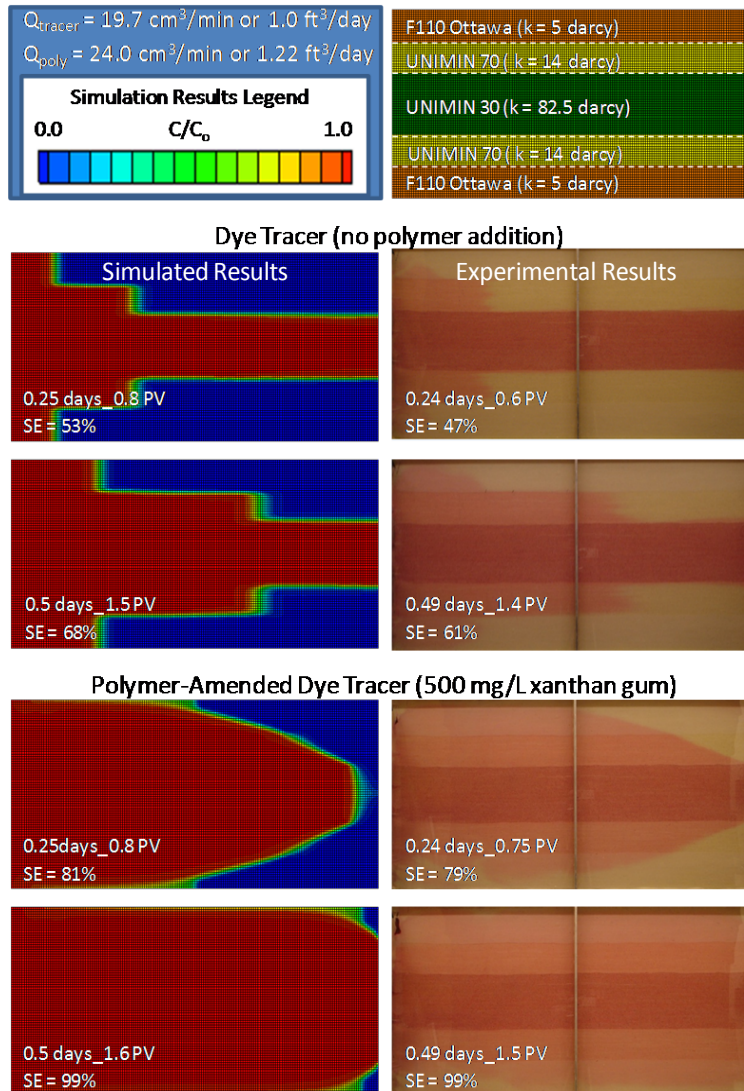


**Figure 5-30.** Example of polymer-improved sweep efficiency within a 2-D sand tank (from Silva, 2011 and Silva et al., 2012b).

### 5.7.2 VOCs in Soil and Groundwater

**Figure 5-31** presents a summary of VOCs concentrations measured pre-, during, and post-treatment for the polymer test plot and **Figure 5-32** presents the same for the permanganate-only control plot. Soil VOCs data plotted along with permanganate distribution are presented in Appendix C. Example data are shown in **Figure 5-33** for the test plot and **Figure 5-34** for the control plot.

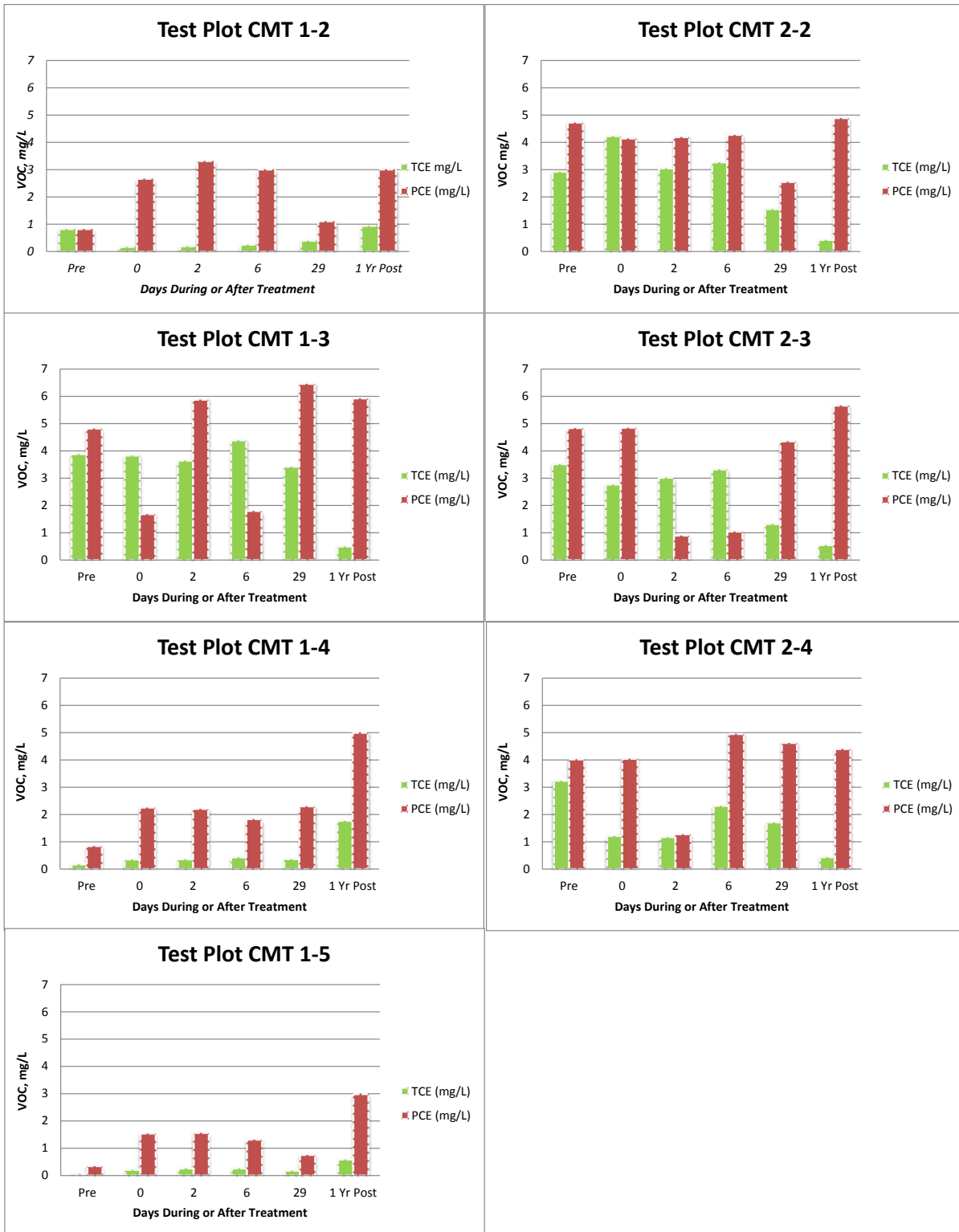


**Figure 5-31.** TCE and PCE concentrations measured in CMT wells 1 and 2 at each screened interval (CMT 2-5 did not produce enough aqueous sample to analyze throughout the demonstration). Values, which are the average of duplicates, are presented for pre-treatment, during treatment, and post-treatment. Delivery occurred until the beginning of Day 6.

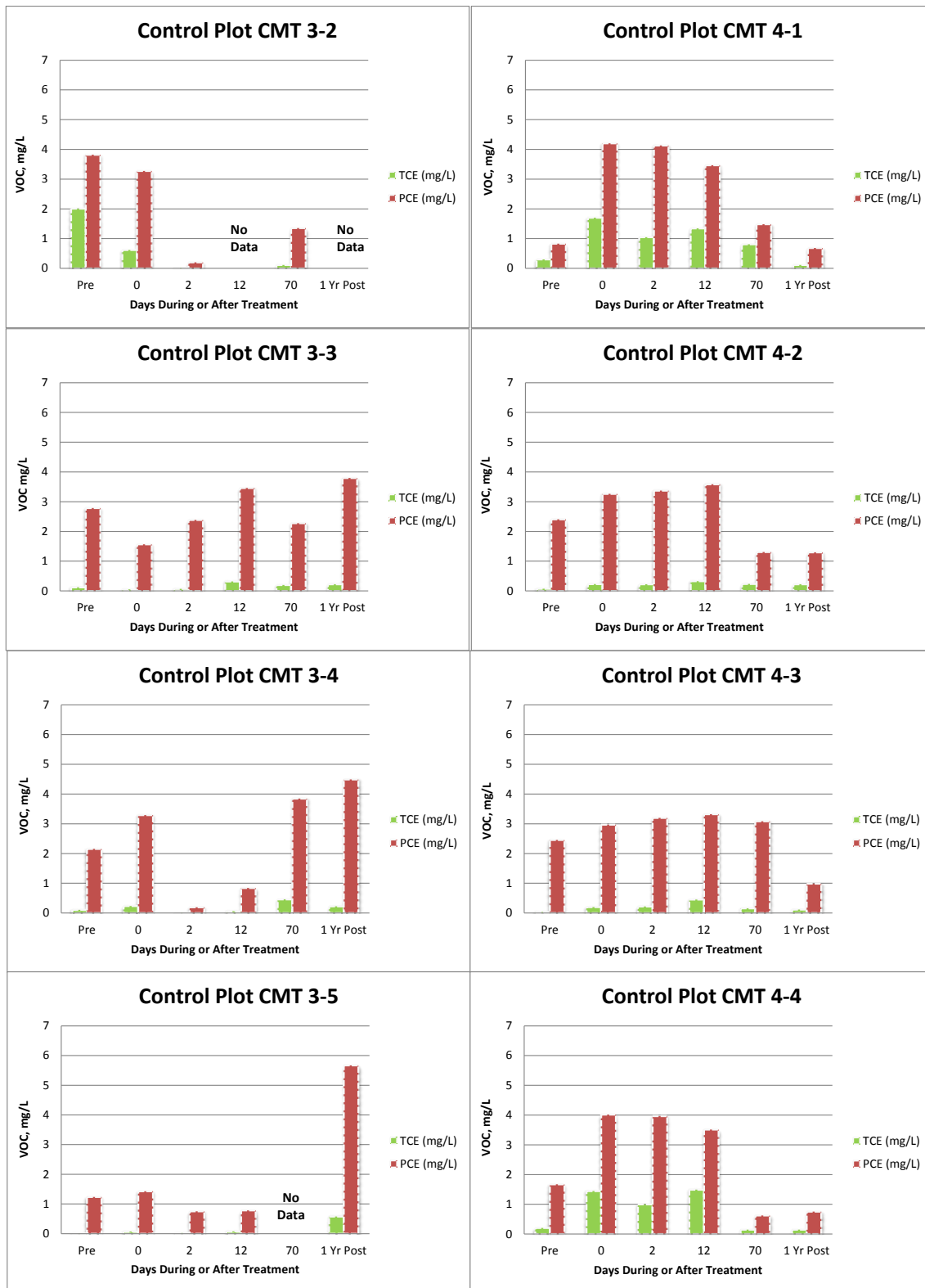


**Figure 5-32.** TCE and PCE concentrations measured in CMT wells 3 and 4 at each screened interval. Values, which are the average of duplicates, are presented for pre-treatment, during treatment, and post-treatment. Delivery occurred until the beginning of Day 6.

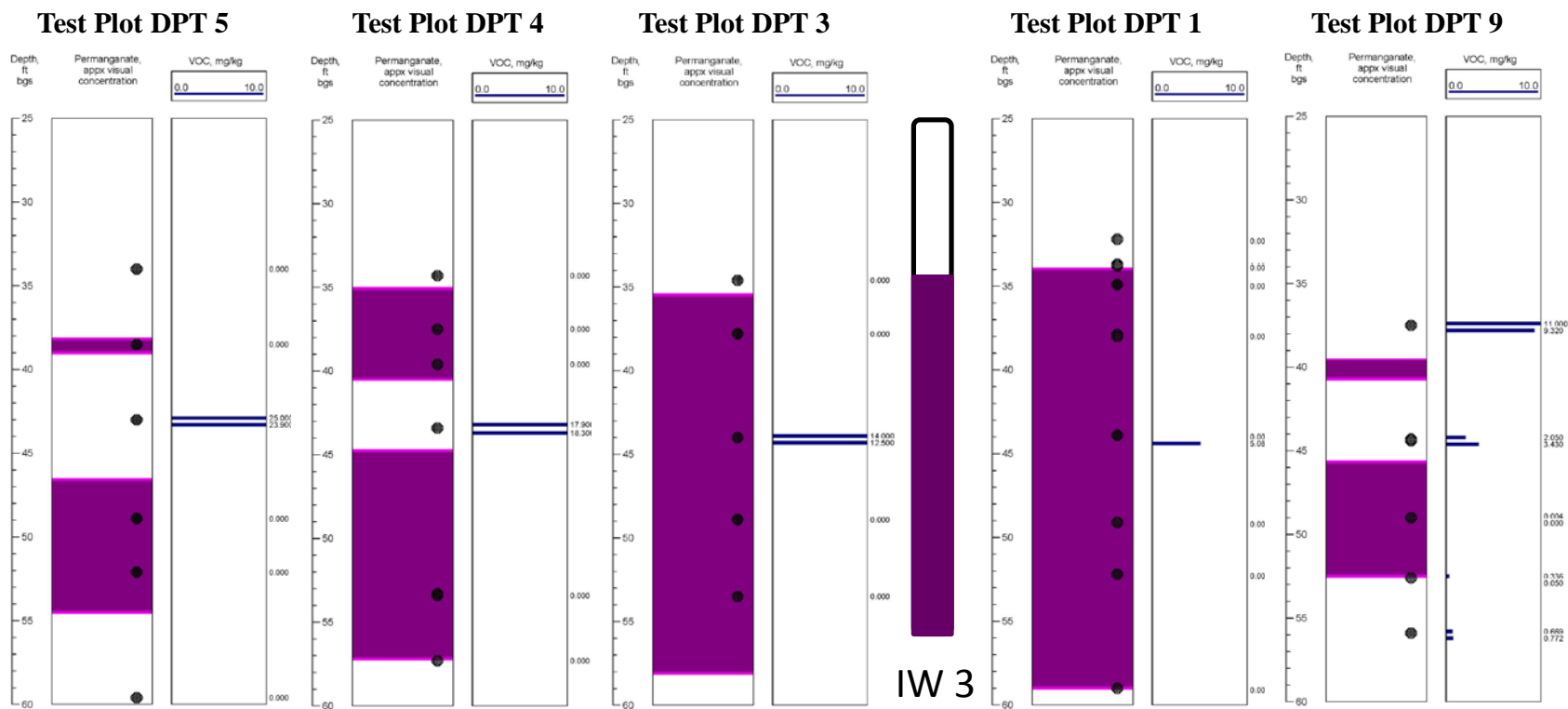


**Figure 5-33.** Soil VOCs concentrations (TCE and PCE) along with permanganate distribution for transect TP-A-TP-A' (Figure 5-19). Dots on the permanganate distribution plot indicate locations where VOCs samples were collected; where no VOCs concentrations are shown on the VOC concentration log, results are below detection (0.05 mg/kg).

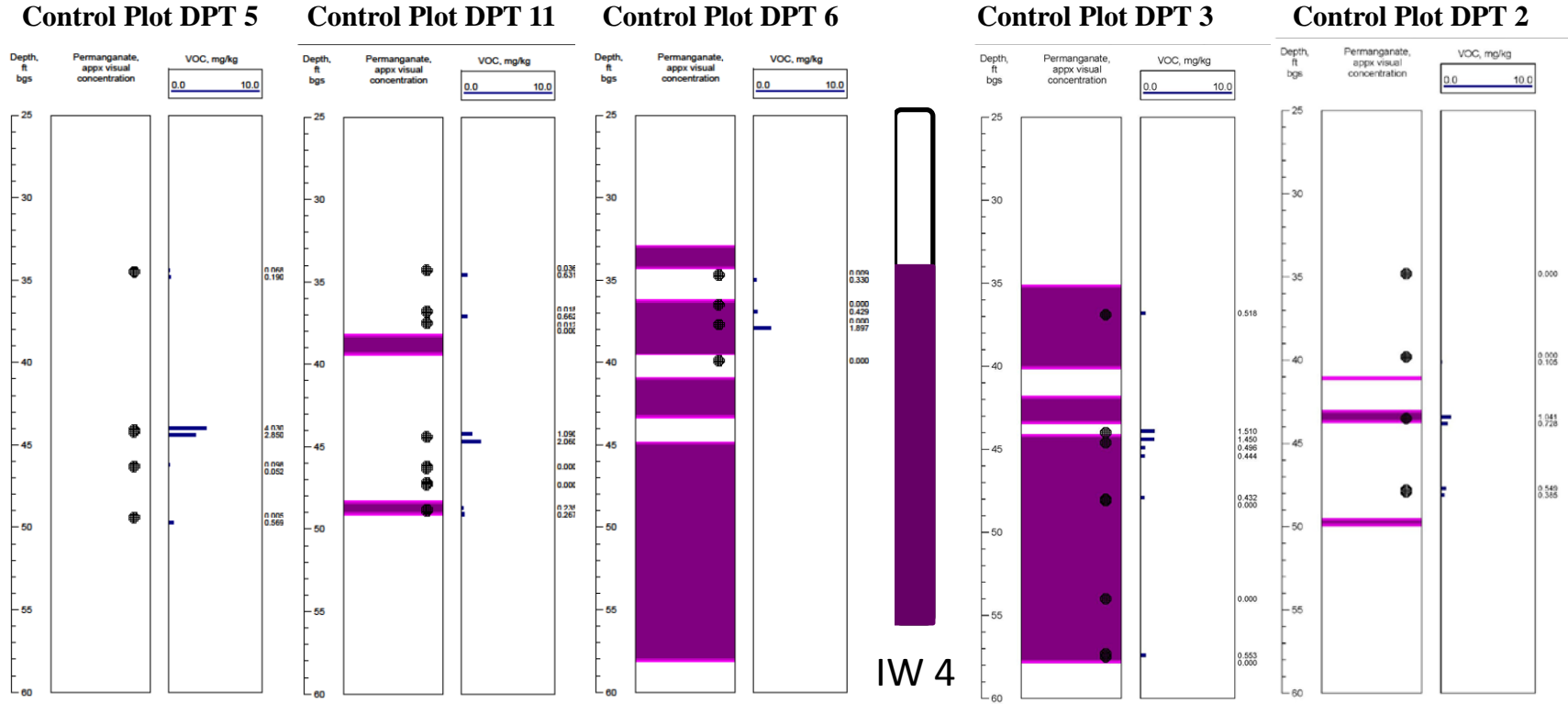


**Figure 5-34.** Soil VOCs concentrations (TCE and PCE) along with permanganate distribution for transect CA-CA' (Figure 5-19). Dots on the permanganate distribution plot indicate locations where VOCs samples were collected; where no VOCs concentrations are shown on the VOC concentration log, results are below detection (0.05 mg/kg).



**Groundwater:** PCE concentrations changed very little relative to the initial concentration over the duration of delivery and one year post-treatment. It is likely that the concentrations did not change during delivery because permanganate did not reach CMTs 1 and 2 during the 5-day delivery period (although it was found within 1-2 ft upon coring). PCE concentrations in the control plot decrease some during delivery in CMT-3, and the decreases generally correspond with the arrival time of the permanganate signature (permanganate itself or its geochemical profile including solids, Eh, and Mn, discussed in Section 5.7.3). The TCE pattern (or lack thereof) is similar to the PCE, in general. However, it is interesting to note that the TCE concentrations were generally higher in the test plot. The cause of this difference is unknown.

**Soils:** Both the test and control plots show lower VOCs concentrations in areas where permanganate is present relative to those where permanganate is not present. In both plots, the effectiveness of treatment generally decreased with distance from injection. This is anticipated in ISCO treatment because the distances closer to injection receive, overall, a greater number of pore volumes of oxidant solution for a longer duration than those distances on the periphery. In comparing the results of the two plots, it is important to note that the test plot was more significantly contaminated than the control plot prior to treatment, as shown in **Figure 4-8** and based on the pre-treatment soil core data for the injection wells and CMT wells associated with the test and control plots (**Table 5-9**).

**Table 5-9. Pre-treatment VOCs Concentrations for Control and Test Plot from Cores Collected During the Drilling of Injection Wells and CMT Wells.**

Control Plot				Test Plot			
Sample ID #	Sample Received	Concentration TCE (mgTCE/kg dry soil)	Concentration PCE (mgPCE/kg dry soil)	Sample ID #	Sample Received	Concentration TCE (mgTCE/kg dry soil)	Concentration PCE (mgPCE/kg dry soil)
IR88-IW04-36-37-1	6/8/2010	0.02	2.05	IR88-IW3-36-37-1	5/26/2010	0.51	1.50
IR88-IW04-36-37-1	6/8/2010	0.02	1.19	IR88-IW3-36-37-1	5/26/2010	0.58	1.77
IR88-IW04-38-40-1	6/8/2010	0.00	0.00	IR88-IW3-38-40-1	5/26/2010	0.58	1.96
IR88-IW04D-38-40-1	6/8/2010	0.00	0.00	IR88-IW3-38-40-1	5/26/2010	1.01	3.47
IR88-IW04-42-43-1	6/8/2010	0.00	0.02	IR88-IW3-45-46-1	5/26/2010	0.80	12.98
IR88-IW04D-42-43-1	6/8/2010	0.00	0.06	IR88-IW3-45-46-1	5/26/2010	0.75	13.18
IR88-IW04D-48-49-1	6/8/2010	0.00	0.11	IR88-IW3-46-48-1	5/26/2010	0.00	0.08
IR88-IW04D-48-49-1	6/8/2010	0.00	0.01	IR88-IW3-46-48-1	5/26/2010	0.00	0.10
IR88-IW04-52-53-1	6/8/2010	0.00	0.00	IR88-IW3-51-51-1	5/26/2010	0.01	0.40
IR88-IW04D-52-53-1	6/8/2010	0.00	0.00	IR88-IW3-51-51-1	5/26/2010	0.00	0.43
IR88-CMT03-36-37-1	5/24/2010	0.00	0.01	IR88-CMT01-38-39-1	5/18/2010	1.71	1.50
IR88-CMT03D-36-37-1	5/24/2010	0.00	0.64	IR88-CMT01D-38-39-1	5/18/2010	2.08	2.39
IR88-CMT03-42-43-1	5/24/2010	0.02	1.38	IR88-CMT01-44-45-1	5/18/2010	1.59	16.27
IR88-CMT03D-42-43-1	5/24/2010	0.04	2.21	IR88-CMT01D-44-45-1	5/18/2010	1.45	13.19
IR88-CMT03-46-47-1	5/24/2010	0.00	0.01	IR88-CMT01-51-52-1	5/18/2010	0.05	0.28
IR88-CMT03D-46-47-1	5/24/2010	0.00	0.10	IR88-CMT01D-51-52-1	5/18/2010	0.10	0.43
IR88-CMT04-39-40-1	5/21/2010	1.26	10.00	IR88-CMT01-55-56-1	5/18/2010	0.07	0.55
IR88-CMT04D-39-40-1	5/21/2010	1.06	4.79	IR88-CMT01D-55-56-1	5/18/2010	0.00	0.11
IR88-CMT04-49-50-1	5/21/2010	0.02	0.45	IR88-CMT02-35-36-1	5/20/2010	1.23	8.07
IR88-CMT04D-49-50-1	5/21/2010	0.00	0.21	IR88-CMT02D-35-36-1	5/20/2010	1.10	5.65
IR88-CMT04-64-65-1	5/21/2010	0.00	0.28	IR88-CMT02-43-44-1	5/20/2010	0.10	2.66
IR88-CMT04D-64-65-1	5/21/2010	0.01	0.38	IR88-CMT02D-43-44-1	5/20/2010	0.00	0.61
				IR88-CMT02-51-52-1	5/20/2010	0.02	0.19
				IR88-CMT02D-51-52-1	5/20/2010	0.02	0.19

With respect to treatment effectiveness, where contact between permanganate and contaminant occurred treatment was effective within both plots except for the most heavily contaminated areas which are predominantly fine sands/silty sands for each plot. The test plot experienced twice the sweep efficiency of the control plot and the overall treatment effectiveness in the test plot is greater.

Because the demonstration/validation was conducted at the pilot scale over a short delivery period (as per scope, project duration, and funding), we did not anticipate complete concentration and/or mass reduction for this particular plot. The site media had a relatively high organic carbon fraction ( $f_{oc} = 0.02 - 0.07\%$ ), with the potential for the majority of contaminant mass to be associated with the solid phase, which in turn serves as a source for groundwater contamination. Also, because of the high organic carbon content, the media exerted a significant demand for the oxidant. At the full scale, these site characteristics would typically call for multiple injections of oxidant to address desorbed mass as the sorbed phase re-equilibrates with the aqueous phase. Furthermore, these conditions call for delivery of multiple pore volumes of solution, requiring a longer injection duration than was practicable for this demonstration. The primary focus of the design, implementation, and subsequent monitoring for this demonstration/validation was the enhanced delivery of the oxidant via viscosity modification by the addition of water soluble polymers. While contaminant treatment effectiveness was captured in the performance criteria set for the demonstration, these criteria were established prior to site selection and characterization.

In general, it is well established that where oxidant and contaminant meet, contaminant destruction will result, particularly for VOCs whose reaction kinetics are rapid (long contact durations are not necessary). This effect can be observed in **Figures 5-33 and 5-34**. The use of polymer offers an advantage over traditional ISCO in that a larger percentage of the treatment volume is contacted by the oxidant (as described in Section 5.7.1). Nonetheless, the presence of sorbed mass will challenge the limits of any remediation technology that involves the delivery of liquid amendments and relies on reaction in the aqueous phase. It is reasonable that more effective treatment could be achieved at this site with a full-scale design that focuses on the sorbed mass by including multiple injections and longer delivery duration. The use of a polymer-amended fluid reduces the number of pore volumes of oxidant necessary to achieve the required contact within the lower permeability strata, thereby decreasing the costs associated with chemical, field time, and return field mobilizations. Furthermore, once the bulk of the initial unproductive demand is met during the initial phase of injection, permanganate concentrations could be reduced within the PA-ISCO fluid formulation (i.e., more efficient use of oxidant) to encourage viscosity retention in situ and provide a longer-term source of oxidant within the swept volume to continue to treat sorbed-phase contamination.

### **5.7.3 Groundwater Quality**

**pH:** According to data collected both during operation real-time and from samples shipped to the lab for next day analysis, low to moderate pH drops (0.1 – 1.5 pH units) occurred in some ports in both the control and test plots during operation (data included in Appendix B). These shifts did not persist beyond a single sampling event and all were within their near-neutral range at the 1-yr post-treatment sampling event. The large majority of samples experienced very little

change in pH (< 0.3 pH units) during and post-treatment. Small decreases in pH are anticipated during oxidation of chlorinated solvents through production of H<sup>+</sup> ion as a byproduct. Aquifers typically attenuate the response via the natural media's buffer capacity, as was the case for these MCIEAST-MCB CAMLEJ sediments.

**ORP and Conductivity:** Figures 5-35 and 5-36 show the ORP and conductivity values for CMT 1 (test plot) and CMT 3 (control plot) at each depth during operation. Both parameters are indicators for the arrival (or near arrival) of oxidant at the well. The data confirm that permanganate or its geochemical signature did not arrive at the monitoring wells during operation (Figure 5-35) (permanganate was found within cores, however, just 1-2 ft from the monitoring wells). The data highlight the preferential flow through the control plot (Figure 5-36), indicating arrival first at depth 2 of CMT 3, followed by depths 3 and 4. One year post-treatment conductivity in CMT 1 and CMT 2 (test plot) were nearly the same as pre- and during treatment. CMT-3 showed a higher conductivity one-year post-treatment at the shallowest depth, however conductivity returned to pre-treatment values in the other depths. CMT-4, however, showed the most dramatic change, with an order of magnitude increase in conductivity one year post-treatment at each depth. While permanganate was not observed to arrive at CMT-4 during treatment (which was further from injection than CMT-3), the influence of permanganate in the direction of CMT-4 toward which a preferential flow path was identified (as described in Section 5.7.1) is clear even one year post-treatment.

**Total Solids:** Laboratory-measured total solids concentrations, presented in Figures 5-37 and 5-38 (note differences in y-axis scale in the two figures), mirror those of the conductivity values measured in the field, as expected. Again, preferential flow of oxidant, reflected in the higher total solids concentration, is clear in CMT 3. This same influence is seen in CMT 4 one year post-treatment. There was little change in CMT 1 and CMT 2. For each of the CMT samples collected, the dissolved concentration samples were > 90% of the total solids concentration, with very few exceptions.

Based on ORP, conductivity, and total solids concentrations of both the test and control plots, and the fact that permanganate was observed in soil cores collected only 1-2 ft. from the CMTs of the test plot, it is apparent that the oxidant travel with polymer present is retarded overall relative to the preferential travel without polymer present. This is expected. The more viscous polymer solution travels more uniformly (as shown in Section 5.7.1) and though a greater percentage of the total volume of the subsurface due to the lack of preferential flow and movement into the less permeable layers. These data support the findings of increased sweep efficiency with the use of polymer. It is interesting to note that there is little to no change in solids and conductivity in the test plot even post-treatment. It is possible that either the passage of the solids (MnO<sub>2</sub> byproduct) occurred after delivery, but before the 1-yr post-treatment sample collection period. It's also possible that some viscosity remains within the treated area, which could result in flow of upgradient groundwater around the treatment area, maintaining the geochemical signature of permanganate treatment within.

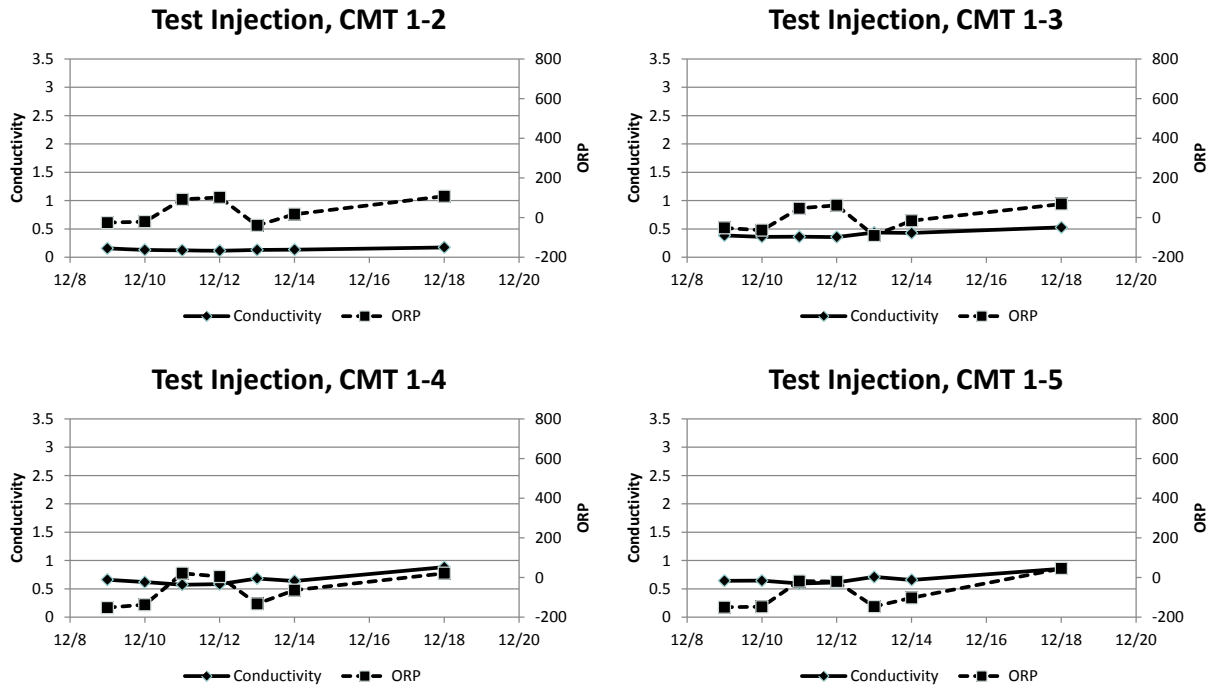


Figure 5-35. Conductivity (mS/cm) and ORP (mV) for CMT 1 (test plot) at each depth.

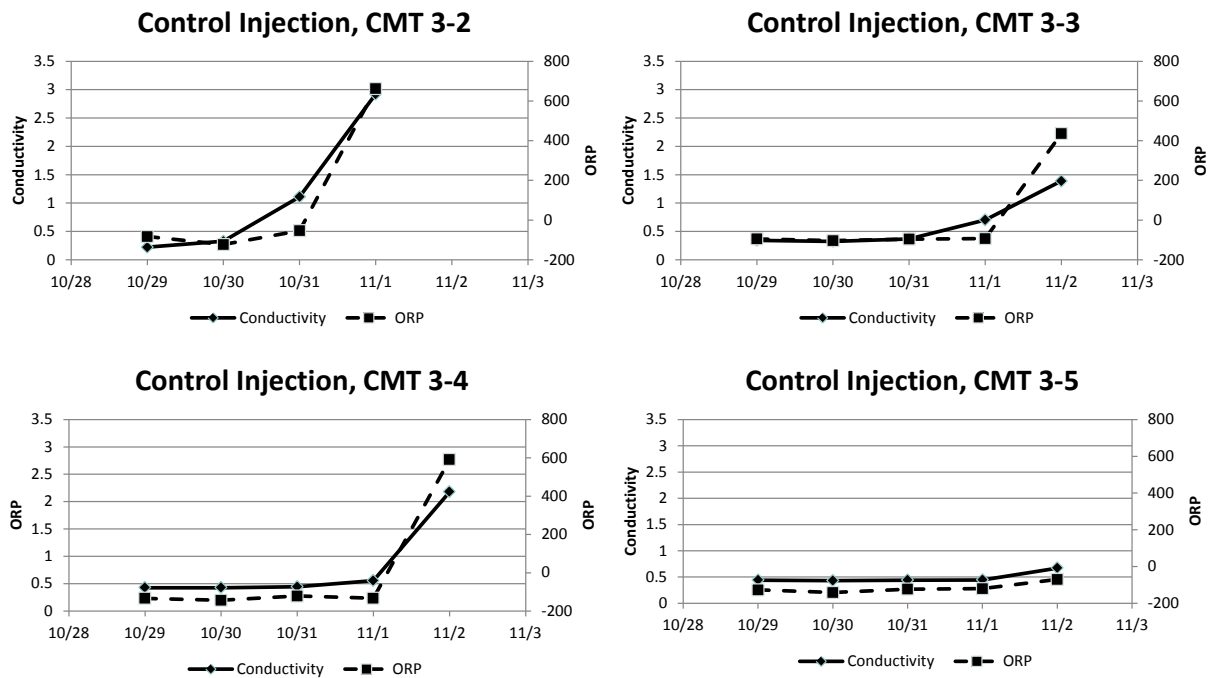
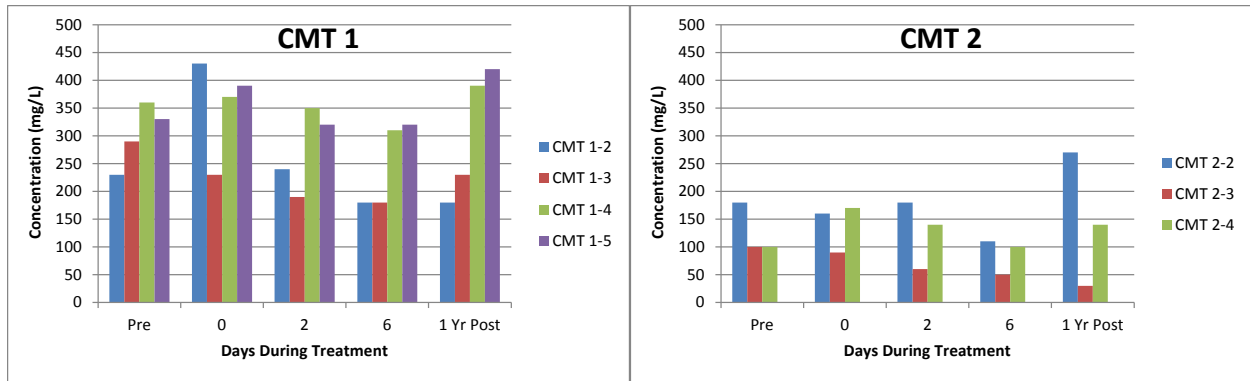
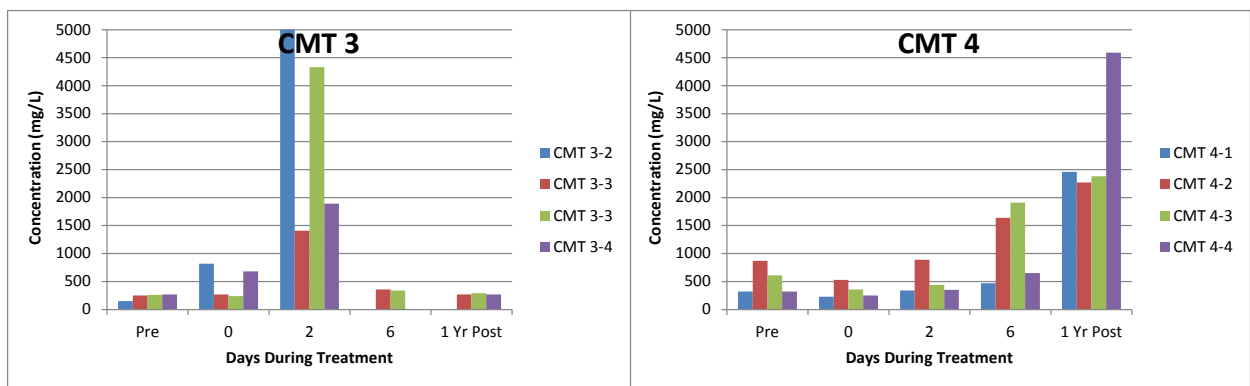


Figure 5-36. Conductivity (mS/cm) and ORP (mV) for CMT 3 (control plot) at each depth.



**Figure 5-37.** Total solids (mg/L) for CMT 1 and CMT 2 (test plot) at each depth.



**Figure 5-38.** Total solids (mg/L) for CMT 3 and CMT 4 (control plot) at each depth.

**Chromium:** Chromium is often of interest at ISCO sites due to its redox-sensitive nature and higher toxicity in its oxidized form. Extremely small, statistically insignificant increases were measured in Cr at shallow depths in the test plot (CMT 1 and 2 **Figure 5-39** below). More significant increases were measured in CMT 3 (control plot) at each depth, generally corresponding with the movement of permanganate front through the screened interval (**Figure 5-40**). Small, less pronounced increases were measured in CMT 4 (control plot), which was further from the injection well than CMT 3. The transient increase of chromium concentration in groundwater in close proximity to injection, which persists only as long as the elevated Eh provided by the oxidant persists, is consistent with other permanganate oxidation sites (Moore, 2008). Because the permanganate injected into the test plot did not reach CMT 1 and 2, we are unable to compare the effect in the test and control plots.

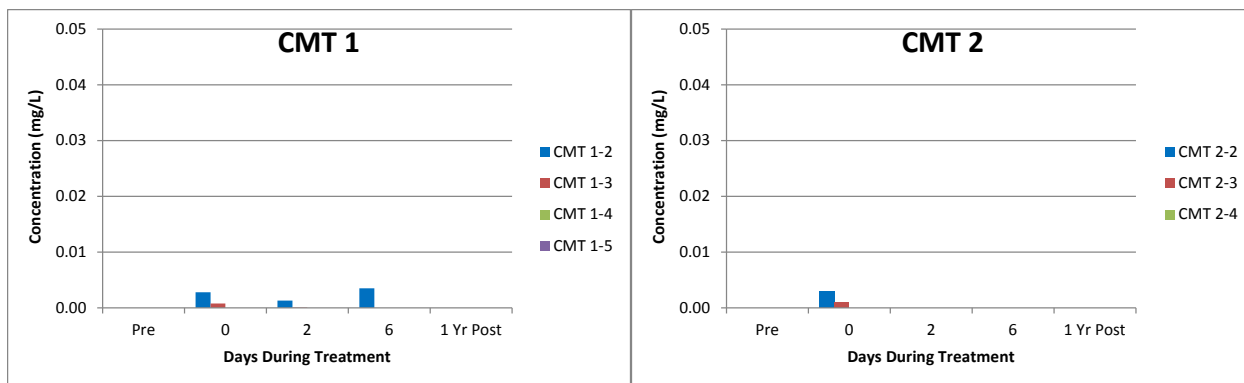


**Figure 5-39.** Chromium concentrations (mg/L) in CMT 1 and CMT 2 (test plot) at each depth.

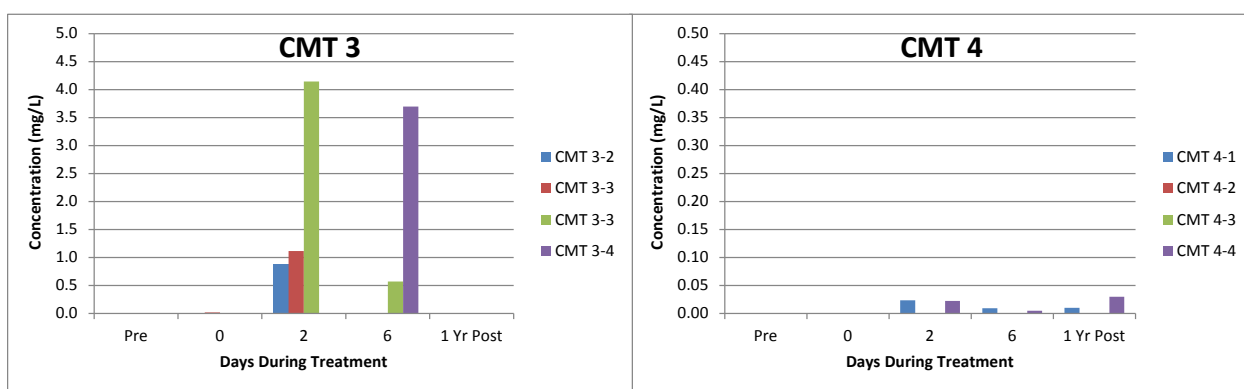


**Figure 5-40.** Chromium concentrations (mg/L) in CMT 3 and CMT 4 (control) at each depth.

**Cations:** Figures 5-41 and 5-42 present cation concentrations measured over time in the test plot, while Figures 5-43 and 5-44 present the same for the control plot. The test plot shows little variation in cation concentrations over time, including Mn (from the permanganate) and Na (from both the sodium permanganate and sodium hexametaphosphate). These findings are consistent with the lack of visual evidence of permanganate arrival, as well as the conductivity and total solids concentrations. Even though permanganate itself did not reach the test plot CMTs, we could anticipate some sign of permanganate approaching the wells, particularly because it was only 1-2 feet from the wells and the natural oxidant demand (i.e., extent of permanganate reaction occurring during its transport) was significant, as measured in our treatability evaluations for the site. Permanganate’s presence, as noted by its purple color, typically lags behind its reaction signature (i.e.,  $MnO_2$  solids, soluble Mn). We do not see this evidence in the test plot. Because viscosity and diffusion are inversely proportional, we postulate that the viscous polymer solution maintains the oxidation signature. This is potentially advantageous as it could prevent a “slug” of solution with high solids concentrations, high Mn concentrations (for which there is an EPA Secondary Water Quality Standard), as well as other cations (including those that may be toxic), from moving downgradient toward a receptor (while also attenuating as it travels).



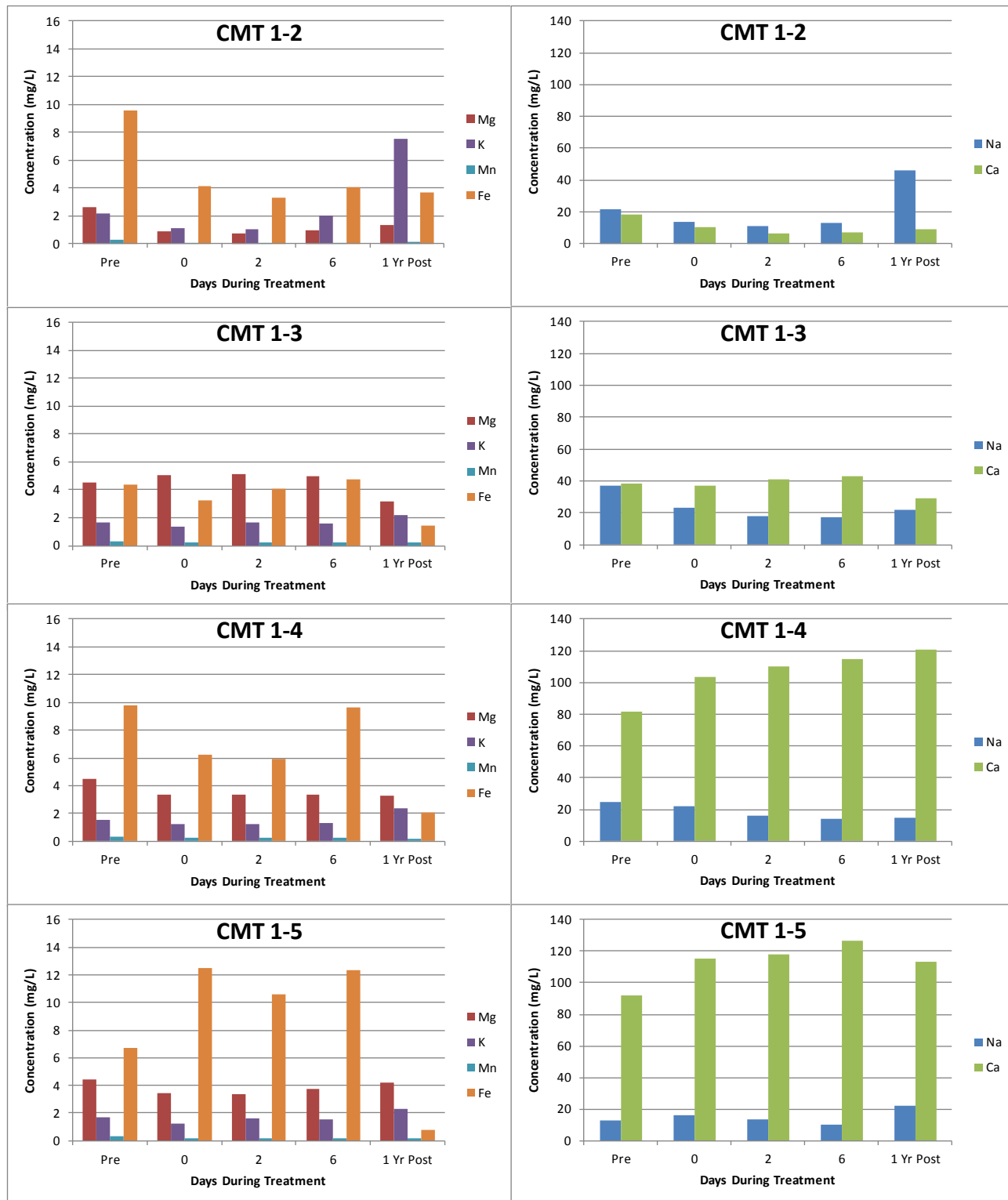


**Figure 5-41.** Concentrations (mg/L) of common cations measured in CMT 1 at each depth. Because of the data range, the left-hand side presents Mg, K, Mn, and Fe data, and the right-hand side presents Na and Ca.

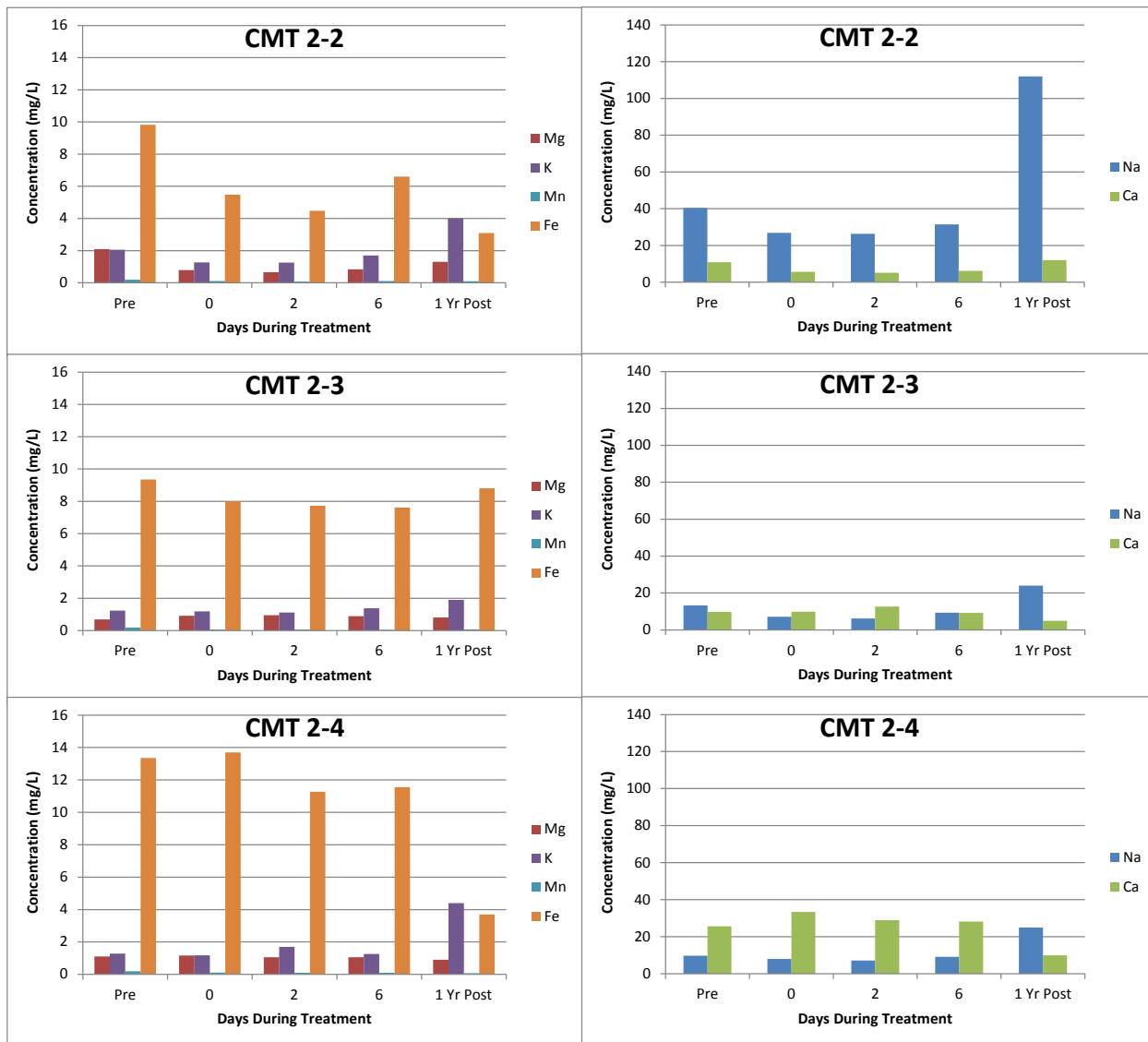


**Figure 5-42.** Concentrations (mg/L) of common cations measured in CMT 2 at each depth. Because of the data range, the left-hand side presents Mg, K, Mn, and Fe data, and the right-hand side presents Na and Ca.

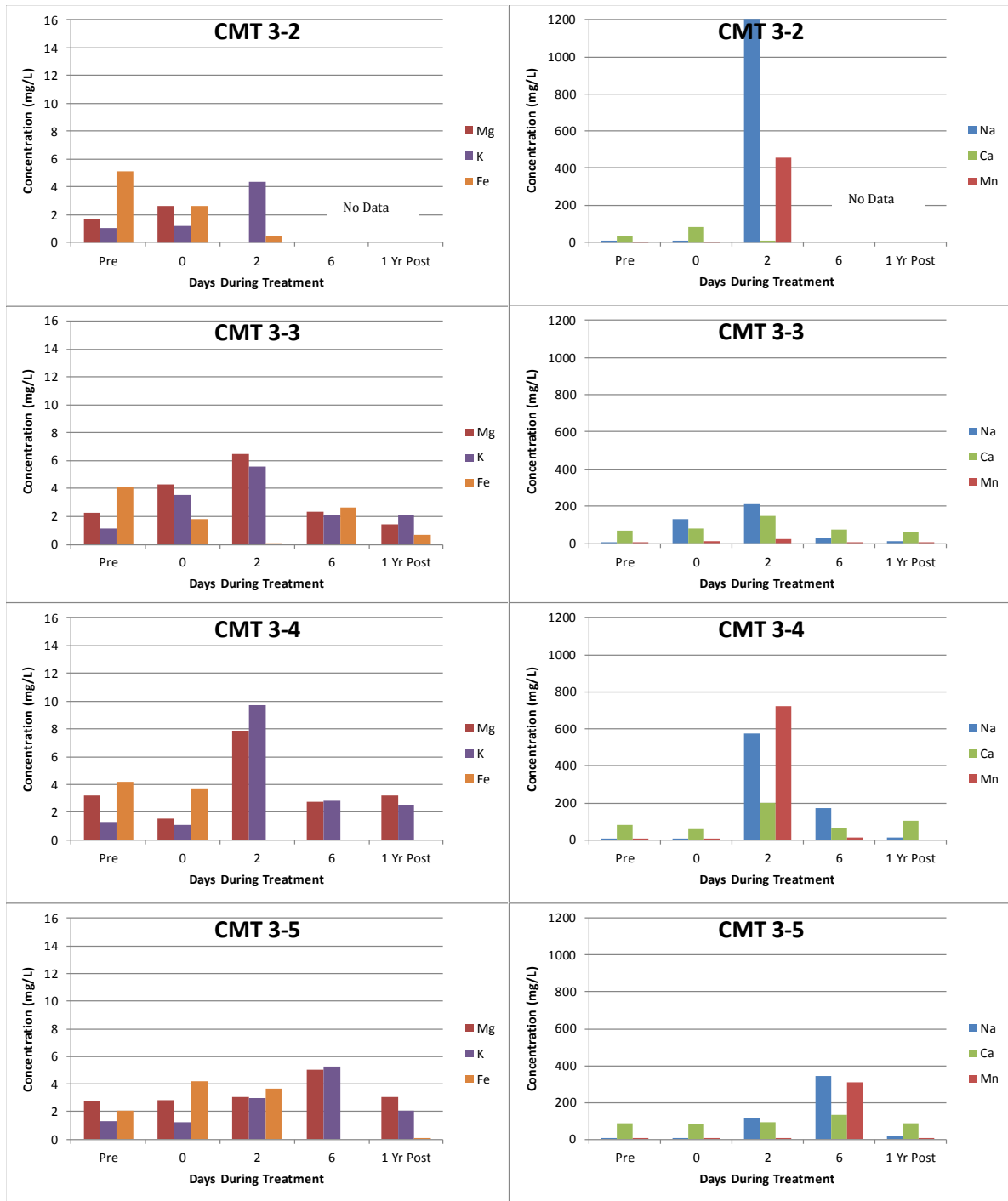


**Figure 5-43.** Concentrations (mg/L) of common cations measured in CMT 3 at each depth. Because of the data range, the left-hand side presents Mg, K, and Fe data, and the right-hand side presents Mn, Na, and Ca.

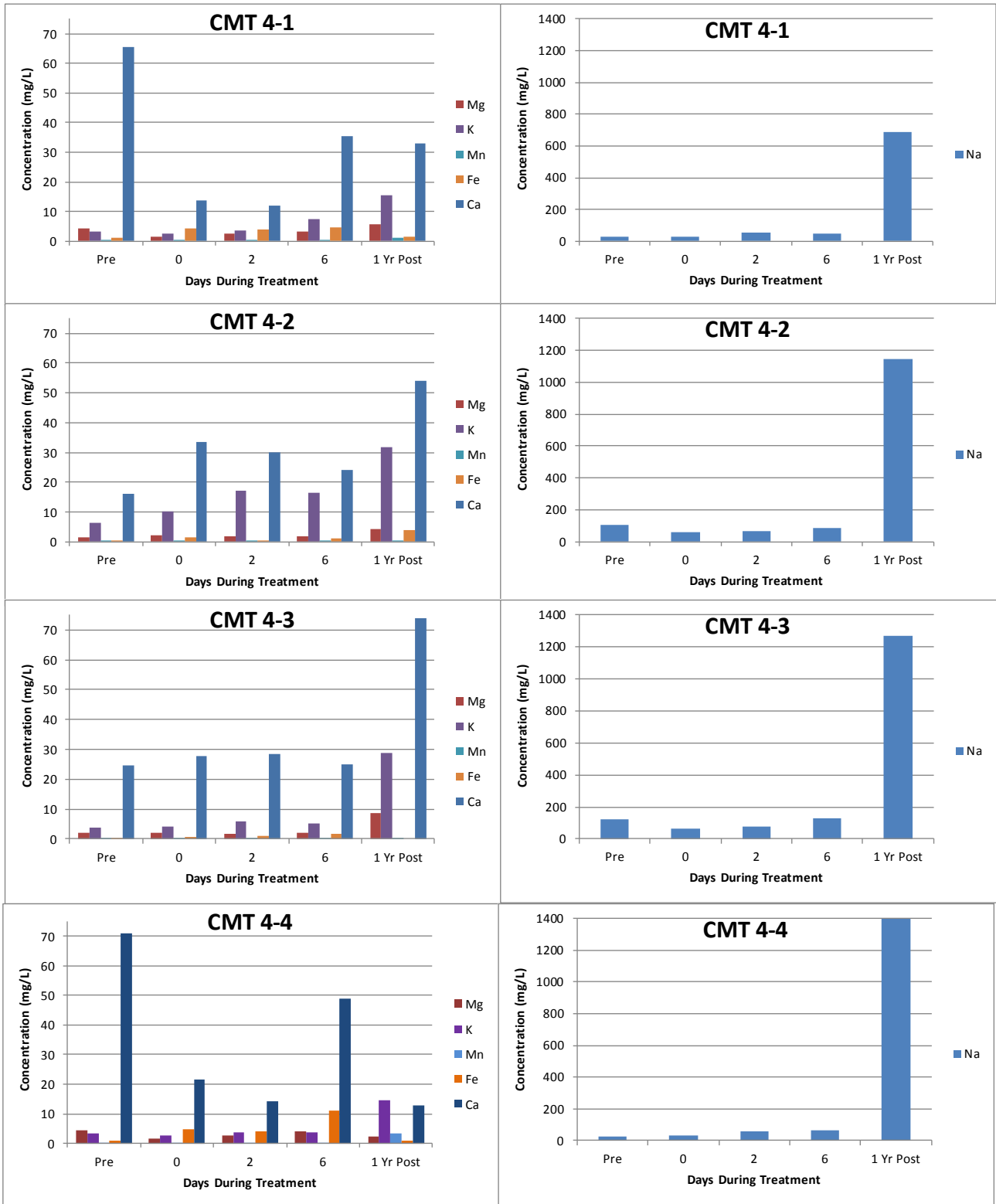


**Figure 5-44.** Concentrations (mg/L) of common cations measured in CMT 4 at each depth. Because of the data range, the left-hand side presents Mg, K, Mn, Fe, and Ca data, and the right-hand side presents Na.

We do expect, as the viscosity dissipates via polymer dissolution, the geochemical signature to “be released”. This effect is perhaps evidenced by the higher 1 year post-treatment Na concentrations measured in CMT 2. We do not see Mn accompany the Na, interestingly. The Mn is likely present as MnO<sub>2</sub> solids 1 year post-treatment rather than soluble Mn, as there was no evidence of permanganate remaining in soil cores collected 1 year post-treatment and the pH and ORP ranges measured are amenable to the MnO<sub>2</sub> form of Mn. While there was little change to cation concentrations as a whole, the iron concentrations decrease with time in CMT 1. The iron here is likely precipitating as iron solids (likely with sulfate, as evidenced by anion data presented below) or is possibly co-precipitating with MnO<sub>2</sub>.

The control plot data, on the other hand, show spikes of Mn and Na that generally correspond with the arrival of permanganate and/or its geochemical signature (e.g., solids, conductivity). These data, too, show the preferential flow of permanganate through different lithology without polymer present, much like the data presented above.

**Anions:** **Figure 5-45** presents anion concentrations measured over time in the test plot, while **Figure 5-46** presents anion concentrations in the control plot. In the test plot, like the cation data, there is little change in anion concentrations with respect to time. The deeper portions of CMT 3 show a possible decrease in sulfate concentrations over time, while the shallowest shows an increase. The control plot data show spikes in concentrations of sulfate the generally correspond with the arrival of permanganate and sodium. It is likely that a naturally reduced form of sulfate is being oxidized and mobilized by the permanganate.

There is very little change in either the chloride or phosphate concentrations in either plot over time. While increases in chloride concentrations would be anticipated with oxidation of PCE and TCE, it is likely the small amounts generated from the low concentrations of oxidation-produced chloride relative to the high natural chloride concentrations of this coastal system are insignificant.

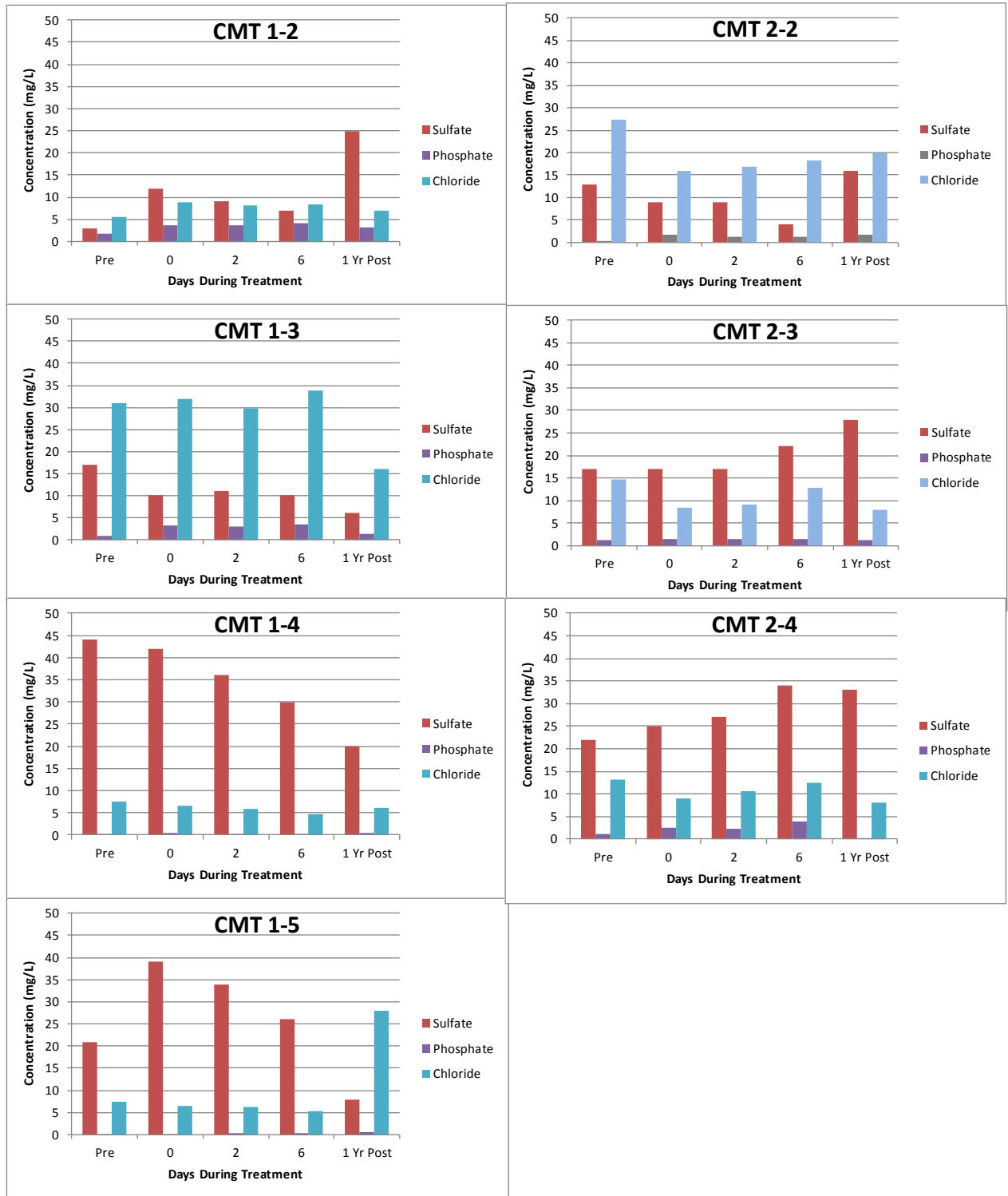


**Figure 5-45.** Concentrations (mg/L) of common anions measured in CMT 1 and CMT 2 at each depth.



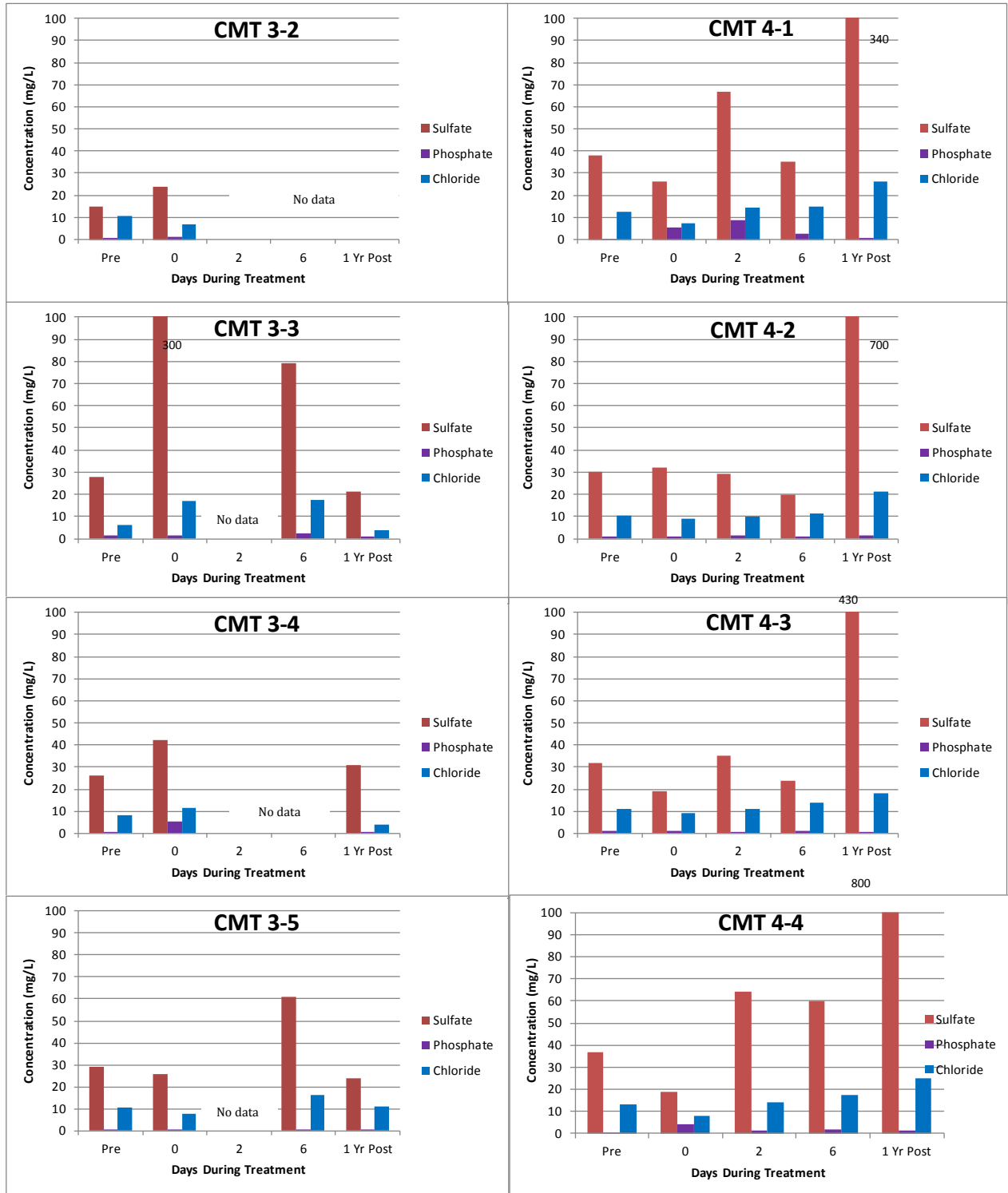


**Figure 5-46.** Concentrations (mg/L) of common anions measured in CMT 3 and CMT 4 at each depth.

### 5.7.4 Deposition and Fate of Manganese

Of particular interest to this demonstration is the influence of SHMP and xanthan polymer on the fate of manganese. A specific objective related to the use of SHMP is to avoid the deposition of MnO<sub>2</sub> within the treated area that could be anticipated to cause preferential flow under conditions where high contaminant concentrations are present. While we wouldn't anticipate such preferential flow with the contamination levels measured for this demonstration, we can expect to see the influence and impact of SHMP on MnO<sub>2</sub> for the purpose of extrapolating results to other systems.

**Figure 5-47** presents dissolved manganese concentrations measured in the test plot's CMTs 1 and 2. **Figure 5-48** presents dissolved manganese concentrations for the control plot's CMTs 3 and 4. Note the difference in the y-axis scales of these two figures. Very little change is measured in dissolved Mn over time in the test plot. For the pH and ORP conditions of these systems (Appendix B), we expect Mn to be predominately present as MnO<sub>2</sub> and not dissolved Mn, therefore results are not surprising, particularly with the strong evidence shown by other geochemical parameter measurements that the oxidation signature did not transport beyond the treatment area within the test plot. In the control plot, like other measured geochemical parameters such as Na and conductivity, we see spikes in Mn. These spikes, which correspond with observations of permanganate's purple color, again, demonstrate the preferential flow of permanganate in the control plot.

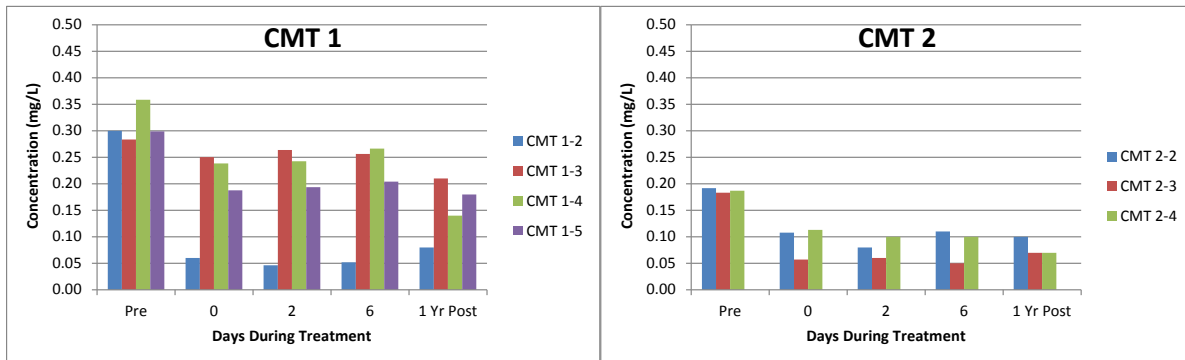


**Figure 5-47.** Manganese concentrations (mg/L) measured in test plot CMT 1 and CMT 2.

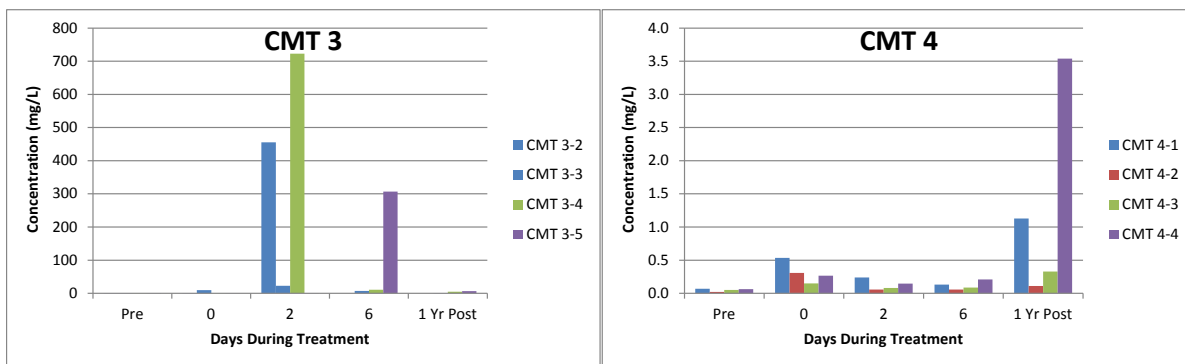


**Figure 5-48.** Manganese concentrations (mg/L) measured in control plot CMT 3 and CMT 4.

**Figure 5-49** and **Figure 5-50** present manganese extraction data for example test plot and control plot cores, respectively (complete data included in Appendix B). Water extractable cations are loosely bound and readily exchangeable (i.e., mobile), Ba-extractable cations are more strongly associated with the soils. Exchange with Ba occurs when the system is overwhelmed by a very high concentration of another cation or by exchange for a more strongly sorbing cation. The Mn as MnO<sub>2</sub> was determined through dissolution of the solids using hydroxylamine hydrochloric acid with nitric acid. **Figure 5-51** presents the total mass of manganese extracted per mass of media for cores collected immediately post treatment for three cores collected at approximately 5, 10, and 15 ft. from injection from top to bottom, respectively. **Figure 5-52** presents the total mass of manganese extracted per mass of media for cores collected one year post-treatment for cores nearly co-located with those shown in **Figure 5-51**. Finally, **Figure 5-53** presents the Mn as MnO<sub>2</sub> concentration for the cores shown in **Figures 5-49 and 5-50** in a different manner for easier interpretation.

Where Mn as MnO<sub>2</sub> concentrations are high due to permanganate reaction (e.g., depth interval 35-40 feet in the test plot (**Figure 5-49**) and depth interval 38-39 feet in the control plot (**Figure 5-50**)), the Mn was nearly 100% as MnO<sub>2</sub>. Where MnO<sub>2</sub> was low and permanganate was not detected (interval 40-45 feet in the test plot (**Figure 5-49**) and the intervals just above and below the 38-39 foot interval in the control plot (**Figure 5-50**)), the percentage as MnO<sub>2</sub> was significantly less, typically between 25 and 50%.

In general, the mass of Mn as MnO<sub>2</sub> and total mass of Mn extracted per mass of media are similar for the test and control plots that were most exposed to permanganate (**Figures 5-49 and 5-50**), particularly the one-year post-treatment samples closest to injection (Charts designated (A) in **Figures 5-51 and 5-52**, and **Figure 5-53**). The one-year post-treatment samples are actually most appropriate to use to make this assessment because the cores collected immediately post-treatment still had significant Mn present as permanganate based on observation. Also, there is greater data density for the one-year samples that were collected in order to intentionally make this assessment. An objective for the use of SHMP was to maintain MnO<sub>2</sub> solids suspended in the aqueous phase. Because of this, and also because we do not see higher concentrations of total solids (indicative of MnO<sub>2</sub>) in the groundwater measured in the CMTs of the test plot relative to the control (**Figures 5-37 and 5-38**), we cannot conclusively demonstrate that SHMP helps to keep MnO<sub>2</sub> suspended in this demonstration. The viscosity of the xanthan polymer, we believe, “holds” the MnO<sub>2</sub> within the bulk solution, which did not reach the monitoring wells. Therefore we also cannot say the SHMP did *not* keep MnO<sub>2</sub> suspended. The coring and extraction method does not differentiate soil-associated and pore water-associated MnO<sub>2</sub>. With the xanthan polymer included in the injection, it is difficult to assess the benefit of SHMP for inhibiting MnO<sub>2</sub> particle deposition, although we do suggest its use with xanthan polymer based on results of the treatability work conducted, which indicated less pressure increase in transport studies with polymer + SHMP than with polymer alone. We cannot extrapolate the findings to the field as we did not conduct a test with polymer and no-SHMP, however we do anticipate scalable results. SHMP not only supports suspension of MnO<sub>2</sub> particles, it will similarly affect any particles carrying a negative charge, thereby inhibiting their deposition and potential build-up of pressure and preferential flow.

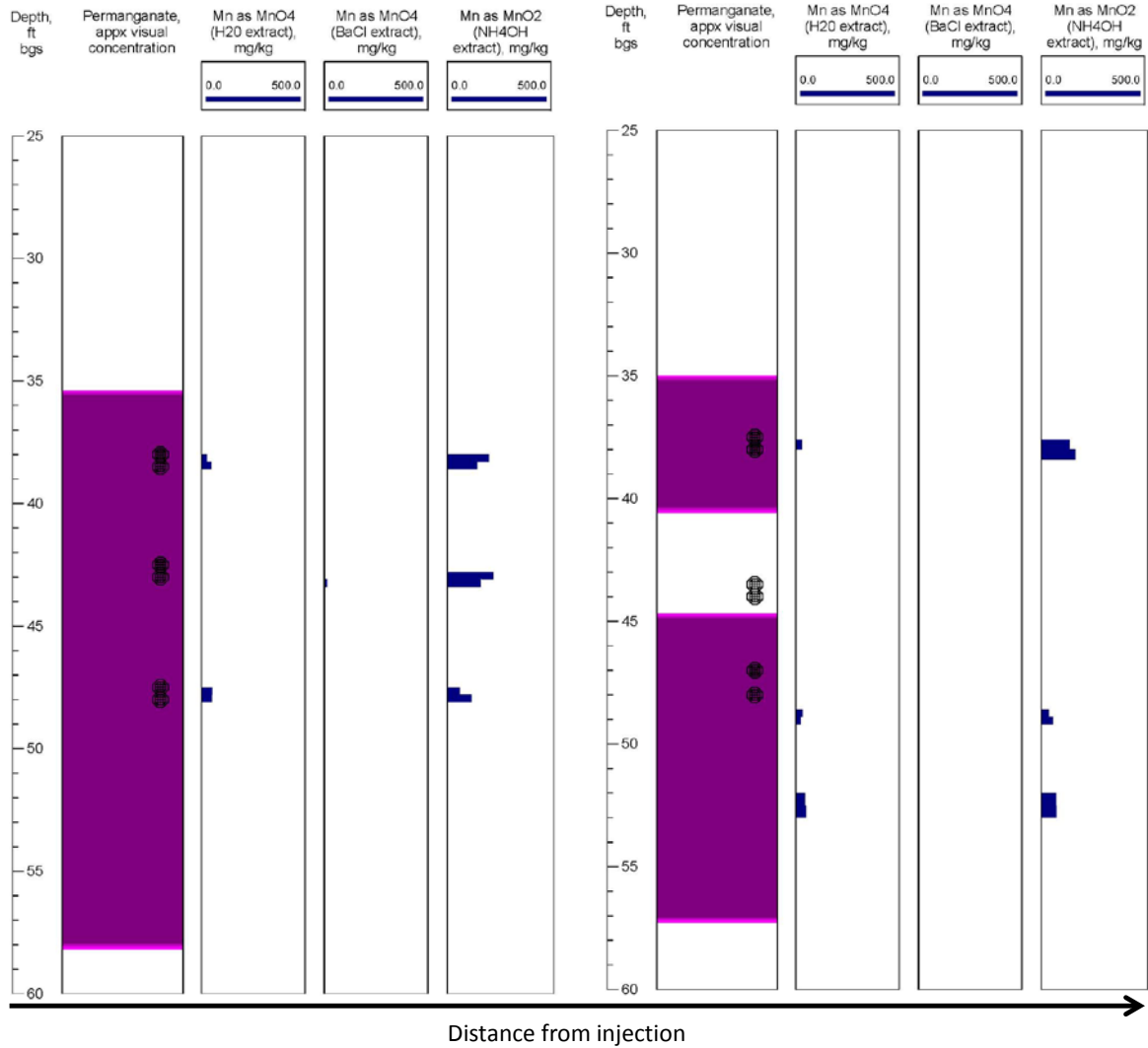


**Figure 5-49.** Manganese as water-extractable, Ba-extractable, and as MnO<sub>2</sub> for example test plot cores post-treatment with distance from injection. Dots on the permanganate distribution plot indicate locations where MnO<sub>2</sub> samples were collected; where no MnO<sub>2</sub> concentrations are shown on the MnO<sub>2</sub> concentration log, results are below detection (0.01 mg/kg).

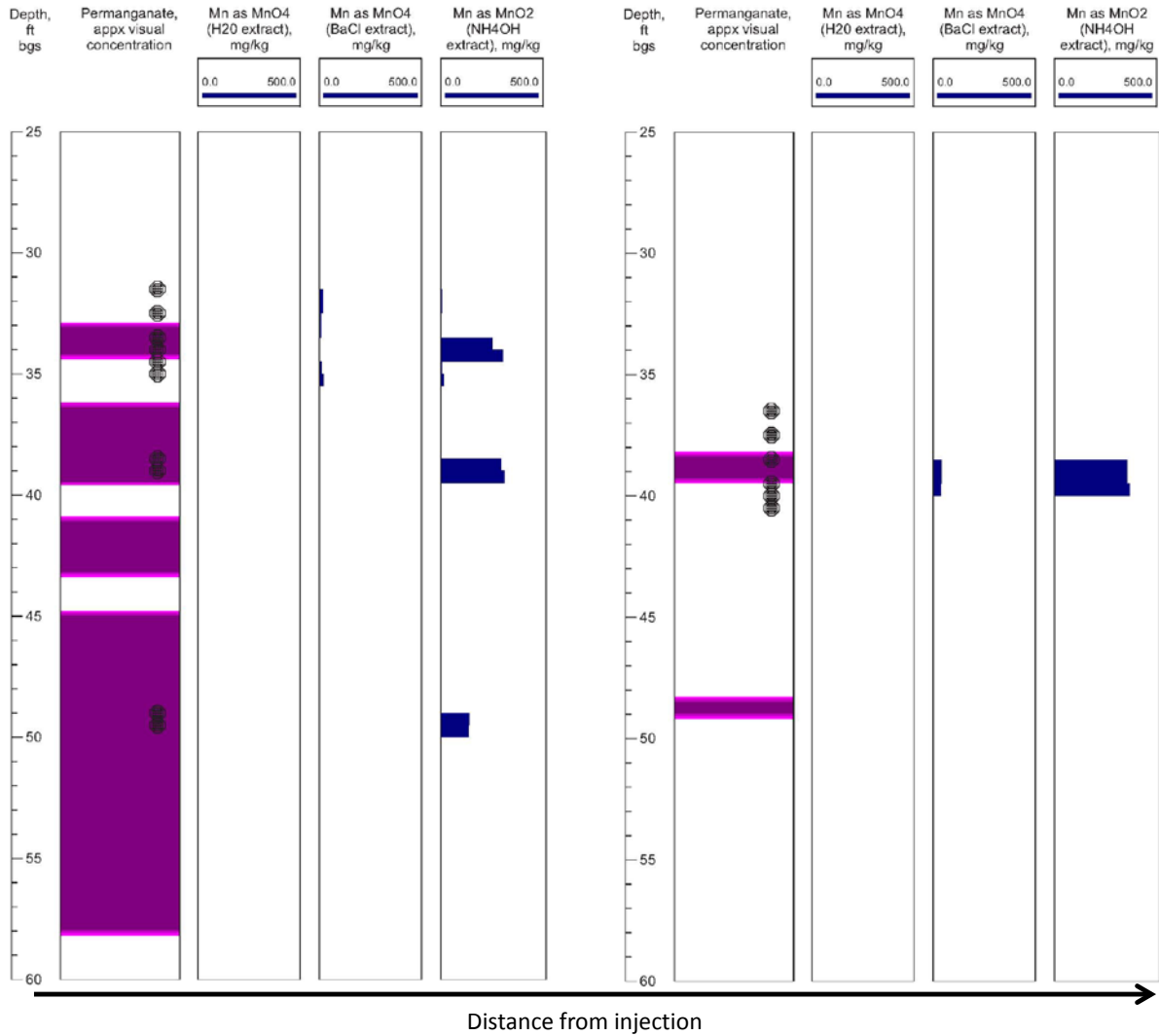


**Figure 5-50.** Manganese as water-extractable, Ba-extractable, and as MnO<sub>2</sub> for example control plot cores post-treatment with distance from injection. Dots on the permanganate distribution plot indicate locations where MnO<sub>2</sub> samples were collected; where no MnO<sub>2</sub> concentrations are shown on the MnO<sub>2</sub> concentration log, results are below detection (0.01 mg/kg).

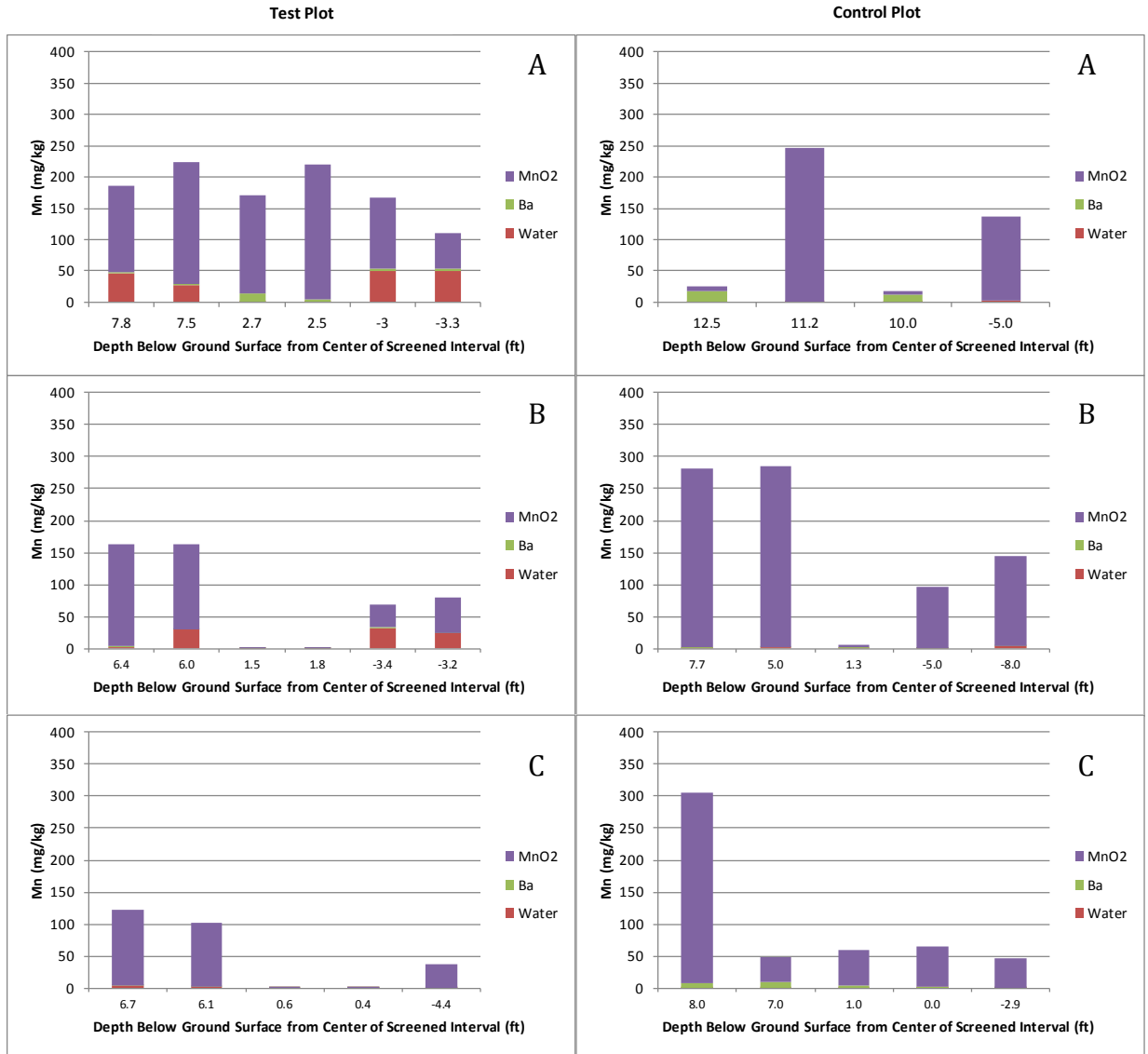


**Figure 5-51.** Manganese as water-extractable, Ba-extractable, and as MnO<sub>2</sub> for test and control plot cores collected immediately post-treatment with respect to depth (relative to the center point of the screened interval). Charts designated (A) are for cores approximately 5 ft. from injection, (B) are approximately 10 ft. from injection, and (C) are approximately 15 ft. from injection.

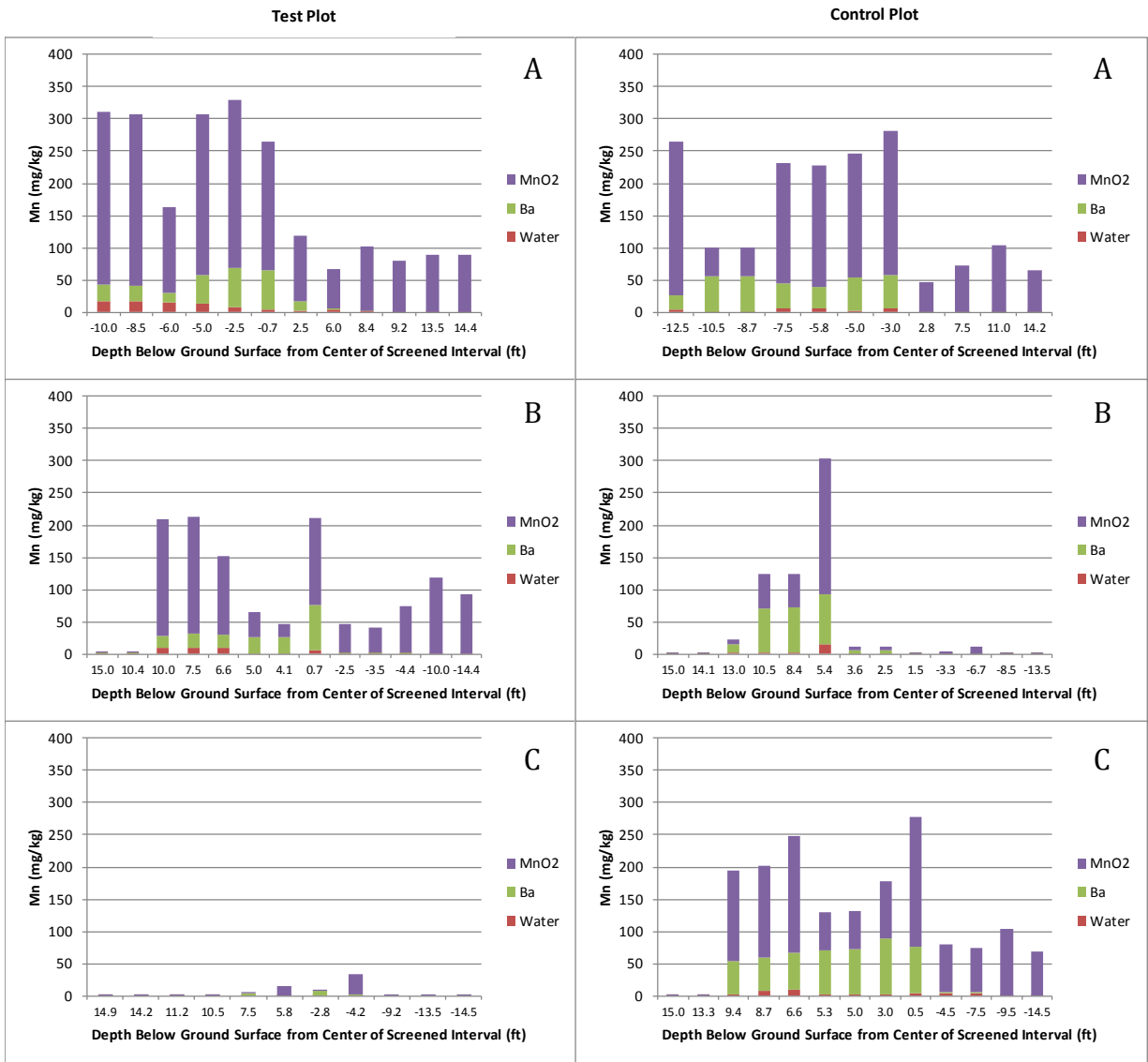


**Figure 5-52.** Manganese as water-extractable, Ba-extractable, and as MnO<sub>2</sub> for test and control plot cores collected one year post-treatment with respect to depth (relative to the center point of the screened interval). Charts designated (A) are for cores approximately 5 ft. from injection, (B) are approximately 10 ft. from injection, and (C) are approximately 15 ft. from injection.



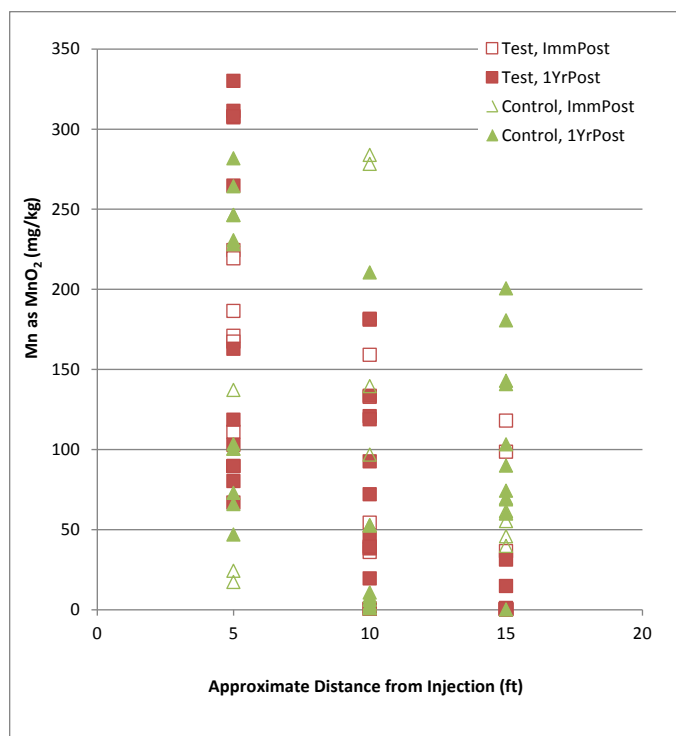


**Figure 5-53.** Mn as MnO<sub>2</sub> with distance from injection for test and control plots immediately post-treatment (Test, ImmPost and Control, ImmPost, respectively) and 1 year post-treatment (Test, 1YrPost and Control, 1YrPost, respectively).

The mass of Mn per mass of media generally decreases with distance in both the test and control plots (**Figure 5-53**). This result is expected for both plots regardless of the presence of polymer because areas closer to injection are exposed to a greater total mass of Mn as permanganate. The effect is more pronounced in the test plot where delivery was more uniform and where closer distances experienced greater permanganate exposure, as opposed to the preferential flow in the control which favored specific depths and traveled further in some layers than others.

**Figure 5-54** presents the molar mass relationship of total sodium and total manganese in the test and control plots cores collected immediately post-treatment (left-hand side) and for cores collected one year post-treatment (right-hand side). The resulting ratios of approximately 2:1 Na:Mn for the test plot and 1:1 Na:Mn for the control plot shown in **Figure 5-54** meet expectations because twice the mass of sodium was used in the test plot (which had sodium as sodium permanganate and sodium hexametaphosphate) than in the control plot (which had sodium only as sodium permanganate). The strength of the 1:1 relationship in the control plot, however, is weaker than the 2:1 relationship in the test plot in both the immediately post-treatment samples and the one-year post-treatment samples. There was greater scatter in the control plot data and the plausible reasons for this are twofold. First, the ratios increase significantly for samples collected where permanganate was not observed and measured MnO<sub>2</sub> concentrations are lower than approximately 2 mg/kg (**Figure 5-55**). Because the control plots had less uniform, more preferential flow, there were more data points that did not conform to the expected ratios that result from oxidant delivery. This translates to greater data scatter for the control plots, even though some (but few) of the Na:Mn ratios in the test plot are quite high.

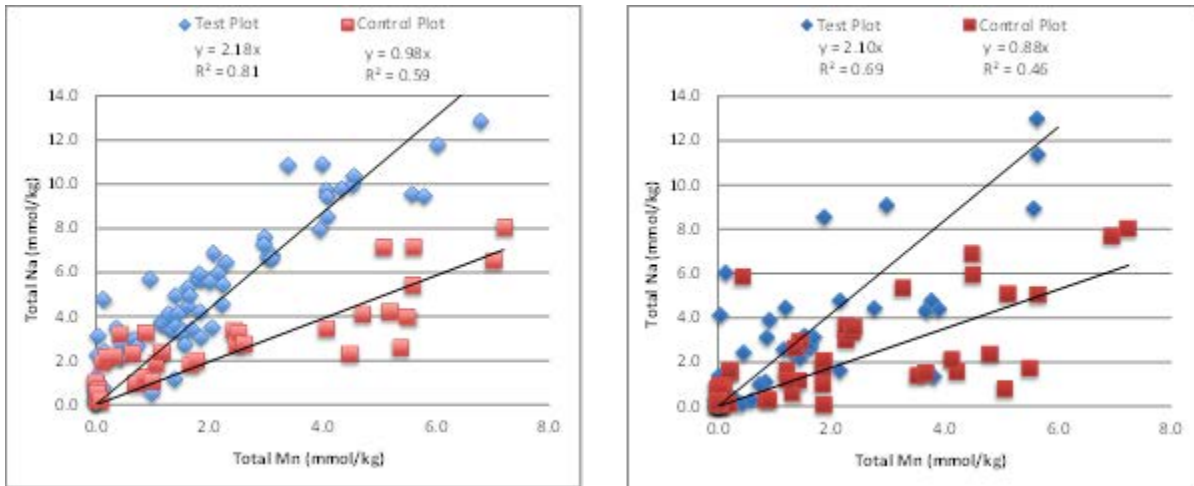


**Figure 5-54.** The relationship of total sodium to total manganese for the test and control plots immediately post-treatment (on the left) and one year post-treatment (on the right).

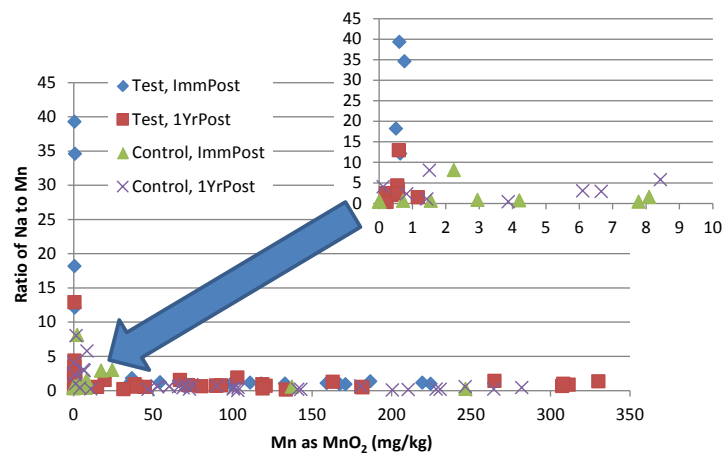


**Figure 5-55.** The ratio of Na to Mn with  $\text{MnO}_2$  concentration for test and control plots immediately post-treatment (Test, ImmPost and Control, ImmPost, respectively) and 1 year post-treatment (Test, 1YrPost and Control, 1YrPost, respectively).

Secondly, in the control plot, the data points indicating higher Mn and lower Na (sitting below the trend line) in **Figure 5-54** generally have a value of 4-6 mmol-Mn/kg and 2-4 mmol-Na/kg. This same grouping with a similar Mn concentration one-year post-treatment has lower associated Na values, though, of around 1-2 mmol-Na/kg, indicating that some sampled areas of the control plot may have experienced significant flushing of the Na (flow through of ambient upgradient groundwater). Sodium would decrease throughout the treated plots as it flushes from the treated areas, while a majority, or least some measurable amount, of  $\text{MnO}_2$  would be retained thereby decreasing the ratio, particularly in the control plot where viscosity isn't an influencing factor. It is possible that the higher viscosity in the test plot would inhibit movement of upgradient water through the treated area to that same extent.

**Figure 5-56** shows the Mn extraction data for all cores (test and control) that were collected immediately post-treatment and one year post-treatment, separated by extractant. The small amounts of dissolved Mn are predominately water-extractable in the test plot and Ba-extractable in the control plot. Because of the highly negative charge associated with the SHMP used in the test plot, cations such as Mn would tend to be loosely (electrostatically) associated with the media and readily exchangeable, whereas in the control plot, the formation of stronger surface complexes that require a stronger extractant to remove them is more likely.

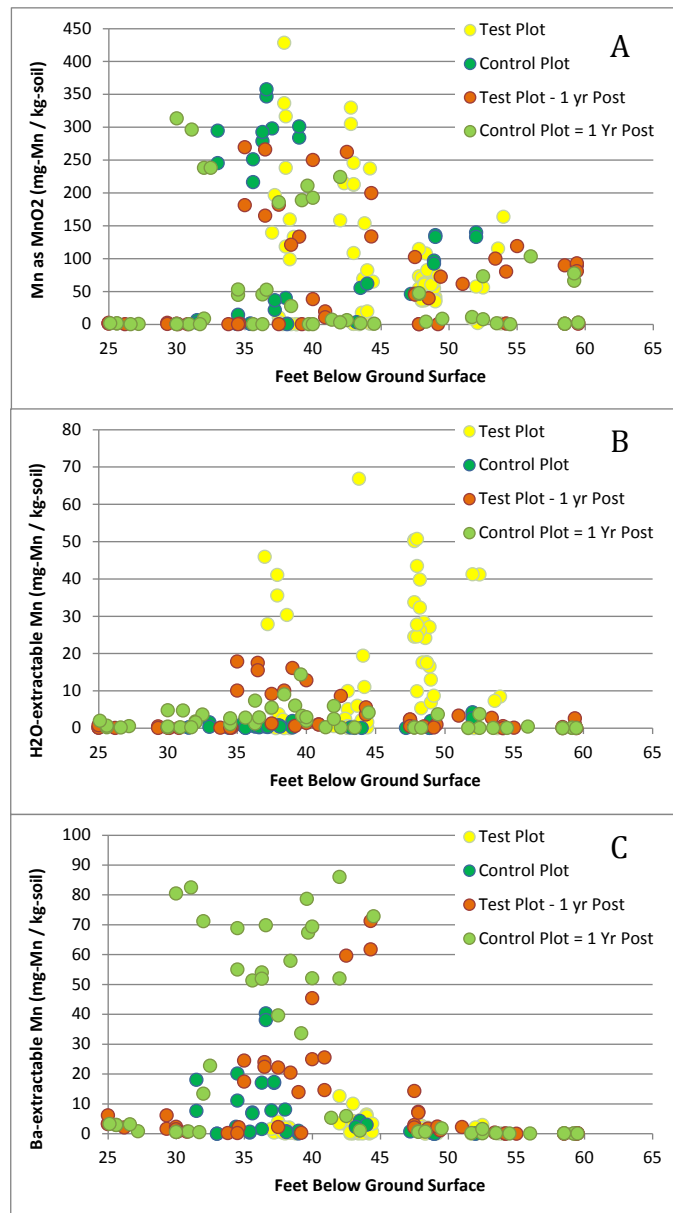


**Figure 5-56.** Mn extraction for test and control plot immediately post-treatment and one year post-treatment by depth. (A) Mn as MnO<sub>2</sub>, (B) water-extractable Mn, and (C) Ba-extractable Mn.

It is interesting to note that the extractability of Mn decreases with depth one year post-treatment (**Figure 5-56; Figures 5-51 and 5-52**). The results for both plots show very little dissolved (water and barium-extractable) manganese for either the control or the test plot at depth. We are investigating the relationship further, but a related geochemical parameter that shows a similar relationship is the cation exchange capacity (CEC). The CEC and anion exchange capacity (AEC) at the media's ambient pH were measured immediately post-treatment and one year post-treatment (**Figure 5-57**). While little difference in AEC is noted between the test and control plot and between the shorter and longer term, the CEC data show a remarkably higher CEC in the test plot one-year post-treatment. The data were further spatially analyzed and results are presented in **Figure 5-58**. The CEC vs. distance plot shows a stratified relationship. For the portion of the data with a higher CEC ( $> 15$  cmol/kg), the CEC increases with distance. For the portion with a lower CEC, the CEC is fairly consistent with distance. The CEC vs. depth profiles further helps to clarify results. The 30-45 foot interval represents the heart of the injection plot's screened interval. Here we see low CEC values, below 5. Surrounding this, above and below the screened interval, we have a significantly higher CEC. It would appear that treatment in the test plot with permanganate and polymer lowers CEC. However, in comparing results to the initial CEC of the test plot, we note that the initial CEC values measured on soil collected upon installation of the injection well, CMT 1, and CMT2 for the test plot are low (Appendix B). The injection well values for the 38-40 ft interval are 2.49 and 3.23. Values for CMT 1 between 38 and 39 ft are 0.89 and 0.71. Values for CMT 2 between 43 and 44 ft are 1.09 and 1.22. Furthermore, the immediately-post treatment sample CEC values do not show such high values even at depths matching those with high CEC one year post-treatment. Results point to a "fringe effect" where high values are measured above and below the intended treatment depth and the higher CEC values increase with distance from injection. The possible reasons for this effect are unclear but are being further investigated.

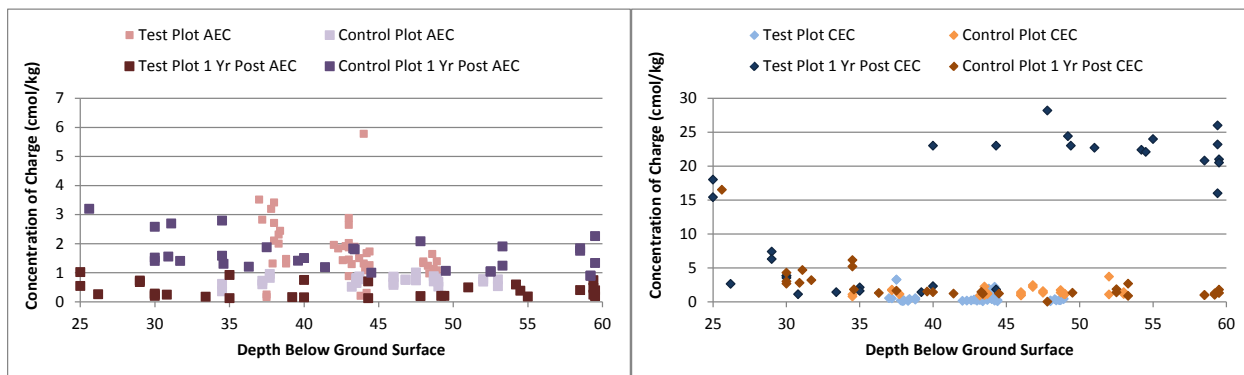


**Figure 5-57.** Anion exchange capacity (left) and cation exchange capacity (right) for test and control plot immediately post-treatment and one year post-treatment.

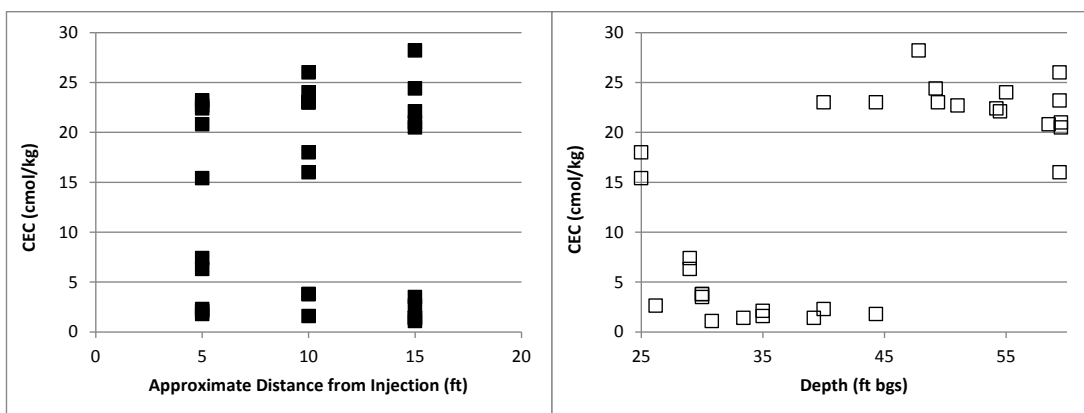


**Figure 5-58.** Cation exchange capacity for the test plot one year post-treatment with respect to distance from injection (left) and depth (right).

In summary, the manganese data for both groundwater and soil demonstrate greater preferential flow in the control plot and more uniform flow in the test plot. Manganese as  $MnO_2$  was similar in both the test and control plots, therefore it was not possible to evaluate the specific influence of SHMP on particle control, however we believe the higher viscosity of the test plot retains the  $MnO_2$  within the bulk solution. Using the two polymers together presents challenges to interpreting the influence of each separately; however experimental results indicate the value of including SHMP in the xanthan/permanganate solution. The value of SHMP alone with permanganate could not be determined. Manganese extraction data show differences in the geochemical effects of permanganate alone vs. permanganate plus polymer, particularly the cation exchange capacity, which increases at the apparent fringe of the polymer's direct influence at the one year post-treatment timeframe.

The Mn-related results actually point to more interesting influences of the polymer than those on Mn itself. Results point to the influence of viscosity on the movement of dissolved or suspended solutions (retaining them relative to surrounding water), indicating the polymer could be valuable in other contexts as an amendment delivery agent. For example, the relatively high natural demand of permanganate in these test and control plots resulted in relatively rapid loss of permanganate over time, however in a media with lower natural demand, we could expect permanganate to persist chemically – higher solution viscosity could also help to retain the permanganate spatially. Results also point to the influence of the polymer solution on media cation exchange. While this influence is less understood, improved understanding could provide guidance on how the polymer could be used to influence metals behavior in the subsurface. For example, if the polymer leaves behind a higher CEC over time, its use could translate to increased removal of metals species over time. This could add significant value in a combined remedies approach that is designed to influence both organics and metals species for a given site.

### 5.7.5 Fate of Polymer

The geochemical signature of oxidation discussed in several sections provides some evidence of the fate of the xanthan polymer (in combination with SHMP). As mentioned throughout sections 5.7.2 and 5.7.3, the polymer appears to retain the geochemical signature of oxidation (solids, Mn,

anions, cations, etc.), likely due to the solution viscosity. We see evidence of greater movement of the polymer-amended permanganate into lower permeability stratum relative to the permanganate control plot, as discussed relative to permanganate itself (Section 5.7.1), geochemistry (5.7.2), and Mn (as MnO<sub>2</sub> and as otherwise extracted) (Section 5.7.3). This section more closely examines measured viscosity in groundwater and results of sodium characterization toward understanding the fate of the polymer.

**Figure 5-59** shows the results of viscosity measurements and calculated biopolymer concentrations based on solution viscosity made on site. These results demonstrate that the biopolymer remains within the test plot, to some degree, one-year post-treatment. This result is somewhat surprising, given the rates of viscosity degradation (i.e. viscosity decreased to near water viscosity in a matter of a week to weeks at design permanganate concentrations) observed during our treatability testing. It would appear that during this field demonstration, the rate and degree of permanganate oxidation of the sediment was rapid and significant enough to effectively reduce the concentration of permanganate within the polymer-amended solution. This reduction in permanganate concentration appears to have been enough to retain a portion of the original injected solution viscosity within the treatment zone one-year post-treatment.

Sodium (from sodium permanganate and from sodium hexametaphosphate) concentrations help to understand the fate of the polymer as well. **Figures 5-60 and 5-61** present sodium concentrations measured in groundwater samples for the control and test plots, respectively. The order of magnitude difference in the concentration scale for the test and control plots is striking, particular because twice the amount of sodium injected into the control was injected into the test plot. The sodium in CMT 3 in the control plot shows the preferential flow of oxidant solution in this area, with the bulk passing through the well during delivery. One year post-treatment, concentrations are back to ambient levels. CMT 3 is in the path of groundwater flow from injection, so this is not surprising. CMT 4, to the northeast of injection and perpendicular to ambient groundwater flow, did not show this same pattern. High concentrations were not measured during injection, but were found there one year post-treatment. Results for other ISCO outcomes, including solids concentrations, PCE concentrations, and sulfate concentrations are similar. Permanganate data from soil cores, **Figures 5-20 through 5-22**, show the bulk movement of permanganate between CMT 3 and 4 well positions. It appears that CMT 3 captured the real-time movement of oxidant in the control plot and CMT 4 is capturing the longer-term influence of diffusion and dispersion of affected groundwater within the control plot.

Polymer Concentration Based on Viscosity Measurement			
Date	Well	Port #	Concentration (mg/L)
11/3/2011	1	2	1.73±0.64
11/3/2011	1	3	1.97±1.4
11/3/2011	1	4	9.03±1.34
11/3/2011	1	5	BDL
11/3/2011	2	2	6.99±0.99
11/3/2011	2	3	3.87±1
11/3/2011	2	4	16.96±1.04

**Figure 5-59.** Polymer concentration as indicated by viscosity measured one year post-treatment in CMT 1 (Well 1 in table) and CMT 2 (Well 2 in table) with depth as designated by the port number.

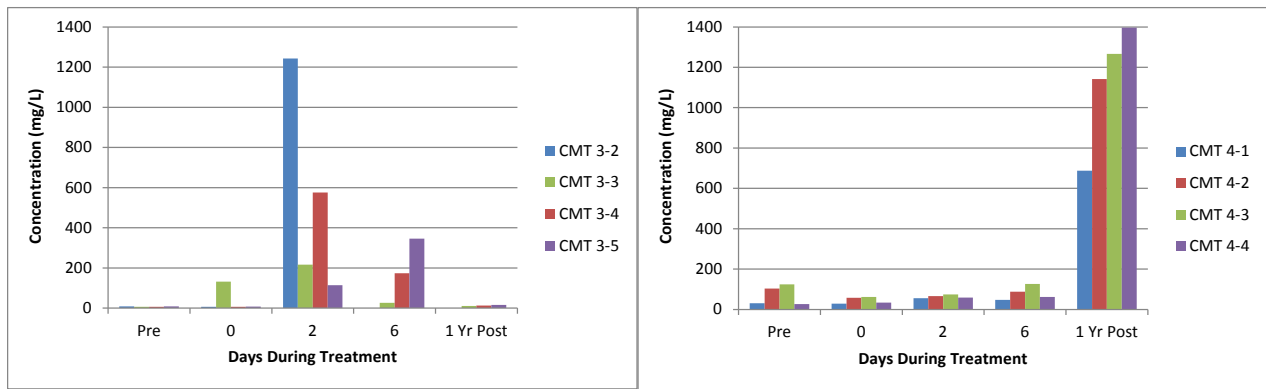


**Figure 5-60.** Sodium concentrations for the control plot's CMT 3 and 4.

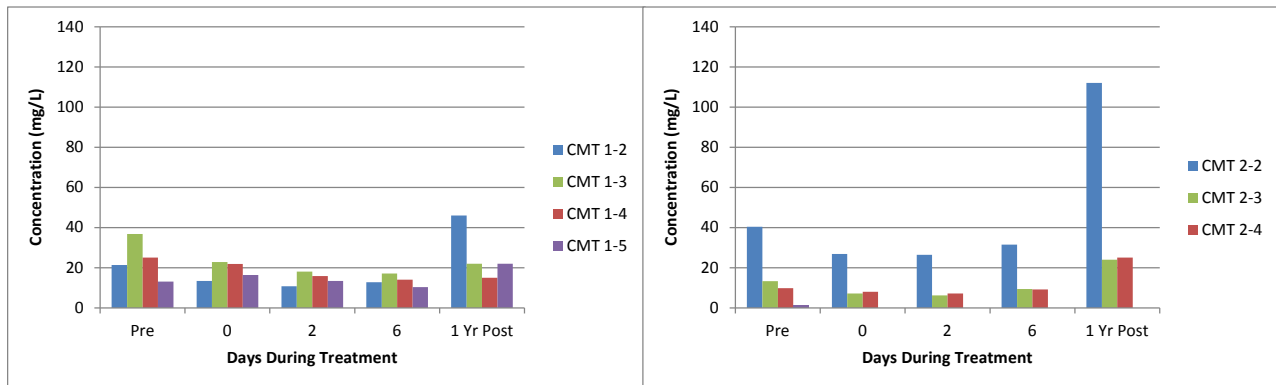


**Figure 5-61.** Sodium concentrations for the test plot's CMT 1 and 2.



The test plot shows little change in measured sodium concentrations in CMTs 1 and 2 during delivery, which is consistent with the fact that permanganate was also not observed in these wells during delivery. It is also consistent with the supposition that the remnant viscosity of the polymer solution retains the geochemical signature of permanganate oxidation that had not yet arrived at these well locations by the end of the injection period. At one-year post-treatment, sodium concentrations are somewhat higher in CMTs 1 and 2, but are still an order of magnitude lower than the highest concentrations measured in the control plot wells (i.e., CMTs 3 and 4). Based on these results for sodium, the following two possibilities present themselves:

1. The sodium initially injected into the test plot has passed out of the treatment zone and ambient conditions were reestablished within one year post-injection, or
2. The injected sodium remains within the test plot as a component of the geochemical signature, described previously, and that the sodium measured at CMT 1 represents a dissolution front of sodium being released from the residual polymer solution.

Measurements of sodium via extraction associated with solids help to clarify which of these possibilities is most likely. **Figure 5-62** presents sodium extraction data for test plot samples collected immediately post-treatment (left) and for samples collected one year post-treatment (right). One year later, sodium concentrations in the test plot are similar to, or even higher than, those for samples collected immediately post-treatment at the distance of approximately 5 ft, which is closest to injection. The concentrations in the farther distances (10 and 15 ft) are lower than those for samples collected immediately post-treatment. This is in indication that the polymer may be retreating via dissolution rather than being flushed from the treated area.

It is important to understand that the elevated post-treatment viscosity described in this section does not exist as a viscous gel within the treated formation. The zero-shear viscosity (maximum) of the injected solution was just 36 cp (or 36 times the viscosity of water), similar to the viscosity of vegetable oil. One-year post treatment this viscosity is likely a fraction of the injected PA-ISCO fluid viscosity (**Table 5-2**). However, given the low hydraulic gradient at this demonstration site (0.0004 ft/ft, **Section 4.2.2**) the remnant viscosity is still viscous enough to partially divert groundwater flow around the treatment zone, resulting in polymer dissolution at the edges of the treated zone at a rate that was slower than anticipated. For a site exhibiting lower natural oxidant demand, viscosity retention would be less significant. In the present case, the implications of this observed viscosity retention is that restoration of the original hydraulic conductivity within the treatment zone will be slowed (under natural hydraulic gradient conditions) and that the rate of migration of the by-products of permanganate oxidation will be slowed. The rate of dissipation of polymer solution viscosity could be greatly accelerated by injecting water into the injection well, as required, to meet site-specific treatment objectives.

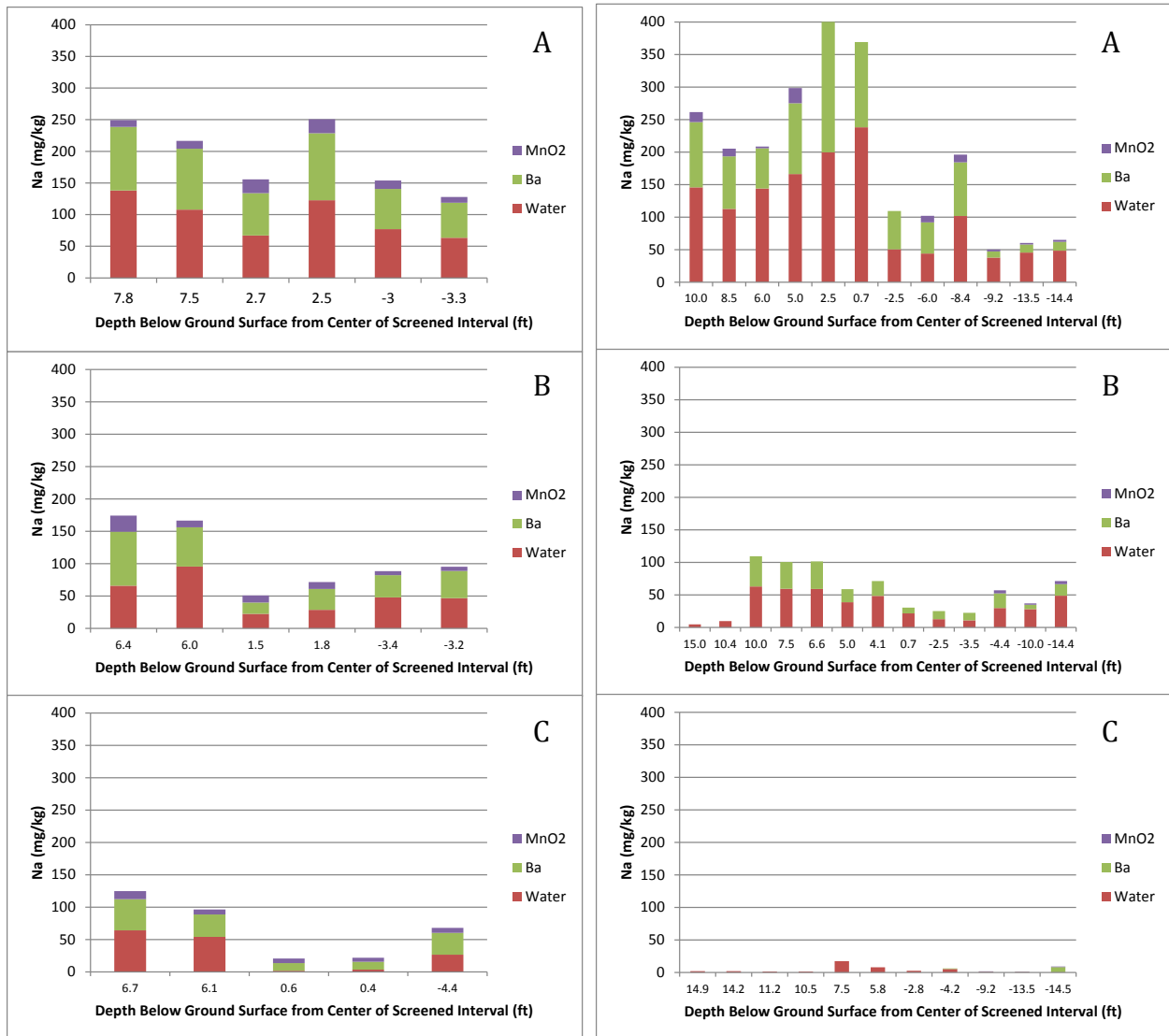


**Figure 5-62.** Sodium as water-extractable, Ba-extractable, and associated with MnO<sub>2</sub> solids structure for the test plot cores collected immediately post-treatment (left) and one year post-treatment (right) with respect to depth (relative to the center point of the screened interval). Charts designated (A) are for cores approximately 5 ft. from injection, (B) are approximately 10 ft. from injection, and (C) are approximately 15 ft. from injection.

## 6.0 PERFORMANCE ASSESSMENT

Table 6-1 shows the performance criteria, data requirements, success criteria, and results for the demonstration/validation of polymer-amended ISCO, which are further described below.

**Table 6-1. Performance Objectives**

Performance Criteria	Data Requirements	Success Criteria (with use of polymer)	Results
<b>Quantitative Performance Objectives</b>			
Increased penetration of oxidant into lower permeability layers/strata	<ul style="list-style-type: none"> <li>- Examination of soil cores for evidence of permanganate or MnO<sub>2</sub></li> <li>- If LPM of thickness appropriate for discrete groundwater sampling is present, then MnO<sub>4</sub><sup>-</sup>/MnO<sub>2</sub> concentrations measured in groundwater over space and time</li> </ul>	<ul style="list-style-type: none"> <li>- 50% longer distance of permanganate penetration into lower permeability layers/strata</li> <li>- 25% higher permanganate concentration at expected time of arrival in each monitoring well</li> <li>- Demonstrated improvement in vertical sweep efficiency within lower permeability layers/strata</li> <li>- Demonstrated improvement in overall vertical sweep efficiency in test plot</li> </ul>	Objective met
Decreased flow bypassing (increased lateral sweep efficiency) of areas of high contaminant mass	<ul style="list-style-type: none"> <li>- Examination of soil cores for evidence of permanganate or MnO<sub>2</sub> in media with high contaminant concentration</li> <li>- Soil core extractions for MnO<sub>2</sub> and measurements of MnO<sub>4</sub><sup>-</sup> and MnO<sub>2</sub> in groundwater over time and distance</li> <li>- Soil core extractions for contaminant with distance</li> </ul>	<ul style="list-style-type: none"> <li>- 50% lower mass of MnO<sub>2</sub> in given mass of media (indicative of inhibition of deposition that can increase bypass)</li> <li>- 25% greater mobile MnO<sub>2</sub> concentration at given time point in monitoring well</li> <li>- 50% lower mass of contaminant in high concentration cores</li> </ul>	Objective partially met; sweep was improved, however not specifically associated with high contaminant mass
Evaluate long-term potential for and short-term occurrence of contaminant rebound	<ul style="list-style-type: none"> <li>- Contaminant concentrations in groundwater over time and distance</li> <li>- Contaminant concentrations in soil cores pre- and post-treatment</li> </ul>	<ul style="list-style-type: none"> <li>- Data collected and are representative of test plots</li> <li>- Post-treatment groundwater monitoring results remain below baseline concentrations</li> </ul>	Objective partially met
Improved contaminant treatment effectiveness	<ul style="list-style-type: none"> <li>- Contaminant concentrations in groundwater over time and distance from injection</li> <li>- Contaminant mass in soil over time and distance</li> </ul>	Statistically significant reduction in contaminant mass as compared to a control plot	Objective met
<b>Qualitative Performance Objectives</b>			
Decreased impact of MnO <sub>2</sub> on injection pressure	Injection well pressure over time	No increase in injection pressure attributable to MnO <sub>2</sub>	Objective met
Improved understanding of impacts of polymers on groundwater quality	pH, ORP, key metals, solids concentrations, conductivity, bioactivity	Note differences	Objective met

## **6.1 INCREASED PENETRATION OF OXIDANT INTO LOWER PERMEABILITY LAYERS/STRATA**

The penetration of oxidant into lower permeability layers/strata was assessed by logging lithology and the distribution of permanganate in soil cores collected immediately post-treatment and comparing these for the control (permanganate only) and test plots (permanganate plus polymer). We evaluated the distance permanganate penetrated lower permeability strata and calculated the sweep efficiency of the oxidant using geostatistical methods. Also, groundwater monitoring wells screened over different lithologic units captured the movement of permanganate through different layers, and these data were compared for the control and test plots.

Soil core and groundwater data demonstrate improved, more uniform distribution of permanganate through the polymer test plot relative to the control plot through multiple lines of evidence including permanganate concentrations and numerous geochemical parameters monitored. Sweep efficiency with delivery of one pore volume of oxidant solution to the control plot (permanganate only) was 33%, whereas sweep efficiency in the test plot with polymer was 67% (**Figures 5-28 and 5-29**).

## **6.2 DECREASE FLOW BYPASSING OF AREAS OF HIGH CONTAMINANT MASS**

This objective was selected prior to selecting the project's site, and relates to the use of SHMP for control of MnO<sub>2</sub> byproduct. Where contaminant mass is high (i.e., NAPL), SHMP can prevent the deposition of MnO<sub>2</sub> around areas where oxidant contacts contaminant where preferential flow can then occur. It was determined that assessment of sweep efficiency with polymer was a higher priority criterion than MnO<sub>2</sub> control, therefore site selection and demonstration design was focused on appropriate conditions for assessing sweep (e.g., heterogeneity distribution and overlying semi-confining layer). While contamination in the area where this demonstration was performed was indeed present, concentrations were not high enough to specifically assess this criterion therefore findings are inconclusive. MnO<sub>2</sub> distributions in soil were measured post-treatment. Similar concentrations of MnO<sub>2</sub> were measured in the control and test plot, however, we believe the viscous polymer solution in the test plot holds the geochemical signature, including MnO<sub>2</sub> solids, therefore we would not be able to detect a difference until the polymer-treated plot is fully restored to pre-treatment conditions (i.e., viscosity dissipated and MnO<sub>2</sub> "released"). Sweep efficiency was improved with polymer as discussed above, however its relationship to contaminant mass is not established.

## **6.3 EVALUATE LONG-TERM POTENTIAL FOR AND SHORT-TERM OCCURRENCE OF CONTAMINANT REBOUND**

Rebound assessment was made by evaluating groundwater concentrations over time in each of the control and test plots, as well as post-treatment soil concentrations. Approximately 1 calculated pore volume (PV) was delivered to each the test and control plot for demonstration purposes. MCIEAST-MCB CAMLEJ sediments in our test area have a high natural demand for oxidant, as determined during treatability evaluations, and a high organic carbon content to which contaminants can be strongly sorbed. While a 1 PV flush is sufficient to assess differences in permanganate distribution, which is the project's focus, we would not expect

100% treatment within these pilot scale plots, making this a challenging success criterion. This objective was partially met.

Measured groundwater concentrations show the influence of preferential flow through the control plot as a function of lithology during treatment. A decrease in concentration corresponds with the arrival of permanganate in the wells at different times for different depths. Concentrations rebounded, however, likely because upgradient groundwater re-entered the plot and/or remaining sorbed mass in the untreated layers re-equilibrated with the aqueous phase. In the test plot, however, evaluation of VOCs is inconclusive because evidence indicates that the polymer remains in the plot and is slowly “releasing” the geochemical signature of oxidation. We suspect preferential flow around the test plot due to presence of polymer. If this is the case, measurements in the well are stagnant until polymer dissolves and ambient flow is returned. This is not a negative result; simply inconclusive. Theory and our understanding of ISCO based on many years of practice and thousands of applications indicate that where oxidant and contaminant meet, reaction occurs. Soil core data do show low to no VOCs in permanganate-impacted soils, while VOCs remain at pre-treatment levels in unaffected soils. The test plot experienced twice the sweep of the control plot and the overall treatment effectiveness in the test plot is greater.

To achieve more effective treatment at the full-scale, multiple injections and pore volumes would be necessary, as it would for most ISCO sites. The advantage of the polymer-addition is that by improving the sweep efficiency, greater contact can be achieved between the oxidant and the existing contaminant with fewer pore volumes and fewer mobilizations. Polymer-addition mitigates the effects of preferential flow and promotes penetration of oxidant into lower permeability geomeia (Silva et al., 2012b). In the absence of polymer-addition, where preferential flow exists, there is a diminished return on the injection of multiple pore volumes as the injected fluids will largely continue through the same preferred pathways, and while beneficial to treat sorbed mass, rebound can occur by back diffusion out of lower permeability zones.

As described in Section 8.4, the more effective mode of PA-ISCO treatment would involve a multiple pore volume treatment strategy that would take advantage of the physics of viscosity-modified fluid transport processes to maximize sweep-efficiency in heterogeneous geomeia. However, if a multiple injection strategy is employed, the timing of re-injection events would not be critical to remnant viscosity (if any) of the previous treatment. This is to say that the remnant viscosity need not completely dissipate prior to another injection. Nonetheless, it could be advantageous to utilize components of the post-treatment geochemical signature to base the timing of subsequent treatments (e.g. absence of permanganate, presence of by-products and rebounding contaminant) from samples collected at monitoring well locations positioned within the treatment area.

#### **6.4 IMPROVED CONTAMINANT TREATMENT EFFECTIVENESS**

As mentioned above, because sweep was greater in the test plot than in the control, a greater mass of media was contacted by permanganate in the test plot. Where permanganate did reach contaminant, low to non-detect concentrations of the VOCs were measured. A statistical

analysis of treatment effectiveness was not possible because of the few number of cores collected pre-treatment, which were limited to the injection well and CMT installation locations to preferential movement of polymer/permanganate to the surface. High concentrations of contaminant remained in the test plot at the 44-45 ft. interval where permanganate movement into this interval was limited. Most other depths, particularly those closer to injection where permanganate presence was nearly uniform were treated effectively, which is significant because the extent of contamination, in terms of both concentration and spatially with depth, was greater for the test plot than for the control. While the control plot had less contamination initially, there were more intervals unaffected by oxidant and left untreated.

## **6.5 DECREASED IMPACT OF $MnO_2$ DEPOSITION ON INJECTION PRESSURE**

Either deposition of  $MnO_2$  due to reaction with natural media and/or contaminants, the viscosity of the PA-ISCO solution itself, or the retention of polymer (via filtration or sorption) within the porous media could result in increased injection pressures. Because of the relatively low contaminant concentrations associated with the solids and also because we used SHMP to alleviate polymer retention and  $MnO_2$  deposition (benefits described in Section 5.3.1 based on treatability study results), we did not anticipate a significant increase in pressure. No significant increases in injection pressure related to  $MnO_2$  and the use of polymer were observed for either the test or the control plot.

## **6.6 PERFORMANCE OBJECTIVE: IMPROVED UNDERSTANDING OF IMPACTS OF THE ENHANCED DELIVERY APPROACH ON GROUNDWATER QUALITY**

Because the use of polymers with oxidant has not been evaluated in the field, it would be generally beneficial to improve the understanding of potential effects of polymer addition on groundwater quality. We collected extensive data on geochemical parameters of the soils and groundwater, as described in Section 5.7. Key findings include:

- Polymer apparently retains the geochemical signature of oxidation, including solids generated, metals (including Mn and Cr), and anions (including sulfate).
- Polymer appears to “retreat” from the leading edge following application rather than flush through the treated area, which can result in a slower “release” of the geochemical signature. Results up to one-year post-treatment are showing the beginning of this release. Both operational and treatment performance monitoring approaches should be adapted accordingly when applied at the full scale.
- Treatment using xanthan with SHMP results in a higher cation exchange capacity in soils around the “fringe” of treatment. The cause of this effect is unclear and warrants further study as it can possibly be manipulated to affect metals naturally present or present as co-contaminants.

## 7.0 COST ASSESSMENT

This section presents the results of an additional costs assessment to implement PA-ISCO. These costs are focused on the costs above and beyond those commonly associated with permanganate ISCO treatments that are well understood. Section 7.1 describes a cost model that was developed to demonstrate the additional costs associated with PA-ISCO application; Section 7.2 presents an assessment of the additional cost drivers for PA-ISCO technology; and Section 7.3 presents the results of an analysis of the cost model.

### 7.1 COST MODEL

A cost model was developed to assist remediation professionals in understanding the costs associated with including polymer-amendment for permanganate ISCO treatment. The cost model identifies the major cost elements specific to the inclusion of polymer-amendment at a site similar to the demonstration site described in this report. Excluded are costs typical of regular permanganate treatment, with the purpose of focusing on the excess costs of including polymer.

A summary of the costs associated with this first pilot-scale field demonstration of PA-ISCO is presented in **Table 7-1**. The cost model was developed for a template site of similar scale and site characteristics observed during this field demonstration. These characteristics are presented in **Table 7-2**. Cost elements and data that were tracked during this first field demonstration focus on those that are above-and-beyond the costs of the typical permanganate-only ISCO approach. Specifically excluded from consideration are the costs associated with pre-remediation activities (e.g., characterizing contaminant distribution using membrane interface probe, risk determination and related needs), treatability testing specific to the optimization of permanganate concentrations, and post-treatment decommissioning. Also excluded are costs associated with well installation (including multi-level screened monitoring wells) and investigation derived waste (e.g., contaminated soil cuttings and well development water) characterization and disposal.

As this field demonstration was led by University employees and associates, actual labor costs were based on student wages. To provide a more realistic cost model, the labor costs presented in **Table 7-1** were based on an assumed loaded hourly rate of \$85 for a typical mid-level Geologist /Scientist/Laboratory Technician and a \$100 hourly rate for a typical Project Engineer.

It is important to remember that PA-ISCO is a new and novel technology and the costs associated with this first field demonstration should be expected to be higher. PA-ISCO costs are expected to decrease as additional implementation experience is gained during future applications. This is true of most novel groundwater remediation technologies when they were first being evaluated.



**Table 7-1. Cost Model for PA-ISCO (16 days total characterization and injection)**

<b>Cost Element</b>	<b>Data Tracked During Demonstration</b>	<b>Costs</b>	
<b>Site Characterization</b>	Vertical Characterization of Permeability (DPT – pneumatic slug testing and or CPT pore pressure dissipation tests plus data analysis <u>performed concurrent with soil sampling</u> )	Subcontractor	\$4,500
		Field Geologist	\$2,040
		Engineer/Scientist Analysis	\$400
	Injectivity Testing (2 field days plus analysis)	Geologist	\$1,360
	Soil Sampling – Treatability Testing	Subcontractor	\$1,500
		Geologist	\$680
Sample shipping		\$800	
<b>Treatability Testing</b>	Labor, materials, and analytical costs for batch experiments, transport experiments, and data analysis	Lumped costs	\$4,300
<b>Materials Costs</b>	Polymer Costs	Xanthan gum	\$3,200
		SHMP	\$1,180
	Polymer Mixing Equipment		\$20,000
	Process Control System*		\$54,000
<b>Installation/ Decommission</b>	Process Control System Subcontractor	Subcontractor (fee)	\$5,000
	Shipping of equipment	To and from site	\$10,000
	Labor	Project Engineer	\$2,400
	Labor	Project Scientist	\$2,040
<b>Operation and Maintenance</b>	Labor – Initial polymer concentrate preparation.	Project Scientist (8 hrs prior to injection operations)	\$680
	Labor – Daily polymer preparation	Project Scientist (4 hrs per day for 4 days)	\$1,360
	Equipment Rental (generator and overhead lighting)	Total per 7 day preparation and injection duration	\$3,000
			<b>\$118,440</b>

\* See discussion of the Process Control System in Section 7.1.3

**Table 7-2. Cost Analysis Design Basis for Template Site MCIEAST-MCB CAMLEJ, North Carolina**

<b>Design Parameter</b>	<b>Units</b>	<b>Quantity</b>
<i>Target Treatment Area Dimensions and Hydrogeology</i>		
Total Depth	ft bgs	60
	m bgs	18.3
Depth to Water	ft bgs	12
	m bgs	3.7
Treatment depth interval	ft bgs	28-60
	m bgs	8.5-18.3
Treatment zone radius	ft	15
	m	4.6
Total treatment area	ft <sup>2</sup>	706.5
	m <sup>2</sup>	65.7
Total treatment volume	ft <sup>3</sup>	22,608
	m <sup>3</sup>	640.7
Average Hydraulic Conductivity	ft/day	6.2
	m/day	1.9
Horizontal Groundwater Gradient	ft/ft	0.002
Average porosity assumed	--	0.35
Treatment pore volume	gallons	59,187
	ft <sup>3</sup>	7,913
	m <sup>3</sup>	224
Sediment bulk density (dry)	kg/m <sup>3</sup>	1,800
Total soil mass in treatment volume	kg	1,153,223
<i>Injection Design</i>		
Number of injection points		1
Injection point ROI	ft	15
	m	4.6
Design Concentration of NaMnO <sub>4</sub>	mg/L	5,000
Design Concentration of SHMP	mg/L	3,000
Design Concentration of xanthan gum	mg/L	500
Number of pore volumes injected	--	1
Number of monitoring wells	--	2
<i>Per Pore Volume Chemical Demands</i>		
Mass of MnO <sub>4</sub> required	kg	1,121
	lb	2,466
Mass of xanthan gum required	kg	112
	lb	246
Mass of SHMP required	kg	670
	lb	1474

### 7.1.1 Cost Element: Site Characterization

Site characterization is required for permanganate ISCO to assess a site's hydraulic properties, contaminant distribution and degree of contamination, and natural oxidant demand to determine dosage requirements and other design parameters necessary for successful in situ treatment. The same is true for PA-ISCO. However, additional site characterization activities are required, including:

1. Discrete vertical characterization of permeability to assess the need for polymer amendment or to optimize polymer concentrations for maximal sweep efficiency improvement.
2. Injectivity testing to determine the maximum injection pressure and the averaged hydraulic conductivity of the formation.
3. Collecting depth-discrete soil and groundwater samples to assist treatability testing related to assessing the potential for permeability reduction.

Therefore, the cost model for this cost element reflects these additional costs. For this demonstration a DPT rig was used to perform depth-discrete slug testing to vertically characterize hydraulic conductivity of the treatment zone. Additional hydraulic testing methods were attempted utilizing pore pressure dissipation tests via high-resolution piezocone but these attempts were largely unsuccessful for the site subsurface conditions. Soil and groundwater samples were collected during the single site characterization event that included hydraulic profiling and well installation for the demonstration. Injectivity testing was performed using a step-injection test mode utilizing the injection well installed for the demonstration and the process control system constructed for the demonstration. Labor and subcontractor costs for the site characterization efforts were tracked as presented in **Table 7-1**.

### 7.1.2 Cost Element: Treatability Test

While oxidant demand tests to determine the rate and extent of permanganate interaction with natural subsurface media are recommended whether or not polymer amendments are added, the use of polymer requires additional testing that involves increased labor, materials, and analytical costs. Additional testing includes the determination of optimal xanthan and SHMP concentrations to use on a site-specific basis at the batch scale, characterization of concentration-specific rates of reaction of xanthan and permanganate (albeit slow), and, ideally, 1-D transport evaluations to assess potential impacts to conductivity and flow. Costs were tracked on a per site basis and will apply to a demonstration of any scale as they appear in **Table 7-1**, which again are those costs additional to those of a typical permanganate ISCO project.

### 7.1.3 Cost Element: Material Cost

Materials costs specific to PA-ISCO that were tracked during this demonstration included polymer chemical costs, the cost of the polymer mixing equipment, and the cost of a process control system (PCS) capable of monitoring and maintaining polymer dosing and injection flow rate for automated 24-hour operation.

The importance of 24-hour injection relates to the physics of viscosity enhancement and its effect on sweep efficiency improvement as described in detail by Silva et al. (2012b). Briefly, the mechanism of sweep improvement involves the maintenance viscous cross-flow potentials between strata of variable permeability. Therefore, a steady and continuous flow condition must be maintained during treatment to maintain solution viscosity at design levels to maintain cross-flow potentials. Additionally, automated 24-hour injection was a necessity for this site because we were not able to staff overnight operations on base.

The PCS designed and constructed for this pilot demonstration possessed a somewhat higher degree of complexity than would be necessary for a more typical permanganate ISCO operation and this degree of complexity is reflected in the cost of the PCS. However, significant cost savings were realized by eliminating the need to staff overnight monitoring of the injection operation. The PCS included separate flow-control, chemical dosing, and injection modules each of which were electronically monitored and linked to a telemetry alarm system. Each of these systems and associated electronics were mounted on a steel skid to minimize on-site installation labor costs. An additional skid-mounted system housed fluid homogenization and filtration modules.

The polymer mixing equipment purchased for this demonstration was a skid-mounted hydrodynamic mixing system with a stainless steel dry chemical hopper and recirculation pump. A polymer concentrate was made on site prior to and during injection and transferred to a 2,500 gallon storage tank. Capital equipment costs for this system are presented in **Table 7-1**. However, costs savings related to polymer concentrate solution preparation could be realized by sourcing a pre-made concentrate solution, of sufficient volume, that could be trucked to the site and contained within a large liquid product tanker trailer throughout the injection period. This would obviate the equipment and labor costs related to on-site polymer concentrate preparation.

Polymer chemical costs were tracked on a mass used per treatment pore volume basis. The polymer mixing and process control system costs were tracked as a lump sum for the demonstration, but will be implemented on a cost per pore volume basis during the cost analysis presented in Section 7.3.

#### **7.1.4 Cost Element: Installation**

Installation costs tracked during this demonstration relate to those associated with the PCS subcontractor supplying a technician to install the PCS and associated systems. Subcontractor costs to decommission the PCS system at project end were rolled into these costs. Additional labor costs were tracked for project personnel on site to assist with the installation and testing of additional system components, including poly tanks, the polymer mixing equipment, and wellhead injection manifolds to record injection pressure response.

Because equipment was used under rental terms, PCS equipment shipping costs were also tracked, and the costs presented in **Table 7-1** include costs associated with shipping all project components to and from the site.

### 7.1.5 Cost Element: Operation and Maintenance

Polymer-specific operations and maintenance (O&M) costs tracked during this pilot demonstration included additional labor costs associated with polymer mixing and preparation of polymer concentrate solution. These costs were tracked on a person-hour basis for the demonstration. The initial mixing and concentrate preparation required 1 field person for 1 day (8-hours) prior to injection to prepare enough polymer concentration to supply uninterrupted overnight injection. Once PA-ISCO fluid injection initiated, polymer concentrate batches were prepared daily requiring 4 person-hours per day. These costs are represented in **Table 7-1**. However, the daily labor costs of polymer concentrate preparation could be rolled into normal daily O&M costs for any in situ groundwater remediation technology. Additionally, costs savings related to polymer concentrate solution preparation could be realized by sourcing a pre-made concentrate solution, of sufficient volume, that could be trucked to the site and contained within a large liquid product tanker trailer throughout the injection period.

Equipment rental costs included in **Table 7-1** for this cost element include those associated with the rental of a diesel generator (supplying power to run the PCS and polymer mixing equipment), overhead lighting for evening operations, and fuel costs. This equipment was rented for a period of 6 weeks during this demonstration. However, rental costs presented in **Table 7-1** are specific to the 2 week period in which the equipment was used during injection and post-injection sampling associated with PA-ISCO specifically.

## 7.2 COST DRIVERS

The cost to implement PA-ISCO is related to the use of permanganate oxidant and the degree of permeability heterogeneity and will vary significantly from site to site. The key cost drivers specific to PA-ISCO application are listed below, along with a brief discussion of their impact on cost.

### Operational Costs

- **Preparation of Polymer Solutions** – As discussed in Section 7.1.5, costs associated with the preparation of the polymer concentrate, using the methods and equipment employed in this demonstration, would increase with increasing scale of remediation. These scaled costs relate to labor needed to prepare the concentrate solutions on-site, as the costs of the mixing equipment would be independent of scale. However, as discussed in Section 7.1.5, we suggest that if a prepared polymer concentrate solution could be sourced and trucked to the site in large liquid product tanker trailers, the costs of this service could offset the cost of on-site preparation and obviate the need for the polymer mixing equipment.
- **Continuous Injection** – Costs associated with providing injection equipment that would provide continuous 24-hour injection is currently required for PA-ISCO treatments. This cost would be a one-time cost per implementation and would be fixed regardless of the scale of the implementation.

## Nature and Extent of Contamination

- **Depth and Extent of the Treatment Zone** – As with any in situ remediation technology, chemical costs will increase with increasing treatment volume. Similarly, costs associated with well installation (increased number of wells) and the treatment duration will increase.
- **Presence of non-aqueous phase liquids (NAPL)** – If polymer sweeps less permeable strata containing NAPL that is not swept by a non-viscous amendment, there is a potential for the PA-ISCO solution to mobilize this NAPL. This has less to do with the viscosity of the PA-ISCO fluid, but rather that the enhanced viscosity promotes access to lower permeability geomeedia that could contain NAPL. However, there is also the potential that PA-ISCO would provide a means of treating this hydraulically isolated NAPL zone that would otherwise not be treated by traditional ISCO application.

## Aquifer Geology and Hydrogeology

- **Vertically averaged hydraulic conductivity** – Relates to the rate of injection achievable and the concentration of polymer (i.e., xanthan gum) needed to achieve the same degree of sweep efficiency improvement. A site with a lower average permeability will require a slower rate of injection and longer treatment duration to maximize sweep efficiency improvement.
- **Implementation within confined and unconfined aquifers** – The present PA-ISCO demonstration was performed in a locally confined aquifer as described in Section 3 of this report. Application within an unconfined, water table aquifer is entirely feasible. The limiting factor would be a shallow water table condition, which would limit the rate of injection possible and necessarily increase the duration of treatment. Careful implementation design is recommended for this application scenario.
- **Degree of heterogeneity** – The principal function of PA-ISCO technology is to mitigate the effects of permeability heterogeneity on sweep efficiency within the treatment zone during injection. However, the degree of permeability heterogeneity can affect the duration of treatment for PA-ISCO, in that longer injection durations will be required to maximize sweep efficiency improvements as the degree of heterogeneity increases. While the relative location of high and low permeability strata is not a significant factor in the effectiveness of PA-ISCO, the degree of permeability contrast can result in increased number of injected pore volumes required to maximize sweep efficiencies. Generally, as the degree of permeability contrast between the bulk media and the target lower permeability zone increase, so does the injection duration. At present, estimating injection duration requires numerical simulation as a design component.

## 7.3 COST ANALYSIS

The primary objective of this first pilot demonstration was to evaluate sweep efficiency improvement for a polymer-amended permanganate solution and learn from the results of this test to better understand the efficacy of the technology for future full-scale application. As a result, the PA-ISCO formulation was not designed to completely remediate the treatment volume, which complicates a comparative analysis of the life cycle costs of PA-ISCO treatment versus traditional permanganate ISCO.

To facilitate this cost analysis, it was assumed that a 2 pore volume PA-ISCO treatment, utilizing the same polymer and oxidant concentrations, would provide maximal sweep efficiency improvement to contact 100 % of the pore volume within the template site described in **Table 7-2**. It is further assumed that this 2 pore volume treatment would provide sufficient oxidant to overcome both the initial instantaneous and slower natural oxidant demand contributions and achieve 100% treatment efficiency

Under this scenario, and utilizing the sum of the costs identified in **Table 7-1**, the additional cost of PA-ISCO (i.e., costs in addition to the normal cost of traditional permanganate ISCO implemented in the same manner) would be \$118,440 or \$185/m<sup>3</sup>.

Approximately 9% of costs (\$11.3 K) were associated with high level site characterization. The ability to assess the applicability of PA-ISCO relies on understanding permeability distribution, and thus this high level of site characterization is warranted. It is good practice, however, to conduct high level site characterization for any *in situ* remediation effort toward improved overall cost-effectiveness.

Roughly 56% (or \$69K) of the total cost was related to the purchase, shipping, and subcontractor labor associated with the process control system used in this pilot demonstration. The requirement of 24-hour injection for PA-ISCO necessitates a similar equipment purchase and therefore would be a fixed cost, regardless of the scale of implementation. However, the unit cost of this equipment would decrease with increasing scale of implementation (e.g., increased number of injection locations within a larger treatment volume or multiple PA-ISCO implementations at additional sites). As PA-ISCO develops, we would expect this equipment, along with the polymer mixing equipment at \$20K (17% of total cost), to become available for rent, with the total costs normalized over multiple sites over multiple years. If, for example, the equipment is purchased by a vendor and wants to realize a return on investment within two years, and we assume the equipment can be applied to a minimum of 6 sites per year, \$89K (75%) of the total costs described in **Table 7-1** would be reduced to approximately \$7.5K. Thus, total costs of PA-ISCO above and beyond traditional ISCO are estimated as \$36,940, or \$58/m<sup>3</sup> (or \$44/yd<sup>3</sup>). Again, because these equipment costs are fixed regardless of scale and these numbers are applied to this relatively small pilot-scale test, we can expect a significant decrease in cost per treated volume with increasing scale.

In a recent review of traditional ISCO application at over 200 individual sites, the average unit cost of ISCO was found to be \$123/m<sup>3</sup> (Krembs et al., 2010). Therefore the unit cost of PA-ISCO (estimated as \$181/m<sup>3</sup> or 138.5/yd<sup>3</sup>) is competitive with traditional ISCO, particularly considering the potential benefit.

The active remediation timeframe for injection of two PVs of amendments is estimated at 10-12 days based on the duration of this 1 PV demonstration. Based on analyses reported in Section 5.7.1, a permanganate-only plot would require approximately 6 PVs and one-month or more field time; and theory dictates that while sweep would be improved without polymer in 6 PVs, there would still be significant preferential flow. Assuming 100% contact, though, the cost savings of PA-ISCO at a minimum are the costs associated with approximately 20 days of field time. A conservative estimate of field costs at \$800/day for labor and travel (hotel, per diem, etc.) translates to a savings of \$16K, or \$25/m<sup>3</sup> (\$19/yd<sup>3</sup>) in the case presented here, which is approximately 40% of the estimated costs associated with use of PA-ISCO above and beyond traditional ISCO (assuming rented equipment with total costs normalized over 2 years and multiple sites, as discussed above). For a worst case scenario, PA-ISCO costs \$33/m<sup>3</sup> (\$25.2/yd<sup>3</sup>) above traditional ISCO for the same benefit as traditional ISCO.

If we assume PA-ISCO achieves treatment goals and results in site closure within 5 years of implementation, but ISCO without polymer does not reach treatment goals because of incomplete sweep (resulting in 30 years of long-term monitoring), the costs saved using PA-ISCO include 25 years of monitoring costs. Assuming a cost of approximately \$50K per year for long-term monitoring, a simple estimate of the associated cost savings indicates savings of up to \$1.25 million per site.



## **8.0 IMPLEMENTATION ISSUES**

This section provides information that will assist in future implementations of this technology. The following are key issues related to implementation of PA-ISCO technology.

### **8.1 POTENTIAL ENVIRONMENTAL ISSUES**

#### **8.1.1 Regulatory Issues**

For this pilot demonstration, an underground injection control (UIC) permit application was completed and submitted to the North Carolina Department of Environment and Natural Resources, although it was not mandated because of MCIEAST-MCB CAMLEJ's status as a CERCLA site (and the intent of the regulation was followed). At full-scale, a UIC permit will be required in most jurisdictions for the injection of permanganate oxidant and for the extraction and re-injection of PA-ISCO fluids and contaminated groundwater if implemented as an inter-well recirculation mode of in situ treatment. Regulatory requirements for permanganate treatment are well known. Xanthan gum, the polymer used in this demonstration is a food grade biopolymer. It is therefore expected that acquiring a UIC permit should not be difficult.

#### **8.1.2 Air Discharge**

The PA-ISCO process described herein will not normally result in the discharge of chemicals to the atmosphere.

#### **8.1.3 Wastewater Discharge**

The PA-ISCO process described will not normally result in the generation of wastewater streams. In this first pilot demonstration of PA-ISCO technology, PA-ISCO fluids were delivered to the subsurface as an injection-only mode of treatment, which did not generate a wastewater stream. Some small quantities of wastewater may be generated during well installation and groundwater sampling events and must be managed as they would be for other investigation derived waste.

#### **8.1.4 Waste Storage, Treatment, and Disposal**

The PA-ISCO process described will not normally result in the generation of significant waste streams. Some waste may be generated during well installation and groundwater sampling and must be managed as they would be for other investigation derived waste. If NAPL areas are targeted for treatment, it is possible that the waste generated will be hazardous and would need to be managed as such.

### **8.2 END-USER ISSUES**

Potential end-users of this technology include responsible parties for sites contaminated by TCE, PCE and potentially other chlorinated solvents. End-users will have an interest in the technology because it can potentially improve the treatment of groundwater aquifers *in situ* by the improved

contact between the contaminant and the injected remedial fluid resulting from improved sweep efficiencies within heterogeneous aquifer environments. PA-ISCO can therefore improve the effectiveness of treatment over traditional permanganate ISCO application. End-users and other stakeholders may have concerns regarding: 1) applicability of the PA-ISCO to sites with more than one-order-of-magnitude variation in hydraulic conductivity/permeability, 2) the effectiveness of the technology in reducing concentrations of target compounds within lower permeability media; 3) potential negative impacts of permanganate and its reaction byproducts in the environment (concern with ISCO in general and not specific to PA-ISCO); and 4) potential negative impacts of xanthan gum on subsurface hydraulics.

Previous SERDP funded research that contributed to this pilot-scale implementation demonstrated that a one or two-order of magnitude variability in media permeability is not a limitation to sweep efficiency improvement via polymer amendment. Rather it is the permeability contrast between adjacent strata that governs the rate of sweep, and therefore the number of pore volumes required to achieve 100% sweep efficiency. The technology is best implemented within sands, silty sands, and silts where the permeability contrasts between these media categories are less severe. Polymer amendment will not drive remedial fluids into clays, wherein the larger polymer molecules will filter out of solution and the viscosifying effect diminishes. However, this does not mean that polymer amendment cannot treat contaminants accumulated within clayey sediments. As observed during this field demonstration, the viscosity of the injected PA-ISCO solution was found to persist within the treatment zone in excess of a year following initial treatment. The low horizontal hydraulic gradient at this site, coupled with the viscosity of the injected solution, appears to have hydraulically isolated the PA-ISCO treatment zone. This result should not be necessarily viewed as a negative consequence of polymer amended fluids. Rather, future remediation designs could be tailored to take advantage of this viscosity retention and hydraulic isolation to sequester permanganate, or other remedial fluids, within the zone of treatment to provide a source continued long-term treatment of contamination within emanating from low-permeability media (e.g., clays, and clayey silts) that were not swept during the initial polymer-amended treatment.

Additionally, the viscosity of the PA-ISCO fluid, and the retention of this viscosity post-treatment, was shown to have sequestered the geochemical signature of ISCO (including metals, which may be of concern at some sites). The expected slow dissipation of viscosity post-treatment could result in slow, low-concentration release of the geochemical signature, preventing “slugs” of high concentrations of metals of concern from passing through monitoring wells.

### **8.3 PROCUREMENT ISSUES**

There are no significant procurement issues related to the purchase of permanganate and/or xanthan gum biopolymer, as there are a number of permanganate and xanthan gum biopolymer vendors in existence. No significant procurement issues were encountered for the purchase of the polymers and polymer mixing equipment. However, the end-user should be cognizant of the need for this type of specialized polymer mixing equipment to ensure proper hydration of these dry polymer products to avoid injectivity issues.

## 8.4 DESIGN ISSUES

Based on the results of the PA-ISCO pilot demonstration conducted at MCIEAST-MCB CAMLEJ (Site 88) potential design issues that should be considered in future applications of PA-ISCO were identified.

- **Daylighting of PA-ISCO Fluids:** Daylighting is a common undesirable occurrence with in situ remediation and, therefore, any condition which may increase it is of design concern. It is a requirement of PA-ISCO, and other polymer-amended remedial fluid applications, that the solutions possess enhanced viscosity. Injection of fluids of increased viscosity naturally evokes concerns over the daylighting of injected fluids at or near the point of injection due to the higher required injection pressures. In this demonstration, however, at most (i.e., static condition) solution viscosities injected did not exceed 36 cP (or 36 times the viscosity of water, which is similar to the viscosity of vegetable oil). Additionally, the polymer used to provide viscosity enhancement possessed shear-thinning rheological character, in which the apparent viscosity of the fluid decreases with increasing hydrodynamic shear (or with increasing pore water velocities). As a result, the location of lowest viscosity would be at the location of greatest pore velocity, or immediately adjacent to the injection well during injection. In fact, pore fluid velocities near the injection well during this pilot demonstration were high enough to provide a near-well fluid viscosity very close to that of water. The purposeful use of a shear-thinning viscous fluid, as in this demonstration, mitigates the potential for daylighting. Daylighting becomes more of a concern for shallow water table aquifers, which could require lower injection flow rates resulting in elevated PA-ISCO fluid viscosities.
- **Delivery Volume and Injection Duration:** The purpose of polymer amendment is to improve the subsurface distribution of injected remedial amendments during in situ treatment. However, throughout this project and prior SERDP-funded work in this area (SERDP Project ER-1486) it has become clear that while polymer amendment can greatly improve the distribution of injected fluids in heterogeneous aquifers, achieving maximal sweep-efficiency improvements most often will require injection of more than a one pore volume injection. The number of pore volumes required depends on the maximum permeability contrast between strata within the treatment volume (Silva et al, 2012b). However, polymer addition will significantly reduce the number of pore volumes required.
- **Mode of PA-ISCO Treatment:** For this first pilot demonstration of PA-ISCO, the mode of introduction of fluids utilized an injection-only mode. This has been a common mode of treatment for traditional permanganate ISCO treatments because of the reduced field time and overall costs of treatment. While we have successfully demonstrated significant sweep efficiency improvement (105% sweep improvement relative to a traditional permanganate injection), we have also estimated that achieving 100% sweep of the demonstration pore volume would require as much as a 2 pore volume injection. This could be a limitation of PA-ISCO application because many practitioners don't recognize or respond to the importance of injection volume in their ISCO designs, or the design of

any treatment system involving the delivery of liquid amendments, in general. PA-ISCO, however, improves the efficiency of treatment by decreasing the total number of pore necessary to achieve sweep. Furthermore, without polymer, preferential flow will continue and we can expect limited movement into the lower permeability layers regardless of how many PVs are delivered. With polymer, movement into lower permeability media will continue. There is greater cost-benefit to a multiple PV injection with polymer than without.

In general, the challenge of high injection volumes for site treatment using any liquid amendment, particularly those with fast reaction rates, could be overcome by implementing the technology in a recirculation mode of treatment (e.g., divergent line-drive well pattern involving a center line of injectors and lines of extraction wells on either side), whereby multiple pore volumes could be introduced to provide maximal sweep efficiency improvement while reducing the duration of treatment.

- **Permeability Reduction Associated with Xanthan Biopolymer:** Polymer amendment not only provides mobility reduction to improve subsurface sweep efficiency, but can also temporarily reduce the permeability of the media it is being injected into as a result of filtration and entrapment of these large polymer molecules within narrow pores and pore pathways. Transport experiments utilizing site aquifer sediments should be conducted as a part of a Treatability Study work scope to evaluate the potential for and degree of permeability reduction as a part of responsible remediation design. The degree of polymer permeability reduction will increase as the media permeability decreases, and the effects of significant polymer permeability reduction could result in lower injection flow rates and an increased potential for daylighting, as described previously. In the present case, including SHMP to the PA-ISCO formulation reduced the potential for permeability reduction (see Table 5-6) as described in Section 5.3.1 of this report.
- **Sorbed-Phase Contamination** – It is widely recognized that ISCO typically requires multiple injections to treat contamination associated with the solid-phase as it diffuses into the treatment pore volume following initial treatment.
- **Equipment to Prepare Xanthan Gum Concentrates:** For this first field demonstration, xanthan gum and SHMP were purchased as dry powdered product and concentrates of these polymers were prepared on-site. Operational and equipment costs associated with preparing these solutions in the field were manageable at the scale of this demonstration, but could become difficult as the scale of the treatment increases. In future applications it may be more appropriate to purchase these polymers as prepared aqueous solutions that could be trucked to the site in large tanker trailers. This action would mitigate labor costs associated with PA-ISCO application and eliminate the need for the relatively expensive (~20-percent of the total equipment cost) hydrodynamic mixing equipment purchased for this demonstration.

## 9.0 REFERENCES

- APHA-AWWA-WPCF, (1998). Standard Methods for Examination of Water and Wastewater, 20th ed., Clesceri, L.S., A.E. Greenberg, and R.R. Trussell, eds. APHA-AWWA-WPCF, Washington, DC.
- ASTM (1991). Standard Practice for Sampling Waste and Soils for Volatile Organics. D4547-91. In: 1992 Annual Book of ASTM Standards, Vol. 11.04, pp. 108-111.
- Baker Environmental, Inc. (Baker) (1998). *Final Focused Remedial Investigation Report, Operable Unit No. 15 (Site 88), Marine Corps Base, Camp Lejeune, North Carolina*. May.
- Battelle Memorial Institute (BMI) (2001). *Reductive Anaerobic Biological In Situ Treatment Technology (RABITT) Treatability Test, Interim Report*. August.
- Carter, M.R. (1993). *Soil Sampling and Methods of Analysis*. Lewis Publishers, Ann Arbor, MI.
- CH2M Hill (2008). *Final Remedial Investigation Report, Site 88, Operable Unit No. 15, Marine Corps Base Camp Lejeune, Jacksonville, North Carolina*.
- CH2M HILL (2002). *Draft Supplemental Site Investigation Report, Operable Unit 15 (Site 88), Building 25 Base Dry Cleaners*. September.
- CH2M HILL (2003). *Supplemental Site Investigation Report, Operable Unit 15 (Site 88), Building 25 Base Dry Cleaners*. December.
- CH2M HILL (2004a). *Membrane Interface Probe Investigation*.
- CH2M HILL (2004b). *Site 88 Building 25 Source Removal Engineering Evaluation/Cost Analysis*. September.
- CH2M HILL (2006). *Draft Site 88 Building 25 Source Removal Non-Time Critical Removal Action Report*. March.
- CH2M HILL (2008a). *Final Remedial Investigation Site 88, Operable Unit No. 15, Building 25*. March.
- CH2M HILL (2008b). *Draft Feasibility Study, Site 88, Operable Unit No. 15*. February.
- Chandrakanth, M.S. and G.L. Amy (1996). Effects of Ozone on the Colloidal Stability and Aggregation of Particles Coated with Natural Organic Matter. *Environmental Science and Technology*, 30(2):431-442.
- Chao, T.T. (1972). Selective Dissolution of Manganese Oxides from Soils and Sediments with Acidified Hydroxylamine Hydrochloride. *Soil Sci. Soc. Am. Proc.* Oct 29-Nov 3, Miami Beach, FL.
- DE&S – Duke Engineering & Services (1999). *DNAPL Site Characterization Using a Partitioning Interwell Tracer Test at Site 88, Marine Corps Base Camp Lejeune, North Carolina (Final Report)*.
- Dominguez, J.G. and Willhite, G.P. (1977) Retention and Flow Characteristics of Polymer solutions in Porous Media. *Soc. Pet. Eng. J.* April, 111-121.
- Doona C.J. and F.W. Schneider (1993). Identification of Colloidal Mn(IV) in Permanganate Oscillating Reactions. *J. Am. Chem. Soc.*, 115:9683-9686.
- Duke Engineering and Services (Duke) (1999). *DNAPL Site Characterization using a Partitioning Interwell Tracer Test at Site 88, Marine Corps Base, Camp Lejeune, North Carolina*. July.
- Duke. 2000. *Surfactant-Enhanced Aquifer Remediation Demonstration at Site 88, Marine Corps Base, Camp Lejeune, North Carolina*. January.

- Insausti, M.J., F. Mata-Perez, and P. Alvarez-Macho (1992). Permanganate Oxidation of Glycine: Influence of Amino Acid on Colloidal Manganese Dioxide. *International Journal of Chemical Kinetics*, 24(5):411-419.
- Insausti, M.J., F. Mata-Perez, and P. Alvarez-Macho (1993). UV-VIS Spectrophotometric Study and Dynamic Analysis of the Colloidal Product of Permanganate Oxidation of  $\alpha$ -Amino Acids. *React. Kinet. Catal. Lett.*, 51(1):51-59.
- Kieft, T.L. and T.J. Phelps (1997). Life in the Slow Lane: Activities of Microorganisms in the Subsurface. CRC Press, Inc. pp. 135-161.
- Klute, A. et al., (ed.) (1986). Methods of Soil Analysis, Part 1. Physical and Mineralogical Methods. Soil Sci. Soc. Am. Madison, WI.
- Krembs FJ, RL Siegrist, M Crimi, RF Furrer, BG Petri. 2010. In Situ Chemical Oxidation for Groundwater Remediation: Analysis of Field Applications and Performance Experiences. *Ground Water Monitoring and Remediation*. 30(4), 42-53.
- Lee E.S., Y.Seol, Y.C. Fang, and F.W. Schwartz (2003). Destruction Efficiencies and Dynamics of Reaction Fronts Associated with Permanganate Oxidation of Trichloroethylene. *Environmental Science and Technology*, 37(11):2540-2546.
- Li X.D. and F.W. Schwartz (2000). Efficiency problems related to permanganate oxidation schemes. In: G.B. Wickramanayake, A.R. Gavaskar, A.S.C. Chen (ed.). Chemical Oxidation and Reactive Barriers: Remediation of Chlorinated and Recalcitrant Compounds. Battelle Press. Columbus, OH. pp. 41-48.
- Lowe, K.S., F.G. Gardner, R.L. Siegrist, and T.C. Houk (2000). EPA/625/R-99/012. US EPA Office of Research and Development, Washington, D.C.
- Moore K. (2008). Geochemical Impacts From Permanganate Oxidation Based on Field Scale Assessments. M.S. Thesis, East Tennessee State University. 138 pp.
- Morgan, J.J. and W. Stumm (1964). Colloid-Chemical Properties of Manganese Dioxide. *Journal of Colloid Science*, 19:347-359.
- OHM Remediation Services Corporation (OHM) (1996). *Contractor's Closeout Report, Underground Storage Tank Removals at Building 25, MCB Camp Lejeune, North Carolina*. October.
- Perez-Benito, J.F. and C. Arias (1991). A Kinetic Study of the Permanganate Oxidation of Triethylamine. Catalysis by Soluble Colloids. *International Journal of Chemical Kinetics*, 23:717-732.
- Perez-Benito, J.F. and C. Arias (1992a). A Kinetic Study of the Reaction Between Soluble (Colloidal) Manganese Dioxide and Formic Acid. *Journal of Colloid and Interface Science*, 149(1):92-97.
- Perez-Benito, J.F. and C. Arias (1992b). Occurrence of Colloidal Manganese Dioxide in Permanganate Reactions. *Journal of Colloid and Interface Science*, 152(1):70-84.
- Perez-Benito, J.F., C. Arias, and E. Brillas (1990). A Kinetic Study of the Autocatalytic Permanganate Oxidation of Formic Acid. *International Journal of Chemical Kinetics*, 22:261-287.
- Perez-Benito, J.F., E. Brillas, and R. Pouplana (1989). Identification of a Soluble Form of Colloidal Manganese (IV). *Inorganic Chemistry*, 28:390-392.
- Phelps T.J., S.M. Pfiffner, K.A. Sargent, and D.C. White (1994b). Factors Influencing the Abundance and Metabolic Capacities of Microorganisms in Eastern Coastal Plain Sediments. *Microb. Ecol.* 28:351-364.

- Phelps T.J., E. Murphy, S.M. Pfiffner, and D.C. Whiate (1994a). Comparison Between Geochemical and Biological Estimates of Subsurface Microbial Activities. *Microbial Ecology*, 28:335-349.
- Reitsma S. and M. Marshall (2000). In: G.B. Wickramanayake, A.R. Gavaskar, A.S.C. Chen (ed.). *Chemical Oxidation and Reactive Barriers: Remediation of Chlorinated Compounds*. Battelle Press. Columbus, OH. p. 25-32.
- Silva, J.A.K., 2011. The utility of polymer-amendment for enhancing in situ remediation effectiveness. Ph.D. Dissertation, Colorado School of Mines, Golden, Colorado.
- Silva, J.A.K., M. Liberatore, and J.E. McCray (2012a). Characterization of Bulk Fluid and Transport Parameters for Simulating Polymer-Improved Aquifer Remediation. *J. Environ. Eng.*, In Press.
- Silva, J.A.K., M. M. Smith, J. Munakata-Marr, and J.E. McCray (2012b). The Effect of System Variables on Sweep-Efficiency Improvements via Viscosity Modification. *J. Contam. Hydrol.*, 136-137, 117-130.
- Sparks D.L., A.L. Page, P.A. Helmke, R.H. Loeppert, P.N. Soltanpour, MA. Tabatabai, C.T. Johnson, and M.E. Sumner (ed.) (1996). *Methods of Soil Analysis: Part 3 – Chemical Methods*. Soil Sci. Soc. Am. Madison, WI.
- Tan, K.H. (1996). *Soil Sampling, Preparation, and Analysis*. Marcel Dekker, Inc. New York. 407 pp.
- USEPA (1986). *Test Methods for the Evaluation of Soil Waste, Physical/Chemical Methods*. SW-846, 3<sup>rd</sup> ed. Off. Solid Waste and Emergency Response, Washington DC.
- USEPA (1990). *Second update to SW-846 Methods Section*. Office of Solid Waste. U.S. Environmental Protection Agency, Washington DC.
- Weaver R.W., S. Angle, P. Bottomley, D. Bezdicek, S. Smith, A Tabatabai, and A. Wollum (ed) (1994). *Methods of Soil Analysis: Part 2 – Microbiological and Biochemical Properties*. Soil Scie. Soc. Am., Madison, WI.
- West, O.R., R.L. Siegrist, S.R. Cline, and F.G. Gardner (2000). The effects of in situ chemical oxidation through recirculation (ISCOR) on aquifer contamination, hydrogeology, and geochemistry. Oak Ridge National Laboratory internal report submitted to the Department of Energy, Office of Environmental Management, Subsurface Contaminants Focus Area.
- West, O.R., S.R. Cline, W.L. Holden, F.G. Gardner, B.M Schlosser, J.E. Thate, D.A. Pickering, T.C. Houk (1998). ORNL/TM-13556, Oak Ridge National Laboratory, Oak Ridge, Tennessee.

## Appendix A: Points of Contact

<b>Point of Contact</b>	<b>Organization</b>	<b>Phone, Email</b>	<b>Role in Project</b>
Michelle Crimi	Institute for a Sustainable Env. Clarkson University	315-268-4174 mcrimi@clarkson.edu	Principal Investigator
Jeffrey Allen Kai Silva	Polymer Methods in Remediation (Colorado School of Mines at time of dem/val)	303-579-1275 jsilva.pmr@gmail.com	Co-PI, Technical Lead
John McCray	Civil and Env Engineering Colorado School of Mines	303-273-3490 jmccray@mines.edu	Co-PI
Tom Palaia	CH2M HILL	303-679-2510 tom.palaia@ch2m.com	Co-PI, CH2M HILL Lead
Monica Fulkerson	CH2M HILL	704-544-5177 monica.fulkerson@ch2m.com	CH2M HILL Project Manager
Narendra De	CH2M HILL	303-771-0900 narendra.de@ch2m.com	CH2M HILL Assistant Project Manager
Simon Kline	CH2M HILL	919-760-1787 simon.kline@ch2m.com	CH2M HILL Field Team Leader
Brooke Probst	CH2M HILL	704-544-5177 brooke.probst@ch2m.com	CH2M HILL Field Team Leader
Saebom Ko	R.S. Kerr Env Res. Center US EPA	580-436-8742 ko.saebom@epa.gov	Collaborator
Matthew Dingens	Carus Corporation	815-224-6556 Matt.dingens@caruscorporation.com	Donated permanganate and SHMP
Charity Rychak	MCIEAST-MCB CAMLEJ	910-451-9385 Charity.rychak@usmc.mil	MCIEAST-MCB CAMLEJ Point of Contact
Nancy Ruiz	NAVFAC Engineering Service Center	805-982-1155 nancy.ruiz@navy.mil	DoD Liaison



**Appendix B: Raw Data for Soil and Groundwater Samples Collected Pre-, Post-, and 1 Year Post-treatment**

## Field Groundwater Quality Data Summary

### Test Plot

CMT - 1						
Date	Port #	Temp.	Conductivity	DO	pH	ORP
12/9/2010	2	20.710	0.158	2.900	5.950	-25.400
12/10/2010	2	20.520	0.130	4.600	5.880	-20.600
12/11/2010	2	19.710	0.123	16.100	6.060	91.900
12/12/2010	2	21.520	0.115	2.900	5.750	101.800
12/13/2010	2	20.110	0.130	9.000	5.820	-39.400
12/14/2010	2	15.05	0.134	126	6.08	17.1
12/15/2010	2	21.44	0.173	4.2	5.79	127.5
11/3/2011	2	26.17	0.208	12.4	6	-278.8
Date	Port #	Temp.	Conductivity	DO	pH	ORP
12/9/2010	3	20.820	0.385	4.100	6.560	-51.900
12/10/2010	3	20.560	0.360	13.800	6.510	-63.500
12/11/2010	3	18.790	0.363	18.300	6.750	47.100
12/12/2010	3	21.230	0.357	7.900	6.550	62.200
12/13/2010	3	20.070	0.436	17.300	6.710	-90.000
12/14/2010	3	16.12	0.428	11.4	6.64	-16.1
12/15/2010	3	21.1	0.503	37.9	6.36	64.8
11/3/2011	3	26.15	0.703	15.7	6.79	-277.4
Date	Port #	Temp.	Conductivity	DO	pH	ORP
12/9/2010	4	21.040	0.661	2.800	7.000	-152.000
12/10/2010	4	18.730	0.618	10.000	7.010	-146.000
12/11/2010	4	20.150	0.573	12.000	7.090	21.300
12/12/2010	4	20.400	0.583	8.400	6.980	13.500
12/13/2010	4	19.520	0.683	12.000	7.110	-133.300
12/14/2010	4	15.54	0.638	10.3	7	-64.2
12/15/2010	4	20.4	0.813	26.4	6.82	13.8
11/3/2011	4	26.79	0.681	13.7	6.78	-287.6
Date	Port #	Temp.	Conductivity	DO	pH	ORP
12/9/2010	5	20.730	0.643	4.900	7.080	-131.700
12/10/2010	5	21.100	0.641	10.900	7.100	-157.200
12/11/2010	5	20.310	0.594	13.700	7.200	-17.800
12/12/2010	5	20.400	0.612	5.300	7.120	-20.400
12/13/2010	5	18.900	0.710	13.600	7.200	-146.800
12/14/2010	5	14.8	0.658	9.9	7.12	-102.6
12/15/2010	5	20.5	0.853	27.7	6.91	21.7
11/3/2011	5	26.24	0.413	19.5	6.59	-291.6

#### UNITS

Temperature      °C  
 Conductivity      mS/cm  
 DO                    mg/L  
 ORP                  mV

## Field Groundwater Quality Data Summary

### Test Plot

CMT - 2						
Date	Port #	Temp.	Conductivity	DO	pH	ORP
12/9/2010	2	19.460	0.325	4.500	6.630	-150.600
12/10/2010	2					
12/11/2010	2					
12/12/2010	2					
12/13/2010	2	21.190	0.269	2.700	4.510	-92.100
12/14/2010	2	18.55	0.478	10.2	6.4	-75.6
12/15/2010	2	22.26	0.332	2.1	7.46	-245
11/3/2011	2	25.54	0.388	7.8	6.43	-88.6
Date	Port #	Temp.	Conductivity	DO	pH	ORP
12/9/2010	3	20.460	0.127	2.900	6.100	-131.700
12/10/2010	3					
12/11/2010	3					
12/12/2010	3					
12/13/2010	3	19.530	0.227	5.800	3.680	-50.300
12/14/2010	3	18.39	0.32	6.1	6.67	-57.7
12/15/2010	3	20.88	0.237	2.1	7.07	-152.6
11/3/2011	3	26	0.16	12.2	5.64	-11
Date	Port #	Temp.	Conductivity	DO	pH	ORP
12/9/2010	4	20.460	0.239	4.800	6.550	-119.600
12/10/2010	4					
12/11/2010	4					
12/12/2010	4					
12/13/2010	4	20.000	0.344	7.100	5.770	-61.900
12/14/2010	4	18.89	0.603	3.8	6.94	-77.2
12/15/2010	4	20.96	0.315	3.4	7.71	-222.8
11/3/2011	4	27.83	0.169	26	5.65	-6.8

### UNITS

Temperature            °C  
 Conductivity            mS/cm  
 DO                        mg/L  
 ORP                        mV

## Field Groundwater Quality Data Summary

### Control Plot

CMT-3						
Date	Port #	Temp.	Conductivity	DO	pH	ORP
10/29/2010	2	22.980	0.271	2.400	7.010	-89.400
10/30/2010	2	23.780	0.397	2.500	6.620	-105.300
10/31/2010	2	23.290	1.105	1.400	6.170	-37.500
11/1/2010	2	24.800	2.922	3.600	6.470	662.100
11/2/2010	2					
11/3/2011	2	Dry Well				
Date	Port #	Temp.	Conductivity	DO	pH	ORP
10/29/2010	3	22.730	0.342	3.200	7.210	-93.600
10/30/2010	3	23.170	0.322	2.200	6.720	-95.800
10/31/2010	3	24.170	0.386	1.700	6.670	-100.700
11/1/2010	3	23.6	0.704	1.7	6.48	-93.2
11/2/2010	3	23.35	1.391	2.4	6.38	435.3
11/3/2011	3	26.49	0.379	20.4	6.81	-97.4
Date	Port #	Temp.	Conductivity	DO	pH	ORP
10/29/2010	4	21.850	0.421	4.000	7.610	-133.000
10/30/2010	4	23.400	0.439	2.000	7.170	-147.800
10/31/2010	4	24.620	0.461	1.700	7.180	-137.200
11/1/2010	4	23.3	0.557	2	7.15	-136.7
11/2/2010	4	22.56	2.178	6.8	6.8	594.5
11/3/2011	4	22.54	0.507	3.3	6.83	-22.1
Date	Port #	Temp.	Conductivity	DO	pH	ORP
10/29/2010	5	22.630	0.449	1.600	7.560	-119.700
10/30/2010	5	23.600	0.457	2.100	7.160	-140.400
10/31/2010	5	24.460	0.424	7.400	7.220	-118.700
11/1/2010	5	22.75	0.448	3.6	7.2	-120.5
11/2/2010	5	22	0.7	4.6	7.13	-102.1
11/3/2011	5	25.87	0.5	15.2	6.98	-63.6

#### UNITS

Temperature      °C  
 Conductivity      mS/cm  
 DO                    mg/L  
 ORP                  mV

## Field Groundwater Quality Data Summary

### Control Plot

CMT - 4						
Date	Port #	Temp.	Conductivity	DO	pH	ORP
10/29/2010	1	23.833	0.311	1.900	6.510	-117.086
10/30/2010	1	23.733	0.228	3.025	6.353	-91.150
10/31/2010	1	24.260	0.211	2.367	6.120	-74.167
11/1/2010	1	24.110	0.219	2.400	5.650	-30.500
11/2/2010	1	22.49	0.315	2.8	5.41	-9.5
11/3/2011	1	22.66	3.086	15.1	6.73	-319.6
Date	Port #	Temp.	Conductivity	DO	pH	ORP
10/29/2010	2	23.168	0.453	1.600	7.560	-179.675
10/30/2010	2	23.704	0.440	2.686	7.766	-173.429
10/31/2010	2	24.537	0.437	3.233	7.565	-156.517
11/1/2010	2	24.31	0.438	2.3	7.07	-150.7
11/2/2010	2	22.78	0.446	3.2	6.79	-104.7
11/3/2011	2	25.67	3.119	11.1	7.04	-311.1
Date	Port #	Temp.	Conductivity	DO	pH	ORP
10/29/2010	3	23.062	0.469	2.744	7.657	-172.211
10/30/2010	3	23.585	0.463	3.050	7.792	-116.250
10/31/2010	3	24.434	0.426	5.229	7.647	-141.814
11/1/2010	3	23.82	0.439	2.7	7.27	-129.3
11/2/2010	3	22.91	0.455	2.4	6.7	-109.3
11/3/2011	3	22.63	1.799	11.5	6.47	-315.9
Date	Port #	Temp.	Conductivity	DO	pH	ORP
10/29/2010	4	22.864	0.293	3.863	6.496	-99.125
10/30/2010	4	23.685	0.280	3.375	6.588	-112.425
10/31/2010	4	24.208	0.241	3.820	6.464	-103.120
11/1/2010	4	24.11	0.254	2.8	5.97	-66.6
11/2/2010	4	22.97	0.363	3.6	5.38	-16.6
11/3/2011	4	25.74	1.32	15.6	6.7	-321.9

#### UNITS

Temperature      °C  
 Conductivity      mS/cm  
 DO                    mg/L  
 ORP                  mV

## Laboratory Groundwater Quality Data Summary

### Pre-treatment

Site Pre-Treatment Groundwater Data, Collected  
from Pre-existing MW 2 in Close Proximity to Demonstration Area  
Laboratory analyses of samples collected in field and shipped to Clarkson University

<b>pH</b>	6.48
<b>Eh (mV)</b>	36
<b>Temp (deg C)</b>	20.5
<b>Cations (mg/L)</b>	
Na	18.17
Al	0.008
K	4.513
Ca	BD
Cr	0.001
Mn	0.566
Fe	BD
Ni	0.018
Zn	0.38
As	0.0017
Sr	0.14
Cd	0.000075
Ba	0.0628
Pb	BD
<b>Anions (mg/L)</b>	
Chloride	59.4
Nitrate	0.17
Nitrite	BD
Sulfate	5.09
Phosphate	*

\*Interference prevented accurate measurement

## **Laboratory Groundwater Quality Data Summary**

## During and Post-treatment – Test Plot

	Depth, feet		Cations (mg/L)												Anions (mg/L)					General Water Quality				
	Date	DTT	DTB	Na	Mg	Ca	K	Mn	Cr	Fe	Ni	As	Se	Cd	Sulfate	NH4	phosphate	Nitrite	Nitrate	Chloride	pH	ORP (mV)	TS (mg/L)	DS (mg/L)
CMT 1 - 2	10/22/2010	32	34	21.31	2.63	18.28	2.13	0.30	BD	9.54	BD	0.022	0.3585	BD	3.00	1.15	1.72	0.002	BD	5.53	6.1	145	230	160
	10/22/2010	32	34	21.45	2.67	18.67	2.14	0.27	BD	9.93	BD	0.025	0.4683	BD	3.00	1.25	1.88	0.003	BD	5.57	6.3	149	230	160
	12/11/2010	32	34	13.43	0.89	10.08	1.08	0.06	0.0028	4.14	0.004	0.007	0.0003	0.0005	12.00	1.05	3.75	0.035	0.5	8.79	5.7	472	430	190
	12/11/2010	32	34	13.22	0.88	10.02	1.19	0.06	0.0028	4.13	0.004	0.004	BD	0.0002	10.00	1.00	3.80	0.029	0.5	8.72	5.6	475	380	190
	12/13/2010	32	34	10.79	0.73	5.99	1.03	0.05	0.0013	3.32	0.002	0.003	0.0056	BD	9.00	0.25	3.66	0.034	0.6	8.19	5.7	335	240	190
	12/13/2010	32	34	11.09	0.73	5.98	1.15	0.05	0.0011	3.26	0.002	0.004	BD	0.0001	9.00	0.24	3.78	0.040	0.7	7.59	5.6	336	230	160
	12/17/2010	32	34	12.75	0.94	6.66	2.01	0.05	0.0035	4.02	0.003	0.003	0.0016	BD	7.00	1.10	4.25	0.020	0.7	8.44	5.6	436	180	90
	12/17/2010	32	34	12.49	0.90	6.54	1.41	0.05	0.0033	3.96	0.002	0.006	0.0036	0.0001	6.00	1.05	3.90	0.020	0.7	8.47	5.5	435	160	80
	10/3/2011	32	34	50.00	1.30	9.00	9.30	0.08	BD	3.90	0.001	0.002	0.0100	0.0007	28.00	1.70	3.00	0.020	0.5	9.00	6.3	360	210	140
	10/3/2011	32	34	46.00	1.30	9.00	7.50	0.08	BD	3.70	0.002	0.003	0.0100	0.0013	25.00	1.10	3.20	0.020	0.6	7.00	6.2	359	180	160
CMT 1 - 3	10/22/2010	43	45	36.75	4.50	38.51	1.65	0.28	BD	4.40	BD	0.012	0.4877	BD	17.00	0.13	0.86	0.001	BD	31.00	6.4	222	290	270
	10/22/2010	43	45	37.23	4.52	38.76	1.67	0.28	BD	3.74	BD	0.018	0.4877	BD	17.00	0.13	0.71	0.001	BD	31.80	6.5	255	270	270
	12/11/2010	43	45	23.03	5.07	37.23	1.46	0.26	BD	3.26	0.002	0.013	0.0015	0.0001	10.00	0.23	3.11	0.002	0.3	31.05	6.2	447	220	220
	12/11/2010	43	45	22.84	5.07	36.82	1.38	0.25	0.0008	3.25	0.003	0.009	0.0044	0.0002	10.00	0.25	3.24	0.003	0.3	31.83	6.2	445	230	230
	12/13/2010	43	45	18.04	5.14	40.71	1.68	0.26	0.0001	4.06	0.002	0.009	0.0068	BD	11.00	0.26	2.90	0.002	0.3	29.81	6.1	364	190	200
	12/13/2010	43	45	18.25	5.15	40.67	1.77	0.27	BD	4.36	0.002	0.006	BD	0.0001	11.00	0.25	2.89	0.003	0.3	30.06	6.1	367	200	200
	12/17/2010	43	45	17.14	5.01	42.49	1.64	0.26	0.0003	4.75	0.002	0.011	0.0023	0.0005	10.00	0.12	3.07	0.006	0.4	32.65	6.1	290	150	160
	12/17/2010	43	45	17.09	4.99	42.71	1.59	0.26	BD	4.75	0.002	0.012	0.0047	0.0002	10.00	0.13	3.44	0.006	0.5	33.82	6.2	277	180	130
	10/3/2011	43	45	12.00	3.00	28.00	22.40	0.19	BD	1.40	0.000	BD	0.0100	0.0014	3.00	0.20	1.30	0.010	0.5	15.00	5.9	349	200	190
	10/3/2011	43	45	22.00	3.20	29.00	22.00	0.21	BD	1.40	0.002	0.003	0.0100	0.0004	6.00	BD	1.40	0.010	0.8	16.00	5.9	356	230	200
CMT 1 - 4	10/22/2010	52	54	25.03	4.47	81.69	1.56	0.36	BD	9.75	BD	0.005	0.6912	BD	44.00	0.05	0.19	0.003	0.1	7.44	7.1	203	360	350
	10/22/2010	52	54	25.83	4.56	83.73	1.55	0.34	BD	10.66	BD	0.006	0.4877	BD	46.00	0.04	0.23	0.004	0.1	8.15	7.1	237	360	330
	12/11/2010	52	54	21.04	3.22	99.81	1.29	0.25	BD	6.66	0.001	0.008	0.0031	0.0006	42.00	0.02	0.69	0.026	1.0	6.59	6.6	435	350	340
	12/11/2010	52	54	21.82	3.33	103.27	1.22	0.24	BD	6.25	0.001	0.005	0.0024	0.0002	42.00	0.01	0.38	0.031	0.8	6.52	6.6	430	370	330
	12/13/2010	52	54	15.86	3.32	110.10	1.22	0.24	BD	5.94	0.001	0.009	BD	0.0003	36.00	BD	0.19	0.052	0.5	5.74	6.7	441	350	340
	12/13/2010	52	54	15.79	3.29	109.67	1.28	0.24	BD	5.78	0.001	0.010	BD	0.0001	37.00	BD	0.19	0.050	0.4	5.96	6.6	449	340	330
	12/17/2010	52	54	13.57	3.42	116.60	1.45	0.27	0.0006	9.41	0.002	0.010	0.0048	0.0012	31.00	BD	0.16	0.008	0.4	4.47	6.6	249	330	260
	12/17/2010	52	54	14.01	3.36	115.00	1.28	0.27	BD	9.65	0.001	0.009	0.0011	0.0005	30.00	BD	0.14	0.010	0.4	4.57	6.7	244	310	270
	10/3/2011	52	54	14.00	3.30	121.00	2.00	0.14	BD	2.90	0.003	0.002	0.0100	0.0038	23.00	0.10	0.50	0.010	0.5	5.00	6.6	367	370	350
	10/3/2011	52	54	15.00	3.30	121.00	2.40	0.14	BD	2.10	0.001	0.001	0.0100	0.0002	20.00	0.10	0.50	0.010	0.3	6.00	6.7	370	390	390
CMT 1 - 5	10/22/2010	57	59	13.07	4.39	92.28	1.68	0.30	BD	6.69	BD	0.008	0.7332	BD	21.00	0.06	0.16	0.003	0.1	7.52	7.2	172	330	300
	10/22/2010	57	59	13.11	4.34	91.19	1.68	0.30	BD	6.56	BD	BD	0.6686	BD	22.00	0.05	0.13	0.002	0.1	7.62	7.3	187	300	190
	12/11/2010	57	59	15.96	3.41	113.50	1.24	0.18	0.0001	12.23	0.001	0.008	BD	0.0007	39.00	BD	0.13	0.013	0.7	5.28	6.7	404	330	330
	12/11/2010	57	59	16.37	3.46	115.30	1.26	0.19	BD	12.46	0.001	0.009	0.0002	0.0007	39.00	0.01	0.20	0.010	0.9	6.38	6.7	394	390	330
	12/13/2010	57	59	13.43	3.34	117.90	1.63	0.19	BD	10.55	0.000	0.008	0.0009	0.0004	34.00	BD	0.32	0.019	0.7	6.27	6.7	448	320	320
	12/13/2010	57	59	13.38	3.37	118.50	1.35	0.20	BD	11.19	0.001	0.010	0.0016	0.0005	34.00	BD	0.32	0.023	0.7	6.10	6.7	443	340	340
	12/17/2010	57	59	9.46	3.70	127.00	1.44	0.19	BD	11.79	0.001	0.009	0.0016	0.0008	27.00	BD	0.13	0.018	0.5	4.36	6.8	266	330	330
	12/17/2010	57	59	10.28	3.72	126.70	1.54	0.20	BD	12.36	0.001	0.008	0.0003	0.0012	26.00	BD	0.42	0.015	0.4	5.32	6.8	253	320	280
	10/3/2011	57	59	22.00	4.20	113.00	2.20	0.17	BD	0.80	BD	BD	0.0100	0.0001	4.00	BD	0.50	0.020	0.9	26.00	6.8	372	410	420
	10/3/2011	57	59	22.00	4.20	113.00	2.30	0.18	BD	0.80	0.001	0.001	0.0100	0.0006	8.00	0.10	0.50	0.020	0.3	28.00	6.7	365	420	410



### During and Post-treatment – Test Plot

	Date	Depth, feet		Cations (mg/L)											Anions (mg/L)					General Water Quality				
		DTT	DTB	Na	Mg	Ca	K	Mn	Cr	Fe	Ni	As	Se	Cd	Sulfate	NH4	phosphate	Nitrite	Nitrate	Chloride	pH	ORP (mV)	TS (mg/L)	DS (mg/L)
CMT 2 - 2	10/22/2010	30	31	40.43	2.09	10.87	2.05	0.19	BD	9.82	BD	0.003	0.4877	BD	13.00	0.33	0.35	0.006	0.2	27.30	6.4	246	180	190
	10/22/2010	30	31	40.26	2.05	10.66	2.11	0.20	BD	10.04	BD	0.005	0.4877	BD	12.00	0.35	0.30	0.006	0.2	25.74	6.4	250	170	180
	12/11/2010	30	31	26.82	0.79	5.69	1.27	0.11	0.0030	5.48	0.004	0.005	0.0060	0.0040	9.00	0.17	1.62	0.004	0.8	15.95	6.2	240	160	160
	12/11/2010	30	31	26.55	0.76	5.59	1.25	0.10	0.0020	5.42	0.003	0.004	0.0030	0.0020	9.00	0.17	2.01	0.004	0.5	15.70	6.1	232	190	150
	12/13/2010	30	31	26.38	0.66	5.15	1.26	0.08	BD	4.48	0.002	0.005	0.0090	BD	9.00	0.19	1.26	0.007	0.6	16.95	6.3	296	180	170
	12/13/2010	30	31	27.43	0.66	5.11	1.28	0.08	BD	4.39	0.001	0.004	0.0050	BD	9.00	0.19	1.17	0.007	0.6	15.42	6.1	241	160	170
	12/17/2010	30	31	31.44	0.84	6.20	1.70	0.11	BD	6.60	0.001	0.004	BD	BD	4.00	0.25	1.13	0.004	0.5	18.22	6.3	252	110	110
	12/17/2010	30	31	32.44	0.85	6.28	2.00	0.11	BD	6.66	0.001	0.004	0.0020	0.0010	5.00	0.22	1.12	0.003	0.6	19.14	6.1	247	120	130
	10/3/2011	30	31	110.00	1.30	12.00	4.00	0.10	BD	4.00	BD	0.002	0.0100	0.0004	17.00	0.50	1.80	0.030	1.3	20.00	6.7	341	240	250
	10/3/2011	30	31	112.00	1.30	12.00	4.00	0.10	BD	3.10	BD	BD	0.0100	BD	16.00	0.50	1.70	0.020	0.9	20.00	6.5	351	270	260
CMT 2 - 3	10/22/2010	35	37	13.27	0.68	9.72	1.23	0.18	BD	9.35	BD	0.003	0.3068	BD	17.00	0.02	1.20	0.002	BD	14.61	5.9	157	100	130
	10/22/2010	35	37	13.25	0.64	9.09	1.24	0.15	BD	8.89	BD	0.005	0.1680	BD	18.00	0.02	1.30	0.003	BD	14.11	5.9	156	100	110
	12/11/2010	35	37	7.16	0.91	9.83	1.19	0.06	0.0010	7.99	0.002	0.008	0.0110	0.0010	17.00	BD	1.35	0.002	0.2	8.30	5.8	244	90	90
	12/11/2010	35	37	6.85	0.92	9.86	1.14	0.05	BD	8.04	0.002	0.005	0.0100	BD	18.00	0.01	1.24	0.002	0.2	8.72	5.6	243	90	90
	12/13/2010	35	37	6.18	0.95	12.66	1.11	0.06	BD	7.72	0.002	0.005	0.0110	0.0010	17.00	BD	1.33	0.002	0.1	9.18	5.8	192	60	60
	12/13/2010	35	37	6.55	0.96	12.79	1.19	0.06	BD	7.81	0.002	0.008	0.0100	0.0010	17.00	0.01	1.18	0.002	0.2	9.50	5.7	179	80	80
	12/17/2010	35	37	9.36	0.89	9.20	1.38	0.05	BD	7.62	0.002	0.005	0.0030	0.0010	22.00	0.03	1.55	0.003	0.4	12.76	5.7	267	50	40
	12/17/2010	35	37	8.56	0.88	9.15	1.32	0.05	BD	7.60	0.001	0.001	0.0080	BD	21.00	0.02	1.35	0.003	0.4	11.91	5.6	258	50	50
	10/3/2011	35	37	23.00	0.80	5.00	1.90	0.06	BD	8.80	BD	0.005	0.0400	0.0003	29.00	0.10	1.20	0.010	0.4	8.00	5.8	352	90	80
	10/3/2011	35	37	24.00	0.80	5.00	1.90	0.07	BD	8.80	BD	0.003	0.0400	0.0002	28.00	0.10	1.10	0.010	0.6	8.00	5.6	354	30	40
CMT 2 - 4	10/22/2010	41	46	9.79	1.11	25.59	1.28	0.19	BD	13.35	BD	0.018	0.4102	BD	22.00	0.03	1.24	0.012	0.3	13.22	6	167	100	140
	10/22/2010	41	46	10.15	1.13	26.26	1.28	0.16	BD	13.85	BD	0.013	0.4619	BD	22.00	0.02	1.01	0.014	0.3	13.08	6	171	150	140
	12/11/2010	41	46	8.00	1.16	33.43	1.17	0.11	BD	13.70	0.001	0.016	0.0040	0.0010	25.00	0.01	2.47	0.010	0.9	8.97	6	227	170	170
	12/11/2010	41	46	8.25	1.14	32.96	1.19	0.11	BD	13.56	0.002	0.020	0.0100	0.0010	24.00	0.01	2.73	0.005	0.7	9.39	6	221	160	160
	12/13/2010	41	46	7.19	1.06	28.91	1.70	0.10	BD	11.27	0.002	0.015	0.0040	0.0010	27.00	0.02	2.38	0.006	0.8	10.67	6	146	140	140
	12/13/2010	41	46	7.05	1.06	29.15	1.18	0.10	0.0010	11.34	0.001	0.013	0.0050	0.0010	26.00	0.03	2.44	0.015	0.9	9.50	6	146	130	140
	12/17/2010	41	46	9.15	1.06	28.22	1.26	0.10	BD	11.55	0.002	0.012	0.0040	0.0010	34.00	BD	3.80	0.006	1.3	12.48	6	200	100	80
	12/17/2010	41	46	9.17	1.08	28.67	1.30	0.10	BD	11.70	0.001	0.010	0.0070	0.0010	28.00	BD	3.80	0.004	0.9	12.73	6.1	198	90	90
	10/3/2011	41	46	25.00	0.90	10.00	4.40	0.08	BD	4.50	0.001	0.003	0.0200	0.0002	35.00	0.10	0.20	BD	0.4	8.00	5.9	353	120	190
	10/3/2011	41	46	25.00	0.90	10.00	4.40	0.07	BD	3.70	BD	0.003	0.0100	0.0002	33.00	BD	0.10	0.010	BD	8.00	5.8	349	140	60

### During and Post-treatment – Control Plot

	Depth, feet		Cations (mg/L)											Anions (mg/L)					General Water Quality							
	Date	DTT	DTB	Na	Mg	Ca	K	Mn	Cr	Fe	Ni	As	Se	Cd	Sulfate	NH4	phosphate	Nitrite	Nitrate	Chloride	pH	ORP (mV)	TS (mg/L)	DS (mg/L)		
CMT 3 - 2	10/22/2010	37	42	8.26	1.72	33.41	1.02	0.12	BD	5.11	BD	0.005	0.4393	BD	15.00	0.21	0.66	0.013	0.3	10.74	6.30	262	150	150		
	10/22/2010	37	42	8.65	1.78	34.63	1.05	0.11	BD	5.46	BD	0.003	0.4683	BD	14.00	0.23	0.60	0.013	0.3	10.56	6.40	243	130	60		
	10/31/2010	37	42	6.63	2.65	79.57	1.15	0.15	BD	2.58	BD	0.013	0.6202	BD	24.00	0.01	1.02	0.009	0.1	6.95	6.30	235	820	740		
	10/31/2010	37	42	6.41	2.63	78.79	1.13	0.16	BD	2.70	BD	0.012	0.4393	BD	26.00	0.01	0.91	0.009	0.1	7.44	6.30	236	810	720		
	11/2/2010	37	42	1242.50	BD	7.65	4.37	455.45	0.8915	0.43	BD	0.035	6.0210	BD	No data available					22.19	6.80	612	5070	3940		
	11/2/2010	37	42	1124.00	BD	8.72	3.94	690.70	0.8650	BD	BD	0.048	6.5410	BD	No data available					22.33	6.80	619	5010	3950		
	11/12/2010	37	42	WELL was dry																						
	11/12/2010	37	42	WELL was dry																						
	10/3/2011	37	42	WELL was dry																						
	10/3/2011	37	42	WELL was dry																						
CMT 3 - 3	10/22/2010	46	48	6.05	2.27	69.27	1.10	0.17	BD	4.18	BD	0.017	0.6105	BD	28.00	0.02	1.22	0.041	0.4	6.20	6.50	256	250	230		
	10/22/2010	46	48	6.12	2.27	70.65	1.15	0.17	BD	4.54	BD	0.014	0.4877	BD	28.00	0.02	1.03	0.049	0.3	6.27	6.60	267	220	230		
	10/31/2010	46	48	131.90	4.30	79.91	3.55	9.43	0.0200	17.93	0.002	0.027	0.7978	BD	295.00	0.02	1.30	0.008	0.1	17.02	7.00	216	270	260		
	10/31/2010	46	48	135.10	4.37	82.02	3.67	8.53	BD	17.41	BD	0.017	0.9780	BD	295.00	0.13	2.45	0.009	0.1	16.13	6.90	214	300	230		
	11/2/2010	46	48	216.40	6.46	147.20	5.60	22.78	1.1160	0.09	0.016	0.015	1.4180	BD	No data available					22.90	6.40	609	1410	1170		
	11/2/2010	46	48	209.00	6.06	135.00	5.38	20.95	0.9182	0.12	0.018	0.018	1.4020	BD	No data available					22.79	6.40	602	1450	1170		
	11/12/2010	46	48	26.67	2.36	73.55	2.14	7.55	0.0021	2.67	0.001	0.014	0.4877	BD	79.00	BD	2.60	0.001	0.1	17.65	6.80	353	360	360		
	11/12/2010	46	48	27.02	2.38	74.35	2.07	7.54	0.0016	2.76	0.000	0.016	0.5620	BD	75.00	BD	1.95	0.001	0.2	17.80	6.90	348	330	340		
	10/3/2011	46	48	11.00	1.45	60.80	20.80	0.07	BD	0.72	BD	0.005	0.0080	BD	21.00	0.10	1.10	0.040	0.5	4.00	6.80	340	270	360		
	10/3/2011	46	48	11.00	1.43	58.20	20.70	0.05	BD	0.64	0.001	0.006	0.0050	0.0010	22.00	0.10	1.30	0.050	0.5	4.00	6.80	352	250	320		
CMT 3 - 4	10/22/2010	52	54	6.94	3.19	79.56	1.25	0.18	BD	4.17	BD	0.008	0.7203	BD	26.00	0.05	0.26	0.016	0.1	8.05	6.90	223	260	250		
	10/22/2010	52	54	6.60	3.18	80.32	1.25	0.18	BD	4.27	BD	0.008	0.7494	BD	27.00	0.05	0.34	0.017	0.1	8.58	6.90	256	260	250		
	10/31/2010	52	54	6.76	1.57	59.42	1.10	0.29	BD	3.69	BD	0.016	0.4328	BD	42.00	BD	5.25	0.001	BD	11.59	6.60	227	240	220		
	10/31/2010	52	54	6.68	1.63	60.85	1.11	0.30	BD	3.66	BD	0.016	0.5394	BD	43.00	BD	4.15	0.001	BD	11.52	6.60	229	230	230		
	11/2/2010	52	54	576.10	7.84	201.30	9.70	722.70	4.1460	BD	BD	0.019	6.3440	BD	No data available					22.90	6.70	630	4330	3610		
	11/2/2010	52	54	572.90	7.90	199.30	9.28	715.90	4.1410	BD	BD	0.027	6.1400	BD	No data available					22.87	6.70	634	4360	3590		
	11/12/2010	52	54	173.60	2.75	66.01	2.85	10.64	0.5700	BD	BD	0.019	1.5700	BD	No data available						7.00	346	340	310		
	11/12/2010	52	54	176.30	2.75	66.61	2.99	12.62	0.6000	BD	BD	0.018	1.5500	BD	No data available						7.00	351	360	310		
	10/3/2011	56.5	57.5	13.00	3.17	104.40	2.50	4.74	BD	0.00	BD	BD	0.0300	BD	31.00	0.10	0.10	0.090	0.6	4.00	7.00	197	290	270		
	10/3/2011	56.5	57.5	12.00	3.11	103.70	2.30	4.54	BD	0.01	0.002	BD	0.0250	BD	31.00	0.10	0.50	0.080	0.6	4.00	7.00	228	310	270		
CMT 3 - 5	10/22/2010	56.5	57.5	8.14	2.74	88.28	1.34	0.10	BD	2.06	0.000	0.006	0.6072	BD	29.00	0.02	0.79	0.030	0.2	10.60	7.00	202	260	270		
	10/22/2010	56.5	57.5	8.02	2.76	87.71	1.30	0.10	BD	2.05	0.001	0.009	0.5652	BD	28.00	0.02	0.89	0.029	0.2	10.35	7.00	217	270	270		
	10/31/2010	56.5	57.5	7.20	2.85	81.01	1.23	0.16	BD	4.22	0.002	0.001	0.4457	BD	26.00	BD	0.79	0.031	0.4	7.80	7.00	417	680	670		
	10/31/2010	56.5	57.5	7.50	2.86	80.74	1.28	0.14	BD	4.33	BD	0.003	0.2972	BD	27.00	BD	0.89	0.031	0.4	7.44	7.00	406	680	650		
	11/2/2010	56.5	57.5	114.60	3.06	93.80	2.97	1.06	0.0044	3.65	0.000	0.015	1.1080	BD	61.00	BD	0.49	0.002	0.2	16.13	7.10	646	1940	1610		
	11/2/2010	56.5	57.5	117.80	3.08	94.87	2.86	0.73	0.0011	3.61	BD	0.017	1.1080	BD	62.00	0.01	0.40	0.003	0.1	15.92	7.00	649	1890	1600		
	11/12/2010	56.5	57.5	345.90	5.03	132.90	5.24	307.10	3.6970	BD	BD	0.019	3.7240	BD	No data available					No data available						
	11/12/2010	56.5	57.5	306.20	6.08	207.20	5.61	270.80	3.1410	BD	BD	0.021	3.8470	BD	No data available					No data available						
	10/3/2011	56.5	57.5	16.00	3.04	87.10	2.10	6.51	0.0030	0.04	0.003	BD	0.0300	BD	24.00	BD	0.30	0.010	0.2	11.00	7.00	354	270	320		
	10/3/2011	56.5	57.5	14.00	3.01	7.50	2.00	6.11	0.0030	0.03	0.002	BD	0.0270	BD	25.00	BD	0.70	BD	0.2	10.00	6.90	363	330	270		

### During and Post-treatment – Control Plot

	Depth, feet		Cations (mg/L)												Anions (mg/L)						General Water Quality			
	Date	DTT	DTB	Na	Mg	Ca	K	Mn	Cr	Fe	Ni	As	Se	Cd	Sulfate	NH4	phosphate	Nitrite	Nitrate	Chloride	pH	ORP (mV)	TS (mg/L)	DS (mg/L)
CMT 4 - 1	10/22/2010	37	42	31.15	4.14	65.66	3.20	0.07	BD	1.32	0.001	0.033	0.4780	BD	38.00	0.04	0.46	0.036	0.3	12.44	7.2	196	320	290
	10/22/2010	37	42	30.94	4.20	66.46	3.04	0.07	BD	1.30	0.001	0.016	0.4005	BD	40.00	0.03	0.45	0.037	0.1	12.16	7.2	210	300	290
	10/31/2010	37	42	28.66	1.38	13.71	2.68	0.54	BD	4.41	0.001	0.007	0.0678	0.0023	26.00	0.15	5.60	0.008	0.1	7.20	6.3	190	230	190
	10/31/2010	37	42	28.26	1.37	13.35	2.11	0.40	BD	4.47	0.000	0.006	0.1227	BD	28.00	0.16	5.30	0.006	0.1	7.02	6.4	203	240	200
	11/2/2010	37	42	55.79	2.51	12.17	3.46	0.24	0.0235	3.90	BD	0.015	0.4877	0.0018	67.00	0.19	8.60	0.005	BD	14.57	5.9	527	340	290
	11/2/2010	37	42	61.19	2.77	12.77	3.81	0.21	0.0275	4.36	BD	0.015	0.5426	BD	63.00	0.17	9.30	0.006	0.2	14.68	5.9	513	330	300
	11/12/2010	37	42	47.38	3.12	35.37	7.59	0.13	0.0096	4.51	0.005	0.010	0.5975	0.0035	35.00	0.09	2.70	BD	0.1	14.89	6.9	436	470	310
	11/12/2010	37	42	50.28	3.07	34.57	8.41	0.12	0.0052	4.18	0.003	0.015	0.5846	0.0018	48.00	0.09	1.70	BD	0.1	14.04	6.7	438	460	310
	10/3/2011	37	42	688.00	5.80	33.00	15.50	1.13	0.0100	1.35	BD	BD	0.1000	BD	340.00	2.30	0.90	0.010	0.4	26.00	6.7	361	2460	1790
	10/3/2011	37	42	699.00	5.90	33.50	14.60	1.13	0.0200	2.19	0.001	0.008	0.1110	BD	320.00	2.50	0.80	0.020	BD	25.00	6.7	360	2260	1800
CMT 4 - 2	10/22/2010	46	48	103.80	1.38	16.18	6.49	0.02	BD	0.52	0.001	0.037	0.4716	BD	30.00	0.07	1.02	0.024	0.2	10.49	8.3	188	870	630
	10/22/2010	46	48	105.60	1.30	14.94	6.37	0.02	BD	0.59	0.000	0.037	0.4877	BD	29.00	0.07	0.95	0.018	0.2	10.28	8.7	145	1060	730
	10/31/2010	46	48	57.75	2.05	33.47	10.01	0.31	BD	1.39	BD	0.005	0.3714	BD	32.00	0.25	1.09	0.001	BD	8.79	7.2	189	530	410
	10/31/2010	46	48	57.00	2.04	33.66	10.58	0.27	BD	1.35	0.000	0.013	0.5652	BD	33.00	0.26	1.17	0.001	BD	8.37	7.4	198	560	410
	11/2/2010	46	48	65.77	1.79	30.17	17.15	0.06	BD	0.15	BD	0.002	0.1098	BD	29.00	0.55	1.20	0.009	BD	9.89	7.2	422	890	510
	11/2/2010	46	48	64.61	2.21	33.39	16.86	0.10	BD	1.86	BD	0.008	0.4748	BD	30.00	0.58	1.00	0.012	BD	9.89	7.2	409	1110	540
	11/12/2010	46	48	87.43	1.92	24.17	16.31	0.06	0.0001	1.21	0.002	0.015	0.7558	BD	20.00	0.42	1.06	BD	BD	11.34	7.7	416	1640	720
	11/12/2010	46	48	87.35	1.87	23.85	16.62	0.05	BD	1.09	0.000	0.014	0.6040	BD	25.00	0.46	0.89	BD	BD	11.66	7.8	415	1460	670
	10/3/2011	46	48	1142.00	4.10	54.10	31.80	0.11	BD	3.83	0.001	0.009	0.0180	0.0010	700.00	1.10	1.20	0.010	0.6	21.00	6.9	364	2270	2370
	10/3/2011	46	48	1143.00	4.00	53.40	31.70	0.11	BD	1.23	0.001	0.003	0.0120	BD	800.00	1.00	0.50	0.020		21.00	7	369	2200	2440
CMT 4 - 3	10/22/2010	52	54	123.90	1.90	24.51	3.95	0.05	BD	0.36	0.005	0.010	0.6525	BD	32.00	0.50	0.92	0.028	0.4	10.92	8.7	152	610	690
	10/22/2010	52	54	123.80	1.93	25.00	4.02	0.05	BD	0.36	0.007	0.011	0.6105	BD	32.00	0.49	0.86	0.027	0.3	11.24	8.6	165	720	620
	10/31/2010	52	54	62.13	1.95	27.85	4.11	0.15	BD	0.59	0.003	0.006	0.4134	BD	19.00	0.25	1.29	0.050	0.3	9.22	7.5	195	360	370
	10/31/2010	52	54	62.12	1.97	28.47	4.11	0.12	BD	0.65	0.003	0.003	0.4264	BD	19.00	0.23	1.12	0.052	0.2	9.08	7.5	196	300	340
	11/2/2010	52	54	74.07	1.87	28.44	5.94	0.08	BD	0.85	0.002	0.010	0.4877	BD	35.00	0.34	0.80	0.039	0.2	11.20	7.2	402	440	390
	11/2/2010	52	54	74.62	1.85	28.42	6.24	0.08	BD	0.83	0.002	0.017	0.4877	BD	30.00	0.30	1.10	0.040	0.2	11.17	7.2	398	520	390
	11/12/2010	52	54	126.20	2.18	24.82	5.09	0.09	BD	1.81	0.003	0.017	0.7978	BD	24.00	0.63	0.96	BD	BD	14.00	7.8	396	1910	810
	11/12/2010	52	54	123.90	2.08	23.88	5.18	0.08	BD	1.57	0.003	0.008	0.6686	BD	30.00	0.65	1.11	BD	BD	14.39	7.7	406	1720	790
	10/3/2011	52	54	1266.00	8.70	73.90	28.80	0.33	BD	BD	2.8320	0.004	0.0040	0.0310	800.00	1.60	0.10	0.020	0.7	18.00	7	372	2380	2880
	10/3/2011	52	54	1252.00	8.70	74.50	28.60	0.32	BD	0.00	2.414	0.002	BD	0.0270	800.00	1.70	0.50	0.020	0.8	19.00	7	375	2360	2810
CMT 4 - 4	10/22/2010	57	57.5	26.85	4.55	71.07	3.23	0.06	BD	0.90	0.001	0.030	0.6169	BD	37.00	0.01	0.29	0.025	0.3	12.94	7.2	166	300	310
	10/22/2010	57	57.5	27.30	4.65	72.85	3.12	0.06	BD	0.87	0.000	0.035	0.5620	BD	38.00	0.01	0.34	0.026	0.3	12.73	7.2	174	320	310
	10/31/2010	57	57.5	34.00	1.74	21.58	2.82	0.27	BD	4.69	0.001	0.005	0.1680	0.0058	19.00	0.18	4.35	0.008	0.1	7.76	7	211	240	230
	10/31/2010	57	57.5	33.89	1.70	21.20	2.82	0.19	BD	3.39	0.001	0.003	0.4748	BD	22.00	0.17	5.25	0.007	0.1	7.91	6.8	218	250	230
	11/2/2010	57	57.5	58.75	2.66	14.10	3.76	0.15	0.0224	4.10	BD	0.011	0.4619	BD	64.00	0.20	1.50	0.011	0.1	14.32	6.1	470	340	290
	11/2/2010	57	57.5	59.25	2.64	13.99	3.92	0.14	0.0225	4.14	BD	0.009	0.6234	BD	65.00	0.19	1.50	0.012	0.2	14.71	6	465	350	310
	11/12/2010	57	57.5	62.26	4.07	48.89	3.89	0.21	0.0050	11.18	0.001	0.016	0.8624	BD	60.00	0.29	2.00	BD	0.1	17.26	6.6	418	650	350
	11/12/2010	57	57.5	66.22	4.08	49.24	3.87	0.21	0.0058	11.27	0.001	0.018	0.8721	BD	62.00	0.34	1.20	BD	0.1	17.65	6.5	416	360	370
	10/3/2011	57	57.5	1396.00	2.20	12.80	14.70	3.54	0.03	1.0970	0.00	0.007	0.338	BD	430.00	5.00	1.40	0.020	1.8	25.00	7.9	358	4590	4090
	10/3/2011	57	57.5	1375.00	2.70	12.50	14.90	3.48	0.08	2.3530	0.00	0.101	0.322	BD	430.00	7.00	1.30	0.020	1.4	26.00	7.9	348	4390	3730

**Absorbance of Groundwater at 418 nm (MnO<sub>2</sub> indicator) and 525 nm (permanganate)**

**Test Plot**

CMT - 1		
Date	A525	A418
12/9/2010		
12/10/2010		
12/11/2010		
12/12/2010	0.221	0.326
12/13/2010	0.233	0.255
12/14/2010		
12/15/2010		
11/3/2011		
Date	A525	A418
12/9/2010		
12/10/2010		
12/11/2010		
12/12/2010	0.001	0.011
12/13/2010	0.007	0.001
12/14/2010		
12/15/2010		
11/3/2011		
Date	A525	A418
12/9/2010		
12/10/2010		
12/11/2010		
12/12/2010	0.007	0.012
12/13/2010	0.003	0.004
12/14/2010		
12/15/2010		
11/3/2011		
Date	A525	A418
12/9/2010		
12/10/2010		
12/11/2010		
12/12/2010	0.001	0.008
12/13/2010	0.004	0.012
12/14/2010		
12/15/2010		
11/3/2011		

CMT - 2		
Date	A525	A418
12/9/2010		
12/10/2010		
12/11/2010		
12/12/2010		
12/13/2010	0.001	0.006
12/14/2010		
12/15/2010		
11/3/2011		
Date	A525	A418
12/9/2010		
12/10/2010		
12/11/2010		
12/12/2010		
12/13/2010	0.000	0.001
12/14/2010		
12/15/2010		
11/3/2011		
Date	A525	A418
12/9/2010		
12/10/2010		
12/11/2010		
12/12/2010		
12/13/2010	0.001	0.005
12/14/2010		
12/15/2010		
11/3/2011		

**Absorbance of Groundwater at 418 nm (MnO<sub>2</sub> indicator) and 525 nm (permanganate)**

**Control Plot**

CMT - 3		
Date	A525	A418
10/29/2010		
10/30/2010	0.006	0.011
10/31/2010	0.113	0.308
11/1/2010	12.700	6.800
11/2/2010	85.1	0.067
11/3/2011	Dry Well	
Date	A525	A418
10/29/2010	0.002	0.001
10/30/2010	0.001	0.005
10/31/2010	0.010	0.020
11/1/2010	0.019	0.045
11/2/2010	0.215	0.562
11/3/2011		
Date	A525	A418
10/29/2010	0.003	0.005
10/30/2010	0.002	0.002
10/31/2010	0.013	0.021
11/1/2010	0.016	0.039
11/2/2010	38.9	1.26
11/3/2011		
Date	A525	A418
10/29/2010	0.001	0.003
10/30/2010	0.005	0.010
10/31/2010	0.011	0.027
11/1/2010	0.012	0.039
11/2/2010	0.014	0.051
11/3/2011		

CMT - 4		
Date	A525	A418
10/29/2010	0.012	0.019
10/30/2010	0.044	0.074
10/31/2010	0.064	0.094
11/1/2010	0.115	0.164
11/2/2010	0.062	0.096
11/3/2011		
Date	A525	A418
10/29/2010	0.070	0.097
10/30/2010	0.150	0.192
10/31/2010	0.176	0.220
11/1/2010	0.169	0.216
11/2/2010	0.352	0.45
11/3/2011		
Date	A525	A418
10/29/2010	0.021	0.035
10/30/2010	0.045	0.058
10/31/2010	0.117	0.147
11/1/2010	0.082	0.108
11/2/2010	0.085	0.117
11/3/2011		
Date	A525	A418
10/29/2010	0.027	0.045
10/30/2010	0.051	0.075
10/31/2010	0.053	0.082
11/1/2010	0.085	0.13
11/2/2010	0.111	0.158
11/3/2011		

## Polymer Concentration in Groundwater

### Test Plot – 1-yr Post-treatment

Polymer Concentration Based on Viscosity Measurement			
Date	Well	Port #	Concentration (mg/L)
11/3/2011	1	2	1.73±0.64
11/3/2011	1	3	1.97±1.4
11/3/2011	1	4	9.03±1.34
11/3/2011	1	5	BDL
11/3/2011	2	2	6.99±0.99
11/3/2011	2	3	3.87±1
11/3/2011	2	4	16.96±1.04

## Groundwater VOCs

### Test Plot

	Date	PCE (mg/L)	TCE (mg/L)	Total VOC (mg/L)		Date	PCE (mg/L)	TCE (mg/L)	Total VOC (mg/L)
CMT 1 - 2	10/22/2010	0.83	0.83	1.66	CMT 2 - 2	10/22/2010	4.73	2.93	7.66
	10/22/2010	0.88	0.89	1.77		10/22/2010	4.66	2.76	7.42
	12/11/2012	2.67	0.17	2.85		12/11/2012	4.14	4.23	8.38
	12/11/2012	2.71	0.19	2.90		12/11/2012	4.34	4.76	9.10
	12/13/2012	3.32	0.20	3.52		12/13/2012	4.19	3.05	7.25
	12/13/2012	3.14	0.18	3.32		12/13/2012	4.18	2.97	7.15
	12/17/2012	3.01	0.26	3.27		12/17/2012	4.28	3.27	7.55
	12/17/2012	3.16	0.28	3.44		12/17/2012	4.07	2.75	6.82
	1/9/2011	1.11	0.41	1.52		1/9/2011	2.56	1.56	4.11
	1/9/2011	1.23	0.43	1.66		1/9/2011	2.63	1.65	4.27
	10/2/2011	3.01	0.95	3.96		10/2/2011	4.89	0.43	5.32
	10/2/2011	2.99	0.96	3.95					
CMT 1 - 3	10/22/2010	4.82	3.88	8.70	CMT 2 - 3	10/22/2010	4.84	3.51	8.35
	10/22/2010	4.89	3.75	8.64		10/22/2010	4.81	3.12	7.93
	12/11/2012	1.68	3.83	5.51		12/11/2012	4.85	2.77	7.61
	12/11/2012	5.78	4.05	9.83		12/11/2012	4.91	2.89	7.79
	12/13/2012	5.88	3.64	9.52		12/13/2012	0.90	3.02	3.91
	12/13/2012	6.15	3.77	9.91		12/13/2012	1.51	3.26	4.77
	12/17/2012	1.80	4.39	6.19		12/17/2012	1.05	3.32	4.37
	12/17/2012	1.47	4.18	5.66		12/17/2012	0.91	3.49	4.40
	1/9/2011	6.45	3.42	9.87		1/9/2011	4.35	1.32	5.67
	1/9/2011	1.92	3.40	5.32		1/9/2011	0.82	1.35	2.17
	10/2/2011	5.92	0.50	6.42		10/2/2011	5.66	0.55	6.21
	10/2/2011	5.84	0.47	6.31					
CMT 1 - 4	10/22/2010	0.85	0.18	1.03	CMT 2 - 4	10/22/2010	4.02	3.24	7.26
	10/22/2010	0.85	0.19	1.04		10/22/2010	4.00	3.11	7.11
	12/11/2012	2.26	0.36	2.61		12/11/2012	4.05	1.22	5.26
	12/11/2012	2.09	0.32	2.41		12/11/2012	4.09	1.26	5.35
	12/13/2012	2.21	0.36	2.57		12/13/2012	1.28	1.18	2.46
	12/13/2012	2.21	0.36	2.57		12/13/2012	4.77	1.16	5.92
	12/17/2012	1.83	0.43	2.27		12/17/2012	4.95	2.32	7.27
	12/17/2012	1.87	0.43	2.30		12/17/2012	4.83	2.03	6.85
	1/9/2011	2.30	0.37	2.67		1/9/2011	4.62	1.72	6.34
	1/9/2011	2.31	0.37	2.68		1/9/2011	4.61	1.65	6.26
	10/2/2011	5.00	1.77	6.77		10/2/2011	4.40	0.44	4.84
	10/2/2011	5.05	1.80	6.85		10/2/2011	5.10	0.43	5.53
CMT 1 - 5	10/22/2010	0.35	0.06	0.42					
	10/22/2010	0.35	0.06	0.42					
	12/11/2012	1.54	0.21	1.76					
	12/11/2012	1.54	0.21	1.76					
	12/13/2012	1.57	0.27	1.83					
	12/13/2012	1.77	0.29	2.06					
	12/17/2012	1.32	0.26	1.58					
	12/17/2012	1.40	0.28	1.68					
	1/9/2011	0.76	0.18	0.94					
	1/9/2011	0.82	0.19	1.01					
	10/2/2011	2.99	0.59	3.58					
	10/2/2011	3.63	0.67	4.30					

## Groundwater VOCs

### Control Plot

	Date	PCE (mg/L)	TCE (mg/L)	Total VOC (mg/L)		Date	PCE (mg/L)	TCE (mg/L)	Total VOC (mg/L)
CMT 3 - 2	10/22/2010	3.82	2.01	5.84	CMT 4 - 1	10/22/2010	0.84	0.30	1.14
	10/22/2010	3.69	2.03	5.72		10/22/2010	0.95	0.35	1.30
	10/31/2010	3.28	0.62	3.90		10/31/2010	4.21	1.71	5.91
	10/31/2010	3.34	0.65	3.99		10/31/2010	4.21	1.68	5.90
	11/2/2010	0.21	0.02	0.23		11/2/2010	4.14	1.05	5.19
	11/2/2010	0.39	0.02	0.42		11/2/2010	4.15	1.10	5.25
						11/12/2010	3.47	1.35	4.82
						11/12/2010	3.31	1.30	4.61
	1/9/2011	1.36	0.12	1.48		1/9/2011	1.49	0.82	2.31
	1/9/2011	1.23	0.11	1.33		1/9/2011	3.34	0.82	4.16
10/3/2011				10/3/2011	0.69	0.12	0.81		
10/3/2011				10/3/2011	0.74	0.13	0.87		
CMT 3 - 3	10/22/2010	2.79	0.13	2.92	CMT 4 - 2	10/22/2010	2.41	0.08	2.49
	10/22/2010	2.67	0.09	2.76		10/22/2010	2.46	0.09	2.55
	10/31/2010	1.57	0.06	1.63		10/31/2010	3.27	0.23	3.50
	10/31/2010	1.54	0.05	1.59		10/31/2010	3.10	0.21	3.31
	11/2/2010	2.39	0.07	2.47		11/2/2010	3.38	0.23	3.61
	11/2/2010	2.12	0.05	2.18		11/2/2010	3.38	0.23	3.61
	11/12/2010	3.47	0.32	3.79		11/12/2010	3.59	0.33	3.92
	11/12/2010	3.45	0.32	3.78		11/12/2010	3.57	0.32	3.89
	1/9/2011	2.28	0.20	2.49		1/9/2011	1.31	0.24	1.55
	1/9/2011	2.22	0.20	2.42		1/9/2011	1.67	0.29	1.96
10/3/2011	3.80	0.23	4.03	10/3/2011	1.30	0.23	1.53		
10/3/2011	2.45	0.32	2.77	10/3/2011	1.19	0.22	1.41		
CMT 3 - 4	10/22/2010	2.16	0.11	2.27	CMT 4 - 3	10/22/2010	2.46	0.04	2.50
	10/22/2010	1.61	0.04	1.65		10/22/2010	2.14	0.02	2.17
	10/31/2010	3.29	0.24	3.53		10/31/2010	2.97	0.20	3.18
	10/31/2010	3.30	0.23	3.54		10/31/2010	3.02	0.21	3.23
	11/2/2010	0.20	0.02	0.21		11/2/2010	3.20	0.22	3.42
	11/2/2010	0.24	0.02	0.26		11/2/2010	3.10	0.21	3.30
	11/12/2010	0.85	0.07	0.91		11/12/2010	3.32	0.46	3.78
	11/12/2010	0.92	0.08	1.00		11/12/2010	3.36	0.44	3.80
	1/9/2011	3.85	0.46	4.31		1/9/2011	3.09	0.16	3.25
	1/9/2011	4.00	0.52	4.52		1/9/2011	3.17	0.17	3.34
10/3/2011	4.49	0.23	4.72	10/3/2011	0.99	0.12	1.11		
10/3/2011	5.05	0.31	5.36	10/3/2011	0.68	0.10	0.78		
CMT 3 - 5	10/22/2010	1.38	0.02	1.40	CMT 4 - 4	10/22/2010	1.68	0.21	1.89
	10/22/2010	1.24	0.02	1.26		10/22/2010	1.59	0.21	1.80
	10/31/2010	1.36	0.07	1.44		10/31/2010	4.02	1.45	5.47
	10/31/2010	1.43	0.08	1.51		10/31/2010	3.99	1.39	5.39
	11/2/2010	0.74	0.02	0.76		11/2/2010	3.97	1.00	4.97
	11/2/2010	0.76	0.02	0.78		11/2/2010	3.75	0.84	4.60
	11/12/2010	0.80	0.09	0.89		11/12/2010	3.52	1.50	5.01
	11/12/2010	0.79	0.08	0.87		11/12/2010	3.49	1.47	4.96
						1/9/2011	0.63	0.15	0.78
						1/9/2011	0.53	0.13	0.66
10/3/2011	5.67	0.58	6.25	10/3/2011	0.76	0.15	0.91		
10/3/2011	1.30	0.11	1.41	10/3/2011	0.87	0.18	1.05		



## **Soil VOCs**

## Test Plot – Pre-treatment

Test Plot			
Sample ID #	Sample Received	Concentration TCE (mgTCE/kg dry soil)	Concentration PCE (mgPCE/kg dry soil)
IR88-IW3-36-37-1	5/26/2010	0.51	1.50
IR88-IW3-36-37-1	5/26/2010	0.58	1.77
IR88-IW3-38-40-1	5/26/2010	0.58	1.96
IR88-IW3-38-40-1	5/26/2010	1.01	3.47
IR88-IW3-45-46-1	5/26/2010	0.80	12.98
IR88-IW3-45-46-1	5/26/2010	0.75	13.18
IR88-IW3-46-48-1	5/26/2010	0.00	0.08
IR88-IW3-46-48-1	5/26/2010	0.00	0.10
IR88-IW3-51-51-1	5/26/2010	0.01	0.40
IR88-IW3-51-51-1	5/26/2010	0.00	0.43
IR88-CMT01-38-39-1	5/18/2010	1.71	1.50
IR88-CMT01D-38-39-1	5/18/2010	2.08	2.39
IR88-CMT01-44-45-1	5/18/2010	1.59	16.27
IR88-CMT01D-44-45-1	5/18/2010	1.45	13.19
IR88-CMT01-51-52-1	5/18/2010	0.05	0.28
IR88-CMT01D-51-52-1	5/18/2010	0.10	0.43
IR88-CMT01-55-56-1	5/18/2010	0.07	0.55
IR88-CMT01D-55-56-1	5/18/2010	0.00	0.11
IR88-CMT02-35-36-1	5/20/2010	1.23	8.07
IR88-CMT02D-35-36-1	5/20/2010	1.10	5.65
IR88-CMT02-43-44-1	5/20/2010	0.10	2.66
IR88-CMT02D-43-44-1	5/20/2010	0.00	0.61
IR88-CMT02-51-52-1	5/20/2010	0.02	0.19
IR88-CMT02D-51-52-1	5/20/2010	0.02	0.19

## Test Plot – Post-treatment

Sample name	Depth (ft bgs)	Date Collected	TCE conc. (mg/kg soil)	PCE conc. (mg/kg soil)	Total VOC (mg/kg soil)
DPT-TP IW 3 1 A	33.7	12/14/2010	BD	BD	BD
DPT-TP IW 3 1 B	33.8	12/14/2010	BD	BD	BD
DPT-TP IW 3 1 A	34.9	12/14/2010	BD	BD	BD
DPT-TP IW 3 1 B	34.9	12/14/2010	BD	BD	BD
DPT-TP IW 3 1 A	38	12/14/2010	BD	BD	BD
DPT-TP IW 3 1 B	37.9	12/14/2010	BD	BD	BD
DPT-TP IW 3 1 A	49.1	12/14/2010	BD	BD	BD
DPT-TP IW 3 1 B	49.1	12/14/2010	BD	BD	BD
DPT-TP IW 3 1 A	43.9	12/14/2010	BD	BD	BD
DPT-TP IW 3 1 B	43.9	12/14/2010	BD	5.08	5.08
DPT-TP IW 3 1 A	52.2	12/14/2010	BD	BD	BD
DPT-TP IW 3 1 B	52.2	12/14/2010	BD	BD	BD
DPT-TP IW 3 1 A	59	12/14/2010	BD	BD	BD
DPT-TP IW 3 1 B	59	12/14/2010	BD	BD	BD
DPT-TP IW 3 2 A	32.8	12/14/2010	BD	BD	BD
DPT-TP IW 3 2 B	32.8	12/14/2010	BD	BD	BD
DPT-TP IW 3 2 A	39.9	12/14/2010	BD	4.97	4.97
DPT-TP IW 3 2 B	39.9	12/14/2010	BD	1.89	1.89
DPT-TP IW 3 2 A	42.7	12/14/2010	BD	1.85	1.85
DPT-TP IW 3 2 B	42.7	12/14/2010	BD	1.61	1.61
DPT-TP IW 3 2 A	43.7	12/14/2010	BD	BD	BD
DPT-TP IW 3 2 B	43.7	12/14/2010	BD	BD	BD
DPT-TP IW 3 2 B	48	12/14/2010	BD	BD	BD
DPT-TP IW 3 2 A	48	12/14/2010	BD	BD	BD
DPT-TP IW 3 2 A	54	12/14/2010	BD	BD	BD
DPT-TP IW 3 2 B	54	12/14/2010	BD	BD	BD
DPT-TP IW 3 3 A	34.6	12/14/2010	BD	BD	BD
DPT-TP IW 3 3 B	34.6	12/14/2010	BD	BD	BD
DPT-TP IW 3 3 A	37.8	12/14/2010	BD	BD	BD
DPT-TP IW 3 3 B	37.8	12/14/2010	BD	BD	BD
DPT-TP IW 3 3 A	44	12/14/2010	BD	13.95	13.95
DPT-TP IW 3 3 B	44	12/14/2010	BD	12.52	12.52
DPT-TP IW 3 3 A	48.9	12/14/2010	BD	BD	BD
DPT-TP IW 3 3 B	48.9	12/14/2010	BD	BD	BD
DPT-TP IW 3 3 A	53.5	12/14/2010	BD	BD	BD
DPT-TP IW 3 3 B	53.5	12/14/2010	BD	BD	BD
DPT-TP IW 3 4 A	34.3	12/15/2010	BD	BD	BD
DPT-TP IW 3 4 B	34.3	12/15/2010	BD	BD	BD
DPT-TP IW 3 4 A	37.5	12/15/2010	BD	BD	BD
DPT-TP IW 3 4 B	37.5	12/15/2010	BD	BD	BD
DPT-TP IW 3 4 A	39.6	12/15/2010	BD	BD	BD
DPT-TP IW 3 4 B	43.4	12/15/2010	0.01	17.90	17.91
DPT-TP IW 3 4 A	43.4	12/15/2010	BD	18.27	18.27
DPT-TP IW 3 4 A	53.3	12/15/2010	BD	BD	BD
DPT-TP IW 3 4 B	53.4	12/15/2010	BD	BD	BD
DPT-TP IW 3 4 A	57.3	12/15/2010	BD	BD	BD
DPT-TP IW 3 4 B	57.3	12/15/2010	BD	BD	BD
DPT-TP IW 3 4 B	59.6	12/15/2010	BD	BD	BD

Sample name	Depth (ft bgs)	Date Collected	TCE conc. (mg/kg soil)	PCE conc. (mg/kg soil)	Total VOC (mg/kg soil)
DPT-TP IW 3 5 A	34	12/15/2010	BD	BD	BD
DPT-TP IW 3 5 B	34	12/15/2010	BD	BD	BD
DPT-TP IW 3 5 A	38.5	12/15/2010	BD	BD	BD
DPT-TP IW 3 5 B	38.5	12/15/2010	BD	BD	BD
DPT-TP IW 3 5 A	43	12/15/2010	1.37	23.61	24.98
DPT-TP IW 3 5 B	43	12/15/2010	1.56	22.30	23.86
DPT-TP IW 3 5 A	48.9	12/15/2010	BD	BD	BD
DPT-TP IW 3 5 B	48.9	12/15/2010	BD	BD	BD
DPT-TP IW 3 5 A	52.1	12/15/2010	BD	BD	BD
DPT-TP IW 3 5 B	52.1	12/15/2010	BD	BD	BD
DPT-TP IW 3 6 A	38.8	12/16/2010	0.04	0.05	0.09
DPT-TP IW 3 6 B	38.8	12/16/2010	0.05	0.04	0.09
DPT-TP IW 3 6 A	48.9	12/16/2010	BD	2.70	2.70
DPT-TP IW 3 6 B	48.9	12/16/2010	BD	3.60	3.60
DPT-TP IW 3 6 A	54.1	12/16/2010	BD	BD	BD
DPT-TP IW 3 6 B	54.1	12/16/2010	BD	BD	BD
DPT-TP IW 3 7 A	38.9	12/16/2010	BD	1.86	1.86
DPT-TP IW 3 7 B	38.9	12/16/2010	0.73	1.24	1.97
DPT-TP IW 3 7 A	48.2	12/16/2010	BD	0.00	0.00
DPT-TP IW 3 7 B	48.2	12/16/2010	BD	0.00	0.00
DPT-TP IW 3 7 A	52.6	12/16/2010	BD	BD	BD
DPT-TP IW 3 7 B	52.6	12/16/2010	BD	BD	BD
DPT-TP IW 3 8 A	33.2	12/16/2010	0.11	0.81	0.92
DPT-TP IW 3 8 B	33.3	12/16/2010	0.02	0.37	0.39
DPT-TP IW 3 8 A	39.5	12/16/2010	1.19	18.80	19.99
DPT-TP IW 3 8 B	39.5	12/16/2010	1.31	19.96	21.27
DPT-TP IW 3 8 A	44.1	12/16/2010	BD	BD	BD
DPT-TP IW 3 8 B	49.1	12/16/2010	BD	BD	BD
DPT-TP IW 3 9 A	37.5	12/16/2010	0.73	10.27	11.00
DPT-TP IW 3 9 B	37.5	12/16/2010	0.67	8.65	9.32
DPT-TP IW 3 9 A	44.3	12/16/2010	0.02	2.03	2.05
DPT-TP IW 3 9 B	44.4	12/16/2010	0.04	3.39	3.43
DPT-TP IW 3 9 A	49	12/16/2010	BD	0.00	0.00
DPT-TP IW 3 9 B	49	12/16/2010	BD	BD	BD
DPT-TP IW 3 9 A	52.6	12/16/2010	BD	0.34	0.34
DPT-TP IW 3 9 B	52.6	12/16/2010	BD	0.05	0.05
DPT-TP IW 3 9 A	55.9	12/16/2010	BD	0.67	0.67
DPT-TP IW 3 9 B	55.9	12/16/2010	0.00	0.77	0.77
DPT-TP IW 3 10 A	34.6	12/17/2010	0.00	BD	0.00
DPT-TP IW 3 10 B	34.6	12/17/2010	BD	BD	0.00
DPT-TP IW 3 10 A	39.2	12/17/2010	0.01	0.71	0.72
DPT-TP IW 3 10 B	39.2	12/17/2010	0.31	1.39	1.70
DPT-TP IW 3 11 A	33.3	12/17/2010	0.37	0.34	0.71
DPT-TP IW 3 11 B	33.3	12/17/2010	0.38	0.63	1.01
DPT-TP IW 3 11 A	39.3	12/17/2010	BD	BD	BD
DPT-TP IW 3 11 B	39.3	12/17/2010	BD	BD	BD
DPT-TP IW 3 11 A	43.3	12/17/2010	BD	BD	BD
DPT-TP IW 3 11 B	43.3	12/17/2010	BD	BD	BD
DPT-TP IW 3 11 A	49.2	12/17/2010	BD	BD	BD
DPT-TP IW 3 11 B	49.2	12/17/2010	BD	BD	BD
DPT-TP IW 3 11 A	53.4	12/17/2010	BD	BD	BD
DPT-TP IW 3 11 B	53.4	12/17/2010	0.00	BD	0.00

## Control Plot – Pre-treatment

Control Plot			
Sample ID #	Sample Received	Concentration TCE (mgTCE/kg dry soil)	Concentration PCE (mgPCE/kg dry soil)
IR88-IW04-36-37-1	6/8/2010	0.02	2.05
IR88-IW04-36-37-1	6/8/2010	0.02	1.19
IR88-IW04-38-40-1	6/8/2010	0.00	0.00
IR88-IW04D-38-40-1	6/8/2010	0.00	0.00
IR88-IW04-42-43-1	6/8/2010	0.00	0.02
IR88-IW04D-42-43-1	6/8/2010	0.00	0.06
IR88-IW04D-48-49-1	6/8/2010	0.00	0.11
IR88-IW04D-48-49-1	6/8/2010	0.00	0.01
IR88-IW04-52-53-1	6/8/2010	0.00	0.00
IR88-IW04D-52-53-1	6/8/2010	0.00	0.00
IR88-CMT03-36-37-1	5/24/2010	0.00	0.01
IR88-CMT03D-36-37-1	5/24/2010	0.00	0.64
IR88-CMT03-42-43-1	5/24/2010	0.02	1.38
IR88-CMT03D-42-43-1	5/24/2010	0.04	2.21
IR88-CMT03-46-47-1	5/24/2010	0.00	0.01
IR88-CMT03D-46-47-1	5/24/2010	0.00	0.10
IR88-CMT04-39-40-1	5/21/2010	1.26	10.00
IR88-CMT04D-39-40-1	5/21/2010	1.06	4.79
IR88-CMT04-49-50-1	5/21/2010	0.02	0.45
IR88-CMT04D-49-50-1	5/21/2010	0.00	0.21
IR88-CMT04-64-65-1	5/21/2010	0.00	0.28
IR88-CMT04D-64-65-1	5/21/2010	0.01	0.38

## Control Plot – Post-treatment

Sample name	Depth (ft bgs)	Date Collected	TCE conc. (mg/kg soil)	PCE conc. (mg/kg soil)	Total VOC (mg/kg soil)
DPT-CP IW4 1 A	37.5	11/4/2010	0.02	2.05	2.07
DPT-CP IW4 1 B	37.5	11/4/2010	0.06	2.76	2.82
DPT-CP IW4 1 A	47.7	11/4/2010	BD	BD	BD
DPT-CP IW4 1 B	47.9	11/4/2010	BD	BD	BD
DPT-CP IW4 1 A	49.5	11/4/2010	BD	BD	BD
DPT-CP IW4 1 B	49.5	11/4/2010	BD	0.30	0.30
DPT-CP IW4 1 A	51.9	11/4/2010	BD	0.19	0.19
DPT-CP IW4 1 B	52	11/4/2010	BD	0.06	0.06
DPT-CP IW4 1 A	56.7	11/4/2010	BD	0.37	0.37
DPT-CP IW4 1 B	56.8	11/4/2010	BD	0.40	0.40
DPT-CP IW4 4 A	37.4	11/6/2010	BD	1.74	1.74
DPT-CP IW4 4 B	37.4	11/6/2010	BD	0.55	0.55
DPT-CP IW4 4 A	42.3	11/6/2010	BD	0.42	0.42
DPT-CP IW4 4 B	42.3	11/6/2010	BD	0.54	0.54
DPT-CP IW4 4 A	46.4	11/6/2010	BD	BD	BD
DPT-CP IW4 4 B	46.4	11/6/2010	BD	0.48	0.48
DPT-CP IW4 7 A	34.3	11/7/2010	BD	0.04	0.04
DPT-CP IW4 7 B	34.3	11/7/2010	BD	0.63	0.63
DPT-CP IW4 7 A	36.8	11/7/2010	BD	0.02	0.02
DPT-CP IW4 7 B	36.8	11/7/2010	BD	0.66	0.66
DPT-CP IW4 7 A	37.5	11/7/2010	BD	0.01	0.01
DPT-CP IW4 7 B	37.5	11/7/2010	BD	BD	BD
DPT-CP IW4 7 A	44.4	11/7/2010	BD	1.09	1.09
DPT-CP IW4 7 B	44.4	11/7/2010	BD	2.06	2.06
DPT-CP IW4 7 A	46.3	11/7/2010	BD	BD	BD
DPT-CP IW4 7 B	46.2	11/7/2010	BD	BD	BD
DPT-CP IW4 7 A	47.2	11/7/2010	BD	BD	BD
DPT-CP IW4 7 B	47.3	11/7/2010	BD	BD	BD
DPT-CP IW4 7 A	48.8	11/7/2010	BD	0.24	0.24
DPT-CP IW4 7 B	48.9	11/7/2010	BD	0.27	0.27
DPT-CP IW4 8 A	38.1	11/7/2010	0.02	1.04	1.06
DPT-CP IW4 8 B	38.1	11/7/2010	BD	0.74	0.74
DPT-CP IW4 8 A	38.8	11/7/2010	BD	BD	BD
DPT-CP IW4 8 B	38.8	11/7/2010	BD	BD	BD
DPT-CP IW4 8 A	44.6	11/7/2010	BD	BD	BD
DPT-CP IW4 8 B	44.6	11/7/2010	BD	0.57	0.57
DPT-CP IW4 8 A	57.3	11/7/2010	BD	BD	BD
DPT-CP IW4 8 B	57.3	11/7/2010	BD	0.37	0.37
DPT-CP IW4 8 A	59.4	11/7/2010	BD	0.51	0.51
DPT-CP IW4 8 B	59.5	11/7/2010	BD	0.60	0.60
DPT-CP IW4 2 A	34.8	11/5/2010	BD	BD	BD
DPT-CP IW4 2 B	34.8	11/5/2010	BD	BD	BD
DPT-CP IW4 2 A	39.8	11/5/2010	BD	BD	BD
DPT-CP IW4 2 B	39.8	11/5/2010	BD	0.11	0.11
DPT-CP IW4 2 A	43.5	11/5/2010	BD	1.04	1.04
DPT-CP IW4 2 B	43.5	11/5/2010	BD	0.73	0.73
DPT-CP IW4 2 A	47.8	11/5/2010	BD	0.55	0.55
DPT-CP IW4 2 B	47.9	11/5/2010	BD	0.39	0.39
DPT-CP IW4 3 A	36.9	11/5/2010	BD	0.52	0.52
DPT-CP IW4 3 B	37.2	11/5/2010	BD	3.06	3.06
DPT-CP IW4 3 A	44	11/5/2010	BD	1.51	1.51
DPT-CP IW4 3 B	44	11/5/2010	BD	1.45	1.45
DPT-CP IW4 3 A	44.6	11/5/2010	BD	0.50	0.50
DPT-CP IW4 3 B	44.6	11/5/2010	BD	0.44	0.44
DPT-CP IW4 3 A	48.1	11/5/2010	BD	BD	BD
DPT-CP IW4 3 B	48	11/5/2010	BD	0.43	0.43
DPT-CP IW4 3 A	54	11/5/2010	BD	BD	BD
DPT-CP IW4 3 B	54	11/5/2010	BD	BD	BD
DPT-CP IW4 3 A	57.5	11/5/2010	BD	BD	BD
DPT-CP IW4 3 B	57.3	11/5/2010	BD	0.55	0.55

Sample name	Depth (ft bgs)	Date Collected	TCE conc. (mg/kg soil)	PCE conc. (mg/kg soil)	Total VOC (mg/kg soil)
DPT-CP IW4 5 A	34.5	11/6/2010	BD	0.07	0.07
DPT-CP IW4 5 B	34.5	11/5/2010	BD	0.19	0.19
DPT-CP IW4 5 A	44.1	11/6/2010	BD	4.03	4.03
DPT-CP IW4 5 B	44.2	11/6/2010	BD	2.85	2.85
DPT-CP IW4 5 A	46.3	11/6/2010	BD	0.10	0.10
DPT-CP IW4 5 B	46.3	11/6/2010	BD	0.05	0.05
DPT-CP IW4 5 A	49.4	11/6/2010	BD	0.01	0.01
DPT-CP IW4 5 B	49.4	11/6/2010	BD	0.57	0.57
DPT-CP IW4 6 A	34.7	11/6/2010	BD	0.01	0.01
DPT-CP IW4 6 B	34.7	11/6/2010	BD	0.33	0.33
DPT-CP IW4 6 A	36.5	11/6/2010	BD	BD	BD
DPT-CP IW4 6 B	36.5	11/6/2010	BD	0.43	0.43
DPT-CP IW4 6 A	37.7	11/6/2010	BD	BD	BD
DPT-CP IW4 6 B	37.7	11/6/2010	1.78	0.12	1.90
DPT-CP IW4 6 A	39.9	11/6/2010	BD	BD	BD
DPT-CP IW4 6 B	39.9	11/6/2010	BD	BD	BD
DPT-CP IW4 11 A	34.4	11/8/2010	0.02	0.83	0.85
DPT-CP IW4 11 B	34.4	11/8/2010	0.01	0.89	0.90
DPT-CP IW4 11 A	38.9	11/8/2010	0.2	BD	0.20
DPT-CP IW4 11 B	38.9	11/8/2010	BD	BD	BD
DPT-CP IW4 11 A	39.8	11/8/2010	0.07	4.46	4.53
DPT-CP IW4 11 B	39.8	11/8/2010	0.14	8.16	8.30
DPT-CP IW4 10 A	44.4	11/7/2010	BD	1.55	1.55
DPT-CP IW4 10 B	44.4	11/7/2010	BD	1.05	1.05
DPT-CP IW4 10 A	46.9	11/7/2010	BD	0.002	0.002
DPT-CP IW4 10 B	46.9	11/7/2010	BD	0.31	0.31
DPT-CP IW4 10 A	47.3	11/7/2010	BD	BD	BD
DPT-CP IW4 10 B	47.3	11/7/2010	BD	BD	BD
DPT-CP IW4 10 A	47.8	11/7/2010	BD	0.58	0.58
DPT-CP IW4 10 B	47.8	11/7/2010	BD	0.28	0.28
DPT-CP IW4 9 A	38.4	11/7/2010	BD	0.70	0.70
DPT-CP IW4 9 B	38.4	11/7/2010	BD	0.70	0.70
DPT-CP IW4 9 A	44.5	11/7/2010	BD	0.13	0.13
DPT-CP IW4 9 B	44.5	11/7/2010	BD	1.13	1.13
DPT-CP IW4 9 A	48.4	11/7/2010	BD	BD	BD
DPT-CP IW4 9 B	48.4	11/7/2010	BD	0.42	0.42
DPT-CP IW4 9 A	53.6	11/7/2010	BD	BD	BD
DPT-CP IW4 9 B	53.6	11/7/2010	BD	0.37	0.37
DPT-CP IW4 9 A	54.3	11/7/2010	BD	0.65	0.65
DPT-CP IW4 9 B	54.3	11/7/2010	BD	0.70	0.70
DPT-CP IW4 9 A	55	11/7/2010	BD	0.39	0.39
DPT-CP IW4 9 B	55	11/7/2010	BD	0.46	0.46
DPT-CP IW4 12 A	39.5	11/8/2010	0.02	2.01	2.03
DPT-CP IW4 12 B	39.5	11/6/2010	BD	0.47	0.47
DPT-CP IW4 12 A	43.4	11/8/2010	BD	BD	BD
DPT-CP IW4 12 B	43.4	11/8/2010	BD	0.32	0.32
DPT-CP IW4 12 A	49.8	11/8/2010	BD	0.41	0.41
DPT-CP IW4 12 B	49.8	11/8/2010	BD	0.50	0.50
DPT-CP IW4 12 A	54.5	11/8/2010	BD	BD	BD
DPT-CP IW4 12 B	54.5	11/8/2010	BD	BD	BD

## Soil Geochemistry

### Pre-treatment

Test Plot							
Location	Depth	Date collected	TOC	pH	Eh	AEC	CEC
IW3	36-37'	5/24/2010		5.66	81.0		
IW3	36-37'	5/24/2010		5.48	89.3		
IW3	38-40'	5/24/2010	0.03	5.17	107.4	7.20	2.49
IW3	38-40'	5/24/2010	0.02	5.08	112.8	7.56	3.23
IW3	44-46'	5/24/2010		4.83	127.1		
IW3	44-46'	5/24/2010		4.88	122.6		
IW3	46-48'	5/24/2010		5.27	101.4		
IW3	46-48'	5/24/2010		5.40	93.5		
IW3	51-52'	5/24/2010		5.95	62.0		
IW3	51-52'	5/24/2010		5.99	59.9		
CMT1	38-39'	5/17/2010		5.42	92.1	6.54	0.89
CMT1	38-39'	5/17/2010		5.60	79.9	6.51	0.71
CMT1	44-45'	5/17/2010		5.53	85.9		
CMT1	44-45'	5/17/2010		5.37	95.4		
CMT1	51-52'	5/17/2010		7.53	-29.0		
CMT1	51-52'	5/17/2010		7.62	-35.7		
CMT1	55-56'	5/17/2010		8.46	-81.1		
CMT1	55-56'	5/17/2010		8.43	-79.3		
CMT2	35-36'	5/19/2010		5.48	89.2		
CMT2	35-36'	5/19/2010		5.41	93.2		
CMT2	43-44'	5/19/2010	0.04	4.94	120.1	7.66	1.09
CMT2	43-44'	5/19/2010	0.05	4.78	129.6	7.71	1.22
CMT2	51-52'	5/19/2010		6.98	1.9		
CMT2	51-52'	5/19/2010		7.20	-10.2		

Control Plot							
Location	Depth	Date collected	TOC	pH	Eh	AEC	CEC
IW4	36-37'	5/25/2010		4.76	130.3		
IW4	36-37'	5/25/2010		4.52	144.0		
IW4	38-40'	5/25/2010	0.04	4.77	129.8	6.24	2.20
IW4	38-40'	5/25/2010	0.05	4.63	137.8	7.55	2.54
IW4	42-43'	5/25/2010		7.22			
IW4	42-43'	5/25/2010		7.67			
IW4	48-49'	5/25/2010		7.95			
IW4	48-49'	5/25/2010		7.98			
IW4	52-53'	5/25/2010		8.02			
IW4	52-53'	5/25/2010		7.99			
CMT3	36-37'	5/21/2010		5.45	91.1		
CMT3	36-37'	5/21/2010		5.76	73.0		
CMT3	42-43'	5/21/2010	0.07	4.98	118.4	7.87	1.69
CMT3	42-43'	5/21/2010	0.05	5.00	117.3	6.82	1.60
CMT3	46-47'	5/21/2010		6.01	58.2		
CMT3	46-47'	5/21/2010		6.23	45.8		
CMT4	39-40'	5/20/2010	0.03	5.99	59.3	7.92	3.19
CMT4	39-40'	5/20/2010	0.97	5.74	73.9	9.89	5.99
CMT4	49-50'	5/20/2010		7.07	-3.2		
CMT4	49-50'	5/20/2010		7.15	-7.8		
CMT4	64-65'	5/20/2010		8.22	-67.6		
CMT4	64-65'	5/20/2010		8.23	-68.0		

AEC = anion exchange capacity (centimoles of charge / kg)

CEC = cation exchange capacity (centimoles of charge / kg)

TOC includes contaminant

### Test Plot – Immediately Post-treatment

Location	Depth (ft bgs)	pH	ORP	AEC	CEC	Extractable Mn (mg/L)			Extractable Na (mg/L)		
						H <sub>2</sub> O	BaCl	Mn as MnO <sub>2</sub>	H <sub>2</sub> O	BaCl	w/ MnO <sub>2</sub>
DPT-TP 1	32.6-32.8	5.61	657								
DPT-TP 1	32.8-33	6.20	576								
DPT-TP 1	37.5-37.8	7.20	633	0.24	3.25	5.3	3.6	10.6	46.7	30.7	2.5
DPT-TP 1	37-37.5	7.86	586	0.16	3.28	0.4	4.0	2.8	50.6	51.1	7.9
DPT-TP 1	44.2-44.4	7.95	584	0.30	2.19	11.0	0.0	237.0	111.7	99.9	17.4
DPT-TP 1	43.8-44.2	7.32	567	0.20	1.91	66.8	3.0	153.5	132.3	80.2	10.9
DPT-TP 1	47.8-48	8.41	558			50.4	3.3	72.8	100.6	41.6	5.7
DPT-TP 1	48-48.3	8.33	584			43.4	2.2	70.2	104.7	45.4	7.4
DPT-TP 1	57.6-58	8.49	538								
DPT-TP 1	57.8-58	9.06	521								
DPT-TP 2	43	7.82	591	2.88	0.46	5.1	0.1	245.5	90.5	125.3	22.4
DPT-TP 2	43	7.83	585	2.64	0.22	9.9	4.3	212.0	70.8	106.9	18.0
DPT-TP 2	48-48.3	6.98	534	1.32	0.17	9.9	2.7	40.0	69.0	51.6	10.1
DPT-TP 2	47.8-48	7.52	505	1.38	0.07	33.8	2.3	42.3	56.0	47.5	10.1
DPT-TP 2	52.2-52.8	8.35	562								
DPT-TP 2	52-52.2	8.15	557								
DPT-TP 2	52.5-53	7.89	588			41.2	2.9	55.9	71.3	53.8	8.4
DPT-TP 2	52-52.5	7.81	589			41.2	2.0	57.1	69.2	52.2	8.8
DPT-TP 2	57.4-57.7	8.85	501								
DPT-TP 2	57.7-58	8.88	503								
DPT-TP 3	32.8-33	6.65	467								
DPT-TP 3	32.5-32.8	6.30	455								
DPT-TP 3	37.2-37.5	7.50	602	2.82	0.49	27.8	0.3	196.4	107.8	96.2	12.6
DPT-TP 3	37-37.2	7.47	623	3.51	0.51	45.9	1.6	139.1	138.1	100.6	10.6
DPT-TP 3	42.3-42.5	7.71	559	1.83	0.16	1.4	3.4	214.5	122.7	106.0	21.9
DPT-TP 3	42-42.3	7.58	582	1.95	0.14	0.7	12.5	157.9	67.1	66.7	21.9
DPT-TP 3	47.8-48	7.70	588			50.1	3.0	114.4	77.1	63.4	13.3
DPT-TP 3	48-48.3	7.70	592			50.7	2.7	57.7	63.3	55.4	9.2
DPT-TP 3	52.4-52.7	7.59	571								
DPT-TP 3	52.7-53	7.52	591								









**Test Plot – One Year Post-treatment**

Location	Depth (ft bgs)	pH	ORP	AEC	CEC	Extractable Mn (mg/L)			Extractable Na (mg/L)		
						H <sub>2</sub> O	BaCl	Mn as MnO <sub>2</sub>	H <sub>2</sub> O	BaCl	w/ MnO <sub>2</sub>
A	25.0-25.5	6.92	10	1.02	15.4	0.07	3.21	0.89	5.54	BD	BD
A	25.0-25.5	6.94	18			0.07	3.33	0.91	5.58	BD	BD
A	27.5-28.2	6.61	125								
A	27.5-28.2	6.29	87								
A	29.3- 30	7.27	58	0.73	7.4	0.44	6.14	1.94	42.79	89.41	6.31
A	29.3- 30	7.35	58	0.68	6.3						
A	30- 31	7.58	122								
A	31.8-32.5	7.66	125								
A	32.5-33	7.13	98			0.03	1.59	0.46	45.28	47.85	1.36
A	32.5-33	7.12	105								
A	34.5-35	7.08	128								
A	35- 35.5	9.08	123	0.92	2.1	17.82	24.46	269.20	145.80	100.40	15.16
A	36.5-37.5	9.20	117			17.48	23.95	266.00	112.80	80.78	11.61
A	36.5-37.5	9.24	116			15.49	22.39	165.12	45.18	51.08	2.76
A	39 - 39.9	8.94	126			16.08	13.88	133.00	144.10	61.94	2.39
A	39 - 39.9	9.00	129								
A	40 - 40.7	8.38	147	0.75	2.3	12.78	45.35	250.00	166.20	108.90	23.30
A	40 - 40.7	8.40	153								
A	41.9 - 42.5	8.64	152								
A	42.5 - 43.1	8.80	151			8.59	59.62	262.00	199.60	220.80	24.97
A	44.3 - 45	8.73	143	0.70	1.8	3.63	61.74	199.42	238.20	130.90	0.00
A	44.3 - 45	8.72	145								
A	47 - 47.5	8.53	142								
A	47.5 - 48	7.90	152			2.28	14.29	102.14	50.81	58.68	BD
A	47.5 - 48	7.98	156			2.29	2.88	46.20	42.77	41.28	5.29
A	51 - 51.6	7.79	175	0.49	22.7	3.33	2.19	61.39	44.10	47.87	10.20
A	51.9 - 52.5	7.55	195								
A	53.4 - 53.9	8.28	191			2.72	0.35	99.88	101.90	82.51	11.86
A	54.2 - 55	8.40	175	0.59	22.4	0.49	0.00	79.85	38.05	9.28	2.92
A	56.9 - 57.5	8.50	174								
A	57. - 58.1	8.32	174								
A	58.5 - 59	8.66	164	0.40	20.8	0.30	0.00	89.41	45.57	12.52	2.43
A	59.4 -60	9.08	390	0.48	23.2	0.29	0.00	89.42	48.63	13.63	2.77

**Test Plot – One Year Post-treatment**

Location	Depth (ft bgs)	pH	ORP	AEC	CEC	Extractable Mn (mg/L)			Extractable Na (mg/L)		
						H <sub>2</sub> O	BaCl	Mn as MnO <sub>2</sub>	H <sub>2</sub> O	BaCl	w/ MnO <sub>2</sub>
B	25 - 25.5	5.68	229	0.54	18.0	0.73	6.09	2.06	13.74	BD	BD
B	25 - 25.5	5.80	220								
B	27.5 - 28	5.42	222								
B	28.8 - 29.3	4.81	310								
B	29.5 - 30	5.11	290								
B	30 - 30.8	5.65	236	0.28	3.8	0.17	2.32	0.80	4.76	BD	BD
B	30 - 30.8	5.82	180	0.20	3.8	0.11	1.48	0.43	3.69	BD	BD
B	32.5 - 33.3	6.43	150								
B	32.5 - 33.3	6.41	149								
B	34.6 - 35	6.43	253			0.11	2.17	0.56	9.77	BD	BD
B	35 - 35.8	9.31	179	0.12	1.6	10.07	17.40	181.06	63.22	46.18	BD
B	36.5 -37.5	9.30	184								
B	37.5 - 38.2	9.29	183			9.14	22.18	181.66	59.69	41.11	BD
B	38.4 - 39.1	8.58	222			10.04	20.44	120.92	59.19	42.39	BD
B	39.2 -40	8.68	221								
B	40 - 40.8	8.22	248	0.15	23.0	1.34	24.92	38.30	38.97	20.07	BD
B	40.9 - 41.9	7.60	269			1.01	25.48	19.56	48.72	22.57	BD
B	40.9 - 41.9	7.39	273			0.92	14.61	10.54	43.86	11.41	BD
B	42.5 - 43.2	7.25	281								
B	43.5 - 44	7.31	274								
B	44.3 - 45	7.73	266	0.12	23.0	5.55	71.25	133.54	21.58	9.14	BD
B	46.7 - 47.1	7.48	285								
B	46.7 - 47.1	7.41	286								
B	47.5 - 48.3	7.11	316			0.50	2.06	44.82	12.83	12.52	BD
B	48.5 - 49.1	6.65	337			0.43	1.66	39.46	11.03	11.54	BD
B	49.4 - 50	6.78	349	0.20	23.0	0.92	1.09	72.09	30.04	22.39	4.83
B	51.4 - 52	7.37	334								
B	52 - 52.5	7.16	336								
B	52 - 52.5	7.13	339								
B	53.3 - 54	7.42	326								
B	54.4 -55	7.64	322								
B	55 -55.5	7.72	310	0.18	24.0	0.11	BD	118.90	28.12	6.79	2.05
B	55.8 - 56.4	7.74	313								
B	57.5 -58	8.89	276								
B	59.4- 60	9.28	482	0.24	26.0	1.02	BD	92.70	48.91	17.64	4.88
B	59.4- 60	9.29	489	0.74	16.0	2.63	BD	80.70	49.77	17.75	5.38

**Test Plot – One Year Post-treatment**

Location	Depth (ft bgs)	pH	ORP	AEC	CEC	Extractable Mn (mg/L)			Extractable Na (mg/L)		
						H <sub>2</sub> O	BaCl	Mn as MnO <sub>2</sub>	H <sub>2</sub> O	BaCl	w/ MnO <sub>2</sub>
C	26.2-26.8	5.84	166	0.26	2.6	0.05	2.09	0.78	5.38	BD	BD
C	26.2-26.8	5.80	179								
C	28.4 - 29.2	4.47	328								
C	29.2 -30	4.55	323								
C	30.1 - 30.6	5.44	250	0.24	3.5	0.05	0.63	0.37	2.14	BD	BD
C	30.8 -31.5	5.81	204	0.24	1.1	0.06	0.60	0.20	2.12	BD	BD
C	30.8 -31.5	5.85	201								
C	32.5 - 33.2	5.07	345								
C	32.5 -33	5.87	230								
C	33.4 - 34	5.78	246	0.17	1.4						
C	33.5 -34	4.86	382								
C	33.5 -34	4.83	383								
C	33.8 - 35	4.82	372			0.06	0.20	0.39	1.51	BD	BD
C	34.5 -35	5.86	250			0.07	0.20	0.38	1.61	BD	BD
C	37.5 - 38.3	8.68	190								
C	37.5 - 38.3	8.72	198			1.25	2.22	0.55	17.52	BD	BD
C	39.2 -40	5.75	330	0.16	1.4	0.58	0.28	14.79	8.23	BD	BD
C	47.8 - 48.3	6.03	360	0.19	28.2	0.29	7.29	0.23	2.75	BD	BD
C	47.8 - 48.3	6.02	355			0.27	7.00	15.97	2.67	BD	BD
C	49.2 - 50	6.06	370	0.20	24.4	0.16	2.36	31.32	5.35	0.87	0.00
C	52- 52.5	5.96	360								
C	52.5 - 53.5	5.98	363								
C	54.2-55	8.69	266	0.38	22.1	0.00	0.05	1.17	0.89	0.06	0.89
C	54.2-55	8.65	260			0.00	0.14	0.89			
C	56.4 - 56.9	8.36	268								
C	56.8 - 57.5	8.56	250								
C	57.5 - 58	9.09	229						11.26	1.92	0.69
C	58.5 - 59.1	8.86	236			0.00	0.08	0.56	0.78	0.11	0.69
C	59.5 -60	9.24	205	0.39	21.0	0.00	0.12	0.59	0.48	8.04	0.66
C	59.5 -60	9.29	210	0.19	20.5	0.01	0.08	1.14	29.29	0.22	1.89

## Control Plot – Immediately Post-treatment

Location	Depth (ft bgs)	pH	ORP	AEC	CEC	Extractable Mn (mg/L)			Extractable Na (mg/L)			
						H <sub>2</sub> O	BaCl	Mn as MnO <sub>2</sub>	H <sub>2</sub> O	BaCl	w/ MnO <sub>2</sub>	
DPT-TP 1	33.0 -34.0											
DPT-TP 1	34.0 - 34.5											
DPT-TP 1	37'					0.44	7.78	298.00	66.26	58.00		BD
DPT-TP 1	38'					0.76	8.09	39.82	46.37	28.24		BD
DPT-TP 1	43.5 - 44.0					0.05	4.21	55.29	26.90	16.24		BD
DPT-TP 1	44.0 -45.0					0.03	2.95	61.57	34.96	19.78		BD
DPT-TP 1	47.2 - 47.9					0.02	0.72	45.86	20.73	5.83		2.18
DPT-TP 1	52.2 - 53.1											
DPT-TP 1	52.7 - 53.1											
DPT-TP 3	36.3 - 37.3					0.51	1.56	278.40	45.53	118.50		BD
DPT-TP 3	36.3 -37.3					0.40	17.08	292.30	53.44	110.80		BD
DPT-TP 3	39 -40					1.90	0.01	284.00	21.89	74.92		BD
DPT-TP 3	39 - 40					0.18	0.97	301.00	29.30	62.06		BD
DPT-TP 3	43.2 - 43.7			0.51	0.91	0.14	2.24	3.06	34.36	9.66		BD
DPT-TP 3	48.9 - 50			0.80	1.15	0.04	0.01	96.79	25.65	17.01		3.30
DPT-TP 3	48.9 - 50					0.03	0.03	92.39	27.68	11.11		2.82
DPT-TP 3	52 -53			0.69	1.07	4.22	0.00	139.60	46.69	13.97		2.26
DPT-TP 3	52 - 53			0.77	3.68	2.58	0.00	132.90	45.26	14.73		2.63
DPT-TP 4	37.7- 38.9	8	411	0.96	1.10							
DPT-TP 4	37.7- 38.9	8	308	0.82	1.14							
DPT-TP 4	42.0 - 43.0	6.8	670									
DPT-TP 4	42.0 - 43.0	6.3	700									
DPT-TP 4	46-46.5	7.3	515									
DPT-TP 4	46-46.5	7.7	487									
DPT-TP 4	58.5 - 59.5	8.2	436									
DPT-TP 4	58.5 - 59.5	8.5	430									
DPT-TP 4	44.0 - 45.0	8.4	555									
DPT-TP 4	44.0 - 45.0	7.9	592									
DPT-TP 4	48.5 - 49.5	7.4	616									
DPT-TP 4	48.5 - 49.5	7.4	615									
DPT-TP 5	43.5 - 44.5			0.65	0.99							
DPT-TP 5	43.5 - 44.5			0.65	2.22							
DPT-TP 5	46.0 - 46.7			0.65	1.42							
DPT-TP 5	46.0 - 46.7			0.57	1.22							
DPT-TP 5	49.0 - 49.7			0.52	1.12							
DPT-TP 5	49.0 - 49.7			0.68	1.11							
DPT-TP 6	31.5 - 32.5					0.17	18.06	6.13	46.90	26.42		BD
DPT-TP 6	31.5 - 32.5					0.16	7.62	1.95	37.13	12.37		BD
DPT-TP 6	33 - 33.8					1.56	BD	245.00	32.07	20.50		0.34
DPT-TP 6	33 -33.8					0.32	BD	294.60	34.28	25.05		BD
DPT-TP 6	34.5 - 35			0.61	1.08	0.17	11.08	6.08	27.24	22.93		BD
DPT-TP 6	34.5 - 35			0.36	0.76	0.31	20.14	14.32	34.31	19.01		BD
DPT-TP 6	49 -50					1.66	BD	135.60	27.54	47.06		BD
DPT-TP 6	49- 50					1.90	BD	132.80	29.31	41.28		6.72



### Control Plot – One Year Post-treatment

Location	Depth (ft bgs)	pH	ORP	AEC	CEC	Extractable Mn (mg/L)			Extractable Na (mg/L)		
						H <sub>2</sub> O	BaCl	Mn as MnO <sub>2</sub>	H <sub>2</sub> O	BaCl	w/ MnO <sub>2</sub>
Z	25.6 -26.1	5.9	254	3.20	16.52	0.20	2.91	0.99	8.27	BD	BD
Z	25.6 -26.1	5.9	254			0.65	2.87	1.39	14.88	6.52	BD
Z	27.2 -27.5	5.8	246								
Z	28.9 - 29.5	5.1	265								
Z	30-30.8	8.7	169	2.58	4.28	4.77	80.46	313.20	104.10	74.39	5.93
Z	31.1 -31.8	8.7	167	2.69	4.68	4.72	82.46	296.00	110.20	61.25	5.43
Z	31.9 - 32.5	8	207								
Z	31.9 - 32.5	8	206			1.78	71.16	238.00	75.28	37.93	2.65
Z	32.5 - 33.2	8.5	170			3.60	22.75	238.00	43.07	6.79	4.33
Z	34.5 - 35	8.5	161	2.79	6.13	1.05	54.98	44.64	21.97	18.12	BD
Z	36.3 - 37	8.1	176			1.25	53.98	45.26	21.33	1.11	BD
Z	37.5 - 38.1	7.5	191	1.87	1.61	5.48	39.62	185.60	26.35	4.34	5.41
Z	39.2 - 40	8.2	175			6.02	33.62	188.52	38.03	10.62	BD
Z	40 -41	8.6	155			1.95	52.02	192.40	89.29	35.85	11.37
Z	40 -41	8.6	149								
Z	42 -42.5	8.6	155			5.90	52.00	224.00	85.25	31.51	BD
Z	43.3 - 44	8.5	166	1.83	1.44						
Z	44.2 - 45	7.8	198								
Z	47.8 - 48.4	7.9	183	2.08	1,56	0.15	0.81	46.00	5.12	1.38	0.51
Z	47.8 - 48.4	7.8	191			0.18	0.60	47.26	5.02	1.18	0.74
Z	49.5 - 50	8.2	185								
Z	52 -52.5	8.6	171								
Z	52.5 -53.3	8.7	170	1.03	1.82	0.04	0.08	72.82	10.48	1.72	1.41
Z	54 - 55.5	9.2	142								
Z	56 -56.8	9.5	131			0.41	0.02	102.98	35.92	9.05	2.59
Z	57.5 -58.3	9	152								
Z	57.5 -58.3	9	160								
Z	59.2 -60	9.5	133	0.89	1.21	0.04	0.01	65.98	20.23	3.46	12.70
Z	59.2 -60	9.5	130	0.90	1.00	0.08	0.01	77.28	20.79	3.45	2.34



**Control Plot – One Year Post-treatment**

Location	Depth (ft bgs)	pH	ORP	AEC	CEC	Extractable Mn (mg/L)			Extractable Na (mg/L)		
						H <sub>2</sub> O	BaCl	Mn as MnO <sub>2</sub>	H <sub>2</sub> O	BaCl	w/ MnO <sub>2</sub>
Y	25.1 - 25.7	5.2	204			1.97	3.29	1.27	19.16	BD	BD
Y	25.1 - 25.7	5.2	201								
Y	27.2 - 28.3	4.5	224			0.51	0.76	0.21	7.04	BD	BD
Y	27.2 - 28.3	4.4	229								
Y	28.5 - 28.9	5	228								
Y	29.5 - 29.8	4.8	240								
Y	30 - 30.8	5.4	206	1.52	2.66	0.24	0.60	0.18	17.41	BD	BD
Y	30.9 - 31.6	5.3	218	1.55	2.77	0.20	0.70	0.16	18.83	BD	BD
Y	32 - 32.5	6.4	144			1.51	13.37	8.44	105.70	28.91	BD
Y	33.5 - 34.2	6.9	154								
Y	33.5 - 34.2	6.9	159								
Y	34.5 - 35	6.9	163	1.58	5.19	2.62	68.80	52.90	47.90	21.23	BD
Y	36.6 - 37.5	8	165			2.87	69.82	52.50	60.55	23.21	BD
Y	37.5 - 38.3	7.2	171								
Y	37.5 - 38.3	7.2	173								
Y	39.6 - 40	6.7	180	1.41	1.51	14.36	78.64	210.60	16.97	2.95	19.42
Y	40 - 41	7.7	183								
Y	41.4 - 42.5	7.7	190	1.19	1.18	0.19	5.27	6.66	28.15	6.11	0.80
Y	42.5 - 43.3	7.6	192			0.13	5.89	6.11	28.22	8.09	0.77
Y	43.5 - 44.3	7.2	220	1.80	1.15	0.13	1.04	1.51	21.48	BD	0.00
Y	48.3 - 48.7	7.2	201	1.90	0.85	0.10	0.65	3.88	1.49	BD	0.25
Y	48.3 - 48.7	7.2	202								
Y	48.7 - 49.3	7.2	206								
Y	49.4 - 49.8	7.4	209								
Y	51.7 - 52	8.1	149			0.04	0.18	10.76	1.33	BD	1.27
Y	51.7 - 52	8.1	145								
Y	52 - 52.5	8.5	135								
Y	53.3 - 53.8	8.8	138			0.01	0.17	1.43	1.08	BD	0.57
Y	53.3 - 53.8	8.8	140	1.24	2.65						
Y	57 - 57.5	8.9	142								
Y	57.5 - 58	8.9	142								
Y	58.5 - 59.1	8.8	150	1.75	0.97	0.00	0.12	0.83	2.11	BD	0.08
Y	58.5 - 59.1	8.9	145	1.84	0.97	0.00	0.08	0.71	1.42	BD	0.25

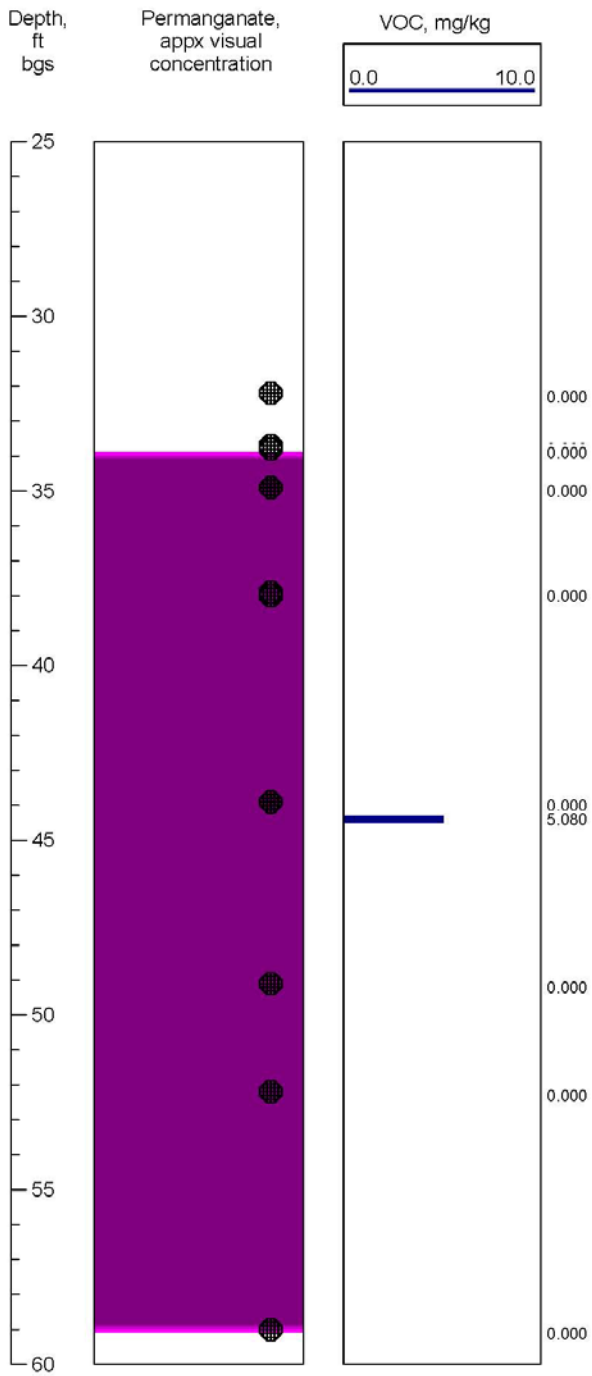
### Control Plot – One Year Post-treatment

Location	Depth (ft bgs)	pH	ORP	AEC	CEC	Extractable Mn (mg/L)			Extractable Na (mg/L)		
						H <sub>2</sub> O	BaCl	Mn as MnO <sub>2</sub>	H <sub>2</sub> O	BaCl	w/ MnO <sub>2</sub>
X	26.6 - 26.9	6.8	295			0.16	3.13	1.49	11.49	5.48	BD
X	26.6 - 26.9	6.8	296								
X	27. - 27.5	6.1	263								
X	27.5 - 28	4.9	312								
X	28.8 - 29.2	4.7	315								
X	28.8 - 29.2	4.7	318								
X	30 - 30.5	4.4	330	1.40	2.98	0.40	0.60	0.18	6.27	BD	BD
X	31.7 - 32.5	4.6	334	1.40	3.16	0.24	0.51	0.12	3.53	BD	BD
X	33.5 - 34	5.3	338								
X	33.5 - 34	5.3	342								
X	34.6 - 35	8.1	309	1.30	1.81	2.81	51.32	140.92	20.57	11.47	BD
X	36.3 -37	8.9	230	1.20	1.28	7.36	51.92	142.92	22.02	12.43	BD
X	36.3 -37	8.9	226								
X	38.4 -38.9	8.8	232			9.03	57.92	180.72	82.54	48.46	27.51
X	38.4 -38.9	8.7	227								
X	39- 39.6	8	284								
X	39.7 - 40	7.8	274			3.26	67.34	60.08	53.39	23.74	BD
X	40 - 40.9	8.2	241	1.50	1.39	2.93	69.34	60.28	57.92	23.95	BD
X	42 -42.5	8.1	245			2.44	86.00	90.02	73.53	46.91	2.61
X	42 -42.5	8.1	246								
X	42.5 -43	8	250								
X	43.5 - 44	7.1	315								
X	44.5-45	7.2	286	1.00	1.20	4.19	72.78	200.60	12.40	4.85	0.69
X	49.5 -50	7.4	275	1.06	1.31	3.68	1.79	74.40	30.01	29.00	8.27
X	52.5-53	7	292	1.05	1.36	3.73	1.57	69.78	28.63	24.36	7.39
X	52.5-53	6.8	292								
X	54.5 -55	7.9	283			0.01	0.02	103.34	1.24	BD	BD
X	56.6-57	8.1	259								
X	57-57.5	8	260								
X	57.5-58	8.9	235								
X	57.5-58	8.9	236								
X	58.5-59	8.7	240								
X	59.5-60	9.2	229	1.33	1.27	0.04	0.02	68.92	20.16	4.83	2.40
X	59.5-60	9.1	227	2.26	1.78						

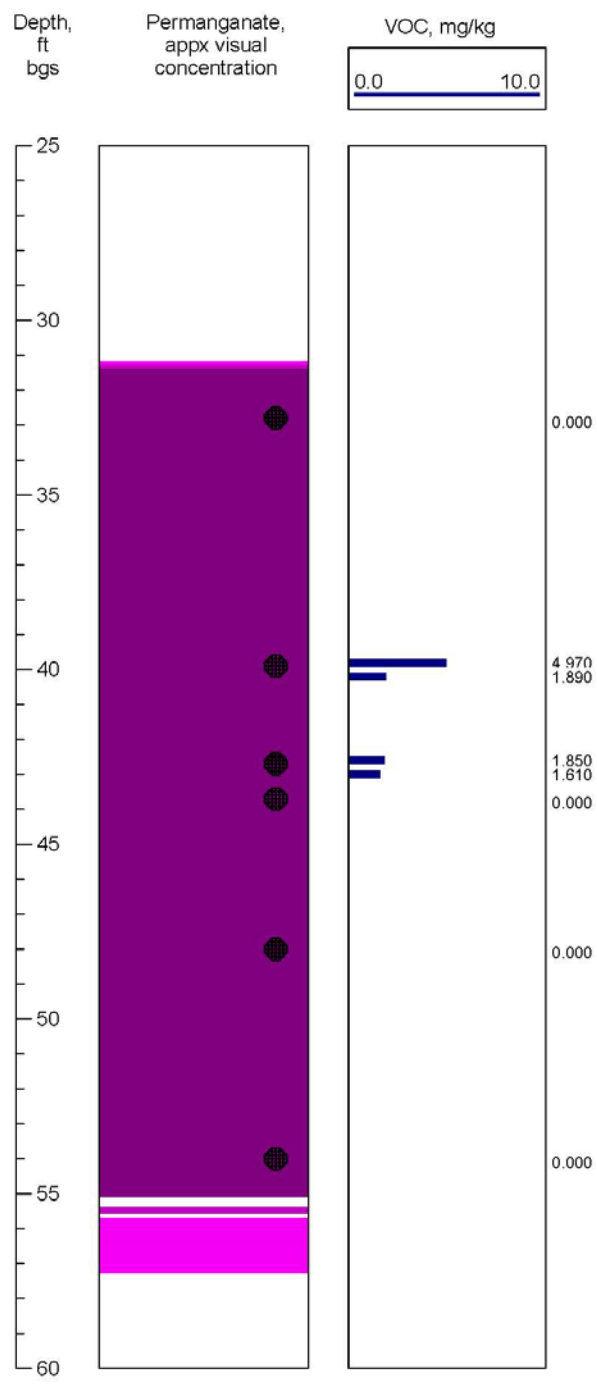
## **Appendix C: DPT Data Plots**

### **Test Plot DPT Data Logs: Permanganate and VOCs**

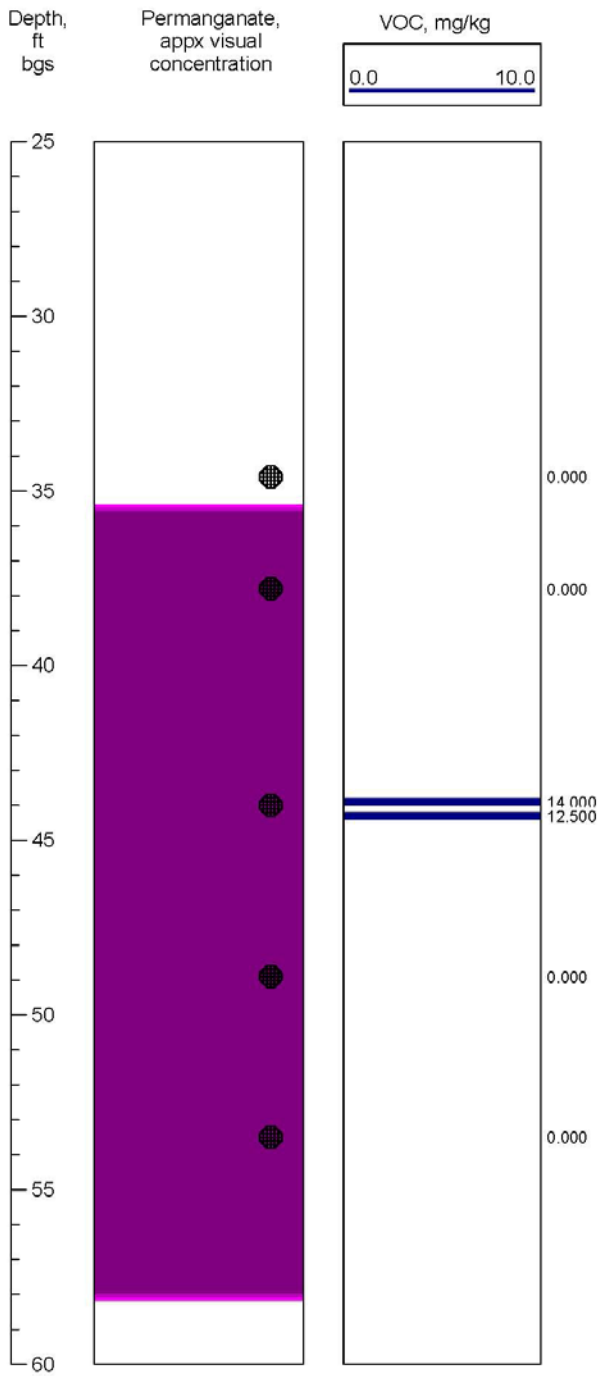
<b>Location:</b>	TP - DPT 01	ESTCP Project ER-0912 Camp Lejeune Field Site
<b>Date Drilled:</b>	12/14/10	



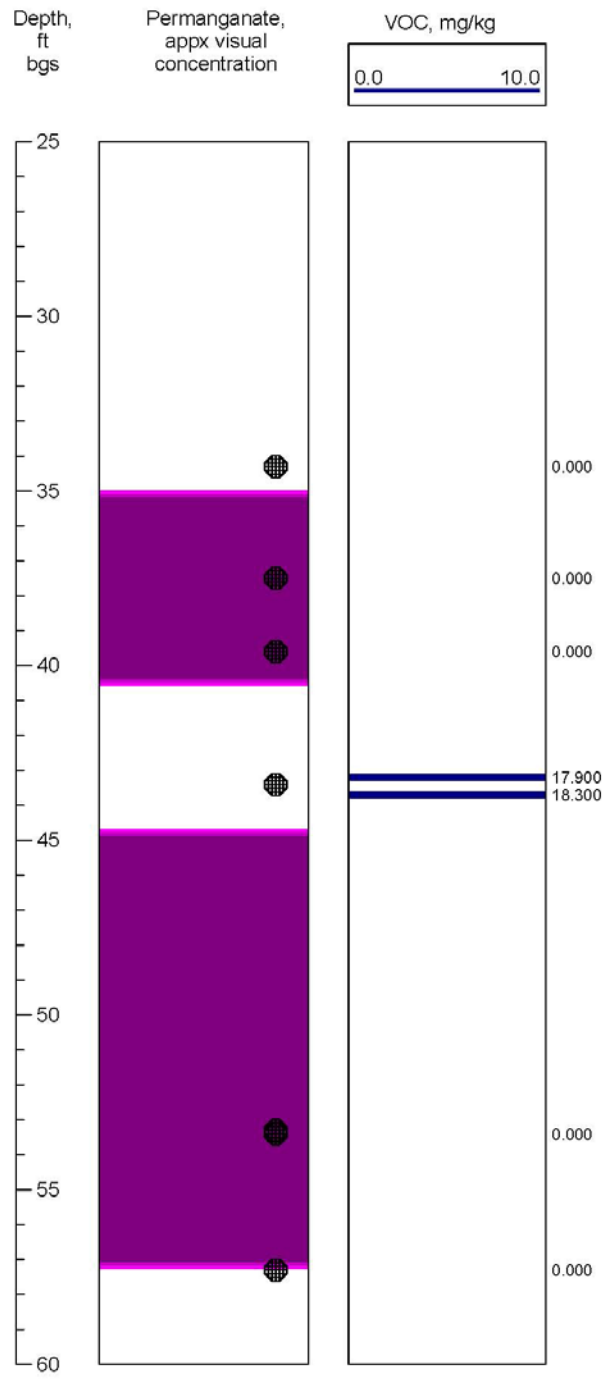
<b>Location:</b> TP - DPT 02	<b>ESTCP Project ER-0912</b>
<b>Date Drilled:</b> 12/14/10	<b>Camp Lejeune Field Site</b>



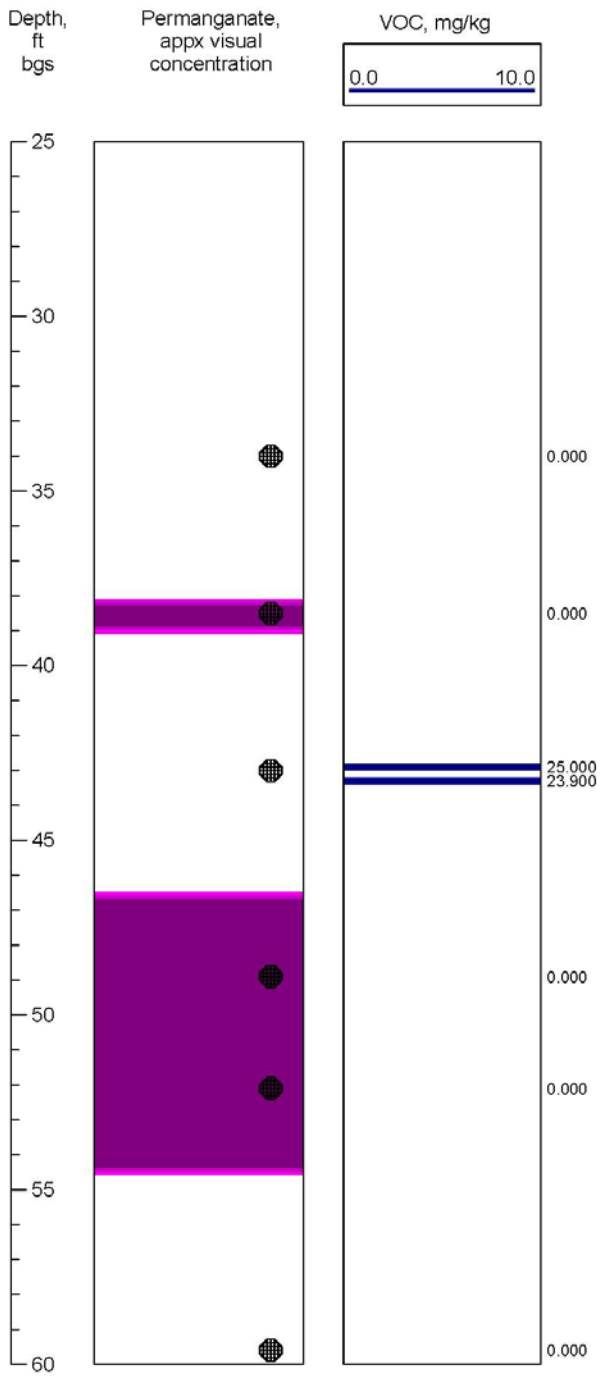
<b>Location:</b>	TP - DPT 03	ESTCP Project ER-0912 Camp Lejeune Field Site
<b>Date Drilled:</b>	12/10/10	



<b>Location:</b>	TP - DPT 04	ESTCP Project ER-0912 Camp Lejeune Field Site
<b>Date Drilled:</b>	12/10/10	

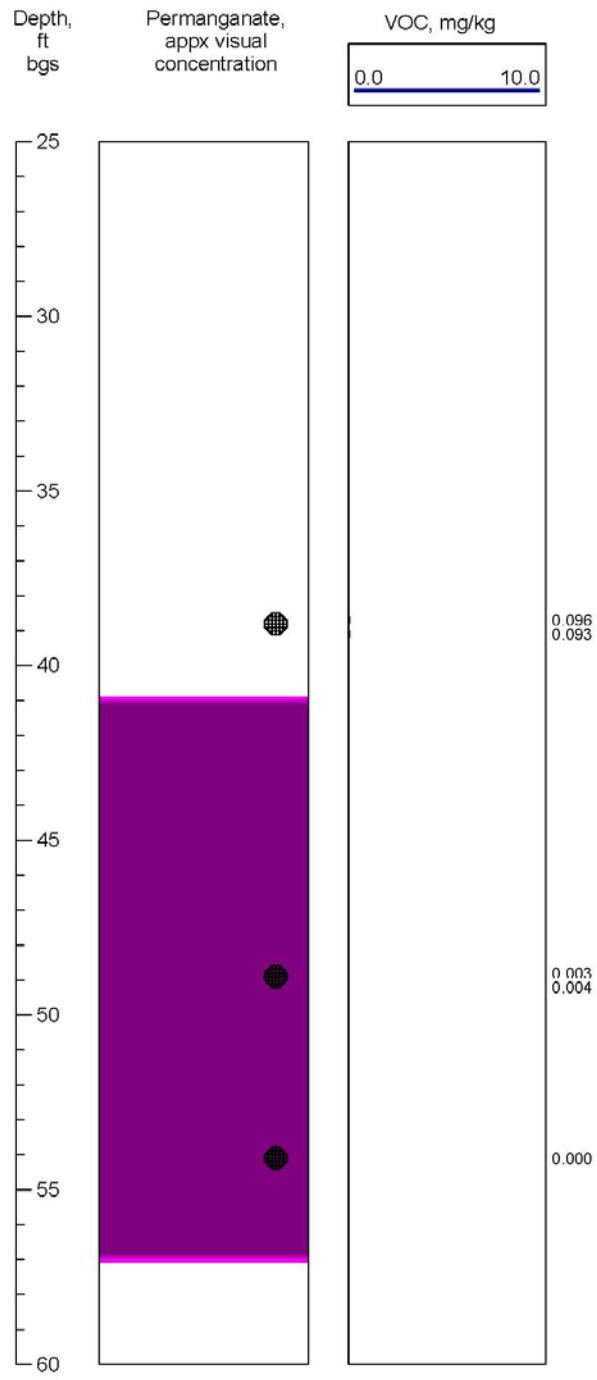


<b>Location:</b>	TP - DPT 05	ESTCP Project ER-0912 Camp Lejeune Field Site
<b>Date Drilled:</b>	12/10/10	

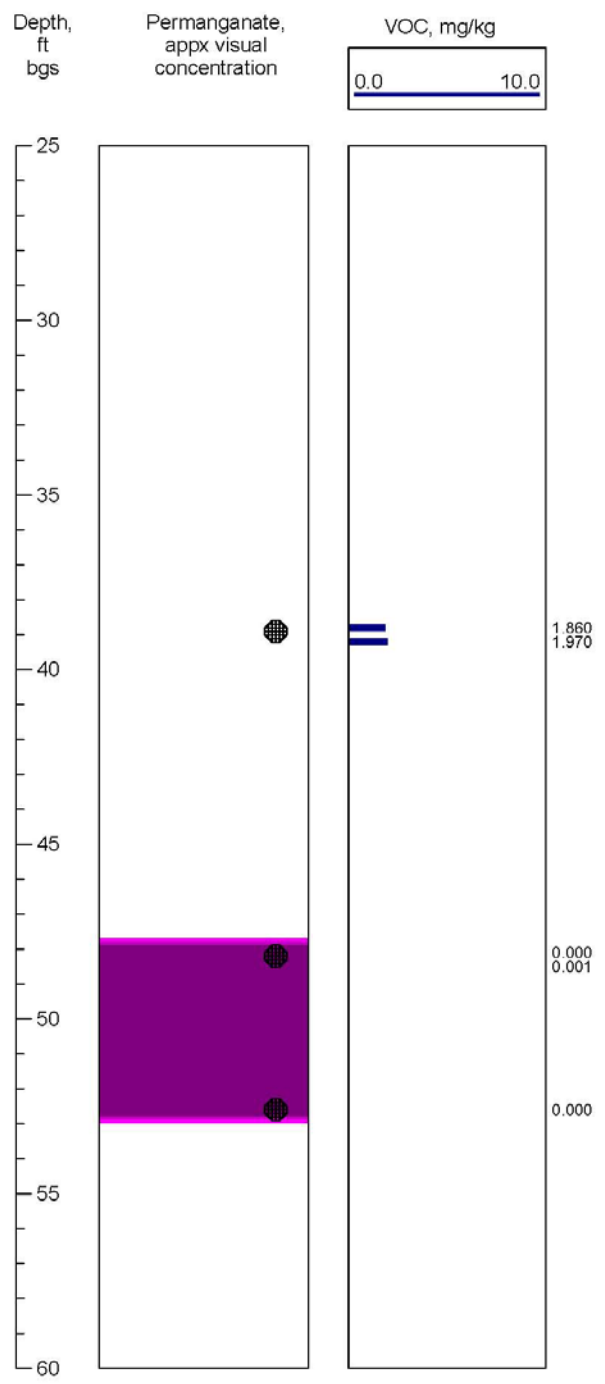




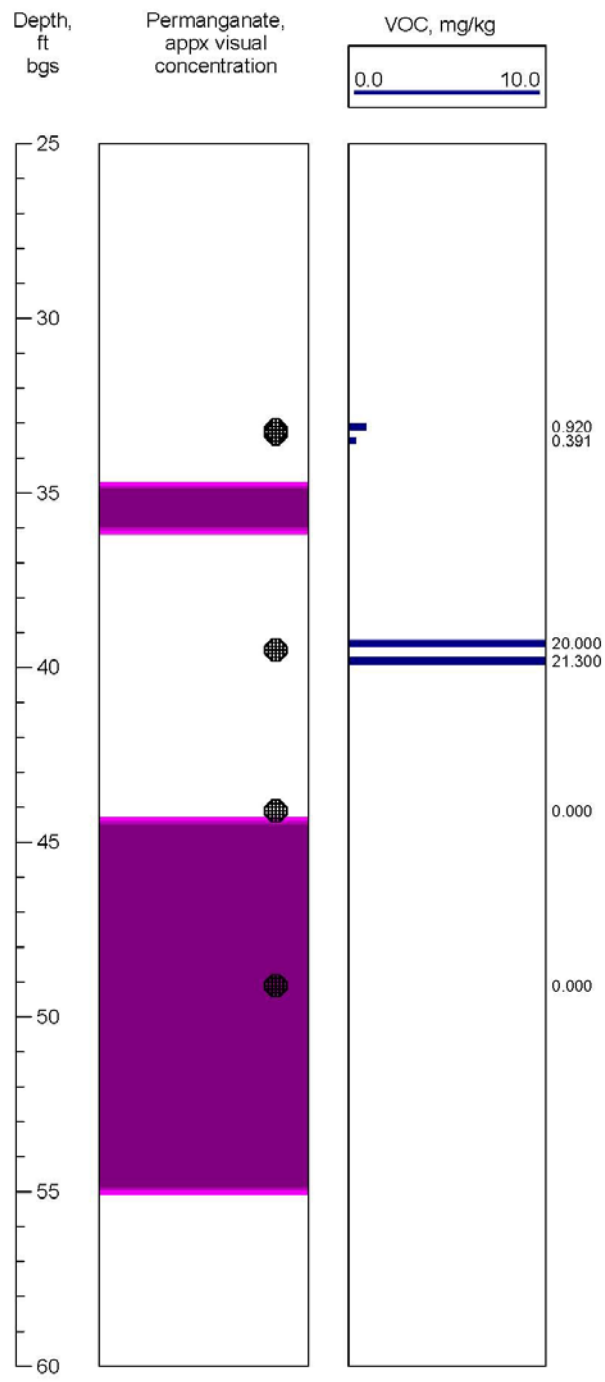
<b>Location:</b>	TP - DPT 06	ESTCP Project ER-0912 Camp Lejeune Field Site
<b>Date Drilled:</b>	12/16/10	



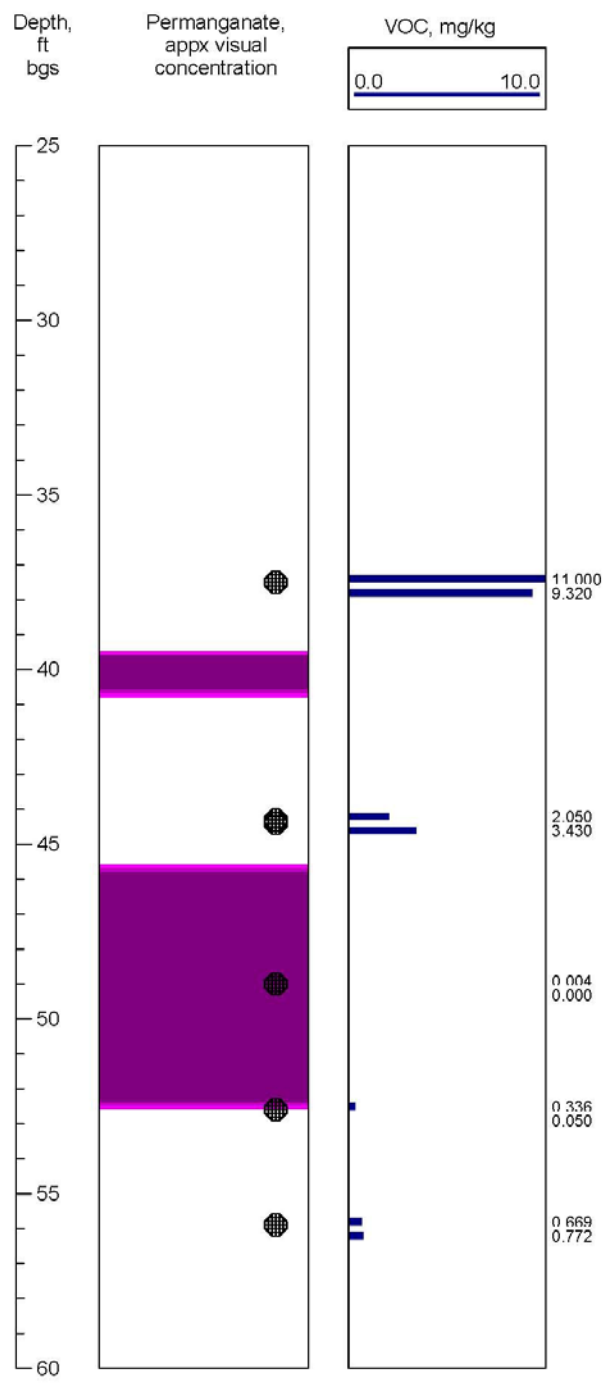
<b>Location:</b>	TP - DPT 07	ESTCP Project ER-0912 Camp Lejeune Field Site
<b>Date Drilled:</b>	12/16/10	



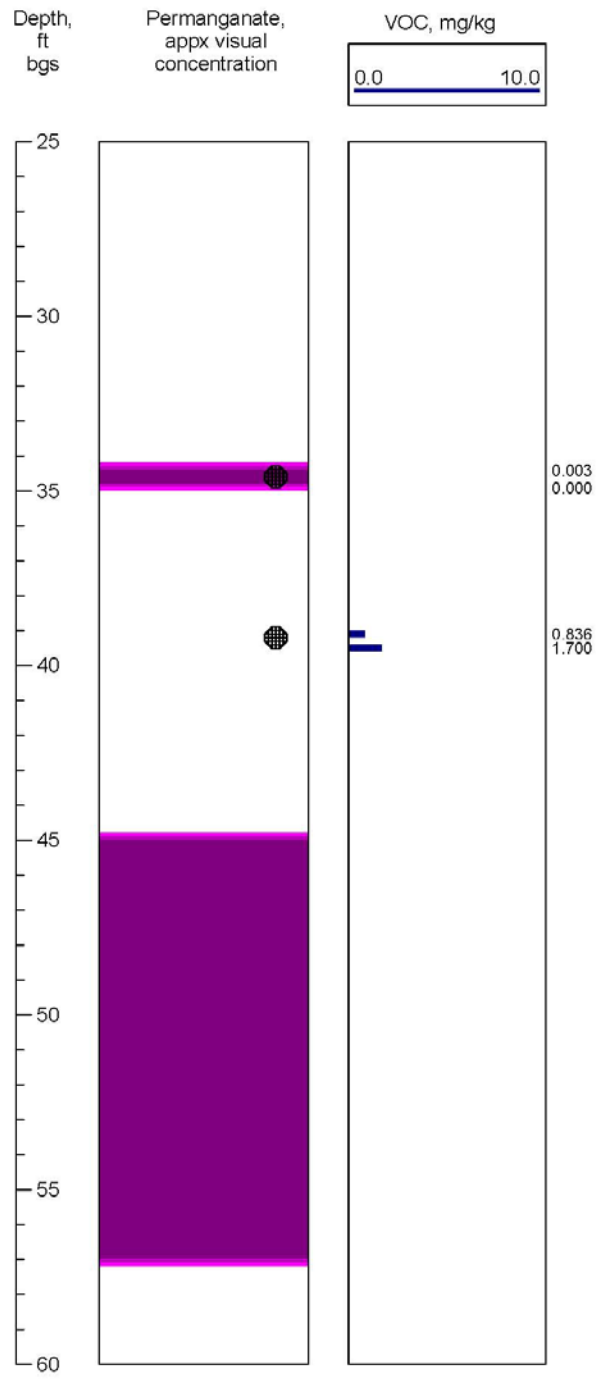
<b>Location:</b>	TP - DPT 08	ESTCP Project ER-0912 Camp Lejeune Field Site
<b>Date Drilled:</b>	12/16/10	



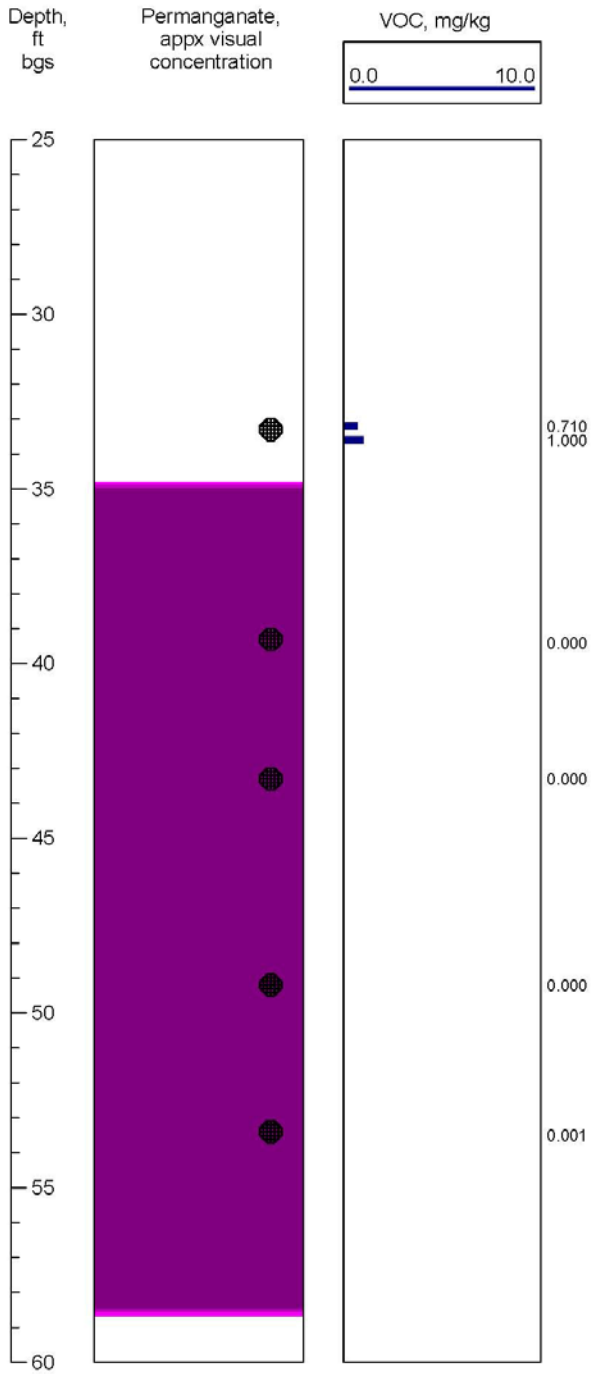
<b>Location:</b> TP - DPT 09	<b>ESTCP Project ER-0912</b>
<b>Date Drilled:</b> 12/16/10	<b>Camp Lejeune Field Site</b>



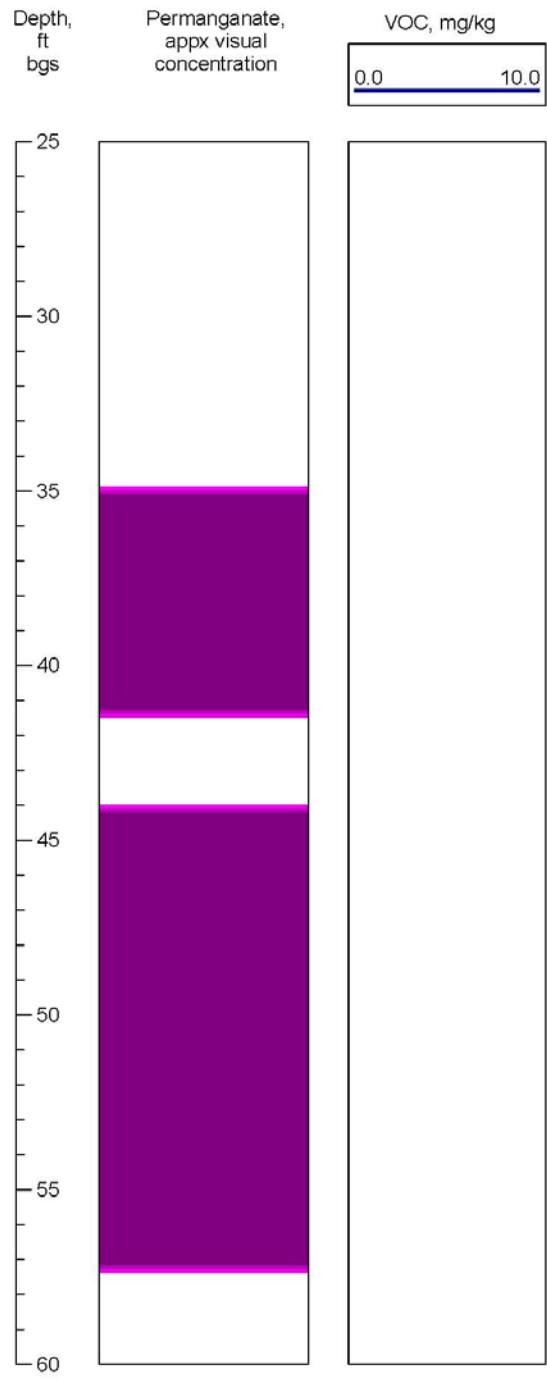
<b>Location:</b>	TP - DPT 10	ESTCP Project ER-0912 Camp Lejeune Field Site
<b>Date Drilled:</b>	12/17/10	



<b>Location:</b>	TP - DPT 11	ESTCP Project ER-0912 Camp Lejeune Field Site
<b>Date Drilled:</b>	12/10/10	



<b>Location:</b>	TP - DPT 12	ESTCP Project ER-0912 Camp Lejeune Field Site
<b>Date Drilled:</b>	12/17/10	

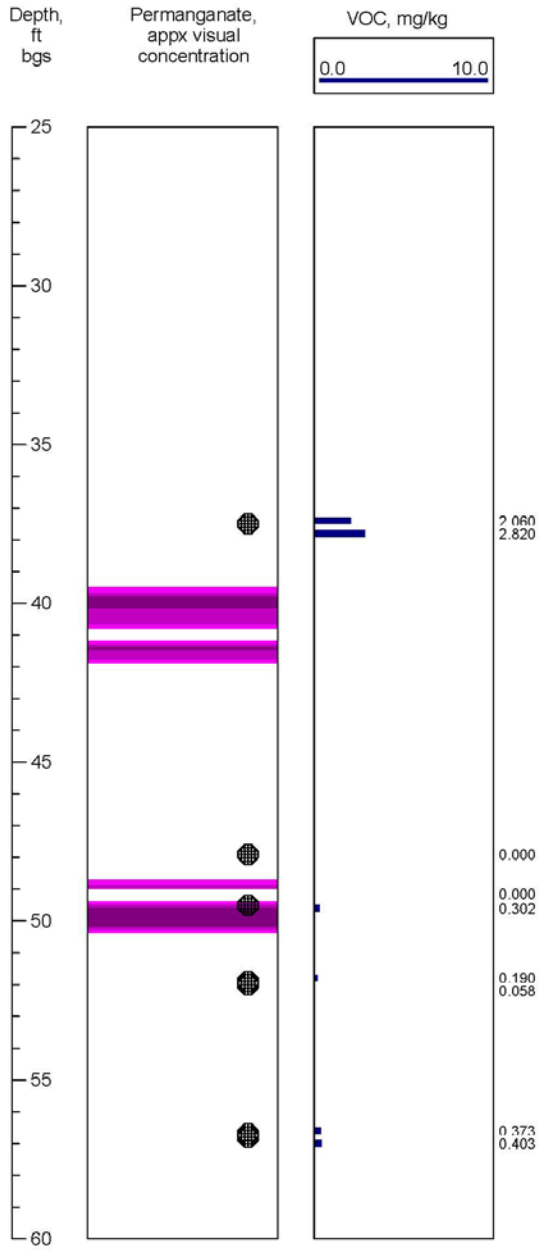


**Appendix C: DPT Data Plots (continued)**

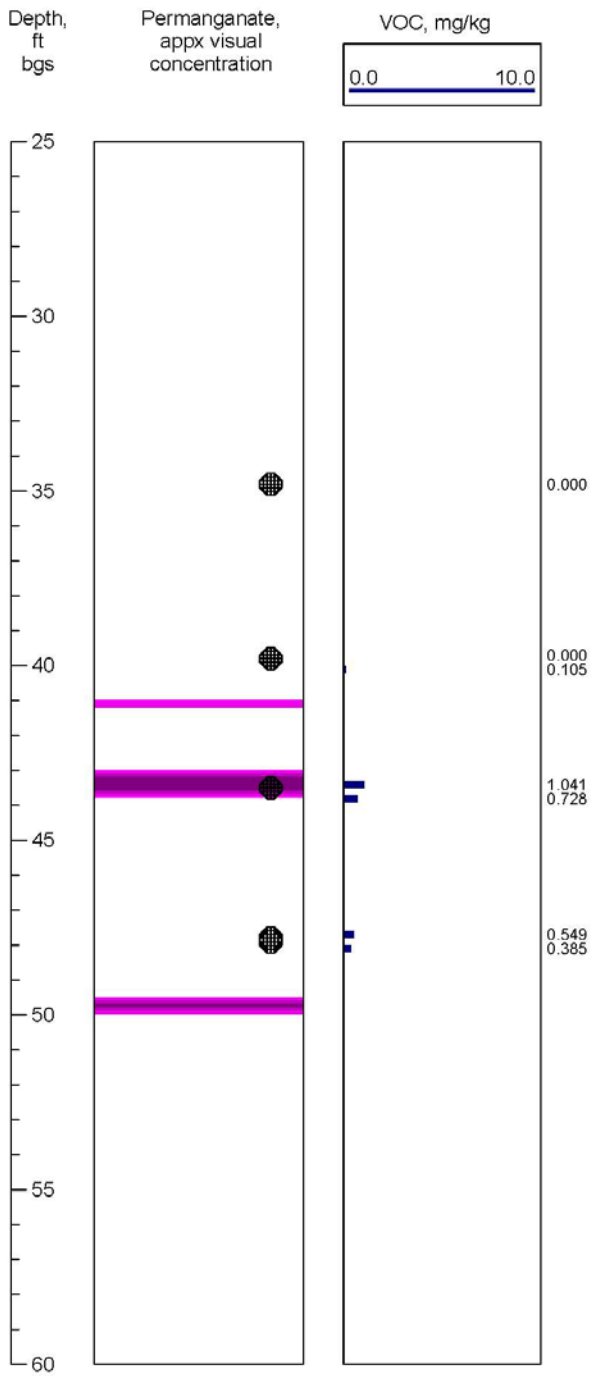
**Control Plot DPT Data Logs: Permanganate and VOCs**



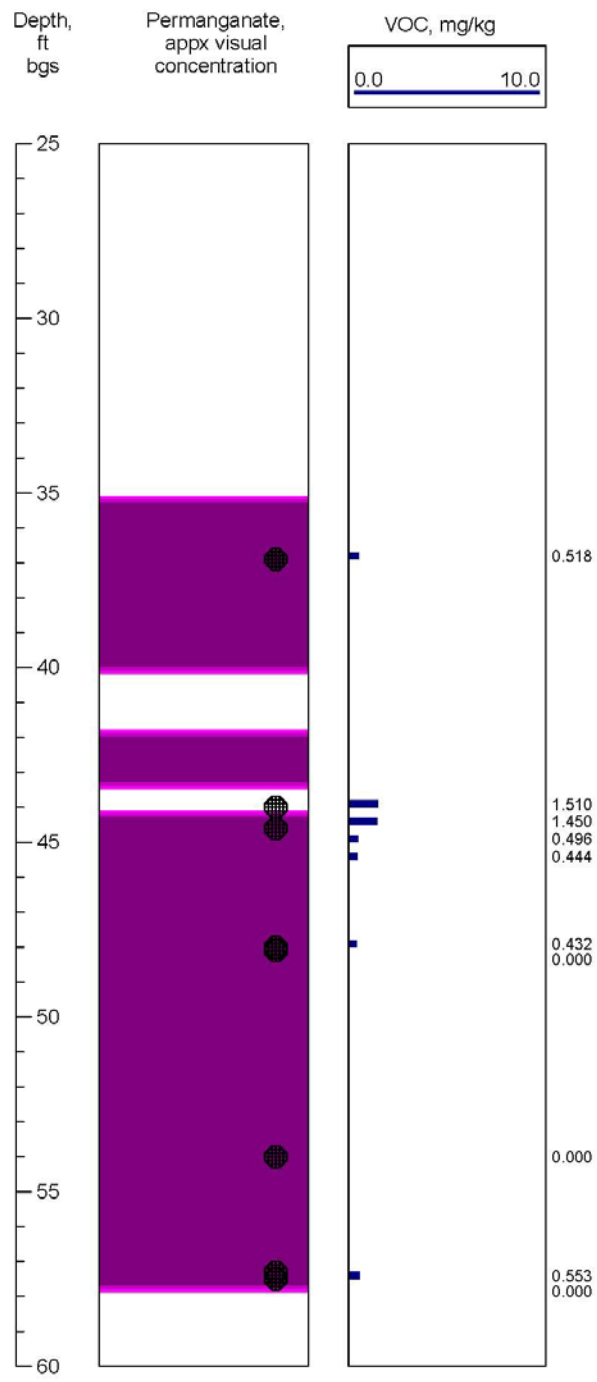
<b>Location:</b> CP - DPT 01	ESTCP Project ER-0912
<b>Date Drilled:</b> 11/4/10	Camp Lejeune Field Site



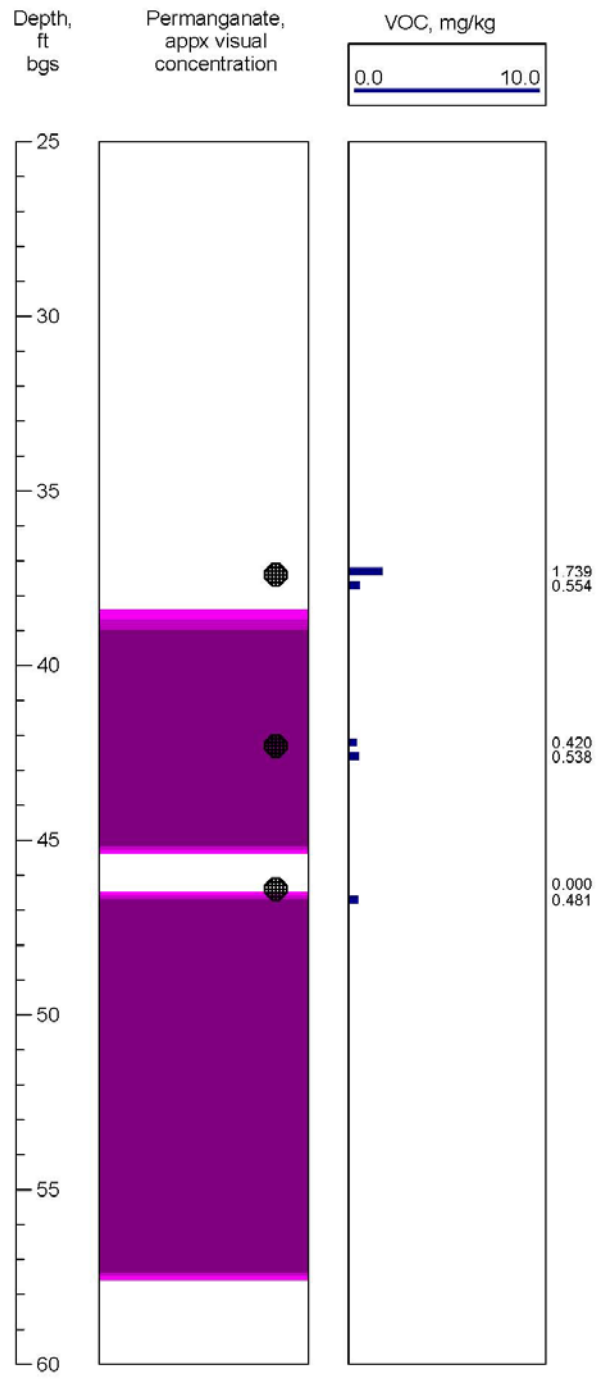
<b>Location:</b>	CP - DPT 02	ESTCP Project ER-0912 Camp Lejeune Field Site
<b>Date Drilled:</b>	11/5/10	



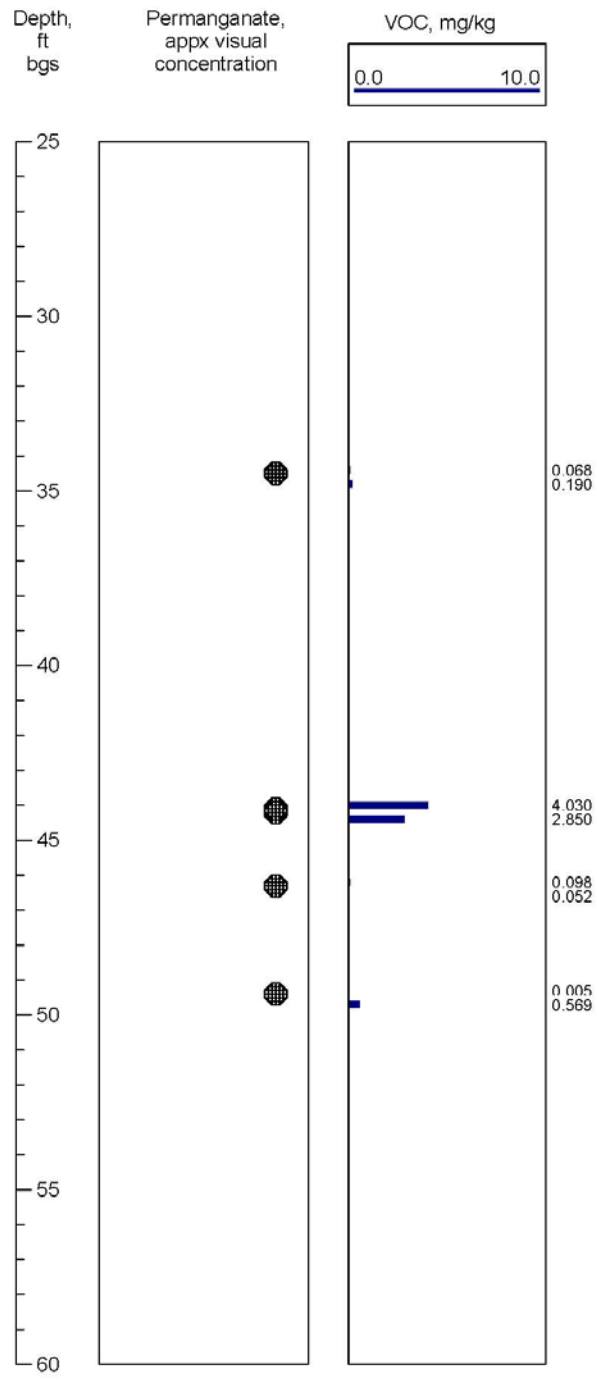
<b>Location:</b>	CP - DPT 03	ESTCP Project ER-0912 Camp Lejeune Field Site
<b>Date Drilled:</b>	11/5/10	



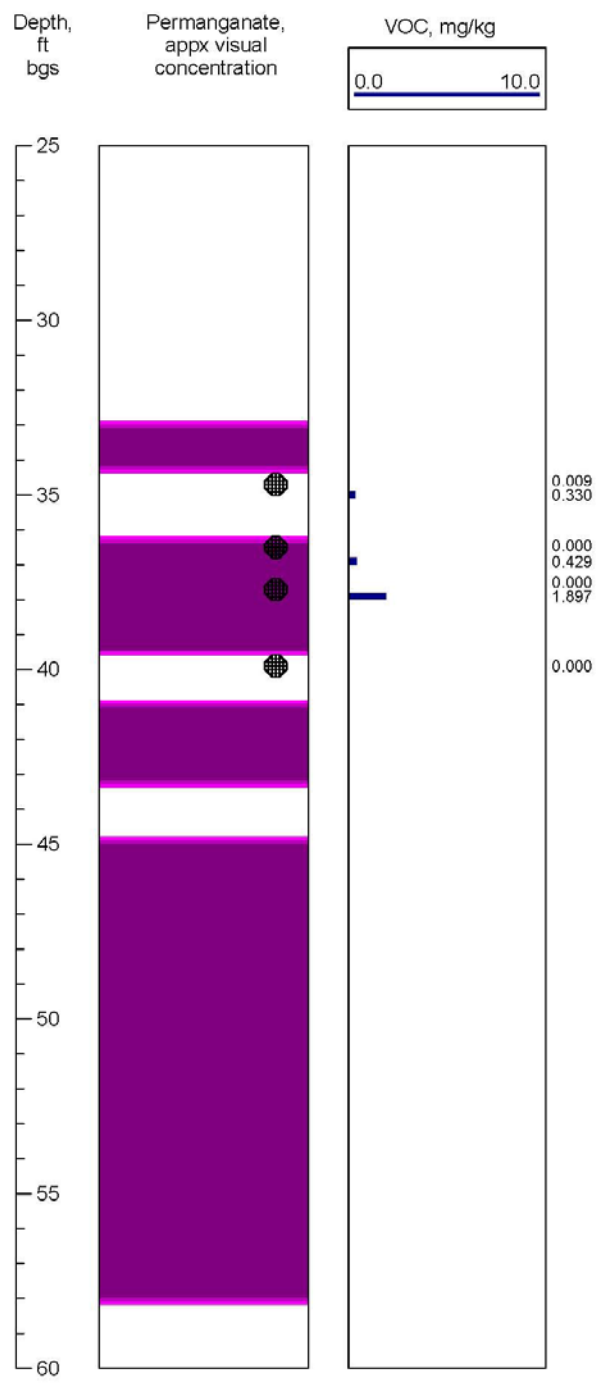
<b>Location:</b>	CP - DPT 04	ESTCP Project ER-0912 Camp Lejeune Field Site
<b>Date Drilled:</b>	11/6/10	



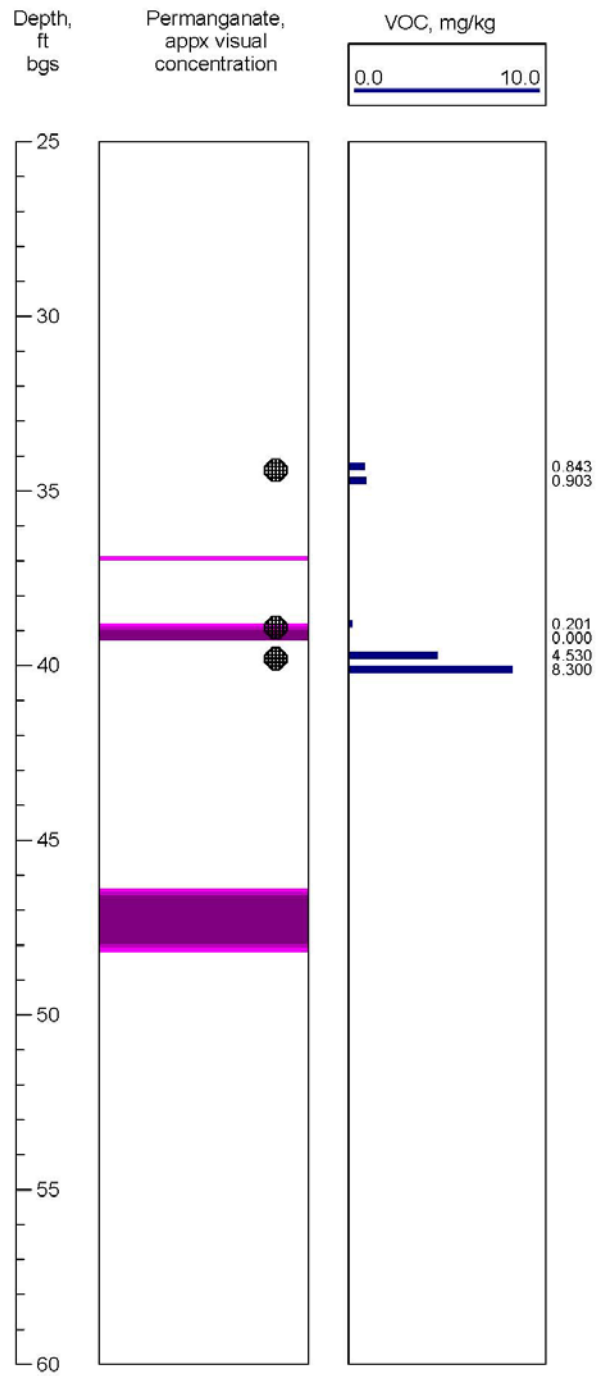
<b>Location:</b>	CP - DPT 05	ESTCP Project ER-0912 Camp Lejeune Field Site
<b>Date Drilled:</b>	11/6/10	



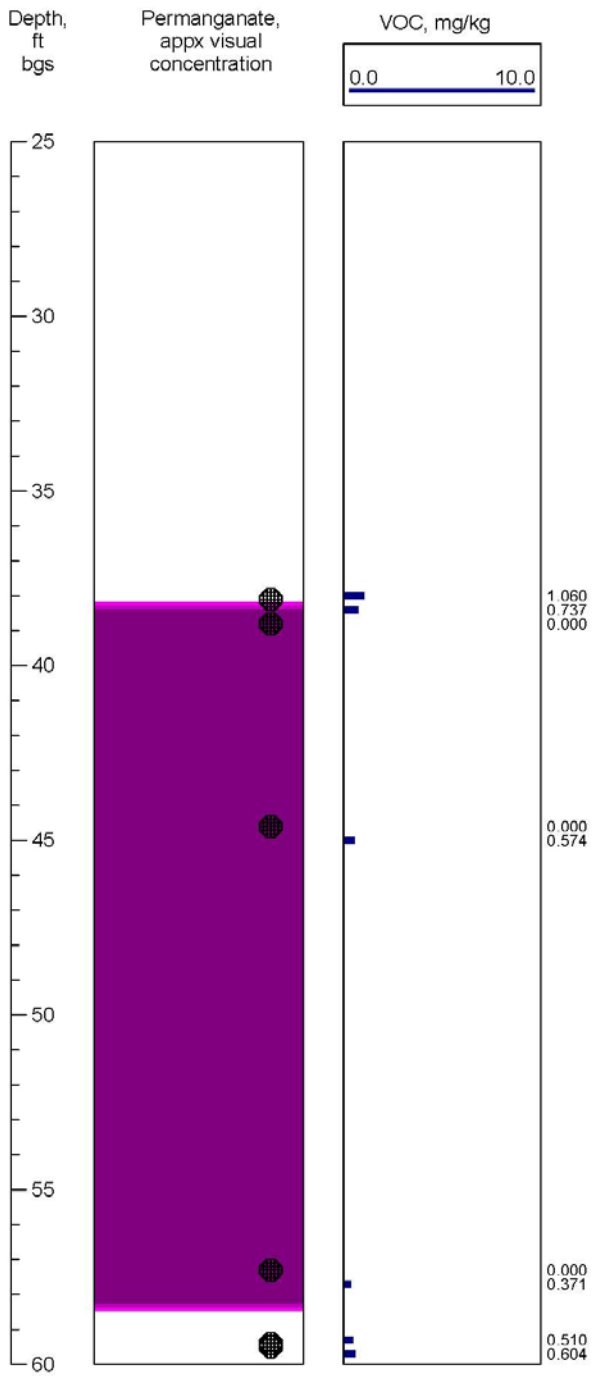
<b>Location:</b>	CP - DPT 06	ESTCP Project ER-0912 Camp Lejeune Field Site
<b>Date Drilled:</b>	11/6/10	



<b>Location:</b>	CP - DPT 07	ESTCP Project ER-0912 Camp Lejeune Field Site
<b>Date Drilled:</b>	11/7/10	

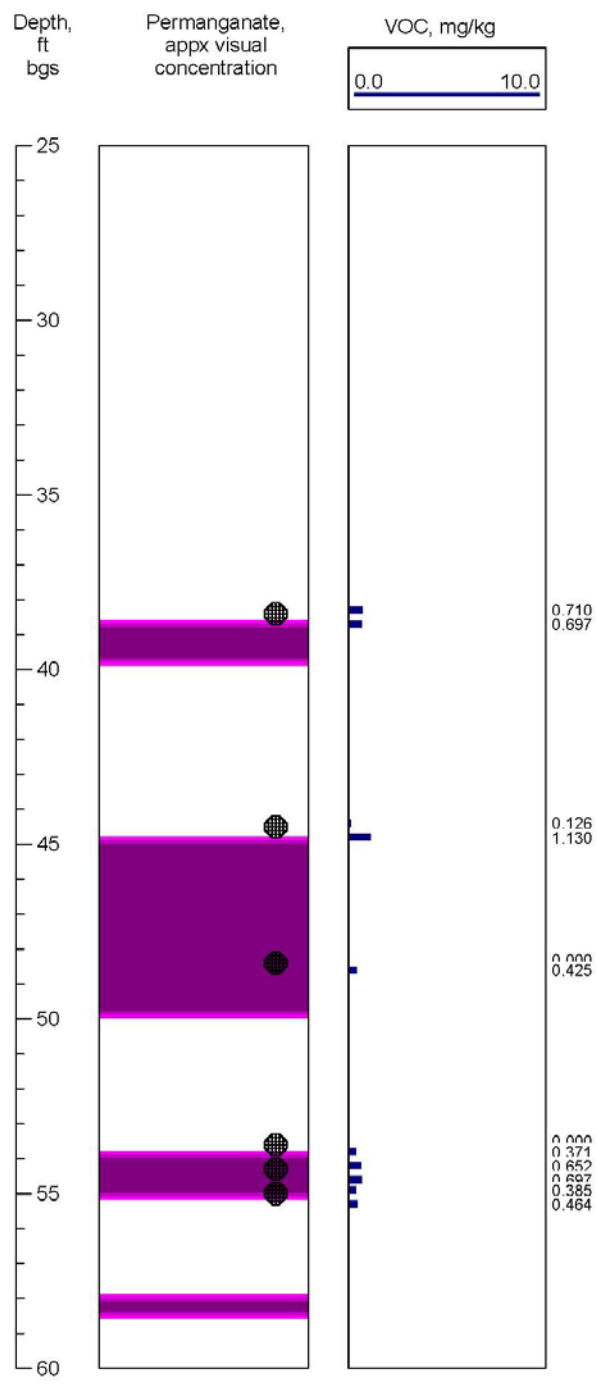


<b>Location:</b>	CP - DPT 08	ESTCP Project ER-0912 Camp Lejeune Field Site
<b>Date Drilled:</b>	11/7/10	

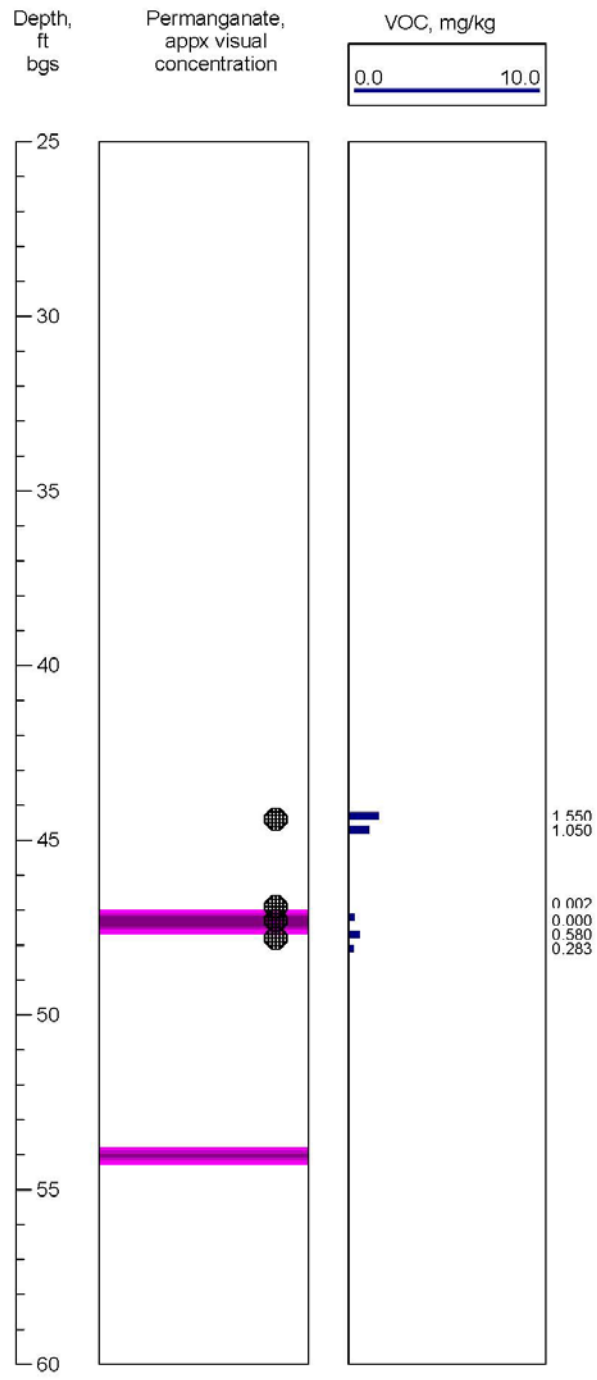




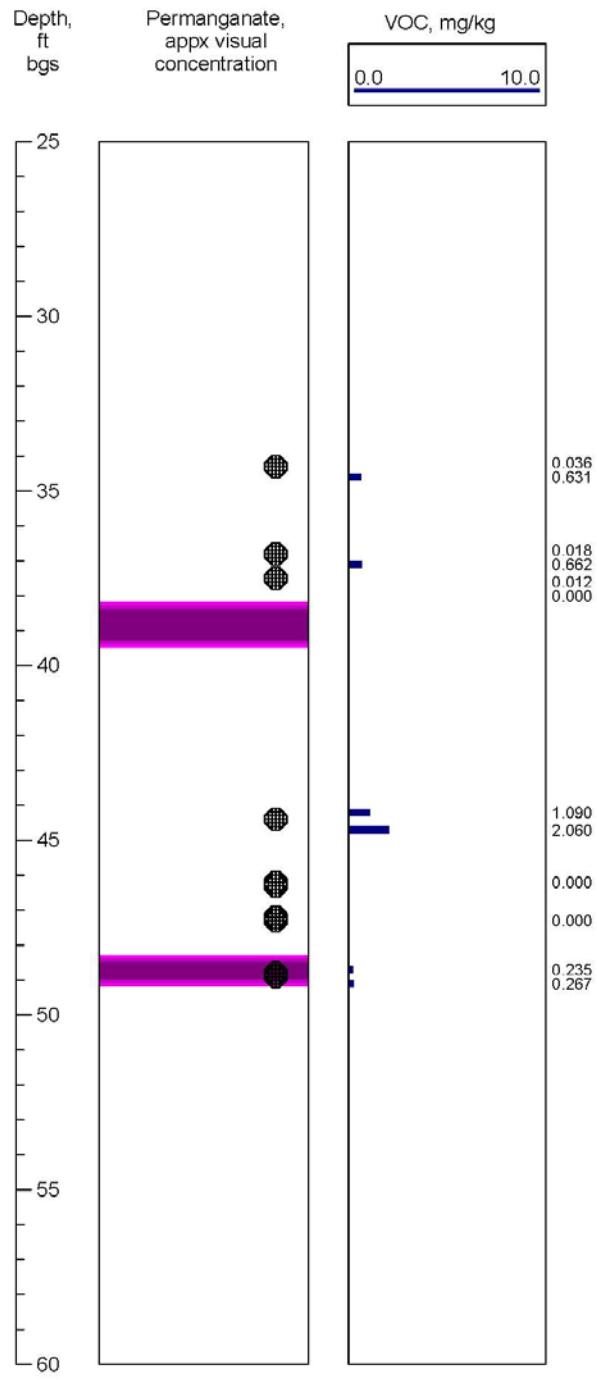
<b>Location:</b> CP - DPT 09	<b>ESTCP Project ER-0912</b>
<b>Date Drilled:</b> 11/7/10	<b>Camp Lejeune Field Site</b>



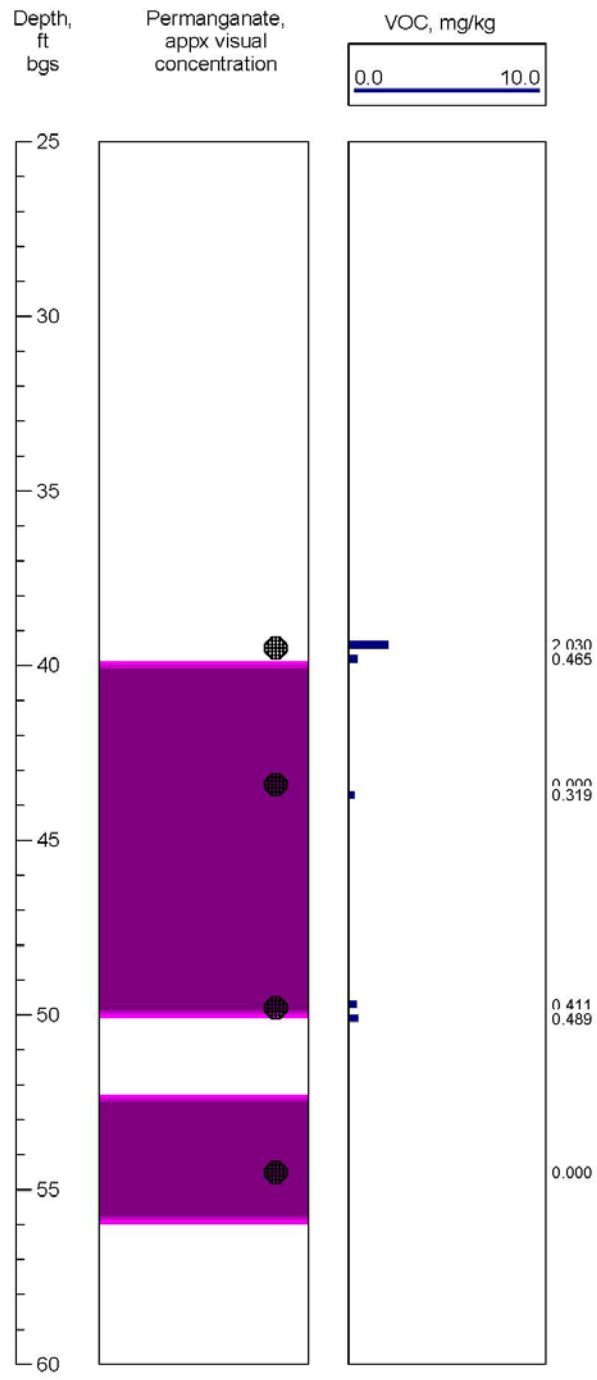
<b>Location:</b>	CP - DPT 10	ESTCP Project ER-0912 Camp Lejeune Field Site
<b>Date Drilled:</b>	11/7/10	



<b>Location:</b>	CP - DPT 11	ESTCP Project ER-0912 Camp Lejeune Field Site
<b>Date Drilled:</b>	11/8/10	



<b>Location:</b>	CP - DPT 12	ESTCP Project ER-0912 Camp Lejeune Field Site
<b>Date Drilled:</b>	11/8/10	



## **Appendix D: Treatability Study Plan**

# **Treatability Study Plan**

---

**ER-0912 Cooperative Technology Demonstration: Polymer-Enhanced Subsurface Delivery and Distribution of Permanganate**

**October 2009  
V.2**

## Contents

List of Tables	ii
List of Figures	ii
Acronyms	iii
<b>1.0 Introduction</b>	<b>1</b>
<b>1.1 Demonstration Objectives</b>	<b>1</b>
<b>1.2 Site Description</b>	<b>1</b>
<b>1.3 Conceptual Site Model (CSM) for Demonstration Area</b>	<b>1</b>
1.3.1 Physical Characteristics	2
1.3.2 Nature and Extent of Contamination	5
<b>2.0 Technology Description (Preliminary Conceptual Design)</b>	<b>9</b>
<b>3.0 Field Characterization Activities</b>	<b>12</b>
<b>4.0 Laboratory Tests and Analyses</b>	<b>19</b>
<b>4.1 Characterization of Site Soil and Groundwater</b>	<b>19</b>
<b>4.2 Laboratory Tests in Support of Objective 1</b>	<b>19</b>
4.2.1 Task 1: Characterize Bulk Solution Rheology	21
4.2.2 Task 2: Characterize Xanthan Oxidant Demand	21
4.2.3 Task 3: Characterize Polymer/Oxidant Transport Conditions in Porous Media	24
4.2.3.1 Polymer/Oxidant Test Solution Injectivity	25
4.2.3.2 Characterize Polymer/Oxidant Solution Rheological Properties in Porous Media	26
4.2.3.3 Characterize Polymer/Oxidant Permeability Reduction	26
4.2.4 Task 4: Optimize Xanthan/KMnO <sub>4</sub> Mixing Strategy for Field Application	27
<b>4.3 Treatability Study Plans for Objective 2</b>	<b>28</b>
4.3.1 Task 1: Identify Optimum Oxidant / Polymer Mixture Concentrations	28
4.3.2 Task 2: Characterize MnO <sub>2</sub> Transport in Porous Media	28
<b>5.0 Summary and Schedule</b>	<b>29</b>
<b>6.0 References</b>	<b>29</b>

## List of Tables

**Table 1. Previous Demonstrations Conducted at Site 88**

**Table 2. Camp Lejeune Demonstration Site Selection Criteria**

**Table 3. Demonstration Performance Objectives**

**Table 4. Summary of Field Data Collection Objectives and Criteria**

**Table 5. Summary of Site Characterization Objectives, Data Needs, and Samples**

**Table 6. Sampling and Analysis Summary Table**

**Table 7. Summary of Laboratory Test Objectives and Criteria**

**Table 8: Treatability Study Schedule**

## List of Figures

**Figure 1.** Site 88 Conceptual Site Model

**Figure 2.** Cross-section location map

**Figure 3.** Cross-section A-A'

**Figure 4.** Cross-section C-C'

**Figure 5.** Two test plots, one treatment (oxidant + polymer) and one control (oxidant only).

**Figure 6.** Schematic of field implementation plan. The left-hand side shows the plan view and the right hand side shows the plan in profile.

**Figure 7.** Initial investigation points for identifying demonstration test plots

**Figure 8.** Schematic diagram of 1-D column test apparatus

**Figure 9.** Schematic of test apparatus for optimizing Xanthan/Permanganate mixing strategy



## Acronyms

<b>APHA</b>	American Public Health Association
<b>AST</b>	Aboveground storage tank
<b>bgs</b>	Below ground surface
<b>CDISCO</b>	Conceptual design for ISCO (modeling tool)
<b>COC</b>	Contaminant of Concern
<b>CPT</b>	Cone penetrometer test
<b>CVOC</b>	Chlorinated volatile organic compound
<b>CSM</b>	Conceptual site model
<b>c-DCE</b>	cis-dichloroethylene
<b>DNAPL</b>	Dense nonaqueous phase liquid
<b>DO</b>	Dissolved oxygen
<b>DPT</b>	Direct push technology
<b>EC</b>	Electrical conductivity
<b>ECD</b>	Electrical conductivity detector
<b>EPA</b>	Environmental Protection Agency
<b>HMP</b>	Hexametaphosphate (used interchangeably with SHMP)
<b>HRP</b>	High-resolution piezocone
<b>ISCO</b>	In situ chemical oxidation
<b>K</b>	Hydraulic conductivity
<b>KMnO<sub>4</sub></b>	Potassium permanganate
<b>LPM</b>	Low permeability media
<b>MCB</b>	Marine Corps base
<b>MIP</b>	Membrane interface probe
<b>MLS</b>	Multi-level sampler
<b>Mn</b>	Manganese
<b>MnO<sub>2</sub></b>	Manganese dioxide
<b>MnO<sub>4</sub><sup>-</sup></b>	Permanganate anion
<b>mV</b>	Millivolts
<b>MW</b>	Monitoring well
<b>NAPL</b>	Nonaqueous phase liquid
<b>NOD</b>	Natural oxidant demand
<b>ORP</b>	Oxidation/Reduction potential
<b>OU</b>	Operable unit
<b>PCE</b>	Tetrachloroethylene (perchloroethylene)
<b>pH</b>	Negative base-10 logarithm of hydronium ion activity
<b>SERDP</b>	Strategic Environmental Research and Development Program
<b>SHMP</b>	Sodium hexametaphosphate
<b>SS</b>	Suspended solids
<b>TCE</b>	Trichloroethylene
<b>TOC</b>	Total organic carbon
<b>TCE</b>	Trichloroethylene
<b>TTI</b>	Target treatment interval
<b>UST</b>	Underground storage tank
<b>VC</b>	Vinyl chloride
<b>VOC</b>	Volatile organic chemical
<b>ZVI</b>	Zero valent iron

## **1.0 Introduction**

### **1.1 Demonstration Objectives**

ISCO using permanganate is an established remediation technology being applied at hazardous waste sites throughout the United States and abroad. Field applications of ISCO continue to grow and have demonstrated that ISCO can achieve destruction of contaminants and achieve clean-up goals. However, some field-scale applications have had uncertain or poor in situ treatment performance. Poor performance is often attributed to poor uniformity of oxidant delivery caused by zones of low permeability media (LPM) and site heterogeneity and excessive oxidant consumption by natural subsurface materials. A second permanganate ISCO challenge is the management of MnO<sub>2</sub> particles, which are a byproduct of the reaction of permanganate with organic contaminants and naturally-reduced subsurface materials. These particles have the potential to deposit in the well and subsurface and impact flow in and around the well screen, filter pack, and the surrounding subsurface formation. This is a particular challenge for sites with excessive oxidant consumption due to the presence of natural materials or large masses of non-aqueous phase liquids (NAPLs). This project focuses on (1) reducing the detrimental effects of site heterogeneities by improving the uniformity of oxidant delivery using the polymer Xanthan gum, and (2) managing MnO<sub>2</sub> aggregation and deposition using the polymer sodium hexametaphosphate (SHMP), hereafter referred to as “Objective 1” and “Objective 2”, respectively. A secondary project objective is to compare post-delivery/treatment groundwater quality for “permanganate only” and “permanganate + polymer” test areas.

### **1.2 Site Description**

The site for the technology demonstration is Site 88 at Marine Corps Base, Camp Lejeune, Jacksonville, North Carolina. MCB Camp Lejeune presently covers approximately 236 square miles and is a training base for the United States Marine Corps. Operable Unit (OU) No. 15, Site 88 consists of the former Base Dry Cleaning facility (former Building 25) and the surrounding paved and grassy areas, located on Post Lane Road, approximately 500 feet east of the intersection of Post Lane Road and McHugh Boulevard. Building 25 was used as a dry cleaning facility from the 1940s until 2004 when operations ceased and the building was demolished. In the 1940s, Varsol™ was stored in underground storage tanks (USTs) located on the north side of the building, and was replaced by PCE in the 1970s. The PCE was stored in an aboveground storage tank (AST). PCE was reportedly stored in the AST from the 1970s until the mid-1980s. Facility employees have reported that spent PCE was disposed of in floor drains that discharged to the sanitary sewer. In March 1995, two self-contained dry cleaning machines were installed in Building 25, eliminating the need for bulk storage of PCE.

### **1.3 Conceptual Site Model (CSM) for Demonstration Area**

The information in this section is based on the data collected and reported in the Site RI by CH2M Hill (included in two volumes as Appendix 1a and 1b). The Conceptual Site Model (CSM) for Site 88 is shown in Figure 1. Previous investigations have been conducted at Site 88 and are summarized in Table 1. This demonstration will be performed in the area surrounding MW02, within the footprint of Former Building 25. It will be located outside of (at least 20 feet)

the source zone at the site that was previously treated (February, 2005) using in situ soil mixing of clay and zero valent iron. Significant tetrachloroethene (PCE) concentrations remain in groundwater outside of the soil mixed zone, as indicated in Table 2, which summarizes the basic site characteristics relative to the objectives of this demonstration. Recent data from the site confirm there is no biogeochemical signature remaining from previous demonstrations or soil mixing activities adjacent to the area of interest for this demonstration (e.g., pH, ORP, dissolved Fe).

### **1.3.1 Physical Characteristics**

Site 88 is underlain by a thick sequence of coastal plain soils consisting of unconsolidated sands, silts, clays, and partially indurated shelly sands. Soils within the surficial aquifer are generally comprised of silty sands, ranging in thickness from 20 to 30 feet, which overlie a discontinuous layer of clayey silt or clay. A clayey silt and clay confining layer, ranging in thickness from 4 to 10 feet, underlies the former location of Building 25 and extends westward as far as Building 3, whereupon it pinches out and appears again further westward. The hydrogeologic setting at Site 88 is that of a two aquifer system, the surficial aquifer and the Castle Hayne aquifer, with the two aquifers occasionally separated by the discontinuous clayey silt and clay layer. Where this layer is absent, the Surficial and Castle Hayne aquifers are in direct hydraulic communication.

Within the Castle Hayne aquifer, a fine grained layer overlies massive beds of fine to medium grained sand with sporadic zones of partial cementation and shell fragments extending to a depth of roughly 180 feet bgs. At Site 88, the Castle Hayne aquifer is divided into the upper Castle Hayne (25-80 feet), the middle Castle Hayne (80-130 feet), and the lower Castle Hayne (130-180 feet). A plastic clay layer, known as the Beaufort confining unit, is beneath the Castle Hayne aquifer; the Beaufort confining unit defines the vertical limit of subsurface investigation at Site 88.

At present, we plan to demonstrate polymer-improved permanganate sweep efficiency (i.e., Objective 1) within the upper Castle Hayne Aquifer unit. Based on previous site characterization efforts within Site 88 (DE&S, 1999; CH2M Hill, 2008) the thickness of the overlying silt/clay layer varies between 6 and 10 feet within this target polymer demonstration area, suggesting it would be a competent upper confining unit. Aquifer testing activities have estimated the geometric mean hydraulic conductivity values for the Surficial, upper Castle Hayne, and lower Castle Hayne aquifers to be 4.1 ft/day, 11.1 ft/day, and 11.5 ft/day, respectively. Corresponding mean seepage velocities for these same aquifers were estimated to be 0.18 ft/day and 0.17 ft/day, respectively. These values are appropriate for our demonstration purposes (Table 2) and equate to permeabilities ranging between 2 and 7 darcy, which is within the range investigated for SERDP Project ER-1486 (foundation for Objective 1) and ER-1484 (foundation for Objective 2). In particular, in the absence of permanganate, the introduction of xanthan gum during ER-1486 studies was found to reduce the intrinsic permeability by a factor of 1.4, which was concluded to be an acceptable permeability reduction for successful technology application. We plan to demonstrate Objective 2 in the Surficial aquifer. For this objective, the physical properties are less critical than the contaminant mass density characteristics described below. To evaluate success related to Objective 1, highly refined data will be collected to characterize hydraulic conductivity / permeability within the test area as described in Section 3.0 below.



**Table 1. Previous Demonstrations Conducted at Site 88**

Activity	Date	Reference	Conclusions
UST and AST Removal	1995	OHM, 1996	Removal of five USTs and one AST. CVOCs and inorganics were detected in subsurface soil samples. CVOCs, TPH, and naphthalene were detected in groundwater.
Focused Remedial Investigation	1996/1997	Baker, 1998	Installation of temporary and permanent wells at varying depth. CVOC contamination identified in subsurface soil beneath and near Building 25 and along the underground industrial sewer line. CVOC impacts were detected in the surficial aquifer and the upper portion of the Castle Hayne aquifer.
DNAPL Characterization using Partitioning Interwell Tracer Tests	1997	Duke, 1999	DNAPL was found beneath Building 25. Approximately 105 gallons of DNAPL were removed.
Reductive Anaerobic In Situ Treatment Technology (RABITT) Testing	2001	BMI, 2001	The RABITT testing concluded that native microbial populations were capable of sequentially reducing PCE to ethene. PCE and TCE concentrations were reduced in the study area.
Supplemental Site Investigation	2002/2003	CH2M HILL 2002, 2003	Installation of 26 monitoring wells at four different depths within the surficial and Castle Hayne aquifers, video inspection of sewer system, soil sampling, aquifer testing, and groundwater sampling. CVOCs were determined to be migrating generally to the northwest. In addition, the vertical distribution of VOCs indicates appreciable volumes of DNAPL have accumulated upon the shallow silt layer. However, this layer was not impermeable; appeared to be allowing dissolved-phase VOCs to migrate vertically.
Membrane Interface Probe (MIP) Investigation	2004	CH2M HILL, 2004a	Used to refine previous source area characterization by evaluating the horizontal and vertical distribution of the DNAPL source area.
Final Engineering Evaluation/Cost Analysis	2004	CH2M HILL, 2004b	The EE/CA recommended shallow soil mixing with clay and zero-valent iron (ZVI) addition for source treatment.
Shallow Soil Mixing with Clay-ZVI	2005	CH2M HILL, 2006	Full-scale implementation of shallow soil mixing with clay-ZVI addition was initiated. The mixture was delivered via a 10-foot diameter auger to a depth of 20 feet bgs over an area of 9,500 square feet (ft <sup>2</sup> ). Approximately 7,050 cubic yards (yd <sup>3</sup> ) of impacted soil was treated. After stabilization, the treatment area was paved and converted into a parking lot. Within the treatment area PCE concentrations in the soil were reduced by greater than 99 percent.
Remedial Investigation	2003-2007	CH2M HILL, 2008a	RI field activities included: DPT groundwater sampling; MIP groundwater profiling; installation of 66 monitoring wells; installation of three multi-screen monitoring wells; sampling of site monitoring wells; and aquifer testing. PCE concentrations in excess of 7,500 µg/L (5 percent of the solubility of PCE), as reported for several Site 88 wells, may indicate the presence of remaining DNAPL PCE.
Draft Feasibility Study	2008	CH2M HILL, 2008b	Groundwater contamination was broken down into three distinct zones (refer to the CSM) for evaluating remedial alternatives.
IR88-MW39MP Re-sample	2008		IR88-MW39MP was re-sampled to evaluate whether the PCE distribution with depth observed in 2007 may have been related to well installation. The data indicate decreasing concentrations with depth.

**Table 2. Camp Lejeune Demonstration Site Selection Criteria**

Parameter	Preferred Value(s)	Relative Importance*	MCB Camp Lejeune
Site Name	-	-	Site 88
Chloroethene concentration	Measured in groundwater above 5 mg/L range	2	~10 mg/L PCE
Depth to groundwater	~10 ft bgs	3	10
Total depth of treatment zone	30 ft bgs	3	60
Utility access	Electrical and water	2	Yes
Bulk hydraulic conductivity	k > 10 ft/day	1	0.4 – 30 ft/day (median 11 ft/day)
Heterogeneous	Measurable or visible difference within several feet of depth	1	Sand with silt and shell fragments and thin discontinuous layers of silt, clay, and peat
Site Project Status	Feasibility Study	1	Feasibility Study
Impediments	Minimal	2	Some – large area, can execute work around to minimize impacts to active facility
US Navy-Owned Site with nearby CH2M HILL office	Yes	3	Yes

Notes:

\*1-5; with 1 being highest

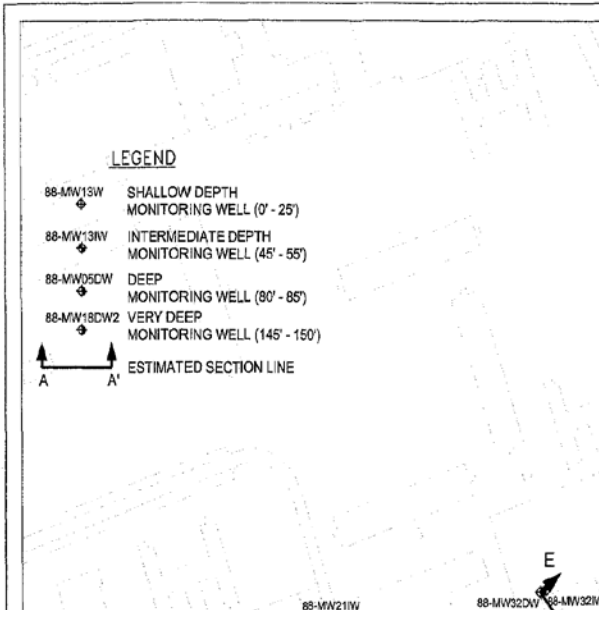
ft bgs – feet below ground surface

ft/day – feet per day hydraulic conductivity

MCB – Marine Corps Base Camp Lejeune, NC

**1.3.2 Nature and Extent of Contamination**

The nature and extent of groundwater contamination at Site 88 was derived from the most recent (August 2007 and October 2008) monitoring data. The primary COCs, the compounds detected at the highest concentrations and with the most frequency, for Site 88 include PCE, TCE, cis-1,2-DCE, and VC. Figure 2 shows cross-sections established for the site. This demonstration is planned for near the junction of cross section A-A' (horizontal) and C-C' (vertical) (adjacent to MW02). Figure 3 shows the contaminant profile with depth for the A-A' cross section. Figure 4 shows the contaminant profile with depth for the C-C' cross section. The MW02 location is highlighted in these figures. These data show PCE concentrations of 12,000 µg/L, TCE 800 µg/L, c-DCE 13,000 µg/L, and VC < 310 µg/L in the Surficial aquifer where Objective 2 will be demonstrated. The contaminant profile is less relevant to Objective 1, which relies more heavily on physical characteristics as described above. While some data are described here for the general vicinity of the planned demonstration, detailed contaminant mass density is critical to evaluating success related to Objective 2. These data will be collected as part of the field characterization activities described below.



  
**MW02**

**Figure 2.** Cross-section location map

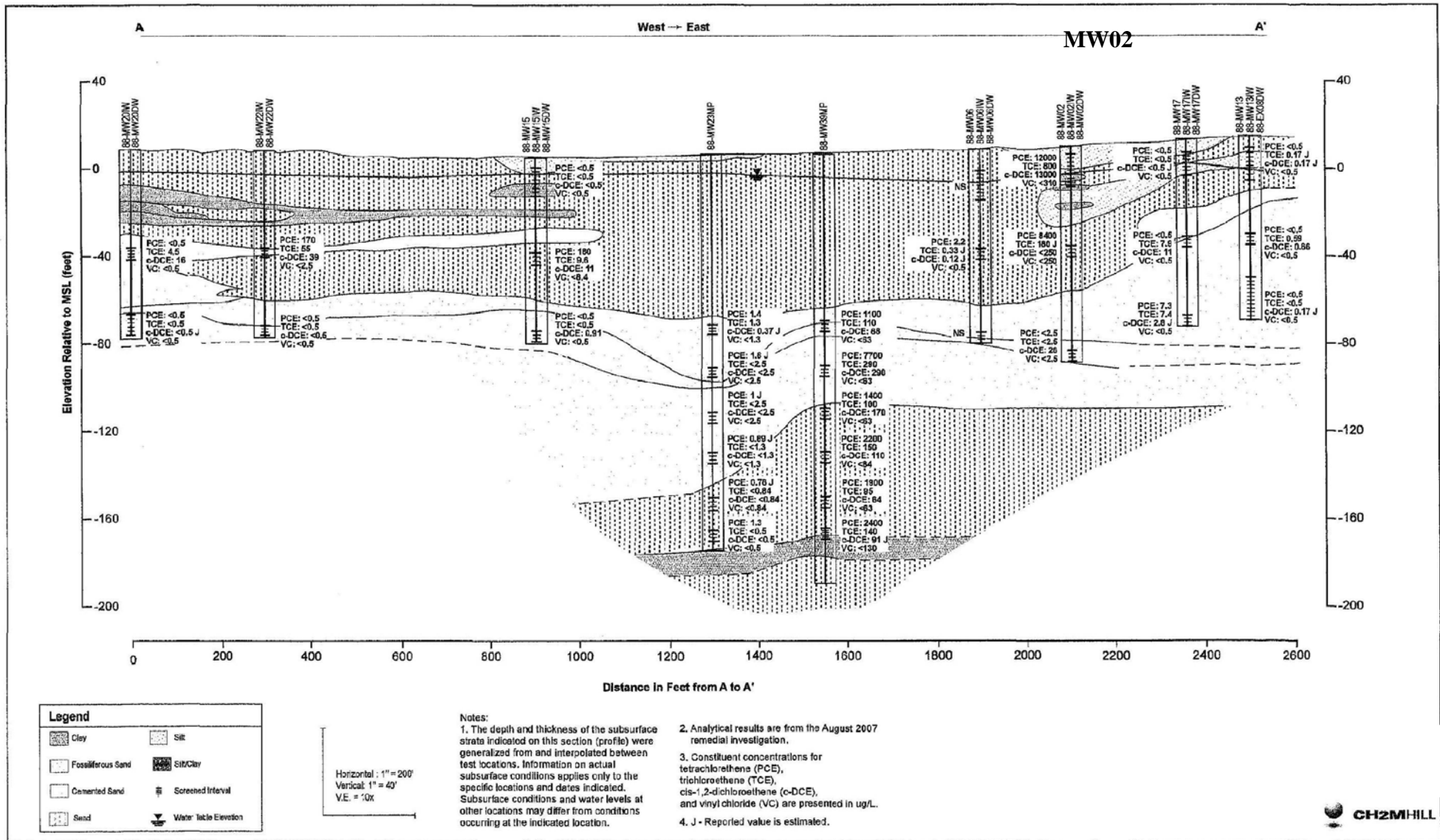


**Figure 3. Cross-section A-A'**





## 2.0 Technology Description (Preliminary Conceptual Design)

To reiterate, the overall objectives for this demonstration (i.e., polymer application) are: Objective 1 - reducing the detrimental effects of site heterogeneities by improving the uniformity of oxidant delivery using the polymer Xanthan gum, and Objective 2 - managing MnO<sub>2</sub> aggregation and deposition using the polymer SHMP. Detailed demonstration performance criteria, data required, and success criteria related to these objectives are presented in Table 3.

**Table 3. Demonstration Performance Objectives**

<b>Performance Criteria</b>	<b>Data Requirements</b>	<b>Success Criteria (with use of polymer)</b>
<b>Quantitative Performance Objectives</b>		
Reducing potential for contaminant rebound	<ul style="list-style-type: none"> <li>Contaminant concentrations in groundwater over time and distance</li> </ul>	<ul style="list-style-type: none"> <li>No contaminant in groundwater attributable to rebound</li> </ul>
Improved contaminant treatment effectiveness	<ul style="list-style-type: none"> <li>Contaminant concentrations in groundwater over time and distance</li> <li>Contaminant mass in soil over time and distance</li> </ul>	<ul style="list-style-type: none"> <li>Statistically significant difference (lower) in contaminant mass</li> </ul>
Increased penetration of oxidant into lower permeability layers/strata	<ul style="list-style-type: none"> <li>Examination of soil cores for evidence of permanganate (purple color, or byproduct brown) in lower permeability layers/strata</li> <li>If LPM of thickness appropriate for discrete groundwater sampling is present, then MnO<sub>4</sub><sup>-</sup> concentrations measured in groundwater over space and time</li> <li>Electrical monitoring probe (ORP and EC) network measurements over space and time</li> </ul>	<ul style="list-style-type: none"> <li>50% longer distance of permanganate penetration/ movement into lower permeability layers/strata</li> <li>25% higher permanganate concentration at expected time of arrival in each monitoring well</li> <li>Demonstrated improvement in vertical sweep efficiency of permanganate within lower permeability layers/strata</li> <li>Demonstrated improvement in overall vertical sweep efficiency of permanganate within the test plot(s)</li> <li>50% greater conductivity and ORP in target media</li> </ul>
Decreased flow bypassing of areas of high contaminant mass	<ul style="list-style-type: none"> <li>Examination of soil cores for evidence of MnO<sub>2</sub> (dark brown) in media with high contaminant saturation</li> <li>Soil core extractions or MnO<sub>2</sub> and spectrophotometric measurements for MnO<sub>2</sub> in groundwater over space and time</li> <li>Soil core extractions for contaminant</li> </ul>	<ul style="list-style-type: none"> <li>50% lower mass of MnO<sub>2</sub> in given mass of media</li> <li>25% greater mobile MnO<sub>2</sub> concentration at given time point in monitoring well</li> <li>50% lower mass of contaminant in high saturation cores</li> </ul>
<b>Qualitative Performance Objectives</b>		
Decreased impact of MnO <sub>2</sub> deposition on injection pressure	<ul style="list-style-type: none"> <li>Field subsurface and injection pressure</li> </ul>	<ul style="list-style-type: none"> <li>No increase in injection pressure attributable to MnO<sub>2</sub> (compared to pressures expected via simulation)</li> </ul>
Improved understanding of impacts of the enhanced delivery approach on groundwater quality	<ul style="list-style-type: none"> <li>pH, ORP, key metals, solids concentrations, conductivity, bioactivity</li> </ul>	<ul style="list-style-type: none"> <li>Note differences</li> </ul>

The two separate overall objectives will be pursued in two separate regions of both a treatment and control plot (Figure 5); a shallow zone (within the Surficial aquifer) and intermediate zone (upper Castle Hayne). The intermediate zone of the site has characteristics suitable for demonstration related to Objective 1, as described above (i.e., hydraulic conductivity, heterogeneity). This is designated as Plot 1. The primary criterion of importance for Objective 2 is a high contaminant mass density/concentration. The shallow zone of the demonstration area meets this criterion with PCE concentrations of ~7-10 mg/L (Table 2).

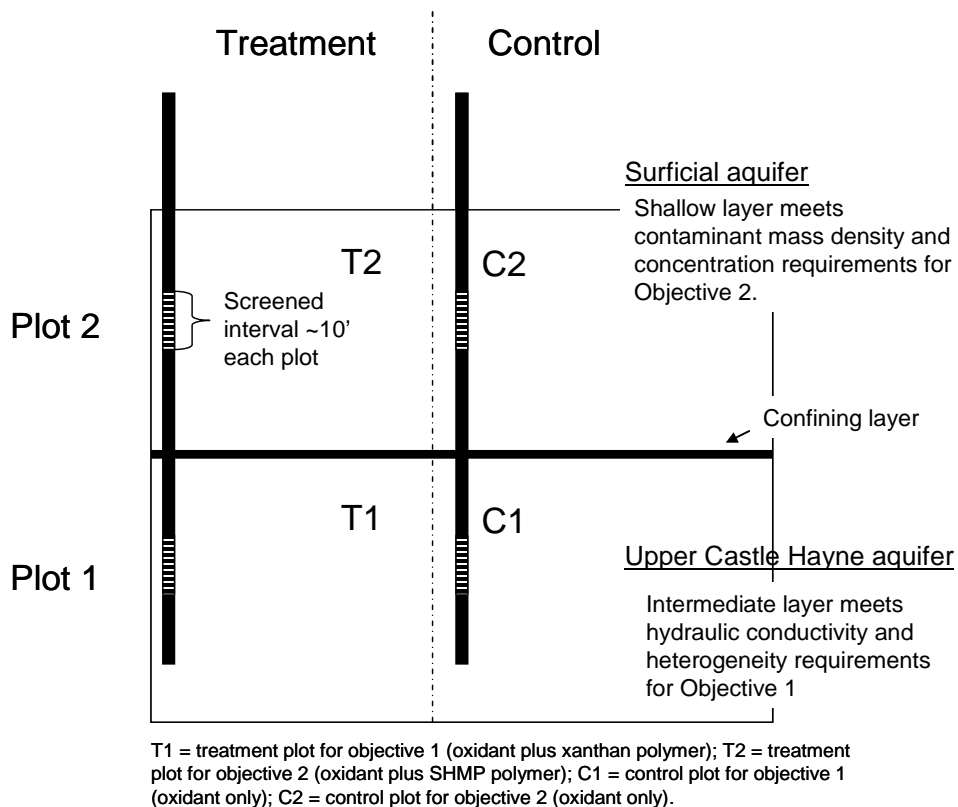


**Figure 5.** Two test plots, one treatment (oxidant + polymer) and one control (oxidant only). The intermediate depth zone (upper Castle Hayne) is suitable for meeting Objective 1, improving sweep efficiency using xanthan polymer. The shallow depth zone (Surficial aquifer) is suitable for meeting Objective 2 controlling MnO<sub>2</sub> particles.

The pilot test plots are planned to be approximately 30-feet in diameter (includes a buffer zone around an expected 15-foot radius of influence) (Figure 6). Four multi-level sampling (MLS) wells will be installed at various distances from the injection well and screened at three depth intervals to monitor the water quality of the targeted zones of high and low permeability. The MLS well screen lengths will range from 6-inches to 5-feet, depending upon the thickness of the target lithology (fine- and coarse-grained) and the thickness of the bentonite seal needed to properly isolate the sample interval from the overburden and/or underlying aquifer zones. The design of the MLS wells will be based upon the results of the cone penetrometer testing (CPT)

investigation and numerical simulation performed during site characterization activities (see Section 3.0 below). The depth and locations of each MLS point will be carefully selected to properly monitor and validate the absence and/or presence of oxidant, polymers, and oxidation by-products within specific heterogeneous strata in order to validate the sweep efficiency of these strata throughout the target treatment zone. Prior to system startup, all new wells will be developed and sampled and direct-push technology (DPT) used to collect discrete groundwater samples from the treatment zone.

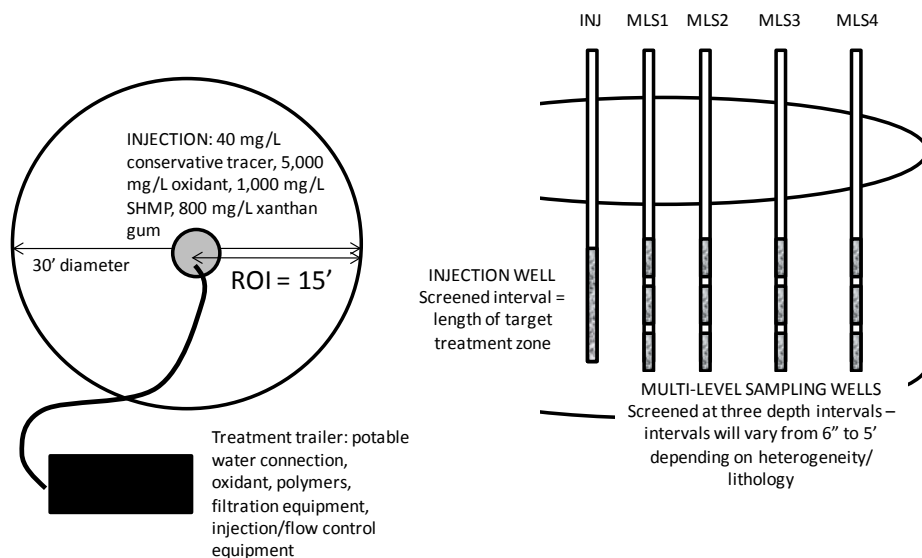


**Figure 6.** Schematic of field implementation plan. The left-hand side shows the plan view and the right hand side shows the plan in profile.

A small treatment trailer will be constructed and used to sequentially implement the test protocol at each of the two pilot test plots. The trailer will contain the potable water connection (from nearby fire hydrant), permanganate, polymers, and conservative tracer dosing, filtration, and injection/flow control equipment. It will be sized to process a maximum of approximately 30 gallons per minute of 5,000 ppm potassium permanganate, 800 ppm of xanthan gum (depending on site permeability conditions), and 1,000 ppm of SHMP and will contain instrumentation and controls to allow for automatic operation and shutdown in case of high tank or injection well pressure (precise concentrations will be determined during site characterization and laboratory evaluations described in Sections 3.0 and 4.0 below). Model simulations will be employed to develop a design basis for oxidant and polymer injection within each test plot using input values measured during site characterization and lab testing. Permanganate injection into the pilot test plots will be operated for the time necessary to achieve oxidant breakthrough at the desired 15-foot radius of influence. During the injection program, water levels and injection pressure will be measured to monitor the physical effectiveness of the delivery system. In addition, MLS wells will be sampled to measure system performance and document oxidant delivery effectiveness. Samples will be collected and analyzed in the field to collect real-time data to assess the demonstration's effectiveness and make adjustments if necessary.

After the active injection is completed, weekly MLS well monitoring will be performed for up to eight weeks to document oxidant persistence and treatment efficiency. Within a couple of weeks of cessation of injection, a DPT-conductivity survey and intact soil coring will be performed. The DPT-conductivity survey results will be used to site the intact coring locations. Five intact soil cores will be collected, visually inspected and logged in the field, and then shipped to the laboratory for quantitative analysis of polymers, permanganate, manganese dioxide, bioactivity, and VOCs. Field groundwater data collection will include permanganate concentrations, ORP, pH, temperature, and conductivity, along with real-time measurements of subsurface (i.e., water levels) and injection pressures. Groundwater samples will be collected and preserved for off-site laboratory measurement of contaminant concentrations, conservative tracer, key metals concentrations, polymer concentration, and MnO<sub>2</sub> concentration. Of interest are potential differences in long-term aquifer quality as a result of permanganate treatment both with and without polymers.

The final sampling will be conducted two months post-demonstration, or as determined by monitoring of the exhaustion of oxidant and adequate aquifer re-equilibration (i.e., field parameter stabilization). The sampling will be conducted using a sampling and analytical program that matches the baseline and 2-week post-injection events. Final sampling of each test plot will consist of intact soil coring, well groundwater sampling, and DPT-Waterloo Profiling within the treatment zone. Post-treatment slug tests will be conducted on the injection well to assess changes in hydraulic conductivity that may have been caused by the pilot test.

While significant data for the site exist as collected during previous investigations, additional data collection is necessary to meet the objectives of this demonstration. The refinement of hydrogeological data (i.e. hydraulic conductivity, permeability, heterogeneity) and contaminant distribution characteristics within the proposed treatment area at the scale appropriate for this pilot-scale demonstration is critical. These data will be collected through field characterization activities (described in Section 3.0 below) and laboratory tests and analyses (described in Section 4.0 below).

### **3.0 Field Characterization Activities**

Table 4 includes field characterization data objectives, along with data needs and criteria for success. Table 5 summarizes the field methods and sample collection to fulfill the data needs. Field characterization will be conducted dynamically with real-time decision-making. Objectives 1A and 1B are to site the demonstration test plots. These must first be completed before the remaining objectives are pursued.

Figure 7 shows initial test points where membrane interface probe (MIP) for profiling contaminant mass distribution, and cone penetrometer testing (CPT) and high-resolution piezocone (HRP) for profiling the lithology/hydraulic conductivity will be initiated. While these characteristics are known roughly for the site and to the certainty that we anticipate a successful demonstration (i.e., basis of site selection criteria), detailed profiles are needed at high resolution in the test plots to evaluate success as per Table 3. Decisions will be made real-time in the field and via team conference (daily) to assess whether data objectives have been met or if additional investigation is necessary (i.e., need for more data points).

**Table 4. Summary of Field Data Collection Objectives and Criteria**

#	Data Objective	Criteria for Achieving Objective	Data Need
1A	Identify a 30-foot diameter location for test plot 1 (Improve permanganate delivery by controlling MnO <sub>2</sub> deposition with soluble polymer)	<ul style="list-style-type: none"> <li>• 30-foot diameter open space with minimal utility interference</li> <li>• High [VOC] &gt; 5 mg/L total chlorinated ethenes</li> <li>• Bulk K &gt; 10 ft/day</li> </ul>	Relative VOC concentrations and lithology in the shallow (0-20' bgs) depth interval and within the vicinity of the 88-MW02 well cluster
1B	Identify a 30-foot diameter location for test plot 2 (Improve permanganate delivery sweep efficiency through heterogeneous zones using a soluble polymer)	<ul style="list-style-type: none"> <li>• 30-foot diameter open space with minimal utility interference</li> <li>• <math>K_v/K_h</math> anisotropy ~ 100</li> <li>• Visible soil heterogeneity within 10-foot depth interval</li> <li>• Bulk K &gt; 10 ft/day</li> </ul>	Relative VOC concentrations and lithology in the intermediate (20-60' bgs) depth interval and within the vicinity of the 88-MW02 well cluster
2	Delineate the volatile organic compound (VOC) distribution including top and bottom of the bulk of contamination (ECD > 1e5 $\mu$ V, for example) within the entire vertical profile of the two test plots at center and three radii within the test plot circle and on 6-inch vertical centers	<ul style="list-style-type: none"> <li>• MIP/ECD &gt; baseline, estimated to be &gt;5e5 <math>\mu</math>V</li> <li>• MIP/ECD measurements at 6-inch to 1-foot vertical spacing</li> <li>• MIP/ECD probe locations at center and three radii within the 30' dia. test plot circle</li> <li>• In 2D only, identify the top and bottom of contamination only. Delineation of the lateral extent is unnecessary. May require probing to depths greater than 60' bgs.</li> </ul>	Relative VOC concentrations in the vicinity of each identified test plot.
3A	Characterize the entire vertical profile of the two test plots at center and three radii within the test plot circle and on 6-inch vertical centers	<ul style="list-style-type: none"> <li>• CPT measurements that differentiate between the types of sand (e.g., fine, medium, silty, etc.) present</li> <li>• HRP measurements as a secondary line-of-evidence to define type of lithology</li> <li>• CPT probe locations at a minimum of 4 locations within each test plot (if data is useful)</li> <li>• HRP probe locations at a minimum of 2 locations within each test plot (shallow and intermediate). May require more probes if the CPT tool is unable to differentiate between the soil types.</li> <li>• In 2D only, monitor the top and bottom of unique lithologic layers only. Delineation of the lateral extent is unnecessary.</li> </ul>	Lithology and hydraulic characteristics in the vicinity of each identified test plot
3B	Characterize the hydraulic characteristics within the entire vertical profile of the two test plots at center and three radii within the test plot circle and on 6-inch vertical centers	<ul style="list-style-type: none"> <li>• HRP measurements to estimate K of each unique lithologic layer</li> <li>• HRP measurements to estimate the horizontal and vertical gradients present within each unique lithologic zone</li> <li>• HRP probe locations at a minimum of 3 locations within each test plot (shallow and intermediate) so that triangulation can be used to estimate lateral gradients within each unique lithologic zone.</li> <li>• In 2D only, monitor the top and bottom of unique lithologic layers only.</li> <li>• Delineation of the lateral extent is unnecessary.</li> </ul>	Lithology and hydraulic characteristics in the vicinity of each identified test plot

**Table 4. Summary of Field Data Collection Objectives and Criteria**

#	Data Objective	Criteria for Achieving Objective	Data Need
4	Identify the possible preferential injection flow pathways within the entire vertical profile of each of the two test plots	<ul style="list-style-type: none"> <li>• Uses CPT and HRP measurements collected for above data objectives. No new data collection is necessary to meet this objective.</li> <li>• Map the MIP, CPT, and HRP data on the same chart and identify (label) the unique horizons in order of highest to lowest conductivity (K) values.</li> </ul>	Lithology and hydraulic characteristics in the vicinity of each identified test plot
5A	Identify target treatment intervals (TTIs) for the shallow depth intervals at each test plot location so that injection well screens can be properly designed	<ul style="list-style-type: none"> <li>• Uses MIP, CPT, and HRP measurements collected for above data objectives. No new data collection is necessary to meet this objective.</li> <li>• Using the collaborative data maps prepared for Objective 4, identify the zones containing [CVOC] &gt; 1e6 µV and a K &gt; 1 ft/day.</li> <li>• Quantify the relative proportion of [CVOC] mass present within each unique zone</li> <li>• The TTI is depth interval that contains [CVOC] &gt; 1e6 µV, K &gt; 1 ft/day, and 90-percent of the mass present within the entire shallow depth interval (0-20' bgs).</li> </ul>	Relative VOC concentrations and lithology in the vicinity of each identified test plot
5B	Identify target treatment intervals (TTIs) for intermediate depth intervals at each test plot location so that injection well screens can be properly designed	<ul style="list-style-type: none"> <li>• Uses MIP, CPT, and HRP measurements collected for above data objectives. No new data collection is necessary to meet this objective.</li> <li>• Using the collaborative data maps prepared for Objective 4, identify the zones containing [CVOC] &gt; 1e6 µV and a K &gt; 0.1 ft/day.</li> <li>• Quantify the <math>K_v/K_h</math> anisotropy within this depth interval</li> <li>• Quantify the relative proportion of [CVOC] mass present within each unique zone</li> <li>• The TTI is 10- to 20-foot (10-foot preferred) depth interval that contains [CVOC] &gt; 1e6 µV, <math>K_{max} &gt; 10</math> ft/day, anisotropy ~100, and 90-percent of the mass present within the entire shallow depth interval (20-60' bgs).</li> </ul>	Relative VOC concentrations and lithology in the vicinity of each identified test plot
6A	Provide detailed information for design of shallow depth test plot injection well and monitoring well network	<ul style="list-style-type: none"> <li>• Uses MIP, CPT, and HRP measurements collected for above data objectives. No new data collection is necessary to meet this objective.</li> <li>• Evaluate the uniformity of [CVOC] distribution within the TTI of each test plot (see Objective 5)</li> <li>• Injection well will be screened across the TTI</li> </ul>	Relative and accurate VOC concentrations and lithology in the vicinity of each identified test plot
6B	Provide detailed information for design of intermediate depth test plot injection well and monitoring well network	<ul style="list-style-type: none"> <li>• Uses MIP, CPT, and HRP measurements collected for above data objectives. No new data collection is necessary to meet this objective.</li> <li>• Evaluate the uniformity of lithology and [CVOC] distribution within the TTI of each test plot (see Objective 5)</li> <li>• Injection well will be screened across the TTI</li> </ul>	Relative and accurate VOC concentrations and lithology in the vicinity of each identified test plot

**Table 4. Summary of Field Data Collection Objectives and Criteria**

#	Data Objective	Criteria for Achieving Objective	Data Need
7A	Provide baseline physical and chemical characteristics from key locations within the shallow depth plots so that post-treatment samples can be co-located and evaluated for treatment performance	<p>Baseline physical and chemical characteristics will be collected to measure baseline parameters necessary to meet the following overall project performance objectives:</p> <ul style="list-style-type: none"> <li>• Eliminate the potential for contaminant rebound               <ul style="list-style-type: none"> <li>– As measured by [CVOC] in groundwater wells. After properly citing the monitoring wells (see Objective 6), baseline water samples will be collected from them using low-flow/micropurge methods and analyzed for [CVOC].</li> <li>– As measured by [CVOC] in DPT grab groundwater samples. Up to 15 DPT grab groundwater samples will be collected with geospatial uniformity across the TTI from each test plot within unique lithologic and [CVOC] zones. Samples will be collected from zones containing high, moderate, and low [CVOC] as indicated by the MIP/ECD results.</li> <li>– As measured by [CVOC] in DPT intact core soil samples. Up to 3 two-foot long intact soil core samples will be collected from the interfaces of low and high permeability zones in each test plot and analyzed for [CVOC]. Multiple subsamples will be taken from each core within the low and higher permeability zones to assess baseline contaminant distribution (MIP confirmation) and serve as a basis for comparison against co-located soil cores to be collected post-ISCO treatment.</li> </ul> </li> <li>• Improve contaminant treatment effectiveness               <ul style="list-style-type: none"> <li>– As measured by [CVOC] in groundwater wells and DPT grab groundwater samples. See above.</li> <li>– As measured by [CVOC] in DPT grab soil samples. Up to 15 DPT grab soil samples will be collected. This baseline monitoring event and used as a point of comparison for future post-ISCO treatment sampling.</li> </ul> </li> <li>• Decreased impact of MnO<sub>2</sub> deposition on injection pressure               <ul style="list-style-type: none"> <li>– As measured by field comparison of injection pressures at the control and test plots in the shallow zone. There is no associated field activity during the site characterization task.</li> </ul> </li> <li>• Improved understanding of impacts of the enhanced delivery approach on groundwater quality               <ul style="list-style-type: none"> <li>– As measured by analyses shown in Table 6</li> <li>– Additional laboratory analyses will be performed on groundwater and soil samples that are noted above for other data objectives.</li> </ul> </li> </ul>	Accurate VOC concentrations and lithology in the vicinity of each identified test plot



**Table 4. Summary of Field Data Collection Objectives and Criteria**

#	Data Objective	Criteria for Achieving Objective	Data Need
7B	Provide baseline physical and chemical characteristics from key locations within the intermediate depth plots so that post-treatment samples can be co-located and evaluated for treatment performance	<p>Baseline physical and chemical characteristics will be collected to measure baseline parameters necessary to meet the following overall project performance objectives:</p> <ul style="list-style-type: none"><li>• Eliminate the potential for contaminant rebound<ul style="list-style-type: none"><li>– Same as above – Objective 7 Shallow Test Plots.</li></ul></li><li>• Improve contaminant treatment effectiveness<ul style="list-style-type: none"><li>– Same as above – Objective 7 Shallow Test Plots.</li></ul></li><li>• Increased penetration of oxidant into LPM<ul style="list-style-type: none"><li>– As measured by visual examination of soil cores for purple color in LPM, <math>[\text{MnO}_4^-]</math> in groundwater within the LPM, and electrical conductivity (EC) response within the LPM. Baseline EC probing will be conducted concurrent with CPT/MIP to record a baseline EC response such that post-ISCO treatment EC probing will have a point of comparison.</li></ul></li><li>• Improved understanding of impacts of the enhanced delivery approach on groundwater quality<ul style="list-style-type: none"><li>– Same as above – Objective 7 Shallow Test Plots.</li></ul></li></ul>	Accurate VOC concentrations and lithology in the vicinity of each identified test plot
8	Provide a data basis for semi-quantitative analysis of contaminant mass distribution within the TTI of each test plot	<ul style="list-style-type: none"><li>• Results of grab groundwater and soil samples will be used to semi-quantitatively estimate a contaminant mass and mass distribution between the permeable and LPM zones within the TTI at each test plot.</li></ul>	Relative and accurate VOC concentrations and lithology in the vicinity of each identified test plot.
9	Define hydraulic input parameters for a numeric model that will be used to predict the delivery/sweep efficiency of polymer and permanganate injection	<ul style="list-style-type: none"><li>• CPT data need to define the lithologic stratification</li><li>• HRP data needed to define the K and head within each unique lithologic horizon</li></ul>	Lithology and hydraulic characteristics in the vicinity of each identified test plot.

**Table 5. Summary of Site Characterization Objectives, Data Needs, and Samples**

No.	Data Need	Description of Field Activity	Sample Support
1.	Relative VOC concentrations and lithology in the shallow (0-20' bgs) and intermediate (20-60' bgs) depth intervals and within the vicinity of the 88-MW02 well cluster	MIP, CPT, HRP	MIP, CPT at up to 4 locations per test plot HRP at up to 3 location per test plot
2.	Relative VOC concentrations in the vicinity of each identified test plot	MIP	MIP at up to 4 locations per test plot
3.	Lithology and hydraulic characteristics in the vicinity of each identified test plot	CPT, HRP	CPT at up to 4 locations per test plot HRP at up to 3 locations per test plot
4.	Lithology and hydraulic characteristics in the vicinity of each identified test plot	CPT, HRP	CPT at up to 4 locations per test plot HRP at up to 3 locations per test plot
5.	Relative VOC concentrations and lithology in the vicinity of each identified test plot	MIP, CPT, HRP	MIP, CPT at up to 4 locations per test plot HRP at up to 3 locations per test plot
6.	Relative and accurate VOC concentrations and lithology in the vicinity of each identified test plot	MIP, CPT, HRP	MIP, CPT at up to 4 locations per test plot HRP at up to 3 locations per test plot
7.	Accurate VOC concentrations and lithology in the vicinity of the each identified test plot	CPT, HRP DPT discrete soil and groundwater sampling Electrical conductivity (EC)	CPT at up to 4 locations per test plot HRP at up to 3 locations per test plot Up to 15 soil samples per test plot Up to 15 groundwater samples per test plot
8.	Relative and accurate VOC concentrations and lithology in the vicinity of each identified test plot	MIP, CPT, HRP DPT discrete soil and groundwater sampling	MIP, CPT at up to 4 locations per test plot HRP at up to 3 locations per test plot Up to 15 soil samples per test plot Up to 15 groundwater samples per test plot
9.	Lithology and hydraulic characteristics in the vicinity of each identified test plot	CPT, HRP	CPT at up to 4 locations per test plot HRP at up to 3 locations per test plot

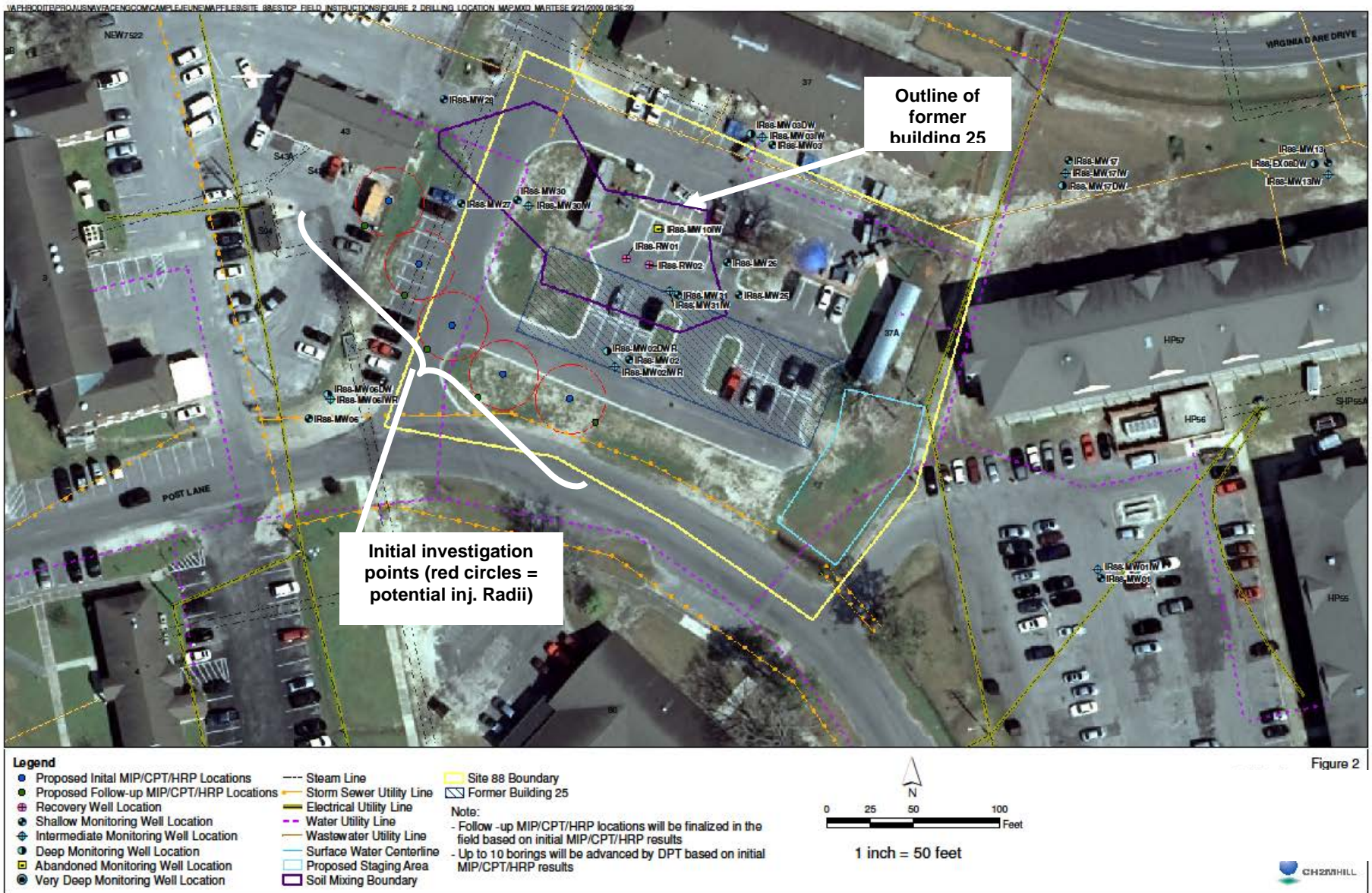


**Figure 7.** Initial investigation points for identifying demonstration test plots

## 4.0 Laboratory Tests and Analyses

A series of laboratory tests will be conducted to better understand pre-treatment site conditions for use as a benchmark for comparison of post-demonstration impacts on groundwater and soil quality. The data will also support system design efforts. A design tool, Conceptual Design for ISCO or CDISCO, will be used to develop the conceptual design for the demonstration. The tool allows the user to vary site and design characteristics, including oxidant concentration, oxidant demand (rate and extent), oxidant delivery rate, etc. and to assess the resulting radius of influence (ROI) of the oxidant delivered. Thus, data collected will serve as model input. Another modeling tool, UTCHEM, will be employed to simulate polymer delivery (sweep in 3D) related to Objective 1, improving permanganate sweep efficiency, and to estimate permanganate sweep efficiency.

### 4.1 Characterization of Site Soil and Groundwater

Table 6 presents a summary of sampling and analyses that will be performed using the samples collected as part of Data Objectives 7 and 8 shown in Tables 4 and 5. These activities are focused on characterization of site soil and groundwater – establishing baseline physical and chemical characteristics of the site. Additionally, the natural oxidant demand (NOD) results will be used to guide oxidant concentration selection for the demonstration by serving as data input for CDISCO.

### 4.2 Laboratory Tests in Support of Objective 1

The primary objectives for the treatability study geared toward improving the sweep efficiency of permanganate using the polymer xanthan gum with potassium permanganate ( $\text{KMnO}_4$ ) are to:

1. Determine an optimal solution formulation for demonstrating polymer-enhanced delivery and sweep-efficiency improvement at our selected test site
2. Collect rheological and transport related data needed to support numerical simulations for implementation design
3. Test our proposed polymer/oxidant mixing strategy at the bench-scale prior to scaling up for the field work

An optimal solution will provide (1) the optimized permanganate concentration based on CDISCO design tool output (effective oxidant distribution, defined for demonstration purposes as a 15' oxidant ROI and persistence of at least 100 mg/L of permanganate for 1 day), while providing (2) a range of viscosities appropriate for demonstrating heterogeneity control given our site conditions (as determined from sensitivity simulations to be conducted), and (3) appropriate rheological stability over our injection time frame (i.e., approximately 5 – 7 days). Much progress has already been made toward identifying optimal Xanthan and permanganate concentrations with respect to rheological stability during the conduct of the nearly completed SERDP Project 1486. However, additional fluid characterization is needed to provide specific data necessary to properly simulate ISCO implementation using the UTCHEM simulator.

**Table 6. Sampling and Analysis Summary Table**

Sample Task	Approx Sample No.	Sampling Equipment	Required Analysis	Analytical Method	Holding Time	Sample Preservation	Containers
<i>Groundwater Sampling</i>							
DPT Sampling with Waterloo Profiler™	15	Waterloo Profiler™	DO, Temperature, pH, Specific Conductance, Turbidity, ORP	Field Direct-Read Meter	N/A	N/A	N/A
DPT Sampling with Waterloo Profiler™	15	Waterloo Profiler™	TCL VOCs	EPA 8260B and 5030	7 Days	Cool to 4°C	(3) 40-ml Vial
DPT Sampling with Waterloo Profiler™	15	Waterloo Profiler™	pH, ORP	APHA 4500, 2580	3 Days	Cool to 4°C	(3) 40-ml Vial
DPT Sampling with Waterloo Profiler™	15	Waterloo Profiler™	Total solids, suspended solids	APHA 2540B, 2540C	ASAP (7 days max)	Cool to 4°C	(3) 40-ml Vial
DPT Sampling with Waterloo Profiler™	15	Waterloo Profiler™	Major cations/metals (Ca, Fe, Mn, Na, K, etc.)	APHA 3125	30 Days	Cool to 4°C	(3) 40-ml Vial
DPT Sampling with Waterloo Profiler™	15	Waterloo Profiler™	Major anions (SO <sub>4</sub> <sup>2-</sup> , PO <sub>4</sub> <sup>3-</sup> , NO <sub>3</sub> <sup>-</sup> , Cl <sup>-</sup> )	APHA 4110	2 Days	Cool to 4°C	(3) 40-ml Vial
DPT Sampling with Waterloo Profiler™	15	Waterloo Profiler™	Total organic carbon	APHA 5310B	15 Days	Cool to 4°C	(3) 40-ml Vial
<i>Soil Sampling</i>							
DPT Soil Sampling	15	Acetate Sleeve, SS Spoon, SS Bowl, (3) Encore Samplers	TCL VOCs	EPA 8260B and 5035	48 hours	Cool to 4°C	(3) Encore Samplers (1) 40-oz jar for moisture content
DPT Soil Sampling	15	Acetate Sleeve, SS Spoon, SS Bowl	Natural Oxidant Demand (NOD)	Siegrist et al., 2009	30 Days	Cool to 4°C	(3) 40-oz jar, minimum headspace
DPT Soil Sampling	15	Acetate Sleeve, SS Spoon, SS Bowl	TOC, Grain Size, Bulk Density, Porosity	EPA 9060	30 Days	Cool to 4°C	(3) 40-oz jar, minimum headspace
DPT Soil Sampling	15	Acetate Sleeve, SS Spoon, SS Bowl	pH, ORP	EPA 9045D	3 Days	Cool to 4°C	(3) 40-oz jar, minimum
DPT Soil Sampling	15	Acetate Sleeve, SS Spoon, SS Bowl	Cation exchange capacity	Sparks et al., 1996	10 Days	Cool to 4°C	(3) 40-oz jar, minimum
DPT Soil Sampling	15	Acetate Sleeve, SS Spoon, SS Bowl	Microbial density, diversity, activity	Kieft and Phelps (1997); Phelps et al. (1994a, 1994b) Weaver et al. (1994)	3 Days	Cool to 4°C	(3) 40-oz jar, minimum
DPT Soil Sampling	15	Acetate Sleeve, SS Spoon, SS Bowl	Mn speciation	Chao, 1972	30 Days	Cool to 4°C	(3) 40-oz jar, minimum

Additionally, the rheological stability of these Xanthan/permanganate solutions will be further tested under conditions of flow through porous media via one-dimensional column experiments. The significance of these column studies is to ensure viscosity-shear rate relationships obtained from rheometer measurements are properly correlated to conditions of dynamic porous media flow. Table 7 summarizes the test method objectives, criteria for success, and approach for the laboratory tests for both Objective 1 and Objective 2. Objective 1 tests are described in further detail below, while Objective 2 tests are described in further detail in Section 4.3.

#### **4.2.1 Task 1: Characterize Bulk Solution Rheology**

A stock solution of Xanthan gum (2 g/L) will be prepared according to the manufacturers recommendations in site source water. Samples of this stock solution will be diluted and added to solutions of potassium permanganate in 40 mL VOA vials to create a test matrix that will span a 500 mg/L to 10,000 mg/L permanganate concentration range and a 250 mg/L to 1,000 mg/L range of Xanthan gum concentrations. Permanganate solutions without polymer addition and Xanthan solutions without permanganate addition will serve as controls.

Once the test solutions are prepared, the viscosity of these solutions will be measured as a function of shear rate using an AR Instruments G-2 rheometer. This rheometer will allow for the characterization of solution viscosities over 4-5 decade change in applied shear rate, enabling model fits to the data needed for UTCHEM simulation. Solution viscosities for all test batches will be similarly measured as a function of time (over a 5 day time period) to monitor the rate of reduction in viscosities that result from the slow oxidation of Xanthan gum. The results of these measurements will allow the selection of an optimal Xanthan and permanganate solution for use during field implementation and implementation design simulation.

#### **4.2.2 Task 2: Characterize Xanthan Oxidant Demand**

For the same solutions described above, the oxidant demand for Xanthan gum will be measured as a function of the reduction in permanganate concentration. Permanganate concentrations will be measured using a spectrophotometric method. These measurements will be made initially after mixing and as a function of time (i.e., at several time points during the first 24h, once per day for several days after initiation, and at approximately weeklong intervals thereafter). A small subsample will be taken from each vial and diluted in DI water to achieve a concentration of permanganate acceptable for spectrophotometry (i.e., < 50 mg/L). After syringe filtration at 0.45um, a Hach DR/4000U Spectrophotometer will be used to measure the absorbance of these diluted samples at 418 and 525 nm. A 10,000 mg/L potassium permanganate solution containing no Xanthan gum will be used as a control. The purpose of these measurements is to obtain data needed to properly design oxidant dosage concentrations in the presence of Xanthan to maintain a target concentration during subsurface injection. NOD measurements described in Section 4.1 will be corrected using these data and results will serve as input to the CDISCO design tool used to estimate the oxidant radius of influence, which is a function of system oxidant demand.



**Table 7. Summary of Laboratory Test Objectives and Criteria**

#	Data Objective	Criteria for Success	Approach	Use of Data and Notes
<i>Demonstration Objective: Improve permanganate delivery sweep efficiency through heterogeneous zones using a soluble polymer</i>				
1.	Characterize bulk solution rheology to provide model input data (UTCHEM simulation)	Viscosity measured over time for range of polymer / oxidant concentration solutions	<ul style="list-style-type: none"> <li>Mix range of solutions of permanganate and Xanthan                             <ul style="list-style-type: none"> <li>Vary permanganate 500 mg/L to 10,000 mg/L</li> <li>Vary Xanthan 250 mg/L to 1,000 mg/L</li> </ul> </li> <li>Measure viscosity vs. shear rate using AR Instruments G-2 Rheometer</li> </ul>	<ul style="list-style-type: none"> <li>As model (simulator) input used for selection of optimum oxidant / polymer solution for use during field implementation</li> <li>Evaluate viscosity modification due to Xanthan oxidation</li> <li>NOTE: This is a measurement that should be typical of an oxidant / polymer delivery scheme when polymer is used for viscosity modification</li> </ul>
2.	Characterize xanthan oxidant demand to provide conceptual design model input (CDISCO)	Oxidant demand measured over time for range of polymer / oxidant concentration solutions	<ul style="list-style-type: none"> <li>Using same samples generated for Objective 1 above, measure permanganate concentration over time and calculate oxidant demand and reaction kinetics</li> </ul>	<ul style="list-style-type: none"> <li>As design tool (Conceptual Design for ISCO or CDISCO tool) input variable – to used to estimate ROI as a function of oxidant delivery concentration and reaction kinetics</li> <li>NOTE: This is a measurement that would only need to be conducted for an oxidant / polymer delivery scheme when polymer is used for viscosity modification when a polymer OTHER THAN xanthan may be employed (note: these data will carry over to field application in general and will be incorporated into guidance accordingly)</li> </ul>
3.	Characterize polymer / oxidant transport conditions in porous media with respect to polymer injectivity, permeability reduction due to polymer entrapment, and rheological behavior	Pressure drop measured across columns packed with field material having oxidant / polymer delivered at optimized concentrations at varied delivery rates	<ul style="list-style-type: none"> <li>Pack 1-D columns with field porous media and saturate with site source water</li> <li>Measure pressure drop across column</li> <li>Introduce oxidant/polymer solution under constant flow rate</li> <li>Evaluate for constant injectivity</li> <li>Calculate shear rate</li> <li>Increase flow rate and note impact on shear rate</li> <li>Flush column with water</li> <li>Measure pressure drop across column</li> <li>Determine permeability loss (permeability reduction factor)</li> </ul>	<ul style="list-style-type: none"> <li>As model (simulator) input used for simulating polymer delivery</li> <li>To describe permeability reduction due to irreversible polymer entrapment and the potential presence of entrapped MnO<sub>2</sub></li> <li>NOTE: If constant injectivity cannot be achieved in the column or injectivity is reduced by more than a factor of 10 compared to no polymer injection, the experiment will stop and a go/no-go decision to proceed with the demonstration will be made</li> <li>NOTE: These measurements will help determine if this approach must always be conducted for an oxidant / polymer delivery scheme when polymer is used for viscosity modification OR if a model can be developed from these data for future applications under alternative sites and site conditions</li> </ul>
4.	Optimize mixing strategy for field application	Maximum concentration of xanthan that can be used as concentrated feed determined	<ul style="list-style-type: none"> <li>Vary concentration of xanthan concentrate solution entering simulated mixing strategy model (physical model)</li> <li>Rheology of solution exiting in-line static mixers characterized (see objective #1)</li> <li>Resulting viscosity-shear rate profiles compared to those for a truly homogeneous xanthan solution</li> <li>Determine max xanthan concentration that has homogeneous solution-like character</li> <li>Repeat with permanganate addition</li> </ul>	<ul style="list-style-type: none"> <li>Provide data to engineer field xanthan delivery system</li> <li>NOTE: These measurements will provide data for any demonstration using oxidant / polymer for viscosity modification (i.e., these measurements would not have to be repeated for other field applications unless a polymer other than xanthan is employed)</li> </ul>

**Table 7. Summary of Laboratory Test Objectives and Criteria**

#	Data Objective	Criteria for Success	Approach	Use of Data and Notes
<i>Demonstration Objective: Improve permanganate delivery by controlling MnO<sub>2</sub> deposition with soluble polymer</i>				
1.	Identify optimum oxidant / HMP mixture concentrations	MnO <sub>2</sub> behavior and Mn speciation characterized for range of oxidant and polymer concentration solutions	<ul style="list-style-type: none"> <li>Repeat NOD measurements (see Table 6) with range of SHMP concentrations (max polymer = solubility concentration; ranges of 0.5 and 0.1 of each of these values will be evaluated) and with optimized permanganate concentration (based on NOD measurements and CDISCO design tool results)</li> <li>Measure MnO<sub>2</sub> in solution spectrophotometrically at 418 nm with and without 0.2 μm filtration (suspended vs. dissolved)</li> <li>Measure permanganate concentration spectrophotometrically at 525 nm</li> <li>Estimate MnO<sub>2</sub> associated with solids via mass balance (Mn as permanganate initial – Mn as MnO<sub>2</sub> suspended – Mn as MnO<sub>2</sub> dissolved – Mn as MnO<sub>4</sub><sup>-</sup> unreacted)</li> <li>Determine ideal solution mixture where MnO<sub>2</sub> dissolved is maximized and MnO<sub>2</sub> associated with solids is minimized</li> </ul>	<ul style="list-style-type: none"> <li>To determine minimum SHMP concentration that offers maximum MnO<sub>2</sub> dissolved concentrations</li> <li>NOTE: This is a measurement that should be typical of an oxidant / polymer delivery scheme when polymer is used to inhibit MnO<sub>2</sub> deposition (i.e., results are site-specific)</li> </ul>
2.	Characterize MnO <sub>2</sub> transport in porous media	MnO <sub>2</sub> behavior and Mn speciation characterized for optimum permanganate and SHMP concentrations in columns packed with field porous media	<ul style="list-style-type: none"> <li>Pack two 1-D columns with field porous media</li> <li>Spike column with PCE</li> <li>Deliver polymer / oxidant solution to one column and oxidant only to the other column</li> <li>Measure MnO<sub>2</sub> dissolved and suspended in effluent</li> <li>Stop polymer / oxidant solution delivery</li> <li>Delivery 1 PV of DI water (or ideally site gw)</li> <li>Extract MnO<sub>2</sub> associated with the solids</li> <li>Measure soil and gw characteristics shown in Table 6 in column materials</li> <li>Assess differences between oxidant only and polymer + oxidant columns</li> </ul>	<ul style="list-style-type: none"> <li>Data used to anticipate field results and guide field monitoring plan</li> <li>NOTE: If there are no measurable differences in MnO<sub>2</sub> content associated with solids, the field demonstration will be NO-GO. This is not anticipated based on review of existing site data and understanding of the oxidant-polymer system.</li> <li>NOTE: These measurements would be considered optional for a polymer / oxidant delivery scheme where polymer is used to inhibit MnO<sub>2</sub> deposition; results are applicable to developing monitoring plans, but typical budgets may not support such efforts.</li> </ul>



### **4.2.3 Task 3: Characterize Polymer/Oxidant Transport Conditions in Porous Media**

One-dimensional column experiments will be performed to determine transport characteristics for the optimal Xanthan gum/permanganate solution selected for this demonstration. These experiments will be performed using porous media collected from the selected test site and will provide data important for assisting implementation design. Specifically, these experiments will be designed to:

1. Characterize polymer/oxidant solution injectivity,
2. Quantify permeability reduction as a result of polymer entrapment and/or manganese dioxide particle deposition during delivery, and
3. Characterize the non-Newtonian rheological behavior of this polymer-amended solution during flow in porous media.

Each of these test variables will be measured during a single column experiment. Multiple column experiments will be performed if our upcoming site characterization activities (described in Section 3.0) discover subsurface strata possessing permeabilities that vary by an order of magnitude within the treatment zone. The specific methodology (described below) that will be employed in this task was developed and successfully implemented as a part SERDP Project ER-1486, to characterize the transport of Xanthan gum solutions in the absence of permanganate. A schematic of the experimental apparatus is presented as Figure 8.

Samples of aquifer material will be collected and shipped to the Colorado School of Mines. These samples will be air-dried at room temperature and homogenized. The test column (dimensions, length = 30 cm, inner diameter = 4.5 cm) will be dry-packed with aquifer material and saturated with site source water. Once saturated, a constant flow rate will be applied to the column inlet. Pressure transducers will be installed at the inlet, outlet, and at two positions along the length of the column. The pressure drop across each column segment will be recorded and used to determine initial media permeability via the application of Darcy's Law. Our goal during the column packing process is to closely match the permeabilities measured in the field during our site characterization activities. Once the initial permeability has been determined the experiment will proceed as described in the following sections.

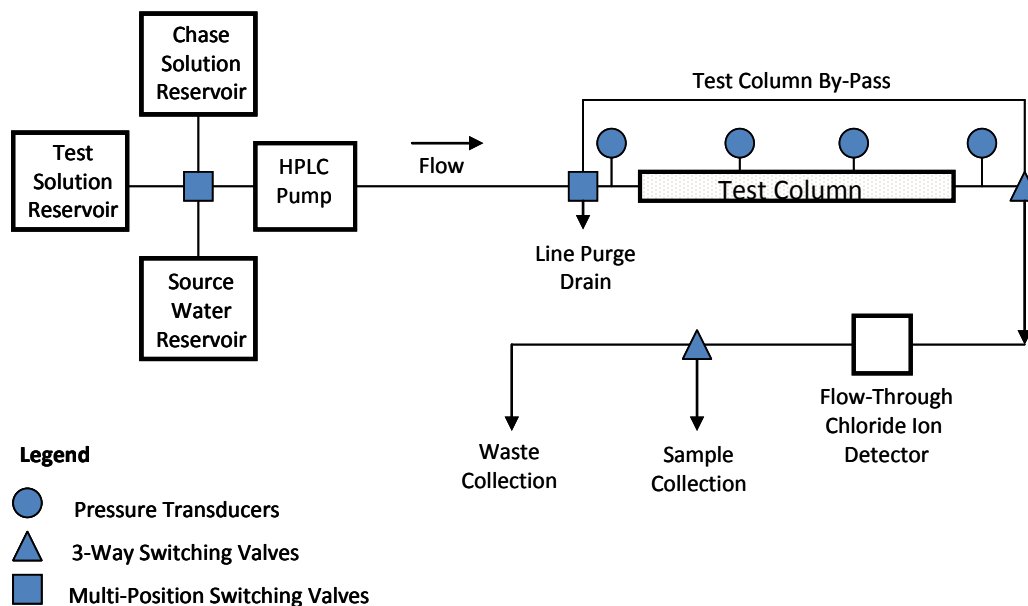


**Figure 8.** Schematic diagram of 1-D column test apparatus

#### 4.2.3.1 Polymer/Oxidant Test Solution Injectivity

These column experiments will begin by first evaluating Xanthan/permanaganate solution injectivity. Injectivity is defined here as the ratio of the volumetric flow rate ( $Q$ ) to the observed pressure drop ( $\Delta P$ ). For the Xanthan/permanaganate solution employed in this demonstration, fluid injectivity can be reduced as a result of polymer entrapment and the potential reduced permeability resulting from entrapped manganese dioxide particles that form during the oxidation of Xanthan, the target contaminant (i.e., chlorinated ethenes) and the oxidant demand of the site porous media. A reduction in permeability results in a reduction in injectivity and requires an increase in injection pressures to maintain a constant volumetric injection flow rate.

Injectivity will be evaluated by introducing the xanthan/permanaganate solution to the test column at a constant flow rate and monitoring the pressure response at each measurement point shown in Figure 8. The results of hydraulic conductivity profiling performed during the proposed site characterization task (described in Section 3.0) within the proposed demonstration area will dictate actual flow rates used in these experiments, with the goal of matching flow velocities for the column test with that anticipated during injection at the field-scale. Based on the available hydraulic properties characterization of the Castle Hayne Aquifer, an assumed injection flow rate of 0.5 gallons/minute, and a 10-foot screened interval, an average linear velocity ( $v = Q/(An)$ , where  $n$  = porosity) is calculated as 0.55 cm/min (26.3 ft/day). Equating this velocity to the column-scale results in a volumetric flow rate of 3.1 cm<sup>3</sup>/min.

Solution introduction and pressure monitoring will continue until the pressures at each monitoring location stabilize and a steady-state flow condition can be assumed. At this steady-state condition, injectivity should be constant at every point along the column length. If a steady-

state flow condition is not achieved and/or the xanthan/permanganate solution injectivity at any point in the column is reduced by more than a factor of 10 from the measured water injectivity, the experiment will stop and a go/no-go decision as to proceed with this demonstration will be made.

#### 4.2.3.2 Characterize Polymer/Oxidant Solution Rheological Properties in Porous Media

The Xanthan/permanganate solution will then be introduced at a low flow rate to one end of the column until the effluent concentration of Xanthan and permanganate equals that of the influent. Actual flow rates used will depend on the permeability of the site soil. At this flow condition, the porous media equivalent shear rate ( $\gamma_{eq}$ ) will be calculated using the following modified Blake-Kozeny capillary bundle equation:

$$\gamma_{eq} = \frac{3.97Cu}{\sqrt{k\Phi}} \quad [1]$$

where C is the shear rate coefficient used to account for non-ideal effects such as slip at the pore walls, u is the water phase frontal velocity (i.e., the average linear velocity of the advecting polymer front), k is the media permeability, and  $\Phi$  is the media porosity. For this same flow condition, the apparent viscosity ( $\mu_{app}$ ) of the solution at this equivalent shear rate will be determined from the measured pressure drops ( $\Delta P$ ), the known intrinsic permeability, and the application of Darcy's law as:

$$\mu_{app} = \frac{k\rho g L}{q \Delta P} \quad [2]$$

where,  $\rho$  and g is the fluid density and gravity constant, q is the Darcy velocity, and L is the column length.

Once  $\gamma_{eq}$  and  $\mu_{app}$  have been determined at this initial flow condition, the applied flow rate will be stepwise increased to obtain measures of apparent viscosity as a function of porous media equivalent shear rate. These data will be compared to the viscosity-shear rate data obtained from the rheometer. Observed deviations from the rheometer dataset will be corrected by adjusting the shear rate coefficient, C, in equation 1. The value of C and the corrected viscosity-shear rate relation will be used at input for the UTCHEM simulator.

#### 4.2.3.3 Characterize Polymer/Oxidant Permeability Reduction

At the completion of the injectivity and rheology tests, the column will be flushed with site source water to remove the Xanthan/permanganate solution from the column porosity. Once the solution is removed and pressures stabilize, the post-flood pressure drops will be used to determine the permeability reduction factor as the ratio of the intrinsic permeability (pre-polymer) to the effective permeability (post-polymer). The permeability reduction factor is needed to simulate polymer delivery and will describe permeability reduction due to irreversible polymer entrapment and the potential presence of entrapped manganese dioxide particles resulting from the oxidation of Xanthan and the oxidant demand of the site soil.

#### 4.2.4 Task 4: Optimize Xanthan/KMnO<sub>4</sub> Mixing Strategy for Field Application

The current strategy for mixing Xanthan and permanganate on-site involves the preparation of a Xanthan gum solution concentrate. A chemical metering pump will then be used to provide the appropriate volume of Xanthan concentrate to a potable water source line to achieve a target diluted Xanthan concentration. This Xanthan mixture will then be homogenized using an array of in-line static mixers. The Xanthan solution will then be introduced to a separate permanganate solution feed line. The two solutions will pass through an additional series of in-line static mixers to achieve a homogeneous Xanthan/permanganate fluid concentration for subsurface injection.

Implementing this strategy requires a given Xanthan concentration for the concentrate in order to size temporary storage tanks and to select an appropriate metering pump. However, the selection of a Xanthan concentration for the concentrate also requires testing to determine what Xanthan concentration the metered concentrate will produce a homogeneous mixture for subsurface injection given our current mixing strategy. Polymers like Xanthan gum do not readily dilute from a concentrate to form homogeneous mixtures like salts. Additional mixing energy is required. The lower the concentration of the concentrate, the less mixing energy required. Therefore, the objective of this subtask is to determine the maximum Xanthan concentrate formulation that will provide a homogeneous mixture of permanganate and Xanthan gum upon mixing.

A scaled-down model of the current mixing strategy will be constructed to achieve this objective. Static mixers most appropriate for homogenizing viscous fluids will be researched, purchased, and tested in the CSM laboratory. A schematic of the test apparatus appears as Figure 9 below.



**Figure 9.** Schematic of test apparatus for optimizing Xanthan/Permanganate mixing strategy

The principal experimental variable in this mixing study will be the concentration of the Xanthan gum concentrate. Flow velocities will be selected to mimic those anticipated during field implementation. Metering pump flows will be set to provide optimal Xanthan and permanganate concentrations as determined from the earlier phases of this treatability study.

Testing will be initiated without the addition of permanganate. The solution exiting the in-line static mixers will be sampled and the solution rheology characterized as described in Section 4.2.1. The resulting viscosity-shear rate profiles will be compared to those for a truly homogeneous Xanthan solution prepared using the methods described in Section 4.2.1. Once a maximum Xanthan concentrate concentration is identified, the same fluid sampling and characterization procedure will be followed for the addition of permanganate.

### **4.3 Treatability Study Plans for Objective 2**

The primary objective for the treatability study geared toward controlling  $\text{MnO}_2$  to improve oxidant delivery and flow, thereby enhancing contaminant destruction, using the polymer SHMP with potassium permanganate ( $\text{KMnO}_4$ ) is to determine an optimal solution of polymer and oxidant for site-specific conditions. Standard methods of analysis (as listed in Section 5.1) will be employed as appropriate.

#### **4.3.1 Task 1: Identify Optimum Oxidant / Polymer Mixture Concentrations**

Using site media from each distinct lithology, batch tests will be conducted to evaluate the impact of varied concentrations of SHMP and permanganate concentrations on  $\text{MnO}_2$  production. Specifically, the amount of suspended  $\text{MnO}_2$  ( $\text{MnO}_{2\text{-sus}}$ ), dissolved  $\text{MnO}_2$  ( $\text{MnO}_{2\text{-diss}}$ ) (filterable at  $0.2\ \mu\text{m}$ ), and settled  $\text{MnO}_2$  ( $\text{MnO}_{2\text{-sett}}$ ) (or  $\text{MnO}_2$  associated with soils) will be determined. Reaction vials (40-mL) will be prepared with site soil and groundwater in a 1:1 (v/v) soil:solution ratio. Oxidant and SHMP will be added spanning ranges between zero and solubility level concentrations of each. The permanganate / no polymer systems will serve as controls. The ideal solution will result in maximum concentrations of  $\text{MnO}_{2\text{-diss}}$  and minimum  $\text{MnO}_{2\text{-sett}}$ . If there are no measurable differences in  $\text{MnO}_2$  content associated with solids, the field demonstration will be NO-GO. This is not anticipated based on review of existing site data and understanding of the oxidant-polymer system.

#### **4.3.2 Task 2: Characterize $\text{MnO}_2$ Transport in Porous Media**

A test column will then be prepared, similar to that described in Section 4.2.3, to evaluate the performance of the optimized solution in a 1-D transport system. The solution will be delivered at a rate deemed appropriate for delivery in the field as per field site characterization results. An identical permanganate-only control column will be prepared alongside.  $\text{MnO}_{2\text{-sus}}$ ,  $\text{MnO}_{2\text{-diss}}$ , and  $\text{MnO}_{2\text{-sett}}$  will be characterized and compared.

Toward fulfilling the secondary project objective of comparing post-delivery/treatment groundwater quality for “permanganate only” and “permanganate + polymer” test areas, soil and groundwater characterizations will also be performed on these columns and those described in

Section 4.2 above post-treatment . These results will aid in anticipating the field-scale effects and guide field-scale monitoring activities during and following the demonstration.

## 5.0 Summary and Schedule

The data collected during previous investigations and remedial activities at Site 88 in MCB Camp Lejeune provide a clear picture of the site conditions on a large scale. The field characterization activities and laboratory tests and analyses described herein will provide data needed on a small scale to achieve the stated demonstration objectives so that the performance of the technology can be properly evaluated. The results of the field and laboratory activities, in addition to the existing data, will be used to develop the Demonstration Plan (system design). This will ensure that the performance criteria can be successfully evaluated when the technology is applied at the site. Table 8 provides the schedule for key activities.

**Table 8: Treatability Study Schedule**

<b>Task</b>	<b>Dates</b>
Field Characterization Activities	Nov 09
Laboratory Tests and Analyses	Nov 09 - Jan 10
Treatability Study Report	Jan 10
Demonstration Implementation Plan	Feb 10
Demonstration Implementation and Monitoring	April 10 - June 10

## 6.0 References

- APHA-AWWA-WPCF, (1998). Standard Methods for Examination of Water and Wastewater, 20th ed., Clesceri, L.S., A.E. Greenberg, and R.R. Trussell, eds. APHA-AWWA-WPCF, Washington, DC.
- ASTM (1991). Standard Practice for Sampling Waste and Soils for Volatile Organics. D4547-91. In: 1992 Annual Book of ASTM Standards, Vol. 11.04, pp. 108-111.
- Baker Environmental, Inc. (Baker). 1998. *Final Focused Remedial Investigation Report, Operable Unit No. 15 (Site 88), Marine Corps Base, Camp Lejeune, North Carolina*. May.
- Battelle Memorial Institute (BMI). 2001. *Reductive Anaerobic Biological In Situ Treatment Technology (RABITT) Treatability Test, Interim Report*. August.
- Carter, M.R. (1993). *Soil Sampling and Methods of Analysis*. Lewis Publishers, Ann Arbor, MI.
- CH2M Hill (2008). *Final Remedial Investigation Report, Site 88, Operable Unit No. 15, Marine Corps Base Camp Lejeune, Jacksonville, North Carolina*.
- CH2M HILL. 2002. *Draft Supplemental Site Investigation Report, Operable Unit 15 (Site 88), Building 25 Base Dry Cleaners*. September.
- CH2M HILL. 2003. *Supplemental Site Investigation Report, Operable Unit 15 (Site 88), Building 25 Base Dry Cleaners*. December.
- CH2M HILL. 2004a. *Membrane Interface Probe Investigation*.

- CH2M HILL. 2004b. *Site 88 Building 25 Source Removal Engineering Evaluation/Cost Analysis*. September.
- CH2M HILL. 2006. *Draft Site 88 Building 25 Source Removal Non-Time Critical Removal Action Report*. March.
- CH2M HILL. 2008a. *Final Remedial Investigation Site 88, Operable Unit No. 15, Building 25*. March.
- CH2M HILL. 2008b. *Draft Feasibility Study, Site 88, Operable Unit No. 15*. February.
- Chandranth, M.S. and G.L. Amy (1996). Effects of Ozone on the Colloidal Stability and Aggregation of Particles Coated with Natural Organic Matter. *Environmental Science and Technology*, 30(2):431-442.
- Chao, T.T. (1972). Selective Dissolution of Manganese Oxides from Soils and Sediments with Acidified Hydroxylamine Hydrochloride. *Soil Sci. Soc. Am. Proc.* Oct 29-Nov 3, Miami Beach, FL.
- DE&S – Duke Engineering & Services (1999). *DNAPL Site Characterization Using a Partitioning Interwell Tracer Test at Site 88, Marine Corps Base Camp Lejeune, North Carolina (Final Report)*.
- Doona C.J. and F.W. Schneider (1993). Identification of Colloidal Mn(IV) in Permanganate Oscillating Reactions. *J. Am. Chem. Soc.*, 115:9683-9686.
- Duke Engineering and Services (Duke). 1999. *DNAPL Site Characterization using a Partitioning Interwell Tracer Test at Site 88, Marine Corps Base, Camp Lejeune, North Carolina*. July.
- Duke. 2000. *Surfactant-Enhanced Aquifer Remediation Demonstration at Site 88, Marine Corps Base, Camp Lejeune, North Carolina*. January.
- Insausti, M.J., F. Mata-Perez, and P. Alvarez-Macho (1992). Permanganate Oxidation of Glycine: Influence of Amino Acid on Colloidal Manganese Dioxide. *International Journal of Chemical Kinetics*, 24(5):411-419.
- Insausti, M.J., F. Mata-Perez, and P. Alvarez-Macho (1993). UV-VIS Spectrophotometric Study and Dynamic Analysis of the Colloidal Product of Permanganate Oxidation of  $\alpha$ -Amino Acids. *React. Kinet. Catal. Lett.*, 51(1):51-59.
- Kieft, T.L. and T.J. Phelps (1997). *Life in the Slow Lane: Activities of Microorganisms in the Subsurface*. CRC Press, Inc. pp. 135-161.
- Klute, A. et al., (ed.) (1986). *Methods of Soil Analysis, Part 1. Physical and Mineralogical Methods*. Soil Sci. Soc. Am. Madison, WI.
- Lee E.S., Y.Seol, Y.C. Fang, and F.W. Schwartz (2003). Destruction Efficiencies and Dynamics of Reaction Fronts Associated with Permanganate Oxidation of Trichloroethylene. *Environmental Science and Technology*, 37(11):2540-2546.
- Li X.D. and F.W. Schwartz (2000). Efficiency problems related to permanganate oxidation schemes. In: G.B. Wickramanayake, A.R. Gavaskar, A.S.C. Chen (ed.). *Chemical Oxidation and Reactive Barriers: Remediation of Chlorinated and Recalcitrant Compounds*. Battelle Press. Columbus, OH. pp. 41-48.
- Lowe, K.S., F.G. Gardner, R.L. Siegrist, and T.C. Houk (2000). EPA/625/R-99/012. US EPA Office of Research and Development, Washington, D.C.
- Morgan, J.J. and W. Stumm (1964). Colloid-Chemical Properties of Manganese Dioxide. *Journal of Colloid Science*, 19:347-359.
- OHM Remediation Services Corporation (OHM). 1996. *Contractor's Closeout Report, Underground Storage Tank Removals at Building 25, MCB Camp Lejeune, North Carolina*. October.

- Perez-Benito, J.F. and C. Arias (1991). A Kinetic Study of the Permanganate Oxidation of Triethylamine. Catalysis by Soluble Colloids. *International Journal of Chemical Kinetics*, 23:717-732.
- Perez-Benito, J.F. and C. Arias (1992a). A Kinetic Study of the Reaction Between Soluble (Colloidal) Manganese Dioxide and Formic Acid. *Journal of Colloid and Interface Science*, 149(1):92-97.
- Perez-Benito, J.F. and C. Arias (1992b). Occurrence of Colloidal Manganese Dioxide in Permanganate Reactions. *Journal of Colloid and Interface Science*, 152(1):70-84.
- Perez-Benito, J.F., C. Arias, and E. Brillas (1990). A Kinetic Study of the Autocatalytic Permanganate Oxidation of Formic Acid. *International Journal of Chemical Kinetics*, 22:261-287.
- Perez-Benito, J.F., E. Brillas, and R. Pouplana (1989). Identification of a Soluble Form of Colloidal Manganese (IV). *Inorganic Chemistry*, 28:390-392.
- Phelps T.J., S.M. Pfiffner, K.A. Sargent, and D.C. White (1994b). Factors Influencing the Abundance and Metabolic Capacities of Microorganisms in Eastern Coastal Plain Sediments. *Microb. Ecol.* 28:351-364.
- Phelps T.J., E. Murphy, S.M. Pfiffner, and D.C. Whiate (1994a). Comparison Between Geochemical and Biological Estimates of Subsurface Microbial Activities. *Microbial Ecology*, 28:335-349.
- Reitsma S. and M. Marshall (2000). In: G.B. Wickramanayake, A.R. Gavaskar, A.S.C. Chen (ed.). *Chemical Oxidation and Reactive Barriers: Remediation of Chlorinated Compounds*. Battelle Press. Columbus, OH. p. 25-32.
- Sparks D.L., A.L. Page, P.A. Helmke, R.H. Loeppert, P.N. Soltanpour, M.A. Tabatabai, C.T. Johnson, and M.E. Sumner (ed.) (1996). *Methods of Soil Analysis: Part 3 – Chemical Methods*. Soil Sci. Soc. Am. Madison, WI.
- Tan, K.H. (1996). *Soil Sampling, Preparation, and Analysis*. Marcel Dekker, Inc. New York. 407 pp.
- USEPA (1986). *Test Methods for the Evaluation of Soil Waste, Physical/Chemical Methods*. SW-846, 3<sup>rd</sup> ed. Off. Solid Waste and Emergency Response, Washington DC.
- USEPA (1990). *Second update to SW-846 Methods Section*. Office of Solid Waste. U.S. Environmental Protection Agency, Washington DC.
- Weaver R.W., S. Angle, P. Bottomley, D. Bezdicek, S. Smith, A. Tabatabai, and A. Wollum (ed) (1994). *Methods of Soil Analysis: Part 2 – Microbiological and Biochemical Properties*. Soil Sci. Soc. Am., Madison, WI.
- West, O.R., R.L. Siegrist, S.R. Cline, and F.G. Gardner (2000). The effects of in situ chemical oxidation through recirculation (ISCOR) on aquifer contamination, hydrogeology, and geochemistry. Oak Ridge National Laboratory internal report submitted to the Department of Energy, Office of Environmental Management, Subsurface Contaminants Focus Area.
- West, O.R., S.R. Cline, W.L. Holden, F.G. Gardner, B.M. Schlosser, J.E. Thate, D.A. Pickering, T.C. Houk (1998). ORNL/TM-13556, Oak Ridge National Laboratory, Oak Ridge, Tennessee.



## **Appendix E: Treatability Study Report**

# **Treatability Study Report**

---

**ER-0912 Cooperative Technology Demonstration: Polymer-  
Enhanced Subsurface Delivery and Distribution of  
Permanganate**

**January 2010**

# Contents

List of Tables	ii
List of Figures	ii
Acronyms	iii
<b>1.0 Introduction</b>	<b>1</b>
<b>1.2 Demonstration Objectives</b>	<b>1</b>
<b>1.2 Site Description</b>	<b>1</b>
<b>1.3 Conceptual Site Model (CSM) for Demonstration Area</b>	<b>1</b>
1.3.1 Physical Characteristics	2
1.3.2 Nature and Extent of Contamination	5
<b>2.0 Technology Description (Preliminary Conceptual Design)</b>	<b>9</b>
<b>3.0 Field Characterization Activities</b>	<b>12</b>
<b>3.1 Objectives and Approach</b>	<b>12</b>
<b>3.2 Results</b>	<b>19</b>
<b>4.0 Laboratory Tests and Analyses</b>	<b>20</b>
<b>4.2 Objectives</b>	<b>20</b>
<b>4.3 Approach and Methods</b>	<b>20</b>
4.2.1 Characterization of Site Soil and Groundwater	20
4.2.2 Objective 1: Improved Sweep Efficiency	20
4.2.2.1 Bulk Solution Rheology	21
4.2.2.2 Xanthan Oxidant Demand	21
4.2.2.3 Polymer/Oxidant Transport Conditions in Porous Media	25
4.2.2.4 Polymer/Oxidant Mixing Strategy	26
4.2.3 Objective 2: Manganese Dioxide Control	28
4.2.3.1 Optimum Oxidant/SHMP Mixture	28
4.2.3.2 Manganese Dioxide Transport	28
<b>4.3 Results</b>	<b>30</b>
4.3.1 Media Characterization	30
4.3.2 Objective 1: Improved Sweep Efficiency	32
4.3.2.1 Bulk Solution Rheology	32
4.3.2.2 Xanthan Oxidant Demand	38
4.3.2.3 Polymer/Oxidant Transport Conditions in Porous Media	40
4.3.2.4 Polymer/Oxidant Mixing Strategy	45
4.3.3 Objective 2: Manganese Dioxide Control	45
4.3.3.1 Optimum Oxidant/SHMP Mixture	45
4.3.3.2 Manganese Dioxide Transport	45
<b>5.0 Summary</b>	<b>47</b>
<b>6.0 References</b>	<b>47</b>
<b>Appendix A – Site Characterization Summary</b>	
<b>Appendix B – HRP Results</b>	
<b>Appendix C – Boring Log for DPT01</b>	
<b>Appendix D – Grain Size Analysis for Surficial Aquifer Media</b>	

## List of Tables

<b>Table 1.</b>	<b>Previous Demonstrations Conducted at Site 88</b>
<b>Table 2.</b>	<b>Camp Lejeune Demonstration Site Selection Criteria</b>
<b>Table 3.</b>	<b>Demonstration Performance Objectives</b>
<b>Table 4.</b>	<b>Summary of Field Data Collection Objectives and Criteria</b>
<b>Table 5.</b>	<b>Summary of Site Characterization Objectives, Data Needs, and Samples</b>
<b>Table 6.</b>	<b>Sampling and Analysis Summary Table</b>
<b>Table 7.</b>	<b>Summary of Laboratory Test Objectives and Criteria</b>
<b>Table 8.</b>	<b>Porous Media Characteristics</b>
<b>Table 9.</b>	<b>Groundwater Characteristics</b>
<b>Table 10.</b>	<b>NOD Test Results Summary</b>
<b>Table 11.</b>	<b>Results of Meter's Equation fits to Viscosity-Shear Rate Profiles</b>
<b>Table 12.</b>	<b>Results of Oxidant Demand for Xanthan Gum (no porous media)</b>
<b>Table A-1.</b>	<b>Hydraulic Conductivity Calculated at Each Slug Test Location</b>
<b>Table A-2.</b>	<b>Analytical Results for Contaminants (GC-MS) in Soils</b>
<b>Table A-3.</b>	<b>Analytical Results for Contaminants (GC-MS) in Groundwater</b>

## List of Figures

<b>Figure 1.</b>	Site 88 Conceptual Site Model
<b>Figure 2.</b>	Cross-section location map
<b>Figure 3.</b>	Cross-section A-A'
<b>Figure 4.</b>	Cross-section C-C'
<b>Figure 5.</b>	Two test plots, one treatment (oxidant + polymer) and one control (oxidant only)
<b>Figure 6.</b>	Schematic of field implementation plan
<b>Figure 7.</b>	Initial investigation points for identifying demonstration test plots
<b>Figure 8.</b>	Schematic diagram of 1-D column test apparatus
<b>Figure 9.</b>	Schematic of test apparatus for optimizing xanthan/permanganate mixing strategy
<b>Figure 10.</b>	1-D packed columns for evaluation of permanganate and SHMP transport through site porous media
<b>Figure 11.</b>	1-D packed columns during permanganate delivery
<b>Figure 12.</b>	Viscosity-shear rate function for a 1000 mg/L xanthan gum solution containing varying concentrations of $\text{KMnO}_4$
<b>Figure 13.</b>	Viscosity-shear rate function for a 500 mg/L xanthan gum solution containing varying concentrations of $\text{KMnO}_4$
<b>Figure 14.</b>	Viscosity-shear rate function for a 250 mg/L xanthan gum solution containing varying concentrations of $\text{KMnO}_4$
<b>Figure 15.</b>	Viscosity-shear rate functions showing viscosity loss due to oxidation of xanthan gum (1000 mg/L polymer case)
<b>Figure 16.</b>	Viscosity-shear rate functions showing viscosity loss due to oxidation of xanthan gum (500 mg/L polymer case)
<b>Figure 17.</b>	Viscosity-shear rate functions showing viscosity loss due to oxidation of xanthan gum (250 mg/L polymer case)
<b>Figure 18.</b>	$\text{KMnO}_4$ demand as a function of time when exposed to 250, 500, and 1000 mg/L xanthan gum

- Figure 19.** Pressure and hydraulic conductivity results measured during oxidant-only injection
- Figure 20.** Measured hydraulic conductivities before, during, and after oxidant injection
- Figure 21.** Pressure and hydraulic conductivity results for the polymer/oxidant injection (no filtration)
- Figure 22.** Measured hydraulic conductivities before and after polymer/oxidant injection (no filtration)
- Figure 23.** Pressure and hydraulic conductivity results for the polymer/oxidant injection (with filtration)
- Figure 24.** Pressure and hydraulic conductivity results for the polymer/oxidant injection (with filtration)
- Figure 25.** Rheometer and porous media equivalent viscosity/shear rate functions (1000 mg/L xanthan gum, 5000 mg/L KMnO<sub>4</sub> solution)
- Figure 26.** Absorbance of samples at 418 nm over time
- Figure 27.** Tracer evaluation for transport columns
- Figure 28.** Column effluent absorbance at 418 nm – indicator of dissolved or suspended MnO<sub>2</sub> concentration passing through column
- 
- Figure A-1.** Test area at MCB CamLej, North Carolina, OU 15, Site 88
- Figure A-2.** Closer view of test area located within and immediately west of the footprint of the former Building 25
- Figure A-3.** Test area conceptual site model
- Figure A-4.** General geologic setting in vicinity of test area
- Figure A-5.** Geologic cross-section within the test area based on most recent characterization activities
- Figure A-6.** Potentiometric map of the Surficial Aquifer
- Figure A-7.** Potentiometric map of the Upper Castle Hayne Aquifer
- Figure A-8.** PCE concentrations in the Surficial Aquifer (2007)
- Figure A-9.** PCE concentrations in the Upper Castle Hayne Aquifer (2007)

## Acronyms

<b>APHA</b>	American Public Health Association
<b>AST</b>	Aboveground storage tank
<b>bgs</b>	Below ground surface
<b>CDISCO</b>	Conceptual design for ISCO (modeling tool)
<b>COC</b>	Contaminant of Concern
<b>CPT</b>	Cone penetrometer test
<b>CVOC</b>	Chlorinated volatile organic compound
<b>CSM</b>	Conceptual site model
<b>c-DCE</b>	cis-dichloroethylene
<b>DNAPL</b>	Dense nonaqueous phase liquid
<b>DO</b>	Dissolved Oxygen
<b>DPT</b>	Direct push technology
<b>EC</b>	Electrical conductivity
<b>ECD</b>	Electrical conductivity detector
<b>EPA</b>	Environmental Protection Agency
<b>HMP</b>	Hexametaphosphate (used interchangeably with SHMP)
<b>HRP</b>	High-resolution piezocone
<b>ISCO</b>	In situ chemical oxidation
<b>k</b>	Hydraulic conductivity
<b>KMnO<sub>4</sub></b>	Potassium permanganate
<b>LPM</b>	Low permeability media
<b>MCB</b>	Marine Corps base
<b>MIP</b>	Membrane interface probe
<b>MLS</b>	Multi-level sampling
<b>Mn</b>	Manganese
<b>MnO<sub>2</sub></b>	Manganese dioxide
<b>MnO<sub>4</sub><sup>-</sup></b>	Permanganate anion
<b>mV</b>	Millivolts
<b>MW</b>	Monitoring Well
<b>NAPL</b>	Nonaqueous phase liquid
<b>NOD</b>	Natural oxidant demand
<b>ORP</b>	Oxidation/Reduction potential
<b>OU</b>	Operable unit
<b>PCE</b>	Tetrachloroethylene (perchloroethylene)
<b>pH</b>	Negative base-10 logarithm of hydronium ion activity
<b>SERDP</b>	Strategic Environmental Research and Development Program
<b>SHMP</b>	Sodium hexametaphosphate
<b>SS</b>	Suspended solids
<b>TCE</b>	Trichloroethylene
<b>TOC</b>	Total organic carbon
<b>TCE</b>	Trichloroethylene
<b>TTI</b>	Target treatment interval
<b>UST</b>	Underground storage tank
<b>VC</b>	Vinyl chloride
<b>VOC</b>	Volatile organic chemical
<b>ZVI</b>	Zero valent iron

## **1.0 Introduction**

### **1.1 Demonstration Objectives**

ISCO using permanganate is an established remediation technology being applied at hazardous waste sites throughout the United States and abroad. Field applications of ISCO continue to grow and have demonstrated that ISCO can achieve destruction of contaminants and achieve clean-up goals. However, some field-scale applications have had uncertain or poor in situ treatment performance. Poor performance is often attributed to poor uniformity of oxidant delivery caused by zones of low permeability media (LPM) and site heterogeneity and excessive oxidant consumption by natural subsurface materials. A second permanganate ISCO challenge is the management of manganese dioxide ( $MnO_2$ ) particles, which are a byproduct of the reaction of permanganate with organic contaminants and naturally-reduced subsurface materials. These particles have the potential to deposit in the well and subsurface and impact flow in and around the well screen, filter pack, and the surrounding subsurface formation. This is a particular challenge for sites with excessive oxidant consumption due to the presence of natural materials or large masses of non-aqueous phase liquids (NAPLs). This project focuses on (1) diminishing the detrimental effects of site heterogeneities with respect to the uniformity of oxidant delivery using the polymer xanthan gum, and (2) managing  $MnO_2$  aggregation and deposition using the polymer sodium hexametaphosphate (SHMP), hereafter referred to as “Objective 1” and “Objective 2”, respectively. A secondary project objective is to compare post-delivery/treatment groundwater quality for “permanganate only” and “permanganate + polymer” test areas.

### **1.2 Site Description**

The site for the technology demonstration is Site 88 at Marine Corps Base, Camp Lejeune, Jacksonville, North Carolina. MCB Camp Lejeune presently covers approximately 236 square miles and is a training base for the United States Marine Corps. Operable Unit (OU) No. 15, Site 88 consists of the former Base Dry Cleaning facility (former Building 25) and the surrounding paved and grassy areas, located on Post Lane Road, approximately 500 feet east of the intersection of Post Lane Road and McHugh Boulevard. Building 25 was used as a dry cleaning facility from the 1940s until 2004 when operations ceased and the building was demolished. In the 1940s, Varsol™ was stored in underground storage tanks (USTs) located on the north side of the building, and was replaced by PCE in the 1970s. The PCE was stored in an aboveground storage tank (AST). PCE was reportedly stored in the AST from the 1970s until the mid-1980s. Facility employees have reported that spent PCE was disposed of in floor drains that discharged to the sanitary sewer. In March 1995, two self-contained dry cleaning machines were installed in Building 25, eliminating the need for bulk storage of PCE.

### **1.3 Conceptual Site Model (CSM) for Demonstration Area**

The information in this section is based on the data collected and reported in the Site RI by CH2M Hill (available upon request). The Conceptual Site Model (CSM) for Site 88 is shown in Figure 1. Previous investigations have been conducted at Site 88 and are summarized in Table 1. This demonstration will be performed in the area surrounding MW02, within the footprint of Former Building 25. It will be located outside of (at least 20 feet) the source zone at the site that

was previously treated (February, 2005) using in situ soil mixing of clay and zero valent iron. Significant tetrachloroethene (PCE) concentrations remain in groundwater outside of the soil mixed zone, as indicated in Table 2, which summarizes the basic site characteristics relative to the objectives of this demonstration. Recent data from the site confirm there is no biogeochemical signature remaining from previous demonstrations in the area of interest for this demonstration (e.g., pH, ORP, dissolved Fe).

### **1.3.1 Physical Characteristics**

Site 88 is underlain by a thick sequence of coastal plain soils consisting of unconsolidated sands, silts, clays, and partially indurated shelly sands. The hydrogeologic setting is that of a two aquifer system, the Surficial aquifer and the Castle Hayne aquifer, with the two aquifers occasionally separated by the discontinuous clayey silt and clay layer. Where this layer is absent, the Surficial and Castle Hayne aquifers are in direct hydraulic communication.

Soils within the Surficial aquifer are generally comprised of silty sands, ranging in thickness from 20 to 30 feet, which overlie a discontinuous layer of clayey silt or clay. A clayey silt and clay confining layer, ranging in thickness from 4 to 10 feet, underlies the former location of Building 25 and extends westward as far as Building 3, whereupon it pinches out and appears again further westward. Within the Castle Hayne aquifer, a fine grained layer overlies massive beds of fine to medium grained sand with sporadic zones of partial cementation and shell fragments extending to a depth of roughly 180 feet bgs. At Site 88, the Castle Hayne aquifer is divided into the upper Castle Hayne (25-80 feet), the middle Castle Hayne (80-130 feet), and the lower Castle Hayne (130-180 feet). A plastic clay layer, known as the Beaufort confining unit, is beneath the Castle Hayne aquifer; the Beaufort confining unit defines the vertical limit of subsurface investigation at Site 88.

At present, we plan to demonstrate polymer-improved permanganate sweep efficiency (i.e., Objective 1) within the upper Castle Hayne Aquifer unit. Based on previous site characterization efforts within Site 88 (DE&S, 1999; CH2M Hill, 2008) the thickness of the overlying silt/clay layer varies between 6 and 10 feet within this target polymer demonstration area, suggesting it would be a competent confining unit. Aquifer testing activities have estimated the geometric mean hydraulic conductivity values for the Surficial, upper Castle Hayne, and lower Castle Hayne aquifers to be 4.1 ft/day, 11.1 ft/day, and 11.5 ft/day, respectively. Corresponding mean seepage velocities for these same aquifers were estimated to be 0.18 ft/day and 0.17 ft/day, respectively. These values are appropriate for our demonstration purposes (Table 2) and equate to permeabilities ranging between 2 and 7 darcy, which is within the range investigated for SERDP Project ER-1486 (foundation for Objective 1) and ER-1484 (foundation for Objective 2).

We plan to demonstrate Objective 2 in the Surficial aquifer. For this objective, the physical properties are less critical than the contaminant mass density characteristics described below. To evaluate success related to Objective 1, highly refined data were recently collected (November 2009) to characterize hydraulic conductivity / permeability within the test area as described in Section 3.0 below.





**Table 1. Previous Demonstrations Conducted at Site 88**

Investigation Phase	Date	Reference	Conclusions
UST and AST Removal	1995	OHM, 1996	Removal of five USTs and one AST. CVOCs and inorganics were detected in subsurface soil samples. CVOCs, TPH, and naphthalene were detected in groundwater.
Focused Remedial Investigation	1996/1997	Baker, 1998	Installation of temporary and permanent wells at varying depth. CVOC contamination identified in subsurface soil beneath and near Building 25 and along the underground industrial sewer line. CVOC impacts were detected in the surficial aquifer and the upper portion of the Castle Hayne aquifer.
DNAPL Characterization using Partitioning Interwell Tracer Tests	1997	Duke, 1999	DNAPL was found beneath Building 25. Approximately 105 gallons of DNAPL were removed.
Reductive Anaerobic In Situ Treatment Technology (RABITT) Testing	2001	BMI, 2001	The RABITT testing concluded that native microbial populations were capable of sequentially reducing PCE to ethene. PCE and TCE concentrations were reduced in the study area.
Supplemental Site Investigation	2002/2003	CH2M HILL 2002, 2003	Installation of 26 monitoring wells at four different depths within the surficial and Castle Hayne aquifers, video inspection of sewer system, soil sampling, aquifer testing, and groundwater sampling. CVOCs were determined to be migrating generally to the northwest. In addition, the vertical distribution of VOCs indicates appreciable volumes of DNAPL have accumulated upon the shallow silt layer. However, this layer was not impermeable; appeared to be allowing dissolved-phase VOCs to migrate vertically.
Membrane Interface Probe (MIP) Investigation	2004	CH2M HILL, 2004a	Used to refine previous source area characterization by evaluating the horizontal and vertical distribution of the DNAPL source area.
Final Engineering Evaluation/Cost Analysis	2004	CH2M HILL, 2004b	The EE/CA recommended shallow soil mixing with clay and zero-valent iron (ZVI) addition for source treatment.
Shallow Soil Mixing with Clay-ZVI	2005	CH2M HILL, 2006	Full-scale implementation of shallow soil mixing with clay-ZVI addition was initiated. The mixture was delivered via a 10-foot diameter auger to a depth of 20 feet bgs over an area of 9,500 square feet (ft <sup>2</sup> ). Approximately 7,050 cubic yards (yd <sup>3</sup> ) of impacted soil was treated. After stabilization, the treatment area was paved and converted into a parking lot. Within the treatment area PCE concentrations in the soil were reduced by greater than 99 percent.
Remedial Investigation	2003-2007	CH2M HILL, 2008a	RI field activities included: DPT groundwater sampling; MIP groundwater profiling; installation of 66 monitoring wells; installation of three multi-screen monitoring wells; sampling of site monitoring wells; and aquifer testing. PCE concentrations in excess of 7,500 µg/L (5 percent of the solubility of PCE), as reported for several Site 88 wells, may indicate the presence of remaining DNAPL PCE.
Draft Feasibility Study	2008	CH2M HILL, 2008b	Groundwater contamination was broken down into three distinct zones (refer to the CSM) for evaluating remedial alternatives.
IR88-MW39MP Re-sample	2008		IR88-MW39MP was re-sampled to evaluate whether the PCE distribution with depth observed in 2007 may have been related to well installation. The data indicate decreasing concentrations with depth.

**Table 2. Camp Lejeune Demonstration Site Selection Criteria**

Parameter	Preferred Value(s)	Relative Importance*	MCB Camp Lejeune
Site Name	-	-	Site 88
Chloroethene concentration	Measured in groundwater above 5 mg/L range	2	~10 mg/L PCE
Depth to groundwater	~10 ft bgs	3	10
Total depth of treatment zone	30 ft bgs	3	60
Utility access	Electrical and water	2	Yes
Bulk hydraulic conductivity	k > 10 ft/day	1	0.4 – 30 ft/day (median 11 ft/day)
Heterogeneous	Measurable or visible difference within several feet of depth	1	Sand with silt and shell fragments and thin discontinuous layers of silt, clay, and peat
Site Project Status	Feasibility Study	1	Feasibility Study
Impediments	Minimal	2	Some – large area, can execute work around to minimize impacts to active facility
US Navy-Owned Site with nearby CH2M HILL office	Yes	3	Yes

Notes:

\*1-5; with 1 being highest

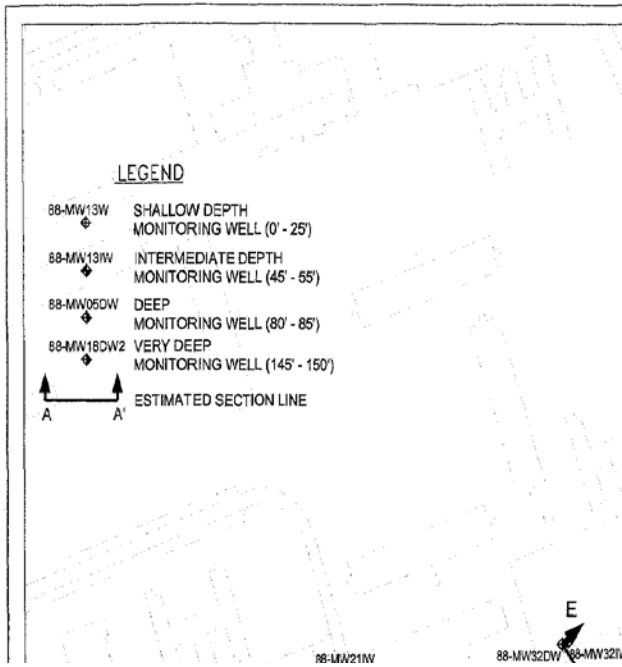
ft bgs – feet below ground surface

ft/day – feet per day hydraulic conductivity

MCB – Marine Corps Base Camp Lejeune, NC

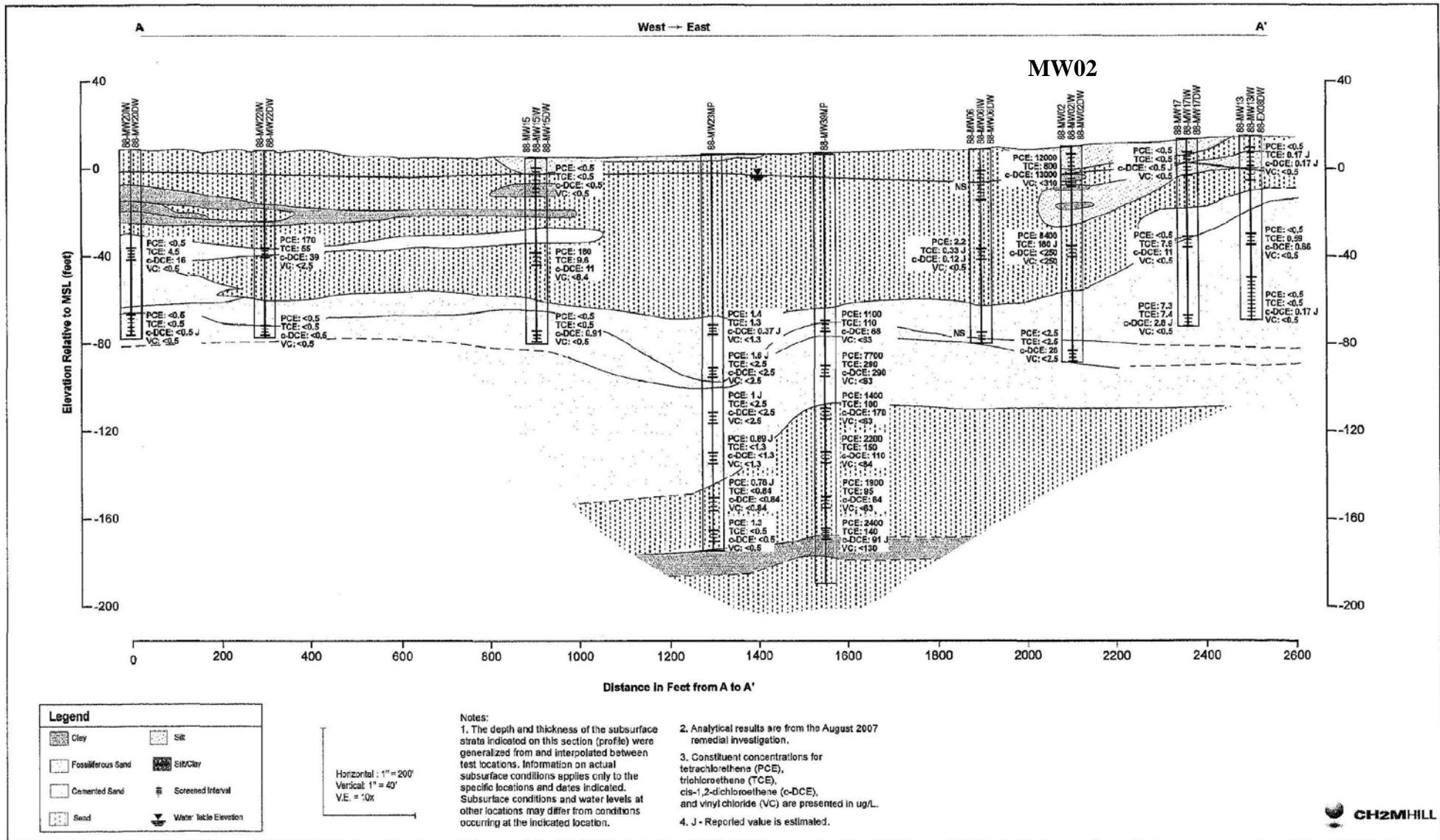
**1.3.2 Nature and Extent of Contamination**

The nature and extent of groundwater contamination at Site 88 was derived from the most recent (August 2007 and October 2008) monitoring data. The primary COCs, the compounds detected at the highest concentrations and with the most frequency, for Site 88 include PCE, TCE, cis-1,2-DCE, and VC. Figure 2 shows cross-sections established for the site. This demonstration is planned near the junction of cross section A-A' (horizontal) and C-C' (vertical) (Near MW02). Figure 3 shows the contaminant profile with depth for the A-A' cross section. Figure 4 shows the contaminant profile with depth for the C-C' cross section. The MW02 location is highlighted in these figures. These data show PCE concentrations of 12,000 µg/L, TCE 800 µg/L, c-DCE 13,000 µg/L, and VC < 310 µg/L in the Surficial aquifer where Objective 2 will be demonstrated. The contaminant profile is less relevant to Objective 1, which relies more heavily on physical characteristics as described above. While some data are described here for the general vicinity of the planned demonstration, detailed contaminant mass information is critical to evaluating success related to Objective 2. These data were recently collected (November 2009) as part of the field characterization activities described below (Section 3.0) and analyzed as part of the laboratory testing activities described below (Section 4.0).



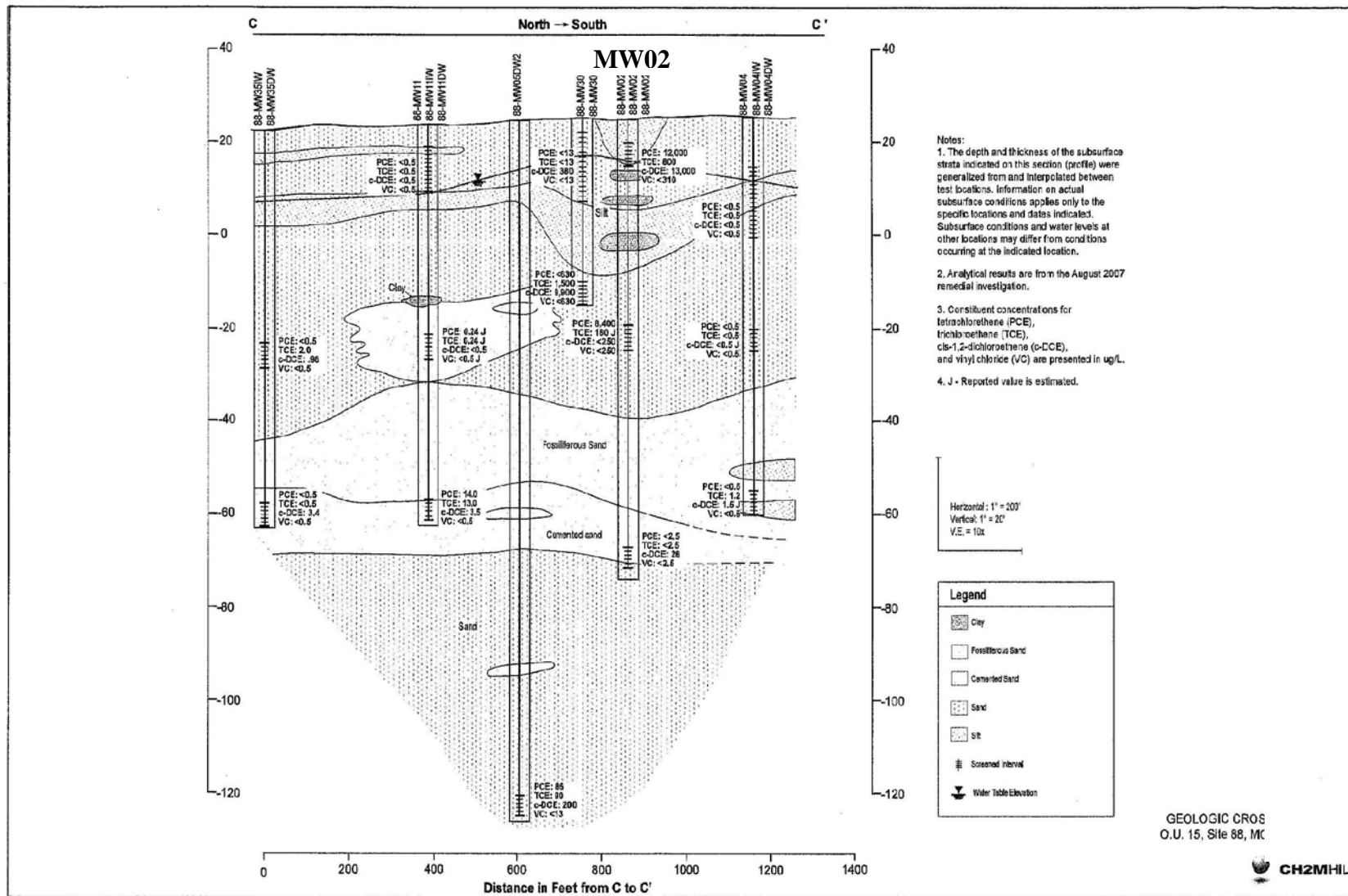
MW02

**Figure 2.** Cross-section location map



ES012008004MKE Site\_88\_Figure\_3-4\_v2.mxd 03.07.08.xls

**Figure 3. Cross-section A-A'**



EGC1200904MNE Site\_88\_Figurs\_3-4\_v2.m 20.07.08 els

Figure 4. Cross-section C-C'

## 2.0 Technology Description (Preliminary Conceptual Design)

To reiterate, the overall objectives for this demonstration (i.e., polymer application) are: Objective 1 - diminishing the detrimental effects of site heterogeneities with respect to the uniformity of oxidant delivery using the polymer Xanthan gum, and Objective 2 - managing MnO<sub>2</sub> aggregation and deposition using the polymer sodium hexametaphosphate (SHMP). Detailed demonstration performance criteria, data required, and success criteria related to these objectives are presented in Table 3.

**Table 3. Demonstration Performance Objectives**

<b>Performance Criteria</b>	<b>Data Requirements</b>	<b>Success Criteria (with use of polymer)</b>
<b>Quantitative Performance Objectives</b>		
Evaluate occurrence of contaminant rebound post-treatment	<ul style="list-style-type: none"> <li>Contaminant concentrations in groundwater over time and distance</li> </ul>	<ul style="list-style-type: none"> <li>Data collected and are representative of test plots</li> </ul>
Improved contaminant treatment effectiveness	<ul style="list-style-type: none"> <li>Contaminant concentrations in groundwater over time and distance</li> <li>Contaminant mass in soil over time and distance</li> </ul>	<ul style="list-style-type: none"> <li>Statistically significant difference (lower) in contaminant mass</li> </ul>
Increased penetration of oxidant into lower permeability layers/strata	<ul style="list-style-type: none"> <li>Examination of soil cores for evidence of permanganate (purple color, or byproduct brown) in lower permeability layers/strata</li> <li>If LPM of thickness appropriate for discrete groundwater sampling is present, then MnO<sub>4</sub><sup>-</sup> concentrations measured in groundwater over space and time</li> <li>Electrical monitoring probe (ORP and EC) network measurements over space and time</li> </ul>	<ul style="list-style-type: none"> <li>50% longer distance of permanganate penetration/ movement into lower permeability layers/strata</li> <li>25% higher permanganate concentration at expected time of arrival in each monitoring well</li> <li>Demonstrated improvement in vertical sweep efficiency of permanganate within lower permeability layers/strata</li> <li>Demonstrated improvement in overall vertical sweep efficiency of permanganate within the test plot(s)</li> <li>50% greater conductivity and ORP in target media</li> </ul>
Decreased flow bypassing of areas of high contaminant mass	<ul style="list-style-type: none"> <li>Examination of soil cores for evidence of MnO<sub>2</sub> (dark brown) in media with high contaminant saturation</li> <li>Soil core extractions for MnO<sub>2</sub> and spectrophotometric measurements for MnO<sub>2</sub> in groundwater over space and time</li> <li>Soil core extractions for contaminant</li> </ul>	<ul style="list-style-type: none"> <li>50% lower mass of MnO<sub>2</sub> in given mass of media</li> <li>25% greater mobile MnO<sub>2</sub> concentration at given time point in monitoring well</li> <li>50% lower mass of contaminant in high saturation cores</li> </ul>
<b>Qualitative Performance Objectives</b>		
Decreased impact of MnO <sub>2</sub> deposition on injection pressure	<ul style="list-style-type: none"> <li>Field subsurface and injection pressure</li> </ul>	<ul style="list-style-type: none"> <li>No increase in injection pressure attributable to MnO<sub>2</sub> (compared to pressures expected via simulation)</li> </ul>
Improved understanding of impacts of the enhanced delivery approach on groundwater quality	<ul style="list-style-type: none"> <li>pH, ORP, key metals, solids concentrations, conductivity, bioactivity</li> </ul>	<ul style="list-style-type: none"> <li>Note differences</li> </ul>

The two separate overall objectives will be pursued in two separate regions of both a treatment and control plot (Figure 5); a shallow zone (within the Surficial aquifer) and intermediate zone (upper Castle Hayne). The intermediate zone of the site has characteristics suitable for demonstration related to Objective 1, as described above (i.e., hydraulic conductivity, heterogeneity). This is designated as Plot 1. The primary criterion of importance for Objective 2 is a high contaminant mass density/concentration. The shallow zone of the demonstration area meets this criterion with reported PCE concentrations of ~7-10 mg/L (Table 2). More detailed contaminant profile information were collected as part of this treatability evaluation and are described further in Sections 3.0 and 4.0 below.

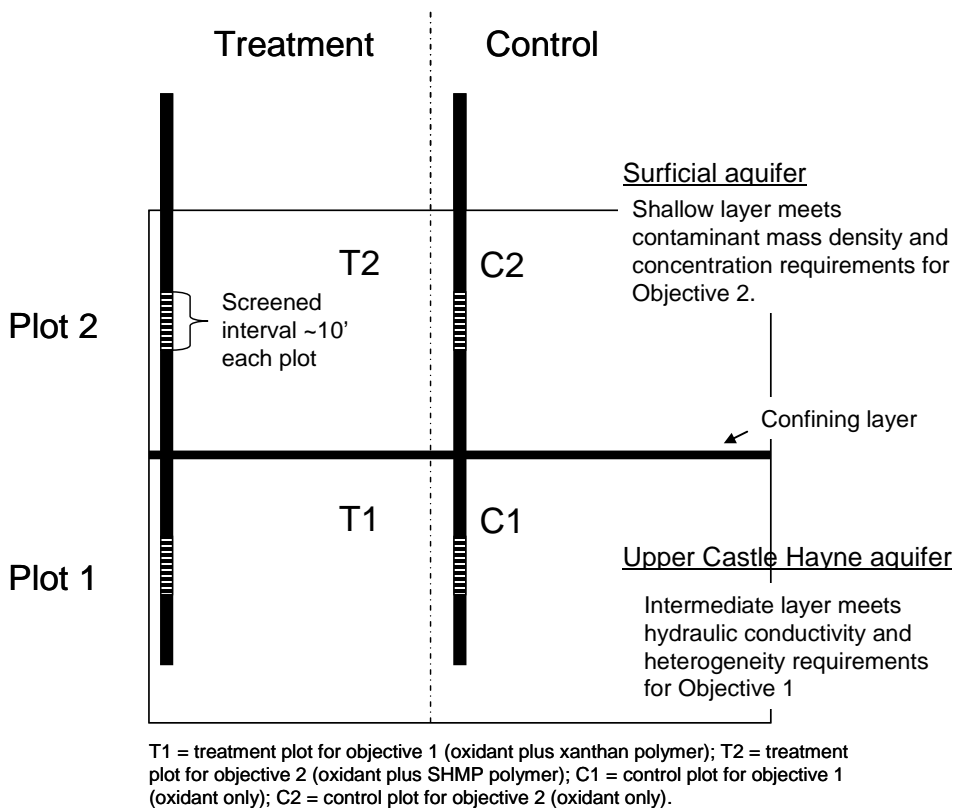


**Figure 5.** Two test plots, one treatment (oxidant + polymer) and one control (oxidant only). The intermediate depth zone (upper Castle Hayne) is suitable for meeting Objective 1, improving sweep efficiency using xanthan polymer. The shallow depth zone (Surficial aquifer) is suitable for meeting Objective 2 controlling MnO<sub>2</sub> particles.

The pilot-scale test plots are planned to be approximately 30-feet in diameter (includes a buffer zone around an expected 15-foot radius of influence) (Figure 6). Four multi-level sampling (MLS) wells will be installed at various distances from the injection well and screened at three depth intervals to monitor the water quality of the targeted zones of high and low permeability. The MLS well screen lengths will range from 6-inches to 5-feet, depending upon the thickness of the target lithology (fine- and coarse-grained) and the thickness of the bentonite seal needed to



properly isolate the sample interval from the overburden and/or underlying aquifer zones. The design of the MLS wells will be based upon the results of the cone penetrometer testing (CPT) investigation and numerical simulation performed during site characterization activities (see Section 3.0 below). The depth and locations of each MLS point will be carefully selected to properly monitor and validate the absence and/or presence of oxidant, polymers, and oxidation by-products within specific heterogeneous strata in order to validate the sweep efficiency of these strata throughout the target treatment zone. Prior to system startup, all new wells will be developed and sampled and direct-push technology (DPT) used to collect discrete groundwater samples from the treatment zone.

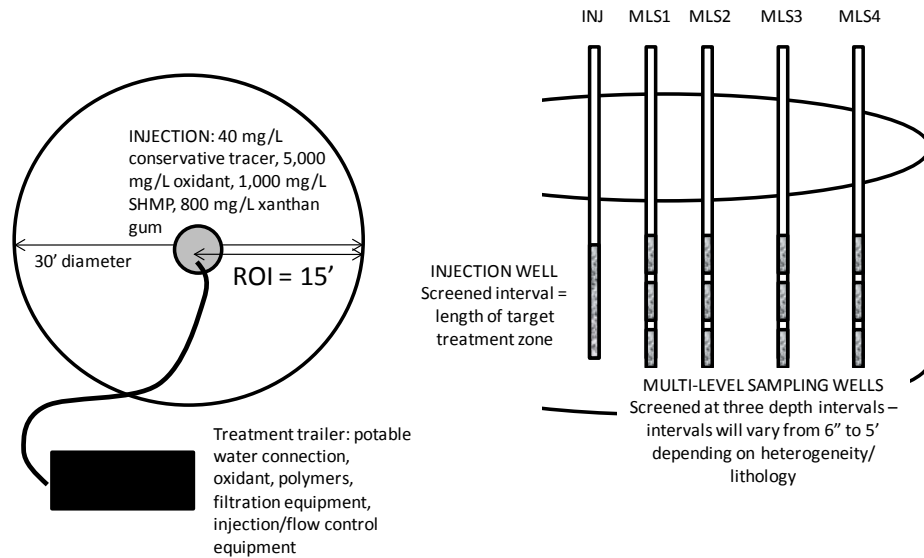


**Figure 6.** Schematic of field implementation plan. The left-hand side shows the plan view and the right hand side shows the plan in profile.

A small treatment trailer will be constructed and used to sequentially implement the test protocol at each of the two pilot test plots. The trailer will contain the potable water connection (from nearby fire hydrant), permanganate, polymers, and conservative tracer dosing, filtration, and injection/flow control equipment. It will be sized to process a maximum of approximately 30 gallons per minute of 5,000 ppm potassium permanganate, 8,000 ppm of xanthan gum (depending on site permeability conditions), and 2,000 ppm of SHMP and will contain instrumentation and controls to allow for automatic operation and shutdown in case of high tank or injection well pressure. Model simulations will be employed to develop a design basis for oxidant and polymer injection within each test plot using input values measured during site characterization and lab testing. Permanganate injection into the pilot test plots will be operated for the time necessary to achieve oxidant breakthrough at the desired 15-foot radius of influence. During the injection program, water levels and injection pressure will be measured to monitor the physical effectiveness of the delivery system. In addition, MLS wells will be sampled to measure system performance and document oxidant delivery effectiveness. Samples will be collected and analyzed in the field to collect real-time data to assess the demonstration's effectiveness and make adjustments if necessary.

After the active injection is completed, weekly MLS well monitoring will be performed for up to eight weeks to document oxidant persistence and treatment efficiency. Within a couple of weeks of cessation of injection, a DPT-conductivity survey and intact soil coring will be performed. The DPT-conductivity survey results will be used to site the intact coring locations. Five intact soil cores will be collected, visually inspected and logged in the field, and then shipped to the laboratory for quantitative analysis of polymers, permanganate, manganese dioxide, bioactivity, and VOCs. Field groundwater data collection will include permanganate concentrations, ORP, pH, temperature, and conductivity, along with real-time measurements of subsurface (i.e., water levels) and injection pressures. Groundwater samples will be collected and preserved for off-site laboratory measurement of contaminant concentrations, conservative tracer, key metals concentrations, polymer concentration, and MnO<sub>2</sub> concentration. Of interest are potential differences in long-term aquifer quality as a result of permanganate treatment both with and without polymers.

The final sampling will be conducted two months post-demonstration, or as determined by monitoring of the exhaustion of oxidant and adequate aquifer re-equilibration (i.e., field parameter stabilization). The sampling will be conducted using a sampling and analytical program that matches the baseline and 2-week post-injection events. Final sampling of each test plot will consist of intact soil coring, well groundwater sampling, and DPT-Waterloo Profiling within the treatment zone. Post-treatment slug tests will be conducted on the injection well to assess changes in hydraulic conductivity that may have been caused by the pilot test.

While significant data for the site were collected during previous investigations, additional data collection was necessary to meet the objectives of this demonstration. The refinement of hydrogeological data (i.e. hydraulic conductivity, permeability, heterogeneity) and contaminant distribution characteristics within the proposed treatment area at the scale appropriate for this pilot-scale demonstration was critical to facilitate design and monitoring plans. These data were collected through field characterization activities (described in Section 3.0 below) and laboratory tests and analyses (described in Section 4.0 below).

### **3.0 Field Characterization Activities**

#### **3.1 Objectives and Approach**

Table 4 includes field characterization data objectives, along with data needs and criteria for success. Table 5 summarizes the field methods and sample collection to fulfill the data needs. Field characterization was conducted dynamically with real-time decision-making (i.e., sampling locations were selected based on results of each prior sampling event). Figure 7 shows initial test points where membrane interface probe (MIP) for profiling contaminant mass distribution, and cone penetrometer testing (CPT) and high-resolution piezocone (HRP) for profiling the lithology/hydraulic conductivity was planned.

**Table 4. Summary of Field Data Collection Objectives and Criteria**

#	Data Objective	Criteria for Achieving Objective	Data Need
1A	Identify a 30-foot diameter location for test plot 1 (Improve permanganate delivery by controlling MnO <sub>2</sub> deposition with soluble polymer)	<ul style="list-style-type: none"><li>• 30-foot diameter open space with minimal utility interference</li><li>• High [VOC] &gt; 5 mg/L total chlorinated ethenes</li><li>• Bulk K &gt; 10 ft/day</li></ul>	Relative VOC concentrations and lithology in the shallow (0-20' bgs) depth interval and within the vicinity of the 88-MW02 well cluster
1B	Identify a 30-foot diameter location for test plot 2 (Improve permanganate delivery sweep efficiency through heterogeneous zones using a soluble polymer)	<ul style="list-style-type: none"><li>• 30-foot diameter open space with minimal utility interference</li><li>• <math>K_v/K_h</math> anisotropy ~ 100</li><li>• Visible soil heterogeneity within 10-foot depth interval</li><li>• Bulk K &gt; 10 ft/day</li></ul>	Relative VOC concentrations and lithology in the intermediate (20-60' bgs) depth interval and within the vicinity of the 88-MW02 well cluster
2	Delineate the volatile organic compound (VOC) distribution including top and bottom of the bulk of contamination (ECD > 1e5 $\mu$ V, for example) within the entire vertical profile of the two test plots at center and three radii within the test plot circle and on 6-inch vertical centers	<ul style="list-style-type: none"><li>• MIP/ECD &gt; baseline, estimated to be &gt;5e5 <math>\mu</math>V</li><li>• MIP/ECD measurements at 6-inch to 1-foot vertical spacing</li><li>• MIP/ECD probe locations at center and three radii within the 30' dia. test plot circle</li><li>• In 2D only, identify the top and bottom of contamination only. Delineation of the lateral extent is unnecessary. May require probing to depths greater than 60' bgs.</li></ul>	Relative VOC concentrations in the vicinity of each identified test plot.
3A	Characterize the entire vertical profile of the two test plots at center and three radii within the test plot circle and on 6-inch vertical centers	<ul style="list-style-type: none"><li>• CPT measurements that differentiate between the types of sand (e.g., fine, medium, silty, etc.) present</li><li>• HRP measurements as a secondary line-of-evidence to define type of lithology</li><li>• CPT probe locations at a minimum of 4 locations within each test plot (if data is useful)</li><li>• HRP probe locations at a minimum of 2 locations within each test plot (shallow and intermediate). May require more probes if the CPT tool is unable to differentiate between the soil types.</li><li>• In 2D only, monitor the top and bottom of unique lithologic layers only. Delineation of the lateral extent is unnecessary.</li></ul>	Lithology and hydraulic characteristics in the vicinity of each identified test plot
3B	Characterize the hydraulic characteristics within the entire vertical profile of the two test plots at center and three radii within the test plot circle and on 6-inch vertical centers	<ul style="list-style-type: none"><li>• HRP measurements to estimate K of each unique lithologic layer</li><li>• HRP measurements to estimate the horizontal and vertical gradients present within each unique lithologic zone</li><li>• HRP probe locations at a minimum of 3 locations within each test plot (shallow and intermediate) so that triangulation can be used to estimate lateral gradients within each unique lithologic zone.</li><li>• In 2D only, monitor the top and bottom of unique lithologic layers only.</li><li>• Delineation of the lateral extent is unnecessary.</li></ul>	Lithology and hydraulic characteristics in the vicinity of each identified test plot

**Table 4. Summary of Field Data Collection Objectives and Criteria**

#	Data Objective	Criteria for Achieving Objective	Data Need
4	Identify the possible preferential injection flow pathways within the entire vertical profile of each of the two test plots	<ul style="list-style-type: none"> <li>• Uses CPT and HRP measurements collected for above data objectives. No new data collection is necessary to meet this objective.</li> <li>• Map the MIP, CPT, and HRP data on the same chart and identify (label) the unique horizons in order of highest to lowest conductivity (K) values.</li> </ul>	Lithology and hydraulic characteristics in the vicinity of each identified test plot
5A	Identify target treatment intervals (TTIs) for the shallow depth intervals at each test plot location so that injection well screens can be properly designed	<ul style="list-style-type: none"> <li>• Uses MIP, CPT, and HRP measurements collected for above data objectives. No new data collection is necessary to meet this objective.</li> <li>• Using the collaborative data maps prepared for Objective 4, identify the zones containing [CVOC] &gt; 1e6 µV and a K &gt; 1 ft/day.</li> <li>• Quantify the relative proportion of [CVOC] mass present within each unique zone</li> <li>• The TTI is depth interval that contains [CVOC] &gt; 1e6 µV, K &gt; 1 ft/day, and 90-percent of the mass present within the entire shallow depth interval (0-20' bgs).</li> </ul>	Relative VOC concentrations and lithology in the vicinity of each identified test plot
5B	Identify target treatment intervals (TTIs) for intermediate depth intervals at each test plot location so that injection well screens can be properly designed	<ul style="list-style-type: none"> <li>• Uses MIP, CPT, and HRP measurements collected for above data objectives. No new data collection is necessary to meet this objective.</li> <li>• Using the collaborative data maps prepared for Objective 4, identify the zones containing [CVOC] &gt; 1e6 µV and a K &gt; 0.1 ft/day.</li> <li>• Quantify the <math>K_v/K_h</math> anisotropy within this depth interval</li> <li>• Quantify the relative proportion of [CVOC] mass present within each unique zone</li> <li>• The TTI is 10- to 20-foot (10-foot preferred) depth interval that contains [CVOC] &gt; 1e6 µV, <math>K_{max} &gt; 10</math> ft/day, anisotropy ~100, and 90-percent of the mass present within the entire shallow depth interval (20-60' bgs).</li> </ul>	Relative VOC concentrations and lithology in the vicinity of each identified test plot
6A	Provide detailed information for design of shallow depth test plot injection well and monitoring well network	<ul style="list-style-type: none"> <li>• Uses MIP, CPT, and HRP measurements collected for above data objectives. No new data collection is necessary to meet this objective.</li> <li>• Evaluate the uniformity of [CVOC] distribution within the TTI of each test plot (see Objective 5)</li> <li>• Injection well will be screened across the TTI</li> </ul>	Relative and accurate VOC concentrations and lithology in the vicinity of each identified test plot
6B	Provide detailed information for design of intermediate depth test plot injection well and monitoring well network	<ul style="list-style-type: none"> <li>• Uses MIP, CPT, and HRP measurements collected for above data objectives. No new data collection is necessary to meet this objective.</li> <li>• Evaluate the uniformity of lithology and [CVOC] distribution within the TTI of each test plot (see Objective 5)</li> <li>• Injection well will be screened across the TTI</li> </ul>	Relative and accurate VOC concentrations and lithology in the vicinity of each identified test plot

**Table 4. Summary of Field Data Collection Objectives and Criteria**

#	Data Objective	Criteria for Achieving Objective	Data Need
7A	Provide baseline physical and chemical characteristics from key locations within the shallow depth plots so that post-treatment samples can be co-located and evaluated for treatment performance	<p>Baseline physical and chemical characteristics will be collected to measure baseline parameters necessary to meet the following overall project performance objectives:</p> <ul style="list-style-type: none"> <li>• Eliminate the potential for contaminant rebound               <ul style="list-style-type: none"> <li>– As measured by [CVOC] in groundwater wells. After properly citing the monitoring wells (see Objective 6), baseline water samples will be collected from them using low-flow/micropurge methods and analyzed for [CVOC].</li> <li>– As measured by [CVOC] in DPT grab groundwater samples. Up to 15 DPT grab groundwater samples will be collected with geospatial uniformity across the TTI from each test plot within unique lithologic and [CVOC] zones. Samples will be collected from zones containing high, moderate, and low [CVOC] as indicated by the MIP/ECD results.</li> <li>– As measured by [CVOC] in DPT intact core soil samples. Up to 3 two-foot long intact soil core samples will be collected from the interfaces of low and high permeability zones in each test plot and analyzed for [CVOC]. Multiple subsamples will be taken from each core within the low and higher permeability zones to assess baseline contaminant distribution (MIP confirmation) and serve as a basis for comparison against co-located soil cores to be collected post-ISCO treatment.</li> </ul> </li> <li>• Improve contaminant treatment effectiveness               <ul style="list-style-type: none"> <li>– As measured by [CVOC] in groundwater wells and DPT grab groundwater samples. See above.</li> <li>– As measured by [CVOC] in DPT grab soil samples. Up to 15 DPT grab soil samples will be collected. This baseline monitoring event and used as a point of comparison for future post-ISCO treatment sampling.</li> </ul> </li> <li>• Decreased impact of MnO<sub>2</sub> deposition on injection pressure               <ul style="list-style-type: none"> <li>– As measured by field comparison of injection pressures at the control and test plots in the shallow zone. There is no associated field activity during the site characterization task.</li> </ul> </li> <li>• Improved understanding of impacts of the enhanced delivery approach on groundwater quality               <ul style="list-style-type: none"> <li>– As measured by analyses shown in Table 6</li> <li>– Additional laboratory analyses will be performed on groundwater and soil samples that are noted above for other data objectives.</li> </ul> </li> </ul>	Accurate VOC concentrations and lithology in the vicinity of each identified test plot

**Table 4. Summary of Field Data Collection Objectives and Criteria**

#	Data Objective	Criteria for Achieving Objective	Data Need
7B	Provide baseline physical and chemical characteristics from key locations within the intermediate depth plots so that post-treatment samples can be co-located and evaluated for treatment performance	<p>Baseline physical and chemical characteristics will be collected to measure baseline parameters necessary to meet the following overall project performance objectives:</p> <ul style="list-style-type: none"><li>• Eliminate the potential for contaminant rebound<ul style="list-style-type: none"><li>– Same as above – Objective 7 Shallow Test Plots.</li></ul></li><li>• Improve contaminant treatment effectiveness<ul style="list-style-type: none"><li>– Same as above – Objective 7 Shallow Test Plots.</li></ul></li><li>• Increased penetration of oxidant into LPM<ul style="list-style-type: none"><li>– As measured by visual examination of soil cores for purple color in LPM, <math>[\text{MnO}_4^-]</math> in groundwater within the LPM, and electrical conductivity (EC) response within the LPM. Baseline EC probing will be conducted concurrent with CPT/MIP to record a baseline EC response such that post-ISCO treatment EC probing will have a point of comparison.</li></ul></li><li>• Improved understanding of impacts of the enhanced delivery approach on groundwater quality<ul style="list-style-type: none"><li>– Same as above – Objective 7 Shallow Test Plots.</li></ul></li></ul>	Accurate VOC concentrations and lithology in the vicinity of each identified test plot
8	Provide a data basis for semi-quantitative analysis of contaminant mass distribution within the TTI of each test plot	<ul style="list-style-type: none"><li>• Results of grab groundwater and soil samples will be used to semi-quantitatively estimate a contaminant mass and mass distribution between the permeable and LPM zones within the TTI at each test plot.</li></ul>	Relative and accurate VOC concentrations and lithology in the vicinity of each identified test plot.
9	Define hydraulic input parameters for a numeric model that will be used to predict the delivery/sweep efficiency of polymer and permanganate injection	<ul style="list-style-type: none"><li>• CPT data need to define the lithologic stratification</li><li>• HRP data needed to define the K and head within each unique lithologic horizon</li></ul>	Lithology and hydraulic characteristics in the vicinity of each identified test plot.

**Table 5. Summary of Site Characterization Objectives, Data Needs, and Samples**

<b>No.</b>	<b>Data Need</b>	<b>Description of Field Activity</b>	<b>Sample Support</b>
1.	Relative VOC concentrations and lithology in the shallow (0-20' bgs) and intermediate (20-60' bgs) depth intervals and within the vicinity of the 88-MW02 well cluster	MIP, CPT, HRP	MIP, CPT at up to 4 locations per test plot HRP at up to 3 location per test plot
2.	Relative VOC concentrations in the vicinity of each identified test plot	MIP	MIP at up to 4 locations per test plot
3.	Lithology and hydraulic characteristics in the vicinity of each identified test plot	CPT, HRP	CPT at up to 4 locations per test plot HRP at up to 3 locations per test plot
4.	Lithology and hydraulic characteristics in the vicinity of each identified test plot	CPT, HRP	CPT at up to 4 locations per test plot HRP at up to 3 locations per test plot
5.	Relative VOC concentrations and lithology in the vicinity of each identified test plot	MIP, CPT, HRP	MIP, CPT at up to 4 locations per test plot HRP at up to 3 locations per test plot
6.	Relative and accurate VOC concentrations and lithology in the vicinity of each identified test plot	MIP, CPT, HRP	MIP, CPT at up to 4 locations per test plot HRP at up to 3 locations per test plot
7.	Accurate VOC concentrations and lithology in the vicinity of the each identified test plot	CPT, HRP DPT discrete soil and groundwater sampling Electrical conductivity (EC)	CPT at up to 4 locations per test plot HRP at up to 3 locations per test plot Up to 15 soil samples per test plot Up to 15 groundwater samples per test plot
8.	Relative and accurate VOC concentrations and lithology in the vicinity of each identified test plot	MIP, CPT, HRP DPT discrete soil and groundwater sampling	MIP, CPT at up to 4 locations per test plot HRP at up to 3 locations per test plot Up to 15 soil samples per test plot Up to 15 groundwater samples per test plot
9.	Lithology and hydraulic characteristics in the vicinity of each identified test plot	CPT, HRP	CPT at up to 4 locations per test plot HRP at up to 3 locations per test plot







## 3.2 Results

Appendix A includes a detailed report of site characterization activity results, including a detailed profile of contaminant and hydraulic conductivity information based on calibrated MIP, HRP, and CPT results. In summary Appendix A and other supporting site data show:

- Soil dominated by silty sand and sand with high natural oxidant demand
  - Silty sand 7-11 ft bgs
  - Sand 11-18 ft bgs
  - Silty sand 33-40 ft bgs
  - Sand 40-60 ft bgs
  
- Hydraulic conductivity (ft/day) in the Surficial Aquifer (7-18 ft bgs):
  - Range = 0.5-5.2
  - Average = 1.8
  - Heterogeneity ( $k_{\max} / k_{\min}$ ) = 10.4
  - Vertical conductivity = 0.00013
  - Anisotropy = 13,846
  - Hydraulic gradient (ft/ft)
    - Horizontal: 0.002, southwest
    - Vertical: 0.25, downward
  
- Hydraulic conductivity (ft/day) in the Upper Castle Hayne Aquifer (33-62 ft bgs):
  - Range = 0.9-18.1
  - Average = 6.6
  - Heterogeneity = 20.1
  - Hydraulic gradient (ft/ft)
    - Horizontal: 0.0004, west
    - Vertical: 0.0015, downward
  
- PCE concentration in Soil
  - 7,100  $\mu\text{g}/\text{kg}$  in the 16-18 ft bgs interval
  - < 720  $\mu\text{g}/\text{kg}$  in the 33-35 ft bgs interval
  - 1,300  $\mu\text{g}/\text{kg}$  in the 53-55 ft bgs interval
  
- PCE concentration in groundwater
  - 220 mg/L in the 7-18 ft bgs interval (NAPL observed in field sample)
  - 230 mg/L in the 33-62 ft bgs interval (NAPL not observed in field sample)
  - NOTE: samples higher than saturation possibly due to enhanced PCE dissolution because of nature of NAPL mixture or presence of small amounts of pure phase within the aqueous (i.e., small “beads” of NAPL suspended in aqueous phase)
  
- Depth interval with greatest contaminant mass as indicated by MIP
  - 16-18 ft bgs in Surficial Aquifer
  - 33-35 ft bgs in Upper Castle Hayne Aquifer

## **4.0 Laboratory Tests and Analyses**

### **4.1 Objectives**

A series of laboratory tests were conducted to better understand pre-treatment site conditions for later determining impacts of the demonstration on groundwater and soil quality post-demonstration and to also support system design efforts. Specifically, the goals for the treatability study geared toward Objective 1, improving the sweep efficiency of permanganate using the polymer xanthan gum with potassium permanganate ( $\text{KMnO}_4$ ), are to (1) determine an optimal solution formulation for demonstrating polymer-enhanced delivery and sweep-efficiency improvement at our selected test site; (2) collect rheological and transport related data needed to support numerical simulations for implementation design; and (3) test our proposed polymer/oxidant mixing strategy at the bench-scale prior to scaling up this strategy at the field scale. The goal for the treatability study geared toward Objective 2, controlling  $\text{MnO}_2$  to improve oxidant delivery and flow, thereby enhancing contaminant destruction using the polymer SHMP with potassium permanganate ( $\text{KMnO}_4$ ), is to determine an optimal solution of polymer and oxidant for site-specific conditions. Standard methods of analysis (as listed in Section 5.1) will be employed as appropriate.

### **4.2 Approach and Methods**

Table 6 presents a summary of sampling and analyses performed using the samples collected as part of the field efforts described in Section 3.0. Table 7 summarizes the test objectives, criteria for achieving the objectives, and approach for the laboratory tests for both Objectives 1 and 2.

#### **4.2.1 Characterization of Site Soil and Groundwater**

Site soil and groundwater were characterized to establish baseline physical and chemical characteristics of the site (Table 6). Additionally, the natural oxidant demand (NOD) results were used to guide oxidant concentration selection for the demonstration by serving as data input for a spreadsheet conceptual design tool, CDISCO (Conceptual Design for ISCO, developed under ESTCP ER-0623). NOD values were collected for specific oxidant and polymer concentration combinations as well to account for potential impacts of oxidant reaction with polymer on oxidant delivery.

#### **4.2.2 Objective 1: Improved Sweep Efficiency**

An optimal solution formulation for enhanced sweep efficiency will provide (1) the optimized permanganate concentration based on CDISCO design tool output (effective oxidant distribution, defined for demonstration purposes as a 15' oxidant ROI and persistence of at least 100 mg/L of permanganate for 1 day), while providing (2) a range of viscosities appropriate for demonstrating heterogeneity control given our site conditions (as determined from sensitivity simulations to be conducted), and (3) appropriate rheological stability over our injection time frame (i.e., approximately 5 – 7 days). Much progress was made toward identifying optimal xanthan and permanganate concentrations with respect to rheological stability during nearly completed

SERDP Project 1486. However, additional fluid characterization was needed for this demonstration to provide specific data necessary to properly simulate implementation using the UTCHEM simulator. The rheological stability of these xanthan/permanganate solutions were further tested under conditions of flow through porous media via one-dimensional column experiments. The column studies were conducted to ensure viscosity-shear rate relationships obtained from rheometer measurements are properly correlated to conditions of dynamic porous media flow.

#### **4.2.2.1 Bulk Solution Rheology**

A stock solution of xanthan gum (2 g/L) was prepared according to the manufacturer's recommendations using site source water collected from a nearby potable water supply source during the initial site characterization effort. Samples of this stock solution were diluted and added to solutions of potassium permanganate in 40 mL VOA vials to create a solution test matrix that spanned a 500 mg/L to 10,000 mg/L permanganate concentration range and a 250 mg/L to 1,000 mg/L range of xanthan gum concentrations. Permanganate solutions without polymer addition, and xanthan solutions without permanganate addition, served as controls.

The viscosity of these solutions was measured as a function of shear rate using an AR Instruments G-2 rheometer. This rheometer allowed for the characterization of solution viscosities over a 4-5 decade change in applied shear rate, enabling model fits to the data needed for UTCHEM simulation. Solution viscosities for all test batches were similarly measured as a function of time (over a 5 day time period) to monitor the rate of reduction in viscosities that result from the slow oxidation of xanthan gum. The results of these measurements allowed for the selection of an optimal xanthan and permanganate solution for use during field implementation and implementation design simulation.

#### **4.2.2.2 Xanthan Oxidant Demand**

For the same solutions described above, the oxidant demand for xanthan gum was measured as the decrease in permanganate concentration. Measurements were made initially after mixing and as a function of time (i.e., at several time points during the first 24h, once per day for several days after initiation, and at approximately weeklong intervals thereafter). A small subsample was taken from each vial and diluted in DI water to achieve a concentration of permanganate acceptable for spectrophotometry (i.e., < 50 mg/L). After syringe filtration at 0.45um, a Hach DR/4000U Spectrophotometer was used to measure the absorbance of these diluted samples at 418 and 525 nm. A 10,000 mg/L potassium permanganate solution containing no xanthan gum was used as a control. The purpose of these measurements was to obtain data needed to properly design oxidant dosage concentrations in the presence of xanthan to maintain a target concentration during subsurface injection. NOD measurements (described in Section 4.1) were also collected for the 5,000 mg/L oxidant and 1,000 mg/L xanthan condition, deemed viable for design based on preliminary UTCHEM modeling results. NOD results serve as input to the CDISCO design tool used to estimate the oxidant radius of influence.

**Table 6. Sampling and Analysis Summary Table**

Sample Task	Approx Sample No.	Sampling Equipment	Required Analysis	Analytical Method	Holding Time	Sample Preservation	Containers
<i>Groundwater Sampling</i>							
DPT Sampling with Waterloo Profiler™	15	Waterloo Profiler™	DO, Temperature, pH, Specific Conductance, Turbidity, ORP	Field Direct-Read Meter	N/A	N/A	N/A
DPT Sampling with Waterloo Profiler™	15	Waterloo Profiler™	TCL VOCs	EPA 8260B and 5030	7 Days	Cool to 4°C	(3) 40-ml Vial
DPT Sampling with Waterloo Profiler™	15	Waterloo Profiler™	pH, ORP	APHA 4500, 2580	3 Days	Cool to 4°C	(3) 40-ml Vial
DPT Sampling with Waterloo Profiler™	15	Waterloo Profiler™	Total solids, suspended solids	APHA 2540B, 2540C	ASAP (7 days max)	Cool to 4°C	(3) 40-ml Vial
DPT Sampling with Waterloo Profiler™	15	Waterloo Profiler™	Major cations/metals (Ca, Fe, Mn, Na, K, etc.)	APHA 3125	30 Days	Cool to 4°C	(3) 40-ml Vial
DPT Sampling with Waterloo Profiler™	15	Waterloo Profiler™	Major anions (SO <sub>4</sub> <sup>2-</sup> , PO <sub>4</sub> <sup>3-</sup> , NO <sub>3</sub> <sup>-</sup> , Cl <sup>-</sup> )	APHA 4110	2 Days	Cool to 4°C	(3) 40-ml Vial
DPT Sampling with Waterloo Profiler™	15	Waterloo Profiler™	Total organic carbon	APHA 5310B	15 Days	Cool to 4°C	(3) 40-ml Vial
<i>Soil Sampling</i>							
DPT Soil Sampling	15	Acetate Sleeve, SS Spoon, SS Bowl, (3) Encore Samplers	TCL VOCs	EPA 8260B and 5035	48 hours	Cool to 4°C	(3) Encore Samplers (1) 40-oz jar for moisture content
DPT Soil Sampling	15	Acetate Sleeve, SS Spoon, SS Bowl	Natural Oxidant Demand (NOD)	Siegrist et al., 2009	30 Days	Cool to 4°C	(3) 40-oz jar, minimum headspace
DPT Soil Sampling	15	Acetate Sleeve, SS Spoon, SS Bowl	TOC, Grain Size, Bulk Density, Porosity	EPA 9060	30 Days	Cool to 4°C	(3) 40-oz jar, minimum headspace
DPT Soil Sampling	15	Acetate Sleeve, SS Spoon, SS Bowl	pH, ORP	EPA 9045D	3 Days	Cool to 4°C	(3) 40-oz jar, minimum
DPT Soil Sampling	15	Acetate Sleeve, SS Spoon, SS Bowl	Cation exchange capacity	Sparks et al., 1996	10 Days	Cool to 4°C	(3) 40-oz jar, minimum
DPT Soil Sampling	15	Acetate Sleeve, SS Spoon, SS Bowl	Microbial density, diversity, activity	Kieft and Phelps (1997); Phelps et al. (1994a, 1994b) Weaver et al. (1994)	3 Days	Cool to 4°C	(3) 40-oz jar, minimum
DPT Soil Sampling	15	Acetate Sleeve, SS Spoon, SS Bowl	Mn speciation	Chao, 1972	30 Days	Cool to 4°C	(3) 40-oz jar, minimum

**Table 7. Summary of Laboratory Test Objectives and Criteria**

#	Data Objective	Criteria for Achieving Objective	Approach	Use of Data and Notes
<i>Demonstration Objective: Improve permanganate delivery sweep efficiency through heterogeneous zones using a soluble polymer</i>				
1.	Characterize bulk solution rheology to provide model input data (UTCHEM simulation)	Viscosity measured over time for range of polymer / oxidant concentration solutions	<ul style="list-style-type: none"> <li>Mix range of solutions of permanganate and Xanthan                             <ul style="list-style-type: none"> <li>Vary permanganate 500 mg/L to 10,000 mg/L</li> <li>Vary Xanthan 250 mg/L to 1,000 mg/L</li> </ul> </li> <li>Measure viscosity vs. shear rate using AR Instruments G-2 Rheometer</li> </ul>	<ul style="list-style-type: none"> <li>As model (simulator) input used for selection of optimum oxidant / polymer solution for use during field implementation</li> <li>Evaluate viscosity modification due to Xanthan oxidation</li> <li>NOTE: This is a measurement that should be typical of an oxidant / polymer delivery scheme when polymer is used for viscosity modification</li> </ul>
2.	Characterize xanthan oxidant demand to provide conceptual design model input (CDISCO)	Oxidant demand measured over time for range of polymer / oxidant concentration solutions	<ul style="list-style-type: none"> <li>Using same samples generated for Objective 1 above, measure permanganate concentration over time and calculate oxidant demand and reaction kinetics</li> </ul>	<ul style="list-style-type: none"> <li>As design tool (Conceptual Design for ISCO or CDISCO tool) input variable – used to estimate ROI as a function of oxidant delivery concentration and reaction kinetics</li> <li>NOTE: This is a measurement that would only need to be conducted for an oxidant / polymer delivery scheme when polymer is used for viscosity modification when a polymer OTHER THAN xanthan may be employed (note: these data will carry over to field application in general and will be incorporated into guidance accordingly)</li> </ul>
3.	Characterize polymer / oxidant transport conditions in porous media with respect to polymer injectivity, permeability reduction due to polymer entrapment, and rheological behavior	Pressure drop measured across columns packed with field material having oxidant / polymer delivered at optimized concentrations at varied delivery rates	<ul style="list-style-type: none"> <li>Pack 1-D columns with field porous media and saturate with site source water</li> <li>Measure pressure drop across column</li> <li>Introduce oxidant/polymer solution under constant flow rate</li> <li>Evaluate for constant injectivity</li> <li>Calculate shear rate</li> <li>Increase flow rate and note impact on shear rate</li> <li>Flush column with water</li> <li>Measure pressure drop across column</li> <li>Determine permeability loss (permeability reduction factor)</li> </ul>	<ul style="list-style-type: none"> <li>As model (simulator) input used for simulating polymer delivery</li> <li>To describe permeability reduction due to irreversible polymer entrapment and the potential presence of entrapped MnO<sub>2</sub></li> <li>NOTE: If constant injectivity cannot be achieved in the column or injectivity is reduced by more than a factor of 10 compared to no polymer injection, the experiment will stop and a go/no-go decision to proceed with the demonstration will be made</li> <li>NOTE: These measurements will help determine if this approach must always be conducted for an oxidant / polymer delivery scheme when polymer is used for viscosity modification OR if a model can be developed from these data for future applications under alternative sites and site conditions</li> </ul>
4.	Optimize mixing strategy for field application	Maximum concentration of xanthan that can be used as concentrated feed determined	<ul style="list-style-type: none"> <li>Vary concentration of xanthan concentrate solution entering simulated mixing strategy model (physical model)</li> <li>Rheology of solution exiting in-line static mixers characterized (see objective #1)</li> <li>Resulting viscosity-shear rate profiles compared to those for a truly homogeneous xanthan solution</li> <li>Determine max xanthan concentration that has homogeneous solution-like character</li> <li>Repeat with permanganate addition</li> </ul>	<ul style="list-style-type: none"> <li>Provide data to engineer field xanthan delivery system</li> <li>NOTE: These measurements will provide data for any demonstration using oxidant / polymer for viscosity modification (i.e., these measurements would not have to be repeated for other field applications unless a polymer other than xanthan is employed)</li> </ul>

**Table 7. Summary of Laboratory Test Objectives and Criteria**

#	Data Objective	Criteria for Achieving Objective	Approach	Use of Data and Notes
<i>Demonstration Objective: Improve permanganate delivery by controlling MnO<sub>2</sub> deposition with soluble polymer</i>				
1.	Identify optimum oxidant / SHMP mixture concentrations	MnO <sub>2</sub> behavior and Mn speciation characterized for range of oxidant and polymer concentration solutions	<ul style="list-style-type: none"> <li>Repeat NOD measurements (see Table 6) with range of SHMP concentrations (max polymer = solubility concentration; ranges of 0.5 and 0.1 of each of these values will be evaluated) and with optimized permanganate concentration (based on NOD measurements and CDISCO design tool results)</li> <li>Measure MnO<sub>2</sub> in solution spectrophotometrically at 418 nm with and without 0.2 μm filtration (suspended vs. dissolved)</li> <li>Measure permanganate concentration spectrophotometrically at 525 nm</li> <li>Estimate MnO<sub>2</sub> associated with solids via mass balance (Mn as permanganate initial – Mn as MnO<sub>2</sub> suspended – Mn as MnO<sub>2</sub> dissolved – Mn as MnO<sub>4</sub><sup>-</sup> unreacted)</li> <li>Determine ideal solution mixture where MnO<sub>2</sub> dissolved is maximized and MnO<sub>2</sub> associated with solids is minimized</li> </ul>	<ul style="list-style-type: none"> <li>To determine minimum SHMP concentration that offers maximum MnO<sub>2</sub> dissolved concentrations</li> <li>NOTE: This is a measurement that should be typical of an oxidant / polymer delivery scheme when polymer is used to inhibit MnO<sub>2</sub> deposition (i.e., results are site-specific)</li> </ul>
2.	Characterize MnO <sub>2</sub> transport in porous media	MnO <sub>2</sub> behavior and Mn speciation characterized for optimum permanganate and SHMP concentrations in columns packed with field porous media	<ul style="list-style-type: none"> <li>Pack two 1-D columns with field porous media</li> <li>Spike columns with PCE</li> <li>Deliver polymer / oxidant solution to one column and oxidant only to the other column</li> <li>Measure MnO<sub>2</sub> dissolved and suspended in effluent</li> <li>Stop polymer / oxidant solution delivery</li> <li>Extract MnO<sub>2</sub> associated with the solids</li> <li>Assess differences between oxidant only and polymer + oxidant columns</li> </ul>	<ul style="list-style-type: none"> <li>Data used to anticipate field results and guide field monitoring plan</li> <li>NOTE: If there are no measurable differences in MnO<sub>2</sub> content associated with solids, the field demonstration will be NO-GO. This is not anticipated based on review of existing site data and understanding of the oxidant-polymer system.</li> <li>NOTE: These measurements would be considered optional for a polymer / oxidant delivery scheme where polymer is used to inhibit MnO<sub>2</sub> deposition; results are applicable to developing monitoring plans, but typical budgets may not support such efforts.</li> </ul>

#### 4.2.2.3 Polymer/Oxidant Transport Conditions in Porous Media

One-dimensional column experiments were performed to determine transport characteristics for the 1,000 mg/L xanthan gum and 5,000 mg/L  $\text{KMnO}_4$  solution. At this point in the treatability study we are considering this polymer/oxidant concentration to be a nearly optimal solution for implementing Objective 1 for this demonstration. Fine tuning of this solution will occur after performing UTCHEM numerical simulations. These experiments were performed using porous media collected from within the Castle Hayne aquifer and provide data important for assisting implementation design. Specifically, these experiments were designed to:

4. Characterize polymer/oxidant solution injectivity,
5. Quantify permeability reduction as a result of polymer entrapment and/or manganese dioxide particle deposition during delivery, and
6. Characterize the non-Newtonian rheological behavior of this polymer-amended solution during flow in porous media.

The specific methodology (described below) employed in this task was based on that developed and successfully implemented as a part SERDP Project ER-1486, to characterize the transport of xanthan gum solutions in the absence of permanganate. The methodology was modified in this work to include three separate column experiments for a single test media sample, each of which were designed to evaluate both permanganate and xanthan gum transport. The goal was to evaluate the potentials for permeability reduction associated with permanganate/sediment reactions and xanthan gum in separate experiments. High oxidant demands were measured for sediments within the upper Castle Hayne aquifer, so it was important to evaluate individual effects. An additional goal was to assess the need to pre-filter the polymer/oxidant solution prior to injection. The motivation behind including pre-filtration arose from the results of hydraulic testing performed during our site characterization activities, which indicated a slightly lower than expected average permeability for the upper Castle Hayne aquifer unit within our test area. Pre-filtration was successfully utilized during SERDP Project ER-1486 as a means of extending the applicability of polymer-amended methods to lower permeability media. Procedurally, these three experiments involved:

1. Packing a test column and performing an oxidant-only flood within the test media.
2. Re-packing the test column and performing a polymer/oxidant flood without filtration.
3. Re-packing the test column and performing a polymer/oxidant flood with filtration.

A schematic of the experimental apparatus is presented as Figure 8. The apparatus was additionally modified from that presented in the Treatability Study Plan in that the pressure drop was not monitored along the length of the column, just at the column inlet and outlet. This modification was necessary because of the limited amount of site sediments collected during our initial site characterization work and the need to pack and re-pack columns. Thus an alternate, and smaller, column was used that did not possess pressure monitoring points along its length.

Samples of aquifer material were collected and shipped to the Colorado School of Mines. These samples were collected from the 35-50 foot depth interval as a continuous vertical core by direct-push methods and arrived within 1-inch acetate sleeves. This depth interval is the upper portion of the Castle Hayne aquifer and is the target interval for implementing Objective 1. Vertically, these sediments were found to grade from a fine-medium grained sand with varying amounts of

very-fine sand and/or silt, to a poorly sorted medium sand within the interval 45-50 feet. Portions of these samples were air-dried at room temperature and homogenized.

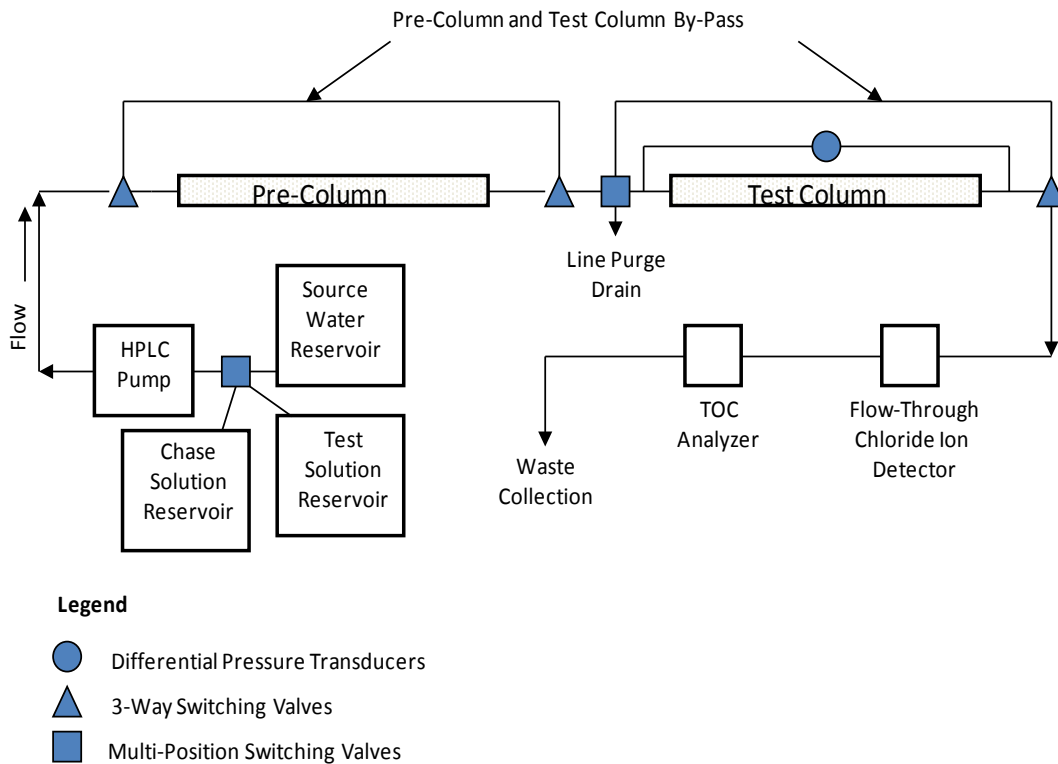


**Figure 8.** Schematic diagram of 1-D column test apparatus

The test column (dimensions, length = 15 cm, inner diameter = 2.5 cm) was dry-packed with aquifer material and saturated with site source water. Once saturated, a constant flow rate was applied to the column inlet. Given the smaller column dimensions, a flow rate of 1 cm<sup>3</sup>/min was used. Pressure transducers were installed at the inlet and outlet of the test column. The pressure drop across the column was recorded and used to determine initial hydraulic conductivity of the sample media via the application of Darcy's Law. Our goal during the column packing process was to closely match permeabilities measured in the field during our site characterization activities within the aquifer section planned for Objective 1.

#### 4.2.2.4 Xanthan/Oxidant Mixing Strategy

Given the large volumes of injection fluids needed for this demonstration, the current strategy for mixing xanthan and permanganate on-site involves the preparation of a xanthan gum solution concentrate. A chemical metering pump will then be used to provide the appropriate volume of xanthan concentrate to a potable water source line to achieve a target diluted xanthan concentration. This xanthan mixture will then be homogenized using an array of in-line static mixers. The xanthan solution will then be introduced to a separate permanganate solution feed line. The two solutions will pass through an additional series of in-line static mixers to achieve a homogeneous xanthan/permanganate fluid concentration for subsurface injection.



Implementing this strategy requires a given xanthan concentration for the concentrate in order to size temporary storage tanks and to select an appropriate metering pump. However, the selection of a xanthan concentration for the concentrate also requires testing to determine what xanthan concentration the metered concentrate will produce a homogeneous mixture for subsurface injection given our current mixing strategy. Polymers like xanthan gum do not readily dilute from a concentrate to form homogeneous mixtures like salts. Additional mixing energy is required. The lower the concentration of the concentrate, the less mixing energy required. Therefore, the objective of this subtask is to determine the maximum xanthan concentrate formulation that will provide a homogeneous mixture of permanganate and xanthan gum upon mixing.

A scaled-down model of the current mixing strategy will be constructed to achieve this objective. Static mixers most appropriate for homogenizing viscous fluids will be researched, purchased, and tested in the CSM laboratory. A schematic of the test apparatus appears as Figure 9 below.

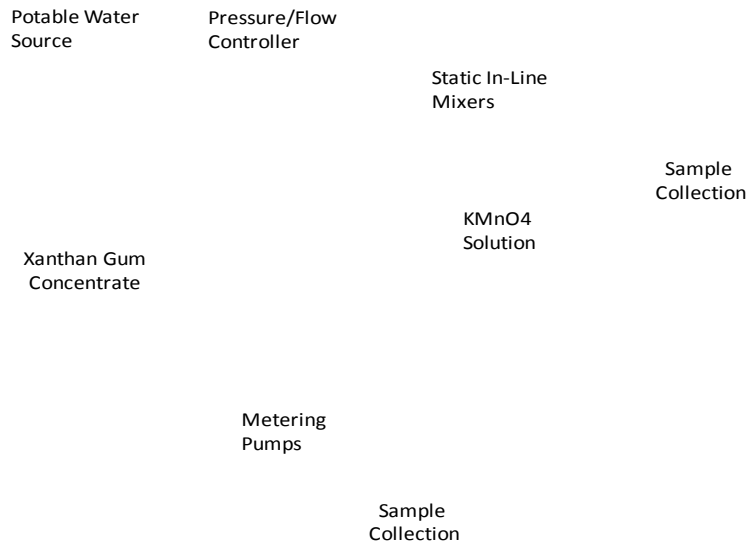


**Figure 9.** Schematic of test apparatus for optimizing Xanthan/Permanganate mixing strategy

The principal experimental variable in this mixing study will be the concentration of the xanthan gum concentrate. Flow velocities will be selected to mimic those anticipated during field implementation. Metering pump flows will be set to provide optimal xanthan and permanganate concentrations as determined from the earlier phases of this treatability study.

Testing will be initiated without the addition of permanganate. The solution exiting the in-line static mixers will be sampled and the solution rheology characterized as described above. The resulting viscosity-shear rate profiles will be compared to those for a truly homogeneous xanthan solution. Once a maximum concentrate concentration is identified, the same fluid sampling and characterization procedure will be followed for the addition of permanganate.

### **4.2.3 Objective 2: Manganese Dioxide Control**

The treatability tests conducted toward Objective 1, Manganese Dioxide Control, included batch tests to evaluate the optimum mixture of oxidant and polymer (concentration ratio) and 1-D transport evaluations to compare MnO<sub>2</sub> deposition for oxidant-only and oxidant + polymer systems.

#### **4.2.3.1 Optimum Oxidant / SHMP Mixture**

Using site media from the Surficial Aquifer collected during Field Characterization Activities (Section 3.0), batch tests were conducted to evaluate the impact of varied concentrations of SHMP and permanganate concentrations on MnO<sub>2</sub> transport. Field-moist aquifer solids were measured into 40 mL amber VOA vials serving as batch reactors (results were later corrected for water content, which was also measured for samples, and results were recorded for an equivalent dry mass). Site groundwater was added to achieve a 1:1 solids to solution ratio. NOD test methods were followed for these tests, however an additional measurement of absorbance at 418 nm were made on the aqueous phase of the samples over time. This measurement is a qualitative indicator of MnO<sub>2</sub> dissolved and/or suspended in solution. Duplicate systems were prepared for the 5,000 mg/L permanganate concentration, deemed the optimum concentration based on the range of conditions evaluated using the conceptual design tool, CDISCO. A key variable in the design tool was the rate of NOD, measured as described in Section 4.2.1. The NOD rate and extent are high for the Surficial Aquifer media, therefore the design tool indicated that a higher oxidant concentration results in nonproductive consumption of oxidant and wouldn't significantly increase a radius of influence for a given delivery rate. A lower oxidant concentration would not be sufficient to meet the design ROI of 15' within 10 days. SHMP concentrations of 500, 1,000, and 2,000 mg/L were evaluated. Note that permanganate demand was measured also for the 500 and 1,000 SHMP systems to verify it did not impact oxidant demand.

#### **4.2.3.2 Manganese Dioxide Transport**

Two columns (60 cm long x 2.5 cm diameter) were packed with well-mixed air-dried media (Figure 10). Initially it was planned for columns to be wet-packed, but the very fine nature of the media prevented settling of the media within the column (i.e., the finest media remained suspended and was thus not representative of site characteristics). Columns were saturated via upflow delivery of deionized water. Water was circulated at 1 mL/min for approximately 10 pore volumes (1 PV ~ 115 mL) to establish flow and assure the delivery flow rate was appropriate.

Next a 0.2 M sodium chloride solution was passed through the column for approximately 1.5 pore volumes to serve as a tracer. The objective was to determine the similarity of flow through the columns and to assure column packing was near identical so that differences in flow during or after delivery can be attributed to oxidant and polymer conditions and not to column packing conditions.



**Figure 10.** 1-D packed columns for evaluation of permanganate and SHMP transport through site porous media. The top column is permanganate-only and the bottom is permanganate + SHMP.

After it was determined that column flow conditions were near identical, 50  $\mu\text{L}$  of field NAPL acquired from the groundwater samples collected as described in Section 3.0 were injected into the gravel influent chamber of the column. This volume is equivalent to the mass of PCE that could occupy approximately 3 pore volumes of water assuming PCE dissolves at solubility-level concentrations ( $\sim 180$  mg/L). Because of the relatively high carbon content of the media (described below in Section 4.3.1) it was anticipated that a significant fraction of this NAPL would remain within the column as water was passed through to distribute it. After NAPL was added, water was re-circulated through the column for approximately 6 pore volumes. At the end of this circulation stage the feed water, which was common to both columns and which had been re-circulated through the columns, and the effluent of each column was sampled for PCE. Each of these three sample concentrations were within 5% of each other in the low mg/L range. Mass balance calculations were performed to estimate that approximately 85% of PCE remained within the column, presumably dissolved or sorbed to media, not accounting for volatilization losses – the potential for which was minimized.

After it was determined that contamination characteristics in the column were similar, 5,000 mg/L permanganate was delivered to one column, while 5,000 mg/L permanganate plus 2,000 mg/L SHMP were delivered to the other. These concentrations were deemed optimum based on results of the batch tests. Oxidant was delivered to each column until back pressure, presumably due to solids generation and loading, prevented additional flow. This occurred just prior to 1 PV of oxidant delivery in the permanganate-only column, where permanganate was observed to reach approximately  $\frac{1}{4}$  of the way into the column, which was anticipated based the NOD rate and oxidant delivery rate; and at approximately 2 PVs in the permanganate and SHMP column where oxidant was observed to reach nearly  $\frac{1}{2}$  of the way into the column as anticipated, but with some preferential flow on one side of the column (Figure 11). During oxidant delivery, absorbance at 418 nm was measured for the column effluent as a qualitative indicator of manganese dioxide passing through the column (dissolved/suspended).

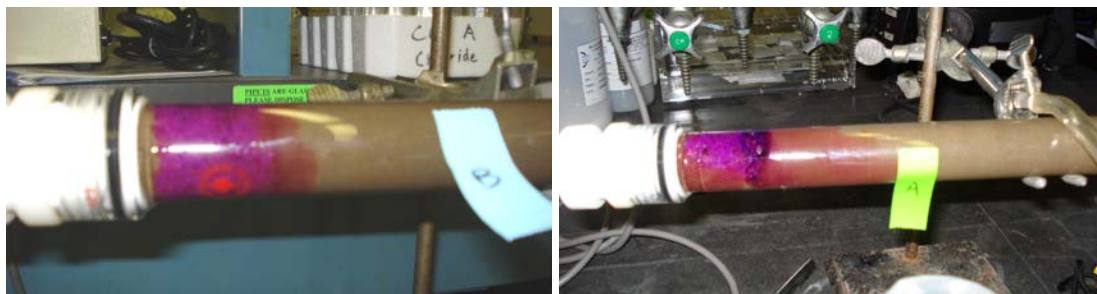


**Figure 11.** 1-D packed columns during permanganate delivery. The left-hand column (B) is permanganate-only and the right-hand is permanganate + SHMP (A).

Once delivery to the columns was complete, they were unpacked and sectioned. Representative samples from sections ranging across the length of the column were subjected to a three phase extraction with the goal of quantifying  $MnO_2$  deposition within the column as a function of distance from the delivery point.

## 4.3 Results

### 4.3.1 Media Characterization

Table 8 provides results of site characterization activities for the porous media, while Table 9 provides results for site groundwater. “Pending” results for porous media are gaps due to (1) instrumentation access/maintenance issues soon to be resolved (Mn speciation and CEC), (2) limited media available through these sample collection efforts (grain size analysis - majority of Castle Hayne porous media was utilized in other laboratory evaluations), and (3) because additional analyses are planned directly prior to treatment during pre-ISCO sample collection efforts that are planned (microbial characteristics). “Pending” results for groundwater are gaps due to instrumentation access/maintenance issues soon to be resolved (TOC). Table 10 includes a summary of NOD test results, including those evaluated with polymer as described in Section 4.2 above. These results include the initial fast oxidant demand in terms of mg-oxidant / kg-media, the % of total NOD attributable to that initial fast demand, and finally the later and slower rate constant. These values serve as input for CDISCO, the conceptual design tool in use for this demonstration.

**Table 8. Porous Media Characteristics**

Parameter	14-18 ft (Surficial)	33-35 ft (Upper Castle Hayne)	53-55 ft (Upper Castle Hayne)
VOCs (µg/kg)			
acetone	1,100	48	40
PCE	7,100	<720	1,300
TCE	600	12	220-540
c-DCE	10,000	22	BDL
VC	38	BDL	BDL
TOC	0.13 %	1.97 %	0.12 %
pH	3.92	5.87	5.57
ORP (mV)	182.5	70.6	87.9
Cation exchange capacity	Pending	Pending	Pending
Mn Speciation	Pending	Pending	Pending
Microbial characteristics	Pending	Pending	Pending

BDL = Below Detection Limit of method

**Table 9. Groundwater Characteristics**

Parameter	Surficial (7-18')	Upper Castle Hayne (33-62')
VOCs (mg/L)	16-18'	33-35'
acetone	75	BDL
PCE	220	230
TCE	BDL	BDL
DCE	BDL	BDL
VC	BDL	BDL
pH	4.42	6.48
ORP (mV)	153.8	36
Total solids (mg/L)	5,570	440
Cations (ppm)		
Na	62.2	16.9
Mg	25.4	3.7
K	3.7	4.3
Fe	64.9	BDL
Cations (ppb)		
Al	2,733	4.8
V	2.9	1.0
Cr	6.1	1.2
Mn	4,410	531
Ni	58.4	17.2
Cu	5.4	2.6
Zn	583	335
As	7.8	1.5
Sr	1,557	134
Ba	1,097	56.3
Pb	0.39	BDL
Anions (mg/L)		
Chloride	1,340	58.4
Nitrate	0.08	0.16
Sulfate	7.5	5.1
TOC	Pending	Pending

**Table 10. NOD Test Results Summary**

Sample Depth	Permanganate Conc. (mg/L)	Polymer, Conc. (mg/L)	Instantaneous NOD (mg/kg)	% Instantaneous of Total NOD	Pseudo 1 <sup>st</sup> order rate (d <sup>-1</sup> )
10-15 ft	1,000	0	421	67	0.25
10-15 ft	5,000	0	894	65	0.114
10-15 ft	10,000	0	1267	46	0.03
15-20 ft	5,000	0	1273	89	0.322
15-20 ft	5,000	HMP, 500	1310	91	0.288
15-20 ft	5,000	HMP, 1,000	1402	98	NA
32-40 ft	5,000	Xanthan, 1000	1430	100	NA
35-40 ft	5,000	Xanthan, 1000	800	63	0.06
40-45 ft	5,000	Xanthan, 1000	902	71	0.16

### 4.3.2 Objective 1: Improved Sweep Efficiency

#### 4.3.2.1 Bulk Solution Rheology

The results of the viscosity-shear rate measurements are presented in Figures 12 through 14 for solutions containing 250, 500, and 1,000 mg/L xanthan gum, respectively. For each case, viscosities were measured within one hour of mixing the oxidant and polymer solutions. Measured viscosities were found to be reasonably insensitive to the concentration of  $\text{KMnO}_4$  added. This is the result of exceeding salinity thresholds for xanthan gum in each case, below which viscosity is more dependent on salinity. The use of 10,000 mg/L  $\text{KMnO}_4$ , at all xanthan concentrations resulted in an initial partial gel formation followed by a rapid return to regular solution behavior upon further mixing. For this reason we decided to limit the oxidant concentration to 5,000 mg/L for this demonstration until such time this phenomenon can be more thoroughly explored.

To provide input data for the UTCHEM simulator, the viscosity results were modeled as a function of shear rate ( $\gamma$ ) using Meter's Equation (Meter and Bird, 1964):

$$\mu_p = \mu_w + \frac{\mu_p^0 - \mu_w}{1 + \left(\frac{\gamma}{\gamma_{1/2}}\right)^{P_\alpha - 1}} \quad [1]$$

where  $\mu_p^0$  is the polymer solution viscosity at zero shear rate (read from the Newtonian plateau region of lowest measurable shear rate change),  $\mu_w$  is the water viscosity (here assumed to be 1 centi-Poise (cP)),  $\gamma_{1/2}$  is the shear rate at which the polymer solution viscosity is half that of the zero shear rate viscosity, and  $P_\alpha$  is an empirical coefficient which governs the abruptness of the change of viscosity with shear. Equation 1 is the viscosity-shear rate equation used by the UTCHEM simulator and was used to fit the experimental shear rate-viscosity data using the UTCHEM input parameters  $P_\alpha$  and  $\gamma_{1/2}$  as fitting parameters. Whenever the Newtonian plateau was not readily discernable from the measured data  $\mu_p^0$  can be employed as an additional fitting parameter. The results of the Meter's equation fits (Equation 1) are presented in Table 11.

The effect of decreasing the concentration of xanthan gum is to decrease the viscosity of the polymer/oxidant solution. Calculations using the radial forms of Darcy's law indicate that realistic in situ shear rates will vary between 1 and 500  $\text{sec}^{-1}$  for our site conditions and range of

injection rates anticipated. As such, these results, and the results of 2-D tank experiments performed during the conduct of SERDP Project ER-1486, suggest that utilizing an injectant polymer concentration between 500 and 1,000 mg/L will provide sufficient range of viscosities to promote improved permanganate sweep efficiencies.

In addition to obtaining initial viscosity-shear rate profiles for these solutions, similar measurements were made as a function of time to better understand the effect of polymer oxidation on solution viscosity. The results of these measurements are presented as Figures 15-17 for a 1,000, 500, and 250 mg/L xanthan solutions, respectively.  $\text{KMnO}_4$  concentrations used were 500, 5000 and 10,000 mg/L to provide a reasonable range of oxidant concentrations from which to assist in selecting an optimal injectate oxidant concentration.

In all cases, solution viscosities decreased with exposure to permanganate over the course of 144 hours (or 6 days). However, it appears from these results that the use of lower permanganate concentrations (e.g., 500 mg/L  $\text{KMnO}_4$ ) provides the best viscosity retention over time. Conversely, the use of permanganate concentrations equal to or greater than 10,000 mg/L results in much more rapid solution viscosity loss which will more significantly impact the potential for polymer sweep efficiency improvements. Again the solutions that exhibit an appropriate combination of initial solution viscosity and temporal viscosity retention over our project's implementation timeline appears to one in which the xanthan gum concentration is within 500 and 1,000 mg/L. Optimal permanganate concentrations for maintaining sufficient viscosity retention appear to range between 500 and 5,000 mg/L.

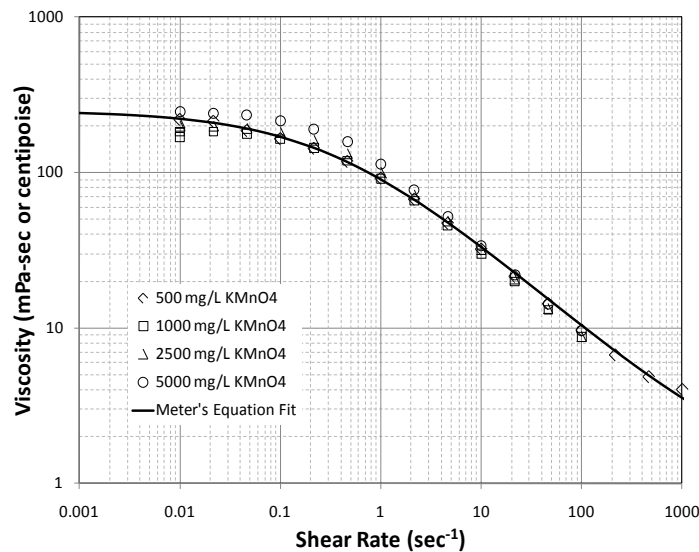


**Figure 12.** Viscosity-shear rate function for a 1,000 mg/L xanthan gum solution containing varying concentrations of  $\text{KMnO}_4$

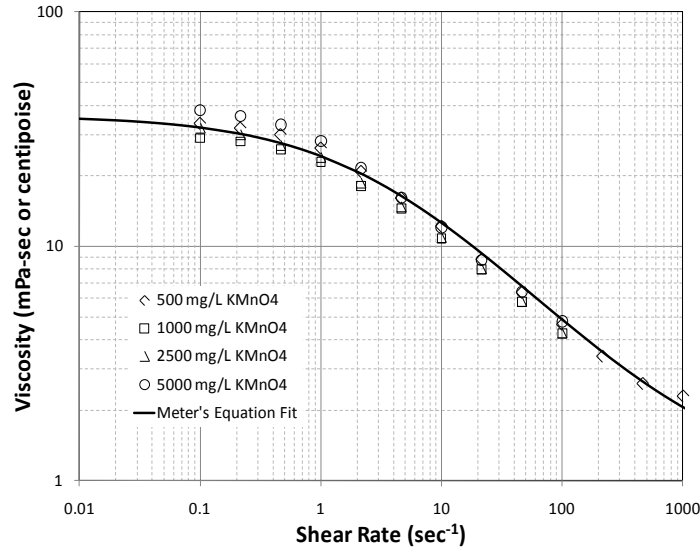


**Figure 13.** Viscosity-shear rate function for a 500 mg/L xanthan gum solution containing varying concentrations of  $\text{KMnO}_4$

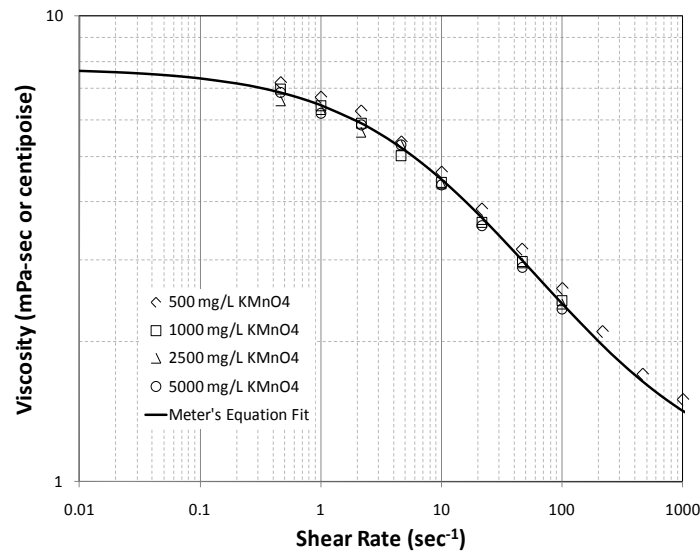


**Figure 14.** Viscosity-shear rate function for a 250 mg/L xanthan gum solution containing varying concentrations of  $\text{KMnO}_4$

**Table 11. Results of Meter's Equation fits to Viscosity-Shear Rate Profiles**

Xanthan Concentration (mg/L)	Zero Shear Viscosity (cP)	Pa	$\gamma_{1/2}$ ( $\text{sec}^{-1}$ )
1000	248	1.6	0.37
500	36	1.6	3
250	7.7	1.6	11



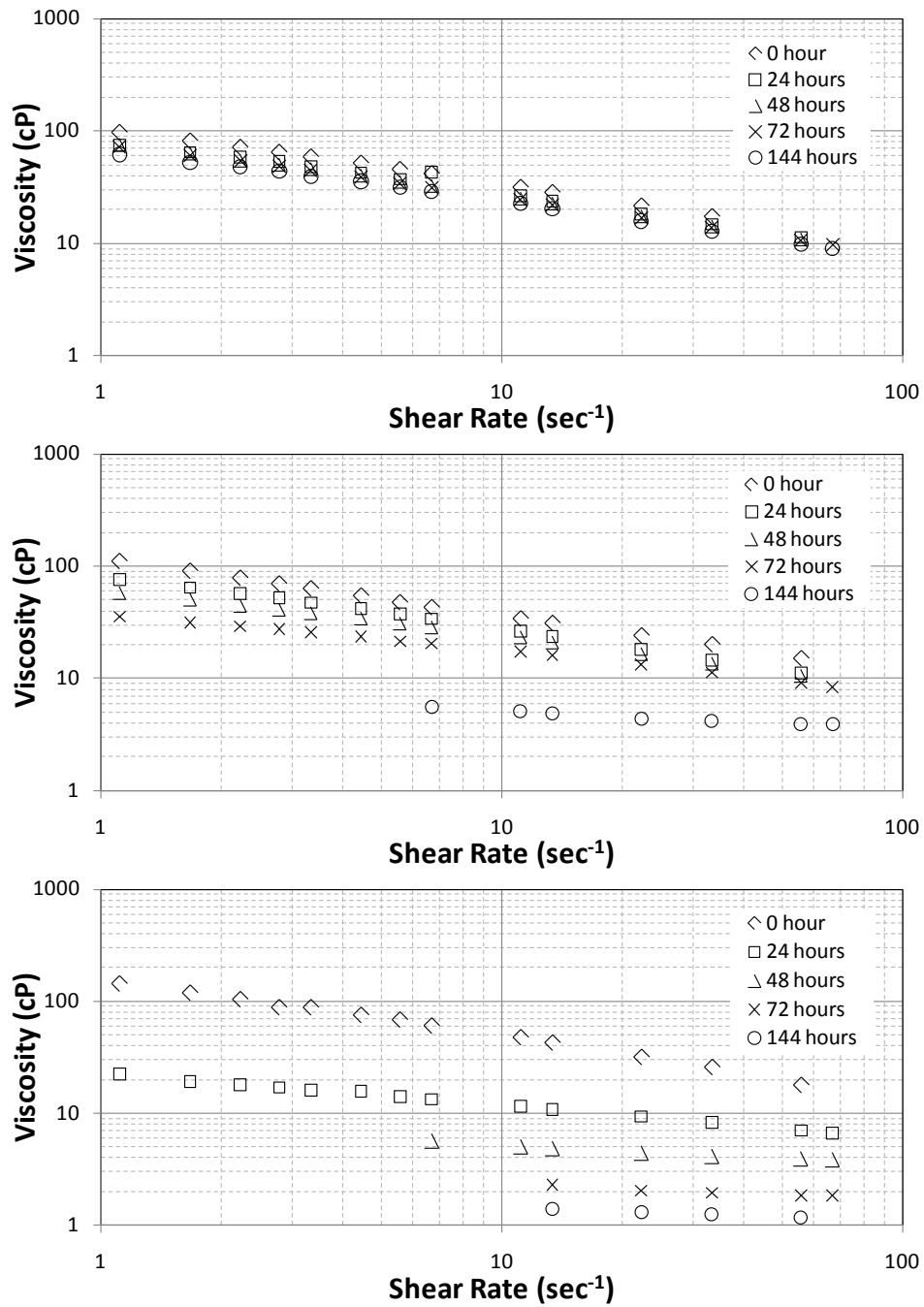


**Figure 15.** Viscosity-shear rate functions showing viscosity loss due to oxidation of xanthan gum (1000 mg/L polymer case)

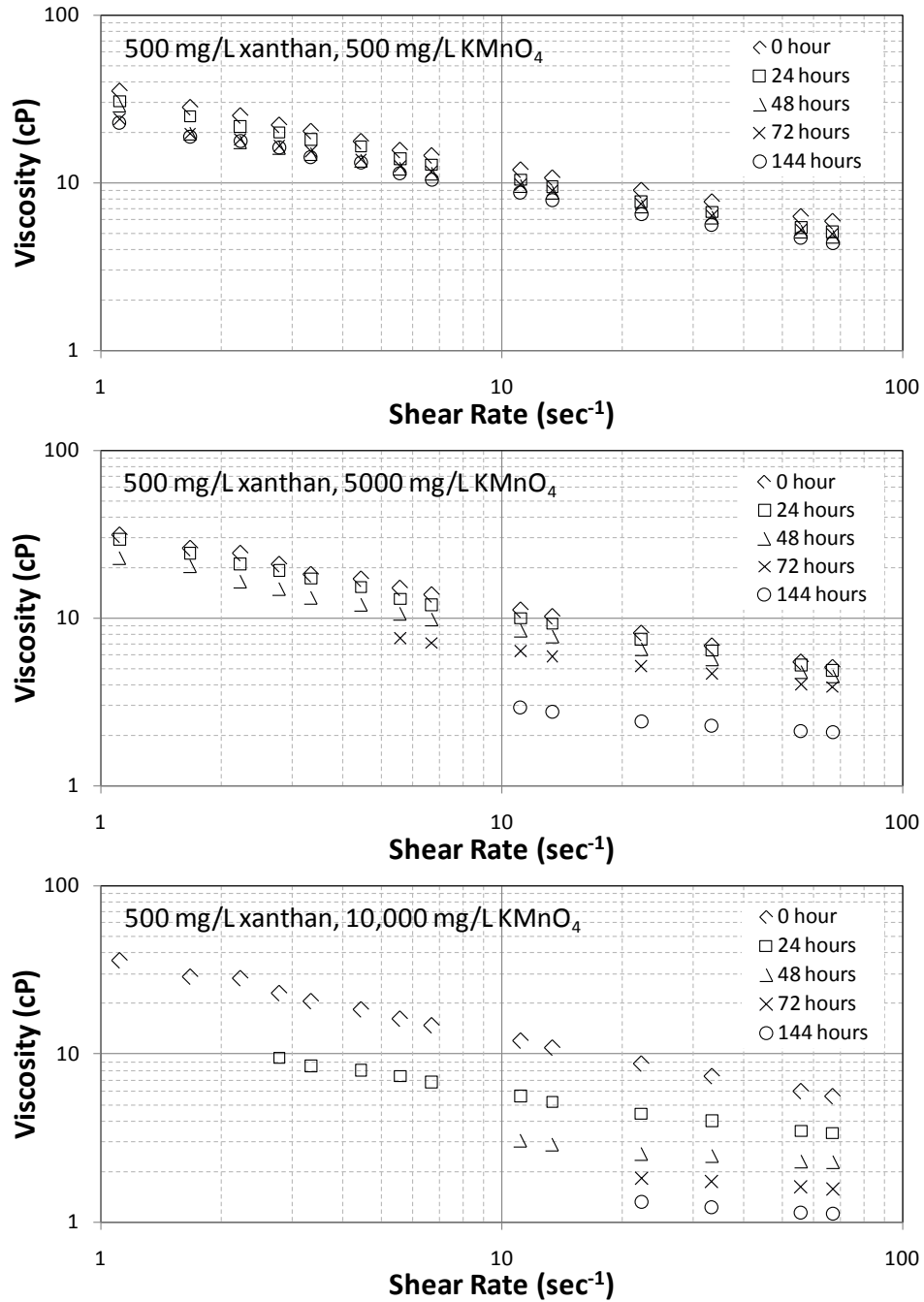


**Figure 16.** Viscosity-shear rate functions showing viscosity loss due to oxidation of xanthan gum (500 mg/L polymer case)

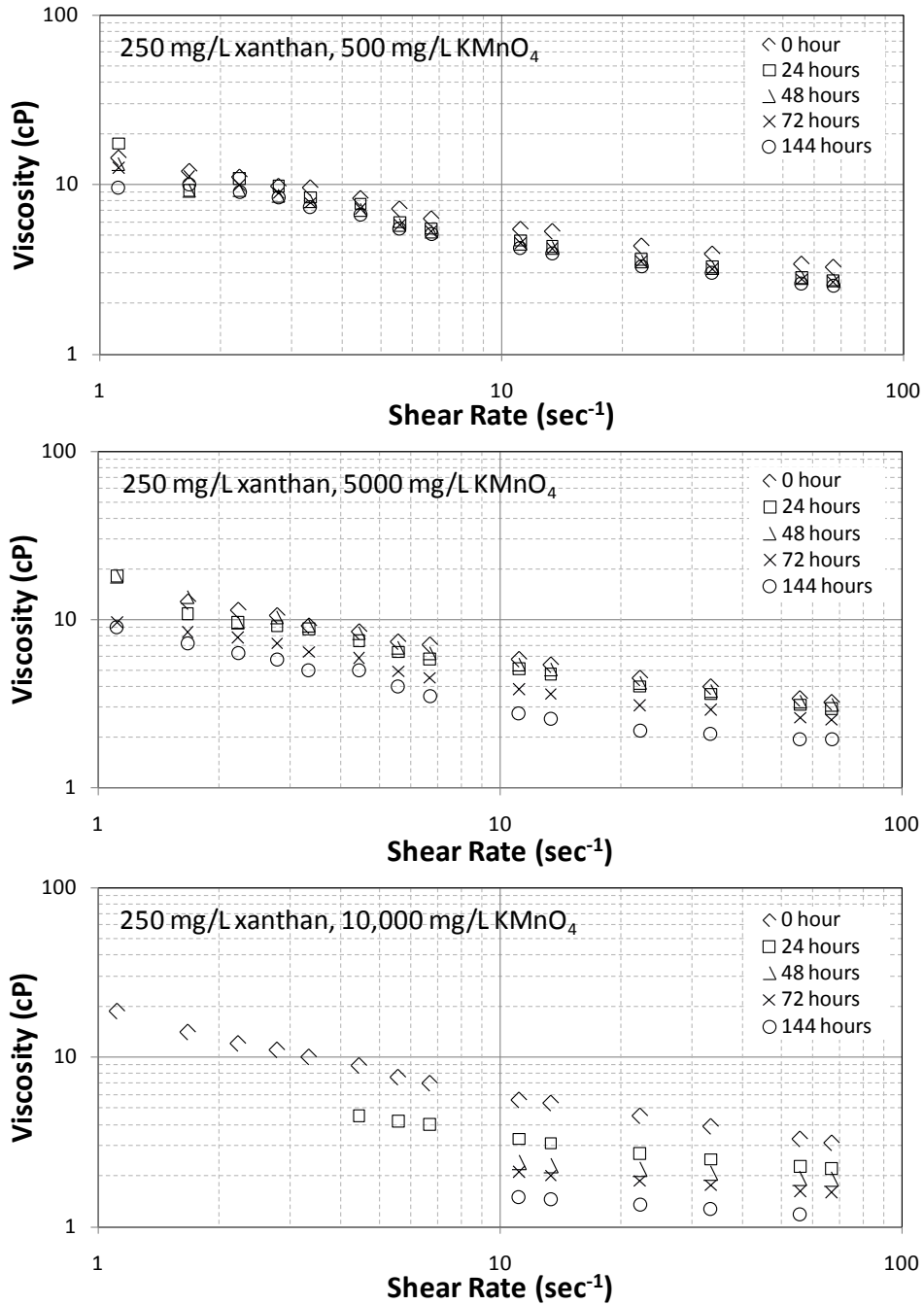


**Figure 17.** Viscosity-shear rate functions showing viscosity loss due to oxidation of xanthan gum (250 mg/L polymer case)

### 4.3.2.2 Xanthan Oxidant Demand

The results of xanthan oxidant demand (no porous media included) measurements are presented in Table 12 and Figure 18. In all cases, the oxidant demand for xanthan gum biopolymer increased with increasing  $\text{KMnO}_4$  concentration. The oxidant demand is also shown to increase with increasing polymer concentration. At most, the percentage oxidant lost was 35% for the highest oxidant/polymer combination at the end of 480 hours (20 days). At minimum, the percentage oxidant lost was 3.5% at the same temporal endpoint. Results compared to those shown in Table 10, indicate that demand of the polymer for oxidant is minimal compared to the natural demand of the media for the oxidant. The selection of an optimal polymer/oxidant still largely depends on maintaining solution viscosity during subsurface injection. As demonstrated previously, the combination of 1,000 mg/L xanthan gum and 5000 mg/L  $\text{KMnO}_4$  oxidant provides both an appropriate viscosity-shear rate function for initial injection and reasonable viscosity retention. It is this polymer/oxidant combination that will be subsequently used for testing during 1-D column experiments. When comparing Table 10 (with porous media) oxidant demand results with Table 12 results (without porous media), it is apparent that while xanthan gum does exert some oxidant demand, the significant demand will be exerted by the porous media itself.

**Table 12. Results of Oxidant Demand for Xanthan Gum (no porous media)**  
**Measured Oxidant Demand (mg/L  $\text{KMnO}_4$ )**

Sample	Hours								
	0	2	4	8	24	48	72	288	480
250 Xanthan, 500 $\text{KMnO}_4$	4.4	2.4	1.9	3.9	12.4	11.4	12.4	16.9	17.0
250 Xanthan, 5000 $\text{KMnO}_4$	193.4	77.2	117.6	127.7	233.8	147.9	158.0	365.1	390.3
250 Xanthan, 10000 $\text{KMnO}_4$	281.4	170.9	180.9	211.0	331.7	70.4	100.5	763.8	1045.2
500 Xanthan, 500 $\text{KMnO}_4$	7.9	5.4	4.4	-3.1	21.4	10.4	21.9	31.9	33.0
500 Xanthan, 5000 $\text{KMnO}_4$	158.0	36.8	57.0	-13.7	279.2	122.7	248.9	521.6	652.9
500 Xanthan, 10000 $\text{KMnO}_4$	402.0	422.1	723.6	361.8	211.0	261.3	381.9	1185.9	1869.3
1000 Xanthan, 500 $\text{KMnO}_4$	20.4	6.9	5.4	9.4	35.4	38.4	41.4	59.9	65.0
1000 Xanthan, 5000 $\text{KMnO}_4$	57.0	173.2	102.5	238.8	395.4	324.7	471.1	930.7	1152.9
1000 Xanthan, 10000 $\text{KMnO}_4$	311.5	371.9	432.2	331.7	321.6	412.0	673.4	2331.6	3447.2

### Percent $\text{KMnO}_4$ Lost

Sample	Hours								
	0	2	4	8	24	48	72	288	480
250 Xanthan, 500 $\text{KMnO}_4$	0.9	0.5	0.4	0.8	2.5	2.3	2.5	3.4	3.4
250 Xanthan, 5000 $\text{KMnO}_4$	3.9	1.5	2.4	2.6	4.7	3.0	3.2	7.3	7.8
250 Xanthan, 10000 $\text{KMnO}_4$	2.8	1.7	1.8	2.1	3.3	0.7	1.0	7.6	10.5
500 Xanthan, 500 $\text{KMnO}_4$	1.6	1.1	0.9	-0.6	4.3	2.1	4.4	6.4	6.6
500 Xanthan, 5000 $\text{KMnO}_4$	3.2	0.7	1.1	-0.3	5.6	2.5	5.0	10.4	13.1
500 Xanthan, 10000 $\text{KMnO}_4$	4.0	4.2	7.2	3.6	2.1	2.6	3.8	11.9	18.7
1000 Xanthan, 500 $\text{KMnO}_4$	4.1	1.4	1.1	1.9	7.1	7.7	8.3	12.0	13.0
1000 Xanthan, 5000 $\text{KMnO}_4$	1.1	3.5	2.0	4.8	7.9	6.5	9.4	18.6	23.1
1000 Xanthan, 10000 $\text{KMnO}_4$	3.1	3.7	4.3	3.3	3.2	4.1	6.7	23.3	34.5

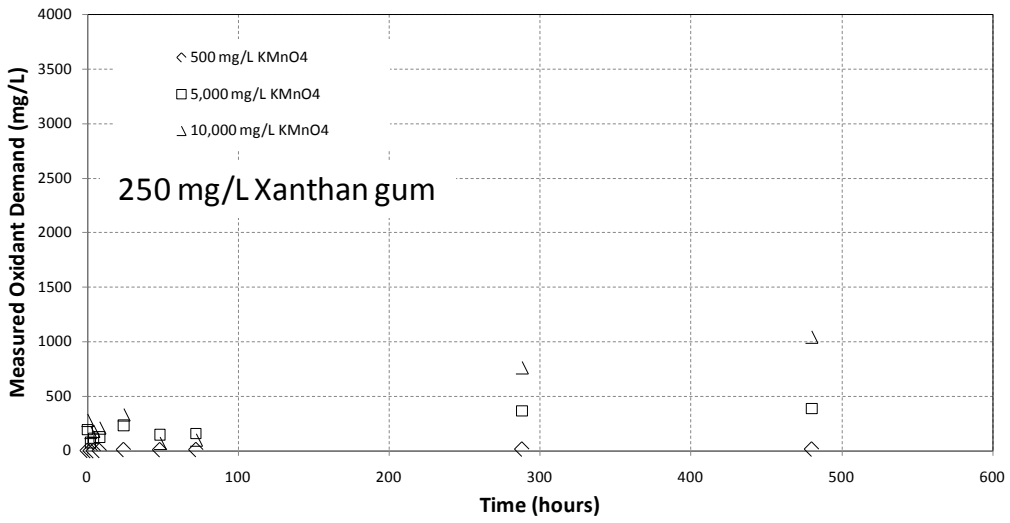
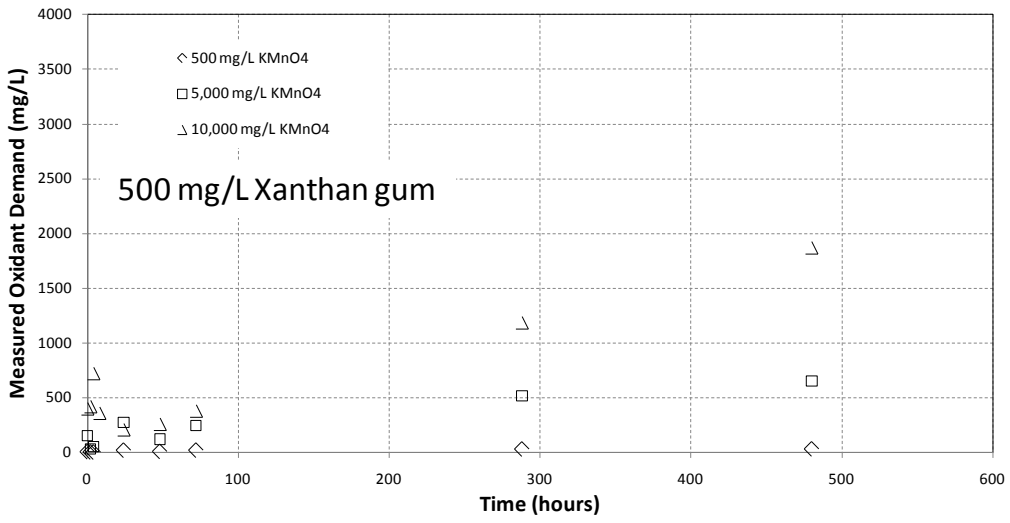
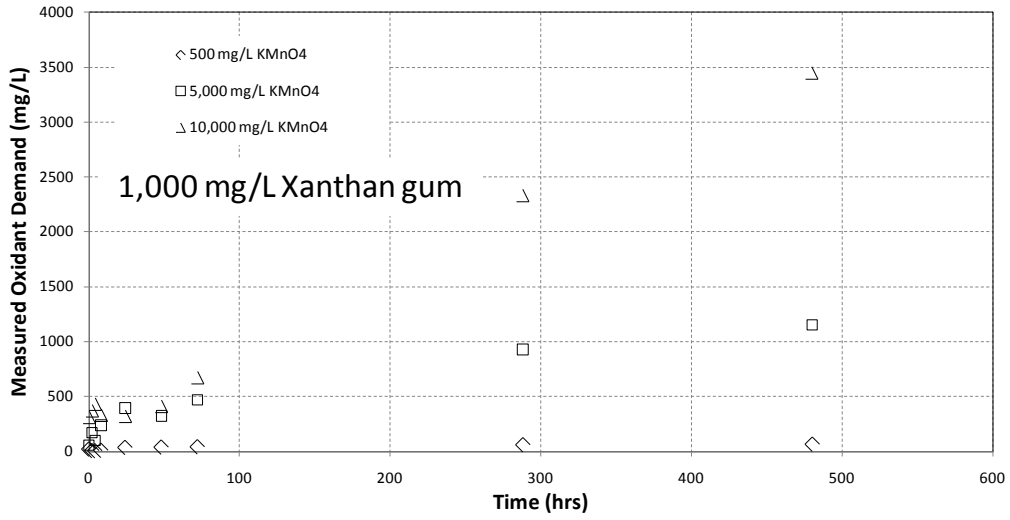


**Figure 18.** KMnO<sub>4</sub> demand as a function of time when exposed to 250, 500, and 1000 mg/L xanthan gum

### 4.3.2.3 Polymer/Oxidant Transport Conditions in Porous Media

***Oxidant-Only Flood.*** The initial hydraulic conductivity of the test sediment was measured at different volumetric flow rates that ranged between 0.25 and 4.5 cm<sup>3</sup>/min. The mean hydraulic conductivity for this sediment pack was  $4.2 \times 10^{-3}$  cm/sec or 11.9 feet/day. Hydraulic conductivities were also measured as a function of flow rate during oxidant injection and after water-flooding to remove the oxidant. Measured pressure drop and the resulting hydraulic conductivity measured during oxidant-only injection are presented in Figures 19 and 20. These results indicate that despite the high natural oxidant demand measured for these sediments the permeability of the test sediment was not reduced when the oxidant is injected alone.

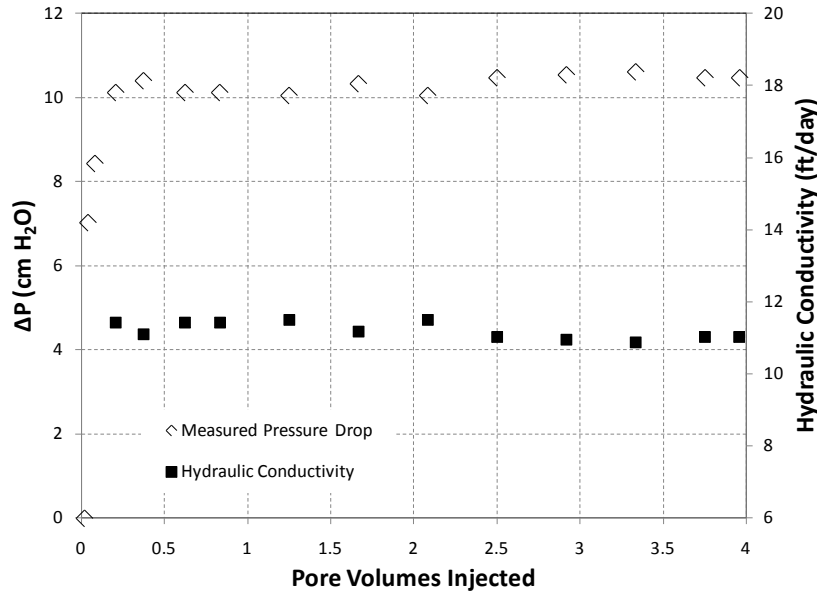


**Figure 19.** Pressure and hydraulic conductivity results measured during oxidant-only injection

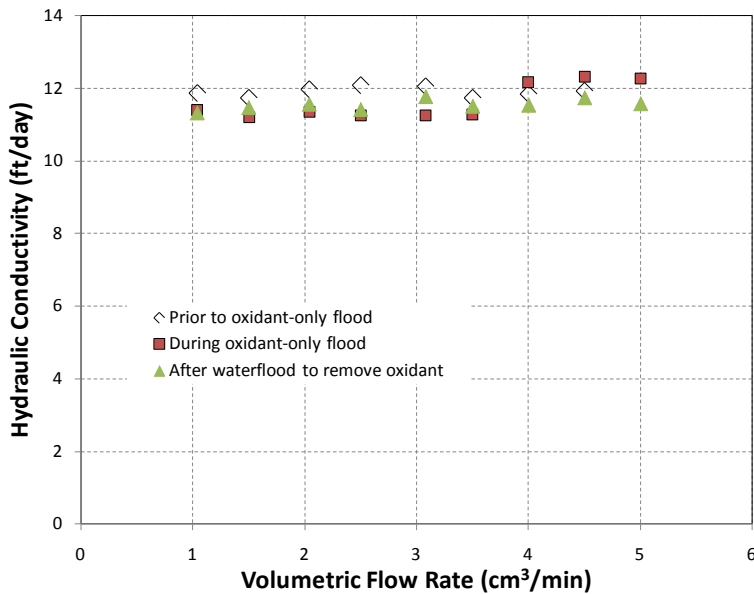


**Figure 20.** Measured hydraulic conductivities before, during, and after oxidant injection

***Polymer/Oxidant Injection without Pre-Filtering Solution.*** After re-packing and saturating the test column, the mean hydraulic conductivity of the sediment pack was measured to be  $3.8 \times 10^{-3}$  cm/sec or 10.8 feet/day. As shown in Figure 21, without pre-filtering the polymer/oxidant solution the pressure drop across the test column increased throughout the 8 pore volume injection, resulting in a continued reduction in hydraulic conductivity for this sediment. The implication of this is reduced injectivity of the polymer/oxidant solution during field implementation. The reduced hydraulic conductivity is, in part, a consequence of the increased viscosity of the polymer/oxidant solution (1,000 mg/L xanthan gum, 50,00 mg/L  $\text{KMnO}_4$ ). However, the continued reduction in conductivity implies *permeability* reduction as a result of partial pore plugging within the sand pack. During the conduct of SERDP Project ER-1486, this process was observed for non-filtered polymer floods within porous media possessing hydraulic conductivities less than  $4 \times 10^{-2}$  cm/sec or 113 feet/day and was determined to be the result of entrapment of polymer multi-molecular aggregates (or “microgels”, *Chauveteau and Kohler, 1984*) and extra-cellular debris common to xanthan gums when hydrated from dry powder form. Here, the results provided in Figure 21 again demonstrate the need for polymer solution filtration prior to subsurface injection to make the technology applicable to lower permeability sediments.

The initial hydraulic conductivity measured for this sediment pack is presented in Figure 22, and is compared the conductivity measured after 12 hours of water flooding to remove the polymer/oxidant solution. Note that the hydraulic conductivity of the sediment has been reduced by a factor of 16, reflecting an unfavorable reduction in sediment permeability and solution injectivity.

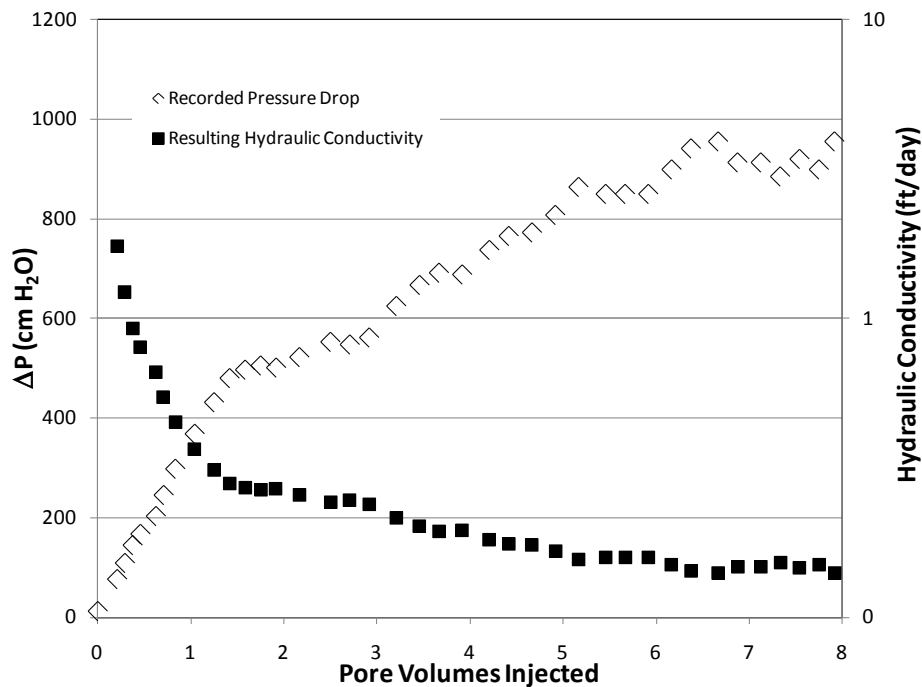


**Figure 21.** Pressure and hydraulic conductivity results for the polymer/oxidant injection (no filtration)

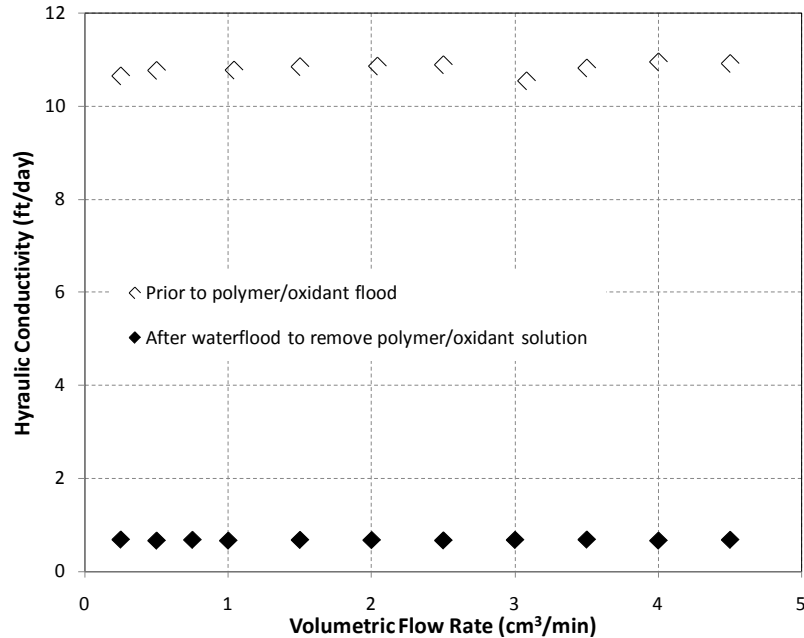


**Figure 22.** Measured hydraulic conductivities before and after polymer/oxidant injection (no filtration)

***Polymer/Oxidant Injection with Pre-Filtering.*** After again re-packing and saturating the test column, the mean hydraulic conductivity of the sediment pack was measured to be  $3.95 \times 10^{-3}$  cm/sec or 11.2 feet/day. Unlike the unfiltered polymer/oxidant flood, the column pressure drop stabilized after 4 pore volumes at about 330 cm H<sub>2</sub>O or 4.7 PSI, as shown in Figure 23. In response, the hydraulic conductivity during filtered polymer/oxidant solution injection stabilized at roughly  $1.45 \times 10^{-4}$  cm/sec or 0.41 feet per day. Filtered polymer/oxidant solution injection continued until 8 pore volumes had been passed through the column. At this point the flow rate was step-wise decreased to obtain a measured column pressure drop at different flow conditions. These data were used to calculate apparent solution viscosities and porous media equivalent shear rates within the sediment pack for each flow condition as described below. Water was then injected over night to remove the polymer/oxidant solution from the test column.

The initial hydraulic conductivity measured for this sediment pack is presented in Figure 24, and is compared the conductivity measured after 12 hours of water flooding. Porous media filtration of the polymer/oxidant solution prior to injection is shown to have reduced the hydraulic conductivity by just a factor of 5, compared to the factor of 16 reduction observed at the end of the unfiltered solution injection experiment. This reduction is attributed to a reduction in sediment permeability. Column experiments, using model sands possessing similar intrinsic permeabilities, were performed during the conduct of SERDP Project ER-1486. In the absence of oxidant, permeability reductions for these sands were found to range within a factor of 1.4 – 2. Significant manganese dioxide staining was observed within the effluent tubing and within the effluent waste collection vessel during the water flooding phase of these experiments. Given the high oxidant demand measured for these sediments, it is possible that MnO<sub>2</sub> precipitation was the cause of the elevated permeability reduction factor. Still, a factor of 5 reduction in permeability is reasonable for injection of these solutions at the field scale.



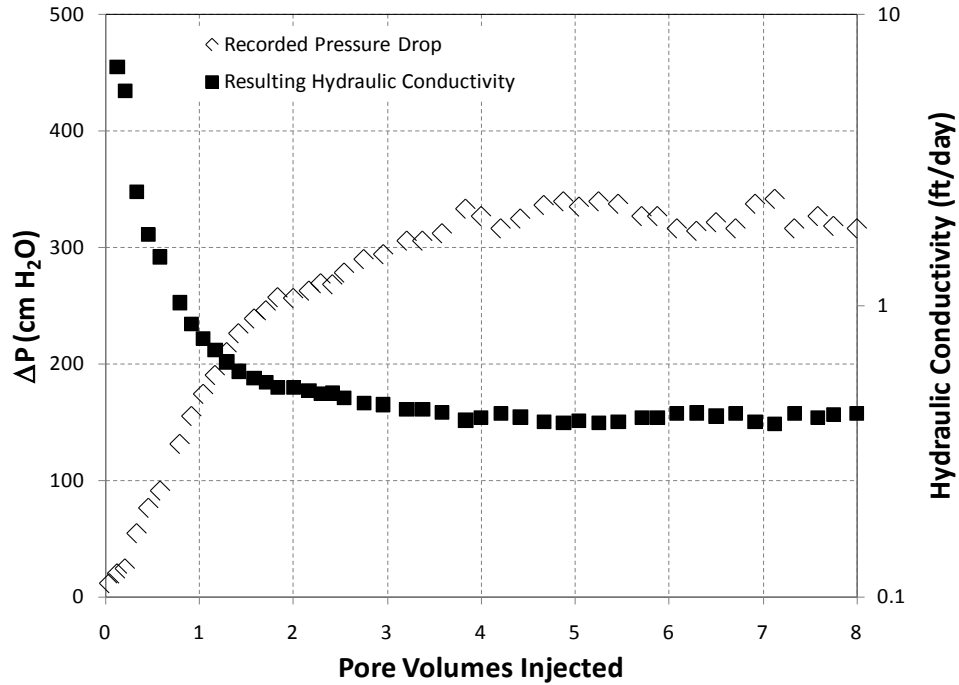


**Figure 23.** Pressure and hydraulic conductivity results for the polymer/oxidant injection (with filtration)

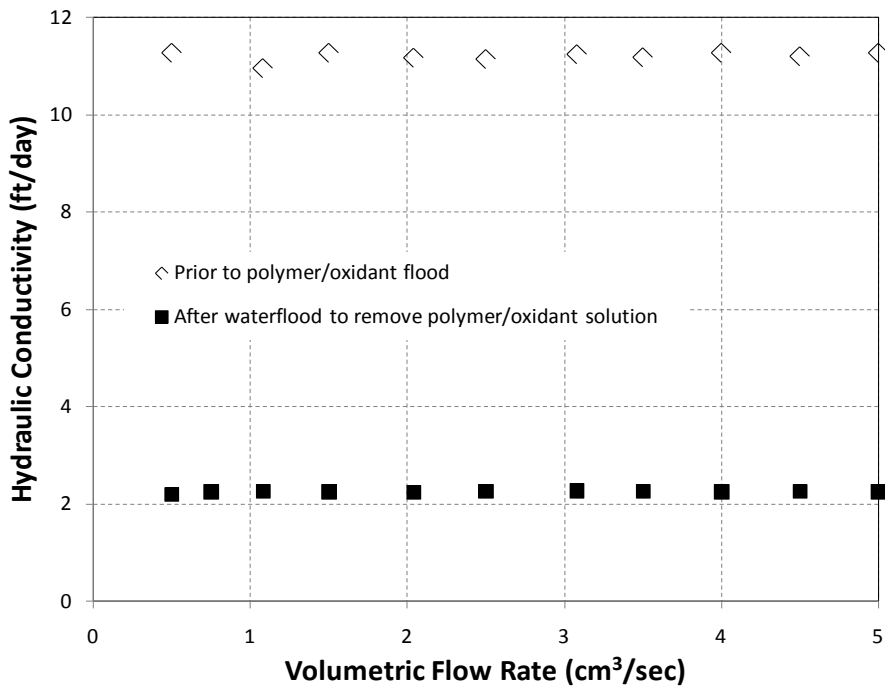


**Figure 24.** Pressure and hydraulic conductivity results for the polymer/oxidant injection (with filtration)

***Polymer/Oxidant Solution Rheological Properties in Porous Media.*** After injecting 8 pore volumes of filtered polymer/oxidant solution into the test column, the column pressure drop was measured as a function of flow rate to provide data needed to evaluate solution rheological behavior during transport within this test sediment. Apparent solution viscosities ( $\mu_{app}$ ) were calculated from this data by applying the following modification of Darcy's law:

$$\mu_{app} = \frac{k\rho g L}{q \Delta P} \quad [2]$$

where,  $\rho$  and  $g$  is the fluid density and gravity constant,  $q$  is the Darcy velocity, and  $L$  is the column length. Porous media equivalent shear rates were additionally calculated at each flow condition using the following modified Blake-Kozeny capillary bundle model:

$$\gamma_{eq} = \frac{3.97Cu}{\sqrt{k\Phi}} \quad [3]$$

where  $C$  is the shear rate coefficient used to account for non-ideal effects such as slip at the pore walls,  $u$  is the water phase frontal velocity (i.e., the average linear velocity of the advecting polymer front),  $k$  is the media permeability, and  $\Phi$  is the media porosity. The purpose of these calculations was to determine if apparent viscosities were changing with variations in shear rate within the sediment pack in a manner similar to the bulk solution viscosity/shear rate function measured by the rheometer. Any departures from the rheometer data could then be adjusted using the shear rate coefficient which would then allow the UTCHEM simulator to appropriately model in situ rheological behavior during our design simulations. The results of these calculations are plotted relative to the rheometer-derived dataset in Figure 25. Porous media equivalent viscosity/shear rate results were found to track closely to the rheometer results without needing to make adjustments to the shear rate coefficient. A value of  $C = 1$  will be used in the design simulations.

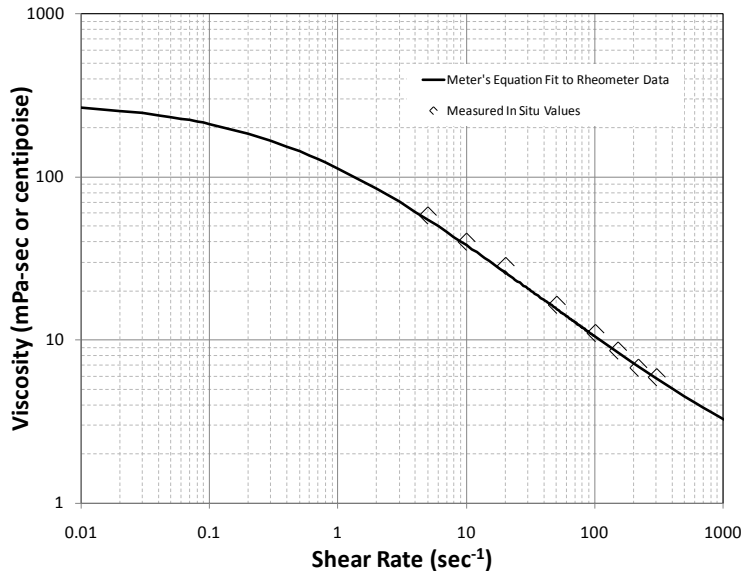


**Figure 25.** Rheometer and porous media equivalent viscosity/shear rate functions (1000 mg/L xanthan gum, 5000 mg/L KMnO<sub>4</sub> solution)

#### 4.3.2.4 Polymer/Oxidant Mixing Strategy

The equipment to complete this task has been acquired and tests will be completed within several weeks. Results will guide the field-scale mixing strategy and do not present a go/no-go challenge.

### 4.3.3 Objective 2: Manganese Dioxide Control

#### 4.3.3.1 Optimum Oxidant/SHMP Mixture

Our objective is to employ the lowest concentration of SHMP as possible (for economic purposes) that will maintain a steady and high concentration of  $\text{MnO}_2$  dissolved or suspended in solution. Data support the use of the highest concentration, 2,000 mg/L, of polymer tested, as shown in Figure 26.

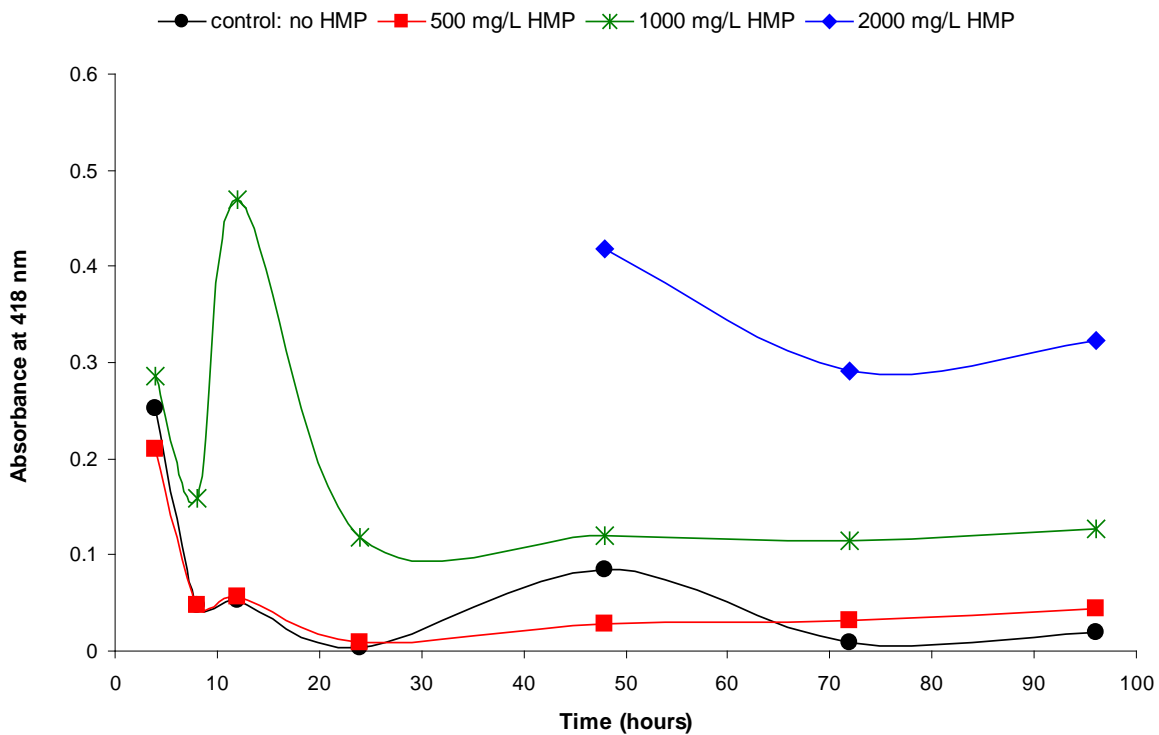


**Figure 26.** Absorbance of samples at 418 nm over time. Absorbance at this wavelength represents light scattering due to dissolved/suspended  $\text{MnO}_2$ , where higher values indicate a higher concentration of smaller particles dissolved or suspended in solution. Note that values prior to 48 hours for the 2,000 mg/L HMP condition (highest concentration) are greater than the instrument's upper detection limit of Absorbance = 1.0.

#### 4.3.3.2 Manganese Dioxide Transport

Figure 27 presents the results of pre-treatment tracer data for the 1-D columns. Note that 1 pore volume of fluid delivery is equivalent to 115-120 minutes. Data indicate a slight difference in flow rate through the columns, but there is no indication of preferential flow or major differences in packed column characteristics.

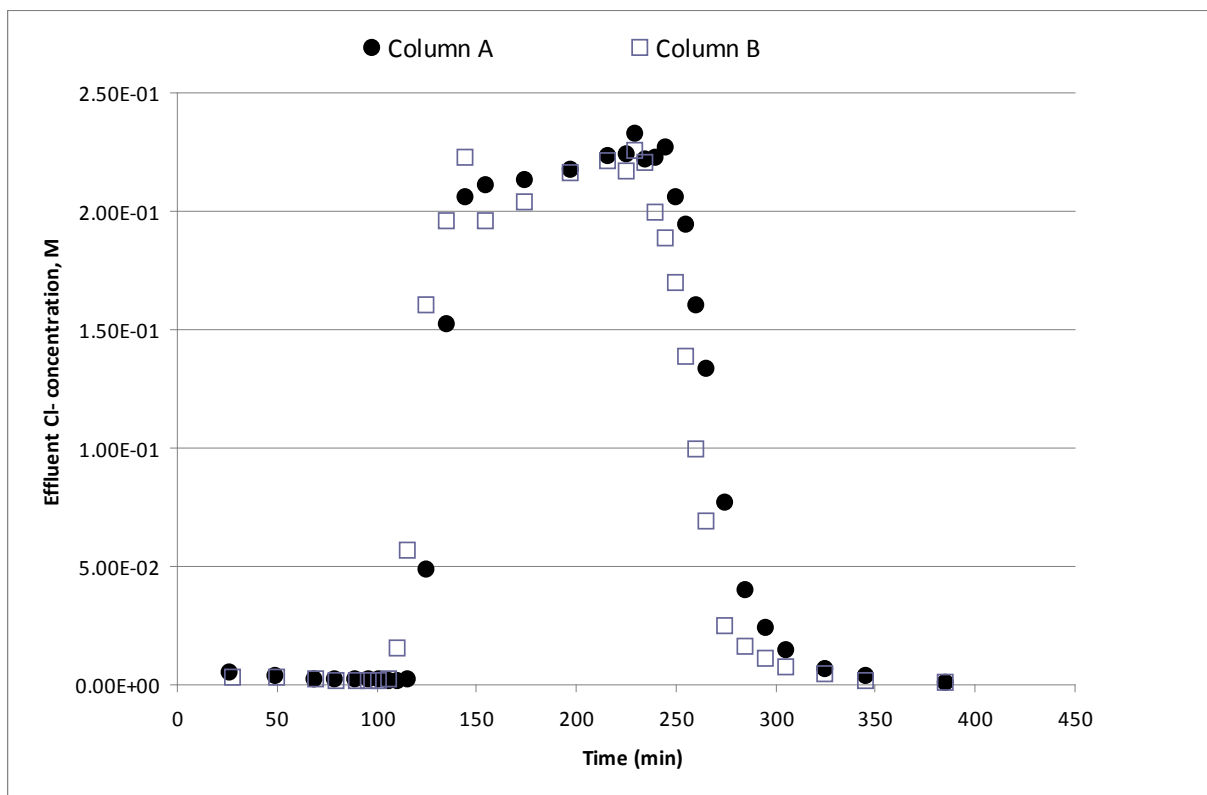


**Figure 27.** Tracer evaluation for transport columns

Figure 28 shows the column effluent absorbance at 418 nm with pore volume throughput, which indicates the relative amount of  $\text{MnO}_2$  (and possibly other aquifer solids) passing through the column. Data are shown until the point where columns plugged: < 1 PV for the permanganate only column and just before 2 PVs for the permanganate plus SHMP column. Note the small scale on the y-axis compared to Figure 19, indicating that an extensive amount of  $\text{MnO}_2$  were likely deposited within the column, even in the SHMP-containing system. It is possible the columns clogged due to the solids loading from  $\text{KMnO}_4$ , the oxidant itself, however this is unlikely because a similar concentration of sodium chloride passed through the column during the tracer test and greater than 99% of the solids were recovered without difficulty. It is more likely that pressure within the column increased due to deposition of  $\text{MnO}_2$ , causing back pressure the laboratory pump could not overcome. An extraction was performed on the media in the column with distance from the influent to help identify where deposition and clogging occurred. These data are pending analysis.

We expected the permanganate only column to plug in this media due to its fine nature and high NOD; however, this was not anticipated in the column with SHMP. Although the SHMP column did outperform the permanganate only column, a higher delivery rate (limiting extent of NOD due to less contact time) and a higher delivery pressure are recommended for field application.

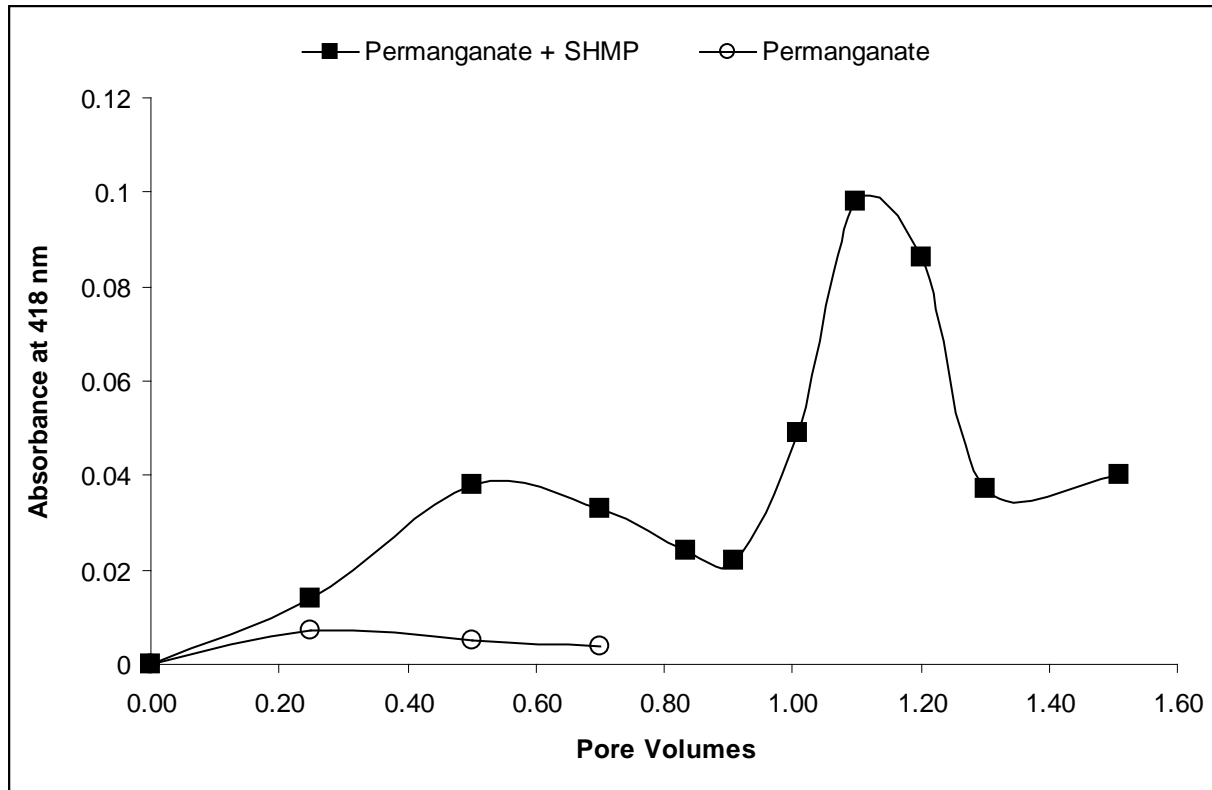


**Figure 28.** Column effluent absorbance at 418 nm – indicator of dissolved or suspended  $MnO_2$  concentration passing through column

## 5.0 Summary

The data collected during previous investigations and remedial activities at Site 88 in MCB Camp Lejeune provide a clear picture of the site conditions on a large scale. The field characterization activities and laboratory tests and analyses described herein have provided the data needed at this pilot demonstration scale to achieve the stated objectives so that the performance of the technologies can be properly evaluated. The results of the field and laboratory activities, in addition to the existing data, will be used to develop the Demonstration Plan (system design). This will ensure that the performance criteria can be successfully evaluated when the technology is applied at the site.

## 6.0 References

- APHA-AWWA-WPCF, (1998). Standard Methods for Examination of Water and Wastewater, 20th ed., Clesceri, L.S., A.E. Greenberg, and R.R. Trussell, eds. APHA-AWWA-WPCF, Washington, DC.
- ASTM (1991). Standard Practice for Sampling Waste and Soils for Volatile Organics. D4547-91. In: 1992 Annual Book of ASTM Standards, Vol. 11.04, pp. 108-111.

- Baker Environmental, Inc. (Baker) (1998). *Final Focused Remedial Investigation Report, Operable Unit No. 15 (Site 88), Marine Corps Base, Camp Lejeune, North Carolina*. May.
- Battelle Memorial Institute (BMI) (2001). *Reductive Anaerobic Biological In Situ Treatment Technology (RABITT) Treatability Test, Interim Report*. August.
- Carter, M.R. (1993). *Soil Sampling and Methods of Analysis*. Lewis Publishers, Ann Arbor, MI.
- CH2M Hill (2008). *Final Remedial Investigation Report, Site 88, Operable Unit No. 15, Marine Corps Base Camp Lejeune, Jacksonville, North Carolina*.
- CH2M HILL (2002). *Draft Supplemental Site Investigation Report, Operable Unit 15 (Site 88), Building 25 Base Dry Cleaners*. September.
- CH2M HILL (2003). *Supplemental Site Investigation Report, Operable Unit 15 (Site 88), Building 25 Base Dry Cleaners*. December.
- CH2M HILL (2004a). *Membrane Interface Probe Investigation*.
- CH2M HILL (2004b). *Site 88 Building 25 Source Removal Engineering Evaluation/Cost Analysis*. September.
- CH2M HILL (2006). *Draft Site 88 Building 25 Source Removal Non-Time Critical Removal Action Report*. March.
- CH2M HILL (2008a). *Final Remedial Investigation Site 88, Operable Unit No. 15, Building 25*. March.
- CH2M HILL (2008b). *Draft Feasibility Study, Site 88, Operable Unit No. 15*. February.
- Chandranth, M.S. and G.L. Amy (1996). Effects of Ozone on the Colloidal Stability and Aggregation of Particles Coated with Natural Organic Matter. *Environmental Science and Technology*, 30(2):431-442.
- Chao, T.T. (1972). Selective Dissolution of Manganese Oxides from Soils and Sediments with Acidified Hydroxylamine Hydrochloride. *Soil Sci. Soc. Am. Proc.* Oct 29-Nov 3, Miami Beach, FL.
- DE&S – Duke Engineering & Services (1999). *DNAPL Site Characterization Using a Partitioning Interwell Tracer Test at Site 88, Marine Corps Base Camp Lejeune, North Carolina (Final Report)*.
- Doona C.J. and F.W. Schneider (1993). Identification of Colloidal Mn(IV) in Permanganate Oscillating Reactions. *J. Am. Chem. Soc.*, 115:9683-9686.
- Duke Engineering and Services (Duke) (1999). *DNAPL Site Characterization using a Partitioning Interwell Tracer Test at Site 88, Marine Corps Base, Camp Lejeune, North Carolina*. July.
- Duke. 2000. *Surfactant-Enhanced Aquifer Remediation Demonstration at Site 88, Marine Corps Base, Camp Lejeune, North Carolina*. January.
- Insausti, M.J., F. Mata-Perez, and P. Alvarez-Macho (1992). Permanganate Oxidation of Glycine: Influence of Amino Acid on Colloidal Manganese Dioxide. *International Journal of Chemical Kinetics*, 24(5):411-419.
- Insausti, M.J., F. Mata-Perez, and P. Alvarez-Macho (1993). UV-VIS Spectrophotometric Study and Dynamic Analysis of the Colloidal Product of Permanganate Oxidation of  $\alpha$ -Amino Acids. *React. Kinet. Catal. Lett.*, 51(1):51-59.
- Kieft, T.L. and T.J. Phelps (1997). *Life in the Slow Lane: Activities of Microorganisms in the Subsurface*. CRC Press, Inc. pp. 135-161.
- Klute, A. et al., (ed.) (1986). *Methods of Soil Analysis, Part 1. Physical and Mineralogical Methods*. Soil Sci. Soc. Am. Madison, WI.

- Lee E.S., Y.Seol, Y.C. Fang, and F.W. Schwartz (2003). Destruction Efficiencies and Dynamics of Reaction Fronts Associated with Permanganate Oxidation of Trichloroethylene. *Environmental Science and Technology*, 37(11):2540-2546.
- Li X.D. and F.W. Schwartz (2000). Efficiency problems related to permanganate oxidation schemes. In: G.B. Wickramanayake, A.R. Gavaskar, A.S.C. Chen (ed.). *Chemical Oxidation and Reactive Barriers: Remediation of Chlorinated and Recalcitrant Compounds*. Battelle Press. Columbus, OH. pp. 41-48.
- Lowe, K.S., F.G. Gardner, R.L. Siegrist, and T.C. Houk (2000). EPA/625/R-99/012. US EPA Office of Research and Development, Washington, D.C.
- Morgan, J.J. and W. Stumm (1964). Colloid-Chemical Properties of Manganese Dioxide. *Journal of Colloid Science*, 19:347-359.
- OHM Remediation Services Corporation (OHM) (1996). *Contractor's Closeout Report, Underground Storage Tank Removals at Building 25, MCB Camp Lejeune, North Carolina*. October.
- Perez-Benito, J.F. and C. Arias (1991). A Kinetic Study of the Permanganate Oxidation of Triethylamine. Catalysis by Soluble Colloids. *International Journal of Chemical Kinetics*, 23:717-732.
- Perez-Benito, J.F. and C. Arias (1992a). A Kinetic Study of the Reaction Between Soluble (Colloidal) Manganese Dioxide and Formic Acid. *Journal of Colloid and Interface Science*, 149(1):92-97.
- Perez-Benito, J.F. and C. Arias (1992b). Occurrence of Colloidal Manganese Dioxide in Permanganate Reactions. *Journal of Colloid and Interface Science*, 152(1):70-84.
- Perez-Benito, J.F., C. Arias, and E. Brillas (1990). A Kinetic Study of the Autocatalytic Permanganate Oxidation of Formic Acid. *International Journal of Chemical Kinetics*, 22:261-287.
- Perez-Benito, J.F., E. Brillas, and R. Pouplana (1989). Identification of a Soluble Form of Colloidal Manganese (IV). *Inorganic Chemistry*, 28:390-392.
- Phelps T.J., S.M. Pfiffner, K.A. Sargent, and D.C. White (1994b). Factors Influencing the Abundance and Metabolic Capacities of Microorganisms in Eastern Coastal Plain Sediments. *Microb. Ecol.* 28:351-364.
- Phelps T.J., E. Murphy, S.M. Pfiffner, and D.C. Whiate (1994a). Comparison Between Geochemical and Biological Estimates of Subsurface Microbial Activities. *Microbial Ecology*, 28:335-349.
- Reitsma S. and M. Marshall (2000). In: G.B. Wickramanayake, A.R. Gavaskar, A.S.C. Chen (ed.). *Chemical Oxidation and Reactive Barriers: Remediation of Chlorinated Compounds*. Battelle Press. Columbus, OH. p. 25-32.
- Sparks D.L., A.L. Page, P.A. Helmke, R.H. Loeppert, P.N. Soltanpour, MA. Tabatabai, C.T. Johnson, and M.E. Sumner (ed.) (1996). *Methods of Soil Analysis: Part 3 – Chemical Methods*. Soil Sci. Soc. Am. Madison, WI.
- Tan, K.H. (1996). *Soil Sampling, Preparation, and Analysis*. Marcel Dekker, Inc. New York. 407 pp.
- USEPA (1986). *Test Methods for the Evaluation of Soil Waste, Physical/Chemical Methods*. SW-846, 3<sup>rd</sup> ed. Off. Solid Waste and Emergency Response, Washington DC.
- USEPA (1990). *Second update to SW-846 Methods Section*. Office of Solid Waste. U.S. Environmental Protection Agency, Washington DC.

- Weaver R.W., S. Angle, P. Bottomley, D. Bezdick, S. Smith, A. Tabatabai, and A. Wollum (ed) (1994). *Methods of Soil Analysis: Part 2 – Microbiological and Biochemical Properties*. Soil Sci. Soc. Am., Madison, WI.
- West, O.R., R.L. Siegrist, S.R. Cline, and F.G. Gardner (2000). The effects of in situ chemical oxidation through recirculation (ISCOR) on aquifer contamination, hydrogeology, and geochemistry. Oak Ridge National Laboratory internal report submitted to the Department of Energy, Office of Environmental Management, Subsurface Contaminants Focus Area.
- West, O.R., S.R. Cline, W.L. Holden, F.G. Gardner, B.M. Schlosser, J.E. Thate, D.A. Pickering, T.C. Houk (1998). ORNL/TM-13556, Oak Ridge National Laboratory, Oak Ridge, Tennessee.



# Appendix A: Field Characterization Report

## A. Site Description

### *A.1 Site Location and History*

The test area is located at MCB CamLej in Jacksonville, North Carolina. MCB CamLej covers approximately 236 square miles and is a training base for the United States Marine Corps. The test area is located within OU 15, Site 88, which consists of the former Base Dry Cleaning facility (former Building 25), located approximately 500 feet east of the intersection of Post Lane Road and McHugh Boulevard (**Figure A-1**). The test area is located within and immediately west of the footprint of the former Building 25 (**Figure A-2**).

Former Building 25 operated as a dry cleaning facility from the 1940s until 2004 when operations ceased and the building was demolished. Five 750-gallon underground storage tanks (USTs) were installed on the north side of the building to store dry cleaning fluids. Initially, Varsol™, a petroleum hydrocarbon-based stoddard solvent, was used in dry cleaning operations at Building 25. Due to flammability concerns, Varsol's use was discontinued in the 1970s and was replaced with tetrachloroethene (PCE). PCE was stored in a 150-gallon aboveground storage tank (AST) adjacent to the north wall of Building 25, in the same vicinity as the USTs. PCE was reportedly stored in the AST from the 1970s until the mid-1990s. Facility employees have reported that during this time, spent PCE was disposed of in floor drains that discharged into the sanitary sewer system on the north side of the building (**Figure A-2**).

In December 1986 and again in March 1995, self-contained dry cleaning machines were installed in Building 25, eliminating the need for bulk storage of PCE. The USTs and AST were removed in November 1995.

During removal of the USTs and ASTs, chlorinated volatile organic compounds (VOCs) were detected in soil and groundwater samples. Subsequent investigations conducted in 1996 and 1997 identified subsurface soil contamination under and near Building 25, and along a line of borings paralleling the underground sanitary sewer line north of Building 25, which was attributed to the leakage of solvent-contaminated wastewater (Baker, 1998a). Groundwater analytical results identified wide-spread chlorinated solvent contamination (PCE, trichloroethene [TCE], and cis-1,2-dichloroethene [cis-1,2-DCE]), which had impacted the Surficial Aquifer (less than 25 ft below ground surface [bgs]) and the upper portion of the Castle Hayne Aquifer (25-80 ft bgs). A distinct contaminant plume was identified, which suggested Building 25 was the source area. The results also suggested the presence of a dense non-aqueous phase liquid (DNAPL) in this area.

In 2005, shallow soil mixing with clay and zero valent iron (ZVI) was implemented at Site 88 in the vicinity of former Building 25, as shown on **Figures A-2** and **A-3**, to contain and treat the DNAPL source area. Approximately 7,050 cubic yards of impacted soil was treated. Within the soil mixing zone, PCE concentrations in the soil were reduced by greater than 99 percent. Despite the significant source area mass flux reduction, residual groundwater contamination remains over a large portion of the surrounding and downgradient areas.





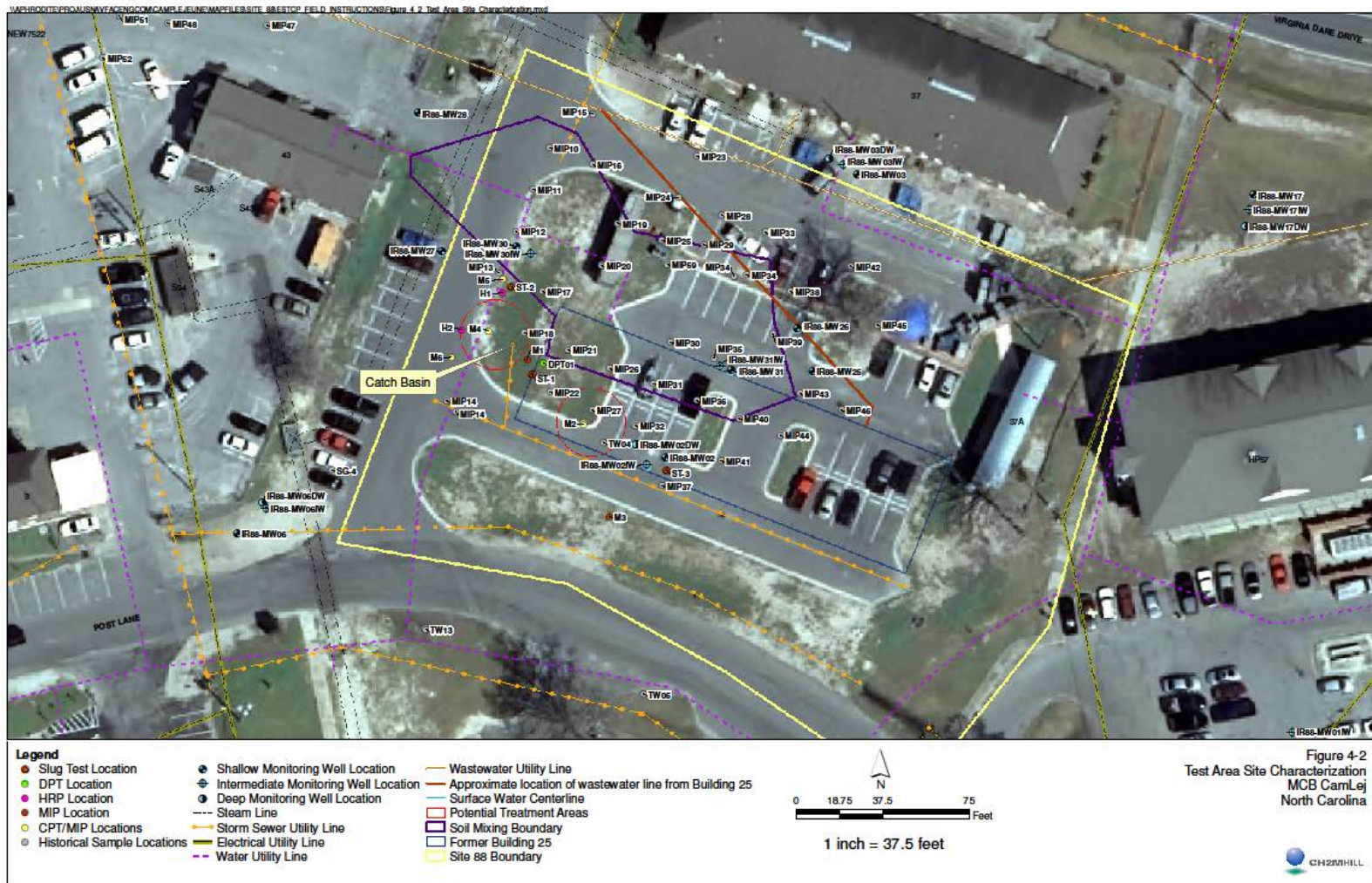


Figure A-2. Closer view of test area located within and immediately west of the footprint of the former Building 25.

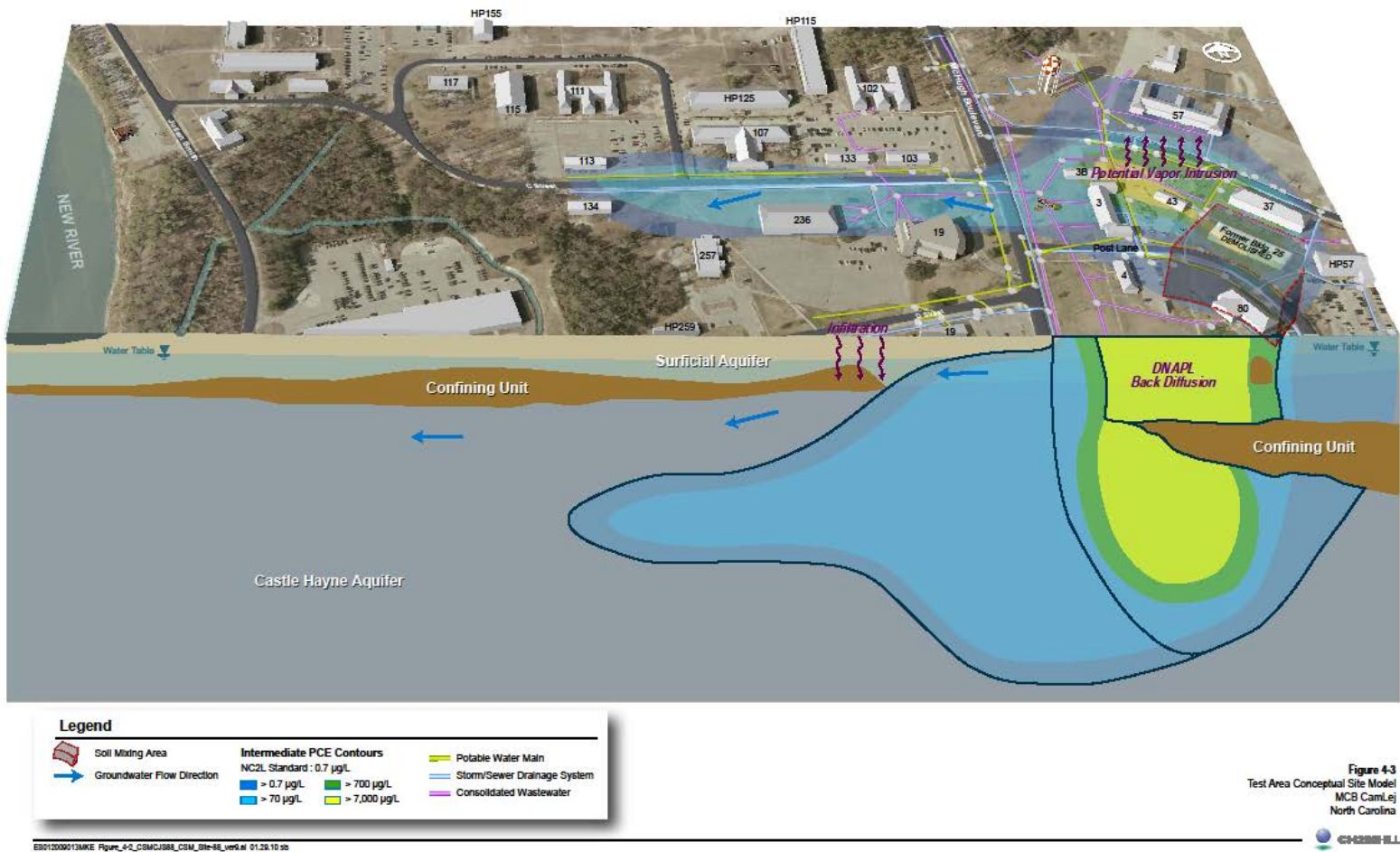


Figure A-3. Test area conceptual site model

Additional investigation and remediation activities conducted at Site 88 include:

- Free Phase DNAPL Recovery, 1998: Conducted north of Building 25
- Partitioning Inter-well Tracer Test (PITT), 1998: Conducted adjacent to the north wall of Bldg. 25
- Surfactant-Enhanced Aquifer Remediation (SEAR), 1998-1999: Conducted adjacent to the north wall of Building 25
- Reductive Anaerobic *In-Situ* Treatment Technology (RABITT), 2001: Conducted at monitoring wells IR88-MW05 and IR88-MW05IW, approximately 200 ft northwest of the test area

Site 88 is currently in the remedial investigation (RI)/feasibility study (FS) phase of the CERCLA process. A pilot study is planned for the summer of 2010 to evaluate in-situ chemical oxidation (ISCO) and enhanced reductive dechlorination (ERD) in the downgradient plume (approximately 400 feet downgradient of the test area). The test area, located within the source zone, will not be affected by on-going site activities.

## ***A.2 Geology and Hydrogeology***

### **A.2.1 Geology**

Southeastern North Carolina and MCB CamLej are within the Tidewater region of the Atlantic Coastal Plain physiographic province. The MCB CamLej area is underlain by a westward (inland) thinning wedge of marine and non-marine sediments ranging in age from early Cretaceous to Holocene. Along the coastline, several thousands of feet of interlayered, unconsolidated sediment are present, consisting of gravel, sand, silt, clay deposits, calcareous clays, shell beds, sandstone and limestone that was deposited over pre-Cretaceous crystalline basement rock.

Site 88 is underlain by a thick sequence of coastal plain soils consisting of unconsolidated sands, silts, clays, and partially indurated shelly sands. Soils within the Surficial Aquifer are generally comprised of silty sands, ranging in thickness from 20 to 30 feet, which overlie a discontinuous layer of clayey silt or clay approximately 20 ft bgs. A clayey silt and clay confining layer, ranging in thickness from 4 to 10 feet, underlies the former location of Building 25 at a depth of approximately 20 ft bgs and extends westward as far as Building 3, whereupon it pinches out and is not encountered again until the 88MW-15 well cluster (**Figure A-1**). Within the Castle Hayne Aquifer, a fine grained layer overlies massive beds of fine to medium grained sand with sporadic zones of partial cementation and shell fragments extending to a depth of roughly 180 feet bgs. At Site 88, the Castle Hayne Aquifer is divided into the upper Castle Hayne (25-80 feet), the middle Castle Hayne (80-130 feet), and the lower Castle Hayne (130-180 feet). A plastic clay layer, known as the Beaufort confining unit, was encountered beneath the Castle Hayne Aquifer; the Beaufort confining unit defines the vertical limit of subsurface investigation at Site 88.

The general geologic setting in the vicinity of the test area is presented on **Figure A-4**. The lithology in the test area was further investigated during site characterization activities conducted in Nov and Dec 2009. Cone penetrometer testing (CPT) was conducted at locations M2, M4, M5 and M6, shown on **Figure 4-2**, to delineate stratigraphic layers in the subsurface. High-resolution piezocone (HRP) profiling was conducted at location H1 to obtain detailed lithologic and hydraulic information. HRP results are provided in **Appendix B**. Additionally, a continuous soil core was collected from 10 to 50 ft bgs via direct push technology (DPT) at soil boring location DPT01, as shown on **Figure A-2**. The boring log for DPT01 is provided in **Appendix C**.



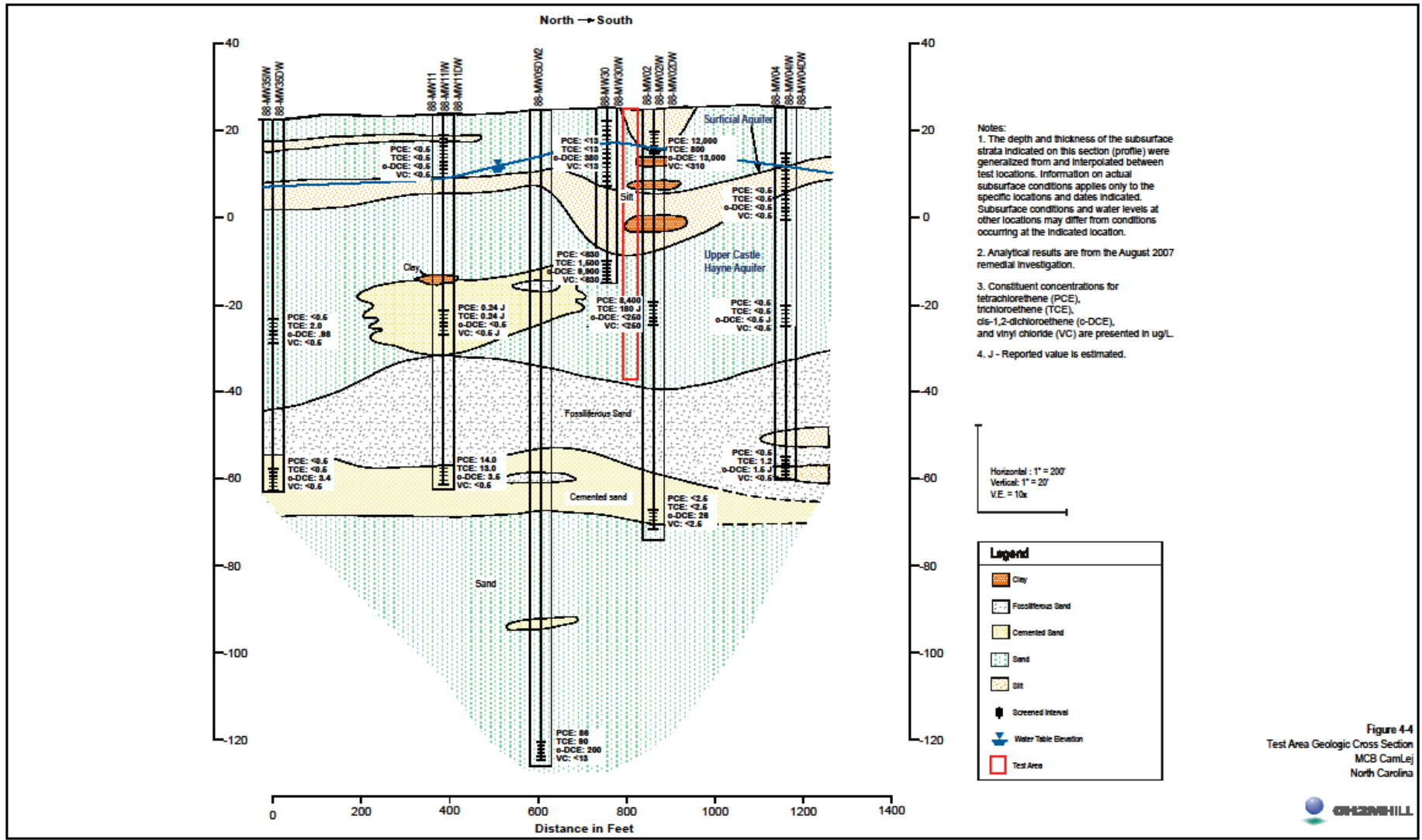


Figure 4-4  
Test Area Geologic Cross Section  
MCB CamLej  
North Carolina



Figure A-4. General geologic setting in vicinity of test area

The data collected during site characterization indicates alternating fine grained silty sand and sand to approximately 20 ft bgs in the vicinity of the test area. Soil particle size analysis has been completed for this shallower area. These data are included as **Appendix D**. The fine grained sediments are underlain by a more dense silty clay and clay layer approximately 7 to 12 feet thick to a depth of approximately 30 ft bgs. Below this unit are alternating layers of silty sand and sand. The sands become more dominate with depth and fewer fines are present, generally between 40 to 60 ft bgs. The boring log for deep monitoring well 88-MW02DW, located adjacent to the test area, indicates that fine grained silty sand is again present between 60 to 88 ft bgs, which is underlain by a layer of partially cemented sand and shells exists from 88 to 90 ft. A geologic cross-section within the vicinity of the test area based on site characterization activities is presented in **Figure 4-5**.

### **A.2.2 Hydrogeology**

The hydrogeologic setting at Site 88 is that of a two aquifer system, the Surficial Aquifer and the Castle Hayne Aquifer, with the two aquifers typically separated by a low permeability clayey silt aquitard (Duke, 1999). This low permeability unit is present under former Building 25 within the test area, and, as noted above, is discontinuous to the west of former Building 25.

In November 2009, depth-to-water measurements were taken across Site 88. In the vicinity of the test area, the water table was found to occur from 7.25 to 10.10 ft bgs. The depth to water in monitoring wells screened within the Upper Castle Hayne Aquifer in the vicinity of the test area, ranged from 14.46 to 15.62 ft bgs.

**Figure 4-6** shows the potentiometric surface of the Surficial Aquifer measured in November 2009, as represented by the shallow monitoring wells (less than 25 ft bgs). **Figure 4-6** shows a highly variable water table surface, which is likely due in part to the heterogeneous nature of the shallow sediments, and also the anthropogenic effects relating to the soil mixing activities. The soil mixing involved addition of a mixture of zero-valent iron and bentonite clay that significantly reduced the hydraulic conductivity of the mixed soil. Shallow groundwater flow in the test area is to the southwest, with a horizontal hydraulic gradient of approximately 0.002 ft/ft. A downward vertical hydraulic gradient of approximately 0.25 ft/ft between the Surficial Aquifer and the Upper Castle Hayne Aquifer in the test area was calculated, based on the November 2009 depth-to-water measurements collected in the IR88-MW02 cluster.

**Figure 4-7** shows the potentiometric surface of the Upper Castle Hayne Aquifer in November 2009, as represented by the intermediate zone wells (45 to 55 ft bgs). The groundwater flow pattern for this aquifer is less complex than that of the Surficial Aquifer, with groundwater flow generally to the west, with an approximate horizontal hydraulic gradient in the vicinity of the test area of 0.0004 ft/ft. A downward vertical gradient of 0.0015 ft/ft between the Upper Castle Hayne and Middle Castle Hayne Aquifers within the test area was calculated, based on the November 2009 depth-to-water measurements collected in the IR88-MW02 cluster.

Aquifer testing was conducted during site characterization activities in November and December 2009. A pneumatic slug test method was employed through DPT-installed steel rod piezometers at three locations across the test area, ST-1, ST-2, ST-3, shown on **Figure 4-2**. A groundwater sampler equipped with a screen was installed in each boring to the terminating depth of the testing interval. The drill rods were then pulled up to expose two feet of the screen and conduct the slug test.

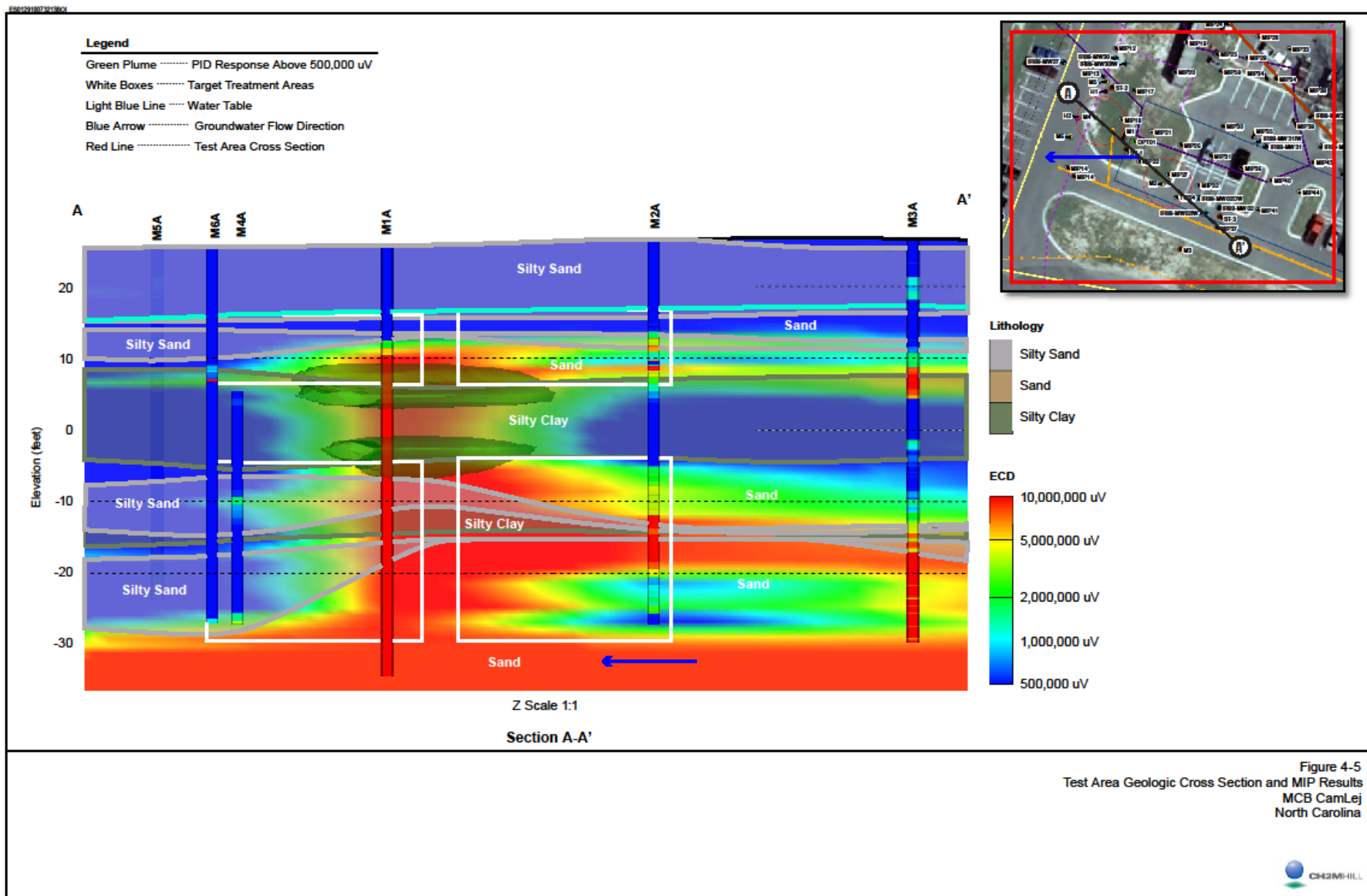
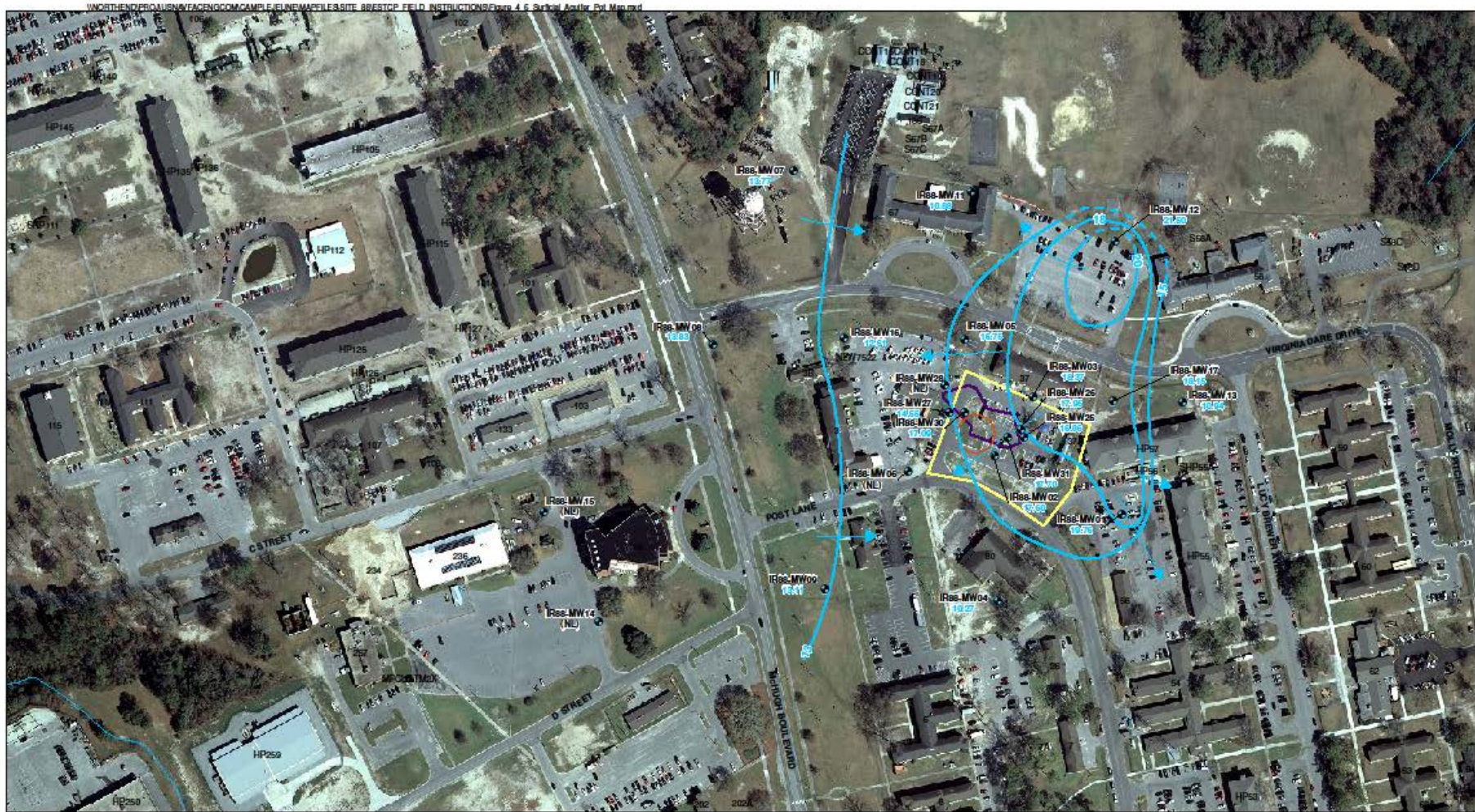


**Figure A-5.** Geologic cross-section within the test area based on most recent characterization activities





- Legend**
- Shallow Monitoring Well Location
  - Shallow Aquifer Potentiometric Contour
  - - - Shallow Aquifer Potentiometric Contour (inferred)
  - ➔ Groundwater Flow Direction
  - Surface Water Centerline
  - ▭ Site 88 Boundary
  - ▭ Test Area
  - ▭ Soil Mixing Boundary
- NL = Not Located

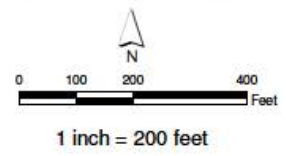


Figure 4-6  
Potentiometric Map  
Surficial Aquifer  
MCB CamLeJ  
North Carolina



Created by: Brooke Props/CLT Checked by: Kari Halberg/CLT

Figure A-6. Potentiometric map of the Surficial Aquifer



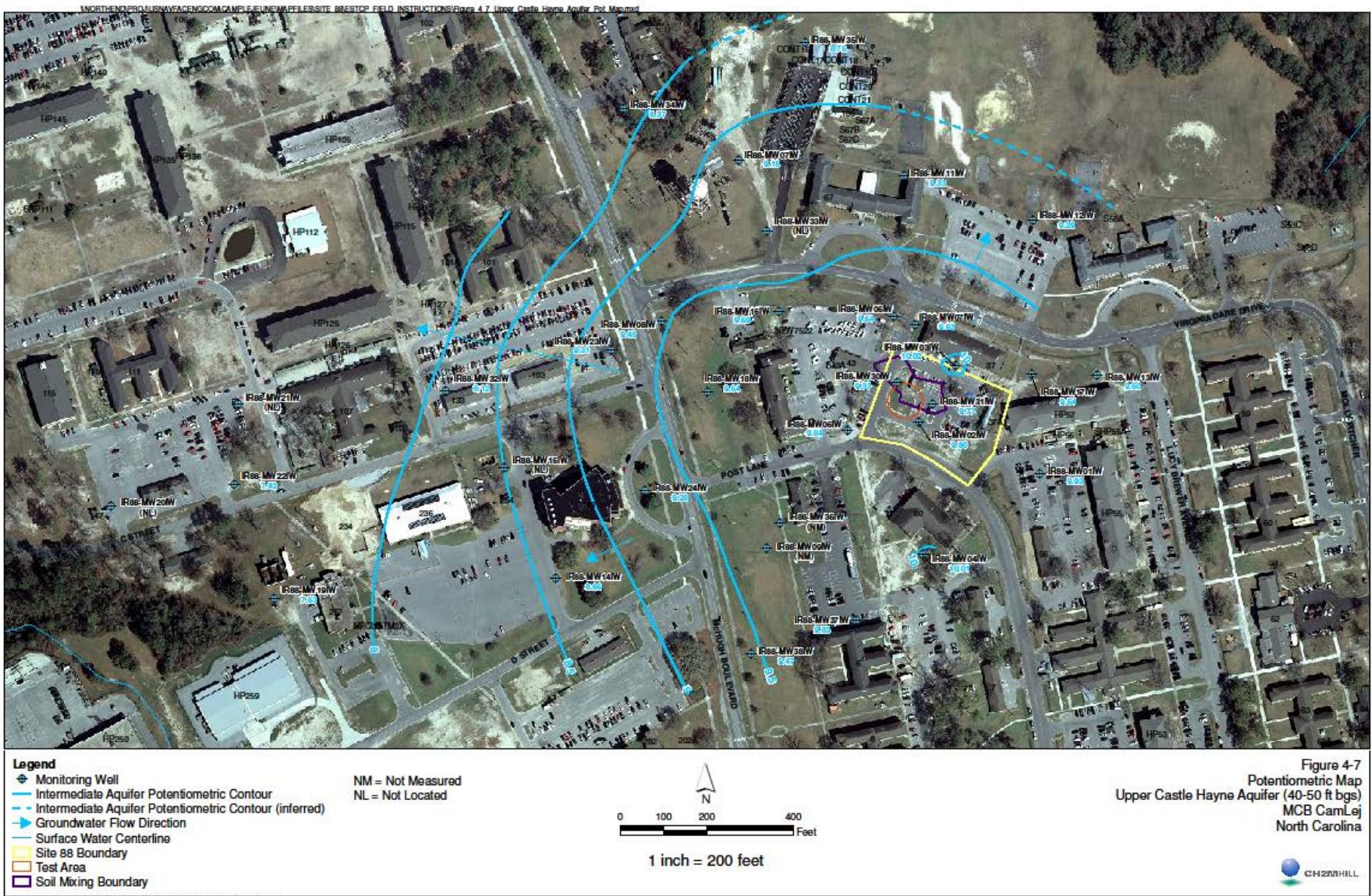


Figure A-7. Potentiometric map of the Upper Castle Hayne Aquifer

Hydraulic conductivity was calculated using the Hvorslev method. The hydraulic conductivity values calculated at each slug test location are summarized in **Table A-1**. The hydraulic conductivity in the Surficial Aquifer ranged from 1.5 ft/day to 5.2 ft/day, with an average hydraulic conductivity of 2.8 ft/day. The hydraulic conductivity in the Upper Castle Hayne Aquifer just below the confining unit ranged from 0.9 ft/day to 4.9 ft/day, with an average hydraulic conductivity of 2.5 ft/day.

**Table A-1. Hydraulic Conductivity Calculated at Each Slug Test Location**

Location	Interval Depth (ft bgs)	Test	Conductivity Results (ft/day)	Average Conductivity (ft/day)
ST-1	33-35	1	4.9	4.6
		2	4.8	
		3	4.2	
	38-40	1	2.6	2.5
		2	2.5	
		3	2.5	
	43-45	1	9.8	9.8
		2	9.8	
		3	9.8	
ST-2	14-16	1	2.2	2.0
		2	1.5	
		3	2.1	
	33-35	1	0.9	1.0
		2	1.0	
		3	1.0	
		4	1.0	
	42-44	1	6.1	6.0
		2	6.1	
		3	5.9	
		4	5.9	
		5	6.0	
	47-49	1	10.7	10.9
		2	10.7	
		3	11.0	
		4	11.0	
	54-56	1	8.7	9.0
		2	8.7	
		3	9.1	
		4	9.4	
		5	9.2	
		6	9.2	
	61-63	1	2.3	2.8
		2	2.4	
3		2.8		
4		3.7		
ST-3	14-16	1	5.2	4.0
		2	2.7	
	33-35	1	1.5	1.5
		2	1.4	
	45-47	1	16.6	17.0
		2	16.4	
		3	18.1	
	54-56	1	8.2	7.4
		2	7.5	
		3	8.0	
		4	6.9	
		5	6.3	
	60-62	1	3.9	3.2
2		2.5		
ST-4 (offset from ST-1)	14-16	1	0.6	0.6
		2	0.6	
		3	0.6	
		4	0.5	

As previously mentioned, HRP profiling was conducted at location H1 to obtain detailed hydraulic information. HRP technology involves the advancement of a probe that continuously logs pore pressure (measured as hydraulic head) and periodically logs pore pressure dissipation during stoppage time. The data are then electronically processed and used to estimate vertical gradients, soil type, and hydraulic conductivity. HRP conductivity values generally ranging from  $1 \times 10^{-5}$  centimeters per second (cm/s) (0.03 ft/day) to 0.001 cm/s (3 ft/day) in the Surficial Aquifer. In the Upper Castle Hayne Aquifer, HRP conductivity values were generally higher, ranging from  $1 \times 10^{-4}$  cm/s (0.3 ft/day) to 0.01 cm/s (30 ft/day) (**Appendix B**).

### ***A.3 Contaminant Distribution***

Based on the chemical data gathered for Site 88, former Building 25 is the source of the chlorinated VOCs that are currently observed in the groundwater within the shallow, intermediate, deep and very deep aquifer zones. The contaminants of concern (COCs) for Site 88 are PCE and its anaerobic biodegradation daughter products TCE, cis-1,2-DCE, and vinyl chloride.

Data obtained from groundwater samples collected as part of the RI in August 2007, indicate the maximum chlorinated VOC concentration within the shallow aquifer in the vicinity of former Building 25 and the test area, was reported at well IR88-MW02 with PCE and cis-1,2-DCE concentrations of 12,000 micrograms per liter ( $\mu\text{g/L}$ ) and 13,000  $\mu\text{g/L}$  respectively. Concentrations in the source area decrease significantly with depth, as shown by the 88-MW02 cluster, on **Figure A-4**. **Figures A-8** and **A-9** show the post-treatment distribution of PCE in the Surficial and Upper Castle Hayne Aquifers across the test area and Site 88 (2007).

During site characterization activities conducted in November and December 2009, membrane interface probe (MIP) profiling was conducted at six locations, M1 through M6 shown on **Figure A-4**, to delineate contaminant concentrations within the test area. Analytical results are shown on **Figure A-5**. MIP results indicate that the highest contaminant concentrations in the Surficial Aquifer exist from 16 to 18 ft bgs at location M1, immediately above an apparent confining unit. MIP results in this area are indicative of DNAPL. Results suggest that contamination in the shallow zone extends approximately 45 feet to the southeast towards location M2. MIP results consistently indicate higher contaminant concentrations throughout the Upper Castle Hayne Aquifer between 40 and 50 ft bgs at locations M1, M2, and M3. Again, the highest contaminant concentrations were detected at location M1 from approximately 33 to 35 ft bgs, immediately below an apparent confining unit. In both the Surficial and Upper Castle Hayne Aquifers, contaminant concentrations appear to decrease significantly to the west towards location M6.

Two groundwater and three soil samples were collected from soil boring DPT01. DPT soil samples were obtained using a 5-foot long, 1.5-inch inner diameter (ID) acetate macro-core sampler. As each borehole was advanced, continuous soil cores were collected and soil samples were collected directly from the acetate liners. The groundwater samples were collected by installing the groundwater sampler equipped with a screen to the terminating depth of the sampling interval. The drill rods were then pulled up to expose two feet of the screen. A peristaltic pump was used to purge the groundwater and collect the groundwater sample. DNAPL, which was dark in color, was observed in the groundwater sample collected in the shallow interval (14-16), immediately above the confining unit. The DNAPL was collected and submitted for laboratory analysis.



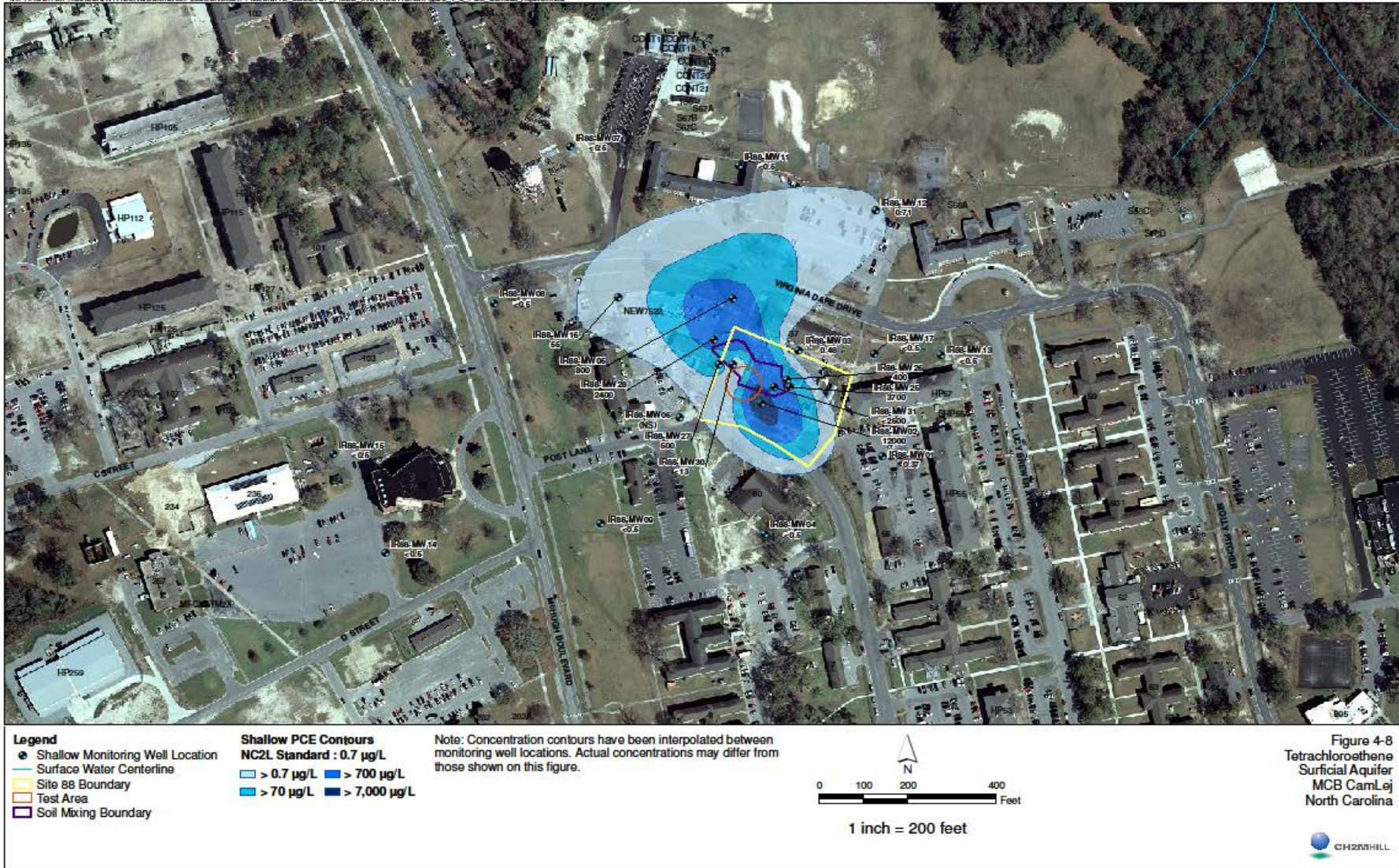


Figure A-8. PCE concentrations in the Surficial Aquifer (2007)



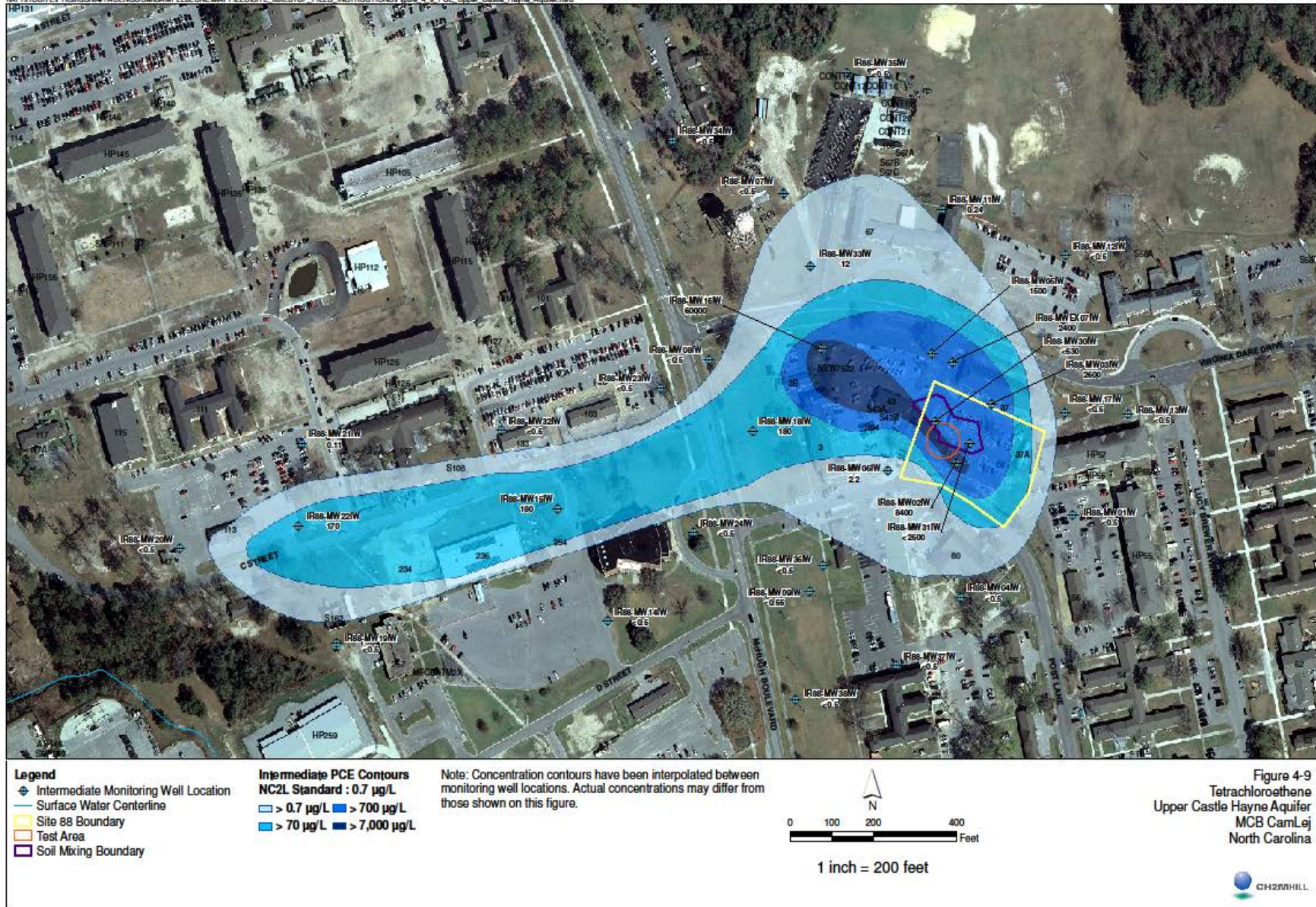


Figure A-9. PCE concentrations in the Upper Castle Hayne Aquifer (2007)

Analytical results are summarized in **Tables A-2 and A-3**. PCE and cis-1,2-DCE were detected at maximum concentrations of 7,100 micrograms per kilogram ( $\mu\text{g}/\text{kg}$ ) and 10,000  $\mu\text{g}/\text{kg}$ , respectively, in the soil sample collected immediately above the confining unit. Below the confining unit, PCE ranged from below the laboratory detection limit (720  $\mu\text{g}/\text{kg}$ ) to 1,300  $\mu\text{g}/\text{kg}$  and cis-1,2-DCE ranged from below the laboratory detection limit (5.2  $\mu\text{g}/\text{kg}$ ) to 22  $\mu\text{g}/\text{kg}$ . PCE was detected in the groundwater sample collected immediately above the confining unit (14-16 ft bgs) at a concentration of 220,000  $\mu\text{g}/\text{L}$ . Below the confining unit (33-35 ft bgs), PCE was detected at a concentration of 230,000  $\mu\text{g}/\text{L}$ . These groundwater concentrations are indicative of DNAPL, which is consistent with observed site conditions described above and the results of the MIP data collected from M1 adjacent to DPT01.

**Table A-2. Analytical Results for Contaminants (GC-MS) in Soils**

Sample ID	DPT01-16-18	DPT01-33-35	DPT01-53-55
Sample Date	11/12/2009	11/12/2009	11/12/2009
<b>Volatile Organic Compounds (<math>\mu\text{g}/\text{kg}</math>)</b>			
2-Butanone	49	14 U	10 U
Acetone	2300 U	48	40
Carbon Disulfide	14	14 U	10
Tetrachloroethene	7,100	720 U	1,300
Toluene	7.6	6.9 U	5.2 U
Trichloroethene	600	12	540 U
cis-1,2-Dichloroethene	10,000	22	5.2 U
trans-1,2-Dichloroethene	21	6.9 U	5.2 U
Vinyl Chloride	38	6.9 U	5.2 U

Notes:

U- Analyte not detected

**Table A-3. Analytical Results for Contaminants (GC-MS) in Groundwater**

Sample ID	DPT01-14-16	DPT01-33-35
Sample Date	11/12/2009	11/12/2009
<b>Chemical Name</b>		
<b>Volatile Organic Compounds (<math>\mu\text{g}/\text{L}</math>)</b>		
Acetone	75,000	50,000 U
Tetrachloroethene	220,000	230,000
Trichloroethene	10,000 U	13,000 U
cis-1,2-Dichloroethene	10,000 U	13,000 U
Vinyl Chloride	10,000 U	13,000 U

Notes:

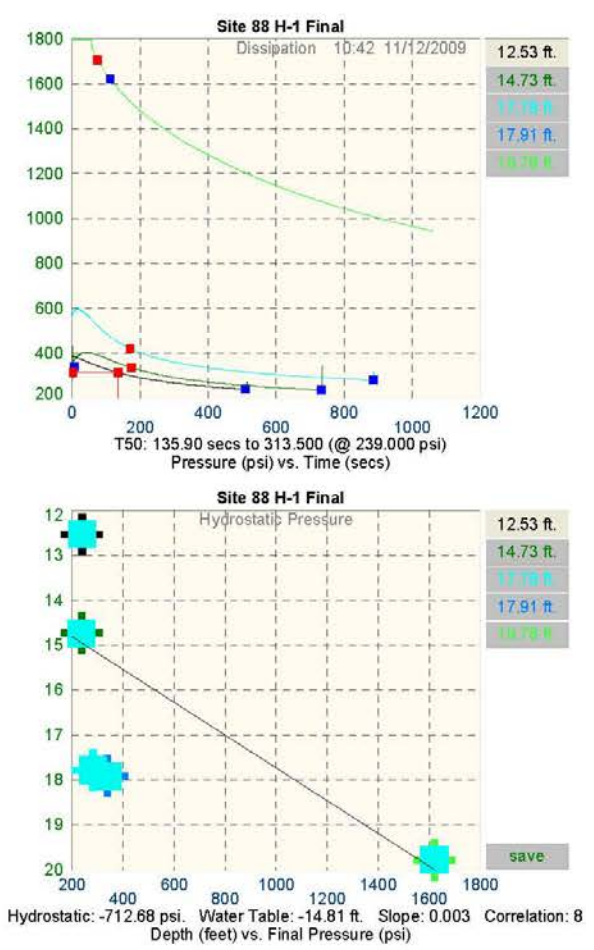
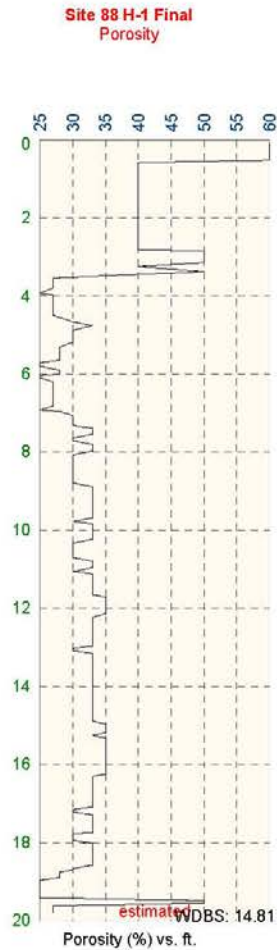
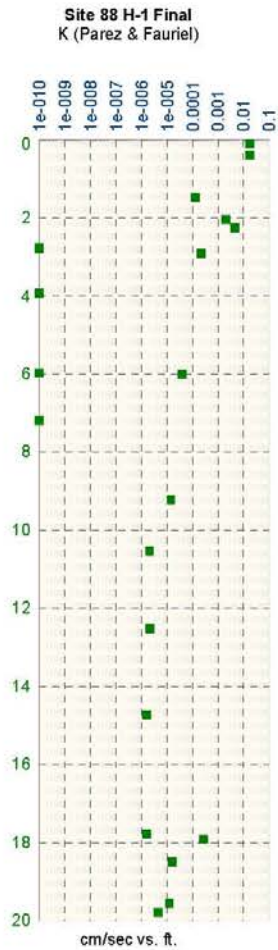
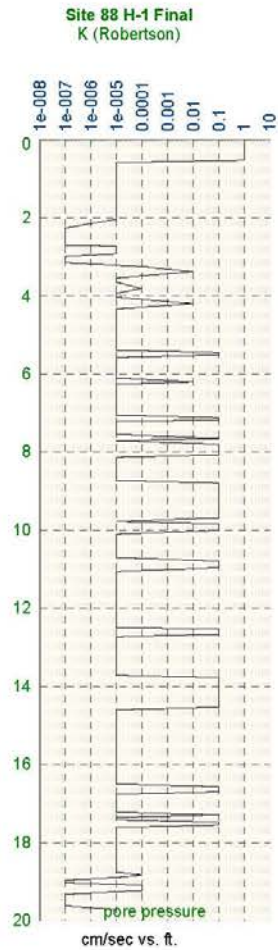
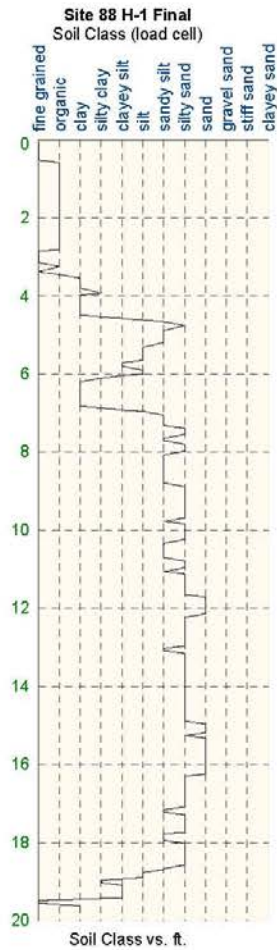
U- Analyte not detected

## **Appendix B: HRP Results**



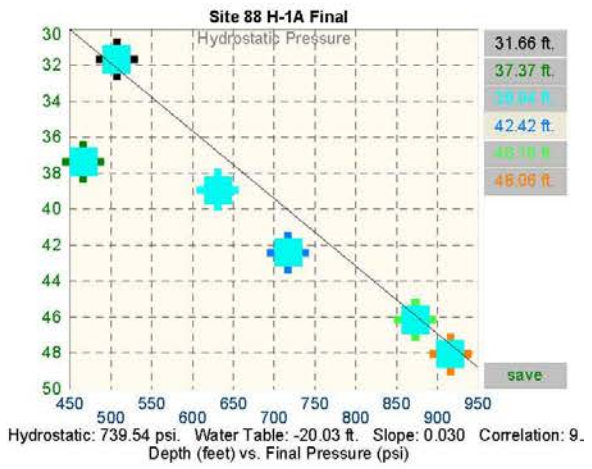
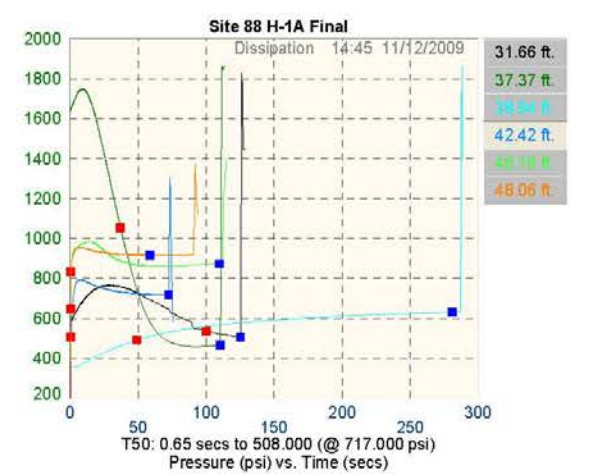
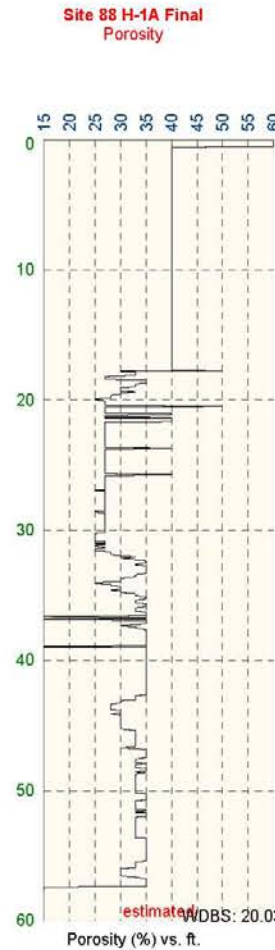
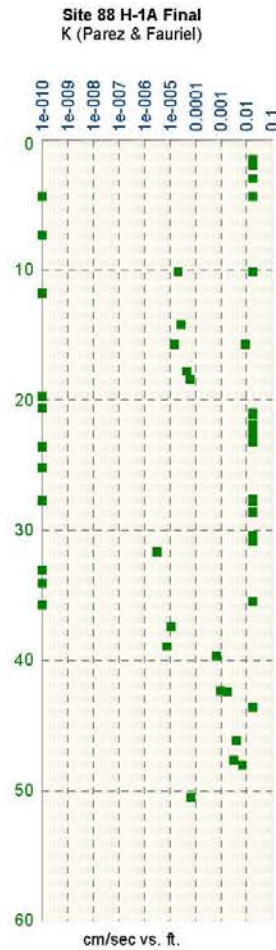
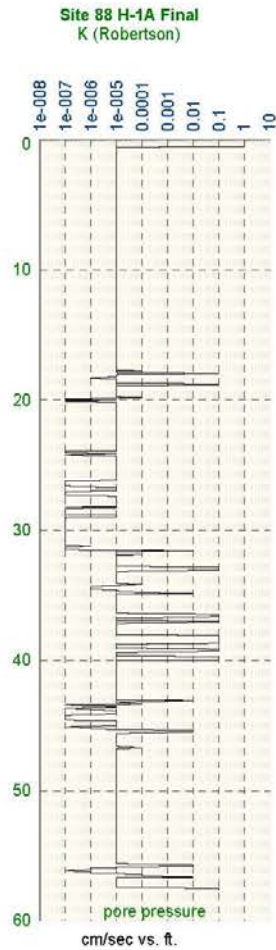
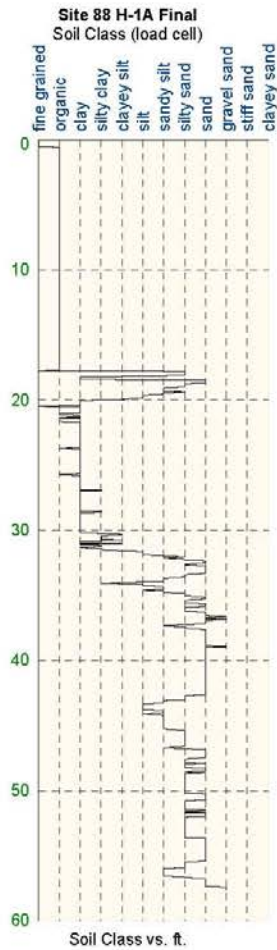
# DIRECT SENSING

H-1



# DIRECT SENSING

H-1A



**Appendix C: Boring Log for DPT01**



CH2MHILL

### Boring Number: DPT-01

Sheet: 1 of 2

Client: Clarkson University  
 Project: ESTCP  
 Location: Site 88, MCB Camp Lejeune  
 Project Number:

Driller: Drill Pro  
 Drilling Method: DPT  
 Sampling Method: macro-core  
 Logged by: B. Propst  
 Start/Finish Date: 11-12-09

Depth (ft)	Sample Information				Soil Log	Soil Description	Comments
	Sample #	Sample Type	Recovery (%)	SPT (6"-6" -ft)			
0						Ground Surface	
0 - 5		HA	100			Silty Sand (SM) Brown, dry, loose, fine grained	
5 - 10						No sample collected	
10 - 15	DP-1	DP	100			Sand (SP) Tan/brown, wet, loose, fine grained	
15 - 20	DP-2	DP	100			Sand (SP) Gray, wet, loose, fine grained	
20 - 23	DP-3	DP	100			Silty Sand (SM) Light brown, wet, loose, fine grained	
23 - 25						Sandy Clay (CL) Light brown, wet, soft, fine grained	
25 - 28	DP-4	DP	100			Clay (CH) Light gray, high plasticity, soft to medium stiff	
28 - 30						Sandy Clay (CL) Brown, wet, stiff	



CH2MHILL

### Boring Number: DPT-01

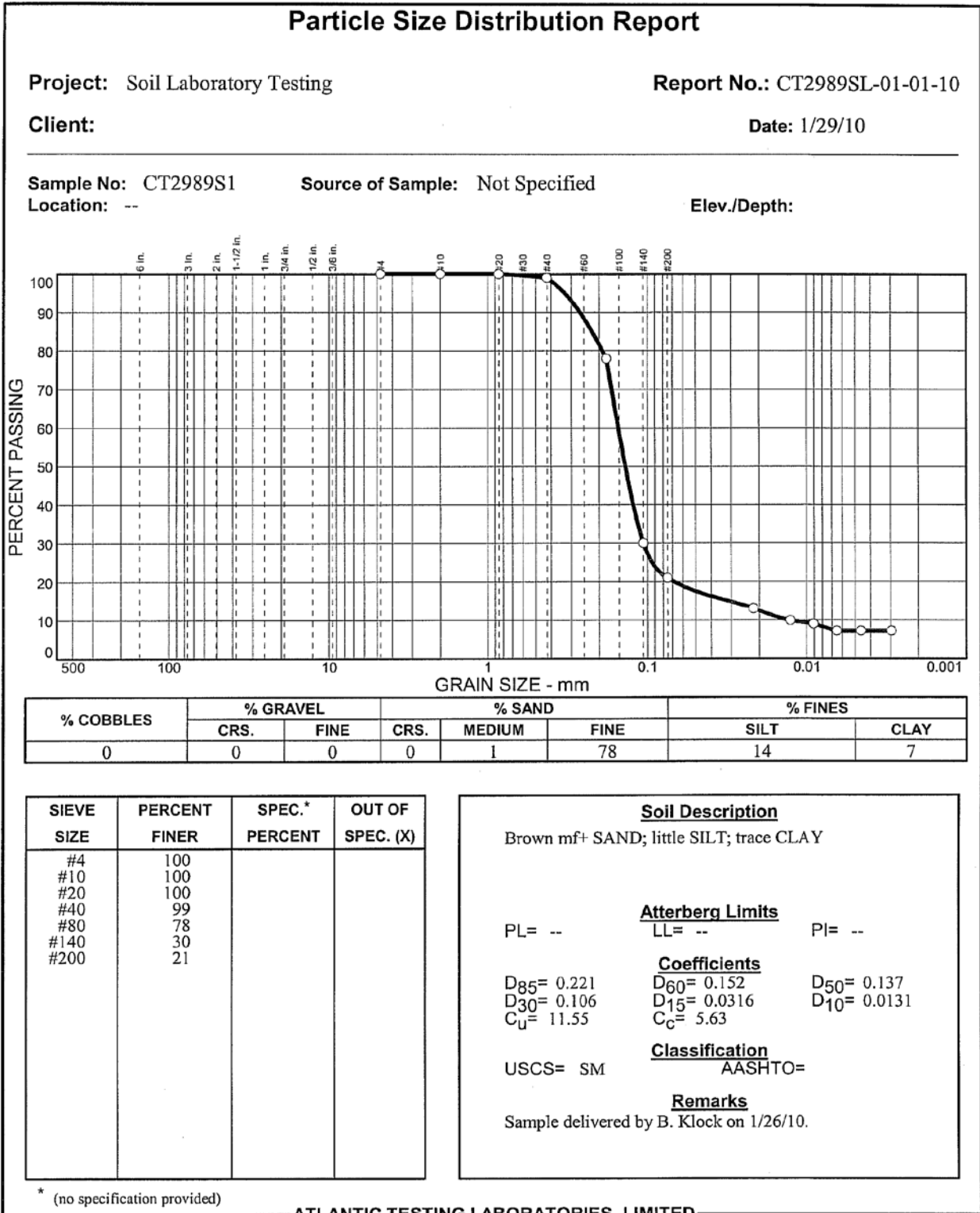
Sheet: 2 of 2

Client: Clarkson University  
 Project: ESTCP  
 Location: Site 88, MCB Camp Lejeune  
 Project Number:

Driller: Drill Pro  
 Drilling Method: DPT  
 Sampling Method: macro-core  
 Logged by: B. Propst  
 Start/Finish Date: 11-12-09

Depth (ft)	Sample Information				Soil Log	Soil Description	Comments
	Sample #	Sample Type	Recovery (%)	SPT (6"-6"-6")			
35	DP-5	DP	100			<b>Sand (SP)</b> Light gray, wet, medium dense, fine grained  <b>Silty Sand (SM)</b> Brown, wet, medium dense, fine grained  <b>Silty Sand (SM)</b> Gray, wet, loose to medium dense, fine grained  <b>Sand (SP)</b> Olive gray, wet, loose to medium dense, fine grained  <b>Sand (SP)</b> Gray, wet, loose, medium grained	
40	DP-6	DP	100				
45	DP-7	DP	100				
50	DP-8	DP	100				
50						Terminate boring at 50' bgs	
55							
60							

# Appendix D: Grain Size Analysis for Surficial Aquifer Media



Reviewed by: *[Signature]*

Date: 1/29/10

